frontiers | Research Topics

Global excellence in ethnopharmacology: Asia

Edited by
Aiping Lyu, Somasundaram Arumugam,
Bey Hing Goh and Uraiwan Panich

Published in
Frontiers in Pharmacology

ISSN 1664-8714
ISBN 978-2-8325-3881-4
DOI 10.3389/978-2-8325-3881-4

About Frontiers

Frontiers is more than just an open access publisher of scholarly articles: it is a pioneering approach to the world of academia, radically improving the way scholarly research is managed. The grand vision of Frontiers is a world where all people have an equal opportunity to seek, share and generate knowledge. Frontiers provides immediate and permanent online open access to all its publications, but this alone is not enough to realize our grand goals.

Frontiers journal series

The Frontiers journal series is a multi-tier and interdisciplinary set of open-access, online journals, promising a paradigm shift from the current review, selection and dissemination processes in academic publishing. All Frontiers journals are driven by researchers for researchers; therefore, they constitute a service to the scholarly community. At the same time, the *Frontiers journal series* operates on a revolutionary invention, the tiered publishing system, initially addressing specific communities of scholars, and gradually climbing up to broader public understanding, thus serving the interests of the lay society, too.

Dedication to quality

Each Frontiers article is a landmark of the highest quality, thanks to genuinely collaborative interactions between authors and review editors, who include some of the world's best academicians. Research must be certified by peers before entering a stream of knowledge that may eventually reach the public - and shape society; therefore, Frontiers only applies the most rigorous and unbiased reviews. Frontiers revolutionizes research publishing by freely delivering the most outstanding research, evaluated with no bias from both the academic and social point of view. By applying the most advanced information technologies, Frontiers is catapulting scholarly publishing into a new generation.

What are Frontiers Research Topics?

Frontiers Research Topics are very popular trademarks of the *Frontiers journals series*: they are collections of at least ten articles, all centered on a particular subject. With their unique mix of varied contributions from Original Research to Review Articles, Frontiers Research Topics unify the most influential researchers, the latest key findings and historical advances in a hot research area.

Find out more on how to host your own Frontiers Research Topic or contribute to one as an author by contacting the Frontiers editorial office: frontiersin.org/about/contact

Global excellence in ethnopharmacology: Asia

Topic editors

Aiping Lyu — Hong Kong Baptist University, Hong Kong, SAR China

Somasundaram Arumugam — National Institute of Pharmaceutical Education and Research, Kolkata, India

Bey Hing Goh — Sunway University, Malaysia

Uraiwan Panich — Mahidol University, Thailand

Citation

Lyu, A., Arumugam, S., Goh, B. H., Panich, U., eds. (2023). *Global excellence in ethnopharmacology: Asia*. Lausanne: Frontiers Media SA.

doi: 10.3389/978-2-8325-3881-4

Table of contents

frontiers | Frontiers in Pharmacology

TYPE Editorial
PUBLISHED 23 October 2023
DOI 10.3389/fphar.2023.1298718

OPEN ACCESS

EDITED AND REVIEWED BY
Michael Heinrich,
University College London,
United Kingdom

*CORRESPONDENCE
Somasundaram Arumugam,
somasundaram.niperk@nic.in,
somasundaram143@gmail.com
Bey Hing Goh,
goh.bey.hing@monash.edu

RECEIVED 22 September 2023
ACCEPTED 12 October 2023
PUBLISHED 23 October 2023

CITATION
Arumugam S, Lyu A, Goh BH and Panich U (2023), Editorial: Global excellence in ethnopharmacology: Asia.
Front. Pharmacol. 14:1298718.
doi: 10.3389/fphar.2023.1298718

Editorial: Global excellence in ethnopharmacology: Asia

Somasundaram Arumugam[1]*, Aiping Lyu[2], Bey Hing Goh[3,4,5]* and Uraiwan Panich[6]

[1]Department of Pharmacology and Toxicology, National Institute of Pharmaceutical Education and Research (NIPER)-Kolkata, Kolkata, West Bengal, India, [2]School of Chinese Medicine, Hong Kong Baptist University, Kowloon, Hong Kong SAR China, [3]Sunway Biofunctional Molecules Discovery Centre (SBMDC), School of Medical and Life Sciences, Sunway University, Sunway, Malaysia, [4]College of Pharmaceutical Sciences, Zhejiang University, Hangzhou, Zhejiang, China, [5]Biofunctional Molecule Exploratory Research Group (BMEX), School of Pharmacy, Monash University Malaysia, Bandar Sunway, Malaysia, [6]Department of Pharmacology, Faculty of Medicine Siriraj Hospital, Mahidol University, Bangkok, Thailand

KEYWORDS

ethnopharmacology, Asia, innovation, trad. chinese medicine (TCM), ayurveda

Editorial on the Research Topic
Global excellence in ethnopharmacology: Asia

Introduction

Ethnopharmacology is a multidisciplinary field combining elements of anthropology, pharmacology, botany, chemistry, and other disciplines to study various cultures' traditional knowledge and medicinal use of plants, animals, and other natural substances (Reyes-García, 2010). It focuses on understanding the relationship between different cultural groups and the plants and substances they use for healing and investigating the scientific basis for the efficacy of these traditional remedies (Fokunang et al., 2011). Ethnopharmacologists study the traditional healing practices of different cultures, including indigenous and local communities. They document the use of specific plants, animals, minerals, and other natural substances in treating various ailments, including botanical and chemical analyses to determine the active metabolites responsible for therapeutic effects. Ethnopharmacologists also focus on conserving medicinal plants and other natural resources used in traditional medicine by promoting sustainable harvesting and cultivation practices to ensure the availability of these resources for future generations. Traditional remedies discovered through ethnopharmacological research can serve as sources of inspiration for developing new pharmaceutical drugs. Most modern medications can be traced back to their origins in traditional remedies. Hence, the established credentials and credibility of ethnopharmacology are widely acknowledged and can contribute to integrating traditional medicine into modern healthcare systems, particularly in areas where traditional remedies are extensively utilized. This integration has the potential to enhance healthcare accessibility and mitigate healthcare disparities. Keeping this in mind, this topic has been chosen to have a collection of ethnopharmacology-based research in Asia, which has the richest history of several traditional medicine systems.

Ethnopharmacology in Asia

Astragalus membranaceus Bunge (Family: Fabaceae), commonly known as Huangqi or Astragalus, is a prominent botanical drug in Traditional Chinese Medicine (TCM) with a long history of use. In TCM, Astragalus is considered a powerful Qi (body's vital energy or life force) tonic. It is frequently used to combat fatigue, boost energy levels, and improve physical endurance. It supports the immune system in addition to its adaptogenic properties. It has anti-inflammatory effects and promotes cardiovascular health by improving blood circulation, reducing blood pressure, and protecting the heart from various forms of stress. Some research suggests that Astragalus may help regulate blood sugar levels and improve insulin sensitivity. Astragalus is often associated with longevity and anti-ageing properties in TCM. It improves digestive health and promotes overall health and wellbeing (Wang et al.).

Similarly, Wen et al. have reviewed the chemical composition, pharmacology, pharmacokinetics and toxicity of *Acorus calamus* var. *angustatus* Besser (Family: Acoraceae) rhizome, a natural product commonly known as "Shi Chang Pu" or "Acori tatarinowii rhizome" in TCM. In TCM, Acori tatarinowii rhizome is classified as a botanical drug that "opens the orifices" and is known for its ability to clear the mind, improve mental clarity, and enhance cognitive function. It also has sedative effects, making it useful for anxiety, insomnia, and restlessness. This botanical drug is also used in TCM to address digestive issues, including abdominal pain, diarrhoea, and bloating. Precaution is necessary since *Acori tatarinowii* contains certain metabolites, such as β-asarone, which can have toxic effects when consumed in large quantities.

Geng et al. reviewed the ethnobotany, phytochemistry and pharmacological properties of *Fagopyrum cymosum* (Trevir.) Meisn. (Family: Polygonaceae), also known as "He Ye" or "*Fagopyri dibotryis* Rhizome" in TCM. It is traditionally used to clear heat and toxins from the body in conditions associated with excessive heat, such as fever, sore throat, and skin rashes. Because of its anti-inflammatory properties, it is helpful in inflammatory skin disorders. Some traditional uses of *F. dibotryis* rhizome involve its diuretic properties. Experiments performed *in vitro* and *in vivo* showed that the extracts or fractions of *F. dibotryis* rhizome had a wide range of pharmacological activities, including antitumor, anti-inflammatory, immunomodulatory, antioxidant, antimicrobial, and antidiabetic. They have concluded that *F. dibotryis* rhizome is worthy of further study and application as a potential antitumor drug.

Apart from these reviews, this topic has five research papers focusing on various traditional or ethnomedicine and their pharmacological activities. Choudhary et al. have studied the antidepressant effects of a natural coumarin antioxidant, 4-methyl esculetin, that is isolated from the peels of *Aesculus hippocastanum* L (Family: Sapindaceae), through the inhibition of LPS-induced NLRP3 inflammasome activation. They have performed *in silico*, *in vitro* and *in vivo* studies and showed the antioxidant, anti-inflammatory and antidepressant effects, possibly through the inhibition of NLRP3 inflammasome activation, suggesting the potential clinical use of 4-methyl esculetin in NLRP3 inflammasome-associated inflammatory diseases such as depression.

The comprehensive metabolomic profiling analysis combined with network analysis of serum pharmacochemistry has revealed the therapeutic mechanism of *Ardisia japonica* (Thunb.) Blume (Family: Primulaceae) also known as "Ardisiae Japonicae Herba (AJH)" against acute lung injury in LPS-induced rats (Han et al.). Metabolomics results showed that AJH effectively treated ALI by alleviating the infiltration of inflammatory cells in alveolar spaces and regulating the expression of inflammatory cytokines. AJH might link to reverse the abnormality of phenylalanine, tyrosine, and tryptophan biosynthesis and linoleic acid metabolism pathways to regulate the concentrations of potential biomarkers to normal levels. Therefore, AJH could alleviate inflammation responses in the Acutlung injury treatment. A similar study evaluated the molecular mechanism of Yinchen Sini decoction in CCl_4-induced acute liver injury in mice using Integrated network analysis and metabolomics (Zheng et al.).

A medical ethnobotanical assessment was conducted to comprehensively understand the single botanical drugs in Ayurvedic Pharmacopoeia of India (API) (Yao et al.). They also highlighted the importance of quantitative ethnobotanic methods in understanding traditional medical knowledge. They have clarified the single botanical drugs, their biological origins, and their standard therapeutic uses. Their work provides ready-to-use medical ethnobotanical information on Ayurvedic botanical drugs.

The extensive exploration study of the traditional knowledge of the Gelao ethnic minority in North Guizhou, China, to gain an in-depth understanding of their botanical drug practices (Liu et al.). The field research in Gelao communities of Daozhen, Wuchuan and Zheng'an counties was done using interviews, surveys and participatory rural appraisal. Though this study had some limitations, including a lack of chemical and pharmacological analysis of the plants to verify their active metabolites and mechanisms of action, they have collected significant information on 187 medicinal plants, including their botanical names, sources, processing methods, primary therapeutic uses, and administration techniques. They also planned to conduct comprehensive and systematic investigations into Gelao traditional medicine and culture, establish appropriate protective measures, and develop high-value pharmaceutical products.

The application of digital intelligence technology in Processing Chinese Materia Medica (PCMM) was analyzed and discussed by Zhang et al. They have addressed the application of digital intellectualization technology in the processing of TCM, which promoted the standardization of the processing, the standardization of the quality of decoction pieces, the digitalization and intellectualization of production, and the safety and effectiveness of clinical use of TCM decoction pieces in addition to providing a theoretical basis for the technical progress and high-quality development of TCM industry in the future.

While valuable in many ways, traditional medicine systems have drawbacks and limitations, such as lack of scientific evidence, limited standardization, safety concerns, inadequate regulation, cultural and geographic limitations, resistance to change, limited documentation, limited accessibility, and lack of integration. It's essential to recognize that traditional medicine can offer valuable insights into treating specific conditions and complement modern medicine. However, addressing these drawbacks through proper

research, regulation, and integration is crucial to ensure the safety and efficacy of traditional medicine practices. One such approach is the recent establishment of guidelines for Phytopharmaceuticals to improve the quality of botanical drugs, though it applies only to plant-based products.

Conclusion

In summary, ethnopharmacology serves as a vital link between traditional wisdom and contemporary scientific exploration. It plays a pivotal role in substantiating and harnessing the healing traditions from diverse cultures, simultaneously enriching our comprehension of natural remedies and their possible advantages. We trust that this Research Topic has comprehensively addressed significant research within the realm of ethnopharmacology and traditional medicinal systems, especially in the Asian context, which may inspire novel concepts and propel future research forward.

Author contributions

SA: Conceptualization, Writing–original draft, Writing–review and editing. AL: Writing–review and editing. BG: Writing–review and editing. UP: Writing–review and editing.

Funding

The author(s) declare that no financial support was received for the research, authorship, and/or publication of this article.

Conflict of interest

The authors declare that the research was conducted in the absence of any commercial or financial relationships that could be construed as a potential conflict of interest.

The handling editor MH declared a past co-authorship/collaboration with the author AL.

The author(s) declared that they were an editorial board member of Frontiers, at the time of submission. This had no impact on the peer review process and the final decision.

Publisher's note

References

Fokunang, C. N., Ndikum, V., Tabi, O. Y., Jiofack, R. B., Ngameni, B., Guedje, N. M., et al. (2011). Traditional medicine: past, present and future research and development prospects and integration in the National Health System of Cameroon. *Afr. J. Tradit. Complement. Altern. Med.* 8 (3), 284–295. doi:10.4314/ajtcam.v8i3.65276

Reyes-García, V. (2010). The relevance of traditional knowledge systems for ethnopharmacological research: theoretical and methodological contributions. *J. Ethnobiol. Ethnomed* 6, 32. doi:10.1186/1746-4269-6-32

frontiers | Frontiers in Pharmacology

TYPE Original Research
PUBLISHED 23 February 2023
DOI 10.3389/fphar.2023.1120508

OPEN ACCESS

EDITED BY
Uraiwan Panich,
Mahidol University, Thailand

REVIEWED BY
Benneth Ben-Azu,
Delta State University, Nigeria
Maria Bove,
University of Foggia, Italy
Wladyslaw - Lason,
Maj Institute of Pharmacology, Polish Academy of Sciences, Poland

*CORRESPONDENCE
Nitesh Kumar,
niteshkumar43@gmail.com

SPECIALTY SECTION
This article was submitted to Ethnopharmacology, a section of the journal Frontiers in Pharmacology

RECEIVED 10 December 2022
ACCEPTED 07 February 2023
PUBLISHED 23 February 2023

CITATION
Choudhary K, Prasad SR, Lokhande KB, Murti K, Singh S, Ravichandiran V and Kumar N (2023), 4-Methylesculetin ameliorates LPS-induced depression-like behavior through the inhibition of NLRP3 inflammasome.
Front. Pharmacol. 14:1120508.
doi: 10.3389/fphar.2023.1120508

4-Methylesculetin ameliorates LPS-induced depression-like behavior through the inhibition of NLRP3 inflammasome

Khushboo Choudhary[1], Surendra Rajit Prasad[2], Kiran Bharat Lokhande[3], Krishna Murti[4], Sanjiv Singh[1], Velayutham Ravichandiran[1,2,4] and Nitesh Kumar[1]*

[1]Department of Pharmacology and Toxicology, National Institute of Pharmaceutical Education and Research–Hajipur, Hajipur, India, [2]Department of Biotechnology, National Institute of Pharmaceutical Education and Research–Hajipur, Hajipur, India, [3]Translational Bioinformatics and Computational Genomics Research Lab, Department of Life Sciences, Shiv Nadar University, GBNagar, Uttar Pradesh, India, [4]Department of Pharmacy Practice, National Institute of Pharmaceutical Education and Research–Hajipur, Hajipur, India

The pathophysiology of depression is heavily dependent on inflammation. Evidence suggests that the etiology of depression is linked with NLRP3 inflammasome-induced inflammation. Therefore, blocking the activated NLRP3 inflammasome may be beneficial for treating depression. Due to the limitations of currently available antidepressants, it is necessary to develop novel, safe, and affordable drugs for the treatment of depression. A natural coumarin derivative named 4-methylesculetin (4-MESC) possesses anti-inflammatory properties. However, the role of 4-MESC as an antidepressant has not been elucidated. Therefore, in this study, we explored the antidepressant-like effects of 4-MESC and its underlying molecular mechanism through the modulation of the NLRP3 inflammasome. The docking and molecular dynamic simulation studies revealed that 4-MESC has a higher affinity for the NLRP3 PYD. Blood–brain barrier permeability was confirmed using the SwissADME pharmacokinetic tool. High doses (50 mg/kg) of 4-MESC significantly reduced the immobility duration in the tail-suspension test (TST) and forced swim test (FST) without changing the overall locomotor activity in the female Swiss albino mice that were subjected to lipopolysaccharide (LPS). LPS-induced pro-inflammatory cytokines such as IL-6 and TNF-α were reduced in serum and brain tissues using 4-MESC. 4-MESC's neuroprotective effects are mediated by increased brain-derived neurotrophic factor (BDNF) and decreased cortisol levels. 4-MESC markedly reduced LPS-induced elevated levels of ROS and lipid peroxidation (malondialdehyde levels) and enhanced the superoxide dismutase (SOD) activity and glutathione levels, which revealed its anti-oxidant potential against oxidative stress. 4-MESC diminished the expression levels of NF-κBp65, IL-6, NLRP3, caspase-1, gasdermin D, and IL-1β in the hippocampus. These findings demonstrated that 4-MESC exhibited antidepressant-like effects by inhibiting the NLRP3 inflammasome. However, other antidepressant mechanisms might also be involved which require further studies.

KEYWORDS

4-methylesculetin, anti-depressant activity, NLRP3 inflammasome, lipopolysaccharide, cytokines

Introduction

Depression is a low-mood situation that happens in everyone's life and impacts the work efficiency of most affected individuals. It is very common among people of all ages and genders in varying degrees of severity. Depending on the severity of the disease, different people experience different symptoms. The most common symptoms are mood swings ranging from emotional bursts to anger, reduced food intake, sometimes overeating, disturbed sleep, an inability to focus on work, a sense of guilt, hopelessness, and loneliness, which can lead to suicidal ideation if left untreated. Depression has become a common disorder worldwide, affecting an estimated 3.8% of the population, including 5% of adults and 5.7% of adults over the age of 60 (World Health Organization, 2022). Depression affects approximately 280 million people, and the numbers exceeded 300 million in 2015, which was equivalent to 4.3% of the world's population (World Health Organization, 2022). According to the National Mental Health Survey 2015–16, one in 20 Indians suffers from depression, and approximately 15% require active intervention for this mental health issue (World Health Organization, 2023). At its worst, depression can result in suicide; every year, over 800,000 individuals commit suicide, and it is the second leading cause of death among people between ages 15–29 years (World Health Organization, 2023). According to estimates, approximately 258,000 suicide cases occurred in India in 2012 among people in the age group of 15–49 (World Health Organization, 2023). It is predicted by the WHO, after examining the existing scenario of depression among people, which currently holds the third rank for the burden of disease, that it may progress to rank first by 2030 (Malhi and Mann, 2018). The progression of depression accelerated during COVID-19, when the entire nation was in lockdown, due to the deaths of numerous people (Santomauro et al., 2021). Many factors are associated with the pathophysiology of depression. The most popular biochemical theory is the monoamine hypothesis, which states that a deficiency of monoamines (norepinephrine, serotonin, and dopamine) leads to depression (Millan, 2004). The monoaminergic system covers a large area of the brain, which suggests that this system is involved in many brain functions. In patients with depression, many of these functions are impaired (Dunlop and Nemeroff, 2007). The stresses of life also contribute to depression. Recurrent stress is an important factor promoting the pathogenesis of depression. Depression can, in turn, lead to more stress and dysfunction and worsen the affected person's life situation (Ben-Azu et al., 2020). In contrast, depression can lead to a higher risk of developing inflammatory disorders, such as diabetes and cardiovascular disorders (Okoh et al., 2020). There is a strong link between aberrant immune functions and depression. It has been noticed for a long time that repeated stress also induces acute changes in the immune system. In the case of stress conditions, the hyperactivation of the corticotropin-releasing factor (CRF) occurs which activates the hypothalamic–pituitary–adrenal (HPA) axis and leads to depression (Gold et al., 2002). Inflammatory responses play a vital role in the pathogenesis of depression. Many studies have found that depressed people have higher levels of pro-inflammatory cytokines (Dantzer et al., 2008). Malondialdehyde (MDA) levels and depression are interlinked. MDA levels are increased in depressed mice compared to normal mice (Pal et al., 2006). Also, gamma-aminobutyric (GABA) levels decreased in the prefrontal and occipital cortex in the depressed patient (Petty et al., 1992). The effect of inflammation and inflammatory cytokines on the monoamines, and the excitatory amino acid glutamate, has received attention because neurotransmission plays an important role in mood regulation. Inflammatory cytokines can reduce synaptic availability of monoamines in various ways, which is thought to be a fundamental factor in the pathogenesis of depression (Miller and Raison, 2016). For instance, in experimental mice, it has been demonstrated that IL-1b and TNF-α activation of p38 mitogen-activated protein kinase (MAPK) increases the expression and functionality of the serotonin reuptake pumps, resulting in the decreased synaptic availability of serotonin and depressive-like behavior (Zhu et al., 2010). Inflammatory cytokines have also been reported to reduce the availability of tetrahydrobiopterin (BH4), an essential enzyme co-factor in the production of all monoamines that is extremely vulnerable to oxidative stress, by producing reactive oxygen and nitrogen species (Neurauter et al., 2008) The treatable drugs mostly have mechanisms for regulating the monoamine levels, which are not adequate for an effective cure, and the conventional drug is the only available treatment for depression, which has certain limitations such as nausea, sexual dysfunction, insomnia, anxiety, dry mouth, and weight gain (Hu et al., 2004). Using the Antidepressant Side-Effect Checklist (ASEC), the reported side effects of antidepressant drugs were categorized as mild, moderate, and severe. A total of 74.13% patients reported antidepressant side effects, with anxiety (17.05%) and sleepiness (17.05%) being the most common ones. More than half of the patients, 52.29%, exhibited low levels of adherence (Marasine et al., 2020). Therefore, the development of safe and effective antidepressants of natural origin is necessary as an alternative therapy. It has been observed in many studies that there is a link between inflammation and depression (Tong et al., 2020). TNF-α, IL-1b, and IL-6, pro-inflammatory cytokines, were more prevalent than usual in clinical samples from depressed patients (Amitai et al., 2016). Additionally, elevated inflammatory mediators may act as indicators that predict antidepressant resistance. Therefore, anti-inflammatory drugs can actually be beneficial for MDD patients who are treatment-resistant and have higher levels of inflammatory mediators (Tong et al., 2020). Recently, the inflammasome has become an unanticipated sensor for metabolic stress and risk (Alcocer-Gómez and Cordero, 2014). The NLRP3 inflammasome is a composite protein mostly composed of three components, namely, the NOD-like receptor NLRP3, central connector ASC, and caspase-1. The effectiveness of this integrated system is to provide protection against the invading microbes *via* the activation of inflaming mediators such as interleukins (ILs: IL-1b and IL-18, further leading to pyroptosis) (Amitai et al., 2016). The pyroptosis-related protein gasdermin D is cleaved, the pro-inflammatory cytokine IL-1b is produced, and microglia are activated as a result of NLRP3 inflammasome activation

(Fu et al., 2013). The NLRP3 inflammasome has been linked to the pathophysiology of depression and may offer a fresh approach to treating the condition. Patients with depression had elevated levels of NLRP3, caspase-1, and IL-1b in their blood samples (Alcocer-Gómez et al., 2014). It has been observed that rodent depression models activate the NLRP3 inflammasome (Alcocer-Gómez et al., 2017). Suppression of the NLRP3 inflammasome improved the depressive-like behavior in mice and decreased IL-1b expression (Xu et al., 2016). Interleukin (IL)-1b, a pro-inflammatory cytokine, was the first cytokine to be identified as enhancing HPA axis activity during an immunological response (Bernton et al., 1987). There are many studies that show depression is associated with increased brain or peripheral IL-1b production, as well as HPA axis hyperactivity (Maes et al., 1993). The report suggested that the NLRP3 inflammasome may be a key mediator of stress-induced depression and a potential novel target for depression as a result of the NLRP3 inflammasome's role in lipopolysaccharide (LPS)-induced depression (Iwata et al., 2013).

Natural coumarin anti-oxidant 4-methylesculetin (4-MESC) has anti-inflammatory effects on intestinal inflammation, whose pathogenesis and oxidative stress are both major contributors to it (Tanimoto et al., 2020). 4-methylesculetin is naturally derived from the peels of *Aesculus hippocastanum* L. It is 6,7-dihydroxy-4-methylcoumarin and can be synthetically derived from other coumarin derivatives. Trinitrobenzenesulfonic acid (TNBS) caused intestinal inflammation, which 4-methylesculetin (4-MESC) prevented by suppressing myeloperoxidase (MPO) activity and preventing glutathione (GSH) depletion (Witaicenis et al., 2010; Witaicenis et al., 2012). In fact, the intestinal anti-inflammatory effects of 4-MESC were also associated with a decrease in malondialdehyde levels *in vivo* and the suppression of a number of pro-inflammatory cytokines *in vitro*, including IL-1, IL-8, IL-2, and IFN-γ (Witaicenis et al., 2012). When compared to esculetin, another coumarin derivative, 4-MESC's anti-oxidant, and anti-inflammatory properties were dependent on the presence of a methyl group at the C-4 position (Zhao and Zhao, 2020). Although its anti-oxidant and anti-inflammatory activity are reported, until date, there is no report of 4-MESC as an antidepressant agent. The present study was designed to assess the anti-depressant effect of 4-MESC and its underlying mechanism through the inhibition of NLRP3 inflammasome activation induced by LPS administration.

Materials and methods

Reagents

LPS (from *Escherichia Coli* 0111: B4) for the *in vivo* study was purchased from Sigma. Mouse Il-6 ELISA Kit, Glutathione Assay Kit, Mouse Tumor Necrosis Factor-alpha ELISA Kit, and SOD Activity Assay Kit were purchased from Sigma. Mice cortisol and BDNF ELISA Kits were purchased from MyBioSource. A BCA protein assay kit was purchased from Merck, and 4-methylesculetin (4-MESC), from TCI Chemicals.

In silico study

Docking and molecular dynamic simulation study

The docking and MD simulation were used to check the interaction between receptor and ligand, as described by Lokhande et al. (2021). The Protein Data Bank was used to find the X-ray crystal structure of the NLRP3 pyrin domains in humans (PDB ID: 3QF2). The SDF file of the structure was retrieved from PubChem. Its energies were reduced using the OPLS-2005 force field and Maestro Schrodinger software until an energetically stable conformation was attained. For a molecular-docking investigation involving the NLRP3 pyrin domain, these energetically stable conformations were used. Small compounds are docked into the protein-binding site using molecular-docking techniques. FlexX software was used for docking studies on natural chemicals to determine how these medications interact with the NLRP3 pyrin domain. Receptor atoms from the PDB database, for example, the NLRP3 pyrin domain (PDB ID: 3QF2), are treated as stiff during docking computations. The binding cavity in the receptor is categorized using the receptor preparation wizard option available in FlexX software. Then, all substances are docked to the NLRP3 pyrin domain's binding site to forecast the binding poses of the retrieved medications. This was performed to assess the docking study's results in the binding pocket of the pyrin domain, which were revealed under conformational dynamics, and the binding potency of crystal ligands and 4-MESC. 4-MESC was the primary natural chemical that we simulated by using full-scale molecular dynamics for 100 nanoseconds using Desmond. The extended simple point charge (SPC), a three-point water model with periodic boundary conditions, is used to immerse the system for complexes in a cubic box filled with water and having water molecules spaced at a distance of one. By adding the proper counter ion randomly to the solvated complex system, the entire charge of the solvent system is neutralized. The steepest descent method is used to minimize energy, which is an essential stage in MD. When applying periodic boundary conditions to a finite system, edge effects are minimized using a cubic box type with a box size of 0.9. Translated copies, which cover the space-filling box, are filled with the atoms of the system that will be replicated. In this work, the OPLS-2005 force field, an enhanced force field suitable for MD simulation of the receptor, is used to characterize the system's potential energy. The Martyna–Tobias–Klein barostat method and the Nose–Hoover chain thermostat method are used in molecular dynamic investigations, which take into account a number of parameters as inputs. The constraints are established as all-bonds. The trajectories of stable conformation are recorded and evaluated to investigate relationship stability after the system has reached equilibrium. The initial conformations and the C-alpha backbone conformational change of the NLRP3 pyrin domain crystal structure have been compared.

Pharmacokinetic measurement

The pharmacokinetic (ADME) characteristics of the substances have been evaluated using the SwissADME online approach. The five principles of Lipinski (molecular weight not exceeding 500 Da, not more than five H-bond donors, not more than 10 H-bond

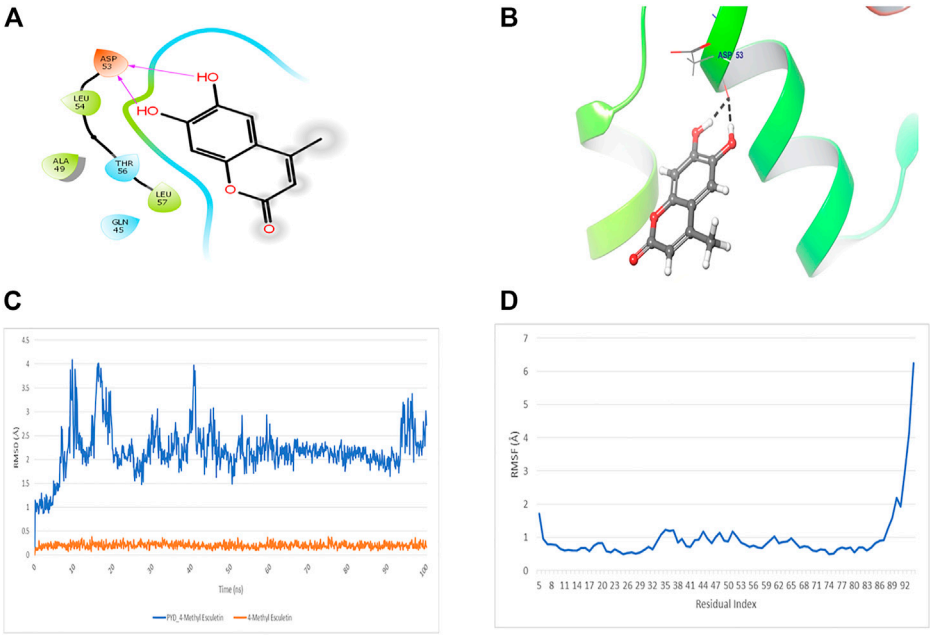

FIGURE 1
Docking and MD simulation study of 4-MESC with NLRP3 PYD. **(A)** 2D image of binding position of 4-MESC within the binding pocket of NLRP3 PYD. **(B)** 3D image. **(C)** Root mean square deviation of the C-α backbone of NLRP3 PYD after binding with 4-MESC. **(D)** Root mean square fluctuation of the C-α backbone of NLRP3 PYD after binding with 4-MESC.

acceptors, molar refractivity between 40 and 130, and LogP value not exceed 5 have been taken into account for the assessment of favorable drug-like characteristics of any substance.

In vitro study

DPPH assay

DPPH solution (1 mg/ml) was prepared in methanol. In a 96-well plate, 50 µl of the DPPH was placed with or without the drug. 4-MESC was added in the concentration range of 25, 50, 100, 200, and 500 µM. The standard anti-oxidant ascorbic acid was taken as the positive control (200 µM). After that, it was incubated at room temperature under dark conditions for 1 h. After incubation, the absorbance was read at 517 nm using a microplate reader (BioTek/Synergy H1). The decrease in absorbance was considered DPPH scavenging activity (More & Makola, 2020).

MTT for cytotoxicity assay

To assess the toxicity of 4-MESC, the MTT assay was performed on the RAW 264.7 cell line. RAW cell lines (1×10^6 cells/ml, per well) were seeded in the 96-well plate and kept for 24 h at 37°C in a CO_2 incubator. After that, drugs were added in the concentration of 0.5, 1, 1.5, 2, 2.5, and 3 mM and incubated for further 24 h under the same condition. After appropriate incubation, the MTT (5 mg/ml, 10 µl) was added to each well and incubated for 4 h at 37°C. DMSO (100 ul) was added to the well to stop the reaction, and after 30 min, with the help of a microplate reader (BioTek/Synergy H1), absorbance was recorded at 570 nm (Sangaran et al., 2021).

Determination of reactive oxygen species

The ROS from the C6 cell line were estimated using the H_2DCFDA dye. The C6 cell line (1×10^6 cells/ml, per well) was seeded in a 96-well plate and incubated for 6 h in a CO_2 incubator with or without the drug. After that, the H_2DCFDA dye (20 µM) was added to each well and kept for 30 min at room temperature. The fluorescence was measured at Ex-495/Emi-530 nm using a microplate reader (BioTek/Synergy H1) (Baek et al., 2020).

In vivo study

Animals and housing

All animals were shipped from Central Drug Research Institute (CDRI), Lucknow. Adult female Swiss albino mice weighing 25–30 g (6–8 weeks old) were acclimatized for weeks before starting the experiment. Mice were kept under a controlled environment with conventional laboratory settings, including 25°C ± 2°C ambient temperature and an equal shift of light and dark exposure. Mice were fed a regular pellet diet and were given tap water. The guidelines for performing experimental work on animals were approved by the Institutional Animal Ethical Committee (IAEC Approval No. NIPER-H/IAEC/03/21).

Experimental outline

A total of 30 female Swiss albino mice were chosen and segregated into five different groups (n = 6). Animals were grouped as follows: normal control (group 1), LPS control (group 2), pretreatment group in low-dose treatment (4-MESC + LPS;

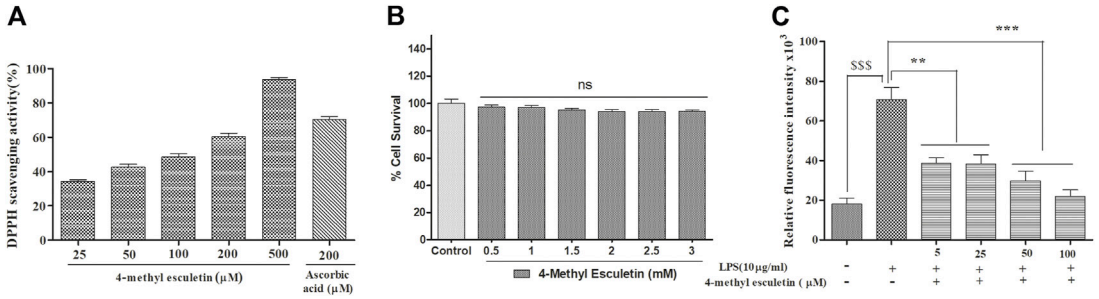

FIGURE 2
Anti-oxidant activity was evaluated by DPPH scavenging, ROS estimation and cytotoxicity by MTT. **(A)** Anti-oxidant efficacy was evaluated by the DPPH assay with an increasing concentration of 4-MESC and ascorbic acid taken as a positive control. **(B)** Cytotoxicity of 4-MESC was evaluated on the RAW cell line up to 3 mM concentration by an MTT assay. **(C)** ROS were estimated by an H_2DCFDA dye after the LPS treatment and along with the different concentrations of 4-MESC. Data were represented as mean ± SD and *$p < 0.05$, ** $0.05 < p < 0.01$, and *** $0.01 < p < 0.001$ were considered significant compared to the LPS control.

group 3), pretreatment group in high-dose treatment (4-MESC + LPS; group 4), and standard group (fluoxetine + LPS; group 5). The experimental plan was carried out for 28 days. Mice of group 1 received normal water. The pretreatment of 4-MESC with low doses (25 mg/kg) and high doses (50 mg/kg) were administered orally to the third and fourth groups, respectively, for 28 days. Fluoxetine (20 mg/kg p.o.) was administered to mice for 28 days as a standard drug. On the 28th day, all mice except those in the control group received a single injection of lipopolysaccharide (0.83 mg/kg i.p.). The day after LPS administration, all mice in each group were evaluated behaviorally using an open-field test (OFT), an immobility test using a tail-suspension test (TST), and a forced swim test (FST). All animals were anesthetized, and retro-orbital blood was withdrawn. Then, the animal was decapitated. The serum and brains of mice were stored at −80°C for biochemical estimations.

Behavioral experiments

Various behavioral parameters were assessed in the open-field test, tail suspension test, and forced swim test after 24 h of LPS administration.

Open-field test

The formal experiments need to be carried out before the open-field test. This test is designed to determine whether the reported side effects of an antidepressant drug are the result of stimulating general motor activity in rodents exposed to unfamiliar surroundings. Mice were individually subjected to an IR actophotometer chamber, which was cleaned and free of bedding and litter. The chamber was divided into nine virtual quadrants, and mice were dropped at predetermined locations for free movement. The locomotor activity of mice was observed by counting the crossings of virtual quadrants and stretching their forelimbs to climb during a 5-min period (Zhao et al., 2019).

Forced swim test

This test is widely used for investigating the behavior of the rodent model of depression and to examine the antidepressant-like effect of novel drugs in rodent models. When mice were forcefully subjected to water for an extended period, they exhibited recognizable immobile behavior. The antidepressant medications reduced the immobility behavior while increasing escape actions such as climbing and swimming. Mice were placed in a transparent cylinder and allowed to swim for 6 min in an experimental test. Video tracking of mice was performed using the ANY-maze software, and the immobility phase was considered for only the last session of 4 mins. Depressed mice showed very little movement and did not try hard to escape that zone. Also, they float motionless by simply keeping their head and noses above the water. Immobility behavior was calculated as the duration of time in which the animal did not show the basic movement to escape. Following the test, the mice were removed from the water and placed in another empty cage, where they were wiped down and dried with a hair dryer. After complete drying, the animal was left in its home cage. The water was changed between testing sessions (Ko et al., 2014).

Tail-suspension test

This test functionally resembles the FST. Before induction with stress, acute antidepressant therapy shortens the TST's immobility period, which is thought to have strong predictive validity. Individual mice were hung by the tail with a fixing tape at the edge of the hook of the burette stand for 6 min. Out of the 6 mins of experimental duration, the immobility phase was recorded for the last 4 min only. The immobility phase of the mice was observed only when they hung passively and stayed motionless (Gill et al., 2018; Redza-Dutordoir and Averill-Bates, 2016).

Estimation of superoxide dismutase activity

The activity of the superoxide dismutase (SOD) enzyme was performed according to the method described in the SOD activity assay kit (Sigma). Around 50 mg of tissue was washed with PBS and homogenized in 500 µl of RIPA buffer, protease, and phosphatase inhibitors. After that, tissue lysates were centrifuged at 14,000 g for 10 min at 4°C. The tissue supernatant was pipetted out in the fresh tube and proceeded further as instructed by the kit protocol. After appropriate

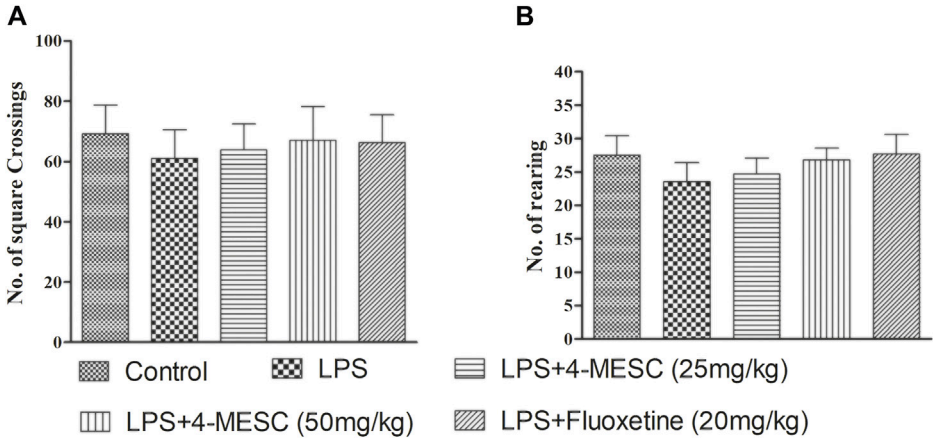

FIGURE 3
Effect of lipopolysaccharide (LPS) and 4-methylesculetin on autonomous activity were evaluated by an open-field test (OFT). **(A)** No. of crossing. **(B)** No. of rearing. Data are expressed as mean ± SD. The results showed no difference between the different groups.

incubation, the absorbance was noted at 450 nm using a microplate reader (BioTek/Synergy H1).

Measurement of the glutathione level

The level of glutathione was estimated as described in the glutathione assay kit (Sigma). The tissue samples were washed with PBS, and 100 mg of tissue was treated with three volumes of 5% sulfosalicyclic acid (SSA) solution (300 µl) and vortex. Then, we added another seven volumes of the 5% sulfosalicyclic acid (SSA) solution and homogenized it. After 10 min at 2°C–8°C, the sample was centrifuged at 10,000 *g* for 10 min. The supernatant was collected and processed further as instructed. Appropriate dilution was performed to stay within the detection range. The absorbance was read at 412 nm by a microplate reader (BioTek/Synergy H1).

MDA level estimation

The oxidative injury of lipids by the interaction of free radicals with phospholipids inside a cell was determined using an MDA assay kit (Sigma). Thiobarbituric acid (TBA) and MDA react to produce colorimetric or fluorometric by-products that are equivalent to the amount of MDA present, which is used to measure lipid peroxidation. Tissue samples (10 mg) are washed in PBS before being homogenized with a 100x mixture of MDA lysis buffer (300 µl) and BHT (3 µl). The samples were processed at 13,000 g for 10 min, and 200 µl of supernatant from each sample was pipetted out for further processing. The relative fluorescence unit was measured at EX/EM-532 nm/553 nm by a microplate reader (BioTek/Synergy H1).

Estimation of pro-inflammatory cytokines, BDNF, and cortisol level by ELISA

According to the instructions provided by the manufacturer, an ELISA kit was used to quantify the levels of pro-inflammatory cytokines, cortisol, and BDNF in both samples (serum and brain tissues). Samples were prepared according to the instruction, and results were shown as pg/ml or ng/ml as per requirement.

NLRP3 inflammasome estimation in gene expression studies using semi-quantitative PCR

In this procedure, 100 mg of whole hippocampal tissue was mixed with 1 ml of TRIzol and allowed for tissue lysis. After homogenization, lysates were allowed to stand for 5 min at room temperature. Then, 200 µl of chloroform was added, and the sample was vigorously shaken for 15 s before being allowed to stand for 15 min. The mixture was centrifuged at 12,000 x g for 15 min at 4°C, separating it into three distinct phases. The top aqueous, colorless phase containing RNA was collected in another sterile tube that had been treated with diethyl-pyrocarbonate (DEPC), to which 500 µl of chilled isopropanol was added and set aside for 10 min. Then, it was centrifuged at 4°C (12,000 x g; 10 min), which resulted in a total RNA pellet at the bottom of the tube. The supernatant was discarded, and the pellet was washed by adding 1 ml of 75% ethanol/ml of TRIzol. To obtain total RNA, the sample was vortexed and centrifuged at 4°C (7500 x g; 5 min). At last, the supernatant was removed, and the final RNA pellet was left for air drying. For longer storage, this RNA pellet was resuspended in 30 µl of RNase-free water with gentle mixing with a pipette and stored at −80°C. The yield of RNA in terms of concentration and purity was determined by the absorbance method (260/280) using NanoDrop (Thermo Fisher), and agarose gel was used further for visualizing the two bands of different sizes of an RNA sample for more clarity of the yield. As per the manufacturer's protocol, cDNA was prepared using the Verso cDNA Synthesis Kit. The sample preparation should be carried out on ice. Except for reverse transcriptase, all of the kit's reagents were thawed on ice and gently spun after being removed from −20°C. The reaction volume was set to 20 µl, and the reagents were added in the following order: nuclease-free water: 12 µl, 5x iScript selected reaction; Mix: 4 µl, Control RNA (up to 1 µg): 1 µl, and oligo (dT) primer: 2 µl; and lastly added iScript reverse transcriptase: 1 µl. The final volume of the reaction was mixed, and the parameter was set (70 min; 42°C for oligo dT). Then, reverse transcriptase was heat-inactivated at 85°C for 5 min. The cDNA product was stored at −20°C. The

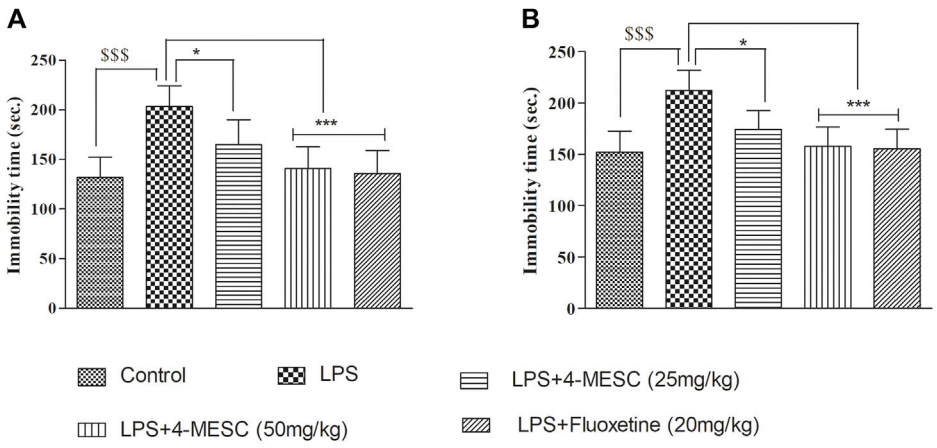

FIGURE 4
Effect of 4-MESC on immobility time. **(A)** Forced swim test (FST). **(B)** Tail-suspension test (TST). Data were represented as mean ± SD. $^{\$\$\$}p < 0.001$ compared to the control and $*p < 0.05$, ** $0.05 < p < 0.01$, and *** $0.01 < p < 0.001$ were considered significant compared to LPS.

semi-quantitative PCR was set for the genes (NLRP3, caspase 1, ASC, gasdermin D, IL-1β, Nf-κBp65, IL-6, GAPDH), which contained 100 µl reaction volume consisting of 1x PCR buffer, a variable concentration of $MgCl_2$, cDNA, forward and reverse primers, 200 µM of dNTPs, and volume makeup with water. Gene amplification was carried out for 28 cycles, initializing with 2 min of initial denaturation (95°C), final denaturation (95°C; 30 s), annealing temperature (55°C–60°C), extension temperature (72°C; 30 s), and final extension (72°C; 7 min). The final amplified product of the gene was stored at 4°C, and it was run on 1% agarose gel with the loading control as GAPDH and visualized in ChemiDoc (Bio-Rad).

Evaluation of the NLRP3 inflammasome inhibition of 4-MESC through western blot

A total of 100 mg of mice brain tissue was taken from each group and homogenized in 500 µl of RIPA buffer with an additional protease inhibitor and phosphatase inhibitor at 4°C. The homogenized sample was allowed to stand for 20 min and centrifuged to 10,000 g for 15 min at 4°C. The supernatant was withdrawn and collected in other tubes. The BCA protein assay kit was used to estimate the protein concentration in the supernatant. A total of 60 µg of total tissue lysate was taken and mixed with the SDS loading dye, boiled for 5–10 min, and then centrifuged and loaded in a 10% SDS page. The protein on the SDS page was then transferred into a PVDF membrane (0.45 µm) for 1.5 h. The PVDF membrane was blocked with 3% BSA in 1% TBST for 1 h and incubated overnight at 4°C with the following primary antibodies: caspase 1(1:2000, Invitrogen), Nf-κBp65 (1:2000, Sigma), NLRP3 (1:1000, Invitrogen), and β-actin (1:5000, Thermo Fisher). The next day, the same PVDF was washed five times with TBST at 5-min intervals and incubated 1 h with the Horse redox peroxidase (HRP)-conjugated secondary antibody goat anti-mouse IgG (1: 10,000, Thermo Fisher) or goat anti-rabbit IgG (1:10,000, Thermo Fisher). The blots were then visualized with ECL chemiluminescent substance in ChemiDoc (Bio-Rad).

Measurement of the NLRP3 level

The level of NLRP3 was estimated as described in the NLRP3 assay kit (Abcam). A total of 100 mg tissue was homogenized with 500 µl of 1x cell extraction buffer and incubated in ice for 20 min. Then, it was centrifuged at 18,000 g for 20 min at 4°C. The supernatant was collected and proceeded for further estimation. The absorbance was taken at 450 nm using a multimode reader.

Statistical analysis

Statistical analysis was carried out by one-way analysis of variance (ANOVA) using GraphPad Prism software (version 5.00; GraphPad software Inc., La Jolla, CA, United States). The results were shown as mean ± SD values. Differences between group data were considered statistically significant at $p < 0.05$.

Results

Docking and MD simulation study reveals high affinity to NLRP3 PYD

The docking study of 4-MESC and NLRP3 PYD was performed to check the affinity. The docking score was found to be −9.879. The binding mode of 4-MESC in the NLRP3 PYD interacting pocket is shown in Figure 1A (2D) and Figure 1B (3D). 4-MESC formed two hydrogen bonds with NLRP3 PYD. An intermolecular force called the hydrogen bond held two or more molecules together. The amino acid Asp 53 was involved in hydrogen bonding with 4-MESC. A docking score of −10 and below using Glide SP is considered to be a good binding for the ligand with protein. In the present study, the binding score was −9.879, which reflected a good binding of 4-MESC with NLRP3 PYD. Since the NLRP3's rigid crystal structure was used for molecular-docking simulations, interaction between the

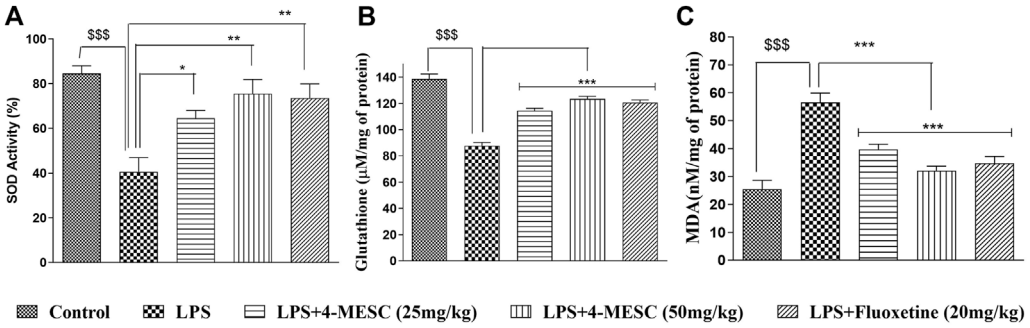

FIGURE 5
4-MESC reduces the LPS-induced oxidative stress. **(A)** Superoxide activity is evaluated with or without LPS and LPS along with 4-MESC and fluoxetine taken as a positive control. **(B)** Glutathione levels were estimated after the LPS treatment and along with 4-MESC. **(C)** Lipid peroxidation (MDA) was also checked after treatment with LPS and in the presence of 4-MESC. Data were represented as mean ± SD and *$p < 0.05$, ** $0.05 < p < 0.01$, and *** $0.01 < p < 0.001$ were considered significant compared to the LPS control.

target receptor and 4-MESC was examined using molecular modeling, and dynamic behavior of the receptor and ligand was used to test the stability of bound conformation using dynamic simulation following compound chemistry in the pocket of NLRP3 PYD. To investigate the protein–ligand conformational stability, we have simulated the changes in complexes and their systems each up to 100 ns In this investigation, the time period which is a sufficient time for the rearranging of NLRP3 PYD's Cα atoms in complexes with 4-MESC. Root mean square deviation (RMSD) and root mean square fluctuation (RMSF) were calculated to demonstrate thermodynamic conformational stability during a 100-ns time frame. An additional 1,000 trajectories were gathered and stored during the MD simulation. The NLRP3 PYD's original crystal structure was overlaid using the SEA panel for the simulation event analysis of Schrodinger's equation, which produced data in the ". dat" format. The RMSD and RMSF graphs were created using the collected RMSF and RMSD values. The RMSD plot suggested that 4-MESC had a mean RMSD value of 2.19 Å which is an acceptable range of RMSD (Figure 1C), indicating that it is strongly bound to NLRP3 PYD. On the other hand, the RMSF values for Cα atoms present in all the residues were calculated to investigate the binding effectiveness of compounds with NLRP3 PYD, based on data from 100 ns of trajectories. The NLRP3 PYD following the binding of 4-MESC, the average RMSFs are 0.95 Å (Figure 1D) which shows the least amount of variation and the NLRP3 relative secondary conformational stability upon the described chemicals' binding. Therefore, the MD research revealed that the 4-MESC had greater potential toward NLRP3 PYD. The pharmacokinetic study using the SwissADME online tool showed that this particular compound followed the Lipinski rule of five (molecular weight: 192.17 g/mol, number of H-bond acceptors: 4, number of H-bond donors: 2, Log *p*-value is 1.45, and molar refractivity is 51.50) and claimed its high GI absorption and blood–brain barrier permeability. It is an inhibitor of cytochrome *CYP1A2* enzyme which will increase the plasma concentrations of the drug. The bioavailability score of the 4-MESC was found to be 0.55 which shows good bioavailability. The LogP value, for oral and intestinal absorption of drugs should be ideally between 1.3–1.8; and for 4-MESC, it is 1.52 which shows its drug -likeness.

Anti-oxidant and cytotoxicity activity of 4-methylesculetin

The anti-oxidant effect of 4-MESC was assessed using a DPPH assay. This assay revealed that the DPPH scavenging activity of 4-MESC increased with increasing concentration. Almost 90% of DPPH was scavenged by 4-MESC at 500 µM concentration (Figure 2A). The standard anti-oxidant compound ascorbic acid was taken as the positive control and showed ~65% scavenging activity at 200 µM (Figure 2A). The cytotoxicity of 4-MESC was assessed by an MTT assay on RAW 264.7 cell lines. The 4-MESC was treated at concentrations ranging from 0.5 mM to 3 mM. The cytotoxicity assay showed that it was not cytotoxic at even high concentrations up to 3 mM (Figure 2B), revealing that it was minimal or not cytotoxic for normal cells. We estimated the ROS production inside the LPS and LPS with 4-MESC-treated C6 cells. We found that ROS production was increased in cells treated with LPS ($p < 0.001$) compared to control cells, but significantly reduced with an increasing concentration of 4-MESC. Almost 60% of ROS production was decreased in 4-MESC and LPS-treated cells at 100 µM concentration compared to LPS-treated cells ($p < 0.001$) (Figure 2C).

Effect of 4-methylesculetin on locomotor activity

The LPS and 4-MESC groups (25 mg/kg and 50 mg/kg) did not show any comparable differences in the movement pattern (number of squares crossing and number of rearing) as compared to the normal control group (Figures 3A, B). Moreover, there was little reduction in motion in LPS-treated mice, but the difference was not significant compared to the control. This result showed that the antidepressant effect of 4-MESC was not due to stimulation of the general motor activity.

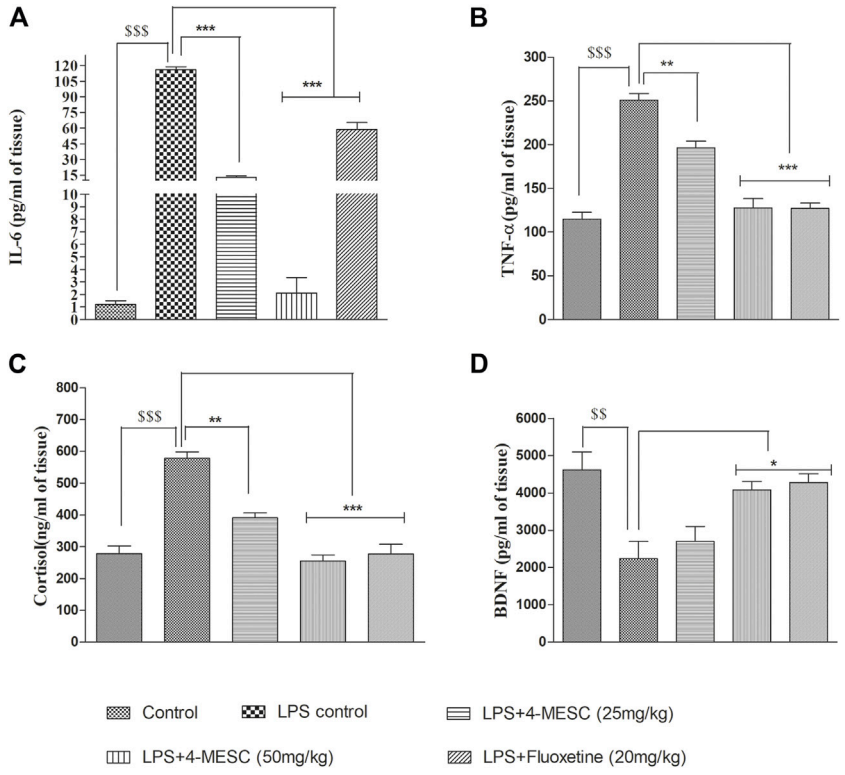

FIGURE 6
Effect of 4-MESC on pro-inflammatory cytokines. **(A)** Estimation of the IL-6 level through ELISA. **(B)** Determination of the level of TNF-α. **(C)** Neuroprotection evaluation of 4-MESC by estimation of BDNF using ELISA. **(D)** Cortisol level estimation. Data were represented as mean ± SD and *p < 0.05, ** 0.05 < p < 0.01, and *** 0.01 < p < 0.001 were considered significant.

Effect of 4-methylesculetin on immobility time in the forced swim test and tail-suspension test

In the present study, LPS-induced stress which caused depression-like behavior, and it was evaluated using the immobility time in the FST and TST. In the FST, our results showed that LPS-induced animals showed less movement with their paws and a significant (p < 0.001) increase in immobility duration compared to that of the normal control group. Similarly, in the TST, the immobility time is increased in the LPS group as compared to the control group (p < 0.001). These findings reflected the successful development of the LPS-induced depression model in mice. Pretreatment with 4-MESC reversed the LPS-induced increased immobility duration at both dosages, 50 mg/kg (p < 0.001) and 25 mg/kg (p < 0.05), significantly in FST and TST studies. Likewise, the standard group (fluoxetine) also showed significant (p < 0.001) decrease in the immobility time as compared to the LPS group. Findings imply that 4-MESC has an antidepressant-like action since it can significantly ameliorate the behavioral despair of depressed animals (Figures 4A, B).

4-Methylesculetin attenuated LPS-induced oxidative stress

Here, we observed that in the case of the LPS-treated group, the SOD activity and glutathione level were significantly (p < 0.001) decreased by 40% and 39%, respectively, as compared to the normal control. However, interestingly, the SOD activity of the 4-MESC group (25 mg/kg and 50 mg/kg) is increased significantly (p < 0.05 and p < 0.01) as compared to that of the LPS group (Figure 5A). Similarly, in the 4-MESC group (25 mg/kg and 50 mg/kg) and the standard group (fluoxetine), the glutathione level was significantly (p < 0.001) increased as compared to that of the LPS control group (Figure 5B). In the LPS-treated group, the MDA level significantly (p < 0.001) increased to 55% compared to the normal control, but significantly (p < 0.001) decreased to 45% in the 4-MESC-treated group (25 mg/kg and 50 mg/kg) and standard group (Fluoxetine) as compared to LPS control (Figure 5C). These studies revealed that it plays a very important role in the defense mechanism against oxidative stress (Figure 5).

4-Methylesculetin reduces pro-inflammatory cytokine production and enhances neuroprotection

Inflammation plays a vital role in brain-related disorders such as depression. NLRP3 inflammasome activation is also associated with the increased production of inflammatory cytokines, such as IL-6 and TNF-α. Therefore, it is necessary to determine the effect of 4-MESC on LPS-induced inflammation.

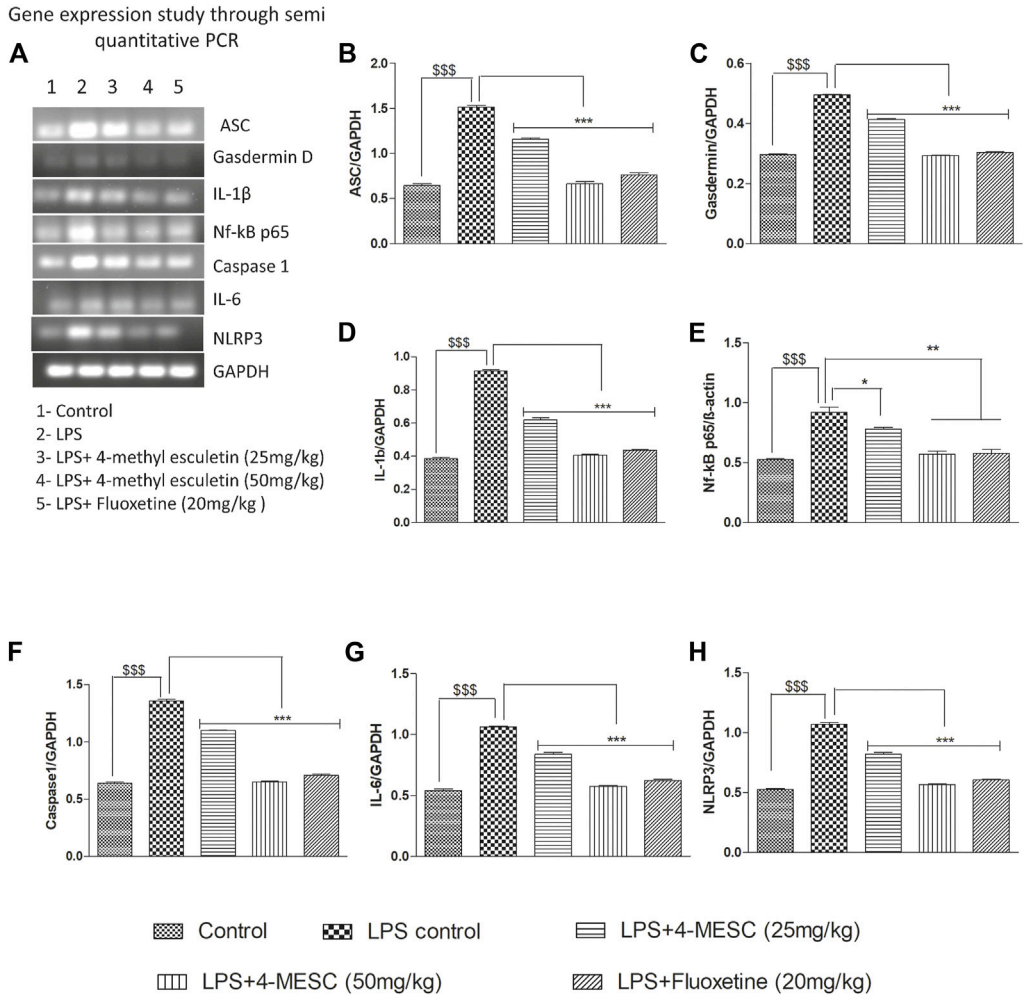

FIGURE 7
Effect of 4-MESC on gene expression involved in the NLRP3 inflammasome pathway evaluated through semi-quantitative PCR. **(A)** Representative agarose gel image of different genes, where lane 1, 2, 3, 4, and 5 represent the control, LPS, LPS +25 mg/kg of 4-MESC, LPS +50 mg/kg of MESC, and LPS+20 mg/kg of the fluoxetine group, respectively. **(B)** ASC, **(C)** caspase-1, **(D)** gasdermin D, **(E)** IL-1b, **(F)** NLRP3, **(G)** IL-6, and **(H)** Nf-κB.

We found that in the LPS control group, the levels of IL-6 and TNF-α significantly ($p < 0.001$) increased as compared to the normal control group, whereas in the 4-MESC group (25 mg/kg and 50 mg/kg) and standard group (fluoxetine), IL-6 decreased significantly ($p < 0.001$) as compared to the LPS control group (Figure 6A). Likewise, TNF-α also decreased significantly ($p < 0.01$ and $p < 0.001$) as compared to the LPS control at 25 mg/kg and 50 mg/kg of the 4-MESC group, respectively. Also, the efficacy was compared to the fluoxetine group, where we observed that fluoxetine reduced significantly ($p < 0.001$) with the level of TNF-α as compared to the LPS control group (Figure 6B). Furthermore, the neuroprotection effect of 4-MESC was evaluated by estimating the brain-derived neurotrophic factor. Our findings also confirmed that LPS-induced neuroinflammation significantly ($p < 0.001$) reduced the expression of BDNF as compared to the normal control group. However, the pretreatment with 4-MESC (50 mg/kg) and fluoxetine significantly ($p < 0.05$) increased the level of BDNF compared to the LPS group and exhibited its neuroprotection activity (Figure 6D). Cortisol level estimation may be the benchmark for the assessment of depression-like behavior. In the present study, LPS treatment-induced neuroinflammation was also significantly ($p < 0.001$) associated with the enhanced level of cortisol as compared to the normal control group, but significantly ($p < 0.001$ and $p < 0.01$) reduced by the 4-MESC treatment at 50 mg/kg and 25 mg/kg as compared to the LPS treatment group, respectively. A fluoxetine treatment also significantly ($p < 0.001$) decreased the level of cortisol (Figure 6C).

4-MESC suppressed NLRP3 inflammasome activation in gene expression studies using PCR

To assess the 4-MESC effect on NLRP3 inflammasome activation in the hippocampus, a semi-quantitative PCR was performed to check the gene expression profile. As compared with the control group, LPS mice showed an aggravated level of nuclear NF-κBp65 ($p < 0.001$) in the hippocampus and significantly

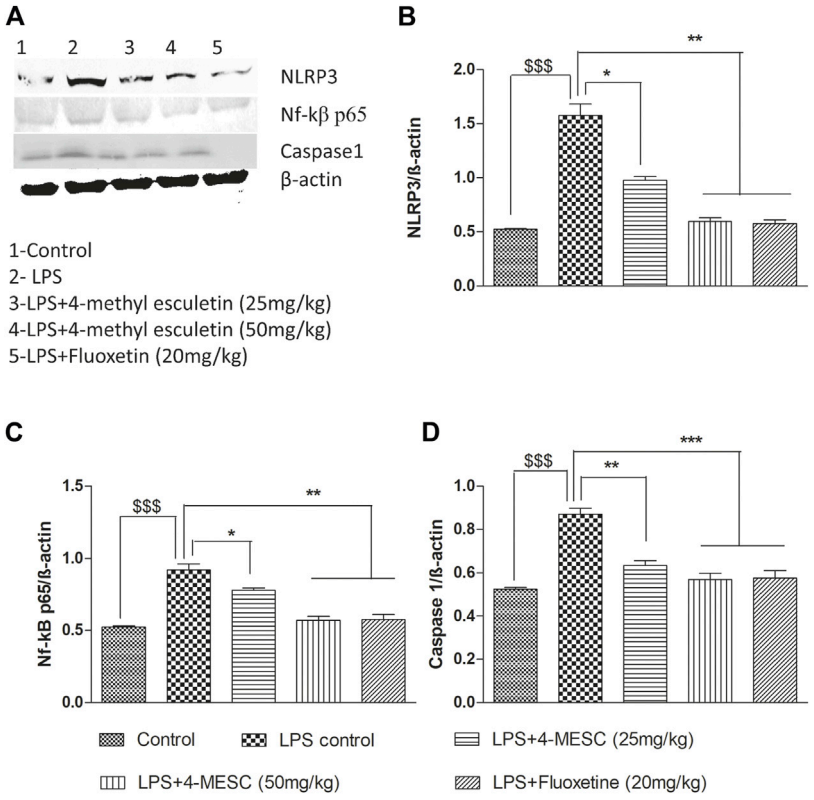

FIGURE 8
Effect of 4-MESC on expression involved in the NLRP3 inflammasome pathway evaluated using western blot. **(A)** Representative western blot image of different proteins, where lane 1, 2, 3, 4, and 5 represent the control, LPS, LPS +25 mg/kg of 4-MESC, LPS +50 mg/kg of MESC, and LPS+20 mg/kg of fluoxetin group, respectively. **(B)** NLRP3, **(C)** caspase-1, **(D)** Nf-κB. b-actin was taken as the loading control.

increased the expression levels of ASC ($p < 0.001$), NLRP3 ($p < 0.001$), IL-6 ($p < 0.001$), IL-1β ($p < 0.001$), and gasdermin D ($p < 0.001$) genes, which indicated the stimulation of the NLRP3 inflammasome after LPS administration having a tendency to enhance the cleavage of caspase-1. However, pretreatment with 4-methylesculetin (25 mg/kg and 50 mg/kg) and fluoxetine reversed the LPS effect and significantly alleviated the expression of NLRP3 ($p < 0.001$), ASC ($p < 0.001$), IL-1b ($p < 0.001$), IL-6 ($p < 0.001$), and gasdermin D ($p < 0.001$) (Figures 7A–H) which were upregulated by LPS. These findings demonstrated that 4-MESC was capable of alleviating the NLRP3 Inflammasome activation driven by LPS-induced pro-inflammatory cytokines release and showed an antidepressant-like effect.

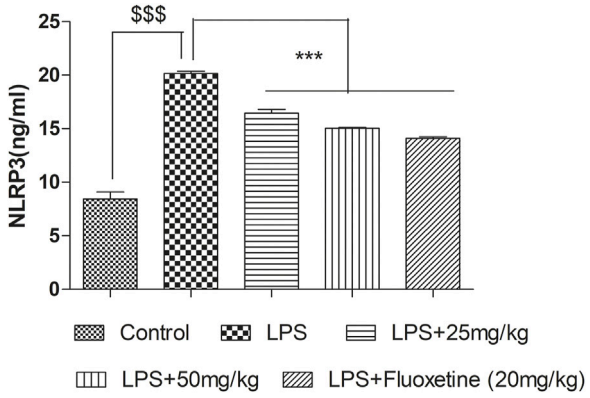

FIGURE 9
Effect of 4-MESC on NLRP3 level evaluated through ELISA Test.

Evaluation of the NLRP3 inflammasome inhibition of 4-MESC through Western blot

To further investigate the NLRP3 inflammasome suppression by 4-MESC, western blotting was used to examine the expression study of proteins such as NLRP3, Nf-kBp65, caspase 1, and b-actin. In the LPS-treated group, NLRP3 ($p < 0.001$), Nf-κBp65 ($p < 0.001$), and caspase 1 ($p < 0.001$) were expressed more than in the control group. The expression levels of NLRP3 and Nf-κBp65 are significantly ($p < 0.05$ and $p < 0.01$) reduced as compared to the LPS group with pretreatment of 4-MESC at 25 mg/kg and 50 mg/kg. Caspase 1 expression also reduced significantly ($p < 0.01$ and $p < 0.001$) as compared to the LPS group at 25 mg/kg and 50 mg/kg of 4-MESC. β-actin was taken as a loading control (Figure 8).

4-MESC attenuated the NLRP3 level

In the LPS-treated group, the NLRP3 level significantly ($p < 0.001$) increased as compared to the control group. Pretreatment with 4-MESC (25 mg/kg and 50 mg/kg) and fluoxetine significantly ($p < 0.001$) reduced the NLRP3 level as compared to the LPS group (Figure 9).

Discussion

Depression is becoming more common because of the increased stress in our daily lives in recent decades. Stress has long been recognized as a significant contributor to the pathophysiology of depression. Stress is responsible for CRF release, which subsequently activates the HPA axis and leads to depression. The deficiency of monoamines at the synaptic cleft is a major contributing factor for depression. Inflammatory responses also play an important role in the pathogenesis of depression. The LPS-induced depression model reflects a sickness-like behavior which applies to both genders. To prevent variation in results, we used only a single gender, i.e., female mice. *In silico* studies were performed to check binding affinity towards NLRP3 PYD. *In vitro* studies, such as DPPH, MTT, and ROS, were performed, and *in vivo* studies of behavioral studies such as the open-field test (OFT), Forced swim test (FST), and tail-suspension test (TST) were performed to check the anti-depressant effect of 4-MESC. Anti-oxidant properties were evaluated by the detection of the level of SOD, glutathione, and MDA through ELISA. Also, ELISA-based studies were also performed to check the level of pro-inflammatory cytokines, such as IL-6 and TNF-α, along with BDNF and cortisol. Gene expression studies were performed by the semi-quantitative and western blot techniques.

Our findings revealed that LPS induces stress, which causes depression-like behavior along with decreased expression of BDNF in the LPS group. There is proof that emotional and physical stressors can trigger inflammatory and immunological responses, which can lead to depression (Iwata et al., 2013). HPA axis dysregulation was proposed as the fundamental mechanism of IL-1's participation in depression, and IL-1b was shown to affect the HPA axis at all levels (Pan et al., 2014). The NLRP3 inflammasome requires two signals to be activated (Pan et al., 2014). A precondition for inflammasome activation, the initial signal is produced by endogenous chemicals or microbes that cause NF-κB to be activated, increasing the production of NLRP3 and proIL-1b (Goshen and Yirmiya, 2009). The second signal causes caspase-1 to be cleaved directly by activating the NLRP3 inflammasome, which in turn causes the maturation of the pro-inflammatory cytokines IL-1b and IL-18 (Bauernfeind et al., 2009). For instance, the previous report depicted the role of the NLRP3 inflammasome in LPS-induced depression (Zhang et al., 2014). In the current investigation, we discovered that 4-MESC decreased the expression of NLRP3, ASC, caspase 1, and proIL-1b which was LPS-induced. These findings show that 4-MESC prevents the NLRP3 inflammasome from being activated. It is thought that the common activator of the NLRP3 inflammasome is the generation of ROS (Schroder and Tschopp, 2010), and also in cells, ROS production is one of the major factors for the stimulation of the apoptosis pathway (Alcocer-Gómez et al., 2016). LPS administration increases the ROS production, but pretreatment with 4-MESC significantly reduces ROS generation. Superoxide dismutase (SOD) enzyme plays a key factor in the anti-oxidant mechanism against oxidative stress in the body. This enzyme has a defensive role in treating illness caused by reactive oxygen species. The enzymes catalyzed the conversion of reactive species, such as free radicals (O_2^-) into stable molecular oxygen and hydrogen peroxide, and hence showed an anti-oxidant effect (T. Wang et al., 2004). In a similar way, GSH is essential for maintaining redox equilibrium, shielding cells against oxidative damage and the toxicity of xenobiotic electrophiles (Forman et al., 2009). In the case of an inflammatory condition, the SOD activity and glutathione level are compromised and the MDA level is increased. Therefore, it is necessary to check the effect of compounds on SOD activity and levels of glutathione and MDA. Here, we found that the 4-MESC significantly enhances the SOD activity and increase the level of glutathione and decrease the level of MDA as compared to the LPS-treated group which reveal its anti-oxidant properties. Additionally, we demonstrated that 4-MESC inhibits central NLRP3 inflammasome activation, which ameliorates the LPS-induced depressive behavior. Numerous studies show that the NLRP3 inflammasome is essential for the development of depression (Martinon, 2010). The NLRP3 inflammasome may therefore constitute a new therapeutic target for the treatment of depression. In this study, we used a mouse model of depression generated by LPS and discovered that LPS activated the NLRP3 inflammasome in the hippocampal region. The systemic administration of LPS resulted in illness and moderate depressive-like behavior, according to our behavioral data. In the current rodent model, it was not able to distinguish between illness and depressive-like behavior due to the overlapping time courses and moderate effects on behavior that is individually associated with depression (Biesmans et al., 2013). With less depressive behavior, including a significant reduction in immobility duration in the TST and FST without affecting spontaneous locomotor activity in OFT, 4-MESC therapy eliminated LPS-induced activation of the NLRP3 inflammasome. These findings imply that the depressed behaviors seen in 4-MESC-treated mice may be attributed to the inhibition of cerebral NLRP3 inflammasome activation. Also, *in silico* studies (docking and MD simulation) showed that 4-MESC strongly binds to the NLRP3 PYD, further proving its NLRP3 inflammasome inhibition. Inflammation has been linked to the etiology of depression, according to the accumulated data, and people with depression have consistently been seen to produce more inflammatory cytokines (Slavich & Irwin, 2014). We examined levels of few inflammatory cytokines in the serum and inflammation-related proteins in the hippocampus in order to investigate the potential mechanism of action of antidepressant 4-MESC. We discovered that LPS administration increased the serum levels of inflammatory cytokines such as TNF-α and IL-6, which have been linked to the etiology of depression. Our findings demonstrated that 4-MESC could successfully decrease the levels of TNF-α and IL-6 caused by LPS, indicating its effectiveness against neuroinflammation. BDNF aids and supports the survival of existing neurons and also stimulates the maturation and differentiation of new neurons (Acheson et al., 1995). Inflammation regulates the BDNF expression in the brain (Acheson et al., 1995). Our findings suggest that LPS administration decreases the expression of BDNF in the brain tissue. However, pretreatment with 4-MESC significantly enhanced the level of BDNF, which showed its neuroprotective nature. Cortisol levels are elevated in the depression-like behavior (Acheson et al., 1995). The LPS treatment caused neuroinflammation and increased cortisol levels in the LPS-treated group but decreased them in the 4-MESC-treated group. The compound 4-methylesculetin is shown to be safe in previous studies on

acute toxicity studies with an LD50 value of 3,200 mg/kg, *p.o.* on mice (Hemshekhar et al., 2013). The observed beneficial effect in this model complements its potential to be a safer antidepressant agent.

Conclusion

In the present study, we evaluated the antidepressant effect of 4-MESC through the inhibition of LPS-induced NLRP3 inflammasome activation. The *in vitro* study showed the safety of the compound and prevention of ROS, along with DPPH inhibition. All of these findings indicated that this molecule has the potential to be useful in inflammasome inhibition. The *in vivo* study reflected the improvement in immobility time induced by LPS. This behavioral parameter was supported by various molecular markers where the compound showed an increase in BDNF expression, which was decreased due to LPS. Our results showed that 4-MESC effectively reduced the levels of TNF-α, IL-6, and cortisol induced by LPS, demonstrating the compound's effect on neuroinflammation. Overall, our study demonstrated the antidepressant effect of 4-MESC through the inhibition of NLRP3 inflammasome activation, suggesting the potential clinical use of 4-MESC in NLRP3 inflammasome-associated inflammatory diseases such as depression.

Data availability statement

The original contributions presented in the study are included in the article/supplementary materials, further inquiries can be directed to the corresponding author.

Ethics statement

The animal study was reviewed and approved by the National Institute of Pharmaceutical Education and Research, and the Export Promotion Industrial Park (EPIP) Jandaha Road, NH322, Hajipur, Bihar 844102.

Author contributions

Conceptualization: KC, VR, and NK; design of the study: KC, KM, and NK; *in silico* study: KC, KL, and NK; *in vitro* study: KC, SP, and NK; *in vivo* study: KC, KM, SS, and NK; manuscript writing: KC, KL, SP, and NK; and reviewing the manuscript: all authors.

Funding

The funding for this research work was provided by the Department of Chemicals and Petrochemicals, Ministry of Chemicals and Fertilizers, India, and Ministry of Education, India.

Acknowledgments

The authors are thankful for the financial assistance in terms of fellowship to KC from the Ministry of Chemicals and Fertilizers, Government of India.

Conflict of interest

The authors declare that the research was conducted in the absence of any commercial or financial relationships that could be construed as a potential conflict of interest.

Publisher's note

References

Acheson, A., Conover, J. C., Fandl, J. P., Dechiara, T. M., Russell, M., Thadani, A., et al. (1995). A BDNF autocrine loop in adult sensory neurons prevents cell death. *Nature* 374 (6521), 450–453. doi:10.1038/374450A0

Alcocer-Gómez, E., Casas-Barquero, N., Williams, M. R., Romero-Guillena, S. L., Cañadas-Lozano, D., Bullón, P., et al. (2017). Antidepressants induce autophagy dependent-NLRP3-inflammasome inhibition in Major depressive disorder. *Pharmacol. Res.* 121, 114–121. doi:10.1016/J.PHRS.2017.04.028

Alcocer-Gómez, E., and Cordero, M. D. (2014). NLRP3 inflammasome: A new target in major depressive disorder. *CNS Neurosci. Ther.* 20 (3), 294–295. doi:10.1111/cns.12230

Alcocer-Gómez, E., de Miguel, M., Casas-Barquero, N., Núñez-Vasco, J., Sánchez-Alcazar, J. A., Fernández-Rodríguez, A., et al. (2014). NLRP3 inflammasome is activated in mononuclear blood cells from patients with major depressive disorder. *Brain, Behav. Immun.* 36, 111–117. doi:10.1016/J.BBI.2013.10.017

Alcocer-Gómez, E., Ulecia-Morón, C., Marín-Aguilar, F., Rybkina, T., Casas-Barquero, N., Ruiz-Cabello, J., et al. (2016). Stress-induced depressive behaviors require a functional NLRP3 inflammasome. *Mol. Neurobiol.* 53 (7), 4874–4882. doi:10.1007/S12035-015-9408-7

Amitai, M., Taler, M., Carmel, M., Michaelovsky, E., Eilat, T., Yablonski, M., et al. (2016). The relationship between plasma cytokine levels and response to selective serotonin reuptake inhibitor treatment in children and adolescents with depression and/or anxiety disorders. *J. Child Adolesc. Psychopharmacol.* 26 (8), 727–732. doi:10.1089/CAP.2015.0147

Baek, S. H., Park, T., Kang, M. G., and Park, D. (2020). Anti-inflammatory activity and ROS regulation effect of sinapaldehyde in LPS-stimulated RAW 264.7 macrophages. *Mol. (Basel, Switz.* 25 (18), 4089. doi:10.3390/MOLECULES25184089

Bauernfeind, F. G., Horvath, G., Stutz, A., Alnemri, E. S., MacDonald, K., Speert, D., et al. (2009). Cutting edge: NF-kappaB activating pattern recognition and cytokine receptors license NLRP3 inflammasome activation by regulating NLRP3 expression. *J. Immunol.* 183 (2), 787–791. doi:10.4049/JIMMUNOL.0901363

Ben-Azu, B., Emokpae, O., Ajayi, A. M., Jarikre, T. A., Orhode, V., Aderibigbe, A. O., et al. (2020). Repeated psychosocial stress causes glutamic acid decarboxylase isoform-67, oxidative-Nox-2 changes and neuroinflammation in mice: Prevention by treatment with a neuroactive flavonoid, morin. *Brain Res.* 1744, 146917. doi:10.1016/j.brainres.2020.146917

Bernton, E. W., Beach, J. E., Holaday, J. W., Smallridge, R. C., and Fein, H. G. (1987). Release of multiple hormones by a direct action of interleukin-1 on pituitary cells. *Science* 238 (4826), 519–521. doi:10.1126/science.2821620

Biesmans, S., Meert, T. F., Bouwknecht, J. A., Acton, P. D., Davoodi, N., de Haes, P., et al. (2013). Systemic immune activation leads to neuroinflammation and sickness behavior in mice. *Mediat. Inflamm.* 2013, 271359. doi:10.1155/2013/271359

Dantzer, R., O'Connor, J. C., Freund, G. G., Johnson, R. W., and Kelley, K. W. (2008). From inflammation to sickness and depression: When the immune system subjugates the brain. *Nat. Rev. Neurosci.* 9 (1), 46–56. doi:10.1038/nrn2297

Dunlop, B. W., and Nemeroff, C. B. (2007). The role of dopamine in the pathophysiology of depression. *Archives General Psychiatry* 64 (3), 327–337. doi:10.1001/archpsyc.64.3.327

Forman, H. J., Zhang, H., and Rinna, A. (2009). Glutathione: Overview of its protective roles, measurement, and biosynthesis. *Mol. Aspects Med.* 30 (1–2), 1–12. doi:10.1016/J.MAM.2008.08.006

Fu, Y., Wang, Y., Du, L., Xu, C., Cao, J., Fan, T., et al. (2013). Resveratrol inhibits ionising irradiation-induced inflammation in MSCs by activating SIRT1 and limiting NLRP-3 inflammasome activation. *Int. J. Mol. Sci.* 14 (7), 14105–14118. doi:10.3390/ijms140714105

Gill, M., Kinra, M., Rai, A., Chamallamudi, M. R., and Kumar, N. (2018). Evaluation of antidepressant activity of methanolic extract of Saraca asoca bark in a chronic unpredictable mild stress model. *Neuroreport* 29 (2), 134–140. doi:10.1097/WNR.0000000000000944

Gold, P. W., Drevets, W. C., Charney, D. S., and Drevets, W. C. (2002). New insights into the role of cortisol and the glucocorticoid receptor in severe depression. *Biol. Psychiatry* 52 (5), 381–385. doi:10.1016/S0006-3223(02)01480-4

Goshen, I., and Yirmiya, R. (2009). Interleukin-1 (IL-1): A central regulator of stress responses. *Front. Neuroendocrinol.* 30 (1), 30–45. doi:10.1016/j.yfrne.2008.10.001

Hemshekhar, M., Sunitha, K., Thushara, R. M., Sebastin Santhosh, M., Shanmuga Sundaram, M., Kemparaju, K., et al. (2013). Antiarthritic and antiinflammatory propensity of 4-methylesculetin, a coumarin derivative. *Biochimie* 95 (6), 1326–1335. doi:10.1016/J.BIOCHI.2013.02.014

Hu, X. H., Bull, S. A., Hunkeler, E. M., Ming, E., Lee, J. Y., Fireman, B., et al. (2004). Incidence and duration of side effects and those rated as bothersome with selective serotonin reuptake inhibitor treatment for depression: Patient report versus physician estimate. *J. Clin. Psychiatry* 65 (7), 959–965. doi:10.4088/JCP.V65N0712

Iwata, M., Ota, K. T., and Duman, R. S. (2013). The inflammasome: Pathways linking psychological stress, depression, and systemic illnesses. *Brain, Behav. Immun.* 31, 105–114. doi:10.1016/J.BBI.2012.12.008

Ko, S.-Y., Kim, D.-H., and Lee, T.-H. (2014). Effect of glycyrrhizae radix water extract on the depression induced by LPS in rats. *Korea J. Herbology* 29 (5), 9–16. doi:10.6116/kjh.2014.29.5.9

Lokhande, K. B., Doiphode, S., Vyas, R., and Swamy, K. V. (2021). Molecular docking and simulation studies on SARS-CoV-2 Mpro reveals Mitoxantrone, Leucovorin, Birinapant, and Dynasore as potent drugs against COVID-19. *J. Biomol. Struct. Dyn.* 39 (18), 7294–7305. doi:10.1080/07391102.2020.1805019

Maes, M., Bosmans, E., Meltzer, H. Y., Scharpé, S., and Suy, E. (1993). Interleukin-1 beta: A putative mediator of HPA axis hyperactivity in major depression? *Am. J. Psychiatry* 150 (8), 1189–1193. doi:10.1176/AJP.150.8.1189

Malhi, G. S., and Mann, J. J. (2018). Depression. *Lancet* 392 (10161), 2299–2312. doi:10.1016/S0140-6736(18)31948-2

Marasine, N. R., Sankhi, S., Lamichhane, R., Marasini, N. R., and Dangi, N. B. (2020). Self-reported antidepressant drug side effects, medication adherence, and its associated factors among patients diagnosed with depression at the psychiatric hospital of Nepal. *Depress. Res. Treat.* 2020, 7024275. doi:10.1155/2020/7024275

Martinon, F. (2010). Signaling by ROS drives inflammasome activation. *Eur. J. Immunol.* 40 (3), 616–619. doi:10.1002/EJI.200940168

Millan, M. J. (2004). The role of monoamines in the actions of established and "novel" antidepressant agents: A critical review. *Eur. J. Pharmacol.* 500 (1–3), 371–384. doi:10.1016/j.ejphar.2004.07.038

Miller, A. H., and Raison, C. L. (2016). The role of inflammation in depression: From evolutionary imperative to modern treatment target. *Nat. Rev. Immunol.* 16 (1), 22–34. doi:10.1038/nri.2015.5

More, G. K., and Makola, R. T. (2020). *In-vitro* analysis of free radical scavenging activities and suppression of LPS-induced ROS production in macrophage cells by Solanum sisymbriifolium extracts. *Sci. Rep.* 10 (1), 6493. doi:10.1038/S41598-020-63491-W

Neurauter, G., Schrocksnadel, K., Scholl-Burgi, S., Sperner-Unterweger, B., Schubert, C., Ledochowski, M., et al. (2008). Chronic immune stimulation correlates with reduced phenylalanine turnover. *Curr. Drug Metab.* 9 (7), 622–627. doi:10.2174/138920008785821738

Okoh, L., Ajayi, A. M., Ben-Azu, B., Akinluyi, E. T., Emokpae, O., and Umukoro, S. (2020). d-Ribose–l-cysteine exhibits adaptogenic-like activity through inhibition of oxido-inflammatory responses and increased neuronal caspase-3 activity in mice exposed to unpredictable chronic mild stress. *Mol. Biol. Rep.* 47 (10), 7709–7722. doi:10.1007/s11033-020-05845-1

Pal, R., Gulati, K., Chakraborti, A., Banerjee, B., and Ray, A. (2006). Role of free radicals in stress-induced neurobehavioural changes in rats. *Indian J. Exp. Biol.* 44 (10), 816–820.

Pan, Y., Chen, X. Y., Zhang, Q. Y., and Kong, L. D. (2014). Microglial NLRP3 inflammasome activation mediates IL-1β-related inflammation in prefrontal cortex of depressive rats. *Brain, Behav. Immun.* 41 (1), 90–100. doi:10.1016/J.BBI.2014.04.007

Petty, F., Kramer, G. L., Gullion, C. M., and John Rush, A. (1992). Low plasma γ-aminobutyric acid levels in male patients with depression. *Biol. Psychiatry* 32 (4), 354–363. doi:10.1016/0006-3223(92)90039-3

Redza-Dutordoir, M., and Averill-Bates, D. A. (2016). Activation of apoptosis signalling pathways by reactive oxygen species. *Biochimica Biophysica Acta (BBA) - Mol. Cell Res.* 1863 (12), 2977–2992. doi:10.1016/j.bbamcr.2016.09.012

Sangaran, P. G., Ibrahim, Z. A., Chik, Z., Mohamed, Z., and Ahmadiani, A. (2021). LPS preconditioning attenuates apoptosis mechanism by inhibiting NF-κB and caspase-3 activity: TLR4 pre-activation in the signaling pathway of LPS-induced neuroprotection. *Mol. Neurobiol.* 58 (5), 2407–2422. doi:10.1007/S12035-020-02227-3

Santomauro, D. F., Mantilla Herrera, A. M., Shadid, J., Zheng, P., Ashbaugh, C., Pigott, D. M., et al. (2021). Global prevalence and burden of depressive and anxiety disorders in 204 countries and territories in 2020 due to the COVID-19 pandemic. *Lancet* 398 (10312), 1700–1712. doi:10.1016/S0140-6736(21)02143-7

Schroder, K., and Tschopp, J. (2010). The inflammasomes. *Cell* 140 (6), 821–832. doi:10.1016/J.CELL.2010.01.040

Slavich, G. M., and Irwin, M. R. (2014). From stress to inflammation and major depressive disorder: A social signal transduction theory of depression. *Psychol. Bull.* 140 (3), 774–815. doi:10.1037/A0035302

Tanimoto, A., Witaicenis, A., Caruso, Í. P., Piva, H. M. R., Araujo, G. C., Moraes, F. R., et al. (2020). 4-Methylesculetin, a natural coumarin with intestinal anti-inflammatory activity, elicits a glutathione antioxidant response by different mechanisms. *Chemico-Biological Interact.* 315, 108876. doi:10.1016/J.CBI.2019.108876

Tong, Y., Fu, H., Xia, C., Song, W., Li, Y., Zhao, J., et al. (2020). Astragalin exerted antidepressant-like action through SIRT1 signaling modulated NLRP3 inflammasome deactivation. *ACS Chem. Neurosci.* 11 (10), 1495–1503. doi:10.1021/ACSCHEMNEURO.0C00156

Wang, T., Qin, L., Liu, B., Liu, Y., Wilson, B., Eling, T. E., et al. (2004). Role of reactive oxygen species in LPS-induced production of prostaglandin E2 in microglia. *J. Neurochem.* 88 (4), 939–947. doi:10.1046/J.1471-4159.2003.02242.X

World Health Organization (2022). https://www.who.int/news-room/fact-sheets/detail/depression (Accessed May 1, 2021).

World Health Organization (2023). https://www.who.int/india/health-topics/depression (Accessed January 1, 2023).

Witaicenis, A., Luchini, A. C., Hiruma-Lima, C. A., Felisbino, S. L., Garrido-Mesa, N., Utrilla, P., et al. (2012). Suppression of TNBS-induced colitis in rats by 4-methylesculetin, a natural coumarin: Comparison with prednisolone and sulphasalazine. *Chemico-Biological Interact.* 195 (1), 76–85. doi:10.1016/J.CBI.2011.11.004

Witaicenis, A., Seito, L. N., and di Stasi, L. C. (2010). Intestinal anti-inflammatory activity of esculetin and 4-methylesculetin in the trinitrobenzenesulphonic acid model of rat colitis. *Chemico-Biological Interact.* 186 (2), 211–218. doi:10.1016/J.CBI.2010.03.045

Xu, Y., Sheng, H., Bao, Q., Wang, Y., Lu, J., and Ni, X. (2016). NLRP3 inflammasome activation mediates estrogen deficiency-induced depression- and anxiety-like behavior and hippocampal inflammation in mice. *Brain, Behav. Immun.* 56, 175–186. doi:10.1016/J.BBI.2016.02.022

Zhang, Y., Liu, L., Peng, Y. L., Liu, Y. Z., Wu, T. Y., Shen, X. L., et al. (2014). Involvement of inflammasome activation in lipopolysaccharide-induced mice depressive-like behaviors. *CNS Neurosci. Ther.* 20 (2), 119–124. doi:10.1111/CNS.12170

Zhao, C., and Zhao, W. (2020). NLRP3 inflammasome-A key player in antiviral responses. *Front. Immunol.* 11, 211. doi:10.3389/FIMMU.2020.00211

Zhao, X., Cao, F., Liu, Q., Li, X., Xu, G., Liu, G., et al. (2019). Behavioral, inflammatory and neurochemical disturbances in LPS and UCMS-induced mouse models of depression. *Behav. Brain Res.* 364, 494–502. doi:10.1016/J.BBR.2017.05.064

Zhu, C.-B., Lindler, K. M., Owens, A. W., Daws, L. C., Blakely, R. D., and Hewlett, W. A. (2010). Interleukin-1 receptor activation by systemic lipopolysaccharide induces behavioral despair linked to MAPK regulation of CNS serotonin transporters. *Neuropsychopharmacology* 35 (13), 2510–2520. doi:10.1038/npp.2010.116

frontiers | Frontiers in Pharmacology

TYPE Review
PUBLISHED 06 March 2023
DOI 10.3389/fphar.2023.1095554

OPEN ACCESS

EDITED BY
Somasundaram Arumugam,
National Institute of Pharmaceutical Education and Research, Kolkata, India

REVIEWED BY
Carlos L. Cespedes-Acuña,
University of Bío-Bío, Chile
Laiba Arshad,
Forman Christian College, Pakistan

*CORRESPONDENCE
Cheng Lu,
lv_cheng0816@163.com

†These authors have contributed equally to this work

SPECIALTY SECTION
This article was submitted to Ethnopharmacology, a section of the journal Frontiers in Pharmacology

RECEIVED 11 November 2022
ACCEPTED 20 February 2023
PUBLISHED 06 March 2023

CITATION
Geng Q, Liu B, Cao Z, Li L, Lu P, Lin L, Yan L and Lu C (2023), Ethnobotany, phytochemistry and pharmacological properties of Fagopyri Dibotryis Rhizoma: A review.
Front. Pharmacol. 14:1095554.
doi: 10.3389/fphar.2023.1095554

Ethnobotany, phytochemistry and pharmacological properties of Fagopyri Dibotryis Rhizoma: A review

Qi Geng†, Bin Liu†, Zhiwen Cao, Li Li, Peipei Lu, Lin Lin, Lan Yan and Cheng Lu*

Institute of Basic Research in Clinical Medicine, China Academy of Chinese Medical Sciences, Beijing, China

Fagopyri Dibotryis Rhizoma (FDR) is an effective Chinese herbal medicine with a long history of use in China. FDR is effective in heat clearing and detoxifying, promotion of blood circulation, relieving carbuncles, dispelling wind, and removing dampness. Its seeds also have high nutritional value, are rich in protein, and contain a variety of mineral elements and vitamins. Therefore, FDR is considered a natural product with medical and economic benefits, and its chemical composition and pharmacological activity are of interest to scientists. The current review provides an overview of the available scientific information on FDR, particularly its botany, chemical constituents, and pharmacological activities. Various sources of valid and comprehensive relevant information were consulted, including the China National Knowledge Infrastructure, Web of Science, and PubMed. Among the keywords used were "*Fagopyri Dibotryis Rhizoma*", "botanical features", "chemical composition", and "pharmacological activity" in combination. Various ailments are treated with FDR, such as diabetes, tumor, sore throat, headache, indigestion, abdominal distension, dysentery, boils, carbuncles, and rheumatism. FDR is rich in organic acids, tannins, flavonoids, steroids, and triterpenoids. Experiments performed *in vitro* and *in vivo* showed that FDR extracts or fractions had a wide range of pharmacological activities, including antitumor, anti-inflammatory, immunomodulatory, antioxidant, antimicrobial, and antidiabetic. The current review provides an integrative perspective on the botany, phytochemistry and pharmacological activities of FDR. FDR may be used as a medicine and food. Based on its chemical composition and pharmacological effects, the main active ingredients of FDR are organic acids, tannins, and flavonoids, and it has obvious antitumor pharmacological activity against a variety of malignant tumors. Therefore, FDR is worthy of further study and application as a potential antitumor drug.

KEYWORDS

Fagopyri Dibotryis Rhizoma, ethnobotany, application, phytochemistry, pharmacology

1 Introduction

Chinese herbal medicine plays a crucial role in the prevention and treatment of diseases as a drug resource for the traditional medical system and as an important raw material for chemical drugs, international botanicals, and the food industry. A significant amount of evidence suggests that medicinal plants may be used to treat a variety of diseases and for the

discovery of novel pharmacologically active molecules. The phytochemicals identified from medicinal plants have provided promising lead compounds for effective new drugs (Ríos and Recio, 2005; Batiha et al., 2019a; Batiha et al., 2020; El-Saber et al., 2020). Medicinal plants have gained wider acceptance in recent years due to the perception that they are natural products and less likely to induce side effects than their synthetic counterparts (Abushouk et al., 2017a; Abushouk et al., 2017b). Various medicinal plants possess anti-inflammatory, antibacterial, antitumor, antiviral, and other activities (Bakkali et al., 2008). Herbal extracts and pharmacologically active molecules extracted from different plant species that were previously used in traditional medicine have received much attention (Essawi and Srour, 2000; Batiha et al., 2019b; Beshbishy et al., 2019).

Fagopyrum dibotrys (D. Don) Hara is a perennial herb of the genus *Fagopyrum* in the family *Polygonaceae*, and it is widely distributed in the Sichuan Basin, the hills of Guangdong and Guangxi, and the Yunnan-Guizhou Plateau in China and Thailand, Nepal, India and other countries (Peng et al., 1996). The dried rhizome is often used as medicine and food because it effectively clears heat, removes toxins, drains pus, removes blood stasis and invigorates the spleen to strengthen the stomach. For several thousand years in China, *Fagopyri Dibotryis Rhizoma* (FDR) has been widely used as a folk medicine to cure forms of chronic bronchitis, lung cancer, sore throat, rheumatic disease, dysentery, and enteritis (Chan, 2003a; Jing et al., 2016; Zhao et al., 2018). The medicinal properties of FDR are attracting the attention of an increasing number of academics due to its tremendous medicinal value. FDR components have been extensively examined, and an increasing number of compounds have been identified and isolated. A variety of components have been identified in FDR, including organic acids, tannins, flavonoids, steroids, and triterpenoids (Shao et al., 2005; Cao et al., 2019). FDR also has a broad spectrum of pharmacological effects, including antitumor, antimicrobial, anti-inflammatory, antioxidant, and immunomodulatory effects (Chan, 2003b; Shen, 2013; Wang et al., 2017).

FDR has a variety of chemical components and diverse pharmacological activities, and it is a highly valuable medicinal resource plant for development. Many studies recently investigated the botany, phytochemistry and pharmacology of FDR and found that organic acids, tannins, and flavonoids were the most important active components underlying the broad-spectrum antitumor, anti-inflammatory, and other effects (Li et al., 2019). However, comprehensive and up-to-date information on FDR is lacking. Therefore, the current review summarizes recent progress on the phytoconstituents, chemical components and pharmacological activity of FDR, especially the organic acids, tannins and flavonoids that inhibit tumors and the specific mechanisms of these effects, and adds its botanical characteristics and clinical applications. Various published data of valid and comprehensive relevant information were consulted, including the China National Knowledge Infrastructure, Web of Science, and PubMed. Among the keywords used were "*Fagopyri Dibotryis Rhizoma*", "botanical features", "chemical composition", and "pharmacological activity" in combination. This review provides references for the further development and use of FDR in traditional Chinese medicine.

2 Botanical characterization and application

2.1 Botanical characterization

Fagopyrum dibotrys (D. Don) Hara is a perennial herb that is native to eastern, central and southwestern China, India, Nepal, Vietnam, Thailand, and other countries. The habitat of *Fagopyrum dibotrys (D. Don) Hara* is 250–3,200 m above sea level in valley wetlands and hillside forests. The rhizomes are black–brown, stout, and ligneous, and the stems are long and erect, green, or brownish, 40–100 cm high, branched, striate, and glabrous. The petiole is 2–10 cm, and the leaf blade is triangular at 4-12 × 3–11 cm. Both surfaces are papillate, the base is nearly hastate, the leaf margin is entire, and the apex is acuminate. The ocrea is brown, 5–10 mm, membranous, and oblique, and the apex is truncate, not ciliate. Plants have terminal, axillary or corymbose inflorescence. Bracts are ovate-lanceolate, ca. 3 mm, with membranous margins, and an acute apex, each 4-flowered and rarely 6-flowered. Pedicels are in equaling bracts that articulate at the middle. Perianth are white, and tepals are narrowly elliptical, ca. 2.5 mm. Stamens are included. The styles are free, and stigmas are much longer than the persistent perianth, capitate, and opaque. During April-August, the chenes are blackish brown, dull, broadly ovoid, 6–8 mm long, trigonous, sometimes narrowly winged, with smooth to repandous angles, and an acute apex (Editorial Committee of Chinese Flora, 1998).

2.2 Application

The anti-inflammatory and antiseptic effects of FDR may be used to treat a variety of respiratory diseases. FDR tablets combined with tiotropium bromide powder nebulizer exhibited clinical efficacy and high safety, and it effectively improved the acute exacerbation of COPD patients with clinical symptoms and blood gas analysis indicators and reduced the inflammatory response (Li et al., 2022). FDR capsules combined with salmeterol ticapone inhalation powder nebulizer for the treatment of bronchial asthma in children had good results, and it effectively relieved clinical symptoms, improved lung and immune functions, regulated serum inflammatory factor levels, and had a good safety profile (Wei et al., 2022). FDR capsules significantly reduced the acute exacerbation of asthma patients' serum EOS and IgE levels, reduced the respiratory inflammatory response, improved the patient's lung ventilation function and the clinical symptoms of patients, which are worthy of clinical promotion (Feng et al., 2021).

The anti-inflammatory, analgesic and antibacterial pharmacological effects of FDR significantly improved the symptoms of infectious diseases of the intestinal tract. FDR tablets combined with cefdinir dispersible tablets effectively improved the symptoms of acute bacterial dysentery patients with diarrhea, purulent stools and other symptoms and reduced the level of serum inflammatory indicators (Zhang and Li, 2019).

3 Phytochemistry

Various parts of FDR have yielded more than 100 compounds, including organic acids, tannins, flavonoids, steroids, and

TABLE 1 Phytochemical constituents of FDR.

No.	Chemical component	Plant Part	Chemistry	Chemical Formula	Chemical Structures	Biological activity
1	(-)-Epicatechin-3-O-gallate acid ester	Rhizome	Organic acids	$C_{22}H_{18}O_{10}$	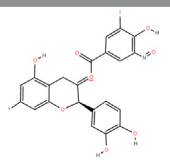	Anti-inflammatory Antioxidant
2	Gallic acid	Rhizome	Organic acids	$C_7H_6O_5$	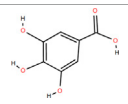	Antitumor Antimicrobial Antioxidant
3	Protocatechuic acid	Rhizome	Organic acids	$C_7H_6O_4$	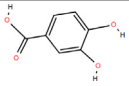	Anti-inflammatory Antimicrobial
4	3,4-Dihydroxy benzamide	Rhizome	Organic acids	$C_7H_7O_3$	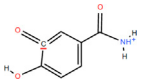	Anti-inflammatory Antimicrobial
5	Monopalmitin	Rhizome	Organic acids	$C_{19}H_{38}O_4$	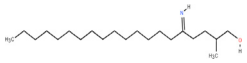	Immunomodulatory
6	Protocatechuic acid methyl ester	Rhizome	Organic acids	$C_8H_8O_4$	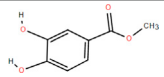	Antioxidant
7	Tans-p-hy-droxy cinnamic methyl ester	Rhizome	Organic acids	$C_{10}H_{10}O_3$	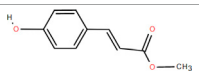	Antitumor Antimicrobial
8	3,5-Dimethoxy benzene carbonic acid-4-O-glucoside	Rhizome	Organic acids	$C_{12}H_{18}O_3$	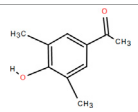	Anti-inflammatory
9	Ferulic acid	Rhizome	Organic acids	$C_{10}H_{10}O_4$	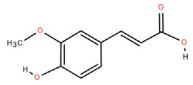	Antioxidant Antimicrobial Anti-viral
10	Syringic acid	Rhizome	Organic acids	$C_9H_{10}O_5$	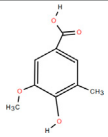	Antimicrobial
11	p-Hydroxyl-benzaldehyde	Rhizome	Organic acids	$C_7H_6O_2$	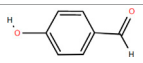	Anti-inflammatory Antimicrobial
12	Succinic acid	Rhizome	Organic acids	$C_4H_6O_4$	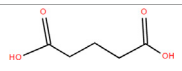	Antimicrobial Immunomodulatory
13	Luteolin	Rhizome	Flavonoids	$C_{15}H_{10}O_6$	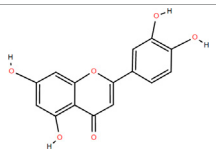	Anti-inflammatory

(Continued on following page)

TABLE 1 (*Continued*) Phytochemical constituents of FDR.

No.	Chemical component	Plant Part	Chemistry	Chemical Formula	Chemical Structures	Biological activity
14	(-)-Epicatechin	Rhizome	Flavonoids	$C_{15}H_{14}O_6$	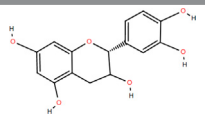	Antitumor Anti-inflammatory
15	3-Galloyl (-) epicatechin	Rhizome	Flavonoids	$C_{22}H_{18}O_{10}$	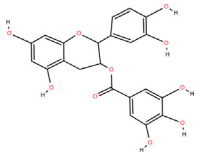	Antitumor Antioxidant Anti-inflammatory
16	Dimeric procyanidin	Rhizome	Flavonoids	$C_{45}H_{38}O_{18}$	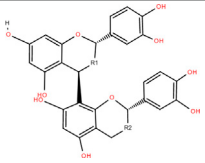	Anti-inflammatory Antimicrobial Immunomodulatory
17	(+)-Catechin	Rhizome	Flavonoids	$C_{15}H_{14}O_6$	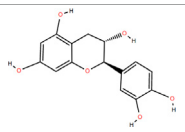	Antitumor Antidiabetic Anti-inflammatory
18	Eriodictyol	Roots	Flavonoids	$C_{15}H_{12}O_6$	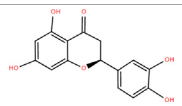	Anti-inflammatory Antioxidant Antidiabetic
19	Quercetin	Seeds, Stems, Roots, Leaves	Flavonoids	$C_{15}H_{10}O_7$	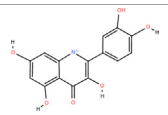	Anti-inflammatory Antioxidant Antimicrobial Immunomodulatory
20	Rutin	Flowers, Seeds, Leaves	Flavonoids	$C_{27}H_{30}O_{16}$	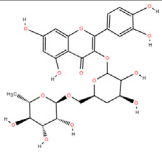	Anti-inflammatory Antioxidant Anti-viral
21	Genkwanin	Rhizome	Flavonoids	$C_{16}H_{12}O_5$	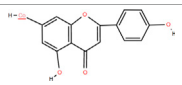	Antitumor Anti-viral
22	Chrysoeriol	Rhizome	Flavonoids	$C_{16}H_{12}O_6$	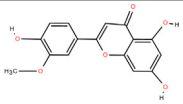	Anti-inflammatory
23	Pratol	Rhizome	Flavonoids	$C_{16}H_{12}O_4$	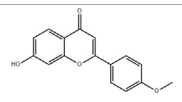	Anti-inflammatory
24	Luteolin-7,4′-dime-thylether	Rhizome	Flavonoids	$C_{17}H_{14}O_6$	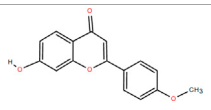	Anti-inflammatory

(Continued on following page)

TABLE 1 (*Continued*) Phytochemical constituents of FDR.

No.	Chemical component	Plant Part	Chemistry	Chemical Formula	Chemical Structures	Biological activity
25	Rhamnetin	Rhizome	Flavonoids	$C_{16}H_{12}O_7$	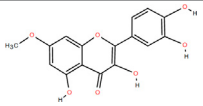	Antitumor Anti-inflammatory
26	3,6,3′,4′-Tetrahydroxy-7-methoxyflavon	Rhizome	Flavonoids	$C_{16}H_{12}O_7$	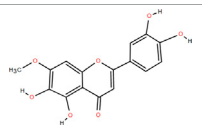	Anti-inflammatory
27	Procyanidin B2	Rhizome	Tannins	$C_{30}H_{26}O_{12}$	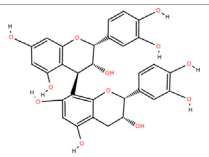	Anti-inflammatory Antimicrobial
28	Procyanidin C1	Rhizome	Tannins	$C_{45}H_{38}O_{18}$	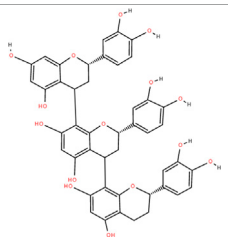	Antitumor Anti-diabetic
29	Procyanidin B4	Rhizome	Tannins	$C_{30}H_{26}O_{12}$	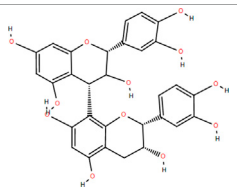	Antitumor Antioxidant
30	3,3'-Digalloyl procyanidin B2	Rhizome	Tannins	$C_{44}H_{34}O_{20}$	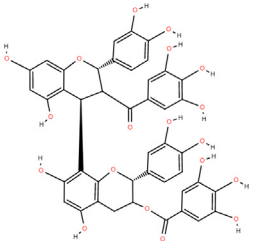	Antitumor Antioxidant
31	*β*-Sitosterol	Rhizome	Steroids	$C_{30}H_{52}O$	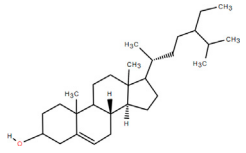	Antitumor
32	*β*-Daucosterol	Rhizome	Steroids	$C_{35}H_{60}O_6$	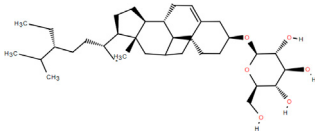	Antitumor

(Continued on following page)

TABLE 1 (*Continued*) Phytochemical constituents of FDR.

No.	Chemical component	Plant Part	Chemistry	Chemical Formula	Chemical Structures	Biological activity
33	Hecogenin	Rhizome	Steroids	$C_{27}H_{42}O_4$	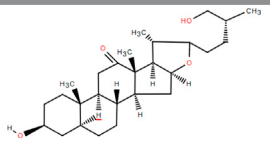	Anti-inflammatory
34	Glutinone	Rhizome	Terpenoids	$C_{19}H_{18}O_3$	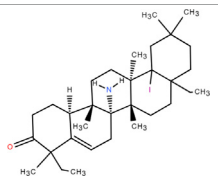	Antimicrobial
35	Glutinol	Rhizome	Terpenoids	$C_{30}H_{50}O_1$	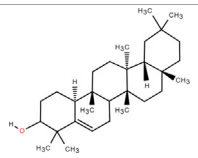	Antimicrobial
36	N-Butyl-β-D-fructopy-ronoside	Rhizome	Others	$C_{10}H_{20}O_6$	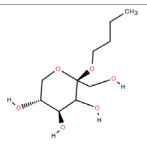	Antitumor
37	Methyl-3,4-dihydroxybenzoatem	Rhizome	Others	$C_8H_8O_4$	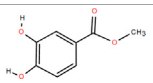	Anti-inflammatory Antioxidant
38	Gglycerol monop-almitate	Rhizome	Others	$C_{19}H_{38}O_4$	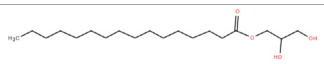	Anti-inflammatory
39	p-Hydroxyl-benzaidehyde	Roots	Others	$C_7H_6O_2$	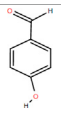	Anti-inflammatory Antimicrobial
40	N-Trans-coumaroyl tyramine	Rhizome	Others	$C_{17}H_{17}NO_3$	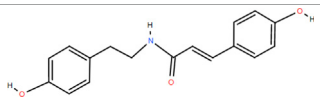	Anti-inflammatory
41	Emodin	Rhizome	Others	$C_{15}H_{10}O_5$	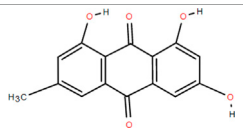	Antimicrobial
42	Diboside A	Rhizome	Others	$C_{49}H_{48}O_{20}$	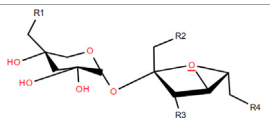	Anti-inflammatory
43	3-Methyl-gossypetin 8-O-d-glucopyranoside	Rhizome	Others	$C_{22}H_{22}O_{13}$	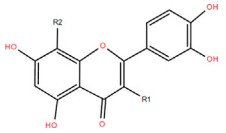	Anti-inflammatory

(Continued on following page)

TABLE 1 (*Continued*) Phytochemical constituents of FDR.

No.	Chemical component	Plant Part	Chemistry	Chemical Formula	Chemical Structures	Biological activity
44	5,5-Di-α-furaldehyde dimethylether	Rhizome	Others	$C_7H_{10}O_3$	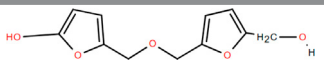	Immunomodulatory

triterpenoids (Lin et al., 2016), which support its potential use as a medicinal and food plant. These compounds likely explain the differentiated pharmacological effects based on the characteristics of these chemical components. A list of phytochemical constituents is presented in Table 1.

3.1 Organic acids

Organic acids are compounds that contain -COOH, -SO_3H, RSOOH, and RCOSH in their molecular structure, and leaves, roots, and Chinese herbs are abundant in these molecular structures. Twelve organic acids have been identified in FDR, including gallic acid, protocatechuic acid, (-)-epicatechin (Li et al., 2020; Huang et al., 2022), (-)-epicatechin-3-O-gallate acid ester, tans-p-hy-droxy cinnamic methyl ester, 3,4-dihydroxy benzamide, monopalmitin, protocatechuic acid methyl ester (Shao et al., 2004), 3,5-dimethoxy benzene carbonic acid-4-O-glucoside, syringic acid, ferulic acid, p-hydroxyl-benzaldehyde, and succinic acid (Zhao et al., 2011).

3.2 Flavonoids

Flavonoids are widely present in naturally growing plants and refer to a class of compounds with two benzene rings connected by three carbon atoms that create the C6-C3-C6 structure (Cook and Samman, 1996). Quercetin, rutin (Tang et al., 2014), luteolin (Shao et al., 2005), genkwanin, chrysoeriol (Yan, 2006), pratol, luteolin-7,4′-dimethylether, rhamnetin, iorhamnetin, 3,6,3′,4′-tetrahydroxy-7-methoxyflavon (Zhang et al., 2016), eriodictyol (Zhao et al., 2011), dimeric procyanidin (Liu et al., 1983), 3-galloyl (+) catechin, 3-galloyl (-) epicatechin (Liu et al., 1998), (+)-catechin, (-) epicatechin (Zhang et al., 1994) and other flavonoids were isolated from FDR using column chromatography and high-performance liquid chromatography (HPLC).

3.3 Tannins

Tannins are phenolic compounds with complex structures that are widely distributed in plants. Procyanidin b2, procyanidin c1 (Huang et al., 2022), procyanidin b4 (Peng et al., 1996), and 3,3′-digalloyl procyanidin b2 were isolated from FDR.

3.4 Steroids

Steroids are a class of natural chemical components that exist widely in nature and have the steroid parent nucleus of cyclopentane-polyhydrophenanthrene in their structure. Chromatography on silica and Sephadex LH-20 columns isolated β-sitosterol and β-daucosterol from FDR (Wu et al., 2008). Liu et al. obtained hecogenin from FDR (Liu et al., 1983).

3.5 Terpenoids

Terpenoid is a general term that summarizes all polymers of isoprene and their derivatives, which are commonly found in plants. Terpenoids have important physiological activities and are an important resource for the study of natural products and the development of new drugs. Silica gel column chromatography, Sephadex LH-20 column chromatography and recrystallization were used to separate the ethyl acetate extract as glutinone and glutinol (Shao et al., 2005).

3.6 Other components

Emodin (Wu et al., 2008), glycerol monop-almitate, n-butyl-β-D-fructopy-ronoside, methyl-3,4-dihydroxybenzoate (Shao et al., 2005), diboside A, 3-methyl-gossypetin 8-O-d-glucopyranoside (Wang et al., 2005), 5,5-di-α-furaldehyde dimethylether (Tian et al., 1997), n-trans-coumaroyl tyramine, and p-hydroxy-benzaidehyde (Zhao et al., 2011) were also isolated from FDR.

4 Pharmacological activities

FDR is widely used in Chinese herbal medicine for its antitumor, anti-inflammatory, antimicrobial, antioxidant, and immunomodulatory properties in recent years (Figure 1). A variety of extracts and their chemical constituents showed various and significant biological and pharmacological activities in previous studies (Yang et al., 2019). Extracts and constituents of FDR were tested, and the results support their renowned applications in the treatment of a variety of ailments. Detailed pharmacological studies are discussed in the following sections.

4.1 Antitumor activity

The antitumor activity of FDR has drawn increasing attention over the past decades. FDR components had beneficial effects in the treatment of a variety of cancers in several studies. As shown in Figure 2, Wang et al. (Wang and Bao, 2020) found that gallic acid prevented non-small cell lung cancer progression *via* inhibition of epidermal growth factor receptor activation and impairment of the

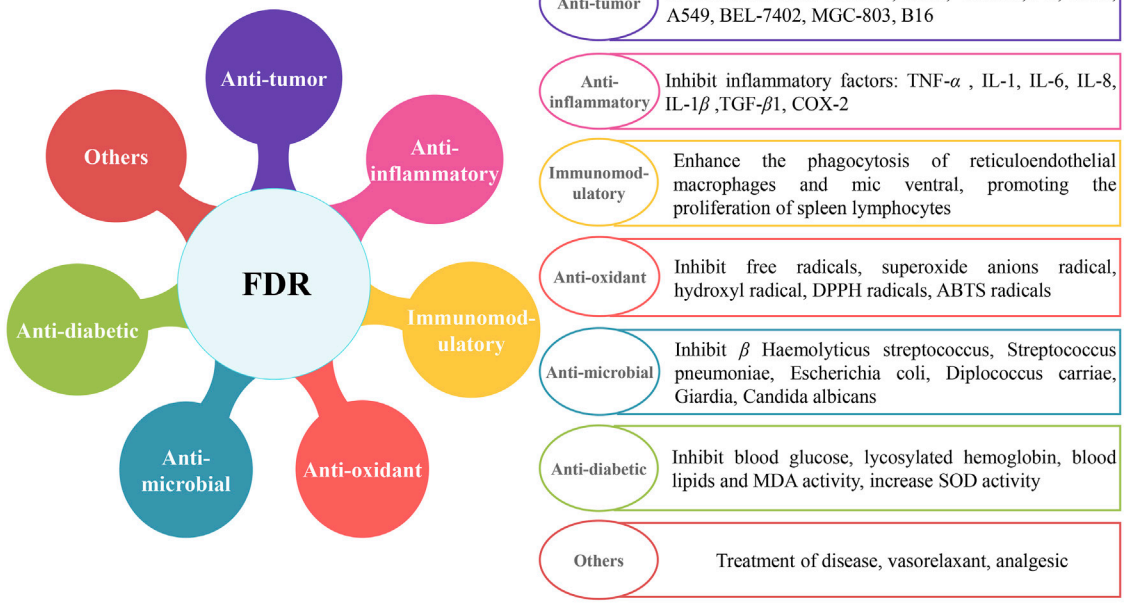

FIGURE 1
Molecular pharmacological activity mechanisms of FDR.

binding of coactivator-associated arginine methyltransferase 1 to proline, glutamic acid, and leucine-rich protein 1. Vergara et al. (Pereyra-Vergara et al., 2020) showed that reactive oxygen species (ROS) mediated (-)-epicatechin-induced apoptosis in human breast cancer cells. Apoptosis and autophagy were induced by procyanidin b2 in colorectal cancer cells (CRC) in a dose-dependent manner *via* downregulation of the expression of phosphorylated-phosphatidylinositol 3-kinase (p-PI3K), phosphorylated-protein kinase B (p-Akt) and phosphorylated-mammalian target of rapamycin (p-mTOR) of the PI3K/Akt pathway (Zhang et al., 2019). Procyanidin b2 prevented the binding of nuclear factor kappa B (NF-κB) to DNA in the H-RS cell line and inhibited NF-κB-driven genes, including anti-apoptotic proteins (Mackenzie et al., 2008). Another study revealed that β-sitosterol regulated the treatment response in CRC by mediating the p53/NF-κB/BCRP signal transduction axis (Wang et al., 2020). Melanoma cell growth inhibition by procyanidin c1 was attributed to activation of the 67LR/PKA/PP2A/CPI17/MRLC pathways (Bae et al., 2020). Genkwanin increased host immunity and decreased the levels of inflammatory cytokines, which may make it an effective chemotherapeutic agent for the treatment of CRC (Wang X et al., 2015). Rhamnetin inhibited the expression of the pregnant x receptor (PXR) by increasing miR-148a levels, which decreased the expression of its downstream genes. Therefore, sorafenib was more effective against hepatocellular carcinoma (Li Y et al., 2021).

The treatment of cancer cells with FDR extract inhibited their growth. FDR extract showed significant proliferation inhibitory activity on HeLa cells, which was primarily associated with modulation of the expression of the apoptotic inducible factor Bcl2-associated X (Bax) and inhibition of the anti-apoptotic factor B-cell lymphoma-2 (Bcl2). The extract of FDR can also activated caspase-8, caspase-9, and caspase-3 and released mitochondrial cytochrome C (Pan et al., 2018). Some extracts from FDR possessed potential antitumor activity. For example, an extract from the FDR rhizome had antiproliferative and proapoptotic effects on the human esophageal cancer cell line CaEs-17 (Zhang et al., 2010). Chen et al. (Chen et al., 2012) revealed that FDR prevented Bowes melanoma cell WM239 proliferation and migration, which was accomplished *via* reduced activation of Src protein, decreased levels of N-cadherin intracellular segment phosphorylation and dissociation of N-cadherin from β-catenin. Fr4 is a polyphenolic substance extracted from FDR. Fr4 reduced tumor weight, increased tumor suppression, and showed good antitumor activity in a mouse Lewis lung cancer model (Chen et al., 2005). Fr4 promoted a dose-dependent increase in the inhibition of HL-60 proliferation in leukemic cells and induced apoptosis (Chen et al., 2006). The FDR extract Fr4 also had an antitumor effect on kidney cancer. Fr4 inhibited the proliferation and induced apoptosis of kidney cancer cells *via* a mechanism related to the upregulation of DNA damage-induced transcript 4 protein expression (Song et al., 2020).

Wei Mai Ning capsules are the main raw material extracts from FDR, which inhibit tumor growth, invasion, and blood flow metastasis, and it has been approved for clinical cancer therapy (Lou et al., 2004a). Wei Mai Ning had effects on the lung cancer cell lines PG, PAa and A549 and inhibited the liver cancer cell line BEL-7402, gastric cancer cell line MGC-803 and melanoma cell line B16 to varying degrees (Lou et al., 2004b). Wei Mai Ning inhibited the adhesion between PG and HUVECs *in vitro via* the dual action of PG cells and HUVECs, which inhibited tumor cell metastasis in the blood channel (Lou et al., 2007).

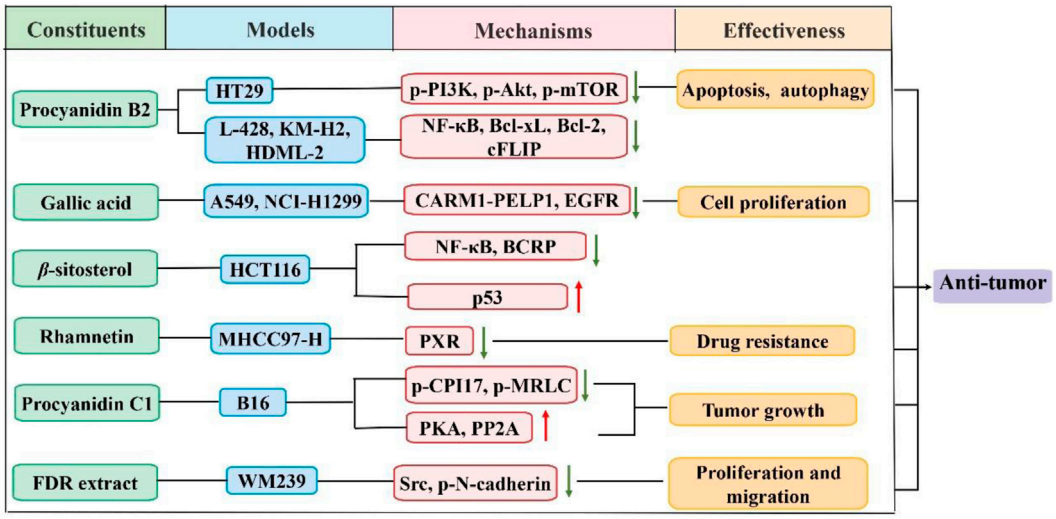

FIGURE 2
Schematic diagram of the antitumor mechanisms of FDR and its constituents.

4.2 Anti-inflammatory activity

Various *in vitro* and *in vivo* experiments investigated the anti-inflammatory effects of FDR extracts (Figure 3). The effects of (-)-epicatechin on lipopolysaccharide (LPS)-induced inflammation in RAW264.7 cells were demonstrated, and its anti-inflammatory effect may be related to a reduction in inflammatory cytokines, such as nitric oxide (NO), tumor necrosis factor-alpha (TNF-α), interleukin-1 and interleukin-6 (IL-6) and inhibition of the expression of nitric oxide synthase, phosphorylation of p38 mitogen-activated protein kinase (p-p38MAPK), extracellular signal regulated kinases 1/2 (ERK1/2) and c-Jun N-terminal kinase (JNK) (Ruan and Mu, 2017). Different (-)-epicatechin metabolites have anti-inflammatory properties that boost vascular health partially by reprogramming epigenetic signaling in endothelial-immune cells and reversing low-grade systemic inflammation (Milenkovic et al., 2020). Protocatechuic acid inhibited BV2 microglia and keratinocytes by reducing the activation of toll-like receptor 4 (TLR4)-dependent Akt, mTOR, and NF-κB transcription factors and activating JNK and p38 MAPK (Wang H. Y et al., 2015; Amini et al., 2018; Nam and Lee, 2018). Rhamnetin treatment inhibited the inflammatory and proatherosclerosis pathways in ApoE−/− mice, and aortic tissue from ApoE−/−mice exhibited amelioration of TLR4 mRNA and components of the TLR4 pathway after treatment with rhamnetin (Wang et al., 2021).

By inhibiting the TLR4-mediated activation of NF-κB and activator protein 1 and suppressing the phosphorylation of PI3K/Akt and MAPK, chrysoeriol inhibited the inflammatory response of LPS-stimulated RAW 264.7 cells (Yoon and Park, 2021). Gallic acid is a promising treatment for gouty arthritis. These effects are induced by suppression of ROS generation, which limits NOD-like receptor protein 3 (NLRP3) inflammasome activation and pyroptosis dependent on nuclear factor erythroid 2-related factor 2 (Nrf2) signaling (Lin et al., 2020). The anti-inflammatory properties of procyanidin b2 are attributed to suppression of NLRP3 inflammasome activation (Jiang et al., 2018). Byun et al. (Byun et al., 2013) indicated that procyanidin c1 inhibited LPS-induced activation of MAPK and NF-κB signaling *via* TLR4 in macrophages. Zhang et al. (Zhang et al., 2020) demonstrated that β-sitosterol suppressed NF-κB and activated heme oxygenase-1 (HO-1)/Nrf-2 pathways to inhibit arthritis.

FDR extract inhibits the transcription factor NF-κB and the induced production of TNF-α, interleukin-8, IL-6, transforming growth factor-β1 and precollagen peptide III activity in chronic obstructive pulmonary disease rats, which improves lung tissue inflammation (Tang et al., 2014; Tang et al., 2016). The FDR extract prevented lung tissue injury in rats with pneumonia by downregulating TLR2/4, myeloid differentiation primary response 88 mRNA and NF-κB inhibitor alpha protein expression (Dong et al., 2011). FDR tablets attenuated inflammatory symptoms and inflammatory damage in colorectal tissues of mice with a dextran sulfate sodium-induced inflammatory bowel disease model by downregulating TNF-α, IL-6 and interleukin-1β factor expression (Shen et al., 2019; Tan et al., 2020).

Clinical studies proposed combination therapy with Chinese medicines as an effective treatment strategy. FDR tablets combined with salazosulfapyridine (SASP) were more effective than SASP alone in ulcerative colitis (UC), and the mechanism may be the anti-inflammatory and immunomodulatory effects of intervening in UC *via* the TLR4/NLRP3 signaling pathway (Ge et al., 2021). FDR tablets were combined with compound kangfuxin solution and showed good efficacy in the treatment of UC (Hua and Yin, 2016). The effectiveness of FDR in controlling lung disease has been demonstrated in several clinical studies, including the treatment of adult and childhood bronchial asthma, and FDR capsules combined with salmeterol xinafoate and fluticasone propionate powder were effective (Li and Wu, 2018; Feng et al., 2021). Some studies also revealed that FDR tablets combined with

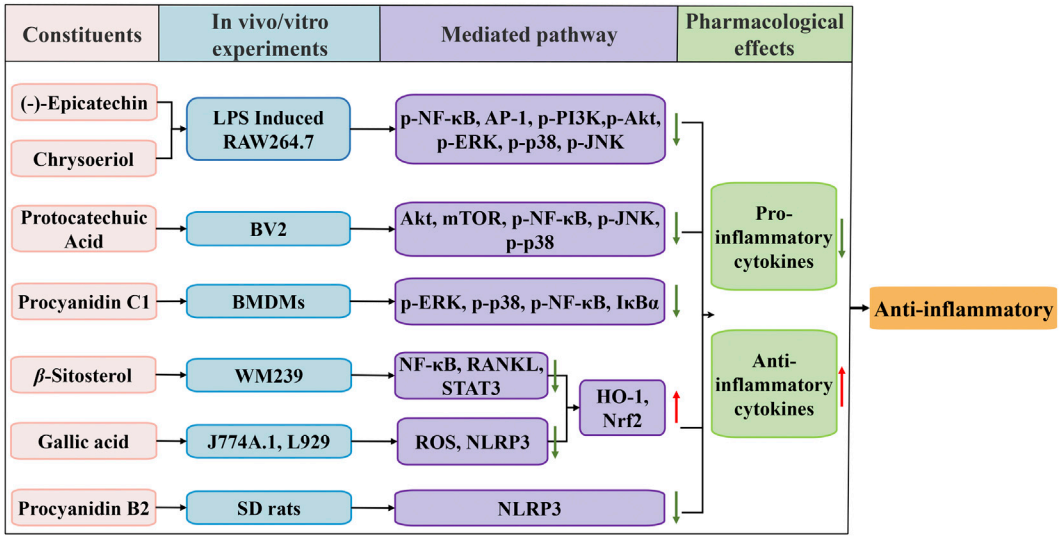

FIGURE 3
Schematic diagram of the anti-inflammatory mechanisms of FDR and its constituents.

cefoperazone and gubenkechuan tablets had a significant effect in chronic bronchial patients (Li, 2010; Han, 2020).

4.3 Immunomodulatory activity

Pharmacological studies confirmed that the extract from FDR showed an anti-rheumatoid arthritis effect, which may be due to its anti-inflammatory and immune activities (Shen, 2013). The polysaccharide content of FDR repairs the immune function of the thymus and spleen, enhances nonspecific immune function, improves specific humoral immunity and cellular immune function, and ultimately enhances the body's immune function *via* multiple pathways, links, and targets (Gu et al., 2015). An extract of FDR reduced the expression of caspase-1, caspase-3, caspase-9, and matrix metallopeptidase-1 (MMP-1) in articular cartilage of a rabbit knee osteoarthritis model, which reduced cartilage damage and had an osteoprotective effect (Pan et al., 2019). FDR enhanced the phagocytosis of ventral and reticuloendothelial macrophages, which showed that it enhanced the immune function of mice (Yang et al., 1992; Zhang and Lin, 1999). Ethanol extract from FDR roots had an immunomodulatory role by promoting the proliferation of chicken spleen lymphocytes and the secretion of interleukin-2 and interferon-γ by peripheral blood T lymphocytes (Qiao et al., 2010).

4.4 Antioxidant activity

Organic acids, flavonoids, and tannins found in FDR demonstrate scavenging properties against free radicals and superoxide anions. Figure 4 shows the antioxidant effect of FDR *via* some pathways. Flavonoids remarkably reduced superoxide anion radicals and hydroxyl radicals in a concentration-dependent manner (Wang et al., 2017). Protoconuic acid is a naturally occurring organic acid that is widely distributed. Han et al. (Han et al., 2018; Han et al., 2019) found that the antioxidant properties of protocatechuic acid were beneficial for reducing the oxidative damage caused by palmitic acid in induced human umbilical vein endothelial cells (HUVECs) or high fat-induced oxidative damage in mice *via* downregulation of the CD36/AMPK-dependent pathway. PA had a beneficial effect on oxidative damage to the gastrointestinal mucosa by upregulating the DJ-1/PI3K pathways, increasing Nrf2 and mTOR expression, reducing ROS levels and lipid peroxidation, downregulating proapoptotic and inflammatory factors, and enhancing antioxidant enzyme activity and cell viability (Farombi et al., 2016; Cheng et al., 2019). (-)-Epicatechin in FDR extract exhibited stronger antioxidant activity and reduced superoxide anion radicals and hydroxyl radicals (Huang R et al., 2014). Procyanidin b2 prevented oxidative injury in aged mice *via* citrate cycle regulation, fatty acid regulation, and bile acid regulation, and procyanidin b2 suppressed intracellular ROS generation by activating Nrf2 expression to prevent oxidative damage (Xiao et al., 2018; Li B et al., 2021). Procyanidin c1 plays an important role in antioxidant activity by mediating the nuclear translocation of Nrf2 and increasing the expression levels of HO-1. Procyanidin c1 also blocks glutamate-induced phosphorylation of MAPKs, including ERK1/2 and p38, but not JNK (Song et al., 2019). Kim et al. (Kim et al., 2021) confirmed that chrysoeriol treatment prevented HO-induced oxidative stress in RPE cells, which significantly decreased the mitochondrial dysfunction caused by HO-induced oxidative stress. A reduction in MMP and an increase in mitochondrial-associated genes and proteins were also observed. Chrysoeriol also markedly induced the transcription factors Nrf2 and NAD(P)H:quinone oxidoreductase 1, which are related to antioxidants.

FDR leaf tea has significant antioxidant scavenging ability against DPPH radicals, ABTS radicals and hydroxyl radicals (Huang et al., 2016). FDR extract reduces cartilage damage by reducing malondialdehyde (MDA) and lipid peroxide content and enhancing superoxide dismutase (SOD) activity, which reduce oxygen free radicals and provide osteoprotective effects (Pan et al., 2020).

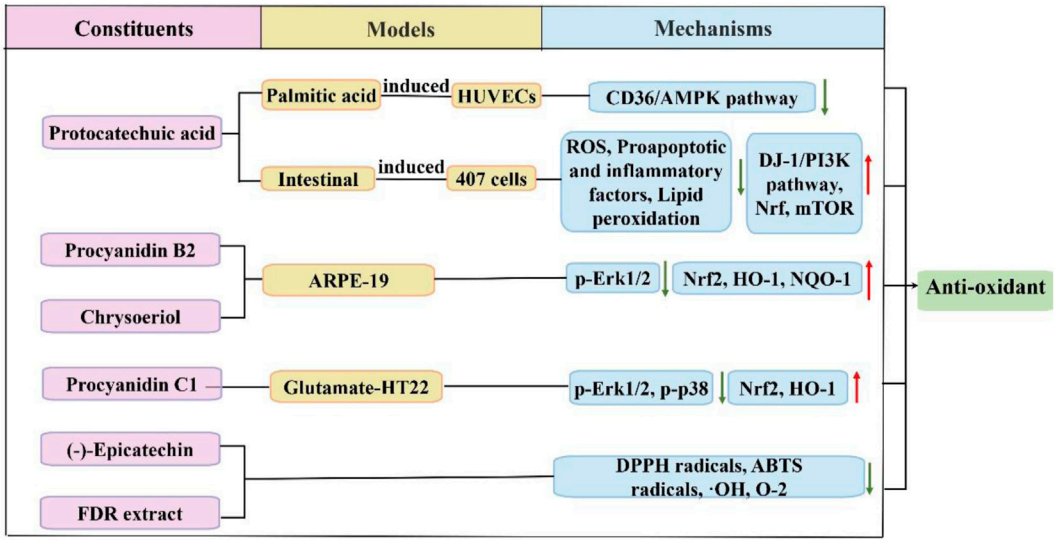

FIGURE 4
Schematic diagram of the antioxidant mechanisms of FDR and its constituents.

4.5 Antimicrobial activity

Ethanol extracts of FDR showed antimicrobial effects (Ai et al., 2002; Zhou et al., 2009). The ethanol extract of FDR showed inhibition of *β Hemolyticus Streptococcus* and *Streptococcus pneumoniae in vitro* and inhibited infections caused by strains of *Streptococcus pneumoniae* in mice *in vivo* (Yan et al., 2006). Fang et al. (Feng et al., 2006) evaluated the inhibitory activities of FDR against bacteria and fungi, and their results indicated that FDR exhibited obvious antibacterial effects on *Staphylococcus aureus*, *Escherichia coli* and *Diplococcus carriae* It also exhibited antifungal activities against *Giardia* and *Candida albicans*. FDR also demonstrated antibacterial activity by scavenging *Staphylococcus aureus, Bacillus subtilis* and *Saccharomyces cerevisiae* (Huang and Yi, 2015). KQH-01, KQH-02 and JQY-1 isolated from FDR showed strong antibiotic activity against some indicator microorganisms, such as *Staphylococcus aureus*, *Escherichia coli*, *Bacillus subtilis* and *Pythium aphanidermatum* (Zhang et al., 2011). FDR powder protected mice from *Salmonella* infection and suggested a dose-activity relationship (Wang et al., 2013).

FDR tablets combined with ceftriaxone had important antimicrobial activities in acute bacillary dysentery, and one of the mechanisms of action was the promotion of inflammatory absorption (Li, 2012). When FDR tablets combined with levofloxacin showed significant antimicrobial activity and may be used for the treatment of acute bacillary dysentery (Bi et al., 2012; Yu, 2014).

4.6 Antidiabetic activity

FDR flavonoids improved objective indices in streptozotocin-induced diabetes mellitus type 2 (T2DM) mice and regulated lipid metabolism and oxidative stress levels in model animals (Ruan et al., 2017). FDR leaf tea reduced blood glucose, blood lipids and MDA activity, increased SOD activity and improved pancreatic and liver lesions in mice with T2DM (Huang X et al., 2014). The FDR mixture significantly improved the clinical symptoms of diabetic nephropathy and significantly reduced the patient's blood glucose, glycosylated hemoglobin and blood lipids (Huang et al., 2009).

4.7 Others

FDR also performs other functions in the above-described pharmacological activities. For example, FDR extract has an obvious antiviral effect *in vitro*, and its active ingredient is the flavonoid of FDR, which is concentration dependent (Zhao et al., 2019). Lianhua Qingwen associated with FDR tablets was more effective, faster and safer than oseltamivir alone in the treatment of patients with influenza A (Guo, 2015). Procyanidin b1 may be an effective treatment for hepatitis C virus, which may be an HCV RNA polymerase inhibitor (Li et al., 2010).

The tannic compound procyanidin b2 has analgesic effects, primarily *via* anti-inflammatory antioxidant free radicals to protect nerve cell membranes and prevent the production and release of the neurotransmitter 5-HT. It also antagonizes the ligand-type receptor 5-HT3A expression or promotes the expression of the G protein-coupled superfamily 5-HT1A receptor *via* the upstream signaling pathway to improve irritable bowel syndrome (IBS). Downregulation of transient receptor potential vanilloid 1 (TRPV1) expression also had a therapeutic effect on hyperalgesia in IBS rats (Liu et al., 2012a; Liu et al., 2012b; Liu et al., 2016). The hot plate test and the acetic acid twist test showed that FDR medicinal liquid had analgesic effects, and it increased the pain threshold and reduced the number of twists in mice (Pan and Wan, 2015). Jia et al. used dysmenorrhea models in mice to evaluate the analgesic effect of FDR extract and found that it showed potential analgesic activity (Jia et al., 2010).

Othman et al. suggested that the vasorelaxant effect of ethyl cinnamate was mediated *via* multiple pathways, and the inhibition of Ca^{2+} influx into vascular cells and release of NO and prostacyclin from endothelial cells were involved (Othman et al., 2002).

5 Conclusions and perspectives

The current review systematically discussed the ethnobotany, phytochemistry, and pharmacology of FDR. Various ailments have traditionally been treated with FDR, including chronic bronchitis, tumor, sore throat, rheumatic disease, dysentery, and enteritis. The predominant natural compounds in FDR are organic acids, tannins, and flavonoids, but over 100 compounds have been identified. FDR exerts antitumor, anti-inflammatory, immunomodulatory, antioxidant, antimicrobial, antidiabetic, and other pharmacological activities. In addition to the phytochemical and pharmacological studies mentioned above, FDR has also received considerable attention because it contains a variety of essential nutrients, and the chemical composition of human health has received widespread attention. Therefore, a better understanding of the phytochemistry and pharmacology of FDR will undoubtedly promote a more rational development and utilization of FDR.

FDR has rich nutritional value and healthcare functions. It is a medicinal resource plant with high developmental value. It contains organic acids, tannins, flavonoids, and other antitumor active ingredients, and gallic acid, procyanidin B2, (-)-epicatechin and genkwanin show significant antitumor activity. However, whether the antitumor effects of FDR are the result of the joint action of various components and the specific antitumor mechanism are not clear. Therefore, there is a need for in-depth research on the following aspects. According to pharmacodynamic studies, the effective site of the antitumor effect of FDR must be clarified *via* separation and purification to improve its antitumor potency. From the molecular or genetic level, more in-depth research is needed to reveal the antitumor effect of FDR. Because FDR has certain anti-invasive and metastatic effects, it is necessary to perform further research to understand the value and significance of its intervention in tumor cell invasion and metastasis. FDR tablets have also been clinically proven to increase the efficacy of pneumonia treatment, pulmonary abscess treatment, and rheumatic disease treatment. However, as a "Chinese Pharmacopoeia" collection, its mechanism of action of "removing heat and toxins and removing pus and stasis" must be further clarified. This pharmacological effect of FDR may be due to the extract or active ingredients as clearing and detoxifying lung agents in drinks and beverages to promote the full use of FDR resources. The antitumor and anti-inflammatory effects and mechanisms of FDR have been widely studied. However, the mechanism of antimicrobial, antidiabetic and immunomodulatory activity of FDR still needs to be further explored. The research on the mechanism of action of FDR should be continuously strengthened, and the potential medicinal function of it should be expanded to promote the development and utilization of its medicinal resources.

Author contributions

QG Designing the review, Writing original draft, Writing—review and editing. BL Designing the review, Revising the pharmacology part, Writing—review and editing. ZC designed the review and revised the botanical characterization and phytochemistry section. LiL designed the review and revised the pharmacological part. PL designed the review and revised the manuscript. LinL preparation table and schematic diagram. LY Preparation schematic diagram and polishing the language and grammar. CL was involved in conception, supervision, manuscript reviewing and editing. Submission of the final version was approved by all authors.

Funding

This study was supported by the Scientific and Technological Innovation Project of the China Academy of Chinese Medical Sciences (CI2021B003), the National Key R&D Program of China (2020YFE0205100) and the Innovation Team and Talents Cultivation Program of the National Administration of Traditional Chinese Medicine (ZYYCXTD-D-202005).

Conflict of interest

The authors declare that the research was conducted in the absence of any commercial or financial relationships that could be construed as a potential conflict of interest.

Publisher's note

References

Abushouk, A. I., Ismail, A., Salem, A., Afifi, A. M., and Abdel-Daim, M. M. (2017a). Cardioprotective mechanisms of phytochemicals against doxorubicin-induced cardiotoxicity. *Biomed. Pharmacother. = Biomedecine Pharmacother.* 90, 935–946. doi:10.1016/j.biopha.2017.04.033

Abushouk, A. I., Negida, A., Ahmed, H., and Abdel-Daim, M. M. (2017b). Neuroprotective mechanisms of plant extracts against MPTP induced neurotoxicity: Future applications in Parkinson's disease. *Biomed. Pharmacother. = Biomedecine Pharmacother.* 85, 635–645. doi:10.1016/j.biopha.2016.11.074

Ai, Q., Wang, B., and Wang, G. (2002). Sterilization function of the abstracting products of rhizom of fagopyrum cymosum maaisn. *Heilongjiang Med. J.* 666. https://kns.cnki.net/kcms2/article/abstract?v=3uoqIhG8C44YLTlOAiTRKgchrJ08w1e7lwLRIsgSA99HxaEcueJ8s_vYdvP1Fwx4fKWzAnkmibK6J7lgRI35sNS7wuNA6hCh&uniplatform=NZKPT

Amini, A. M., Spencer, J., and Yaqoob, P. (2018). Effects of pelargonidin-3-O-glucoside and its metabolites on lipopolysaccharide-stimulated cytokine production by THP-1 monocytes and macrophages. *Cytokine* 103, 29–33. doi:10.1016/j.cyto.2017.12.031

Bae, J., Kumazoe, M., Murata, K., Fujimura, Y., and Tachibana, H. (2020). Procyanidin C1 inhibits melanoma cell growth by activating 67-kDa laminin receptor signaling. *Mol. Nutr. Food Res.* 64 (7), e1900986. doi:10.1002/mnfr.201900986

Bakkali, F., Averbeck, S., Averbeck, D., and Idaomar, M. (2008). Biological effects of essential oils–a review. *Food Chem. Toxicol.* 46 (2), 446–475. doi:10.1016/j.fct.2007.09.106

Batiha, G. E., Beshbishy, A. M., Alkazmi, L., Adeyemi, O. S., Nadwa, E., Rashwan, E., et al. (2020). Gas chromatography-mass spectrometry analysis, phytochemical screening and antiprotozoal effects of the methanolic Viola tricolor and acetonic Laurus nobilis extracts. *Ther* 20 (1), 87. doi:10.1186/s12906-020-2848-2

Batiha, G. E., Beshbishy, A. M., Tayebwa, D. S., Adeyemi, O. S., Shaheen, H., Yokoyama, N., et al. (2019a). The effects of trans-chalcone and chalcone 4 hydrate on the growth of Babesia and Theileria. *Plos Negl. Trop. Dis.* 13, e0007030. doi:10.1371/journal.pntd.0007030

Batiha, G. E., Beshbishy, A. M., Tayebwa, D. S., Shaheen, H. M., Yokoyama, N., and Igarashi, I. (2019b). Inhibitory effects of Syzygium aromaticum and Camellia sinensis methanolic extracts on the growth of Babesia and Theileria parasites. *Ticks Tick-Borne Dis.* 10 (5), 949–958. doi:10.1016/j.ttbdis.2019.04.016

Beshbishy, A. M., Batiha, G. E., Yokoyama, N., and Igarashi, I. (2019). Ellagic acid microspheres restrict the growth of Babesia and Theileria *in vitro* and Babesia microti *in vivo*. *Parasites Vectors* 12 (1), 269. doi:10.1186/s13071-019-3520-x

Bi, C., Gao, X., and Zhang, Q. (2012). Therapeutic efficacy of fagopyrum cymosum tabletcombined with levofloxacin on acute bacillary dysentery. *Infect. Dis. Inf.* 25 (1), 31–33.

Byun, E. B., Sung, N. Y., Byun, E. H., Song, D. S., Kim, J. K., Park, J. H., et al. (2013). The procyanidin trimer C1 inhibits LPS-induced MAPK and NF-κB signaling through TLR4 in macrophages. *Immunopharmacol* 15 (2), 450–456. doi:10.1016/j.intimp.2012.11.021

Cao, T., Zhao, L., Luo, H., Shi, J., and Jiang, Y. (2019). Study on the extraction and purification technology for active ingredients of JinQiaoMai by taking epicatechin as the marker. *West. J. Traditional Chin. Med.* 32 (03), 36–40. https://kns.cnki.net/kcms2/article/abstract?v=M5zCgC8QIcrbD1bgB8dzzWR2b3IZcBSNp-89zD9F4u7iLCgaMNvaiUS-49gqyL94w3B1MqpUjf9SYmG8Ynn-_AN1WcrGj4gUuw8wlkQ31wg4OuUj56s0zg==&uniplatform=NZKPT&language=CHS

Editorial Committee Of Chinese Flora (1998). "Editorial committee of Chinese Flora," in *Flora of China*. (Beijing: Science Press). http://www.cn-flora.ac.cn/

Chan, P. (2003b). Inhibition of tumor growth *in vitro* by the extract of Fagopyrum cymosum. *J. Chin. Integr. Med.* 1 (2), 128–131. doi:10.3736/jcim20030213

Chan, P. (2003a). Inhibition of tumor growth *in vitro* by the extract of fagopyrum cymosum (fago-c). *Life Sci.* 72 (16), 1851–1858. doi:10.1016/s0024-3205(03)00013-4

Chen, H., Zou, Z., Xu, X., Zhang, J., Zhang, X., Meng, D., et al. (2012). Inhibitory effect of Fagopyri Dibotryis Rhizoma extract on migration of WM239 and phosphorylation of N-cadherin in co-culture system of WM239 and Huvec. *Chin. J. Cell. Mol. Immunol.* 28 (1), 37–39. doi:10.13423/j.cnki.cjcmi.006300

Chen, X., Gu, Z., Yang, H., and Liang, Z. (2005). *The effect of Fr4 on expression of matrix metalloproteinase-9 and tissue inhibitors of metallproteinase-1 in mouse Lewis lung cancer tissue*, 25. China: Suzhou University Journal of Medical Science, 383–386. https://kns.cnki.net/kcms/detail/detail.aspx?FileName=SYXU200503011&DbName=CJFQ2005

Chen, X., Gu, Z., Yang, H., Liang, Z., Zhu, M., and Chen, B. (2006). Effect of Fagopyri Dibotryis Rhizoma Fr4 on apoptosis and telomerase activity of HL-60 cells induced. *Chin. Pharmacol. ical Bull.* 22 (7), 836–840. https://kns.cnki.net/kcms2/article/abstract?v=3uoqIhG8C44YLTlOAiTRKgchrJ08w1e7eWoVfj7plMzGtzV4keeauUu5P4TXrh2R22DCg6Mt70DPAe5itXyMOOMlDzJoEbVF&uniplatform=NZKPT

Cheng, Y. T., Lin, J. A., Jhang, J. J., and Yen, G. C. (2019). Protocatechuic acid-mediated DJ-1/PARK7 activation followed by PI3K/mTOR signaling pathway activation as a novel mechanism for protection against ketoprofen-induced oxidative damage in the gastrointestinal mucosa. *Free Radic. Biol. Med.* 130, 35–47. doi:10.1016/j.freeradbiomed.2018.10.415

Cook, N. C., and Samman, S. J. (1996). Flavonoids Chemistry, metabolism, cardioprotective effects, and dietary sources. *J. Nutr. Biochem.* 7 (2), 66–76. doi:10.1016/0955-2863(95)00168-9

Dong, L., Wang, C., Wu, C., Jiang, Q., and Zhang, Z. (2011). [Effect of jinqiaomai on expression of TLR2/4, MyD88 mRNA and IkappaB-alpha in lung tissue of rats with Klebsiella pneumonia]. *China J. Chin. Materia Medica* 36 (2), 200–204. https://kns.cnki.net/kcms2/article/abstract?v=3uoqIhG8C44YLTlOAiTRKgchrJ08w1e7tvjWANqNvp86QERf2Ty5clht06VmARYrSkr8coldZTKr1AdVj66cbPy0UKAbAa7U&uniplatform=NZKPT

El-Saber, B. G., Magdy, B. A., Stephen, A. O., Nadwa, E., Rashwan, E., Yokoyama, N., et al. (2020). Safety and efficacy of hydroxyurea and eflornithine against most blood parasites Babesia and Theileria. *PLoS One* 15, e0228996. doi:10.1371/journal.pone.022899

Essawi, T., and Srour, M. (2000). Screening of some Palestinian medicinal plants for antibacterial activity. *J. Ethnopharmacol.* 70 (3), 343–349. doi:10.1016/s0378-8741(99)00187-7

Farombi, E. O., Adedara, I. A., Awoyemi, O. V., Njoku, C. R., Micah, G. O., Esogwa, C. U., et al. (2016). Dietary protocatechuic acid ameliorates dextran sulphate sodium-induced ulcerative colitis and hepatotoxicity in rats. *Food Funct.* 7 (2), 913–921. doi:10.1039/c5fo01228g

Feng, B., Huang, X., Pang, X., and Long, Q. (2021). Clinical efficacy of jinqiaomai capsules combined with salmeterol xinafoate and fluticason propionate powder for inhalation in the treatment of children with bronchial asthma. *China Pharm.* 30 (7), 46–48. https://kns.cnki.net/kcms/detail/detail.aspx?FileName=YYGZ202107012&DbName=CJFQ2021

Feng, L., Chen, F., and Bai, J. (2006). Study of antimicrobial *in vitro* from fagopyrum dibotrys extracts. *J. Wuhan Botanical Res.* 24 (3), 240–244. https://kns.cnki.net/kcms2/article/abstract?v=3uoqIhG8C44YLTlOAiTRKgchrJ08w1e7eWoVfj7plMwamtZ5XYOWUW_egjbGHE7JlQO6DfGdNRAMmO4umUjbu3e5dR7Nz3yO&uniplatform=NZKPT

Ge, F., Liu, L., Yan, J., Kang, A., Zhu, S., Tian, Z., et al. (2021). *Influence of jinqiaomai pill combined with SASP on treating UC with dampness-heat in large intestine*, 37. Nanjing, China: Journal of Nanjing University of Traditional Chinese Medicine, 16 (1)–20. https://kns.cnki.net/kcms2/article/abstract?v=3uoqIhG8C44YLTlOAiTRKibYlV5Vjs7iy_Rpms2pqwbFRRUtoUImHdXb0YLgRehclWyfiCiFAKvqIeaItVyGYM9i1fkEfrsN&uniplatform=NZKPT

Gu, F., Huang, R., and Liu, Y. (2015). Effect of Fagopyri Dibotryis polysaccharide on immune function of immunocompromised mice induced by cyclophosphamide. *J. Chin. Med. Mater.* 38 (2), 370–372. doi:10.13863/j.issn1001-4454.2015.02.040

Guo, W. (2015). Clinical observation of lianhua-qingwen capsule joint with jingqiaomai tablet in treatment of influeza A (H1N1). *J. Chengdu Med. Coll.* 10 (3), 357–359. doi:10.3969/j.issn.1674-2257.2015.03.027

Han, J. (2020). Effect of Gubenkechuan tablet combined with Fagopyri Dibotryis Rhizoma tablet on symptom score and lung function in patients with chronic bronchitis. *Contemp. Med.* 26 (27), 170–171. doi:10.3969/j.issn.1009-4393.2020.27.073

Han, L., Yang, Q., Li, J., Cheng, F., Zhang, Y., Li, Y., et al. (2019). Protocatechuic acid-ameliorated endothelial oxidative stress through regulating acetylation level via CD36/AMPK pathway. *J. Agric. Food Chem.* 67 (25), 7060–7072. doi:10.1021/acs.jafc.9b02647

Han, L., Yang, Q., Ma, W., Li, J., Qu, L., and Wang, M. (2018). Protocatechuic acid ameliorated palmitic-acid-induced oxidative damage in endothelial cells through activating endogenous antioxidant enzymes via an adenosine-monophosphate-activated-protein-kinase-dependent pathway. *J. Agric. Food Chem.* 66 (40), 10400–10409. doi:10.1021/acs.jafc.8b03414

Hua, M., and Yin, Z. (2016). Clinical observation on the treatment of mild and moderate ulcerative colitis by oral administration of Fagopyri Dibotryis Rhizoma tablets combined with rectal drip of compound Kangfuxin solution. *J. Med. Theory Pract.* 29 (24), 3354–3356. doi:10.19381/j.issn.1001-7585.2016.24.025

Huang, G., Huang, M., Chen, W., Huang, Y., Yang, Z., and You, Y. (2009). Clinical study on the treatment of early diabetic nephropathy with Fagopyri dibotryis mixture. *J. Chin. Med. Mater.* 32 (12), 1932–1935. doi:10.13863/j.issn1001-4454.2009.12.011

Huang, J., Wang, L., Tang, B., Ren, R., Shi, T., Zhu, L., et al. (2022). Integrated transcriptomics and wide targeted metabolomics analyses provide insights into flavonoid biosynthesis in the rhizomes of golden buckwheat (fagopyrum cymosum). *Front. Plant Sci.* 20, 803472. doi:10.3389/fpls.2022.803472

Huang, R., and Yi, F. (2015). Bacteriostasis of epicatechin active substances from Buckwheat (-) *in vitro*. *Jiangsu Agric. Sci.* 43 (01), 308–310. doi:10.15889/j.issn.1002-1302.2015.01.103

Huang, R., Yi, F., He, H., Wu, S., Fang, J., and Yang, M. (2014). Antioxidant activity of (-)-Epicatechin from the root tubers of fagopyrum dibotrys. *Food Sci.* 35 (15), 118–121. doi:10.7506/spkx1002-6630-201415024

Huang, S., Wang, J., Chen, Q., and Huang, X. (2016). Study on the antioxidant effect of the active components of Fagopyri Dibotryis Rhizoma leaf tea. *Cereals & Oils* 29 (2), 30–32. https://kns.cnki.net/kcms2/article/abstract?v=3uoqIhG8C44YLTlOAiTRKibYlV5Vjs7ijP0rjQD-AVm8oHBO0FTadjrjgFLq8hawP0ZrsKTTc6ko7kCFohVL7vTz86B1tgYI&uniplatform=NZKPT

Huang, X., Wang, J., and Chen, Q. (2014). Golden buckwheat (Fagopyrum cymosum) leaf tea function and mechanism of resistance to type II diabetes. *Lishizhen Med. Materia Medica Res.* 25 (6), 1334–1337. doi:10.3969/j.issn.1008-0805.2014.06.020

Jia, W., Lu, J., Li, X., and Li, C. (2010). Effects of rhizoma fagopyrum dibotryis extraction on dysmenorrhea models in mouse. *J. LIAONING Univ. TRADITIONAL Chin. Med.* 12 (2), 198–199. doi:10.13194/j.jlunivtcm.2010.02.200.jiaw.069

Jiang, Y., Yang, W., and Gui, S. (2018). Procyanidin B2 protects rats from paraquat-induced acute lung injury by inhibiting NLRP3 inflammasome activation. *Immunobiology* 223 (10), 555–561. doi:10.1016/j.imbio.2018.07.001

Jing, R., Li, H. Q., Hu, C. L., Jiang, Y. P., Qin, L. P., and Zheng, C. J. (2016). Phytochemical and pharmacological profiles of three fagopyrum buckwheats. *Int. J. Mol. Sci.* 17, 589. doi:10.3390/ijms17040589

Kim, M. H., Kwon, S. Y., Woo, S. Y., Seo, W. D., and Kim, D. Y. (2021). Antioxidative effects of chrysoeriol via activation of the Nrf2 signaling pathway and modulation of mitochondrial function. *Molecules* 26, 313. doi:10.3390/molecules26020313

Li, H., Wen, D., Zhou, M., Wang, H., Peng, X., and Gao, L. (2019). Advances in extraction and mechanism of antitumor active components from Fagopyrum dibotrys. *Chin.*

J. Clin. Pharmacol. Ther. 24 (7), 833–840. https://kns.cnki.net/kcms2/article/abstract?v=3uoqIhG8C44YLTlOAiTRKibYlV5Vjs7iLik5jEcCI09uHa3oBxtWoDKPjZvajtk0U5H0I2RWOF3DfyjnCdAmn4dUKqJentv6&uniplatform=NZKPT

Li, J., Hossain, M. S., Ma, H., Yang, Q., Gong, X., Yang, P., et al. (2020). Comparative metabolomics reveals differences in flavonoid metabolites among different coloured buckwheat flowers. *J. Food Compos. Anal.* 85, 103335. doi:10.1016/j.jfca.2019.103335

Li, L. (2012). Treatment of 32 cases of acute bacillary dysentery with Fagopyri Dibotryis Rhizoma tablets combined with ceftriaxone sodium. *Guid. J. Traditional Chin. Med. Pharm.* 18 (3), 90. doi:10.13862/j.cnki.cn43-1446/r.2012.03.061

Li, L., and Wu, X. (2018). Clinical observation of jinqiaomai capsules combined with salmeterol xinafoate and fluticasone propionate powder for inhalation in treatment of bronchial asthma. *Drugs & Clin.* 33 (12), 3234–3237. doi:10.7501/j.issn.1674-5515.2018.12.034

Li, S. (2010). Observation on the curative effect of gold buckwheat tablet combined with cefoperazone in treating acute attack of chronic bronchitis. *J. Clin. Pulm. Med.* 15 (4), 466–467. https://kns.cnki.net/kcms2/article/abstract?v=3uoqIhG8C44YLTlOAiTRKgchrJ08w1e7_IFawAif0mxIaKhd5F2gn6ZFPc9juEyia0jox23Zn4iBpAhSuhp4ar1a_vqOp23F&uniplatform=NZKPT

Li, S., Kodama, E. N., Inoue, Y., Tani, H., Matsuura, Y., Zhang, J., et al. (2010). Procyanidin B1 purified from Cinnamomi cortex suppresses hepatitis C virus replication. *Antivir. Chem. Chemother.* 20 (6), 239–248. doi:10.3851/IMP1597

Li, X., Wu, J., Liu, Z., Zhu, H., and Zhang, Z. (2022). Clinical study on the treatment of acute exacerbation of chronic ObstructivePulmonary disease with jinqiaomai tablets combined with tiotropium BromidePowder for inhalation. *Chin. J. Ration. Drug Use* 19 (04), 59–64. doi:10.3969/j.issn.2096-3327.2022.04.011

Li, Y., Cheng, Z., Wang, K., Zhu, X., Ali, Y., Shu, W., et al. (2021). Procyanidin B2 and rutin in Ginkgo biloba extracts protect human retinal pigment epithelial (RPE) cells from oxidative stress by modulating Nrf2 and Erk1/2 signalling. *Exp. Eye Res.* 207, 108586. doi:10.1016/j.exer.2021.108586

Li, B, B., Feng, F., Jia, H., Jiang, Q., Cao, S., Wei, L., et al. (2021). Rhamnetin decelerates the elimination and enhances the antitumor effect of the molecular-targeting agent sorafenib in hepatocellular carcinoma cells via the miR-148a/PXR axis. *Food Funct.* 12 (6), 2404–2417. doi:10.1039/d0fo02270e

Lin, J., Zhao, L., Guo, J., Liu, L., Kuang, Y., and Yang, S. (2016). Chemical constituents from aerial parts of cagopyrum dibotrys. *Chin. Traditional Herb. Drugs* 46 (11), 1841–1844. doi:10.7501/j.issn.0253-2670.2016.11.005

Lin, Y., Luo, T., Weng, A., Huang, X., Yao, Y., Fu, Z., et al. (2020). Gallic acid alleviates gouty arthritis by inhibiting NLRP3 inflammasome activation and pyroptosis through enhancing Nrf2 signaling. *Immunol* 11, 580593. doi:10.3389/fimmu.2020.580593

Liu, L., Sun, Z., Zhang, X., Zhou, L., Tian, C., Chen, L., et al. (2012a). Analgesic mechanisms of Fagopyrum cymosum extracts in rats with irritable bowel syndrome. *World Chin. J. Dig.* 20 (15), 1290–1295. https://kns.cnki.net/kcms2/article/abstract?v=3uoqIhG8C44YLTlOAiTRKgchrJ08w1e7fm4X_1ttJAmcliuAXHuQoTp9KWtxk6uq-JqpQKMnByXyHvO9qN9HXmCaMwsp_uWK&uniplatform=NZKPT

Liu, L., Yan, J., Lu, W., Chen, G., Lu, Y., and Sun, Z. (2016). Effects of Fagopyrum cymosum extracts on visceral hyperalgesia of IBS rats and themechanism. *West China J. Pharm. Sci.* 31 (2), 135–138. doi:10.13375/j.cnki.wcjps.2016.02.008

Liu, L., Zhou, L., Tian, C., Chen, L., Guo, H., and Sun, Z. (2012b). Improvement of IBS rats'hyperalgesia by total flavones of Fagopyrum cymosum via down - regulation of NR2B expression. *Chin. Pharmacol. Bull.* 28 (9), 1289–1293. doi:10.3969/j.issn.1001-1978.2012.09.024

Liu, S., Tian, L., and Chen, L. (1998). Research progress of buckwheat aureus. *Prim. J. Chin. Mater Med.* 3, 46–47. doi:10.13728/j.1673-6427.1998.03.035

Liu, Y., Fang, Q., Zhang, X., Feng, X., Zhang, L., and He, X. (1983). Study on active components of Fagopyri dibotryis rhizoma. *Acta Pharm. Sin.* 18 (7), 545–547. doi:10.16438/j.0513-4870.1983.07.013

Lou, J., Lin, H., Qiu, Q., Pei, Y., Qi, X., and He, X. (2004b). Experimental study on the antitumor effect of Weimining *in vitro*. *Chin. Archives Traditional Chin. Med.* 22 (5), 810–811. doi:10.13193/j.archtcm.2004.05.39.loujl.025

Lou, J., Lin, H., Qiu, Q., Pei, Y., Qi, X., and He, X. (2004a). The molecular mechanism of inhibition of murine Lewis lung carcinoma metastasis by weimaining *in vivo*. *Chin. J. Pathophysiol.* 20 (4), 627–631. https://kns.cnki.net/kcms2/article/abstract?v=3uoqIhG8C44YLTlOAiTRKgchrJ08w1e7eeyE9jLkqq9HoZSVvnrpXjWT2L1a8vL_JroqhLyR_wAc82w9iKit0cGTyG5xf3mW&uniplatform=NZKPT

Lou, J., Qiu, Q., Lin, H., Pei, Y., Qi, X., Wu, X., et al. (2007). *Effect of Weimaining on adhesion between PG cell and human umbilical vein endothelial cells*, 30. Beijing, China: Journal of Beijing University of Traditional Chinese Medicine, 29–31.1. https://kns.cnki.net/kcms/detail/detail.aspx?FileName=JZYB200701009&DbName=CJFQ2007

Mackenzie, G. G., Adamo, A. M., Decker, N. P., and Oteiza, P. I. (2008). Dimeric procyanidin B2 inhibits constitutively active NF-kappaB in Hodgkin's lymphoma cells independently of the presence of IkappaB mutations. *Biochem. Pharmacol.* 75 (7), 1461–1471. doi:10.1016/j.bcp.2007.12.013

Milenkovic, D., Declerck, K., Guttman, Y., Kerem, Z., Claude, S., Weseler, A. R., et al. (2020). (-)-Epicatechin metabolites promote vascular health through epigenetic reprogramming of endothelial-immune cell signaling and reversing systemic low-grade inflammation. *Biochem. Pharmacol.* 173, 113699. doi:10.1016/j.bcp.2019.113699

Nam, Y. J., and Lee, C. S. (2018). Protocatechuic acid inhibits Toll-like receptor-4-dependent activation of NF-κB by suppressing activation of the Akt, mTOR, JNK and p38-MAPK. *Int. Immunopharmacol.* 55, 272–281. doi:10.1016/j.intimp.2017.12.024

Othman, R., Ibrahim, H., Mohd, M. A., Awang, K., Gilani, A. U., and Mustafa, M. R. (2002). Vasorelaxant effects of ethyl cinnamate isolated from Kaempferia galanga on smooth muscles of the rat aorta. *Planta Med.* 68 (7), 655–657. doi:10.1055/s-2002-32900

Pan, C., and Wan, J. (2015). *Study on analgesic and anti - inflammatory effects of Fagopyri Dibotryis Rhizoma medicinal liquor*, 22. Hezhou, China: Journal of Ezhou University, 110–112. https://kns.cnki.net/kcms/detail/detail.aspx?FileName=EZDX201509034&DbName=CJFQ2015

Pan, C., Wang, W., Qi, X., Yang, J., and Zhou, X. (2018). Anti-proliferative and apoptosis-inducing activity of rhizoma Fagopyri cymosi extract in cervical cancer hela cells. *Pharmacol. Clin. Chin. Materia Medica* 34 (5), 96–100. doi:10.13412/j.cnki.zyyl.2018.05.023

Pan, C., Wang, W., Wan, J., Ji, D., and Qing, L. (2019). Effects of Fagopyri Dibotryis Rhizoma extract on caspase-1 39 and MMP-1 of articular cartilage in rabbits with knee osteoarthritis. *Chin. J. Gerontology* 39 (20), 5066–5069. https://kns.cnki.net/kcms/detail/detail.aspx?FileName=ZLXZ201920059&DbName=CJFQ2019

Pan, C., Yang, J., Ji, D., and Wan, J. (2020). *Effect of Fagopyri Dibotryis Rhizoma extract on oxygen free radical in rat model of knee osteoarthritis*, 27. Hezhou, China: Journal of Ezhou University, 106–108.5. doi:10.16732/j.cnki.jeu.2020.05.033

Peng, Y., Sun, Z., and Xiao, P. (1996). Research and development of fagopyrum dibotrys (D.don) Hara. *Chin. Traditional Herb. Drugs* 27 (10), 629–631. https://kns.cnki.net/kcms2/article/abstract?v=3uoqIhG8C44YLTlOAiTRKjkpgKvIT9NkZNmQNo4kSVpbdjw7UNKfQ-1kzAb7Yq9-LI70Ck2x-j41l-1716-RaQuMuOwJRw0r&uniplatform=NZKPT

Pereyra-Vergara, F., Olivares-Corichi, I. M., Perez-Ruiz, A. G., Luna-Arias, J. P., and García-Sánchez, J. R. (2020). Apoptosis induced by (-)-Epicatechin in human breast cancer cells is mediated by reactive oxygen species. *Molecules*. 25. 1020. doi:10.3390/molecules25051020

Qiao, H., Li, C., and Wang, G. (2010). Serum pharmacological study on the effect of Rhizoma Fagopyri dibotryis root extract on th1-like lymphofactor mRNA expression in chicken. *Heilongjiang Animal Sci. Veterinary Med.* 22, 130–132. doi:10.13881/j.cnki.hljxmsy.2010.09.056

Ríos, J. L., and Recio, M. C. (2005). Medicinal plants and antimicrobial activity. *J. Ethnopharmacol.* 100 (1-2), 80–84. doi:10.1016/j.jep.2005.04.025

Ruan, H., Ji, T., Ji, W., Ma, S., and Zhang, Z. (2017). Effects of flavonoids from Fagopyri dibotryis rhizoma on the glycolipidmetabolism and antioxidation in type 2 diabetic rats. *Pharmacol. Clin. Chin. Materia Medica* 33 (5), 73–76. doi:10.13412/j.cnki.zyyl.2017.05.020

Ruan, H., and Mu, J. (2017). Effect of epicatechin on inflammatory cytokines in LPS-induced RAW264.7 cell. *Chin. J. Exp. Traditional Med. Formulae* 32, 159–163. doi:10.13422/j.cnki.syfjx.2017040159

Shao, M., Yang, Y., Gao, H., Wu, B., Wang, L., and Wu, L. (2004). Phenolic acid derivatives from the rhizome of Fagopyrum cymosum. *China J. Chin. Materia Medica* 30 (20), 1591–1593. https://kns.cnki.net/kcms2/article/abstract?v=3uoqIhG8C44YLTlOAiTRKgchrJ08w1e7F1IFNsBV5UtgR4AbwGdxZneHv9jhpZXpwlxY5V9dwWzUOIEEAGjbNxYbpvhbVpSv&uniplatform=NZKPT

Shao, M., Yang, Y., Gao, H., Wu, B., Wang, L., and Wu, L. (2005). *Study on chemical constituents of Fagopyri Dibotryis rhizoma*, 22. Shenyang, China: Journal of Shenyang Pharmaceutical University, 1006–2858.2. https://kns.cnki.net/kcms2/article/abstract?v=3uoqIhG8C44YLTlOAiTRKgchrJ08w1e7F1IFNsBV5Uu2KAJBLaRynTuLXOBKO2uWV2l-Png5drI8NNUUNdDGqNb1fp3Tyg3A&uniplatform=NZKPT

Shen, L. (2013). *The anti-rheumatoid arthritis activity of Fagopyrum cymosum and its mechanism study*. Wuhan, China: Huazhong University Of Science And Technology. https://kns.cnki.net/kcms/detail/detail.aspx?FileName=1014025348.nh&DbName=CDFD2014

Shen, Y., Bian, Z., and Shao, J. (2019). Effect of fagopyrum cymosum tablets on the level of inflammatory factor in DSS-induced inflammation model mice. *Acta Chin. Med.* 34 (9), 1916–1920. doi:10.16368/j.issn.1674-8999.2019.09.448

Song, H., Li, L., and Zhang, J. (2020). Effect of Fagopyri Dibotryis Rhizoma extract on apoptosis of renal carcinoma cells regulated by DDIT4. *Chin. J. Integr. Traditional West. Nephrol.* 21 (8), 708–711. https://kns.cnki.net/kcms/detail/detail.aspx?FileName=JXSB202008020&DbName=CJFQ2020

Song, J. H., Lee, H. J., and Kang, K. S. (2019). Procyanidin C1 activates the Nrf2/HO-1 signaling pathway to prevent glutamate-induced apoptotic HT22 cell death. *Int. J. Mol. Sci.* 20, 142. doi:10.3390/ijms20010142

Tan, Y., Gan, M., Fan, Y., Wang, J., Zhang, X., Huang, B., et al. (2020). Protective effects of Fagopyri dibotryis on lipopolysaccharide - induced intestinal inflammation in mice. *China Animal Husb. Veterinary Med.* 47 (2), 597–604. doi:10.16431/j.cnki.1671-7236.2020.02.032

Tang, Y., Gao, X., Jiang, F., Guo, S., You, J., Zhu, J., et al. (2014). Effect of extract of fagopyrum dibotrys on serum cytokines and pulmonary histopathological changes in chronic obstructive pulmonary disease rats. *Traditional Chin. Drug Res. Clin. Pharmacol.* 25 (6), 679–683. doi:10.3969/j.issn.1003-9783.2014.06.008

Tang, Y., Gao, X., Jiang, F., Guo, S., Su, C., and Hou, H. (2016). Effect of the Wild Buckwheat Rhizome Extract on the serum inflammatory cytokines and the expression of NF-κB in chronic obstructive pulmonary disease model of rats. *Mod. J. Integr. Traditional Chin. West. Med.* 25 (15), 1600–1603. doi:10.3969/j.issn.1008-8849.2016.15.002

Tang, Y., Jia, H., Sun, J., Zhong, Z., and Shao, J. (2014). Study on active components and content change of Fagopyri Dibotryis Rhizoma. *Hubei Agric. Sci.* 53 (3), 672–675. doi:10.14088/j.cnki.issn0439-8114.2014.03.010

Tian, L., Xu, L., and Shilin, Y. (1997). Study on Chemical constituents of the aboveground part of Buckwheat. *China J. Chin. Materia Medica* 22 (12), 100–102.

Wang, D., and Bao, B. (2020). Gallic acid impedes non-small cell lung cancer progression via suppression of EGFR-dependent CARM1-PELP1 complex. *Drug Des. Devel Ther.* 14, 1583–1592. doi:10.2147/DDDT.S228123

Wang, H., Tang, C., and Yue, H. (2013). Studies on antibacterial function of superfine powder fagopyrum dibotryis *in vivo* in mice. *Prog. Veterinary Med.* 34 (10), 130–132. doi:10.16437/j.cnki.1007-5038.2013.10.029

Wang, H. Y., Wang, H., Wang, J. H., Wang, Q., Ma, Q. F., and Chen, Y. Y. (2015). Protocatechuic acid inhibits inflammatory responses in LPS-stimulated BV2 microglia via NF-κB and MAPKs signaling pathways. *Neurochem. Res.* 40 (8), 1655–1660. doi:10.1007/s11064-015-1646-6

Wang, K. J., Zhang, Y. J., and Yang, C. R. (2005). Antioxidant phenolic constituents from Fagopyrum dibotrys. *J. Ethnopharmacol.* 99 (2), 259–264. doi:10.1016/j.jep.2005.02.029

Wang, M., Wu, Y., and Li, W. (2021). Rhamnetin ameliorates macrophage-mediated inflammation and pro-atherosclerosis pathways in apolipoprotein E-deficient mice. *J. Physiol. Pharmacol.* 72, 10. doi:10.26402/jpp.2021.2.10

Wang, P., Wang, Y., and Fang, Y. (2017). Study on anti-oxidantion activity of the total flavone extract from fagopyrum dibotrys(D.Don)Hara. *Anhui Agric. Sci. Bull.* 23 (8), 23–24. doi:10.16377/j.cnki.issn1007-7731.2017.08.011

Wang, Z., Zhan, Y., Xu, J., Wang, Y., Sun, M., Chen, J., et al. (2020). β-Sitosterol reverses multidrug resistance via BCRP suppression by inhibiting the p53-MDM2 interaction in colorectal cancer. *J. Agric. Food Chem.* 68 (12), 3850–3858. doi:10.1021/acs.jafc.0c00107

Wang, X, X., Song, Z. J., He, X., Zhang, R. Q., Zhang, C. F., Li, F., et al. (2015). Antitumor and immunomodulatory activity of genkwanin on colorectal cancer in the APC(Min/+) mice. *Int. Immunopharmacol.* 29 (2), 701–707. doi:10.1016/j.intimp.2015.09.006

Wei, W., Sun, J., and Shuai, X. (2022). Effect of Jinqiaomai Capsules on the pulmonary ventilation function and the EOSlgE levels in the patients with mild to moderate asthma during its acute attack. *Jilin J. Traditional Chin. Med.* 41 (06), 751–754. doi:10.13463/j.cnki.jlzyy.2021.06.015

Wu, H., Zhou, J., and Pan, H. (2008). Study on chemical constituents of fagopyrumdibotrys (D.don) Hara. *Chin. J. Hosp. Pharm.* 28 (21), 1829–1831. https://kns.cnki.net/kcms2/article/abstract?v=3uoqIhG8C44YLTlOAiTRKgchrJ08w1e7VSL-HJEdEx3onS7wCSmyabHM2q82d4k-b7YwTR-EwQ9tBXiWUQc2MXh-MfrFedt2&uniplatform=NZKPT

Xiao, Y., Dong, J., Yin, Z., Wu, Q., Zhou, Y., and Zhou, X. (2018). Procyanidin B2 protects against d-galactose-induced mimetic aging in mice: Metabolites and microbiome analysis. *Food Chem. Toxicol.* 119, 141–149. doi:10.1016/j.fct.2018.05.017

Yan, J. (2006). *Study on Chemical constituents & HPLC fingerprint of buckwheat*. Shenyang, China: Shenyang Pharmaceutical University. https://kns.cnki.net/kcms2/article/abstract?v=3uoqIhG8C475KOm_zrgu4lQARvep2SAk6X_k1IQGNCLwAgnuJ-hC0_lcpntt3h-DHUcgEmqBCCkz8iejljMj5jLDULva8NQD&uniplatform=NZKPT

Yan, J., Wang, L., Li, W., Gao, H., and Wu, L. (2006). Study on bacteriostasis of fagopyrum dibotrys (D.don) Hara. *Mod. Chin. Med.* 8 (6), 21–23. doi:10.13313/j.issn.1673-4890.2006.06.008

Yang, T., Rong, Z., and Wu, Y. (1992). Effect of Fagopyri Dibotryis Rhizoma E on phagocytosis of reticuloendothelial system in mice. *Sichuan J. Physiological Sci.* 22, 9–12. https://kns.cnki.net/kcms2/article/abstract?v=3uoqIhG8C44YLTlOAiTRKjkpgKvIT9NkyGkCpOZCCaeYi10YmvBDhlGCMGoEFfVYjcBPb-oTRtrumQOj7cHoS2uvLlFeYB_6&uniplatform=NZKPT

Yang, X., Zhang, Y., and Li, L. (2019). Advances in studies on medicinal plant of fagopyrum dibotrys. *Mod. Chin. Med.* 21 (6), 837–846. doi:10.13313/j.issn.1673-4890.20180709003

Yin, D., and Lin, S. (1999). Effect of Fagopyri Dibotryis Rhizoma on phagocytic function of mouse peritoneal macrophages. *Cap. Med.* 6 (12), 28–29. https://kns.cnki.net/kcms2/article/abstract?v=3uoqIhG8C44YLTlOAiTRKjkpgKvIT9Nkm5tS6uBYqSGHbvWnFosSPHb_Qf7ezhOT0DOH1YfuehruJzt_RqjoCUwV1AidIvYZ&uniplatform=NZKPT

Yoon, H. S., and Park, C. M. (2021). Chrysoeriol ameliorates COX-2 expression through NF-κB, AP-1 and MAPK regulation via the TLR4/MyD88 signaling pathway in LPS-stimulated murine macrophages. *Exp. Ther. Med.* 22 (1), 718. doi:10.3892/etm.2021.10150

Yu, J. (2014). Effect of Fagopyri Dibotryis Rhizoma tablet combined with levofloxacin on acute bacillary dysentery. *Chin. Foreign Med. Res.* 12 (10), 49–50. doi:10.14033/j.cnki.cfmr.2014.10.039

Zhang, C., Chen, R., Yin, Y., and Wang, Z. (2011). Isolation and identification of endophytic fungi with antimicrobial activity from Fagopyrum dibotrys. *Microbiol. China* 38 (1), 70–77. doi:10.13344/j.microbiol.china.2011.01.016

Zhang, F., Liu, Z., He, X., Li, Z., Shi, B., and Cai, F. (2020). β-Sitosterol-loaded solid lipid nanoparticles ameliorate complete freund's adjuvant-induced arthritis in rats: Involvement of NF-κB and HO-1/Nrf-2 pathway. *Drug Deliv.* 27 (1), 1329–1341. doi:10.1080/10717544.2020.1818883

Zhang, H., and Li, L. (2019). Clinical study on Jinqiaomai Tablets combined with cefdinir in treatment of acute bacterial dysentery. *Drugs & Clin.* 34 (02), 499–503. doi:10.7501/j.issn.1674-5515.2019.02.050

Zhang, H., Li, S., Cui, J., and Zhao, T. (2010). Effects of extract from rosa roxburghir tratt or extract of fagopyrum cymosum meissn on cell prolife. *J. Oncol.* 16 (01), 35–39. https://kns.cnki.net/kcms2/article/abstract?v=3uoqIhG8C44YLTlOAiTRKgchrJ08w1e7_IFawAif0mz-Ilz_uHmWlNMTZhzl0zx7_vOJm9bBco2au0067CUXs1uK2se5uYba&uniplatform=NZKPT

Zhang, J., Kuang, Y., Liu, L., Yang, S., and Zhao, C. (2016). Chemical constituents from root tubers of Fagopyrum dibotrys. *Chin. Traditional Herb. Drugs* 47 (5), 722–725. doi:10.7501/j.issn.0253-2670.2016.05.005

Zhang, R., Yu, Q., Lu, W., Shen, J., Zhou, D., Wang, Y., et al. (2019). Grape seed procyanidin B2 promotes the autophagy and apoptosis in colorectal cancer cells via regulating PI3K/Akt signaling pathway. *OncoTargets Ther.* 12, 4109–4118. doi:10.2147/OTT.S195615

Zhang, W., Li, X., Liu, Y., Yao, R., Nonaka, G., and Yang, C. (1994). Phenolic constituents from fagopyrum dibotrys. *Acta Bot. Yunnanica* 16 (4), 354–356. https://kns.cnki.net/kcms2/article/abstract?v=3uoqIhG8C44YLTlOAiTRKjkpgKvIT9NkGsvn6cq9Bo0GTEcJPCg6sx7krNckKfvPcY49x34luPbmxOqhjwEttn-fvNXzSoTZ&uniplatform=NZKPT

Zhao, J., Jiang, L., Tang, X., Peng, L., Li, X., Zhao, G., et al. (2018). Chemical composition, antimicrobial and antioxidant activities of the flower volatile oils of fagopyrum esculentum. *Fagopyrum tataricum Fagopyrum Cymosum. Mol.* 23, 182. doi:10.3390/molecules23010182

Zhao, L., Zhang, X., and Zhang, C. (2011). Fractionation and identification of ethyl ecetate extract from rhizoma Fagopyri cymosi. *Food Sci.* 32 (19), 16–22. https://kns.cnki.net/kcms/detail/detail.aspx?FileName=SPKX201119005&DbName=CJFQ2011

Zhao, Y., Liu, Y., Xie, S., and Wu, Q. (2019). Study on the anti-influenza virus of extracts from fagopyrum dibotrys(D. Don) Hara *in vitro*. *Chin. J. Mod. Appl. Pharm.* 36 (21), 2648–2651. doi:10.16368/j.issn.1674-8999.2019.09.448

Zhou, Y., Qiao, H., Li, C., and Wang, G. (2009). Study on antibacterial activity of Fagopyri dibotryis rhizoma extract *in vitro*. *J. Traditional Chin. Veterinary Med.* 28 (5), 44–46. doi:10.13823/j.cnki.jtcvm.2009.05.045

frontiers | Frontiers in Pharmacology

TYPE Review
PUBLISHED 16 March 2023
DOI 10.3389/fphar.2023.1090526

OPEN ACCESS

EDITED BY
Uraiwan Panich,
Mahidol University, Thailand

REVIEWED BY
Thomas Heinbockel,
Howard University, United States
Shuang Zhang,
Hefei University of Technology, China

*CORRESPONDENCE
Jianxia Wen,
wenjx32@163.com
Junjie Hao,
2005102238@163.com

SPECIALTY SECTION
This article was submitted to Ethnopharmacology, a section of the journal Frontiers in Pharmacology

RECEIVED 05 November 2022
ACCEPTED 06 March 2023
PUBLISHED 16 March 2023

CITATION
Wen J, Yang Y and Hao J (2023), *Acori Tatarinowii* Rhizoma: A comprehensive review of its chemical composition, pharmacology, pharmacokinetics and toxicity.
Front. Pharmacol. 14:1090526.
doi: 10.3389/fphar.2023.1090526

Acori Tatarinowii Rhizoma: A comprehensive review of its chemical composition, pharmacology, pharmacokinetics and toxicity

Jianxia Wen[1]*, Yi Yang[1] and Junjie Hao[2]*

[1]School of Food and Bioengineering, Food Microbiology Key Laboratory of Sichuan Province, Xihua University, Chengdu, China, [2]College of Pharmaceutical Science, Yunnan University of Chinese Medicine, Kunming, China

Acori Tatarinowii Rhizoma (ATR, *Shi Chang Pu* in Chinese), a natural product with multiple targets in various diseases. This review provides the comprehensive summary of the chemical composition, pharmacological effects, pharmacokinetics parameters and toxicity of ATR. The results indicated that ATR possesses a wide spectrum of chemical composition, including volatile oil, terpenoids, organic acids, flavonoids, amino acids, lignin, carbohydrates and so on. Accumulating evidence from various studies has shown that ATR exerts a wide range of pharmacological properties, including protecting nerve cells, alleviating learning and memory impairment, anti-ischemic, anti-myocardial ischemia, anti-arrhythmic, anti-tumor, anti-bacterial, and anti-oxidant activities. Currently, ATR is widely used in the central nervous system, cardiovascular system, gastrointestinal digestive system, respiratory system in China, and for the treatment of epilepsy, depression, amnesia, consciousness, anxiety, insomnia, aphasia, tinnitus, cancers, dementia, stroke, skin diseases, and other complex diseases. Pharmacokinetic studies indicated that β-asarone, α-asarone, *cis*-methylisoeugenol, and asarylaldehyde, the active components of ATR, were absorbed slowly after oral administration of ATR. Moreover, toxicity studies have suggested that ATR has no carcinogenic, teratogenic and mutagenic toxicity. Nevertheless, long term or high-dose toxicity testing in animals to explore the acute and chronic toxicity of *acori Tatarinowii* Rhizoma is still lacking. In view of good pharmacological activities, ATR is expected to be a potential drug candidate for the treatment of Alzheimer's disease, depression, or ulcerative colitis. However, further studies are needed to elucidate its chemical composition, pharmacological effects, molecular mechanisms and targets, improve its oral bioavailability, and clarify its potential toxicity.

KEYWORDS

Acori tatarinowii rhizoma, chemical composition, pharmacology, pharmacokinetics, toxicity, review

Introduction

Acori Tatarinowii Rhizoma (ATR, *Shi Chang Pu* in Chinese) is the dried rhizome of *Acorus tatarinowii* Schott., a perennial herb of the Araceae Juss (Yan et al., 2020b). It is first recorded in the classic works of traditional Chinese medicine "Shen Nong's Materia Medica," and is listed as a top grade. The effects of ATR are mainly to resuscitate, calm the mind, resolve *shi* (dampness) and harmonize the *wei* (stomach) (Lam et al., 2016b). Clinically, ATR is widely used for neurological disorders, cardiovascular system, gastrointestinal digestive system, respiratory system in China (Lam et al., 2016b; Li et al., 2018a), and for the treatment of epilepsy, depression, amnesia, consciousness, anxiety, insomnia, aphasia, tinnitus, cancers, dementia, stroke, skin diseases, and other complex diseases (Lee et al., 2004; Liu et al., 2013; Lam et al., 2019; Li J. et al., 2021). In recent years, its pharmacological research has shown that ATR has a variety of pharmacological effects, including anti-epileptic, sedative, hypnotic, anti-convulsant, anti-tussive, anti-asthmatic, anti-oxidant, anti-tumor and so on (Wu et al., 2015; Lam et al., 2017a; Fu et al., 2020; Shi et al., 2020; Zhang W. et al., 2022). Previous studies indicated that ATR is promising as a potential drug candidate for the treatment of Alzheimer's disease (AD), depression, or ulcerative colitis. In view of the exact clinical efficacy of ATR and the continuous discovery of new pharmacological activities and active ingredients, it has been widely concerned worldwide in recent years and has become one of the hot researched Chinese medicine varieties in the medical field.

The chemical composition and pharmacological effects of ATR have been extensively reported over the past few decades, and its pharmacokinetics and toxicity have also been studied in varying degrees. However, most of the previous reports are scattered, lacking systematic summary and induction of ATR. Therefore, this review aims to provide a comprehensive summary and discussion of its chemical composition, pharmacology, pharmacokinetics and toxicity characteristics, thereby contributing to the further clinical practice and application of ATR.

Chemical composition of ATR

The chemical composition of ATR are mainly volatile components and non-volatile components. The ATR essential oil (ATEO) is considered to be the active component of ATR, and the content of ATEO is the only indicator for the determination of ATR content. At present, there are various researches on volatile parts and relatively less research on non-volatile parts. The volatile components are relatively complex, and the main structural types are phenylpropanoids (simple phenylpropanoids, lignans and coumarins) and terpenoids (monoterpenes, sesquiterpenes, diterpenoids and triterpenes). Non-volatile components are mainly alkaloids, aldehydes and acids, quinones and ketones, sterols, amino acids, and carbohydrates. The results of the ATR chemical composition study will contribute to the development of its quality research.

Volatile composition

Researchers used analytical testing techniques such as chromatography and GC-MS to analyze the chemical components of ATR from different origins, different batches, different extraction methods and different parts. Previous studies indicated that the main chemical constituents in ATR were volatile oils, which are the important indicator for quality evaluation of ATR. α-Asarone and β-asarone accounted for 95% of ATR volatile oils and were identified as characteristic components (Figure 1) (Lam et al., 2016a). The "Pharmacopoeia of The People's Republic of China" (2020 Edition) records that the volatile oil content of ATR should not be less than 1.0% (mL/g). Currently, multiple kinds of volatile oil components were found in ATR (Table 1).

Non-volatile components

Most of the non-volatile components of ATR are in its aqueous extraction and organic solvent extraction parts, and the *n*-butanol fraction of the ethanol extract can be separated and purified to obtain alkaloids, phenylpropanoid derivatives, and furan compounds, pyrone compounds, organic acid compounds and diterpene glycoside compounds (Dong et al., 2008; Yang et al., 2021). This study summarizes the terpenoids, organic acids, and flavonoids components in ATR. Among them, the terpenoids in ATR include shyobunone, acoronene, cycloartenol, lupeol, and daucosterol (Table 2). The organic acids in ATR include fumaric acid, benzoic acid, nicotinic acid, 4-hydroxybenzoic acid, protocatechuic acid, vanillic acid, suberic acid, caffeic acid. (Table 3). The flavonoids in ATR include astragalin, rhodionin, rhoifolin, kaempferol-3-rutinoside (Table 4).

In addition to the above components, ATR also contains amino acids, lignin, carbohydrates and other chemical components. Among the amino acids, both human essential amino acids, and human semi-essential amino acids are contained. In addition, ATR also contains glucose and trace elements, alkaloids, etc. (Hu et al., 2019). The lignan components include bergapten, marmesin, eudesmin and so on. Its carbohydrate components are mainly glucose, maltose, fructose and mannose (Shi et al., 2021). Zhang et al., focused on large molecular components such as polysaccharides in ATR, speculating that the immune activity of ATR may be related to active polysaccharide components. In their study, DEAE-52 cellulose and Sephadex G-100 column chromatography were used to separate and purify polysaccharide from water chestnut base extracted polysaccharide. The eluent with absorbance greater than 0.3 in polysaccharide is collected and freeze-dried, and is named RATAPW. The average molecular weight of RATAPW was 2.51×10^4 Da, and the total carbohydrate content of RATAPW was 98.23% ± 0.29%. Monosaccharide composition, methylation and nuclear magnetic resonance (NMR) analysis showed that the polysaccharide was α-1,4-glucan with short α-1,6 branches (Zhang Y. et al., 2022).

Pharmacological effects of ATR

Effects on the central nervous system

The regulation of ATR on the central nervous system is particularly significant and has a bidirectional regulatory effect. Modern research shows that ATR and its active components

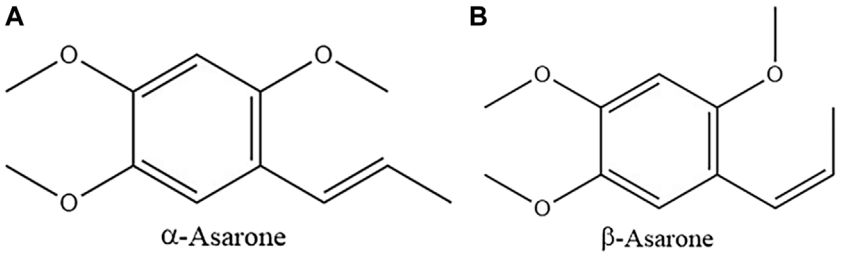

FIGURE 1
The chemical structure of α-asarone (PubChem CID: 636822) **(A)**, and β-asarone (PubChem CID: 5281758) **(B)**.

α-asarone and β-asarone have effects on calming the nerves, anti-epileptic, anti-depression, anti-AD, anti-convulsant, and anti-dementia (Yang et al., 2021). Moreover, ATR and its active components also have a good protective effect on brain tissue and nerve cells, and can improve the permeability of the blood-brain barrier (BBB), promote the entry of other substances into the brain tissue through the BBB, and improve the blood concentration and bioavailability of drugs in the brain tissue (Jiang et al., 2018). The high safety and obvious curative effect of ATR in the treatment of central nervous system disease make it have a good development and application prospect. However, studies also showed that α-asarone and β-asarone could shrink the endothelial cells and loosen the tight connection, thus increasing the permeability of the BBB and assisting the drug to enter the brain tissue, which is in contradiction with the above research mechanism (Huang et al., 2016). Thus, whether asarone has protective effect on BBB needs further research to confirm.

Protective effect on nerve cells

α-Asarone and β-asarone are considered to be the main active components of ATR as a Chinese herbal medicine, and both can be potential candidates for drug development in neurodegenerative diseases. Lam et al., found that when performed to cultured rat astrocytes, ATR volatile oil, α-asarone and β-asarone could dose-dependently stimulate the expression and secretion of neurotrophic factor, namely, nerve growth factor (NGF), brain-derived neurotrophic factor (BDNF) and glial-derived neurotrophic factor (GDNF) in cultured PC12 cells (Lam et al., 2016a; Lam et al., 2017a; Lam et al., 2019). In addition, β-asarone could protect PC12 cells from amyloid beta (Aβ)-induced damage and regulates the expression of autophagy factors. Simultaneously, the cytoprotective effects of ATR oil, α-asarone and β-asarone on tert-butyl hydroperoxide (tBHP)-induced astrocyte injury were also revealed, which reduced tBHP-induced accumulation of reactive oxygen species (ROS) in astrocytes. Moreover, the activity of the transfected anti-oxidant response element (ARE) promoter construct (pARE-Luc) and the mRNAs encoding anti-oxidant enzymes were regulated by ATR oil and asarones, whose gene expression may be mediated by Akt phosphorylation (Lam et al., 2017a; Lam et al., 2017b). Moreover, ATR volatile oil, α-asarone, or β-asarone induces the transcriptional activation of neurofilament promoters and potentiates NGF-induced neurite outgrowth and neurofilament expression. Mechanism research found ATR volatile oil, α-asarone or β-asarone, induces phosphorylation of cAMP-response element binding protein (CREB) and cAMP-mediated transcriptional activity. Above all, α-asarone and β-asarone synergistically increase transcriptional activation of neurofilament promoters (Lam et al., 2016a). α-Asarone and β-asarone, as the main active ingredient in volatile oil, play a wide and important pharmacological role protecting nerve cells. Asarones or ATR volatile oil promoting axons might help to find potential agents for treating various neurodegenerative diseases.

β-Asarone could improve the degree of cerebral edema in rats with ischemia-reperfusion injury, and it have effects on reducing oxidative stress injury, inhibiting brain cell apoptosis, regulating amino acid levels and excitatory amino acid toxicity (Huang et al., 2020). Furthermore, it could increase the expression levels of Glutamic acid, Aspartic acid, and gamma-aminobutyric acid, and improve cerebral ischemia tolerance (Ke and Fang, 2003), thereby reducing the damage to neurons caused by the above substances during cerebral ischemia-reperfusion, thus playing a role in brain protection. Li et al., established a PC12 cell line with APPswe-overexpressing as a cellular model of Aβ-induced injury and assessed autophagic flux-related proteins as well as the number and morphology of autophagosomes and autolysosomes (Li Z. et al., 2021). The results indicated that β-asarone could reduce the expression levels of Beclin-1, p62, LC3-II, and $A\beta_{1\text{-}42}$. β-Asarone decreased the number of autophagosomes and increased the number of autolysosomes. Studies have shown that β-asarone can protect PC12 cells from Aβ-induced damage by promoting autophagic flux, which can be achieved by enhancing autophagosome-lysosome fusion and/or lysosomal function. In addition, the essential oil is also considered as the active fraction of ATR. To investigate the anti-oxidative stress effects of ATEO, a H_2O_2-stressed neuronal cell model was established by Yan et al.,. ATEO treatment increased the viability of cells affected by H_2O_2-mediated injury, inhibited the accumulation of ROS, and induced the expression of several anti-oxidant proteins (SOD, GPx, and UCPs). It was suggested that ATEO may effectively prevent H_2O_2-induced cell damage by activating CREB/peroxisome proliferator-activated receptor gamma coactivator 1-alpha (PGC-1α) signaling in PC12 cells and exerting an anti-oxidative stress effect (Yan et al., 2020b). In addition, the ATR polysaccharides could protect PC12 cells from H_2O_2-induced injury, which could substantially stimulate nitric oxide (NO) production and phagocytic activity in RAW264.7, and promoted splenocyte proliferation (Zhang W. et al., 2015). The results showed that ATR polysaccharide could serve as a novel natural source of anti-oxidant and immune enhancer (Table 5; Figure 2).

TABLE 1 The volatile oil composition in ATR.

Compounds	Formula	Molecular weight	CAS No.	References
o-Cymene	$C_{10}H_{14}$	134.218	527-84-4	Lam et al. (2017a), Yan et al. (2020a)
α-Pinene	$C_{10}H_{16}$	136.234	2,437-95-8	Xiaojuan Zhang et al. (2015), Lam et al. (2017a), Liu et al. (2017), Yan et al. (2020a)
β-Pinene	$C_{10}H_{16}$	136.234	127-91-3	Xiaojuan Zhang et al. (201b), Yan et al. (2020a)
(−)-Camphene	$C_{10}H_{16}$	136.234	5,794-04-7	Xiaojuan Zhang et al. (2015), Yan et al. (2020a)
3-Carene	$C_{10}H_{16}$	136.234	13,466-78-9	Wu et al. (2013)
Limonene	$C_{10}H_{16}$	136.234	138-86-3	Lam et al. (2017a), Yan et al. (2020a)
α-Terpinene	$C_{10}H_{16}$	136.234	99-86-5	Lam et al. (2017a), Yan et al. (2020a)
γ-Terpinene	$C_{10}H_{16}$	136.234	99-85-4	Xiaojuan Zhang et al. (2015), Yan et al. (2020a)
Estragole	$C_{10}H_{12}O$	148.202	140-67-0	Lam et al. (2017a), Yan et al. (2020a)
Camphor	$C_{10}H_{16}O$	152.233	76-22-2	Xiaojuan Zhang et al. (2015), Lam et al. (2017a)
(−)-Borneol	$C_{10}H_{18}O$	154.249	464-45-9	Xiaojuan Zhang et al. (2015), Zhang et al. (2020)
α-terpineol	$C_{10}H_{18}O$	154.249	98-55-5	Yan et al. (2020a), Zhang et al. (2020)
Cineole	$C_{10}H_{18}O$	154.249	406-67-7	Wu et al. (2013)
4-Terpineol	$C_{10}H_{18}O$	154.249	562-74-3	Liu et al. (2006), Wu et al. (2013), Shi et al. (2021)
Linalool	$C_{10}H_{18}O$	154.249	78-70-6	Xiaojuan Zhang et al. (2015), Lam et al. (2017a), Yan et al. (2020a)
Eucalyptol	$C_{10}H_{18}O$	154.249	470-82-6	Xiaojuan Zhang et al. (2015), Yan et al. (2020a)
Menthol	$C_{10}H_{20}O$	156.265	1,490-04-6	Wu et al. (2013), Shi et al. (2021)
Methyl eugenol	$C_{11}H_{14}O_2$	178.228	93-15-2	Liu et al. (2006), Wu et al. (2013), Tang et al. (2014), Wang et al. (2015), Shi et al. (2021)
cis-methylisoeugenol	$C_{11}H_{14}O_2$	178.228	6,380-24-1	Xiaojuan Zhang et al. (2015), Lam et al. (2017a), Liu et al. (2017), Song et al. (2018), Yan et al. (2020a), Zhang et al. (2020)
trans-methylisoeugenol	$C_{11}H_{14}O_2$	178.228	6,379-72-2	Lam et al. (2017a), Liu et al. (2017), Xiaojuan Zhang et al. (2015), Zhang et al. (2020)
2,4,5-Trimethoxybenzaldehyde	$C_{10}H_{12}O_4$	196.200	4,460-86-0	Wu et al. (2017), Shi et al. (2021)
α-Calacorene	$C_{15}H_{20}$	200.319	21,391-99-1	Lam et al. (2017a), Liu et al. (2017), Wu et al. (2017), Yan et al. (2020a), Shi et al. (2021)
(−)-β-Caryophyllene	$C_{15}H_{24}$	204.351	87-44-5	Xiaojuan Zhang et al. (2015), Lam et al. (2017a), Yan et al. (2020a)
(+)-β-Caryophyllene	$C_{15}H_{24}$	204.351	87-44-5	Xiaojuan Zhang et al. (2015), Lam et al. (2017a), Zhang et al. (2020)
α-Caryophyllene	$C_{15}H_{24}$	204.351	6,753-98-6	Yan et al. (2020a)
β-Caryophyllene	$C_{15}H_{24}$	204.351	87-44-5	Liu et al. (2006), Wu et al. (2013), Tang et al. (2014), Shi et al. (2021)
α-Gurjunene	$C_{15}H_{24}$	204.351	489-40-7	Wu et al. (2013), Tang et al. (2014), Shi et al. (2021)
γ-Gurjunene	$C_{15}H_{24}$	204.351	22,567-17-5	Wu et al. (2013), Wang et al. (2015), Shi et al. (2021)
α-Cadinene	$C_{15}H_{24}$	204.351	24,406-05-1	Wu et al. (2013), Shi et al. (2021)
β-Cadinene	$C_{15}H_{24}$	204.351	523-47-7	Wu et al. (2013), Lam et al. (2017a), Shi et al. (2021)
γ-Cadinene	$C_{15}H_{24}$	204.351	39,029-41-9	Wu et al. (2013), Lam et al. (2017a), Shi et al. (2021)
δ-Cadinene	$C_{15}H_{24}$	204.351	483-76-1	Wu et al. (2013), Tang et al. (2014), Xiaojuan Zhang et al. (2015), Wang et al. (2015), Liu et al. (2017), Yan et al. (2020a), Shi et al. (2021)

(Continued on following page)

TABLE 1 (*Continued*) The volatile oil composition in ATR.

Compounds	Formula	Molecular weight	CAS No.	References
α-Patchoulene	$C_{15}H_{24}$	204.351	560-32-7	Lam et al. (2017a), Yan et al. (2020a)
α-Panasinsen	$C_{15}H_{24}$	204.351	56,633-28-4	Yan et al. (2020a)
α-Longipinene	$C_{15}H_{24}$	204.351	5,989-08-2	Lam et al. (2017a), Yan et al. (2020a)
α-Acoradiene	$C_{15}H_{24}$	204.351	28,400-13-7	Yan et al. (2020a)
Longifolene	$C_{15}H_{24}$	204.351	475-20-7	Yan et al. (2020a)
Longicyclene	$C_{15}H_{24}$	204.351	1,137-12-8	Xiaojuan Zhang et al. (2015), Lam et al. (2017a), Song et al. (2018), Yan et al. (2020a)
β-Elemene	$C_{15}H_{24}$	204.351	515-13-9	Xiaojuan Zhang et al. (2015), Lam et al. (2017a), Yan et al. (2020a)
δ-Elemene	$C_{15}H_{24}$	204.351	20,307-84-0	Xiaojuan Zhang et al. (2015), Yan et al. (2020a)
Calarene	$C_{15}H_{24}$	204.351	17,334-55-3	Xiaojuan Zhang et al. (2015), Song et al. (2018), Yan et al. (2020a)
Germacrene D	$C_{15}H_{24}$	204.351	317,819-80-0	Xiaojuan Zhang et al. (2015), Yan et al. (2020a)
α-Asarone	$C_{12}H_{16}O_3$	208.254	2,883-98-9	Zhu et al. (2010), Xiaojuan Zhang et al. (2015), Lam et al. (2017a), Liu et al. (2017), Lam et al. (2019), Yan et al. (2020a), Zhang et al. (2020)
β-Asarone	$C_{12}H_{16}O_3$	208.254	5,273-86-9	Zhu et al. (2010), Xiaojuan Zhang et al. (2015), Lam et al. (2017a), Liu et al. (2017), Li et al. (2018a), Song et al. (2018), Lam et al. (2019), Yan et al. (2020a), Zhang et al. (2020)
γ-Asarone	$C_{12}H_{16}O_3$	208.254	5,353-15-1	Xiaojuan Zhang et al. (2015), Lam et al. (2017a), Liu et al. (2017), Song et al. (2018), Yan et al. (2020a)
Elemisin	$C_{12}H_{16}O_3$	208.254	487-11-6	Tang et al. (2014), Wang et al. (2015), Shi et al. (2021)
Shyobunone	$C_{15}H_{24}O$	220.350	21,698-44-2	Xiaojuan Zhang et al. (2015), Lam et al. (2017a), Yan et al. (2020a)
Isoshyobunone	$C_{15}H_{24}O$	220.350	21,698-46-4	Lam et al. (2017a), Liu et al. (2017), Yan et al. (2020a)
Caryophyllene oxide	$C_{15}H_{24}O$	220.350	1,139-30-6	Song et al. (2018), Yan et al. (2020a)
Eremophila ketone	$C_{15}H_{24}O$	220.350	158,930-41-7	Yan et al. (2020a)
Spathulenol	$C_{15}H_{24}O$	220.350	6,750-60-3	Lam et al. (2017a), Yan et al. (2020a)
α-Cadinol	$C_{15}H_{26}O$	222.366	481-34-5	Xiaojuan Zhang et al. (2015), Lam et al. (2017a), Yan et al. (2020a)
α-Bisabolol	$C_{15}H_{26}O$	222.366	515-69-5	Liu et al. (2006), Shi et al. (2021)
Viridiflorol	$C_{15}H_{26}O$	222.366	51,371-47-2	Yan et al. (2020a)
Dihydroagarofuran	$C_{15}H_{26}O$	222.366	20,053-66-1	Wu et al. (2013), Shi et al. (2021)
Aihydroagarofuran	$C_{15}H_{26}O$	222.366	5,956-09-2	Yan et al. (2020a)
Elemol	$C_{15}H_{26}O$	222.366	639-99-6	Xiaojuan Zhang et al. (2015), Yan et al. (2020a)
Germacrene D-4-ol	$C_{15}H_{26}O$	222.366	74,841-87-5	Yan et al. (2020a)
Isocalamendiol	$C_{15}H_{26}O_2$	238.366	25,330-21-6	Wu et al. (2013), Shi et al. (2021)
Linoleic acid	$C_{18}H_{32}O_2$	280.445	60-33-3	Dong et al. (2007), Li et al. (2013), Wang et al. (2015), Shi et al. (2021)
Elaidic Acid	C18H34O2	282.461	112-79-8	Wang et al. (2015)

Effects on learning and memory impairment

ATR extract and its active ingredient, asarones could promote aberrant neural progenitor cell (NPC) proliferation. Oral administration of ATR enhanced NPC proliferation and neurogenesis in the hippocampus of adult and aged mice as well as in transgenic AD model mice. ATR and its components also enhanced the proliferation of cultured NPCs *in vitro*. Mechanistic studies have shown that ATR and asarones could activate the key

TABLE 2 The terpenoids composition in ATR.

Compounds	Formula	Molecular weight	CAS No.	References
Shyobunone	$C_{15}H_{24}O$	220.350	21,698-44-2	Ni and Yu (2013), Shi et al. (2021)
Acoronene	$C_{15}H_{22}O_2$	234.33	33,983-45-8	Ni and Yu (2013), Shi et al. (2021)
(3beta,24S)-stigmast-5-en-3-ol	$C_{29}H_{50}O$	414.707	83-47-6	Ni and Yu (2013), Shi et al. (2021)
Cycloartenol	$C_{30}H_{50}O$	426.717	469-38-5	Ni and Yu (2013), Song et al. (2018), Shi et al. (2021)
Lupeol	$C_{30}H_{50}O$	426.717	545-47-1	Ni and Yu (2013), Shi et al. (2021)
Daucosterol	$C_{35}H_{60}O_6$	576.847	474-58-8	Ni and Yu (2013), Shi et al. (2021)

TABLE 3 The organic acids composition in ATR.

Compounds	Formula	Molecular weight	CAS No.	References
Fumaric acid	$C_4H_4O_4$	116.072	110-17-8	Dong et al. (2007), Li et al. (2013), Shi et al. (2021)
Benzoic acid	$C_7H_6O_2$	122.120	65-85-0	Dong et al. (2007), Li et al. (2013), Shi et al. (2021)
Nicotinic acid	$C_6H_5NO_2$	123.110	59-67-6	Dong et al. (2007), Li et al. (2013), Shi et al. (2021)
4-Hydroxybenzoic acid	$C_7H_6O_3$	138.121	99-96-7	Dong et al. (2007), Li et al. (2013), Shi et al. (2021)
Protocatechuic acid	$C_7H_6O_4$	154.120	99-50-3	Dong et al. (2007), Li et al. (2013), Shi et al. (2021)
Vanillic acid	$C_8H_8O_4$	168.147	121-34-6	Dong et al. (2007), Li et al. (2013), Shi et al. (2021)
Suberic acid	$C_8H_{14}O_4$	174.194	505-48-6	Dong et al. (2007), Li et al. (2013), Shi et al. (2021)
Caffeic acid	$C_9H_8O_4$	180.157	331-39-5	Dong et al. (2007), Li et al. (2013), Shi et al. (2021)
Ferulic acid	$C_{10}H_{10}O_4$	194.184	537-98-4	Dong et al. (2007), Li et al. (2013), Shi et al. (2021)
Myristoleic acid	$C_{14}H_{26}O_2$	226.355	544-64-9	Dong et al. (2007), Li et al. (2013), Shi et al. (2021)
Palmitic acid	$C_{16}H_{32}O_2$	256.424	60,605-23-4	Dong et al. (2007), Li et al. (2013), Wu et al. (2013), Shi et al. (2021)
Cryptochlorogenic acid	$C_{16}H_{18}O_9$	354.309	905-99-7	Dong et al. (2007), Li et al. (2013), Shi et al. (2021)

TABLE 4 The flavonoids composition in ATR.

Compounds	Formula	Molecular weight	CAS No.	References
Astragalin	$C_{21}H_{20}O_{11}$	448.377	480-10-4	Tong and Cheng (2011), Shi et al. (2021)
Rhodionin	$C_{21}H_{20}O_{11}$	448.377	85,571-15-9	Tong and Cheng (2011), Shi et al. (2021)
Rhoifolin	$C_{27}H_{30}O_{14}$	578.519	17,306-46-6	Tong and Cheng (2011), Shi et al. (2021)
kaempferol-3-rutinoside	$C_{27}H_{30}O_{15}$	594.518	17,650-84-9	Tong and Cheng (2011), Shi et al. (2021)

kinase cascades in neurogenesis, extracellular signal-regulated kinase (ERK), but not Akt. Studies have shown that oral administration of ATR and asarones could be used as preventive and regenerative therapeutics to promote neurogenesis against age-related neurodegeneration and neurodegenerative disorders (Mao et al., 2015). Ning et al. (2021) explored the protective effect of Polygoni Multiflori Radix Praeparata (PMRP) combined with ATR (PA) on scopolamine-induced cognitive impairment in mice and its potential mechanism. PA was found to increase the concentration of neurotransmitters in the hippocampus, activate the BDNF/ERK/CREB signaling pathway, and increase the p90 ribosome expression of S6 kinase (p90RSK) and postsynaptic density (PSD) 95 proteins. Therefore, PA alleviates cognitive deficits by enhancing synapse-associated proteins, suggesting its therapeutic potential for the treatment of aging-related diseases such as AD (Table 5; Figure 2).

System biology research could predict the active components of ATR, as well as its corresponding targets and potential mechanism, and provide new ideas and directions for further research on the mechanism of ATR. Studies have (Song et al., 2018; Liu et al., 2020; Zhang et al., 2020) revealed a multicomponent synergistic mechanism and molecular targets of ATR in AD using a system pharmacology strategy. The results showed that the active

TABLE 5 Effects of ATR on the central nervous system.

Effects	Animals/cells	Experimental model	Dosage/ concentrations	Pharmacological effects	Targets/pathways
AD (Li et al., 2021b)	PC12 cells	PC12 cell line with APPswe-overexpressing as a cellular model of Aβ-induced injury	72 μM β-asarone treatment for 24 h	Promote autophagic flux, enhance autophagosome-lysosome fusion and/or lysosomal function	Reduce the expression levels of Beclin-1, p62, LC3-II and $A\beta_{1-42}$
AD (Mao et al., 2015)	C57BL/6 mice, APP/PS1 transgenic mice, adult hippocampal NPCs	APP/PS1 mice and their wild-type littermates	10 g/kg ATR, 10 mg/kg α-asarone, 30 mg/kg β-asarone in mice (*i.g.*) 0.1–1 mg/mL ATR, 0.3–10 μM α-asarone or β-asarone *in vitro*	Promote NPC proliferation and neurogenesis	activated ERK but not Akt
ROS-mediated damage in neuronal cells (Yang et al., 2021)	PC12 cells	H_2O_2-induced injury	1.5, 5, and 15 μg/mL for 48 h	Suppresse the accumulation of ROS and induces the expression of anti-oxidant proteins	Activation of CREB/ PGC-1α signaling
Neurotrophin deficiency (Lam et al., 2016a)	PC12 cells	Low concentration NGF-induced neurite outgrowth and neurofilament expression	30 μg/mL for 48 h	Induces the transcriptional activation of neurofilament promoters and potentiates NGF-induced neurite outgrowth and neurofilament expression	Induces phosphorylation of CREB and cAMP-mediated transcriptional activity
Anti-oxidative and immunopotentiating (Zhang et al., 2015a)	Mice, PC12 cells	H_2O_2-induced PC12 cell death	10, 100, 200 μg/mL for 12 h	Promotes splenocyte proliferation, anti-oxidant	Stimulates NO production and phagocytic activity
Defective neurotrophic factor expression (Lam et al., 2017a; Lam et al., 2019)	Astrocytes	Neurotrophic factor expression partially blocked by PKA inhibitor, H89	50 μM	Stimulates the expression and secretion of neurotrophic factors	PKA signaling
Astrocytes cell injury (Lam et al., 2017a; Lam et al., 2017b)	Astrocytes	tBHP-induced intracellular ROS accumulation	0.5–15 μg/mL α-asarone, β-asarone or ATR oil	Reduce astrocytes cell injury and ROS accumulation	Akt phosphorylation
AD (Ning et al., 2021)	Mice	Scopolamine-induced cognitive impairment (*i.p.*)	1.56, 6.24 g/kg/d PA (*i.g.*) 0.78, 3.12 g/kg/d ATR (*i.g.*)	Increase neurotransmitter concentrations in the hippocampus, increase synapse-associated proteins to alleviate cognitive deficits	Activated BDNF/ERK/ CRE signaling pathway, and increased p90RSK and PSD95 protein expression

Notes: ATR, acori tatarinowii rhizoma; AD, anti-Alzheimer's disease; ROS, reactive oxygen species; NPC, neural progenitor cell; NGF, nerve growth factor; ERK, extracellular signal-regulated kinase; CREB, cAMP-response element binding protein; BDNF, brain-derived neurotrophic factor.

components of ATR were involved in cancer, inflammation, cell metabolism, metabolic pathways and other related biological processes (Zhang et al., 2020), and were associated with a variety of predicted targets, such as amyloid precursor protein (APP), estrogen receptor 1 (ESR1), peroxisome proliferator activated receptor gamma (PPARG), androgen receptor (AR), muscarinic acetylcholine receptor M1 (CHRM1), caspase 3 (CASP3), janus kinase 2 (JAK2), mitogen-activated protein kinase 14 (MAPK14), prostaglandin G/H synthase 1 (PTGS1), protein kinase cAMP-activated catalytic subunit alpha (PRKACA). Moreover, most compounds in ATR have anti-fibrillar amyloid plaque, anti-inflammatory and anti-tau phosphorylation effects (Song et al., 2018). The potential mechanisms were found to be mainly involved in phosphoinositide 3-kinase (PI3K)-Akt, JAK2, MAPK, protein tyrosine phosphatase non-receptor type 1 (PTPN1) signaling pathway, neuroactive ligand-receptor interaction, as well as fluid shear stress and atherosclerosis (Liu et al., 2020; Zhang et al., 2020). ATR mainly acts on the kinase domain receptor (*KDR*) gene. Organ distribution showed that the targets of active ingredients were mainly located in AD-related whole blood, heart, liver, brain and muscle (Song et al., 2018; Liu et al., 2020). The network pharmacology technology has been systematically applied to the study of the target and potential mechanism corresponding to the active components of ATR, providing a new idea and direction for further study of the mechanism of ATR in AD. These findings suggested that ESR1, JAK2, PRKACA, and PTPN1 were considered as therapeutic targets for further research on ATR treatment of AD. However, more molecular biological methods are needed to demonstrate these targets.

Effects on the cardiovascular system

In recent years, the in-depth development and application of ATR in the cardiovascular field has become a research hotspot. ATR is widely used in the prevention and treatment of cardiovascular diseases such as coronary heart disease, hypertension and hyperlipidemia due to its multi-channel, multi-target and comprehensive regulation characteristics in the treatment of diseases. A series of *in vitro* studies have shown that ATR and its chemical components can effectively protect vascular endothelium and cardiomyocytes, and play an important role in anti-platelet

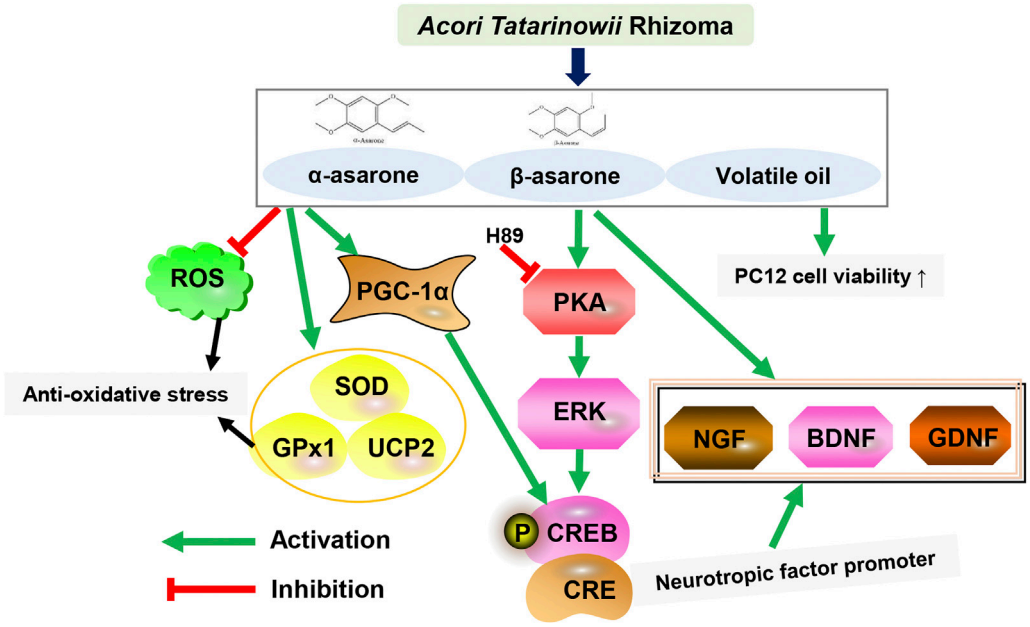

FIGURE 2
The main biological activities and potential mechanism of ATR on the central nervous system.

aggregation, improving blood rheology, regulating blood lipids, resisting arrhythmia, lowering blood pressure, resisting myocardial hypertrophy and atherosclerosis. The current research is mainly manifested in the following aspects.

Anti-myocardial ischemia effect

Myocardial ischemia-reperfusion injury refers to the interruption of myocardial blood supply in a short period of time, and the restoration of blood supply within a certain period of time. This is an unavoidable anomaly that is clearly contrary to the purpose of treatment (Tsao et al., 2022). The volatile oil of ATR and β-asarone have anti-myocardial ischemia effects, which can reduce the levels of endothelin (ET), calcitonin gene-related peptide (CGRP), and norepinephrine (NE) in rats with myocardial ischemia, and increase NO level. In addition, it could increase serum superoxide dismutase (SOD) levels, decreased malondialdehyde (MDA) and creatine kinase (CK) levels (Zhong et al., 2019). Furthermore, Wang et al., used sodium dithionite ($Na_2S_2O_4$) to induce myocardial ischemia/reperfusion injury (MI/RI) in cardiomyocytes, and explored the protective effect of the active ingredient β-asarone of ATR on myocardial cells from ischemia-reperfusion injury. It was found that β-asarone could significantly improve cell viability, reduce the content of lactate dehydrogenase (LDH) and CK in culture medium, stabilize mitochondrial membrane potential (MMP), and effectively inhibit mitochondrial damage in cardiomyocytes. The results showed that β-asarone had a significant protective effect on MI/RI cardiomyocytes (Wang et al., 2008a; Wang et al., 2008b).

Anti-arrhythmic effect

ATR has a certain anti-arrhythmic effect. Studies have found that aconitine could cause atrial, ventricular premature beats or the formation atrial tachycardia, short paroxysmal ventricular tachycardia, and ventricular tachycardia in rats. Epinephrine could cause single or multi-source premature ventricular contractions, paroxysmal ventricular tachycardia in rabbits. Barium chloride can induce bidirectional ventricular tachycardia-based arrhythmia in rabbits. The production of these arrhythmias is related to changes in autonomic nerves, mediators and myocardial excitability and automaticity. Shen et al., found that the volatile oil components of ATR may antagonize aconitine-induced arrhythmia in rats. Simultaneously, it is resistant to arrhythmias induced by epinephrine or barium chloride in rabbits (Shen et al., 1993). A certain concentration of ATR volatile oil could reduce the beating frequency of myocardial cells and improve the vitality of myocardial cells, so as to achieve the purpose of anti-arrhythmia. Specifically, 100–160 mg/L volatile oil from ATR can improve the survival rate of normal cardiomyocytes. The concentration of volatile oil from ATR is 140 mg/L, the survival rate of cardiac myocytes is at the top of the parabola. When the concentration is lower than 160 mg/L, there is no abnormal change in the morphology of cardiomyocytes. However, there are phenomena such as cell synapse thinning, retraction, and cytoplasmic shrinkage while the concentration is higher than 180 mg/L (Wu et al., 2009). Therefore, the volatile oil of ATR could reduce the beating frequency and enhance the viability of cardiomyocytes in a certain concentration, but it might have a certain adverse effect on normal cardiac myocytes when the concentration is too high.

Anti-tumor effects

The main component volatile oil of ATR, β-asarone inhibited the growth of colon cancer cells and the proliferation of gastric

TABLE 6 Anti-tumor effects of ATR.

Chemical composition	Animals/cells	Experimental model	Dosage/ concentrations	Pharmacological effects	Biological mechanism
β-Asarone (Tao et al., 2020)	Human gastric cancer cell lines MGC803, SGC7901, and MKN74	$Cocl_2$ (200 μM, 24 h) to induce hypoxia conditions while H_2O_2 (100 μM, 1 h) to induce peroxide condition	60 μg/mL β-asarone for 24 h	Induces apoptosis in gastric cancer cells and affects tumor glycolysis	Reduce the expression of PDK1, phospho(p)-PDK1, PDK4, HIF1α, c-myc, STAT5, and p-STAT5
β-Asarone (Li et al., 2018a)	human glioma U251 cells	-	30, 60 μM β-asarone for 48 h	Inhibits migration, invasion and adhesion of U251 cells	Regulate hnRNP A2/ B1 signaling pathway
β-Asarone (Li et al., 2018b)	human glioma U251 cells	-	60–480 μM β-asarone for 48 h	Inhibits cell viability, proliferation and colony-forming ability of U251 cells	Inhibit hnRNPA2/B1-mediated signaling pathway
β-Asarone (Wu et al., 2015)	Human gastric cancer cell lines SGC-7901, BGC-823 and MKN-28	-	0.12, 0.24 mM β-asarone for 24 h	Inhibits cell proliferation and induces apoptosis, reducing its ability to invade, migrate and adhere	Upregulating caspase-3, caspase-8, caspase-9, Bax, Bak, RECK, E-cadherin and downregulating MMP-2, MMP-9, MMP-14, Bcl-2, Bcl-xL and N-cadherin

cancer cells (Zou et al., 2012; Wu et al., 2015). Studies have shown that 30–60 μM asarone inhibited the cell viability, proliferation, colony-forming ability, migration, invasion, and adhesion of human glioma U251 cells. It regulated the levels of key proteins involved in the death receptor pathway and mitochondrial apoptosis pathway. Simultaneously, β-asarone regulated cell cycle-related proteins and inhibited tumor growth and induces apoptosis. It inhibits epithelial-mesenchymal transition (EMT) by up-regulating E-cadherin and down-regulating vimentin, and reduces the expression of the oncogenic protein hnRNPA2/B1 in a concentration- and time-dependent manner, which may be the effect of β-asarone on glioma cell invasion and EMT (Li et al., 2018a; Li et al., 2018b). In addition, β-asarone had a significant dose-dependent inhibitory effect on the cell proliferation and induction on cell apoptosis of human gastric cancer cell lines (SGC-7901, BGC-823, and MKN-28), as well as inhibiting effect on the invasion, migration and adhesion of BGC-823 cells. Furthermore, β-asarone inhibited the gastric cancer cell growth by upregulating the expression of caspase-3, caspase-8, caspase-9, Bcl2-associated X (Bax), Bcl-2 homologous antagonist/killer (Bak), reversion-inducing cysteine-rich protein with kazal motifs (RECK), E-cadherin and downregulating MMP-2, MMP-9, MMP-14, Bcl-2, Bcl-xL, and N-cadherin (Wu et al., 2015). Tao et al. (2020) investigated the exact mechanism of β-asarone in gastric cancer. The current study showed that β-asarone had a dose-dependent inhibitory effect on three gastric cancer cell lines (MGC803, SGC7901, and MKN74) at different differentiation stages. Meanwhile, under both normoxia and CoCl2-induced hypoxia, β-asarone could induce apoptosis of gastric cancer cells and block gastric cancer cells in G2/M phase of cell cycle. Besides, it decreased LDH activity in gastric cancer cells. Mechanistically, β-asarone reduces the expression of pyruvate dehydrogenase kinase (PDK) 1, phospho(p)-PDK1, PDK4, hypoxia-inducible factor 1-α (HIF-1α), c-myc, STAT5, and p-STAT5 to influence tumor glycolysis. Ultimately, β-asarone increased chemosensitization and inhibited tumor glycolysis (Table 6). In general, there are few studies on the pharmacology and clinical application of ATR in anti-tumor, and more studies are needed to investigate the effective components, pharmacological effects and molecular biological mechanisms of ATR in anti-tumor.

Effects on the digestive system

The free-volatile oil decoction of ATR, total volatile oil, β-asarone and α-asarone could inhibit the spontaneous contraction of isolated rabbit intestine, antagonize the intestinal spasm caused by acetylcholine (Ach), histamine phosphate (Hist) and $BaCl_2$, and enhance intestinal peristalsis in rats and intestinal propulsion in mice. In addition, these components could also promote bile secretion in rats and promote the advancement of intestinal contents in mice. The above-mentioned effect is the strongest with total volatile oil, followed by α-asarone, β-asarone, and the free-volatile oil decoction of ATR was the weakest (Hu et al., 1999). The α-asarone and β-asarone contained in the volatile oil of ATR could improve the intestinal absorption of 3,4,5-trimethoxycinnamic acid (TMCA), the active ingredient of Polygalae Radix (PR), by inhibiting the function of p-glycoprotein (P-gp) in the intestinal segment (Meng et al., 2019). At the same time, the volatile oil of calamus could inhibit the intestinal absorption of saikosaponin a and promote the intestinal absorption of ginsenosides. The mechanism of promoting absorption may be related to the inhibition of P-gp (Yang et al., 2018; Wang et al., 2019). ATR could promote digestion and regulate gastrointestinal movement. It is mainly used for stomachache and abdominal pain in clinic.

Effects on the respiratory system

Modern research shows that ATR indeed have a therapeutic effect on respiratory diseases. Li et al., investigated the anti-asthmatic effect of β-asarone on guinea pig asthma induced by ovalbumin aerosol inhalation sensitization (Li et al., 2006). The results showed that β-asarone could prolong the asthma attack latency and fall latency of model guinea pigs by spraying and

gavage. However, the effect of β-asarone in spray administration was better than that in gavage administration. Xu studied the cough-relieving, phlegm-relieving and asthmatic effects of β-asarone, the active ingredient of calamus volatile oil, through experiments such as phlegm-relieving experiments in mice, cough-relieving experiments in mice, and effects on immune organs in mice (Xu, 2007). The results showed that β-asarone can increase the excretion of phenol red, which could reduce the incubation period and the number of cough attacks in cough-induced mice. Moreover, it could increase the immune organ indices of mice.

Anti-bacterial and anti-oxidant effects

To date, several publications have reported the anti-oxidant capacity of α-asarone, β-asarone (Mukherjee et al., 2008), and isoshyobunone, calacorene, and isocalamendiol are essential oils with anti-oxidant activity (Lubsandorzhieva et al., 2013). γ-asarone shows fungitoxicity against *Aspergillus flavus* (Varma et al., 2002). δ-Cadinene in Psidium cattleianum Sabine has anti-microbial and anti-oxidant activities (Scur et al., 2016). The volatile oil of ATR has a good inhibitory effect on *staphylococcus* epidermidis, group A *streptococcus* and *shigella* flexneri (Zheng et al., 2015). Qiu et al., found that the microwave water extract of ATR has effective anti-bacterial components (Liu and Qiu, 2012). The microwave water extract of ATR has obvious anti-bacterial effect on *staphylococcus aureus* and *pseudomonas aeruginosa*. Secondly, it has a certain inhibitory effect on *salmonella* paratyphi B, *shigella* sonnei, *staphylococcus* epidermidis, *salmonella typhi*, *acinetobacter*, *shigella* flexneri and *escherichia coli*. In addition, α-asarone could regulate the activity of matrix metalloproteinases and anti-oxidant activities (Park and Kim, 2018).

Other pharmacological effects

The RATAPW isolated from ATR by Zhang et al., can promote the production of tumor necrosis factor alpha (TNF-α) in RAW264.7 macrophages through the nuclear factor kappa B (NF-kB) molecular signaling pathway (Zhang Y. et al., 2022). Treatment with 200 μg/mL RATAPW increased the proliferation rate of spleen lymphocytes by 38.77%. RATAPW also enhanced ConA-induced T cell and lipopolysaccharide (LPS)-induced B cell proliferation in a dose-dependent manner. The research lays the foundation for the discovery of natural polysaccharide immunomodulators or functional foods from ATR.

Clinical application of compound prescription containing ATR

The composition of traditional Chinese medicine is relatively complex. In traditional Chinese medicine, which advocates syndrome differentiation and treatment, reasonable compatibility will make it play the advantage of multi-target simultaneous action. The compound formula with ATR as the main component will produce the effect of "1 plus one is greater than two" to a certain extent. Some compounds preparations, including Kaixin San (KXS), Xian-He-Cao-Chang-Yan formula (XHCYF), Longshengzhi capsule (LSZ), Smart Soup etc. contain ATR, which are also widely used in clinical treatment for various diseases.

Kaixin San (KXS)

KXS is a traditional Chinese herbal preparation with memory-enhancing properties that has been used for thousands of years in the medical care of depression, senile dementia, forgetfulness, and dizziness (Zhu et al., 2013). It consists of two functional pairs of herbs: Ginseng Radix (GR), PR, ATR, and Poria cum Radix Pini (PRP) (Zhu et al., 2016a; Zhu et al., 2016b; Yan et al., 2017; Cao et al., 2018; Dong et al., 2020; Qu et al., 2021). Qu et al., found that KXS exerts anti-depressant effects in chronic unpredictable mild stress-induced depression-like mice (Qu et al., 2021). It inhibits the activation of microglia and reduces the expression of pro-inflammatory cytokines in the mouse hippocampus. Kaixin powder extract decreased lipopolysaccharide-induced expression of inflammatory factors in BV2 cells by inhibiting toll-like receptor 4/inhibitor of kappa B kinase/nuclear factor kappa-B (TLR4/IKK/NF-κB) pathway in mice BV2 microglia cell lines. (Dong et al. (2021) also investigated the anti-depressant mechanism of KXS in a rat model of chronic mild stress induced by different stress methods. The results identified 33 differentially expressed proteins: seven upregulated and 26 downregulated. Functional analysis revealed that these differentially expressed proteins are involved in synaptic plasticity, neurodevelopment, and neurogenesis. In chronic mild stress (CMS)-induced depression in rats and in H_2O_2-stressed astrocytes model, KXS treatment could significantly alleviate CMS-induced depression symptoms, restore neurotransmitter quality, and increase the expressions of neurotrophic factors and their corresponding receptors, promote neurogenesis (Zhu et al., 2012). Moreover, KXS had the highest tendency to increase NGF, GDNF, and BDNF expression by activating cAMP-dependent signaling pathways as well as stimulating enzymes responsible for neurotrophic factor synthesis (Zhu et al., 2013; Zhu et al., 2016b; Cao et al., 2018). These therapeutic effects might be related to the modification of Erk1/2 and CREB phosphorylation (Yan et al., 2016). The anti-depressant-like effects of KXS might be mediated by increased neurotrophic factor expression in astrocytes and weren't dependent on estrogen receptor or protein kinase-mediated signaling (Zhu et al., 2013). KXS could significantly enhance the expression levels of synaptotagmin and PSD95 by stimulating the cAMP-dependent pathway in chronic unpredictable mild stress (CUMS)-induced depressive rats, which is beneficial to synaptogenesis by inducing synaptic expression, possibly accounting for its anti-depressant effect *in vivo* and *in vitro* (Zhu et al., 2016a). In PC12 cultures, a single application of KXS had no effect on the neuronal differentiation, but showed robust effects in enhancing NGF-induced neurite outgrowth and neurofilament expression. Enhancement by KXS is mediated through the NGF receptor, tropomyosin receptor kinase (Trk) A (Yan et al., 2017). KXS might exert anti-depressant-like effects that induce neuronal differentiation (Zhu et al., 2016b; Yan et al., 2017; Dong et al., 2020; Qu et al., 2021), which supports the clinical use of this decoction.

TABLE 7 Clinical application of compound prescription containing ATR.

Compound prescription	Formulation	Effects	Animals/ cells	Experimental model	Dosage/ concentrations	Pharmacological effects	Targets/ pathways
Kaixin San (Qu et al., 2021)	GR, PR, ATR, PRP	Major depressive disorder (MDD)	Mice Mice BV2 microglia cell lines	Chronic unpredictable mild stress-induced depression-like mice	3, 10 g/kg/d (*i.g.*)	Inhibits the activation of microglia and reduces the expression of pro-inflammatory cytokines	Inhibite TLR4/IKK/ NF-κB pathways
Kaixin San (Dong et al., 2020)	GR, PR, ATR, PRP	Depression	Rats	different stress methods-induced chronic mild stress	600 mg/kg/d (*i.g.*)	Regulation of synaptic plasticity, neurodevelopment and neurogenesis	Synaptic plasticity, neurodevelopment, and neurogenesis-related proteins
Kaixin San (Zhu et al., 2016a)	GR, PR, ATR, PRP	Depression	Rats	CUMS-induced depressive rats	1.5, 5 g/kg/d (*i.g.*)	Beneficial for synaptogenesis	Stimulation of cAMP-dependent pathways
Kaixin San (Zhu et al., 2012)	GR, PR, ATR, PRP	Depression	Rats	CMS-induced depressive	0.9, 2.7 g/kg/d (*i.g.*)	anti-depressant-like action	Increase of neurotransmitters and expression of neurotrophic factors
Kaixin San (Cao et al., 2018)	GR, PR, ATR, PRP	AD	Mouse astrocytes	-	1–10 μg/mL for 48 h	Increases NGF and BDNF expression and stimulates enzymes responsible for neurotrophic factor synthesis	activating cAMP-dependent signaling pathway
Kaixin San (Zhu et al., 2013)	GR, PR, ATR, PRP	Depression	Cultured astrocytes	Day *in vitro* (DIV) 12	0.5–50 ?g/mL for 24 h	Stimulates the expression and secretion of neurotrophic factors including NGF, BDNF and GDNF	Increases neurotrophic factor expression in astrocytes
Kaixin San (Zhu et al., 2016b)	GR, PR, ATR, PRP	Depression	PC12 cells	NGF-induced neuronal differentiation in PC12 cells	0.1–10 μg/mL for 48 h	Potentiate the NGF-induced neurite outgrowth	cAMP-dependent pathway
Kaixin San (Yan et al., 2017)	GR, PR, ATR, PRP	Depression	PC12 cells	NGF-induced neuronal differentiation in PC12 cells	0–100 μg/mL for 48 h or 24 h	Robust effects in NGF-induced neurite outgrowth and neurofilament expression	Trk A signaling
Kaixin San (Yan et al., 2016)	GR, PR, ATR, PRP	Depression	Rats, cultured neurons and astrocytes	CMS-induced depressive rats and H_2O_2-stressed astrocytes	60.9, 182.7, 548.1 mg/kg/d in rats (*i.g.*), 0.3–3 μ g/mL for 96 h in cultured neurons, 1.5–15 μ g/mL for 48 h in cultured astrocytes	Promote neurogenesis and induced neurotrophic factors expression	Modification of Erk1/2 and CREB phosphorylation
Xian-He-Cao-Chang-Yan formula (Li et al., 2021a)	Agrimoniae Herba, Coptidis Rhizoma, Aucklandiae Radix, Cicadae Periostracum, ATR, and Platycodonis Radix	UC	Mice RAW 264.7 cells	DSS-induced UC LPS-stimulated RAW 264.7 cells	2.5, 5, 10 g/kg/d (*i.g.*) for mice 3, 0.8, 0.2 mg/mL for cells	Regulate macrophage polarization and inhibit glycolysis	The modulation of macrophage metabolic reprogramming *via* AMPK pathway
Longshengzhi capsule (Yin et al., 2020)	Hirudo, Astmgali Radix, Carthami Flos, Persicae Semen, ATR, and Acanthopanax Senticosus	AD	Mice HT-22 cells	Double transgenic mice expressing the APP/PS1 to model AD	850, 2000 mg/100 g food in mice 0, 10, and 20 μg/mL for 3 h in HT-22 cell	Anti-oxidative stress, anti-inflammatory and neuroprotective effects	In part by regulating the FAS/Bcl-2/ p53 and NF-kB pathway

(Continued on following page)

TABLE 7 (*Continued*) Clinical application of compound prescription containing ATR.

Compound prescription	Formulation	Effects	Animals/cells	Experimental model	Dosage/concentrations	Pharmacological effects	Targets/pathways
Smart Soup (Hou et al., 2014)	ATR, PR, PRP	AD	APPswe/PS1dE9 (APP/PS1) double-transgenic mice	Aβ-induced AD	10 g/kg (*i.g.*)	Improves cognitive impairment and reduces brain gliosis and neuronal loss in AD mice	Neuroprotective effects against Aβ

Notes: GR, ginseng radix; PR, ATR, acori tatarinowii rhizoma; PRP, poria cum radix pini; MDD, major depressive disorder; CUMS, chronic unpredictable mild stress; NGF, nerve growth factor; BDNF, brain-derived neurotrophic factor; GDNF, glial-derived neurotrophic factor; UC, ulcerative colitis; DSS, dextran sulfate sodium; LPS, lipopolysaccharide.

TABLE 8 Pharmacokinetic parameters of ATR.

Compounds	Species	Dose of ATR	Pharmacokinetics parameter
cis-Methylisoeugenol (Ning et al., 2021)	Rats	2.16 g/kg ATR, *p.o*	C_{max} (ng/mL): 19.432 ± 18.798
			T_{max} (h): 3.514 ± 3.753
			$T_{1/2}$ (h): 7.493 ± 2.55
			$AUC_{0-\infty}$ (ng·h/mL): 93.824 ± 20.379
			$AUC_{0-\infty}$ (ng·h/mL): 123.263 ± 30.025
β-Asarone (Ning et al., 2021)	Rats (Ning et al., 2021)	2.16 g/kg ATR, *p.o*	C_{max} (ng/mL): 49.752 ± 16.049
			T_{max} (h): 4.778 ± 3.777
			$T_{1/2}$ (h): 10.662 ± 6.942
			$AUC_{0-\infty}$ (ng·h/mL): 603.44 ± 280.969
			$AUC_{0-\infty}$ (ng·h/mL): 1,045.247 ± 910.63
α-Asarone (Ning et al., 2021)	Rats (Ning et al., 2021)	2.16 g/kg ATR, *p.o*	C_{max} (ng/mL): 73.456 ± 25.933
			T_{max} (h): 3.542 ± 3.736
			$T_{1/2}$ (h): 11.797 ± 12.574
			$AUC_{0-\infty}$ (ng·h/mL): 599.674 ± 360.384
			$AUC_{0-\infty}$ (ng·h/mL): 1,042.098 ± 614.716
Asarylaldehyde (Ning et al., 2021)	Rats (Ning et al., 2021)	2.16 g/kg ATR, *p.o*	C_{max} (ng/mL): 119.288 ± 52.23
			T_{max} (h): 2.208 ± 3.217
			$T_{1/2}$ (h): 7.177 ± 1.232
			$AUC_{0-\infty}$ (ng·h/mL): 1,439.382 ± 492.857
			$AUC_{0-\infty}$ (ng·h/mL): 1,547.283 ± 482.098

Notes: ATR, acori tatarinowii rhizoma; C_{max}, peak concentration of drug; T_{max}, peak time; $T_{1/2}$, half-life of elimination; $AUC_{0-\infty}$, area under the plasma concentration-time curve.

Xian-He-Cao-Chang-Yan formula

Li et ai., investigated the bioactive ingredients and therapeutic mechanisms of Xian-He-Cao-Chang-Yan formula (XHCF) (composition: Agrimoniae Herba, Coptidis Rhizoma, Aucklandiae Radix, Cicadae Periostracum, ATR, and Platycodonis Radix) on dextran sulfate sodium (DSS)-induced ulcerative colitis (UC) and LPS-stimulated RAW 264.7 cells (Li J. et al., 2021). The results indicated that XHCF could effectively improve DSS-induced acute colitis. It regulates macrophage polarization and inhibits glycolysis, downregulating HK2 expression in LPS-challenged macrophages. Furthermore, XHCF enhanced the phosphorylation of adenosine 5′-monophosphate (AMP)-activated protein kinase (AMPK) both *in vivo* and *in vitro*, suggesting that AMPK is involved in XHCF function.

Longshengzhi capsule (LSZ)

LSZ has been approved by the China Food and Drug Administration for treatment of patients with cardiovascular/cerebrovascular disease. Yin et al., determined the effect of LSZ on AD processes using double transgenic mice expressing the amyloid-β precursor protein and mutant human presenilin 1 (APP/PS1) to mimic AD (Yin et al., 2020). Studies have demonstrated anti-oxidative stress, anti-inflammatory and neuroprotective effects of LSZ in AD-like pathology, and its potential

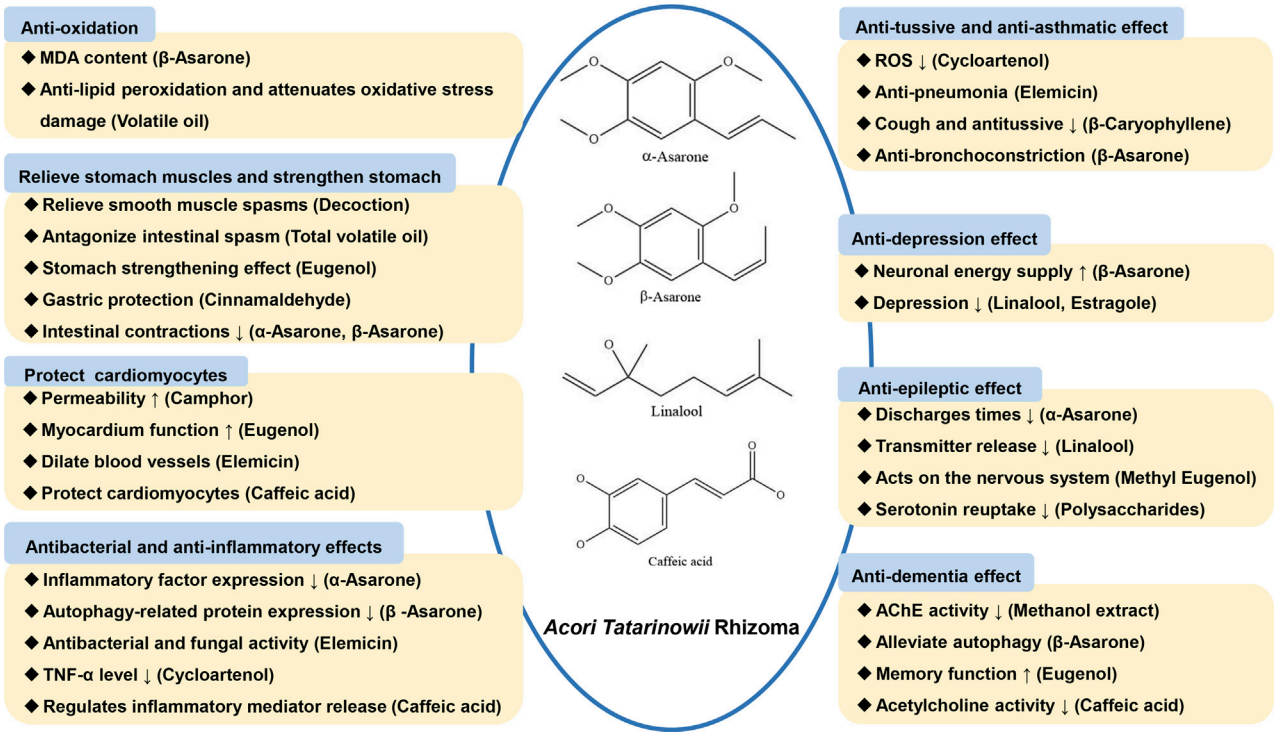

FIGURE 3
Active chemical constituents and pharmacological mechanism of ATR.

mechanism was to enhance neuronal survival in HT-22 cells by partially modulating the FAS/Bcl-2/p53 pathway.

Smart Soup

Smart Soup is a traditional Chinese medicine formula composed of ATR, PRP, and PR, which is a typical anti-memory disorder prescription. Hou et al. (2014), evaluated the efficacy of SS on AD. Oral administration of SS ameliorates cognitive impairment in AD transgenic mice, reduces Aβ levels, delays Aβ amyloidosis, and reduces Aβ-induced brain gliosis and neuronal loss in AD mice. Consistently, SS treatment reduced amyloid-related motor dysfunction and premature death in AD transgenic flies. Mechanistic studies show that ATR exerts neuroprotective effects on antibodies and plays a role in the treatment of AD (Table 7).

Pharmacokinetics of ATR

Literature studies have found that there are relatively few pharmacokinetic studies on ATR and its active components. Ning et al. investigated the pharmacokinetic parameters of active components such as *cis*-methyl isoeugenol, β-asarone, α-asarone, and asarylaldehyde in ATR (2.16 g/kg, *p. o.*) in rats. The results indicated that β-asarone, α-asarone, *cis*-methylisoeugenol, and asarylaldehyde were absorbed slowly after oral administration of ATR (T_{max} = 4.78, 3.54, 3.51, and 2.21 h, respectively) (Ning et al., 2021) (Table 8). Due to the limited references reporting on the pharmacokinetic parameters of ATR, more studies need to be designed to further clarify the pharmacokinetic parameters of the absorption, distribution, metabolism and excretion processes of ATR as well as its active components.

Toxicity of ATR

Currently, the toxicological studies on ATR focus on its active components. The median lethal dose (LD_{50}) of ATR volatile oil to mice was 0.22 ± 0.055 mL/kg. At the therapeutic dose, ATR volatile oil could significantly slow down the heart rate and prolong the P-R interval (Wu et al., 2009). Preliminary experiments found that the beating frequency of cardiomyocytes cultured *in vitro* was slowed down. Therefore, it is speculated that ATR volatile oil acts by inhibiting myocardial excitability and automaticity (Shen et al., 1993). It is worth noting that the existing research has proved that α-asarone and β-asarone may have carcinogenicity, teratogenicity and mutagenicity toxicity (Chellian et al., 2017). Therefore, it is necessary to pay attention to the contraindications and dosage of drugs. Simultaneously, the balance between curative effect and toxic and side effects should be grasped in clinical use. According to the literature reports, ATR has anti-cancer activity (Wu et al., 2004). Nevertheless, long term or high-dose toxicity testing in animals to explore the acute and chronic toxicity of ATR is still lacking. Thus, more meaningful studies need to be further designed to explore the toxicology of ATR.

Conclusion and perspective

Summary of evidence

As a traditional Chinese medicine in China, ATR has a long history of medicinal use and a wide range of pharmacological effects. ATR treatment of diseases has the characteristics of multi-component, multi-target, and multi-pathway synergy, among which there are many active monomer components, and the potential mechanism is complex and diverse. The volatile drugs with aromatic odor are administered through nasal inhalation and smell, which has become an effective way to prevent and treat diseases of the central nervous system (Zhang et al., 2021). The volatile oil of ATR is the main pharmacological component, and it has shown definite curative effect and good application prospect in the prevention and treatment of central nervous system diseases. Modern pharmacological studies have shown that ATR has an extremely wide range of pharmacological effects, and has a good preventive effect on a variety of diseases, especially central nervous system diseases, such as anti-depression, anti-AD, anti-Parkinson's disease (PD), anti-epileptic, anti-cerebral ischemia-reperfusion injury and other effects, which has gradually become one of the hot studies in the field of medicine (Chellian et al., 2017).

At present, the central nervous system effect of ATR is mainly related to its regulation of cholinergic system, regulation of synaptic plasticity, antioxidation and protection of neurons. ATR is often used in combination with PR and GR in the treatment of central nervous system diseases. It is composed of KXS, PR powder and other well-known prescription for intelligence. It is the representative and basic prescription for future generations of prescription for intelligence. It has a good development and application prospect because of its high safety and obvious curative effect. However, since the pathogenesis of central nervous system diseases and the chemical components of ATR are relatively complex, more comprehensive and systematic research on the pathogenesis and pharmacological effects of central nervous system diseases should be strengthened in the future to provide more sufficient theoretical basis for ATR to treat central nervous system diseases.

α-Asarone and β-asarone are isomers of each other. Because of their volatile oil properties, α-asarone and β-asarone can quickly pass through the BBB to exert pharmacological effects on the central nervous system (Lam et al., 2019), and showing a very promising application prospect. Based on the aromatic odor of α-asarone and β-asarone and their easy penetration through the BBB, nasal inhalation and olfactory administration has opened up a new way for the volatile oil of ATR to prevent and treat central nervous system diseases, especially mental diseases. This is an efficient, low-toxic, safe and simple route of administration, which is worthy of in-depth research and exploration.

Correlation between the chemical constituents and pharmacological mechanism of ATR

From this study, ATR can be used to prevent and treat central nervous system diseases, cardiovascular system diseases, gastrointestinal digestive system diseases, respiratory system diseases, etc. Therefore, this study summarizes the correlation between its chemical constituents and its pharmacological mechanism of action. A large number of experiments have shown that the volatile oil of ATR has a two-way regulation of excitation and inhibition on the central nervous system. It has antiarrhythmic, antithrombotic and protective effects on cardiac cells and blood vessels. Besides, ATR has anti-spasmodic and anti-asthmatic effects on the respiratory system and can promote digestion and regulate gastrointestinal movement for the digestive system. In terms of anti-epilepsy, α-asarone can reduce the number of discharges; linalool reduces transmitter release; methyl eugenol acts on the nervous system; polysaccharides inhibit serotonin reuptake. In terms of anti-depressant effects, β-asarone can improve behavioral disorders and increase neuronal energy supply. β-pinene can interact with monoamine systems. Linalool and artemisinin can reduce depression. Volatile oils and their aqueous extracts, methanol extracts, β-asarone, eugenol, caffeic acid, etc. can play an anti-dementia role by inhibiting β-amyloid aggregation and fiber formation, inhibiting acetylcholine esterase (AChE) activity, relieving autophagy, improving memory, and inhibiting acetylcholine activity, etc. In terms of cardiovascular activity, volatile oil, β-asarone, camphor, eugenol, elemene and caffeic acid have effect on reducing atherosclerotic blood lipids cholesterol (CHOL) and low-density lipoprotein cholesterol (LDL-C), enhancing permeability, exciting myocardium, dilating blood vessels, protecting cardiomyocytes. ATR water extract, total volatile oil, eugenol, cinnamic aldehyde, β-asarone, α-asarone block the receptors, relieve smooth muscle spasm, antagonize intestinal spasm, protect gastric function, inhibit intestinal contraction, etc. Gastrointestinal muscles and play a role in stomach. For the respiratory system, ATR can inhibit the generation of ROS, increase tracheal secretion, dilute sputum, inhibit bronchoconstriction, relax tracheal smooth muscle, block MAPK and NF-κB to exert anti-tussive and asthmatic effects. Other chemical basis and pharmacological mechanism of action are shown in Figure 3.

Research limitations and problems

Currently, the research on ATR mainly focuses on the volatile components. The traditional usage is to boil it into a water decoction, and its volatile components will be lost (Yang et al., 2021). Whether and to what extent the loss of volatile components of ATR and related preparations has an impact on the quality of the drug is unknown. Some studies have reported that its volatile components are present in both oil and water media. Whether these two media are the same and what are the similarities and differences when they exert their medicinal effects is worthy of further study. There are various studies on the volatile components of ATR, such as α-asarone and β-asarone, but less research on its non-volatile components. Thus, there are still insufficient studies on the systemic activity and pharmacological mechanism, active ingredients, pharmacokinetic characteristics of volatile and non-volatile components of ATR. Besides, the qualitative and quantitative analysis of various chemical components in ATR still needs to be detected and analyzed by ultrahigh performance liquid chromatography quadrupole time of flight mass spectrometry (UHPLC/Q-TOF-MS). In addition, there are few reports on

pharmacokinetics and toxicology of ATR and its active components in the current study. Therefore, a more comprehensive and in-depth excavation of the effect of ATR will promote its new clinical use, thereby providing useful guidance for improving its medicinal value. The further study can combine ATR with modern pharmaceutical technology to explore whether it can be used as a drug carrier to assist chemical medicine to achieve the leap of BBB, reduce the dosage of chemical medicine, reduce adverse reactions, and make ATR more widely applicable. It is expected to provide scientific basis for the promotion and application of ATR in the prevention and treatment of various diseases, and can become an antiepileptic drug with significant clinical efficacy, low toxicity and more safety.

As a common traditional Chinese medicine, ATR has a long history of application in China, and is widely used in the treatment of diseases of the central nervous system, cardiovascular system, digestive system and respiratory system. However, the chemical components, pharmacological activity, toxicological effect and molecular mechanism of ATR need to be further explored. The future study should focus on clarifying the chronic toxicity and acute toxicity of ATR to further clarify its safety, so as to guide the clinical rational use of drugs and the development of new drugs. In addition, nanotechnology and chemical modification can improve the oral bioavailability of ATR and expand the scope of drug clinical treatment.

Author contributions

JW wrote and amended the manuscript. YY conceived and designed the study. JH checked crucial information of this manuscript. All data were generated in-house, and no paper mill was used. All authors agree to be accountable for all aspects of work ensuring integrity and accuracy.

Funding

This study was supported by the Xihua University Talent Introduction Project (Z211060), the introduction of talents research start-up and supporting funds of Yunnan University of Chinese Medicine, and Yunnan Provincial Science and Technology Department-Applied Basic Research Joint Special Funds of Chinese Medicine (202101AZ070001-028).

Conflict of interest

The authors declare that the research was conducted in the absence of any commercial or financial relationships that could be construed as a potential conflict of interest.

Publisher's note

All claims expressed in this article are solely those of the authors and do not necessarily represent those of their affiliated organizations, or those of the publisher, the editors and the reviewers. Any product that may be evaluated in this article, or claim that may be made by its manufacturer, is not guaranteed or endorsed by the publisher.

References

Cao, C., Xiao, J., Liu, M., Ge, Z., Huang, R., Qi, M., et al. (2018). Active components, derived from kai-xin-san, A herbal formula, increase the expressions of neurotrophic factor NGF and BDNF on mouse astrocyte primary cultures via cAMP-dependent signaling pathway. *J. Ethnopharmacol.* 224, 554–562. doi:10.1016/j.jep.2018.06.007

Chellian, R., Pandy, V., and Mohamed, Z. (2017). Pharmacology and toxicology of α- and β-asarone: A review of preclinical evidence. *Phytomedicine* 32, 41–58. doi:10.1016/j.phymed.2017.04.003

Dong, X. Z., Wang, D. X., Zhang, T. Y., Liu, X., Liu, P., and Hu, Y. (2020). Identification of protein targets for the antidepressant effects of Kai-Xin-San in Chinese medicine using isobaric tags for relative and absolute quantitation. *Neural Regen. Res.* 15, 302–310. doi:10.4103/1673-5374.265555

Dong, Y., Shi, R., and Liu, B. (2007). Study on chemical compositions of acorus tatarinowii schott (I). *J. Beijing Univ. Traditional Chin. Med.* 30, 61–63.

Dong, Y., Shi, R., and Liu, B. (2008). Study on chemical constituents of non-volatile parts of acorus calamus. *China Pharm.* 17, 18–20. doi:10.3969/j.issn.1006-4931.2008.20.015

Fu, Y., Yang, Y., Shi, J., Bishayee, K., Lin, L., Lin, Y., et al. (2020). Acori tatarinowii rhizoma extract ameliorates Alzheimer's pathological syndromes by repairing myelin injury and lowering Tau phosphorylation in mice. *Pharmazie* 75, 395–400. doi:10.1691/ph.2020.0492

Hou, Y., Wang, Y., Zhao, J., Li, X., Cui, J., Ding, J., et al. (2014). Smart Soup, a traditional Chinese medicine formula, ameliorates amyloid pathology and related cognitive deficits. *PLoS One* 9, e111215. doi:10.1371/journal.pone.0111215

Hu, J., Gu, J., and Wang, Z. (1999). Effects of Acori Tatarinowii Rhizoma and its active ingredients on the digestive system. *Pharmacol. Clin. Chin. Materia Medica* 15, 16–18. doi:10.1016/B978-008043005-8/50012-3

Hu, X., Tang, Y., and Yuan, J. (2019). Isolation and identification the compositions of alkaloids in Acorus tatarinowii. *China Pharm.* 30, 642–645.

Huang, L., Deng, M., He, Y., Lu, S., Ma, R., and Fang, Y. (2016). β-asarone and levodopa co-administration increase striatal dopamine level in 6-hydroxydopamine induced rats by modulating P-glycoprotein and tight junction proteins at the blood-brain barrier and promoting levodopa into the brain. *Clin. Exp. Pharmacol. Physiol.* 43, 634–643. doi:10.1111/1440-1681.12570

Huang, L., Zhu, C., Lin, L., Wang, J., and Li, L. (2020). Effects of different resuscitation-inducing herbs on excitation-sedation condition of nervous system. *Acta Chin. Med.* 35, 1501–1504. doi:10.16368/j.issn.1674-8999.2020.07.335

Jiang, C., Liu, X., Gong, J., and Cai, G. (2018). The research progress of calamus to regulate the permeability of blood-brain barrier and the mechanism. *Ginseng Res.* 30, 44–45. doi:10.19403/j.cnki.1671-1521.2018.01.013

Ke, X., and Fang, Y. (2003). Effects of volatile oil of acorus tatarinowii schott on amino acids in cerebral ischemia-reperfusion. *Chin. J. Gerontology* 23, 302–303.

Lam, K. Y., Chen, J., Lam, C. T., Wu, Q., Yao, P., Dong, T. T., et al. (2016a). Asarone from acori tatarinowii rhizoma potentiates the nerve growth factor-induced neuronal differentiation in cultured PC12 cells: A signaling mediated by protein kinase A. *PLoS One* 11, e0163337. doi:10.1371/journal.pone.0163337

Lam, K. Y. C., Huang, Y., Yao, P., Wang, H., Dong, T. T. X., Zhou, Z., et al. (2017a). Comparative study of different acorus species in potentiating neuronal differentiation in cultured PC12 cells. *Phytother. Res.* 31, 1757–1764. doi:10.1002/ptr.5904

Lam, K. Y. C., Wu, Q. Y., Hu, W. H., Yao, P., Wang, H. Y., Dong, T. T. X., et al. (2019). Asarones from Acori Tatarinowii Rhizoma stimulate expression and secretion of neurotrophic factors in cultured astrocytes. *Neurosci. Lett.* 707, 134308. doi:10.1016/j.neulet.2019.134308

Lam, K. Y. C., Yao, P., Wang, H., Duan, R., Dong, T. T. X., and Tsim, K. W. K. (2017b). Asarone from acori tatarinowii rhizome prevents oxidative stress-induced cell injury in cultured astrocytes: A signaling triggered by Akt activation. *PLoS One* 12, e0179077. doi:10.1371/journal.pone.0179077

Lam, K. Y., Ku, C. F., Wang, H. Y., Chan, G. K., Yao, P., Lin, H. Q., et al. (2016b). Authentication of Acori Tatarinowii Rhizoma (Shi Chang Pu) and its adulterants by morphological distinction, chemical composition and ITS sequencing. *Chin. Med.* 11, 41. doi:10.1186/s13020-016-0113-x

Lee, J. Y., Lee, J. Y., Yun, B. S., and Hwang, B. K. (2004). Antifungal activity of beta-asarone from rhizomes of Acorus gramineus. *J. Agric. Food Chem.* 52, 776–780. doi:10.1021/jf035204o

Li, G., Chen, F., Shen, L., Shen, S., Zhang, J., and Si, J. (2013). Study on chemical constituents from roots and rhizomes of Acorus tatarinowii. *Chin. Traditional Herb. Drugs* 44, 808–811. doi:10.7501/j.issn.0253-2670

Li, J., Li, M., Ye, K., Jiang, Q., Wang, M., Wen, X., et al. (2021). Chemical profile of Xian-He-Cao-Chang-Yan formula and its effects on ulcerative colitis. *J. Ethnopharmacol.* 267, 113517. doi:10.1016/j.jep.2020.113517

Li, L., Wu, M., Wang, C., Yu, Z., Wang, H., Qi, H., et al. (2018a). β-Asarone inhibits invasion and EMT in human glioma U251 cells by suppressing splicing factor HnRNP A2/B1. *Molecules* 23, 671. doi:10.3390/molecules23030671

Li, L., Yang, Y., Wu, M., Yu, Z., Wang, C., Dou, G., et al. (2018b). Beta-asarone induces LoVo colon cancer cell apoptosis by up-regulation of caspases through a mitochondrial pathway *in vitro* and *in vivo*. *Molecules* 23, 5291–5298. doi:10.7314/apjcp.2012.13.10.5291

Li, L., Zou, Y., Shi, C., Wei, G., Lin, S., Jiang, H., et al. (2006). Research on the asthma-reducing effect of asthma model in Guinea pigs treated with β-asarone through stomach-perfusion and spray administration. *Chin. Archives Traditional Chin. Med.* 24, 2244–2245. doi:10.13193/j.archtcm.2006.12.86.lil.040

Li, Z., Ma, J., Kuang, Z., and Jiang, Y. (2021). β-Asarone attenuates aβ-induced neuronal damage in PC12 cells overexpressing APPswe by restoring autophagic flux. *Front. Pharmacol.* 12, 701635. doi:10.3389/fphar.2021.701635

Liu, C., Liu, X., and Yang, H. (2006). GC-MS analysis of essential oils from Acorus Tatarinowii Schott. *Chin. Archives Traditional Chin. Med.* 24, 1280–1281. doi:10.13193/j.archtcm.2006.07.98.liuchh.043

Liu, L., Wang, J., Shi, L., Zhang, W., Du, X., Wang, Z., et al. (2013). β-Asarone induces senescence in colorectal cancer cells by inducing lamin B1 expression. *Phytomedicine* 20, 512–520. doi:10.1016/j.phymed.2012.12.008

Liu, S., He, C., Liao, Y., Liu, H., Mao, W., and Shen, Z. (2020). Enhancing and complementary mechanisms of synergistic action of acori tatarinowii rhizoma and codonopsis radix for Alzheimer's disease based on systems pharmacology. *Evid. Based Complement. Altern. Med.* 2020, 6317230. doi:10.1155/2020/6317230

Liu, W., Zhang, B., Xin, Z., Ren, D., and Yi, L. (2017). GC-MS fingerprinting combined with chemometric methods reveals key bioactive components in acori tatarinowii rhizoma. *Int. J. Mol. Sci.* 18, 1342. doi:10.3390/ijms18071342

Liu, Y., and Qiu, T. (2012). Study on anti-inflammatory and *in vitro* antibacterial effects of microwave water extract of Acori Tatarinowii Rhizoma. *Strait Pharm. J.* 24 (6), 2. doi:10.3969/j.issn.1006-3765.2012.06.008

Lubsandorzhieva, P. B., Boldanova, N. B., and Dashinamzhilov, Z. B. (2013). Chemical composition and *in vitro* antioxidant activity of essential oil from a hepatoprotective herbal mix. *Pharm. Chem. J.* 47, 58–61. doi:10.1007/s11094-013-0897-2

Mao, J., Huang, S., Liu, S., Feng, X. L., Yu, M., Liu, J., et al. (2015). A herbal medicine for Alzheimer's disease and its active constituents promote neural progenitor proliferation. *Aging Cell.* 14, 784–796. doi:10.1111/acel.12356

Meng, X., Jia, P., Zhang, Y., Wang, S., Zheng, X., Chen, Z., et al. (2019). Effects of Acori Tatarinowii Rhizome on intestinal absorption characteristics of Polygalae Radix based on the regulation of p-glycoprotein. *Res. Pract. Chin. Med.* 33, 19–23. doi:10.13728/j.1673-6427.2019.05.006

Mukherjee, P. K., Kumar, V., Mal, M., and Houghton, P. J. (2008). Acorus calamus.: Scientific validation of ayurvedic tradition from natural resources. *Pharm. Biol.* 45, 651–666. doi:10.1080/13880200701538724

Ni, G., and Yu, D. (2013). Chemical constituents from rhizomes of Acorus tatarinowii. *China J. Chin. Materia Medica* 38, 569–573. doi:10.4268/cjcmm20130420

Ning, F., Chen, L., Liu, X., Zhu, Y., Hu, J., Xie, G., et al. (2021). Combination of Polygoni Multiflori radix Praeparata and acori tatarinowii rhizoma alleviates learning and memory impairment in scopolamine-treated mice by regulating synaptic-related proteins. *Front. Pharmacol.* 12, 679573. doi:10.3389/fphar.2021.679573

Park, H. J., and Kim, M. M. (2018). α-asarone modulates activity of matrix metalloproteinase as well as antioxidant activity. *J. Life Sci.* 25, 1000–1006. doi:10.5352/jls.2015.25.9.1000

Qu, S., Liu, M., Cao, C., Wei, C., Meng, X. E., Lou, Q., et al. (2021). Chinese medicine formula kai-xin-san ameliorates neuronal inflammation of CUMS-induced depression-like mice and reduces the expressions of inflammatory factors via inhibiting TLR4/IKK/NF-κB pathways on BV2 cells. *Front. Pharmacol.* 12, 626949. doi:10.3389/fphar.2021.626949

Scur, M. C., Pinto, F. G., Pandini, J. A., Costa, W. F., Leite, C. W., and Temponi, L. G. (2016). Antimicrobial and antioxidant activity of essential oil and different plant extracts of Psidium cattleianum Sabine. *Braz J. Biol.* 76, 101–108. doi:10.1590/1519-6984.13714

Shen, J., Xiao, L., and Zhang, D. (1993). Experimental study on antiarrhythmic effect of volatile oil from Acori Tatarinowii Rhizoma. *Guangzhou Med. J.* 24, 44–45.

Shi, B., Liu, J., Zhang, Q., Wang, S., Jia, P., Bian, L., et al. (2020). Effect of co-administration of Acori Tatarinowii Rhizoma volatile oil on pharmacokinetic fate of xanthotoxol, oxypeucedanin hydrate, and byakangelicin from Angelicae Dahuricae Radix in rat. *J. Sep. Sci.* 43, 2349–2362. doi:10.1002/jssc.201901250

Shi, J., Ji, L., Luo, Q., Yu, H., Huang, S., and Li, C. (2021). Research progress on the prediction and analysis of chemical constituents, pharmacological effects and quality markers of *Acori Tatarinowii Rhizoma*. *Chin. Tradit. Pat. Med.* 43, 1286–1290. doi:10.3969/j.issn.1001-1528.2021.05.033

Song, Z., Yin, F., Xiang, B., Lan, B., and Cheng, S. (2018). Systems pharmacological approach to investigate the mechanism of acori tatarinowii rhizoma for Alzheimer's disease. *Evid. Based Complement. Altern. Med.* 2018, 5194016. doi:10.1155/2018/5194016

Tang, Y., Ren, G., Huang, Q., Yang, G., Liu, J., Yuan, J., et al. (2014). GC-MS analysis of the chemical constituents of Acori Tatarinowii Rhizoma volatile oil. *Jiangxi J. Traditional Chin. Med.* 45, 60–62.

Tao, H., Ding, X., Wu, J., Liu, S., Sun, W., Nie, M., et al. (2020). β-Asarone increases chemosensitivity by inhibiting tumor glycolysis in gastric cancer. *Evid. Based Complement. Altern. Med.* 2020, 6981520. doi:10.1155/2020/6981520

Tong, X., and Cheng, Y. (2011). Chemical constituents from Acorus tatarinowii. *Nat. Prod. Res. Dev.* 23, 404–409. doi:10.16333/j.1001-6880.2011.03.004

Tsao, C. W., Aday, A. W., Almarzooq, Z. I., Alonso, A., Beaton, A. Z., Bittencourt, M. S., et al. (2022). Heart disease and stroke statistics-2022 update: A report from the American heart association. *Circulation* 145, e153–e639. doi:10.1161/CIR.0000000000001052

Varma, J., Tripathi, M., Ram, V. J., Pandey, V. B., and Dubey, N. K. (2002). γ-Asarone-the fungitoxic principle of the essential oil of Caesulia axillaris. *World J. Microbiol. Biotechnol.* 18, 277–279. doi:10.1023/A:1014905111973

Wang, B., Pei, K., Wang, X., Chen, L., Qin, K., Wang, Y., et al. (2015). Determination of 26 volatile components in Acori Tatarinowii Rhizoma by gas chromatography-mass spectrometry. *Lishizhen Med. Materia Medica Res.* 26, 2627–2630.

Wang, D., Liu, X., Ji, J., Peng, D., and Zhou, A. (2019). Effect of acori tatarinowii rhizoma on intestinal absorption of ginsenosides in dingzhi xiaowan. *Chin. J. Exp. Traditional Med. Formulae* 25, 7–13. doi:10.13422/j.cnki.syfjx.20190552

Wang, Q., Wu, Q., and Chen, Y. (2008a). Effects of β-asarone mitochondrial membrane potential of cardiac myocytes with ischemia reperfusion injury. *Traditional Chin. Drug Res. Clin. Pharmacol.* 19, 451–454. doi:10.19378/j.issn.1003-9783.2008.06.012

Wang, Q., Wu, Q., and Chen, Y. (2008b). Protective effects of β-asarone against myocardial ischemia/reperfusion injury in cultured cardiac myocytes. *Chin. J. Inf. TCM* 15, 44–46.

Wu, H., Fang, Y., and Li, R. (2004). Pharmacological action and toxicology of acori tatarinowii rhizoma on CNS. *Chin. Archives Traditional Chin. Med.* 22, 127–128+132. doi:10.13193/j.archtcm.2004.01.126.wuhb.059

Wu, J., Zhang, X. X., Sun, Q. M., Chen, M., Liu, S. L., Zhang, X., et al. (2015). β-Asarone inhibits gastric cancer cell proliferation. *Oncol. Rep.* 34, 3043–3050. doi:10.3892/or.2015.4316

Wu, Q., Wang, S., Yuan, D., and Wu, X. (2013). Quality study of volatile oils from rhizoma acori tatarinowii. *J. Guangzhou Univ. Traditional Chin. Med.* 30, 72–77. doi:10.13359/j.cnki.gzxbtcm.2013.01.028

Wu, Q., Yuan, D., Wang, Q., and Wu, X. (2009). Effects of volatile oil of Rhizoma Acori Tatarinowii on morphology and cell viability in cultured cardiac myocytes. *J. Chin. Med. Mater.* 32, 242–245. doi:10.13863/j.issn1001-4454.2009.02.037

Wu, X., Liang, H., Wu, X., Huang, Y., Chen, J., and Liu, C. (2017). The chemical constituents of Acorus tatarinowii. *J. Ningxia Med. Univ.* 39, 53–55. doi:10.16050/j.cnki.issn1674-6309.2017.01.014

Xu, J. (2007). Experimental study on the therapeutic effect of Acori Tatarinowii Rhizoma on bronchial asthma. Hubei. *J. Traditional Chin. Med.* 29, 7–8. doi:10.3969/j.issn.1000-0704.2007.09.003

Yan, L., Hu, Q., Mak, M. S., Lou, J., Xu, S. L., Bi, C. W., et al. (2016). A Chinese herbal decoction, reformulated from Kai-Xin-San, relieves the depression-like symptoms in stressed rats and induces neurogenesis in cultured neurons. *Sci. Rep.* 6, 30014. doi:10.1038/srep30014

Yan, L., Liu, Z., Xu, L., Qian, Y., Song, P., and Wei, M. (2020). Identification of volatile active components in Acori Tatarinowii Rhizome essential oil from different regions in China by C6 glioma cells. *BMC Complement. Med. Ther.* 20, 255. doi:10.1186/s12906-020-03020-4

Yan, L., Mahady, G., Qian, Y., Song, P., Jian, T., Ding, X., et al. (2020). The essential oil from acori tatarinowii rhizome (the dried rhizome of acorus tatarinowii schott) prevents hydrogen peroxide-induced cell injury in PC12 cells: A signaling triggered by CREB/PGC-1 α activation. *Evid. Based Complement. Altern. Med.* 2020, 4845028. doi:10.1155/2020/4845028

Yan, L., Wei, M., Gong, A. G., Song, P., Lou, J., Bi, C. W., et al. (2017). A modified Chinese herbal decoction (Kai-Xin-San) promotes NGF-induced neuronal differentiation in PC12 cells via up-regulating trk A signaling. *Front. Cell. Dev. Biol.* 5, 118. doi:10.3389/fcell.2017.00118

Yang, F., Wang, Z., Li, C., and Liang, J. (2018). The effect of volatile oil of Acori Tatarinowii Rhizoma on the absorption and transport of saikosaponin in Caco-2 cell model. *Mod. Med. Health Res.* 2, 152–154.

Yang, H., Wu, S., Li, H., and Li, G. (2021). Research progress of calamus and prediction analysis of quality markers. *Chin. J. New Drugs* 30, 1213–1219. doi:10.3969/j.issn.1003-3734.2021.13.010

Yin, Z., Wang, X., Zheng, S., Cao, P., Chen, Y., Yu, M., et al. (2020). LongShengZhi capsule attenuates alzheimer-like pathology in APP/PS1 double transgenic mice by

reducing neuronal oxidative stress and inflammation. *Front. Aging Neurosci.* 12, 582455. doi:10.3389/fnagi.2020.582455

Zhang, W., He, J., Hu, Y., Lu, J., Zhao, J., and Li, P. (2022). Chemical structure and immune activation of a glucan from rhizoma acori tatarinowii. *Front. Nutr.* 9, 942241. doi:10.3389/fnut.2022.942241

Zhang, W., Song, D., Xu, D., Wang, T., Chen, L., and Duan, J. (2015). Characterization of polysaccharides with antioxidant and immunological activities from Rhizoma Acori Tatarinowii. *Carbohydr. Polym.* 133, 154–162. doi:10.1016/j.carbpol.2015.07.018

Zhang, X., Yi, L., Deng, B., Chen, L., Shi, S., Zhuang, Y., et al. (2015). Discrimination of Acori Tatarinowii Rhizoma and Acori Calami Rhizoma based on quantitative gas chromatographic fingerprints and chemometric methods. *J. Sep. Sci.* 38, 4078–4085. doi:10.1002/jssc.201500730

Zhang, Y., Long, Y., Yu, S., Li, D., Yang, M., Guan, Y., et al. (2021). Natural volatile oils derived from herbal medicines: A promising therapy way for treating depressive disorder. *Pharmacol. Res.* 164, 105376. doi:10.1016/j.phrs.2020.105376

Zhang, Y., Tong, L., Chen, G., Deng, J., Zhang, L., Li, H., et al. (2022). Analysis of medication rule of primary epilepsy based on xiaocheng yan's clinical experience collection of epilepsy. *Evid. Based Complement. Altern. Med.* 2022, 9539944. doi:10.1155/2022/9539944

Zhang, Y., Wu, Y., Fu, Y., Lin, L., Lin, Y., Ji, L., et al. (2020). Anti-Alzheimer's disease molecular mechanism of acori tatarinowii rhizoma based on network pharmacology. *Med. Sci. Monit. Basic Res.* 26, e924203. doi:10.12659/MSMBR.924203

Zheng, Y., Yu, A., Xu, S., and Qiu, T. (2015). *In vitro* antibacterial activity and anti-inflammatory effect of volatile oil of Acori Tatarinowii Rhizoma. *Strait Pharm. J.* 27, 260–263.

Zhong, R., Wang, X., Wan, L., Shen, C., Shen, B., Wang, J., et al. (2019). Study on preparation of volatile oil from Acorus tatarinowii self-nanoemulsion dropping pills and its protective effect on acute myocardial ischemia injury. *China J. Chin. Materia Medica* 44, 1357–1362. doi:10.19540/j.cnki.cjcmm.20181220.006

Zhu, K. Y., Fu, Q., Xie, H. Q., Xu, S. L., Cheung, A. W., Zheng, K. Y., et al. (2010). Quality assessment of a formulated Chinese herbal decoction, kaixinsan, by using rapid resolution liquid chromatography coupled with mass spectrometry: A chemical evaluation of different historical formulae. *J. Sep. Sci.* 33 (23-24), 3666–3674. doi:10.1002/jssc.201000498

Zhu, K. Y., Mao, Q. Q., Ip, S. P., Choi, R. C., Dong, T. T., Lau, D. T., et al. (2012). A standardized Chinese herbal decoction, kai-xin-san, restores decreased levels of neurotransmitters and neurotrophic factors in the brain of chronic stress-induced depressive rats. *Evid. Based Complement. Altern. Med.* 2012, 149256. doi:10.1155/2012/149256

Zhu, K. Y., Xu, S. L., Choi, R. C., Yan, A. L., Dong, T. T., and Tsim, K. W. (2013). Kai-xin-san, a Chinese herbal decoction containing ginseng radix et rhizoma, polygalae radix, acori tatarinowii rhizoma, and poria, stimulates the expression and secretion of neurotrophic factors in cultured astrocytes. *Evid. Based Complement. Altern. Med.* 2013, 731385. doi:10.1155/2013/731385

Zhu, Y., Duan, X., Cheng, X., Cheng, X., Li, X., Zhang, L., et al. (2016a). Kai-Xin-San, a standardized traditional Chinese medicine formula, up-regulates the expressions of synaptic proteins on hippocampus of chronic mild stress induced depressive rats and primary cultured rat hippocampal neuron. *J. Ethnopharmacol.* 193, 423–432. doi:10.1016/j.jep.2016.09.037

Zhu, Y., Duan, X., Huang, F., Cheng, X., Zhang, L., Liu, P., et al. (2016b). Kai-Xin-San, a traditional Chinese medicine formula, induces neuronal differentiation of cultured PC12 cells: Modulating neurotransmitter regulation enzymes and potentiating NGF inducing neurite outgrowth. *J. Ethnopharmacol.* 193, 272–282. doi:10.1016/j.jep.2016.08.013

Zou, X., Liu, S. L., Zhou, J. Y., Wu, J., Ling, B. F., and Wang, R. P. (2012). Beta-asarone induces LoVo colon cancer cell apoptosis by up-regulation of caspases through a mitochondrial pathway *in vitro* and *in vivo*. *Asian Pac J. Cancer Prev.* 13, 5291–5298. doi:10.7314/apjcp.2012.13.10.5291

Glossary

ATR Acori Tatarinowii Rhizoma
CNKI China National Knowledge Infrastructure
VMIS VIP medicine information system
CBM Chinese Biomedical Database
ATEO The essential oil of ATR
NMR Nuclear magnetic resonance
AD Anti-Alzheimer's disease
BBB Blood-brain barrier
NGF Nerve growth factor
BDNF Brain-derived neurotrophic factor
GDNF Glial-derived neurotrophic factor
Aβ Amyloid beta
tBHP Tert-butyl hydroperoxide
ROS Reactive oxygen species
ARE Anti-oxidant response element
CREB cAMP-response element binding protein
SOD Superoxide dismutase
NO Nitric oxide
NPC Neural progenitor cell
ERK Extracellular signal-regulated kinase
APP Amyloid precursor protein
ESR1 Estrogen receptor 1
PPARG Peroxisome proliferator activated receptor gamma
AR Androgen receptor
CHRM1 Muscarinic acetylcholine receptor M1
CASP3 Caspase 3
JAK2 Janus kinase 2
MAPK14 Mitogen-activated protein kinase 14
PTGS1 Prostaglandin G/H synthase 1
PTPN1 Protein tyrosine phosphatase non-receptor type 1
KDR Kinase domain receptor
ET Endothelin
CGRP Calcitonin gene-related peptide
NE Norepinephrine
MDA Malondialdehyde
CK Creatine kinase
MI/RI Myocardial ischemia/reperfusion injury
LDH Lactate dehydrogenase
MMP Mitochondrial membrane potential
EMT Epithelial-mesenchymal transition
Bax Bcl2-associated X
Bak Bcl-2 homologous antagonist/killer
PDK Pyruvate dehydrogenase kinase
Ach Acetylcholine
Hist Histamine phosphate
TMCA 3,4,5-trimethoxycinnamic acid
PR Polygalae Radix
P-gp P-glycoprotein
TNF-α Tumor necrosis factor alpha
NF-kB Nuclear factor kappa B
LPS Lipopolysaccharide
KXS Kaixin San
XHCYF Xian-He-Cao-Chang-Yan formula5
LSZ Longshengzhi capsule
GR Ginseng Radix
PRP Poria cum Radix Pini
TLR4/IKK/NF-κB Toll-like receptor 4/inhibitor of kappa B kinase/nuclear factor kappa-B
CMS Chronic mild stress
CUMS Chronic unpredictable mild stress
NGF Nerve growth factor
Trk Tropomyosin receptor kinase
XHCF Xian-He-Cao-Chang-Yan formula
DSS Dextran sulfate sodium
UC Ulcerative colitis
AMP Adenosine 5'-monophosphate
AMPK Activated protein kinase
APP Amyloid-β precursor protein
PS1 Presenilin 1
PD Anti-Parkinson's disease
AChE Acetylcholine esterase
CHOL Cholesterol
LDL-C Low-density lipoprotein cholesterol.

frontiers | Frontiers in Pharmacology

TYPE Original Research
PUBLISHED 11 May 2023
DOI 10.3389/fphar.2023.1136446

OPEN ACCESS

EDITED BY
Bey Hing Goh,
Monash University Malaysia, Malaysia

REVIEWED BY
Francis-Alfred Unuagbe Attah,
University of Ilorin, Nigeria
Elaine Elisabetsky,
Federal University of Rio Grande do Sul, Brazil

*CORRESPONDENCE
Yaodong Qi,
ydqi@implad.ac.cn
Weiwei Gao,
wwgao@implad.ac.cn

RECEIVED 03 January 2023
ACCEPTED 04 May 2023
PUBLISHED 11 May 2023

CITATION
Yao R, Heinrich M, Zhang B, Wei X, Qi Y and Gao W (2023), Single botanical drugs in the Ayurvedic Pharmacopoeia of India—A quantitative ethnobotanical analysis.
Front. Pharmacol. 14:1136446.
doi: 10.3389/fphar.2023.1136446

Single botanical drugs in the Ayurvedic Pharmacopoeia of India—A quantitative ethnobotanical analysis

Ruyu Yao[1], Michael Heinrich[2], Bengang Zhang[1], Xueping Wei[1], Yaodong Qi[1]* and Weiwei Gao[1]*

[1]Institute of Medicinal Plant Development, Chinese Academy of Medical Sciences and Peking Union Medical College, Beijing, China, [2]Research Group "Pharmacognosy and Phytotherapy", UCL School of Pharmacy, University of London, London, United Kingdom

Developing evidence-based uses of herbal medicines and natural product-based drug discovery are two core aims of ethnopharmacology. This requires an understanding of the medicinal plants and the traditional medical knowledge associated with them which is a basis for cross-cultural comparison. The botanical drugs of traditional medical systems are still not understood well, even for well-known and widely respected traditions like Ayurveda. In this study, a quantitative ethnobotanical analysis was performed on the single botanical drugs included in the Ayurvedic Pharmacopoeia of India (API), presenting an overview on the medicinal plants of Ayurveda from perspectives of plant systematics and medical ethnobotany. Part-I of API includes 621 single botanical drugs, which are sourced from 393 species (323 genera in 115 families). Of these, 96 species yield two or more drugs, together accounting for 238 drugs. Taking the traditional concepts, biomedical uses and the pragmatic disease classification into account, therapeutic uses of these botanical drugs are sorted into 20 categories, which meet primary health demands. The therapeutic uses of the drugs sourced from the same species may differ considerably, but 30 of the 238 drugs are used in highly similar way. The comparative phylogenetic analysis identifies 172 species with high potential for specific therapeutic uses. This medical ethnobotanical assessment for the first time provides a comprehensive understanding on the single botanical drugs in API from the perspective of medical botany using an "etic" (scientist-oriented) approach. This study also highlights the importance of quantitative ethnobotanic methods in understanding traditional medical knowledge.

KEYWORDS

botanical drug, medical flora, Pharmacopoeia, ayurveda, quantitative ethnobotany

Introduction

Botanical drugs are the most common medical resources used in traditional medical systems, have played a key role in primary healthcare and are still the main sources for new drug discovery (Heinrich and Jäger, 2015; Newman and Cragg, 2020; Atanasov et al., 2021). Single botanical drugs, the botanical drugs sourced from a single plant, are the basic traditional medical materials. The medical usages of one plant are generally based on diverse factors, thus, one given medicinal species will often be used for several purposes, which complicate the evidence-based uses of herbal medicines and natural product-based drug discovery. Consequently, the historical/traditional uses

of botanical drugs provide important clues for new drug discovery and are a core basis for their legal acceptance by regulatory agencies (Jutte et al., 2017; Lenssen et al., 2019). However, the regional knowledge on botanical drugs is often interpreted with heterogenous terms, which may lead to inadequate uses or even the misidentification of the plant species especially in a cross-cultural environment (Rivera et al., 2014; Yao et al., 2021; Heinrich et al., 2022b). A comprehensive understanding the botanical drugs of a medical flora, the botanical drugs used within a tradition, and the traditional and local knowledge associated with this is critical for developing evidence-based uses of herbal medicines and natural product-based drug discovery.

Today 65% of people in rural India still rely on traditional medicines (Sen and Chakraborty, 2015), especially using botanical drugs derived from Ayurveda, but also Siddha and Unani traditions. Globally, Ayurveda is among the most popular traditional medicinal practices. It originated in South Asia and has been known since the Vedic era (ca. 1500 to 600 BCE), as evidenced in the ancient literature such as Charaka Samhita and Sushruta Samhita (National Health Portal of India, 2016; Jaiswal and Williams, 2017). Ayurvedic medical interventions rely on botanical drugs, with approximately ninety percent of its preparations being plant-based, and eighty percent of the Ayurvedic medicines being sourced from plants (Joshi et al., 2017; Kumar et al., 2017). Approximately 7,500 plant species are used medicinally in India, and 2,000 of those are used in Ayurveda, with 700 being used frequently (Sen et al., 2011; Pan et al., 2014). Since 1989, part I of the Ayurvedic Pharmacopoeia of India (API) has published nine volumes (the last one in 2016). It is a crucial reference for the identification and quality control of single drugs used in Ayurveda (Joshi et al., 2017). Part II of API is for the medicated formulations with multi-ingredients, so we did not include it in the present study on single botanical drugs. Previously, Jia et al. (2012) have described the single drugs in the first 7 volumes of part I of API, while Jaiswal et al. (2016) discussed the different usages and processing of selected single botanical drugs in API and China. The above studies have provided an initial understanding on the single botanical drugs in API. However, a systematic scientific understanding on these drugs is still not available, which limits their broader cross-cultural use.

Plants with close phylogenetic relationship are likely to be similar in their metabolome (i.e., share classes of metabolites) and often have similar traditional uses (Zaman et al., 2021). In practice, this complexity might be overlooked in scientific processes which do not encompass an approach capturing a species chemical complexity. One option to overcome this is through comparative phylogeny, which enables the identification of taxa with high potential for specific therapeutic uses, as indicated by phylogenetic clustering (Lei et al., 2020; Zaman et al., 2021). In the present study, the single botanical drugs in API are studied systematically using a quantitative ethnobotanic approach. Moreover, borrowing methods of comparative phylogeny, taxa with high potential for specific therapeutic uses are suggested.

Materials and methods

Data collection

Data of the single botanical drugs were collected from the Part I of API, including 9 volumes as shown in Table 1. For each of the herbal monographs, information on the herbal name, biological origin(s), medicinal plant-part(s), therapeutic use(s) were extracted. The scientific names of the biological origins were then checked against World Flora Online (WFO) using R package "U.Taxonstand" (Zhang and Qian, 2022) with R 4.2.0 (R Core Team, 2022). Since the therapeutic uses of the herbal drugs in volume one to five were only available in Latinized Sanskrit, these terms were translated as follows: 1) to build a Sanskrit-English dictionary with the therapeutic use data in volume six to nine; 2) to translate the therapeutic uses into English with the above dictionary; 3) for those terms which were not included in the above dictionary, search in Wisdom Library (https://www.wisdomlib.org/) manually and cross-checked with the standardization of non-clinical terminologies of ayurveda (National Institute of Ayurveda, 2011). As a result, data including the drug names, biological origins, medicinal plant-parts, as well as the therapeutic uses of all the single botanical drugs in API were compiled (Supplementary Materials S1, S2).

Therapeutic use categorization

While understanding traditional practice clearly and essential aim of any ethnopharmacological study, there now is a long tradition of using an etic categorization in order to allow an understanding of biomedical uses and the future potential of these species (Staub et al., 2015). In anthropological terms "etic" approaches (borrowed from the term phonetic in linguistics) investigate elements of a culture from an outsider's perspective focusing on cross-cultural differences and similarities. Since it provides a global standard, it also enables a comparative analysis (Yao et al., 2021). Additionally, we suggest that the categorization should also consider the traditional concept and the pragmatic category in modern hospital. Finally, these therapeutic uses were sorted into 20 categories, including AND (andrology and male reproductive system), ANT (antidote and problems due to poisoning), CAR (cardiovascular disorders, blood-related diseases), DER (dermatologic disorders, skin problems), EAR (ear and hearing problems), EYE (eye and vision disorders), GAS (gastrointestinal and digestive disorders), GYN (gynecology and female reproductive system), GNR (general complaints including cold, fever, inflammation, headache, etc.), IMM (immune disorders and rheumatism), MET (metabolic and endocrine disorders), NER (nervous system, memory and sleeping problems), ORA (oral and dental problems), PAR (parasitic disease), PED (pediatrics disorders), PSY (psychiatric disorders and mental illness), RES (respiratory system disorders), SKE (skeleto-muscular system disorders), TRA (traditional uses that were not related to modern indications), URO (urinary disorders).

Data analysis

To generate a phylogenetic tree of all species, R package "V.PhyloMaker2" (Jin and Qian, 2022) was used with R 4.2.0 (R Core Team, 2022). And then, with formatted tables (i.e., "sample" and "traits") generated from the data obtained above, this phylogenetic tree was loaded into Phylocom 4.2 (Webb et al., 2008). According to the manual, the following indices for each therapeutic use category were calculated: Faith's phylogenetic diversity (PD), diversity weighted by interspecific phylogenetic distances (Dp), mean pairwise

TABLE 1 The 9 volumes of the Ayurvedic Pharmacopoeia of India (part I).

Volume	Contents	References
1	80 monographs for single drugs	Ministry of HFW (1986)
2	78 monographs for single drugs	Ministry of HFW (1999)
3	100 monographs for single drugs	Ministry of HFW (2001)
4	68 monographs for single drugs	Ministry of HFW (2004)
5	92 monographs for single drugs	Ministry of HFW (2006)
6	101 monographs for single drugs	Ministry of HFW (2008a)
7	21 monographs for single drugs (minerals or metals)	Ministry of HFW (2008b)
8	60 monographs, for 15 single drugs and their extracts	Ministry of HFW (2011)
9	45 monographs, for 15 single drugs and their extracts	Ministry of AYUSH (2016)

trait distance among taxa (MPD), net relatedness index (NRI), mean distance to nearest neighbor trait distance (MNTD) and nearest taxon index (NTI). Additionally, "hot nodes," which mean the nodes with significantly more taxa than random probability for specific therapeutic uses were detected as marked with "SIGMORE" (Webb et al., 2008). Data visualization was performed using iTOL (Letunic and Bork, 2021).

To evaluate the therapeutic similarity of drugs sourced from the same species, the pairwise Jaccard Index (JI) was calculated based on their categorized therapeutic uses data, using the R package "sets." And then, those JI of the same species were selected manually (as highlighted in Supplementary Material S3), thereafter, a distribution histogram of these JI values were plotted with interval of 0.1 was plotted using Microsoft Excel 365. A Cullen and Frey graph was then mapped to test the distribution pattern using R package "fitdistrplus" (Delignette-Muller & Dutang, 2015) with R 4.2.0 (R Core Team, 2022).

Results

An overview of the single drugs in API

Part I of API consists of 645 monographs for single drugs or extracts, and almost all of these are single botanical drugs except the following 27: 1) Volume VII records 21 drugs sourced exclusively from minerals or metals; 2) volume VI includes three non-botanical drugs (i.e., butter, water and honey; 3) volume VI includes two drugs which are the mixture of plant extracts from two families thus they are not "single"; 4) volume III includes one drug which is the fungal part of a lichen. Besides, different parts of three botanical drugs were with distinguishable therapeutic uses, so these different parts were treated as individual botanical drugs. As a result, 621 single botanical drugs were identified in API in total (A list of these 621 drugs is provided in Supplementary Material S1).

Taxonomic diversity of biological sources for the single botanical drugs in API

The 621 single botanical drugs in API are sourced from 393 species in 323 genera and 115 families based on APG IV—the current Angiosperm Phylogeny Group's classification (Figure 1). With 47 species, Fabaceae is the largest source family of these botanical drugs, which is followed by Apiaceae (16), Poaceae (15), Euphorbiaceae (13), Lamiaceae (13), Asteraceae (13), Apocynaceae (13), Cucurbitaceae (11), Malvaceae (10), Zingiberaceae (10), Solanaceae (9), and Moraceae (8). The top 12 families together contribute 178 species which constitute 45.3% of the total source species. Other families such as Acanthaceae, Arecaceae, Anacardiaceae, Rubiaceae, Amaranthaceae, Araceae, Combretaceae, Convolvulaceae and Piperaceae contribute less species to the Ayurvedic medical flora.

As expected, some large families with distinct species like the Fabaceae, Euphorbiaceae, Lamiaceae and Asteraceae are commonly included, but some with a less distinct characteristics like the Poaceae and some smaller but very characteristic families like the Zingiberaceae are also present. It is worth noting that as many as 75 families contribute only one or two species, and these families have increased the phylogenetic diversity of the Ayurvedic medical flora largely.

Medicinal plant-parts of the single botanical drugs in API

In terms of the medicinal part, the 621 single botanical drugs (Figure 2) include125 roots, (20%) making it the most commonly used medicinal part. Fruit rank second (85 drugs; 14%). These are followed by whole plant (13%), stem (12%), leaf (11%), bark (10%), and seed (10%).

Therapeutic uses of the single botanical drugs in API

Taking the traditional concepts, biomedical uses and the pragmatic disease classification into account, therapeutic uses of the botanical drugs were sorted into 20 categories (Figure 3). There are 293 species of 95 families used in GAS (75% of all species and 82% of all families). This is followed by that of GNR (255 species, 89 families), DER (250 species, 91 families), MET (227 species,

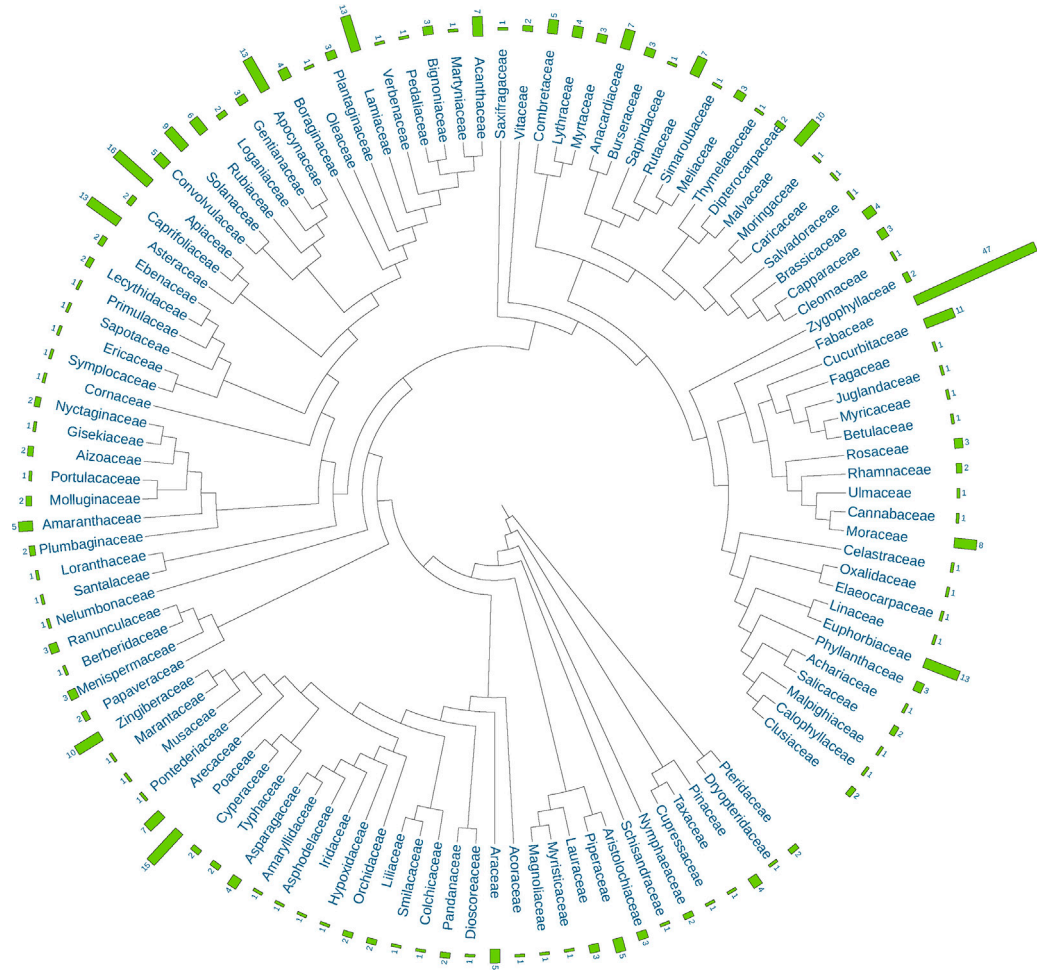

FIGURE 1
Composition of plant families and species for single botanical drugs in the Ayurvedic Pharmacopoeia of India (API).

81 families), CAR (201 species, 81 families), RES (181 species, 68 families), PAR (134 species, 58 families), and URO (125 species, 61 families). Interestingly, the above-mentioned therapeutic uses, which are linked to more species or families than the rest, are with a higher average species per family, ranging from 3.1 to 2.0; conversely, for those uses linking to less species and families, the average species per family are below 2.0.

The similarity in therapeutic uses of drugs sourced from the same species

Different parts of 96 plant species are used as two or more drugs. For example, the root and the seed of *Abrus precatorius* L. are used as two drugs, separately; the ripe and unripe fruit of *Diospyros malabarica* (Desr.) Kostel are recorded as one drug but with different therapeutic uses, so we treat them as two single drugs. Volumes VIII and IX of API include 15 botanical drugs and their processed products (*i.e.*, powder, hydro-alcoholic extract, and water extract) respectively, and we treat these powders and extracts as the same drug with their original drug. In total, 238 single botanical drugs of API are sourced from these 96 species. The pairwise Jaccard Index (JI) was calculated to evaluate the similarity between every two drugs (Supplementary Material S3, note the ones sourced from the same species are highlighted). Figure 4 shows the distribution of pairwise JI values of the drugs from the same species.

Accordingly, the average value of all the 215 JI values is 0.54617, suggesting that drugs of the same species differ in their therapeutic uses. However, these values fit for beta distribution instead of Normal distribution. There are 30 JI values at the region (0.9–1.0], indicating that many of these drugs from the same species are still used highly similarly. For example, leaf, stem, aerial part and flower of *Dendrophthoe falcata* (L.f.) Ettingsh are recorded as four drugs separately, but they have very similar therapeutic uses; however, the therapeutic uses of its fruit are distinguishable. In other cases, the low JI values indicate the different therapeutic uses of drugs from the same species. For example, the seed and whole plant of *Datura metel* L. only have one common therapeutic use for PAR, and their JI value is 0.1. As is shown in Figure 4A, only four of these drugs are with distinct therapeutic uses, *viz.* the seed and whole plant of *D. metel* L., and the root and the stem of *Saccharum officinarum* L. As a result, the

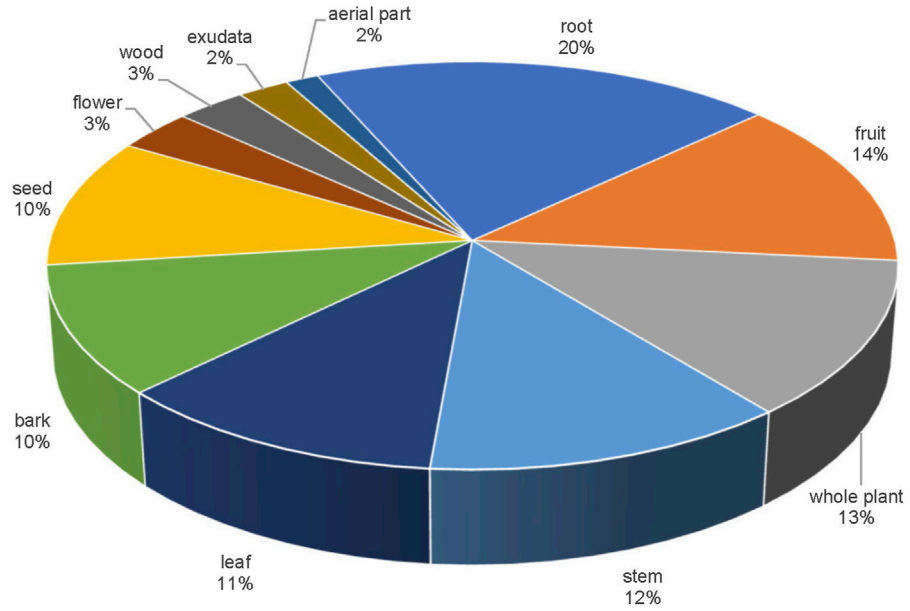

FIGURE 2
Constitution of medicinal parts for the single botanical drugs in API.

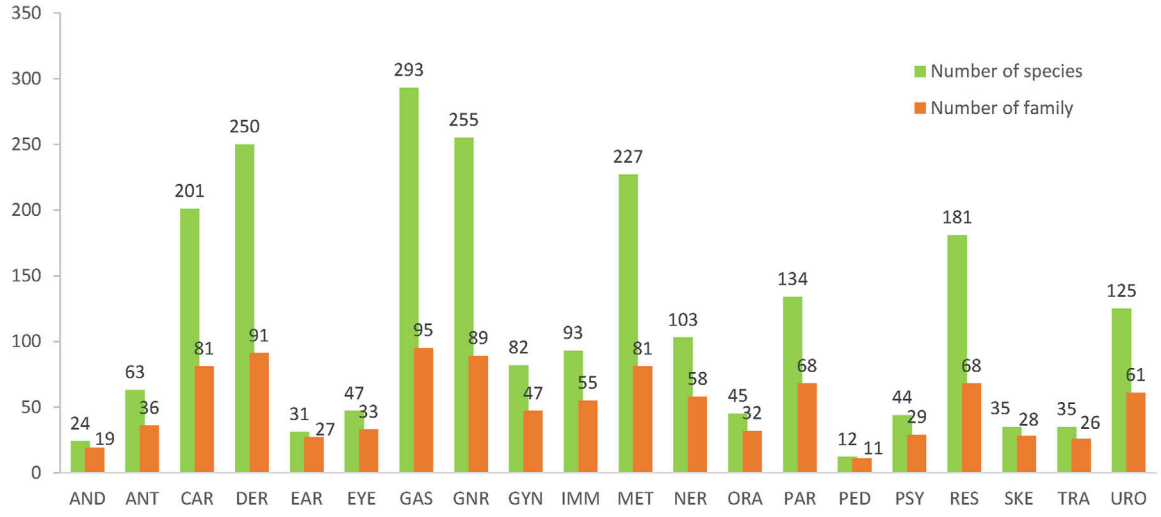

FIGURE 3
The numbers of species/families used for the therapeutic uses in API.

therapeutic uses of the drugs sourced from the same species may differ to different extent.

Phylogenetic diversity and structure of the source plants of the single botanical drugs in API

Indices for phylogenetic diversity and structure of the source species of the single botanical drugs in API (Table 2) indicate the Ayurvedic medicinal plants for different therapeutic uses distribute evenly in the perspective of phylogeny. Faith's phylogenetic diversity (PD) correlates with the numbers of species (Nsp) positively, fitting the formula PD = 44.836*Nsp +2,197.3 (R^2 = 0.9833) and this linear relationship hints that the phylogenetic distances between the species are even. This evenness is also supported by the similar Dp values which range from 110 to 142. Similarly, values of mean pairwise trait distance among taxa (MPD) also fluctuate slightly, while values of the mean distance to nearest neighbor trait distance (MNTD) are with relative larger fluctuation. Net Relatedness Index

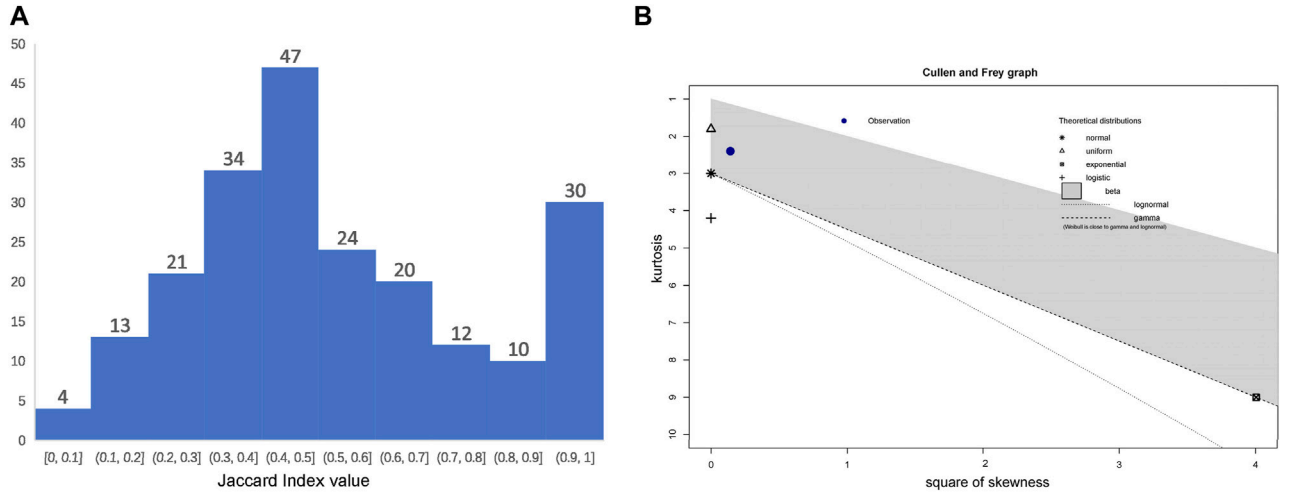

FIGURE 4
Distribution of Jaccard Index (JI) values of the botanical drugs from the same species. **(A)** the histogram; **(B)** a Cullen and Frey graph.

TABLE 2 Indices for phylogenetic diversity and structure of the source plants of the single botanical drugs in API.

Site	Nsp	PD	Dp	MPD	NRI	MNTD	NTI
ALL	393	18765.34	131.88	264.43	0.9995	61.68	0.9995
AND	24	2480.24	117.39	244.98	0.6997	157.66	0.2298
ANT	63	5044.97	133.93	272.17	−0.5123	105.79	1.3870
CAR	201	11966.57	132.83	267.00	−0.4594	74.86	1.5728
DER	250	13495.03	130.95	262.95	0.2306	71.16	1.2967
EAR	31	3198.60	128.78	266.15	−0.0890	156.61	−0.2516
EYE	47	4184.65	125.91	257.28	0.3816	132.53	0.1500
GAS	293	15082.26	132.10	265.10	−0.1841	65.45	2.0526
GNR	255	13565.71	129.71	260.44	0.9152	71.98	0.7149
GYN	82	5978.06	129.91	263.03	0.1332	96.41	1.6847
IMM	93	7497.75	134.63	272.19	−0.6370	111.51	−0.5217
MET	227	12305.72	132.67	266.50	−0.3181	67.28	2.9931
NER	103	7643.13	135.95	274.56	−0.9384	106.09	−0.3789
ORA	45	4297.89	127.04	259.85	0.2454	146.78	−0.7199
PAR	134	9205.82	138.41	278.90	−1.5691	96.78	−0.4259
PED	12	1477.36	110.68	241.49	0.5930	166.16	0.8324
PSY	44	4191.30	137.91	282.23	−0.8910	140.39	−0.1611
RES	181	10411.27	132.77	267.02	−0.3242	77.24	1.6584
SKE	35	3692.30	142.50	293.39	−1.3157	141.90	0.3498
TRA	35	3205.85	118.51	243.99	0.9674	127.97	1.0970
URO	125	8299.06	125.44	252.91	1.1770	94.45	0.3384

Nsp, number of species; PD, faith's phylogenetic diversity; Dp, diversity weighted by interspecific phylogenetic distances; MPD, mean pairwise trait distance among taxa; NRI, net Relatedness Index; MNTD, mean distance to nearest neighbor trait distance; NTI, nearest Taxon Index.

TABLE 3 Number of species in hot nodes by family and the hot nodes hits of each therapeutic category.

Family	Hot nodes hits[#]	Number of species in hot nodes	AND	ANT	CAR	DER	EAR	EYE	GNR	GYN	IMM	MET	NER	ORA	PAR	PSY	RES	SKE	TRA	URO
Moraceae	32	8	0	0	8	8	0	0	0	8	0	8	0	0	0	0	0	0	0	0
Apocynaceae	31	13	0	0	0	13	0	0	13	0	0	0	0	5	0	0	0	0	0	0
Poaceae	29	15	0	0	0	0	0	0	0	0	0	15	0	0	0	0	0	0	0	14
Fabaceae	22	18	18	0	0	0	0	2	0	0	0	0	0	0	0	2	0	0	0	0
Asteraceae	20	13	0	0	0	0	0	0	13	0	0	0	7	0	0	0	0	0	0	0
Apiaceae	19	11	0	0	0	0	0	0	11	0	0	0	5	0	0	0	0	0	3	0
Lamiaceae	18	7	0	4	0	0	0	0	0	0	0	0	0	0	4	3	0	0	3	4
Acanthaceae	14	7	0	0	0	0	7	0	0	0	7	0	0	0	0	0	0	0	0	0
Cucurbitaceae	11	11	0	0	0	0	0	0	0	0	0	11	0	0	0	0	0	0	0	0
Zingiberaceae	10	10	0	0	0	0	0	0	0	0	0	0	0	0	0	0	10	0	0	0
Pinaceae	6	4	0	0	0	0	0	0	0	0	0	0	0	0	4	0	0	2	0	0
Piperaceae	5	5	0	0	0	0	0	0	5	0	0	0	0	0	0	0	0	0	0	0
Convolvulaceae	5	5	0	0	0	0	0	0	0	0	0	0	5	0	0	0	0	0	0	0
Dipterocarpaceae	4	2	0	2	0	0	2	0	0	0	0	0	0	0	0	0	0	0	0	0
Cyperaceae	4	2	0	0	0	0	0	0	0	0	0	2	0	0	0	0	0	0	0	2
Typhaceae	4	2	0	0	0	0	0	0	0	0	0	2	0	0	0	0	0	0	0	2
Ebenaceae	4	2	0	0	0	0	0	0	0	0	0	0	0	0	0	0	0	2	2	0
Lauraceae	3	3	3	0	0	0	0	0	0	0	0	0	0	0	0	0	0	0	0	0
Meliaceae	3	3	0	3	0	0	0	0	0	0	0	0	0	0	0	0	0	0	0	0
Gentianaceae	3	3	0	0	0	3	0	0	0	0	0	0	0	0	0	0	0	0	0	0
Bignoniaceae	3	3	0	0	0	0	3	0	0	0	0	0	0	0	0	0	0	0	0	0
Aristolochiaceae	3	3	0	0	0	0	0	0	3	0	0	0	0	0	0	0	0	0	0	0
Pteridaceae	2	2	0	2	0	0	0	0	0	0	0	0	0	0	0	0	0	0	0	0
Brassicaceae	2	2	0	0	0	0	0	2	0	0	0	0	0	0	0	0	0	0	0	0
Cannabaceae	2	1	0	0	0	0	0	0	0	1	0	1	0	0	0	0	0	0	0	0
Rhamnaceae	2	2	0	0	0	0	0	0	0	0	0	2	0	0	0	0	0	0	0	0

(Continued on following page)

10.3389/fphar.2023.1136446

TABLE 3 (*Continued*) Number of species in hot nodes by family and the hot nodes hits of each therapeutic category.

Family	Hot nodes hits[#]	Number of species in hot nodes	AND	ANT	CAR	DER	EAR	EYE	GNR	GYN	IMM	MET	NER	ORA	PAR	PSY	RES	SKE	TRA	URO
Caprifoliaceae	2	2	0	0	0	0	0	0	0	0	0	0	0	0	0	2	0	0	0	0
Magnoliaceae	1	1	1	0	0	0	0	0	0	0	0	0	0	0	0	0	0	0	0	0
Simaroubaceae	1	1	0	1	0	0	0	0	0	0	0	0	0	0	0	0	0	0	0	0
Martyniaceae	1	1	0	0	0	0	1	0	0	0	0	0	0	0	0	0	0	0	0	0
Pedaliaceae	1	1	0	0	0	0	1	0	0	0	0	0	0	0	0	0	0	0	0	0
Verbenaceae	1	1	0	0	0	0	1	0	0	0	0	0	0	0	0	0	0	0	0	0
Loranthaceae	1	1	0	0	0	0	0	1	0	0	0	0	0	0	0	0	0	0	0	0
Santalaceae	1	1	0	0	0	0	0	1	0	0	0	0	0	0	0	0	0	0	0	0
Ulmaceae	1	1	0	0	0	0	0	0	0	0	0	1	0	0	0	0	0	0	0	0
Cupressaceae	1	1	0	0	0	0	0	0	0	0	0	0	0	0	1	0	0	0	0	0
Taxaceae	1	1	0	0	0	0	0	0	0	0	0	0	0	0	1	0	0	0	0	0
Marantaceae	1	1	0	0	0	0	0	0	0	0	0	0	0	0	0	0	1	0	0	0
Musaceae	1	1	0	0	0	0	0	0	0	0	0	0	0	0	0	0	1	0	0	0
Pontederiaceae	1	1	0	0	0	0	0	0	0	0	0	0	0	0	0	0	1	0	0	0
Total	276	172	22	12	8	24	15	6	45	9	7	42	17	5	10	7	13	4	8	22

"Hot nodes" were found by phylocom 4.2, one species may be "hot nodes" of several therapeutic categories. A detailed list of these species in hot nodes is presented in Supplementary Material S4.

10.3389/fphar.2023.1136446

(NRI) and Nearest Taxon Index (NTI) are indices for indicating the significant clustering. Specifically, values below −1.96 indicate significant "over-dispersal" while values above 1.96 indicate significant "clustering." As are shown in Table 2, there is no significant "over-dispersal" or "clustering" except for those of GAS and MET, which are clustering significantly.

The algorithm "nodesig" in phylocom allows for finding the taxa of "hot nodes," which were hypothesized to have higher potential for specific therapeutics. Accordingly, 172 species were found out in "hot nodes," contributing 276 "hot nodes" hits for 20 of the therapeutic categories. Table 3 shows the number of these species by family and their hot nodes hits of each therapeutic category.

The results show many useful clues for the relationship between families and therapeutic uses. Eight species of Moraceae contributing the most hot nodes hits (32) to CAR, DER, GYN and MET, suggesting Moraceae's potential functions in the above therapeutic uses; 13 species of Apocynaceae are found to be hot nodes of DER, GNR and ORA; almost all the hot nodes species of Poaceae are found to linked with MET and URO; 18 species of Fabaceae are with high potential for the therapeutic use of AND, which 2 of them are also for EYE. Several species are found to be related to more than one therapeutic use. For example, *Artocarpus heterophyllus* Lam. (Moraceae) is "hot" for CAR, DER, GYN and MET, *Coleus forskohlii* (Willd.) Briq. (Lamiaceae) for ANT, PAR, PSY and URO, *Ocimum tenuiflorum* L. (Lamiaceae) for ANT, PAR, PSY and URO, highlighting their multiple functions. With regards to the therapeutic categories, GNR and MET have the most hot nodes species (45 and 42 separately), this might because of the frequent occurrence rate of related diseases such as fever. Hot nodes species of GNR are commonly found in the Apocynaceae (13), Asteraceae (13), Apiaceae (11) and Piperaceae (5), while those for MET are from the Moraceae (8), Poaceae (15), Cucurbitaceae (11), Cyperaceae (2) and Typhaceae (2). Additionally, there are 13 families that have only one hot nodes species for one therapeutic category. It is worth noting that no hot taxon was found for GAS or PED, which can be accounted for based on different reasons: (a) There are 293 species (accounting for 74.5% of all the 393 species) with the therapeutic use for GAS, while the algorithm "nodesig" does not detect any "hot nodes," hinting that no taxonomic preference for these species; (b) differently, only 12 species are used for PED, which is not sufficient for finding out the phylogenetic distribution pattern.

Discussion

Ayurveda has provided medical services for people of South Asia for thousands of years. Currently, Ayurveda is embedded in the Indian national traditional medical system, and has been increasingly accepted globally since it offers a perspective on a "healthy lifestyle" instead of allopathy (Jaiswal and Williams, 2017). As a key reference for identification and quality control, part I of API records the most commonly used Ayurvedic single drugs. While it was reported that 70% of the Indian medicines are sourced from natural sources, and plant-derived drugs comprise 80% of the Ayurvedic medicines (Joshi et al., 2017; Sen and Chakraborty, 2017). Here, we find 621 single botanical drugs from all the 645 pharmacopeial monographs, and this high proportion highlights the importance of botanical drugs in Ayurveda.

The biological sources of the single botanical drugs are highly diverse. Previous studies have provided partial understanding on Ayurvedic medicines (Jia et al., 2012; Jaiswal et al., 2016). By systematizing the biological sources and indications of all the single botanical drugs in API and analysing their uses in terms of plant systematics, our study has made a vital step forward for a cross-cultural understanding of these medicinal knowledge system. It is expected that this fundamental information on Ayurvedic medical flora provided by the current study will foster the further development of Indian herbal resources.

The application of comparative phylogeny allows for refining the high potential taxa for specific therapeutic uses. This method has been used for comparative studies among medical floras and is found to be sufficient for predicting the plants with high medical value from a regional flora (Saslis-Lagoudakis et al., 2012; Lei et al., 2020). Differently, the present study focuses on the commonly used single botanical drugs without considering the regional flora, and the analysis is for refining of the traditional medicinal information. This is similar to the study on exploration of Chinese medical flora (Zaman et al., 2021). However, unpredicted results are also found. As a result, our directional results provide useful clues for bioprospecting of the botanical drugs. Our study also indicates that this method is a pragmatic tool for quantitative ethnobotanic studies, especially in compiling the traditional uses of a large number of plants with different levels of phylogenetic relationship.

The sharing of traditional medical knowledge and cross-cultural collaboration is essential in an era of globalization since health threats are a common challenge to all. However, without a cross-culturally usable or "standard" terminology transforming, the traditional health knowledge is difficult to be accepted cross-culturally or developed scientifically (Yao et al., 2021; Heinrich et al., 2022a; Heinrich et al., 2022b; Yao et al., 2023). While we clearly need a culture-specific expression of medical uses, as soon as such uses are to be compared cross-culturally, a standard terminology is essential. This study systematises the traditional herbal knowledge of Ayurveda using an etic view, which is expected to accelerate the global recognition of Ayurvedic botanical drugs.

Conclusion

For the first time, the present work reports a systematic understanding on the single botanical drugs in API, which represent the medical flora of Ayurveda and are important global medical resources. We have clarified the single botanical drugs and their biological origins, as well as their standard therapeutic uses; additionally, the taxa with high potential of medical values for some specific therapeutic uses are predicted. Finally, we provide a ready-to-use medical ethnobotanical information on the Ayurvedic botanical drugs.

An increasing number of traditional, local herbal medicines are entering markets globally. The cross-cultural understanding on their traditional herbal knowledge is a core foundation for understanding such developments. Quantitative ethnobotanic methods are useful in understanding traditional herbal knowledge by providing standard outcomes which can form a basis for a cross-cultural comparison. Of course, such approaches are science- oriented (etic) and we do not address culture specific meaning aspects. The extending use of this methodology is expected to help in understanding the regional used traditional herbal medicines.

Data availability statement

The original contributions presented in the study are included in the article/Supplementary Material, further inquiries can be directed to the corresponding authors.

Ethics statement

This study does not use animal or human subjects, or any special genetic resources. All data are already in the public domain and readily available whit no confidential or personal information being included. All assessments are performed conforming to the national/international legislation, and no special permission was required.

Author contributions

RY, YQ, WG, BZ, and MH developed the initial idea of this study. RY, XW, and YQ performed the data collection and data analysis. RY, YQ, and MH drafted the manuscript. BZ and WG supervised the work. All authors revised the manuscript. All authors listed have made a substantial, direct, and intellectual contribution to the work and approved it for publication. All authors contributed to the article and approved the submitted version.

Funding

This study is supported financially by Chinese National Science and Technology Fundamental Resources Investigation Program (2018FY100703) and Senior Foreign Expert Introduction Program 2022 (G2022194013L).

Acknowledgments

The author RY would like to thank Prof. Peigen Xiao from IMPLAD for his insightful suggestions, Roy Upton RH, DipAyu from American Herbal Pharmacopoeia for his kind help in data collection, and Dr. Xinning Zhao for her valuable help in editing.

Conflict of interest

The authors declare that the research was conducted in the absence of any commercial or financial relationships that could be construed as a potential conflict of interest.

Publisher's note

All claims expressed in this article are solely those of the authors and do not necessarily represent those of their affiliated organizations, or those of the publisher, the editors and the reviewers. Any product that may be evaluated in this article, or claim that may be made by its manufacturer, is not guaranteed or endorsed by the publisher.

Supplementary material

The Supplementary Material for this article can be found online at: https://www.frontiersin.org/articles/10.3389/fphar.2023.1136446/full#supplementary-material

References

Atanasov, A. G., Zotchev, S. B., Dirsch, V. M., and Supuran, C. T.International Natural Product Sciences Taskforce (2021). Natural products in drug discovery: Advances and opportunities. *Nat. Rev. Drug Discov.* 20 (3), 200–216. doi:10.1038/s41573-020-00114-z

Delignette-Muller, M. L., and Dutang, C. (2015). **Fitdistrplus**: An*R*Package for fitting distributions. *Stat. Softw.* 64 (4), 1–34. doi:10.18637/jss.v064.i04

Heinrich, M., and Jäger, A. K. (2015). *Ethnopharmacology*. New York, NY: John Wiley & Sons, Ltd.

Heinrich, M., Kum, K. Y., and Yao, R. (2022a). "Decontextualized Chinese medicines – their uses as health foods and medicines in the 'global west," in *Routledge handbook of Chinese medicine*. Editors V. Lo and M. Stanley-Baker (Abingdon: Routledge), 721–741.

Heinrich, M., Yao, R., and Xiao, P. (2022b). 'Food and medicine continuum' – why we should promote cross-cultural communication between the global east and west. *Chin. Herb. Med.* 14 (1), 3–4. doi:10.1016/j.chmed.2021.12.002

Jaiswal, Y., Liang, Z., and Zhao, Z. (2016). Botanical drugs in ayurveda and traditional Chinese medicine. *J. Ethnopharmacol.* 194, 245–259. doi:10.1016/j.jep.2016.06.052

Jaiswal, Y. S., and Williams, L. L. (2017). A glimpse of ayurveda - the forgotten history and principles of Indian traditional medicine. *J. Tradit. Complement. Med.* 7 (1), 50–53. doi:10.1016/j.jtcme.2016.02.002

Jia, M., Wang, Z., Kuang, T., and Zhang, Y. (2012). A comparative study on the drugs in the ayurvedic pharmacopoeia of India and the corresponding traditional medicines in China (in Chinese). *J. Chin. Ethn. Med.* 18 (5), 14–25. doi:10.16041/j.cnki.cn15-1175.2012.05.039

Jin, Y., and Qian, H. (2022). V.PhyloMaker2: An updated and enlarged R package that can generate very large phylogenies for vascular plants. *Plant Divers.* 44, 335–339. doi:10.1016/j.pld.2022.05.005

Joshi, V. K., Joshi, A., and Dhiman, K. S. (2017). The ayurvedic pharmacopoeia of India, development and perspectives. *J. Ethnopharmacol.* 197, 32–38. doi:10.1016/j.jep.2016.07.030

Jutte, R., Heinrich, M., Helmstadter, A., Langhorst, J., Meng, G., Niebling, W., et al. (2017). Herbal medicinal products - evidence and tradition from a historical perspective. *J. Ethnopharmacol.* 207, 220–225. doi:10.1016/j.jep.2017.06.047

Kumar, S., Dobos, G. J., and Rampp, T. (2017). The significance of ayurvedic medicinal plants. *J. Evid. Based Complement. Altern. Med.* 22 (3), 494–501. doi:10.1177/2156587216671392

Lei, D., Al Jabri, T., Teixidor-Toneu, I., Saslis-Lagoudakis, C. H., Ghazanfar, S. A., and Hawkins, J. A. (2020). Comparative analysis of four medicinal floras: Phylogenetic methods to identify cross-cultural patterns. *Plants, People, Planet* 2 (6), 614–626. doi:10.1002/ppp3.10131

Lenssen, K. G. M., Bast, A., and de Boer, A. (2019). International perspectives on substantiating the efficacy of herbal dietary supplements and herbal medicines through evidence on traditional use. *Compr. Rev. Food Sci. Food Saf.* 18 (4), 910–922. doi:10.1111/1541-4337.12446

Letunic, I., and Bork, P. (2021). Interactive tree of life (iTOL) v5: An online tool for phylogenetic tree display and annotation. *Nucleic. Acids Res.* 49 (1), W293–W296. doi:10.1093/nar/gkab301

Ministry of AYUSH (2016). *The ayurvedic pharmacopoeia of India (Part I, volume IX)*. Ghaziabad: Pharmacopoeia Commission for Indian Medicine & Homoeopathy.

Ministry of HFW (1986). *The ayurvedic pharmacopoeia of India (Part I, volume I)*. New Delhi: Ministry of Health and Family Welfare, Government of India.

Ministry of HFW (1999). *The ayurvedic pharmacopoeia of India (Part I, volume II)*. New Delhi: Ministry of Health and Family Welfare, Government of India.

Ministry of HFW (2001). *The ayurvedic pharmacopoeia of India (Part I, volume III)*. New Delhi: Ministry of Health and Family Welfare, Government of India.

Ministry of HFW (2004). *The ayurvedic pharmacopoeia of India (Part I, volume IV)*. New Delhi: Ministry of Health and Family Welfare, Government of India.

Ministry of HFW (2006). *The ayurvedic pharmacopoeia of India (Part I, volume V)*. New Delhi: Ministry of Health and Family Welfare, Government of India.

Ministry of HFW (2008a). *The ayurvedic pharmacopoeia of India (Part I, volume VI)*. New Delhi: Ministry of Health and Family Welfare, Government of India.

Ministry of HFW (2008b). *The ayurvedic pharmacopoeia of India (Part I, volume VII)*. New Delhi: Ministry of Health and Family Welfare, Government of India.

Ministry of HFW (2011). *The ayurvedic pharmacopoeia of India (Part I, volume VIII)*. New Delhi: Ministry of Health and Family Welfare, Government of India.

National Health Portal of India (2016). Origin of ayurveda. Available at: https://www.healthonnet.org/HONcode/Conduct.html?HONConduct878982.

National Institute of Ayurveda (2011). *Standardization of non-clinical terminologies of ayurveda*. Jaipur: National Institute of Ayurveda.

Newman, D. J., and Cragg, G. M. (2020). Natural products as sources of new drugs over the nearly four decades from 01/1981 to 09/2019. *J. Nat. Prod.* 83 (3), 770–803. doi:10.1021/acs.jnatprod.9b01285

Pan, S. Y., Litscher, G., Gao, S. H., Zhou, S. F., Yu, Z. L., Chen, H. Q., et al. (2014). Historical perspective of traditional indigenous medical practices: The current renaissance and conservation of herbal resources. *Evid. Based Complement. Altern. Med.* 2014, 525340. doi:10.1155/2014/525340

R Core Team (2022). *R: A language and environment for statistical computing R foundation for statistical computing*. Vienna, Austria: R Core Team.

Rivera, D., Allkin, R., Obon, C., Alcaraz, F., Verpoorte, R., and Heinrich, M. (2014). What is in a name? The need for accurate scientific nomenclature for plants. *J. Ethnopharmacol.* 152 (3), 393–402. doi:10.1016/j.jep.2013.12.022

Saslis-Lagoudakis, C. H., Savolainen, V., Williamson, E. M., Forest, F., Wagstaff, S. J., Baral, S. R., et al. (2012). Phylogenies reveal predictive power of traditional medicine in bioprospecting. *Proc. Natl. Acad. Sci. U. S. A.* 109 (39), 15835–15840. doi:10.1073/pnas.1202242109

Sen, S., Chakraborty, R., and De, B. (2011). Challenges and opportunities in the advancement of herbal medicine: India's position and role in a global context. *J. Herb. Med.* 1 (3-4), 67–75. doi:10.1016/j.hermed.2011.11.001

Sen, S., and Chakraborty, R. (2017). Revival, modernization and integration of Indian traditional herbal medicine in clinical practice: Importance, challenges and future. *J. Tradit. Complement. Med.* 7 (2), 234–244. doi:10.1016/j.jtcme.2016.05.006

Sen, S., and Chakraborty, R. (2015). Toward the integration and advancement of herbal medicine: A focus on traditional Indian medicine. *Botanics Targets Ther.* 5, 33–44. doi:10.2147/BTAT.S66308

Staub, P. O., Geck, M. S., Weckerle, C. S., Casu, L., and Leonti, M. (2015). Classifying diseases and remedies in ethnomedicine and Ethnopharmacology. *J. Ethnopharmacol.* 174, 514–519. doi:10.1016/j.jep.2015.08.051

Webb, C. O., Ackerly, D. D., and Kembel, S. W. (2008). Phylocom: Software for the analysis of phylogenetic community structure and trait evolution. *Bioinformatics* 24 (18), 2098–2100. doi:10.1093/bioinformatics/btn358

Yao, R., He, C., and Xiao, P. (2023). 'Food and medicine continuum' in the east and west: Old tradition and current regulation. *Chin. Herb. Med.* 15 (1), 6–14. doi:10.1016/j.chmed.2022.12.002

Yao, R., Heinrich, M., Wei, J., and Xiao, P. (2021). Cross-cultural ethnobotanical assembly as a new tool for understanding medicinal and culinary values - the genus *lycium* as a case study. *Front. Pharmacol.* 12, 708518. doi:10.3389/fphar.2021.708518

Zaman, W., Ye, J., Saqib, S., Liu, Y., Shan, Z., Hao, D., et al. (2021). Predicting potential medicinal plants with phylogenetic topology: Inspiration from the research of traditional Chinese medicine. *J. Ethnopharmacol.* 281, 114515. doi:10.1016/j.jep.2021.114515

Zhang, J., and Qian, H. (2022). U.Taxonstand: An R package for standardizing scientific names of plants and animals. *Plant Divers.* 45, 1–5. doi:10.1016/j.pld.2022.09.001

frontiers | Frontiers in Pharmacology

TYPE Original Research
PUBLISHED 24 July 2023
DOI 10.3389/fphar.2023.1131479

OPEN ACCESS

EDITED BY
Uraiwan Panich,
Mahidol University, Thailand

REVIEWED BY
Bin Yang,
Zaozhuang University, China
Maria Bove,
University of Foggia, Italy
Laiba Arshad,
Forman Christian College, Pakistan

*CORRESPONDENCE
Su-Xiang Feng,
fengsx221@163.com
Jian-Sheng Li,
li_js8@163.com

†These authors have contributed equally to this work and share first authorship

RECEIVED 25 December 2022
ACCEPTED 07 July 2023
PUBLISHED 24 July 2023

CITATION
Han X-X, Tian Y-G, Liu W-J, Zhao D, Liu X-F, Hu Y-P, Feng S-X and Li J-S (2023), Metabolomic profiling combined with network analysis of serum pharmacochemistry to reveal the therapeutic mechanism of Ardisiae Japonicae Herba against acute lung injury.
Front. Pharmacol. 14:1131479.
doi: 10.3389/fphar.2023.1131479

Metabolomic profiling combined with network analysis of serum pharmacochemistry to reveal the therapeutic mechanism of Ardisiae Japonicae Herba against acute lung injury

Xiao-Xiao Han[1,2†], Yan-Ge Tian[2,3†], Wen-Jing Liu[1,2], Di Zhao[2,3], Xue-Fang Liu[2,3], Yan-Ping Hu[1,2], Su-Xiang Feng[2,3*] and Jian-Sheng Li[2,4*]

[1]College of Pharmacy, Henan University of Chinese Medicine, Zhengzhou, Henan, China, [2]Collaborative Innovation Center for Chinese Medicine and Respiratory Diseases Co-constructed by Henan Province and Education Ministry of P. R. China, Zhengzhou, Henan, China, [3]Academy of Chinese Medical Sciences, Henan University of Chinese Medicine, Zhengzhou, Henan, China, [4]The First Affiliated Hospital, Henan University of Chinese Medicine, Zhengzhou, Henan, China

Introduction: Acute lung injury (ALI) is a common and devastating respiratory disease associated with uncontrolled inflammatory response and transepithelial neutrophil migration. In recent years, a growing number of studies have found that Ardisiae Japonicae Herba (AJH) has a favorable anti-inflammatory effect. However, its serum material basis and molecular mechanism are still unknown in ALI treatment. In this study, metabolomics and network analysis of serum pharmacochemistry were used to explore the therapeutic effect and molecular mechanism of AJH against lipopolysaccharide (LPS)-induced ALI.

Methods: A total of 12 rats for serum pharmacochemistry analysis were randomly divided into the LPS group and LPS + AJH-treated group (treated with AJH extract 20 g/kg/d), which were administered LPS (2 mg/kg) by intratracheal instillation and then continuously administered for 7 days. Moreover, 36 rats for metabolomic research were divided into control, LPS, LPS + AJH-treated (5, 10, and 20 g/kg/d), and LPS + dexamethasone (Dex) (2.3×10^{-4} g/kg/d) groups. After 1 h of the seventh administration, the LPS, LPS + AJH-treated, and LPS + Dex groups were administered LPS by intratracheal instillation to induce ALI. The serum pharmacochemistry profiling was performed by UPLC-Orbitrap Fusion MS to identify serum components, which further explore the molecular mechanism of AJH against ALI by network analysis. Meanwhile, metabolomics was used to select the potential biomarkers and related metabolic pathways and to analyze the therapeutic mechanism of AJH against ALI.

Results: The results showed that 71 serum components and 18 related metabolites were identified in ALI rat serum. We found that 81 overlapping targets were frequently involved in AGE-RAGE, PI3K-AKT, and JAK-STAT signaling pathways in network analysis. The LPS + AJH-treated groups exerted protective effects against ALI by reducing the infiltration of inflammatory cells and achieved anti-inflammatory efficacy by significantly regulating the interleukin (IL)-6 and IL-10 levels. Metabolomics analysis shows that the therapeutic effect of AJH on ALI

10.3389/fphar.2023.1131479

involves 43 potential biomarkers and 14 metabolic pathways, especially phenylalanine, tyrosine, and tryptophan biosynthesis and linoleic acid metabolism pathways, to be influenced, which implied the potential mechanism of AJH in ALI treatment.

Discussion: Our study initially elucidated the material basis and effective mechanism of AJH against ALI, which provided a solid basis for AJH application.

KEYWORDS

Ardisiae Japonicae Herba, serum pharmacochemistry, network analysis, metabolomics, acute lung injury

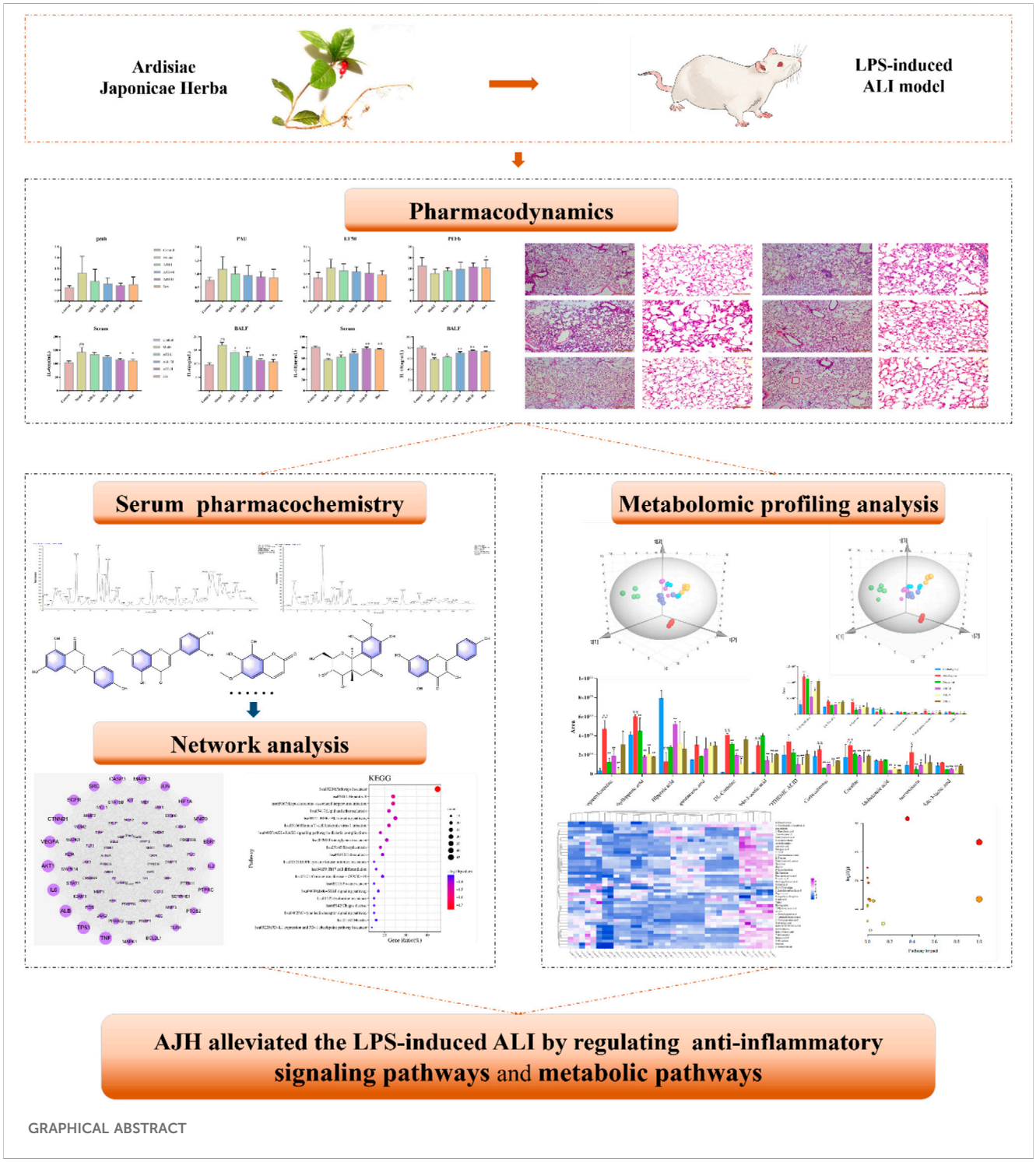

GRAPHICAL ABSTRACT

1 Introduction

Acute lung injury (ALI), a common and devastating respiratory disease, is induced by inhalation injury, acute pneumonia, trauma, sepsis, pulmonary edema, and acute pancreatitis (Savino et al., 2019; Bin et al., 2022; Ying et al., 2022). ALI is the leading cause of morbidity and mortality in intensive care units (SeungHye and Mallampalli, 2015; Huang et al., 2018), and the mortality rate is 35%–55% (Levitt et al., 2013). The pathological characteristics are associated with excessive immune cell activation, oxidative stress, inflammation, hypoxemia, bilateral lung infiltration, and electrolyte disturbances (Jiang et al., 2020; liu et al., 2021; Ying et al., 2022). ALI is considered an acute lung disease and has severe inflammatory response outbreaks in the lung accompanied by widespread damage to epithelial and endothelial cells, macrophage activation, and neutrophil infiltration (Wu et al., 2022; Zhang et al., 2022). Zhang et al. (2019) demonstrated that dexmedetomidine can inhibit the inflammatory response by regulating GSK-3β/STAT3-NF-κB. In addition, several studies demonstrated that some Chinese medicines (CMs) improve ALI by regulating relevant inflammatory cytokines and pathways. Scutellariae Radix can improve ALI by reducing the expression of nitric oxide (NO), tumor necrosis factor alpha (TNF-α), interleukin (IL)-6, and IL-8 (Hu et al., 2020). In addition, *Sarcandra glabra* combined with lycopene ameliorates histopathological injuries and decreases the levels of TNF-α and IL-6. Mitogen-activated protein kinase (MAPK) and transcription factor NF-kB were activated in lipopolysaccharide (LPS)-induced ALI rats, which exhibit a significant effect in protecting and improving LPS-induced ALI rats (Liu and Chen, 2016). Therefore, deregulating inflammatory response may play a significant role and be available for ALI treatment.

Ardisiae Japonicae Herba (AJH, *Ardisia japonica* (Thunb.) Blume), having a slightly bitter taste, belongs to the genus Ardisia and family Primulaceae. AJH converges the lung and liver meridians and has detoxification effects and activates blood circulation, which is recorded in the Materia Medica based on Chinese medical theory. On the basis of its anti-inflammatory (Liu et al., 2009), anti-cancer (Chang et al., 2007; Li et al., 2012), and anti-viral effects (Tien et al., 2007), AJH is widely used to improve chronic bronchitis (Xi, 2006) and hepatoma carcinoma (Gong et al., 2021). Cao et al. (2021) demonstrated that flavonoids in AJH showed an anti-inflammatory effect by regulating the levels of TNF-α and IL-1β, which could inhibit the proliferation and activation of hepatic stellate cells, and affect the immune function. In our previous study, we found that three components in AJH, namely, bergenin, luteolin, and kaempferol, decreased the IL-6 and matrix metalloproteinase (MMP) 9 levels, which showed a significant anti-inflammatory effect in a TNF-α-induced A549 cell model (Feng et al., 2022). Therefore, it can be deduced that AJH was effective against ALI through the anti-inflammatory mechanism. In order to confirm this hypothesis, we investigated the therapeutic effect and molecular mechanism of AJH on LPS-induced ALI rats by network analysis and metabolomics.

Due to the complexity of serum components of CMs, network analysis is often applied to study the pharmacological action and molecular mechanism of components or serum components by computer algorithms and network databases, including Metascape, GeneCards, and STRING (Societies, 2021; Han et al., 2022; Xiong et al., 2022). Moreover, metabolomics can comprehensively identify and quantify endogenous metabolites to systematically investigate the metabolic response and pathway by multivariate statistical analysis, which has been widely used in disease diagnosis and toxicology (Liu and Chen, 2016).

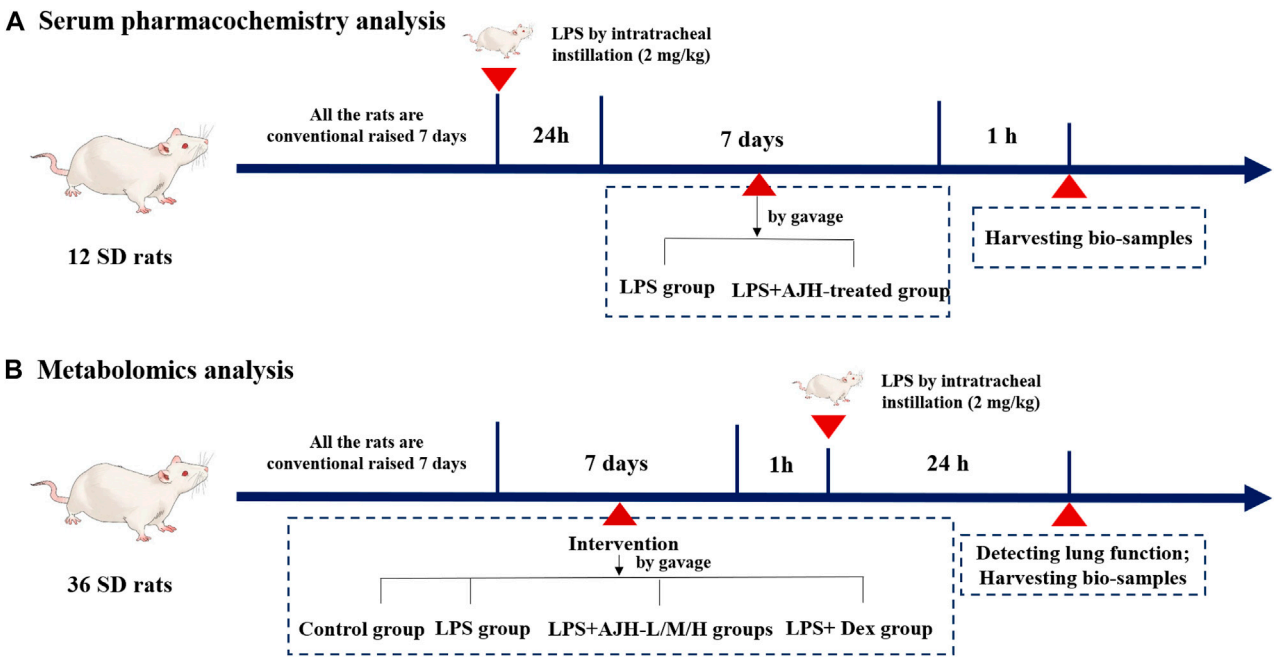

FIGURE 1
Process of animal grouping and treatment in serum pharmacochemistry and metabolomics tests. ((**A**) serum pharmacochemistry analysis; (**B**) metabolomics analysis).

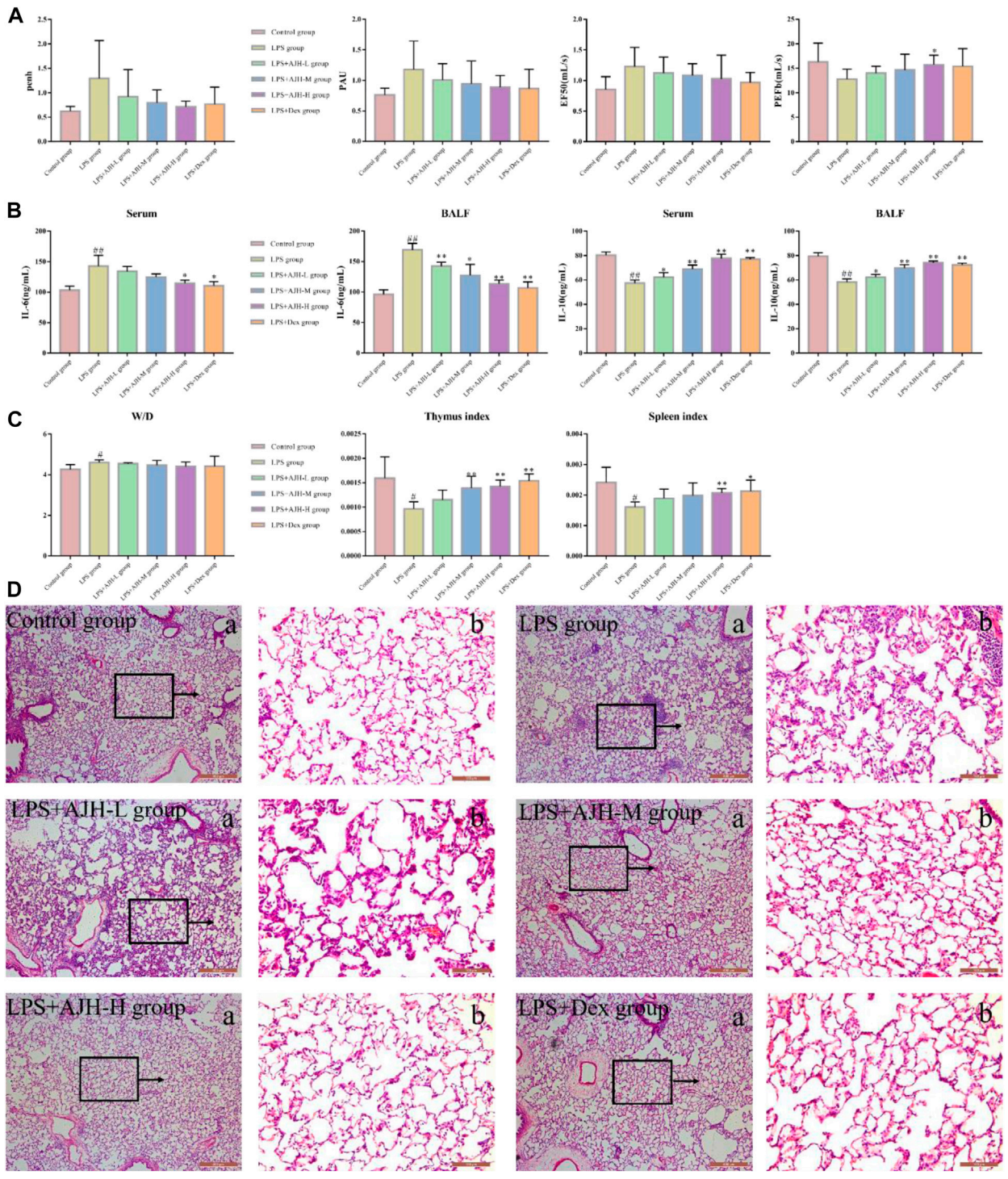

FIGURE 2
Effect of AJH intervention on ALI based on general characteristics, biochemical analysis, and pathological changes. **(A)** Measurement of the relevant indexes of lung function analysis in rats, including penh, PAU, EF50, and PEFb. **(B)** AJH regulated the expression levels of IL-6 and IL-10 in serum and BALF. **(C)** Lung W/D ratio and thymus and spleen indexes. $^{\#}p < 0.05$, $^{\#\#}p < 0.01$ vs the control group; $^{*}p < 0.05$, $^{**}p < 0.01$ vs the LPS group. **(D)** Histopathological changes in lung tissue and effects of AJH on the ALI model rat ((a) magnification ×50, (b) magnification ×200).

Therefore, we integrate network analysis and metabolomics to investigate the material basis and the anti-inflammatory molecular mechanism of AJH against ALI. First, the serum components of AJH in the ALI model rat were identified by UPLC-Orbitrap Fusion MS. Subsequently, we further systematically hypothesized and incorporated the potential therapeutic targets and molecular mechanism based on the network analysis. Finally, the therapeutic mechanisms of AJH

10.3389/fphar.2023.1131479

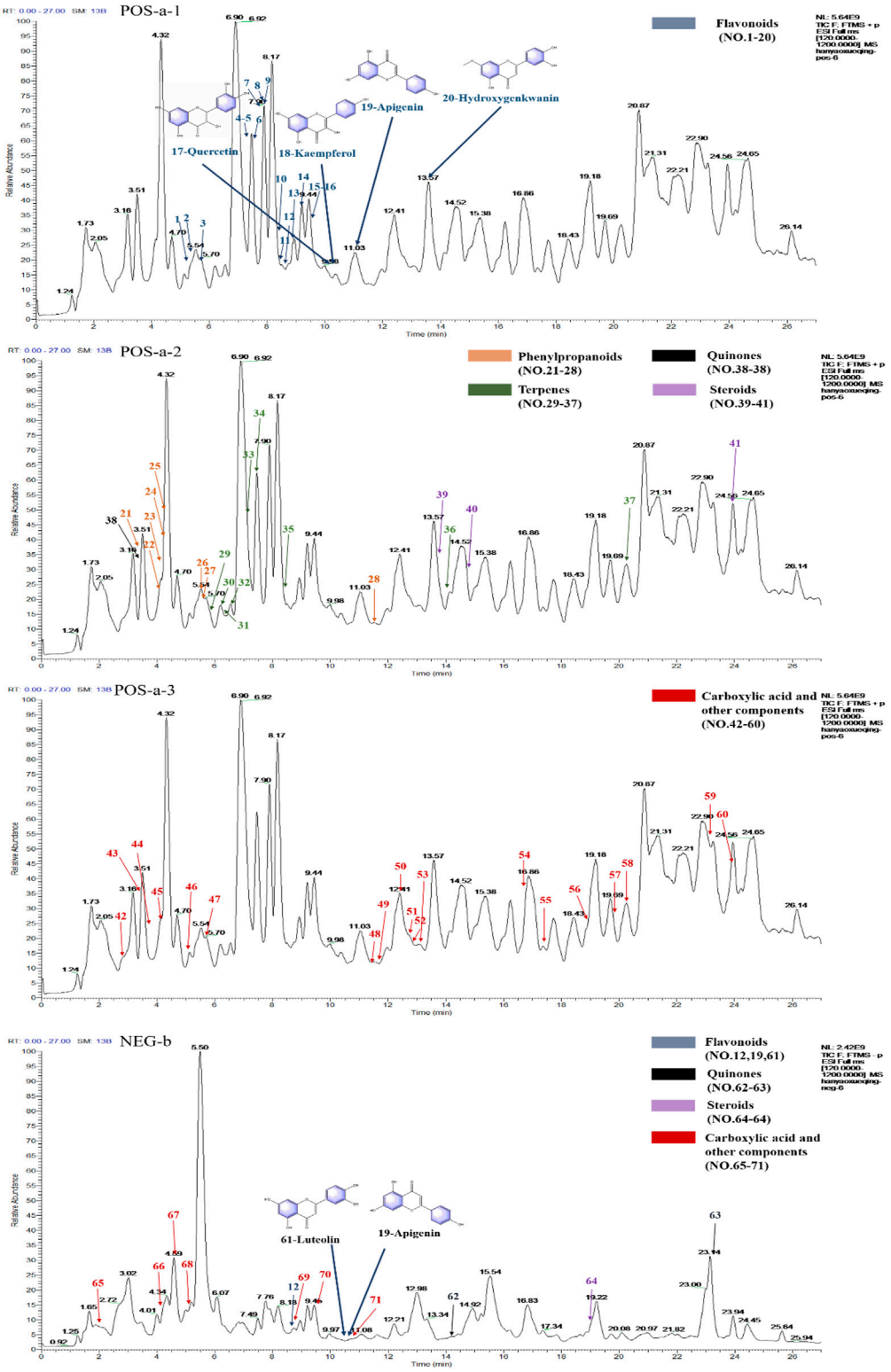

FIGURE 3
Total ion chromatograms (TICs) of serum pharmacochemistry of AJH in ALI model rats; flavonoids (21 in total) are marked in blue, phenylpropanoids (eight in total) are marked in orange, terpenes (nine in total) are marked in green, quinones (three in total) are marked in black, steroids (4 in total) are marked in purple, and carboxylic acid and other components (26 in total) are marked in red. (a1–3. positive ion mode; b. negative ion mode).

TABLE 1 Details about 71 serum components of AJH in ALI rats.

No.	Identification	Formula	Experimental MS (m/z)	Measured MS (m/z)	Ion mode	Rt (min)	NL	UPLC-Orbitrap Fusion MS/MS fragments (m/z)
1	Cianidanol	$C_{15}H_{14}O_6$	291.08631	291.08603	$[M + H]^+$	5.22	8.21E+06	139.03833,123.04332,119.04829
2	Epigallocatechin gallate	$C_{22}H_{18}O_{11}$	459.09219	459.09281	$[M + H]^+$	5.47	1.29E+05	229.04925,163.03815,153.01743,139.03825,135.04340,125.02317
3	Epigallocatechin	$C_{15}H_{14}O_7$	307.08123	307.08092	$[M + H]^+$	5.74	5.27E+05	229.04886,169.04962, 163.03816,139.03824,127.03838,111.04329
4	Myricitrin	$C_{21}H_{20}O_{12}$	465.10275	465.10231	$[M + H]^+$	7.53	3.71E+05	449.10737,331.04511,319.04493,127.03986
5	Hyperoside	$C_{21}H_{20}O_{12}$	465.10275	465.10231	$[M + H]^+$	7.53	3.71E+05	361.05469,318.03699,165.01767,153.01761
6	Taxifolin	$C_{15}H_{12}O_7$	305.06558	305.06523	$[M + H]^+$	7.57	2.40E+06	167.03305,161.02266,153.01746,151.03816,149.02257,123.04352
7	Cynaroside	$C_{21}H_{20}O_{11}$	449.10784	449.10804	$[M + H]^+$	7.8	1.35E+06	341.06534,287.05411,285.03873,153.01759,137.02287
8	Rutin	$C_{27}H_{30}O_{16}$	611.16066	611.16063	$[M + H]^+$	7.85	3.73E+05	434.31986,303.04828,153.01752,151.03825
9	Astilbin	$C_{21}H_{22}O_{11}$	451.12349	451.12301	$[M + H]^+$	8	2.10E+05	305.06528,287.05326,247.05983,183.02783,177.01764,165.01741
10	Apigenin-7-O-rutinoside	$C_{27}H_{30}O_{14}$	579.17083	579.17279	$[M + H]^+$	8.33	4.95E+06	271.06042,251.09155,167.07050
11	Epicatechin gallate	$C_{22}H_{18}O_{10}$	443.09727	443.09705	$[M + H]^+$	8.47	1.15E+06	319.04459,163.03907,149.02328,137.05978,135.04411,127.03901
12	Myricetin	$C_{15}H_{10}O_8$	319.04484	319.04459	$[M + H]^+$	8.55	1.59E+06	194.02125,193.01260,165.01741,153.01741,139.03819,137.02272
	Myricetin	$C_{15}H_{10}O_8$	317.03029	317.03061	$[M-H]^-$	8.58	1.20E+06	289.03586,237.11314,219.10246,178.99829,151.00334,137.02409
13	Luteolin-7-o-rutinoside	$C_{27}H_{30}O_{15}$	595.16575	595.16514	$[M + H]^+$	8.79	1.09E+05	395.07574,287.05328,163.05959,145.04890,135.04378
14	Eriodictyol	$C_{15}H_{12}O_6$	289.07066	289.07045	$[M + H]^+$	9.17	6.38E+05	163.03786,153.01738,137.05890,123.04350
15	Apigenin-7-O-glucoside	$C_{21}H_{20}O_{10}$	433.11292	433.113	$[M + H]^+$	9.86	1.24E+05	287.05341,165.01737,153.01752,137.02246
16	Afzelin	$C_{21}H_{20}O_{10}$	433.11292	433.113	$[M + H]^+$	9.86	1.24E+05	287.05341,165.01737,153.01752,137.02246
17	Quercetin	$C_{15}H_{10}O_7$	303.04993	303.04997	$[M + H]^+$	10.18	3.50E+06	195.02780,165.01746,153.01744,149.02246,137.02271
18	Kaempferol	$C_{15}H_{10}O_6$	287.05501	287.05489	$[M + H]^+$	10.72	3.41E+06	287.05493,269.04440,259.05978,231.06528,153.01827
19	Apigenin	$C_{15}H_{10}O_5$	271.0601	271.05987	$[M + H]^+$	11.84	3.03E+06	163.03876,153.01738,145.02841,121.02782,119.04863
	Apigenin	$C_{15}H_{10}O_5$	269.04555	269.04553	$[M-H]^-$	11.86	1.13E+06	269.04486,253.04996,117.03370
20	Hydroxygenkwanin	$C_{16}H_{12}O_6$	301.07066	301.07037	$[M + H]^+$	13.37	1.23E+07	283.05939,167.03323,107.04848
21	Bergenin	$C_{14}H_{16}O_9$	329.08671	329.08684	$[M + H]^+$	3.31	1.03E+07	293.06567,275.05524,263.05508,251.05508,237.03936
22	Fraxetin	$C_{10}H_8O_5$	209.04445	209.04461	$[M + H]^+$	4.07	2.35E+05	194.01999,181.04860,166.02537,163.03799,153.05370,149.02237
23	4-Methoxycinnamic acid	$C_{10}H_{10}O_3$	179.07027	179.0704	$[M + H]^+$	4.12	2.93E+06	161.05899,133.06421,118.04059,109.06401,105.06937
24	Methyl cinnamate	$C_{10}H_{10}O_2$	163.07536	163.07558	$[M + H]^+$	4.18	5.75E+06	145.06491,131.04929,107.04924
25	(2E)-3-(2,3-Dihydro-1,4-benzodioxin-6-yl)acrylic acid	$C_{11}H_{10}O_4$	207.06518	207.06514	$[M + H]^+$	4.22	2.33E+05	163.03816,161.05965,147.04341,135.04344
26	Myristicin	$C_{11}H_{12}O_3$	193.08592	193.08606	$[M + H]^+$	5.55	1.28E+06	193.08583,165.05429,160.05147,135.04312,117.06930

(Continued on following page)

10.3389/fphar.2023.1131479

TABLE 1 (*Continued*) Details about 71 serum components of AJH in ALI rats.

No.	Identification	Formula	Experimental MS (m/z)	Measured MS (m/z)	Ion mode	Rt (min)	NL	UPLC-Orbitrap Fusion MS/MS fragments (m/z)
27	Scopoletin	$C_{10}H_8O_4$	193.04953	193.0497	$[M + H]^+$	5.67	1.92E+06	178.02512,150.03026,137.05913,133.02785,122.03581
28	Umbelliferone	$C_9H_6O_3$	163.03897	163.03903	$[M + H]^+$	11.86	3.28E+06	163.03911,135.04419,121.02788,109.02848,95.04936
29	DL-Carvone	$C_{10}H_{14}O$	151.11174	151.11185	$[M + H]^+$	5.82	1.42E+06	123.07984,109.06389,107.08508,95.08512,93.06918
30	Thymoxyacetic acid	$C_{12}H_{16}O_3$	209.11722	209.11732	$[M + H]^+$	6.01	2.12E+06	149.09509,133.10080,109.06394,105.06921
31	p-Cymene	$C_{10}H_{14}$	135.11683	135.11678	$[M + H]^+$	6.29	1.70E+06	135.11687,93.06999
32	Perillic acid	$C_{10}H_{14}O_2$	167.10666	167.10674	$[M + H]^+$	6.62	1.81E+06	125.05868,121.10059,111.04363,109.06443,107.08519
33	4-Tert butylbenzoic acid	$C_{11}H_{14}O_2$	179.10666	179.10671	$[M + H]^+$	7.02	5.19E+06	133.10049,123.04314,119.08498,91.05397
34	Carvacrol	$C_{10}H_{14}O$	151.11174	151.11179	$[M + H]^+$	7.52	9.02E+05	109.06396,105.06938,93.06905,91.05400
35	Nootkatone	$C_{15}H_{22}O$	219.17434	219.17434	$[M + H]^+$	8.3	3.42E+06	201.16319,189.12659,177.12662,161.13178,149.13248,109.06479
36	Iso-E Super	$C_{16}H_{26}O$	235.20564	235.20541	$[M + H]^+$	14.2	1.43E+05	191.17917,151.11130,147.11610,135.11632,123.11609
37	Oleanolic acid	$C_{30}H_{48}O_3$	457.36762	457.36827	$[M + H]^+$	20.33	4.94E+07	289.21579,275.19968,191.17848,181.12321,179.10584,163.14749
38	5,8-Dihydroxy-2,3,6-trimethoxy-1,4-naphthoquinone	$C_{13}H_{12}O_7$	281.06558	281.0658	$[M + H]^+$	3.31	1.90E+05	263.05228,235.05891,219.02913,139.03922
39	Hydroxyprogesterone	$C_{21}H_{30}O_3$	331.22677	331.22673	$[M + H]^+$	13.71	4.82E+06	331.22699,313.21619,295.20575,271.20587,191.14323
40	Epiallopregnanolone	$C_{21}H_{34}O_3$	335.25807	335.25793	$[M + H]^+$	14.84	1.88E+06	165.12691,159.11597,123.07957,121.10042,109.10036,107.08513
41	3-Hydroxycholest-5-en-7-one	$C_{27}H_{44}O_2$	401.34141	401.34103	$[M + H]^+$	24.54	4.71E+06	343.26334,341.24781,235.16939,221.15350,161.09619
42	Caffeic acid	$C_9H_8O_4$	181.04953	181.04959	$[M + H]^+$	2.88	2.05E+07	181.01306,163.08649,138.03114,125.05968
43	1-Salicylate glucuronide	$C_{13}H_{14}O_9$	315.07106	315.07088	$[M + H]^+$	3.39	1.20E+06	165.05453,153.05463,145.04943,143.03388
44	Gallic acid	$C_7H_6O_5$	171.0288	171.02865	$[M + H]^+$	3.87	5.60E+04	169.01334,125.02361,124.01605,123.00786,108.02087
45	3-Oxocyclopentanecarboxylic acid	$C_6H_8O_3$	129.05462	129.05459	$[M + H]^+$	4.19	2.13E+06	101.05936,83.04877,59.04896,55.05402
46	Ethyl gallate	$C_9H_{10}O_5$	199.0601	199.06022	$[M + H]^+$	5.29	2.10E+06	185.04442,171.02890,153.01829,127.03909,125.02340
47	3,4-Dimethoxybenzoic acid	$C_9H_{10}O_4$	183.06518	183.0651	$[M + H]^+$	5.64	2.41E+06	183.06540,167.03389,165.05461,151.03899,139.07542,137.02339
48	(±)-Abscisic acid	$C_{15}H_{20}O_4$	265.14343	265.1433	$[M + H]^+$	11.61	1.85E+06	249.14854,247.13275,233.15354,231.13814,223.13283
49	Monobutyl phthalate	$C_{12}H_{14}O_4$	223.09648	223.09632	$[M + H]^+$	11.87	1.18E+06	163.03863,149.02251,135.04327,131.08472,121.02756
50	Phenylbutyric acid	$C_{10}H_{12}O_2$	165.09101	165.09096	$[M + H]^+$	12.42	1.86E+07	147.08006,137.09532,121.10033,119.08482,103.05366
51	Mycophenolic acid	$C_{17}H_{20}O_6$	321.13326	321.13301	$[M + H]^+$	12.57	6.55E+05	285.11115,275.12698,109.06411
52	Ardisinol II	$C_{19}H_{30}O_2$	291.23186	291.23205	$[M + H]^+$	12.65	2.62E+06	178.08191,147.06284,119.08478,107.08492
53	Hexylresorcinol	$C_{12}H_{18}O_2$	195.13796	195.13792	$[M + H]^+$	13.3	2.72E+06	135.07948,109.02810,107.04833,95.04876
54	4-Heptylbenzoic acid	$C_{14}H_{20}O_2$	221.15361	221.15354	$[M + H]^+$	16.78	2.70E+06	177.16296,175.14723,147.11607,133.10062,121.10062,119.08498
55	9S,13R-12-Oxophytodienoic acid	$C_{18}H_{28}O_3$	293.21112	293.21103	$[M + H]^+$	17.49	1.23E+07	247.20465,173.13164,163.11095,161.13155,159.11589

(Continued on following page)

10.3389/fphar.2023.1131479

TABLE 1 Details about 71 serum components of AJH in ALI rats.

No.	Identification	Formula	Experimental MS (m/z)	Measured MS (m/z)	Ion mode	Rt (min)	NL	UPLC-Orbitrap Fusion MS/MS fragments (m/z)
1	Cianidanol	$C_{15}H_{14}O_6$	291.08631	291.08603	$[M + H]^+$	5.22	8.21E+06	139.03833,123.04332,119.04829
2	Epigallocatechin gallate	$C_{22}H_{18}O_{11}$	459.09219	459.09281	$[M + H]^+$	5.47	1.29E+05	229.04925,163.03815,153.01743,139.03825,135.04340,125.02317
3	Epigallocatechin	$C_{15}H_{14}O_7$	307.08123	307.08092	$[M + H]^+$	5.74	5.27E+05	229.04886,169.04962, 163.03816,139.03824,127.03838,111.04329
4	Myricitrin	$C_{21}H_{20}O_{12}$	465.10275	465.10231	$[M + H]^+$	7.53	3.71E+05	449.10737,331.04511,319.04493,127.03986
5	Hyperoside	$C_{21}H_{20}O_{12}$	465.10275	465.10231	$[M + H]^+$	7.53	3.71E+05	361.05469,318.03699,165.01767,153.01761
6	Taxifolin	$C_{15}H_{12}O_7$	305.06558	305.06523	$[M + H]^+$	7.57	2.40E+06	167.03305,161.02266,153.01746,151.03816,149.02257,123.04352
7	Cynaroside	$C_{21}H_{20}O_{11}$	449.10784	449.10804	$[M + H]^+$	7.8	1.35E+06	341.06534,287.05411,285.03873,153.01759,137.02287
8	Rutin	$C_{27}H_{30}O_{16}$	611.16066	611.16063	$[M + H]^+$	7.85	3.73E+05	434.31986,303.04828,153.01752,151.03825
9	Astilbin	$C_{21}H_{22}O_{11}$	451.12349	451.12301	$[M + H]^+$	8	2.10E+05	305.06528,287.05326,247.05983,183.02783,177.01764,165.01741
10	Apigenin-7-O-rutinoside	$C_{27}H_{30}O_{14}$	579.17083	579.17279	$[M + H]^+$	8.33	4.95E+06	271.06042,251.09155,167.07050
11	Epicatechin gallate	$C_{22}H_{18}O_{10}$	443.09727	443.09705	$[M + H]^+$	8.47	1.15E+06	319.04459,163.03907,149.02328,137.05978,135.04411,127.03901
12	Myricetin	$C_{15}H_{10}O_8$	319.04484	319.04459	$[M + H]^+$	8.55	1.59E+06	194.02125,193.01260,165.01741,153.01741,139.03819,137.02272
	Myricetin	$C_{15}H_{10}O_8$	317.03029	317.03061	$[M-H]^-$	8.58	1.20E+06	289.03586,237.11314,219.10246,178.99829,151.00334,137.02409
13	Luteolin-7-o-rutinoside	$C_{27}H_{30}O_{15}$	595.16575	595.16514	$[M + H]^+$	8.79	1.09E+05	395.07574,287.05328,163.05959,145.04890,135.04378
14	Eriodictyol	$C_{15}H_{12}O_6$	289.07066	289.07045	$[M + H]^+$	9.17	6.38E+05	163.03786,153.01738,137.05890,123.04350
15	Apigenin-7-O-glucoside	$C_{21}H_{20}O_{10}$	433.11292	433.113	$[M + H]^+$	9.86	1.24E+05	287.05341,165.01737,153.01752,137.02246
16	Afzelin	$C_{21}H_{20}O_{10}$	433.11292	433.113	$[M + H]^+$	9.86	1.24E+05	287.05341,165.01737,153.01752,137.02246
17	Quercetin	$C_{15}H_{10}O_7$	303.04993	303.04997	$[M + H]^+$	10.18	3.50E+06	195.02780,165.01746,153.01744,149.02246,137.02271
18	Kaempferol	$C_{15}H_{10}O_6$	287.05501	287.05489	$[M + H]^+$	10.72	3.41E+06	287.05493,269.04440,259.05978,231.06528,153.01827
19	Apigenin	$C_{15}H_{10}O_5$	271.0601	271.05987	$[M + H]^+$	11.84	3.03E+06	163.03876,153.01738,145.02841,121.02782,119.04863
	Apigenin	$C_{15}H_{10}O_5$	269.04555	269.04553	$[M-H]^-$	11.86	1.13E+06	269.04486,253.04996,117.03370
20	Hydroxygenkwanin	$C_{16}H_{12}O_6$	301.07066	301.07037	$[M + H]^+$	13.37	1.23E+07	283.05939,167.03323,107.04848
21	Bergenin	$C_{14}H_{16}O_9$	329.08671	329.08684	$[M + H]^+$	3.31	1.03E+07	293.06567,275.05524,263.05508,251.05508,237.03936
22	Fraxetin	$C_{10}H_8O_5$	209.04445	209.04461	$[M + H]^+$	4.07	2.35E+05	194.01999,181.04860,166.02537,163.03799,153.05370,149.02237
23	4-Methoxycinnamic acid	$C_{10}H_{10}O_3$	179.07027	179.0704	$[M + H]^+$	4.12	2.93E+06	161.05899,133.06421,118.04059,109.06401,105.06937
24	Methyl cinnamate	$C_{10}H_{10}O_2$	163.07536	163.07558	$[M + H]^+$	4.18	5.75E+06	145.06491,131.04929,107.04924
25	(2E)-3-(2,3-Dihydro-1,4-benzodioxin-6-yl)acrylic acid	$C_{11}H_{10}O_4$	207.06518	207.06514	$[M + H]^+$	4.22	2.33E+05	163.03816,161.05965,147.04341,135.04344
26	Myristicin	$C_{11}H_{12}O_3$	193.08592	193.08606	$[M + H]^+$	5.55	1.28E+06	193.08583,165.05429,160.05147,135.04312,117.06930

(Continued on following page)

10.3389/fphar.2023.1131479

TABLE 2 Details about 18 related metabolites of AJH serum components in ALI rats.

No.	Formula	Experimental MS (m/z)	Measured MS (m/z)	Ion mode	RT (min)	UPLC-Orbitrap Fusion MS/MS fragments (m/z)	Metabolic sequestration	Resource
1	$C_{16}H_{12}O_6$	301.07066	301.07037	$[M + H]^+$	13.37	286.04721,258.05237,167.03403	Methylation	Kaempferol
2	$C_{16}H_{12}O_6$	299.05611	299.0559	$[M-H]^-$	13.35	284.03262,212.04758,148.01617	Methylation	Luteolin
3	$C_{16}H_{18}O_{10}$	371.09727	371.09769	$[M + H]^+$	5.76	275.05511,247.06015,233.04451,205.04968	Methylation + glucuronide conjugation	Caffeic acid
4	$C_{15}H_{16}O_{10}$	357.08162	357.08185	$[M + H]^+$	4.56	261.03955,233.04457,219.02892,199.03398	Glucuronide conjugation	Caffeic acid
5	$C_{12}H_{13}NO_3$	220.09682	220.09702	$[M + H]^+$	9.23	159.11691,125.09621,107.08566,97.10132	Glycine conjugation	Methyl cinnamate
6	$C_{21}H_{20}O_{11}$	449.10784	449.10804	$[M + H]^+$	7.8	303.05026,257.04456,229.04973	Oxidation	Apigenin-7-O-glucoside
7	$C_{15}H_{10}O_6$	287.05501	287.05489	$[M + H]^+$	10.72	287.05493,259.08517,241.07463,153.01826	Hydroxylation + glucuronide conjugation	Apigenin-7-O-glucoside
8	$C_{21}H_{22}O_{11}$	451.12349	451.12301	$[M + H]^+$	8	259.06033,231.06540,195.02905,165.01845,153.01846	Hydration	Apigenin-7-O-glucoside
9	$C_{21}H_{20}O_{10}$	433.11292	433.113	$[M + H]^+$	9.86	329.06628,213.05504,153.01845	Deglucosylation	Luteolin-7-o-rutinoside
10	$C_{27}H_{30}O_{16}$	611.16066	611.16063	$[M + H]^+$	7.85	303.05011,177.05482,153.01840	Oxidation	Luteolin-7-o-rutinoside
11	$C_{28}H_{32}O_{16}$	625.17631	625.17841	$[M + H]^+$	8.94	317.06573,255.12033,207.06532,175.03914	Hydroxylation + methylation	Luteolin-7-o-rutinoside
12	$C_{27}H_{30}O_{15}$	595.16575	595.16514	$[M + H]^+$	8.79	303.05029,287.05542,153.05487	Oxidation	Apigenin-7-O-rutinoside
13	$C_{21}H_{20}O_{10}$	433.11292	433.113	$[M + H]^+$	9.86	287.05548,241.04991,185.05965,129.05496	Hydroxylation + glucuronide conjugation	Apigenin-7-O-rutinoside
14	$C_{28}H_{32}O_{16}$	625.17631	625.17841	$[M + H]^+$	8.94	317.06573,255.12033,207.06532,175.03914	Methylation	Apigenin-7-O-rutinoside
15	$C_{28}H_{32}O_{16}$	625.17631	625.17841	$[M + H]^+$	8.94	317.06573,255.12033,207.06532,175.03914	Methylation	Quercetin-3-O-rutinoside
16	$C_{21}H_{20}O_{11}$	449.10784	449.10804	$[M + H]^+$	7.8	345.06165,287.05524,247.06033,183.02893	Deglucosylation	Quercetin-3-O-rutinoside
17	$C_{26}H_{43}NO_5$	448.30685	448.30862	$[M-H]^-$	15.01	448.30679,404.31696,402.30160	Glycine conjugation	Deoxycholic acid
18	$C_9H_{10}O_3$	165.05572	165.05534	$[M-H]^-$	6.51	147.04488,119.04997,106.04213	Oxidation	Apigenin

10.3389/fphar.2023.1131479

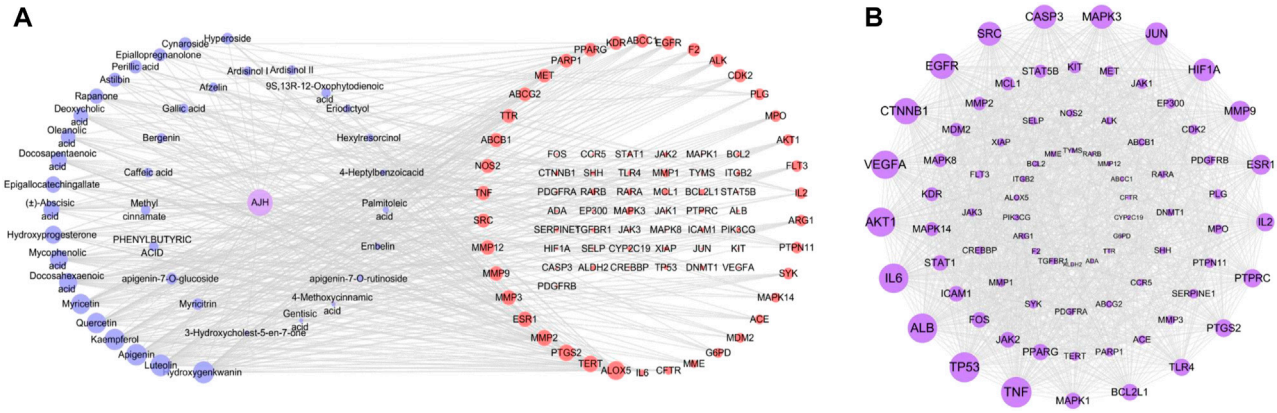

FIGURE 4
Network pharmacology prediction for AJH intervention in ALI. **(A)** AJH–serum component–target–ALI network. **(B)** PPI network.

against ALI were evaluated by biochemical indexes and histopathology of the lung. Furthermore, the serum metabolic profile was confirmed to analyze the metabolic pathways.

2 Materials and methods

2.1 Materials

AJH (*Ardisia japonica* (Thunb.) Blume) was purchased from Zhangshu Tianqitang Chinese medicine Co., Ltd (Jiangxi, China; batch: 201909001) and authenticated by Dr. Suiqing Chen, Henan University of Chinese Medicine. The voucher specimen was stored at the Scientific Research Center, Henan University of Chinese Medicine, Zhengzhou. The reference standards of methyl salicylate (batch: CHB190925), kaempferol (batch: CHB190127), embelin (batch: CHB190829), hydroxygenkwanin (batch: CHB180611), rapanone (batch: CHB190723), (−)-epigallocatechin gallate (batch: CHB180307), myricitrin (batch: CHB180611), 3,4-dimethoxybenzoic acid (batch: CHB190820), ethyl gallate (batch: CHB180116), myricetin (batch: CHB180614), astilbin (batch: CHB190107), apigenin (batch: CHB180103), and (−)-epicatechin gallate (batch: CHB180305) (purity ≥98%) were obtained from Chengdu Chroma-Biotechnology Co., Ltd (Chengdu, China). Quercetin (batch: MUST-20101104, purity ≥99.35%) was purchased from Chengdu Must Bio-technology Co., Ltd. Bergenin (batch: 111532–201604, purity ≥94.1%) was obtained from National Institutes for Food and Drug Control (Beijing, China). HPLC-grade methanol and formic acid of mass grade were purchased from Thermo Fisher (United States). Ultra-pure water was prepared using a Milli-Q purification system (Millipore, Merck).

Dexamethasone acetate tablets were purchased from Anhui Jintaiyang Pharmaceutical Company Ltd (batch: 2104082; specification: 0.75 mg * 100 pills; usage and dosage: 0.75–3 mg/times and 2–4 times/day; experimental usage and dosage: 0.75 mg/times and 3 times/day). Whole-value grain feedstuff was purchased from SPF (Beijing) Biotechnology Company Ltd (SCXK (Jing) 2019–0010). LPS (batch: 039M4004V) was obtained from Sigma-Aldrich Company Ltd. The levels of IL-6 and IL-10 were quantified by the enzyme-linked immunosorbent assay (ELISA) kits obtained from Wuhan Boster Biological Technology Company Ltd.

2.2 Preparation of sample solution

2.2.1 AJH sample preparation

An accurately weighed sample (500 g) of AJH was extracted twice with 5,000 mL ethanol–water (7:3, v/v) under reflux for 1 h each time. The AJH extract was concentrated under reduced pressure to 2.4 g/mL.

2.2.2 Standard solution preparation

A total of 15 reference standards, such as methyl salicylate, kaempferol, and embelin, were accurately weighed, dissolved in methanol to prepare a mixed stock solution with appropriate concentration, and stored at 4°C until further use.

2.3 Animals and treatments

Male Sprague–Dawley rats (body weight 200 ± 20 g) (NO.: 1107261911004350) were purchased from the Animal Experimental Center of Huaxing (Henan, China, SCXK(Yu) 2019–0002). The experimental protocol was reviewed and approved by the Experimental Animal Care and Ethics Committee of Henan University of Chinese Medicine (Henan, China, SYXK(Yu) 2020–0004). The rats were housed at the Center of Experimental Animals in Henan University of Chinese Medicine, maintained under a 12 h light–dark cycle, temperature of 23°C ± 2°C, and humidity of 50%–60%, with free access to water and food (Han et al., 2022). For serum pharmacochemistry analysis, 12 rats were randomly divided into two groups (n = 6 each): LPS (treated with 10 mL/kg/d distilled water by gavage) and LPS + AJH-treated groups (treated with AJH extract 20 g/kg/d by gavage). The rats in the groups were administered LPS by intratracheal instillation (2 mg/kg) to induce ALI. After 24 h of LPS exposure, the LPS and LPS + AJH-treated groups were continuously administered for

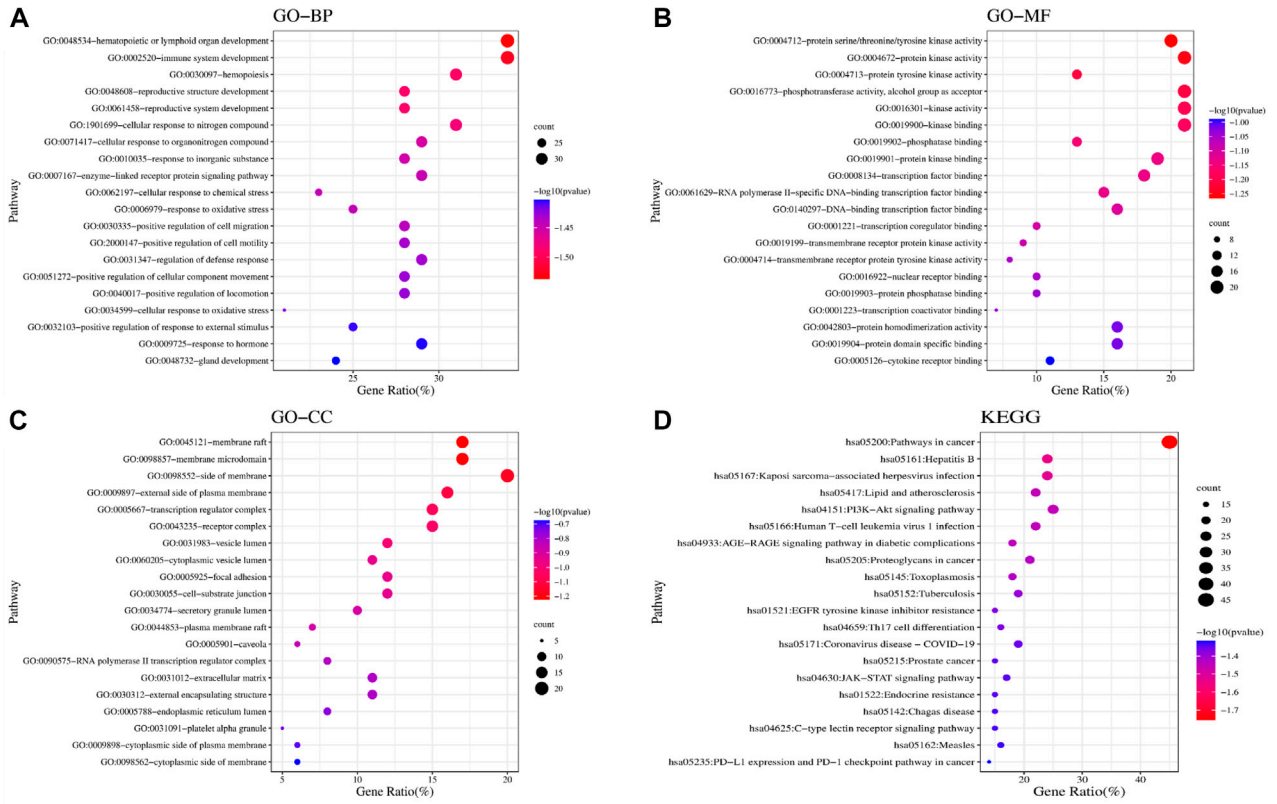

FIGURE 5
Results of GO and KEGG enrichment analyses. Bubble charts of **(A)** GOBP; **(B)** GOMF; **(C)** GOCC; and **(D)** KEGG enrichment analysis.

7 days (Figure 1A). After 1 h of the last administration, the serum samples were collected, separated by centrifugation at 3,000 rpm for 15 min, and then stored at −80°C. A total of 36 rats for metabolomics analysis were divided into control (treated with 10 mL/kg/d distilled water by gavage), LPS (treated with 10 mL/kg/d distilled water by gavage), LPS + AJH-low (LPS + AJH-L) (treated with AJH extract 5 g/kg/d by gavage), LPS + AJH-medium (LPS + AJH-M) (treated with AJH extract 10 g/kg/d by gavage), LPS + AJH-high (LPS + AJH-H) (treated with AJH extract 20 g/kg/d by gavage), and LPS + dexamethasone (LPS + Dex) (treated with Dex 2.3×10^{-4} g/kg/d by gavage). The LPS + AJH-treated and LPS + Dex groups were continuously administered for 7 days. After 1 h of the last administration, the LPS, LPS + AJH-treated, and LPS + Dex groups were anesthetized by intraperitoneal injection of 20% urethane and administered LPS by intratracheal instillation (2 mg/kg) to establish an ALI model (Figure 1B). Furthermore, the LPS doses were selected as previously described (Hu et al., 2020). Subsequently, 24 h after modeling, 36 rats for metabolomic research were tested for lung function and then euthanized after anesthesia to harvest bio-samples including serum, lung tissues, and bronchoalveolar lavage fluid (BALF). Furthermore, BALF was centrifuged for 15 min at 3,000 rpm and stored at −80°C for evaluation of the inflammatory cytokine levels. The serum samples of metabolomics were collected and separated by centrifugation at 3,000 rpm for 15 min and then stored at −80°C and were used to evaluate the inflammatory cytokine levels and metabolomics analysis.

2.4 Pathological parameters

According to related studies, several pathological parameters were investigated in our study, including histopathologic evaluation stained with hematoxylin and eosin (H&E), lung wet/dry (W/D) ratio, indexes of the thymus and spleen, lung function, and the levels of inflammatory cytokines (IL-6 and IL-10) in serum and BALF, to assess AJH intervention effects for the ALI model.

2.5 Serum sample preparation

For serum pharmacochemistry analysis, 1,500 μL methanol solution was mixed with 500 μL serum sample, vortexed for 6 min, and then centrifuged at 14,000 rpm for 15 min at 4°C. The supernatant was collected and dehydrated under vacuum conditions. Furthermore, dried samples were mixed with 200 μL methanol–water (1:1, v/v), followed by 6 min vortex and 15 min centrifugation (14,000 rpm, 4°C). The supernatant was then analyzed by UPLC-Orbitrap Fusion MS.

In addition, 200 μL rat serum was added to 600 μL methanol, vortexed for 6 min, centrifuged for 15 min at 14,000 rpm and 4°C,

TABLE 3 Metabolites in serum samples.

No.	Rt (min)	Observed (m/z)	Ion mode	Identification	Formula	Tendency in model samples *versus* control samples	VIP
1	1.21	145.1579	$[M + H]^+$	Spermidine	$C_7H_{19}N_3$	↓	0.9996
2	1.43	103.0999	$[M + H]^+$	Choline	$C_5H_{13}NO$	↓	0.7434
3	1.58	131.0695	$[M + H]^+$	Creatine	$C_4H_9N_3O_2$	↑	1.0110
4	1.58	113.0591	$[M + H]^+$	Creatinine	$C_4H_7N_3O$	↓	0.6972
5	1.58	161.1053	$[M + H]^+$	DL-Carnitine	$C_7H_{15}NO_3$	↑	1.2442
6	1.59	111.0434	$[M + H]^+$	Cytosine	$C_4H_5N_3O$	↓	0.8123
7	1.59	159.1259	$[M + H]^+$	Pregabalin	$C_8H_{17}NO_2$	↓	0.9559
8	1.59	117.0790	$[M + H]^+$	Valine	$C_5H_{11}NO_2$	↑	1.0165
9	1.60	261.1211	$[M + H]^+$	Lotaustralin	$C_{11}H_{19}NO_6$	↑	0.9396
10	1.67	153.0900	$[M + H]^+$	Acetylhistamine	$C_7H_{11}N_3O$	↑	1.0611
11	1.75	149.0510	$[M + H]^+$	L-(−)-Methionine	$C_5H_{11}NO_2S$	↓	0.5381
12	1.88	122.0480	$[M + H]^+$	Nicotinamide	$C_6H_6N_2O$	↓	0.7372
13	1.88	168.0283	$[M + H]^+$	Uric acid	$C_5H_4N_4O_3$	↓	0.8517
14	1.89	257.1010	$[M + H]^+$	5-Methylcytidine	$C_{10}H_{15}N_3O_5$	↑	0.8651
15	1.89	241.1062	$[M + H]^+$	5-Methyldeoxycytidine	$C_{10}H_{15}N_3O_4$	↑	0.8870
16	2.09	125.0590	$[M + H]^+$	5-Methylcytosine	$C_5H_7N_3O$	↑	1.1157
17	2.09	181.0739	$[M + H]^+$	L-Tyrosine	$C_9H_{11}NO_3$	↑	1.3252
18	2.15	118.0418	$[M + H]^+$	Coumarone	C_8H_6O	↓	0.9755
19	2.22	132.0975	$[M + H]^+$	1-Heptanethiol	$C_7H_{16}S$	↓	0.7524
20	2.23	131.0946	$[M + H]^+$	L-Isoleucine	$C_6H_{13}NO_2$	↓	0.8602
21	2.44	164.0472	$[M + H]^+$	(E)-p-Coumaric acid	$C_9H_8O_3$	↑	0.8918
22	2.68	217.1314	$[M + H]^+$	Propionylcarnitine	$C_{10}H_{19}NO_4$	↑	1.1635
23	3.10	174.0793	$[M + H]^+$	Edaravone	$C_{10}H_{10}N_2O$	↑	0.4934
24	3.18	173.1051	$[M + H]^+$	N-Acetyl-L-leucine	$C_8H_{15}NO_3$	↓	0.7597
25	3.18	315.1291	$[M + H]^+$	Neosaxitoxin	$C_{10}H_{17}N_7O_5$	↑	1.2204
26	3.39	191.0582	$[M + H]^+$	5-Hydroxyindole-3-acetic acid	$C_{10}H_9NO_3$	↑	1.1850

(Continued on following page)

10.3389/fphar.2023.1131479

TABLE 3 (*Continued*) Metabolites in serum samples.

No.	Rt (min)	Observed (m/z)	Ion mode	Identification	Formula	Tendency in model samples *versus* control samples	VIP
27	3.48	126.0428	$[M + H]^+$	Thymine	$C_5H_6N_2O_2$	↓	0.8188
28	3.50	168.0875	$[M + H]^+$	Pyridoxamine	$C_8H_{12}N_2O_2$	↓	0.9556
29	3.59	165.0789	$[M + H]^+$	L-Phenylalanine	$C_9H_{11}NO_2$	↑	1.1184
30	3.87	194.1153	$[M + H]^+$	PEG-4	$C_8H_{18}O_5$	↑	0.8846
31	3.98	219.1106	$[M + H]^+$	D-Pantothenic acid	$C_9H_{17}NO_5$	↑	1.1255
32	5.13	243.1469	$[M + H]^+$	Tiglylcarnitine	$C_{12}H_{21}NO_4$	↑	1.0748
33	5.28	187.0607	$[M + H]^+$	Desethylatrazine	$C_6H_{10}ClN_5$	↓	0.7858
34	5.29	220.0846	$[M + H]^+$	5-Hydroxy-DL-tryptophan	$C_{11}H_{12}N_2O_3$	↓	0.9817
35	5.29	204.0899	$[M + H]^+$	DL-Tryptophan	$C_{11}H_{12}N_2O_2$	↓	0.7795
36	5.80	262.1314	$[M + H]^+$	Methohexital	$C_{14}H_{18}N_2O_3$	↓	0.7853
37	5.80	382.1966	$[M + H]^+$	Tofisopam	$C_{22}H_{26}N_2O_4$	↑	0.6902
38	5.95	173.0476	$[M + H]^+$	2-Quinolinecarboxylic acid	$C_{10}H_7NO_2$	↓	1.1023
39	5.95	179.0582	$[M + H]^+$	Hippuric acid	$C_9H_9NO_3$	↓	1.2751
40	6.05	260.1370	$[M + H]^+$	L-gamma-Glutamyl-L-leucine	$C_{11}H_{20}N_2O_5$	↓	0.7021
41	6.05	218.1055	$[M + H]^+$	N-Acetylserotonin	$C_{12}H_{14}N_2O_2$	↑	1.0294
42	6.53	257.1625	$[M + H]^+$	2-Hexenoylcarnitine	$C_{13}H_{23}NO_4$	↓	0.9174
43	6.56	189.0425	$[M + H]^+$	Kynurenic acid	$C_{10}H_7NO_3$	↓	0.8463
44	6.59	294.1213	$[M + H]^+$	Aspartame	$C_{14}H_{18}N_2O_5$	↓	0.7352
45	8.52	259.1782	$[M + H]^+$	Hexanoylcarnitine	$C_{13}H_{25}NO_4$	↓	0.8575
46	8.54	177.0281	$[M + H]^+$	Sulforaphane	$C_6H_{11}NOS_2$	↑	1.1457
47	9.32	205.0738	$[M + H]^+$	Indole-3-lactic acid	$C_{11}H_{11}NO_3$	↑	1.2161
48	10.41	337.1861	$[M + H]^+$	Istamycin AO	$C_{13}H_{27}N_3O_7$	↑	1.2429
49	12.85	219.1292	$[M + H]^+$	Pentahomomethionine	$C_{10}H_{21}NO_2S$	↓	0.7331
50	13.01	129.0579	$[M + H]^+$	Quinoline	C_9H_7N	↑	1.3006
51	15.74	313.2253	$[M + H]^+$	9-Decenoylcarnitine	$C_{17}H_{31}NO_4$	↓	0.7838
52	15.90	346.2144	$[M + H]^+$	Corticosterone	$C_{21}H_{30}O_4$	↑	1.2626

(Continued on following page)

10.3389/fphar.2023.1131479

TABLE 3 (*Continued*) Metabolites in serum samples.

No.	Rt (min)	Observed (m/z)	Ion mode	Identification	Formula	Tendency in model samples *versus* control samples	VIP
53	15.95	341.2564	$[M + H]^+$	Trans-2-Dodecenoylcarnitine	$C_{19}H_{35}NO_4$	↓	0.8213
54	16.00	367.2721	$[M + H]^+$	3, 5-Tetradecadiencarnitine	$C_{21}H_{37}NO_4$	↓	0.8208
55	16.04	210.1232	$[M + H]^+$	Jasmonic acid	$C_{12}H_{18}O_3$	↑	0.9176
56	16.04	301.2979	$[M + H]^+$	Sphinganine	$C_{18}H_{39}NO_2$	↓	0.7849
57	16.13	360.2298	$[M + H]^+$	Iloprost	$C_{22}H_{32}O_4$	↑	1.3640
58	16.18	423.3347	$[M + H]^+$	Linoleyl carnitine	$C_{25}H_{45}NO_4$	↓	0.7149
59	16.24	399.3347	$[M + H]^+$	Palmitoylcarnitine	$C_{23}H_{45}NO_4$	↓	0.7318
60	16.45	314.2219	$[M + H]^+$	THC	$C_{21}H_{30}O_2$	↑	0.8493
61	16.58	262.1568	$[M + H]^+$	3″-Hydroxy-geranylhydroquinone	$C_{16}H_{22}O_3$	↑	0.9573
62	16.69	308.2326	$[M + H]^+$	Eicosapentaenoic acid	$C_{20}H_{30}O_2$	↑	1.0847
63	16.70	304.2399	$[M + H]^+$	Arachidonic acid	$C_{20}H_{32}O_2$	↓	0.8450
64	18.04	110.0368	$[M + H]^+$	Hydroquinone	$C_6H_6O_2$	↓	0.8630
65	13.02	189.0789	$[M + H]^+$	Methyl indole-3-acetate	$C_{11}H_{11}NO_2$	↑	1.2827
66	1.60	117.0420	$[M-H]^-$	N-Acetylglycine	$C_4H_7NO_3$	↑	1.0214
67	1.67	117.0784	$[M-H]^-$	5-Aminovaleric acid	$C_5H_{11}NO_2$	↓	0.9335
68	1.78	118.0261	$[M-H]^-$	Methylmalonic acid	$C_4H_6O_4$	↑	1.0963
69	1.78	202.0949	$[M-H]^-$	Ser-pro	$C_8H_{14}N_2O_4$	↑	1.1308
70	2.02	129.0420	$[M-H]^-$	4-Oxoproline	$C_5H_7NO_3$	↑	0.6355
71	2.06	192.0262	$[M-H]^-$	Citric acid	$C_6H_8O_7$	↑	0.6741
72	2.82	183.0525	$[M-H]^-$	4-Pyridoxic acid	$C_8H_9NO_4$	↓	0.3797
73	2.84	116.0469	$[M-H]^-$	Methyl acetoacetate	$C_5H_8O_3$	↓	0.6839
74	4.68	145.0732	$[M-H]^-$	4-Acetamidobutanoic acid	$C_6H_{11}NO_3$	↑	1.0323
75	5.24	204.0895	$[M-H]^-$	D-(+)-Tryptophan	$C_{11}H_{12}N_2O_2$	↓	1.2278
76	5.39	214.0117	$[M-H]^-$	L-Aspartyl-4-phosphate	$C_4H_9NO_7P$	↓	1.0156
77	5.98	260.1371	$[M-H]^-$	Leu-Glu	$C_{11}H_{20}N_2O_5$	↓	0.6926
78	6.14	130.0624	$[M-H]^-$	6-Oxohexanoic acid	$C_6H_{10}O_3$	↓	0.8673

(Continued on following page)

10.3389/fphar.2023.1131479

TABLE 3 (*Continued*) Metabolites in serum samples.

No.	Rt (min)	Observed (m/z)	Ion mode	Identification	Formula	Tendency in model samples *versus* control samples	VIP
79	8.57	193.0733	$[M-H]^-$	2-Methylhippuric acid	$C_{10}H_{11}NO_3$	↑	1.1274
80	8.70	166.0623	$[M-H]^-$	3-Phenyllactic acid	$C_9H_{10}O_3$	↑	1.0823
81	9.84	174.0885	$[M-H]^-$	Suberic acid	$C_8H_{14}O_4$	↓	1.1495
82	16.00	194.0936	$[M-H]^-$	Butylparaben	$C_{11}H_{14}O_3$	↑	1.8263
83	16.01	370.2355	$[M-H]^-$	Thromboxane B2	$C_{20}H_{34}O_6$	↑	1.4778
84	16.14	188.1405	$[M-H]^-$	3-Hydroxydecanoic acid	$C_{10}H_{20}O_3$	↑	1.3511
85	16.37	244.2034	$[M-H]^-$	2-Hydroxymyristic acid	$C_{14}H_{28}O_3$	↑	1.6081
86	16.46	216.1719	$[M-H]^-$	12-Hydroxylauric acid	$C_{12}H_{24}O_3$	↑	1.2065
87	16.56	318.2192	$[M-H]^-$	5-HEPE	$C_{20}H_{30}O_3$	↑	1.3855
88	16.61	242.1877	$[M-H]^-$	3-Oxotetradecanoic acid	$C_{14}H_{26}O_3$	↓	0.4613
89	16.61	296.2350	$[M-H]^-$	13S-Hydroxyoctadecadienoic acid	$C_{18}H_{32}O_3$	↓	0.8055
90	16.63	272.2349	$[M-H]^-$	16-Hydroxyhexadecanoic acid	$C_{16}H_{32}O_3$	↓	0.9383
91	16.75	346.2504	$[M-H]^-$	Ginkgoic acid	$C_{22}H_{34}O_3$	↑	1.1884
92	16.88	348.2662	$[M-H]^-$	Anacardic acid	$C_{22}H_{36}O_3$	↑	1.2482
93	17.44	328.2406	$[M-H]^-$	Docosahexaenoic acid	$C_{22}H_{32}O_2$	↓	0.9610
94	17.61	280.2402	$[M-H]^-$	Linoleic acid	$C_{18}H_{32}O_2$	↑	1.0674
95	17.62	330.2553	$[M-H]^-$	Docosapentaenoic acid	$C_{22}H_{34}O_2$	↑	1.0961
96	17.86	306.2554	$[M-H]^-$	8Z,11Z,14Z-Eicosatrienoic acid	$C_{20}H_{34}O_2$	↓	0.8787
97	17.88	256.2402	$[M-H]^-$	Ethyl myristate	$C_{16}H_{32}O_2$	↓	0.9412
98	17.99	332.2711	$[M-H]^-$	Adrenic acid	$C_{22}H_{36}O_2$	↓	0.8615
99	18.01	282.2558	$[M-H]^-$	Oleic acid	$C_{18}H_{34}O_2$	↓	0.9214
100	18.58	284.2717	$[M-H]^-$	Stearic acid	$C_{18}H_{36}O_2$	↓	1.0277
11	18.64	310.2870	$[M-H]^-$	11(Z)-Eicosenoic acid	$C_{20}H_{38}O_2$	↓	0.8998
102	19.37	312.3023	$[M-H]^-$	Arachidic acid	$C_{20}H_{40}O_2$	↓	0.8624

10.3389/fphar.2023.1131479

and evaporated to dryness. Next, 100 μL methanol–water (1:1, v/v) was added after a vortex and centrifugation according to similar conditions, and the supernatant was analyzed by UPLC-Orbitrap Fusion MS for metabolomics analysis.

2.6 UPLC-Orbitrap Fusion MS conditions of serum pharmacochemistry and metabolomics analysis

For serum pharmacochemistry analysis, the sample was separated for analysis on the UPLC-Orbitrap Fusion MS (Thermo Scientific, United States) equipped with a UPLC column (Hypersil GOLD 100 mm × 2.1 mm, 3 μm). The mobile phase system was composed of methanol (A) and 0.1% formic acid in water (B). The flow rate was controlled at 0.2 mL/min with a gradient program of 0–2 min, 93–70%B; 2–12 min, 70–30%B; 12–16 min, 30–20%B; and 16–27 min, 20–0%B. The column temperature and the injection volume were preset at 30°C and 5 μL, respectively. Mass spectral data acquisition was performed on Orbitrap Fusion MS equipped with an electrospray ionization source (ESI) in positive and negative ion modes. The optimal conditions of the ion source was set as follows: evaporation temperature, 275°C; sheath gas, 35 Arb; spray voltage, 3.50 Kv (in the positive ion mode) and −2.50 Kv (in the negative ion mode); auxiliary gas, 7 Arb; capillary temperature, 300°C. Scan mode: full mass (±) (resolution: 120,000); scan range: m/z 120–1,200.

For metabolomics analysis, the mobile phase system was composed of methanol (A) and 0.1% formic acid in water (B). The flow rate was controlled at 0.2 mL/min with a gradient program of 0–5 min, 93–70%B; 5–13 min, 70–48%B; 13–14 min, 48–6%B; 14–17 min, 6–3%B; and 17–20 min, 3–0%B. The temperature of the column was maintained at 30°C, and the injection volume was 5 μL. The scan range of Orbitrap Fusion MS was preset at m/z 100–1,000. The other parameters of UPLC and Orbitrap Fusion MS were consistent with serum pharmacochemistry analysis conditions.

2.7 Network analysis based on serum pharmacochemistry in ALI rats

The raw data of serum pharmacochemistry analysis were preprocessed using Compound Discoverer 3.3 software to identify the structure of serum components and further determine the aforementioned components by comparing the fragmentation pathways in Thermo Scientific™ Mass Frontier 7.0 software. The targets of the serum components were predicted from the Swiss Target Prediction database (http://www.swisstargetprediction.ch/). The GeneCards database (https://www.genecards.org/) and the Online Mendelian Inheritance in Man (OMIM) database (https://omim.org/) were used to collect the ALI-associated targets, which were searched using the keywords “acute lung injury”. To find 81 overlapping targets of AJH treatment for ALI from Venny obtained using the bioinformatics analysis platform (http://www.bioinformatics.com.cn/), which were entered into the STRING database (https://cn.string-db.org/cgi/input.pl) for protein–protein interaction (PPI) analysis, a TSV file was downloaded. The AJH–serum component–target–ALI network and PPI network were constructed using Cytoscape 3.2.1 software (Cytoscape Consortium, National Institute of General Medical Sciences, United States). Then, enrichment analysis was carried out in the Metascape database (https://metascape.org/) to predict and analyze Gene Ontology (GO) and the related signaling pathways.

2.8 Metabolomics data processing based on multivariate data analysis

Principal component analysis (PCA) was used to visualize the global chemical variations among the control, LPS, LPS + AJH-L, LPS + AJH-M, LPS + AJH-H, and LPS + Dex groups, while partial least squares-discriminant analysis (PLS-DA) was utilized to discover the potential biomarkers, which were defined as the components displaying a variable importance in projection (VIP) > 1.0 in the current work. Then, the potential biomarkers were identified by comparing the Human Metabolome Database (http://www.hmdb.ca/) and the Kyoto Encyclopedia of Genes and Genomes (http://www.kegg.ca/). The potential biomarkers were inputted into MetaboAnalyst 5.0 to reveal the related metabolic pathway. The metabolic pathways with an impact value >0.10 were considered to be the potential target pathway.

2.9 Statistical analysis

All data were expressed as the mean ± standard deviation, and statistical analysis was carried out by one-way analysis of variance using SPSS Statistics 26.0. Least significant difference analysis was applied to groups that conformed to the homogeneity test of variance, while Dunnett’s T3 test was performed for groups inconsistent with the homogeneity test of variance. $\alpha < 0.05$ was considered statistically significant. All metabolomics data preprocessed using Compound Discoverer 3.3 and Mass Frontier 7.0. were inputted into SIMCA 14.1 software for the multivariate statistical analysis, including PCA and PLS-DA.

3 Results

3.1 Biochemical parameters and histopathologic analysis

Compared with the control group, IL-6 in serum and BALF was significantly upregulated and IL-10 was downregulated in the LPS group, indicating successful modeling of ALI ($p < 0.01$), as shown in Supplementary Table S1. The level of IL-6 in serum and BALF was decreased; however, the IL-10 expression significantly increased in LPS + AJH groups and LPS + Dex group compared with the LPS group (Figure 2B). Results of IL-6 and IL-10 levels indicated that the protective effects of AJH showed obvious improvement. In addition, AJH groups improved the parameters of lung function by regulating bronchoconstriction and airway resistance, with no significant difference, as shown in Figure 2A and Supplementary Table S2. In order to further identify the therapeutic effect of AJH, the lung

W/D ratio and indexes of the thymus and spleen were detected and calculated (Figure 2C and Supplementary Table S3). Compared with the control group, the indexes of the thymus and spleen were decreased in the LPS group ($p < 0.05$ and 0.01). The thymus and spleen indexes of LPS + AJH-H and LPS + Dex groups were significantly increased compared with those of the LPS group ($p < 0.05$ and 0.01). In addition, compared with the control group, the W/D ratio in the LPS group was markedly increased, indicating severe edema ($p < 0.01$). The LPS + AJH-treated groups could improve lung, thymus, and spleen injury. Pathological results further indicated that the LPS group showed distinct histological changes, including alveolar ectasia, alveolar fusion, airway wall thickening, and infiltration of a mass of inflammatory cells into alveolar spaces. Pathological changes were alleviated in the LPS + AJH-treated groups (Figure 2D) compared with the LPS group. All these results showed that the ALI model was successfully established, and the LPS + AJH-L, LPS + AJH-M, and LPS + AJH-H groups have a therapeutic effect on ALI (lung function, lung W/D ratio, indexes of the thymus and spleen, and histological changes), which appeared to be dose-dependent. The AJH-treated groups could also reduce the inflammation on ALI. The anti-inflammatory activity of LPS + AJH-H and LPS + AJH-M groups was better than that of the LPS + AJH-L group.

3.2 Characterization and identification of serum components in the ALI rat model

The UPLC-Orbitrap Fusion MS, an instrument with high sensitivity and accuracy, was employed to identify the serum components in the ALI rat model. The total ion chromatogram (TIC) is shown in Figure 3. A total of 71 serum components and 18 related metabolites were identified in ALI rats, and the details including name, retention time, and fragments ions are presented in Tables 1, 2. Among them, 21 components, including kaempferol, myricitrin, and hydroxygenkwanin, were classified as flavonoids; eight components, including bergenin, fraxetin, and scopoletin, were identified as phenylpropanoids; and nine terpenes and three quinones, four steroids, 26 carboxylic acids, and other components were also observed. In addition, 15 serum components were identified by comparing with the reference standards.

3.3 Network analysis based on serum components in the ALI rat model

In network analysis, we analyzed and selected 40 components among 71 serum components identified by UPLC-Orbitrap Fusion MS, which have acted on 81 overlapping targets. The AJH–serum component–target–ALI network (Figure 4A) included 122 nodes (one AJH, 40 serum components, and 81 targets) and 422 edges. The mean degree value of the components was 6.9, which indicated that the components regulated multiple targets to achieve therapeutic effects of AJH against ALI. In addition, hydroxygenkwanin, luteolin, apigenin, kaempferol, and quercetin acted on 28, 27, 27, 26, and 24 targets, respectively. Due to their important positions in this network, the aforementioned five components were selected as core components.

We found 81 overlapping targets to construct the PPI network (Figure 4B). The average node degree was 34.5, in which 36 targets (degree >34.5) were selected as core targets. The core targets with topological significance, including TNF, tumor protein (TP) 53, albumin (ALB), IL-6, AKT serine/threonine kinase (AKT)1, vascular endothelial growth factor A (VEGFA), epidermal growth factor receptor (EGFR), mitogen-activated protein kinase (MAPK), and toll-like receptor (TLR) 4, might play an important role in the molecular mechanism of AJH against ALI. The number of Gene Ontology (GO) biological processes (BP), GO cellular components (CC), and GO molecular functions (MF) was 1,499, 62, and 108, respectively. GOBP, GOCC, and GOMF with all top 20 *p*-values were screened and represented by a graphical bubble with the *p*-value, as shown in Figures 5A–C and Supplementary Table S4. Finally, we found 171 related signaling pathways. The top 20 *p*-values were represented by a graphical bubble, as shown in Figure 5D and Supplementary Table S5, which included the PI3K-Akt, AGE-RAGE, and JAK-STAT signaling pathways.

3.4 Metabolomics analysis

According to the established UPLC-Orbitrap Fusion MS analysis method, the serum sample data of the control, LPS, LPS + Dex, LPS + AJH-L, LPS + AJH-M, and LPS + AJH-H groups were analyzed, and the TIC spectra are shown in Figure 6A with a total of 102 metabolites annotated and identified (Table 3). PCA can reduce the dimensionality of complex datasets to form several main components, reflect the natural distribution of different groups, and find outliers (Huang et al., 2018). The data of 102 metabolites in each group were performed using SIMCA 14.1 software to establish the PCA score plot (Figure 6B). The control, LPS, LPS + Dex, and LPS + AJH-treated groups were significantly scattered and clustered. In addition, the control group was significantly separated from the LPS group, which further proved that the ALI rat model was successfully replicated, as shown in Figure 6B. Compared with the control group and LPS group, the LPS + Dex and LPS + AJH-treated groups are close to the control group and away from the LPS group. The aforementioned PCA results illustrated the effectiveness of AJH in the intervention of ALI.

In order to further select potential biomarkers and determine the difference between the control group and LPS group, between control, LPS groups, and LPS + AJH-treated groups, and between control, LPS groups, and LPS + Dex group, the metabolomics data were placed in a supervised method of PLS-DA (Figure 6C). The R^2X, R^2Y, and Q^2 in the PLS-DA model were 0.782, 0.964, and 0.916, respectively ($Q^2 > 0.5$). After setting permutations at 200 times, the permutation test of the PLS-DA model was applied to further assess the reliability level. As shown in Supplementary Figure S1, all the Q^2 and R^2 values of Y-permuted models were lower than those of the original models, which showed that the PLS-DA model has a significant explanation or prediction ability and is not over-fitted. Based on VIP >1.0 (Figure 6D), 43 components were selected as potential biomarkers and are presented in Table 3.

In Figure 7A, the control group and LPS group were scattered and clustered, which showed that the ALI rat model was successfully established. Then, the control, LPS, and LPS + Dex/AJH-H/AJH-M/AJH-L groups were obviously clustered into three individual groups

10.3389/fphar.2023.1131479

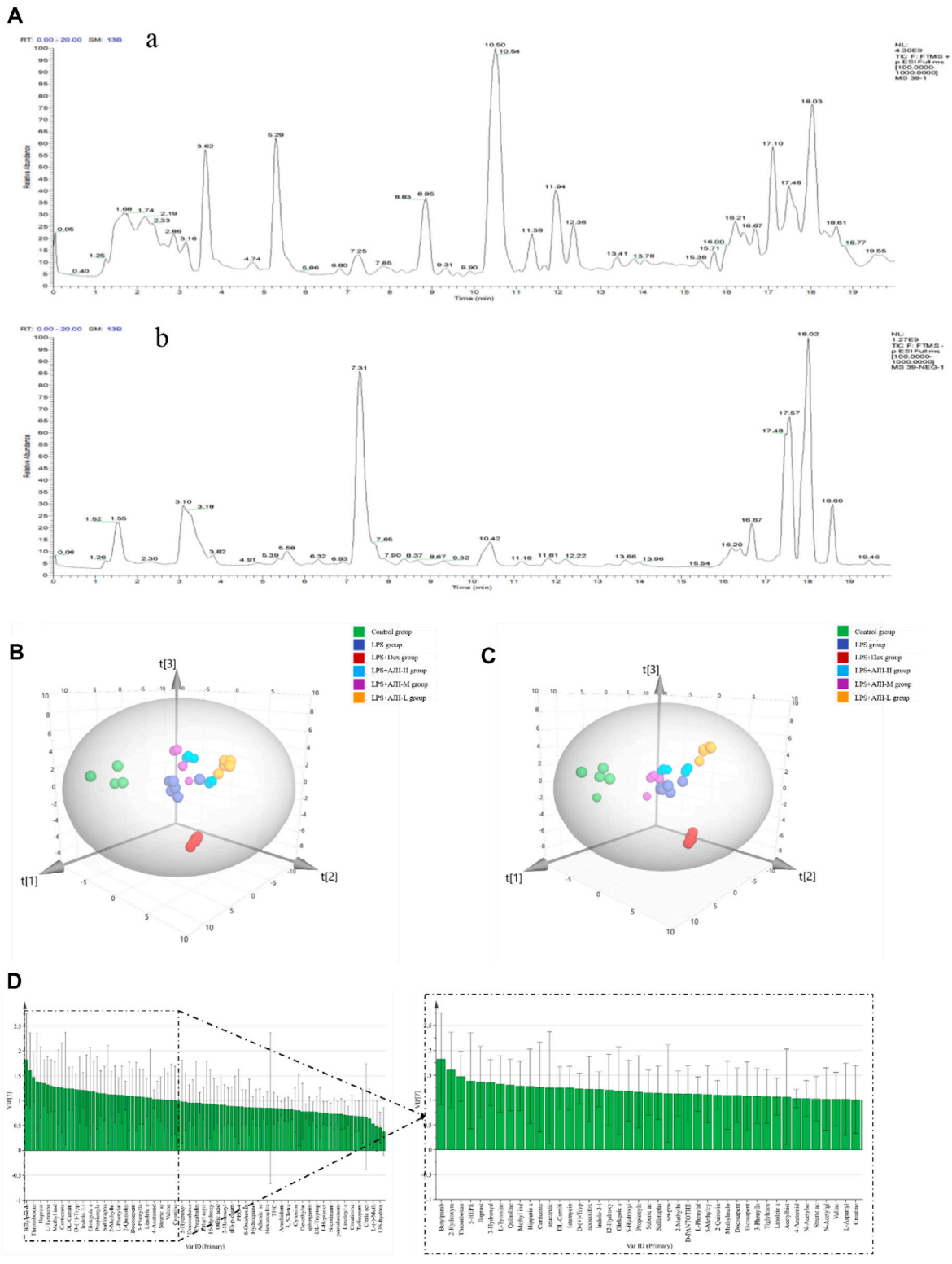

FIGURE 6
Metabolomics analysis based on the multivariate statistical method. **(A)** Total ion chromatograms (TICs) of metabolic samples (a. positive ion mode; b. negative ion mode); **(B)** 3D PCA score plot; **(C)** 3D PLS-DA score plot; **(D)** VIP chart.

and separated from each other (Figure 7A), and the results of the permutation test indicated that the PLS-DA model was reliable and not over-fitted (Figure 7B). According to the cleavage law of mass spectrometry, HCDM, Compound Discoverer database, and references, we identified 43 potential biomarkers. The further analysis was aimed at the content level and tendency of the

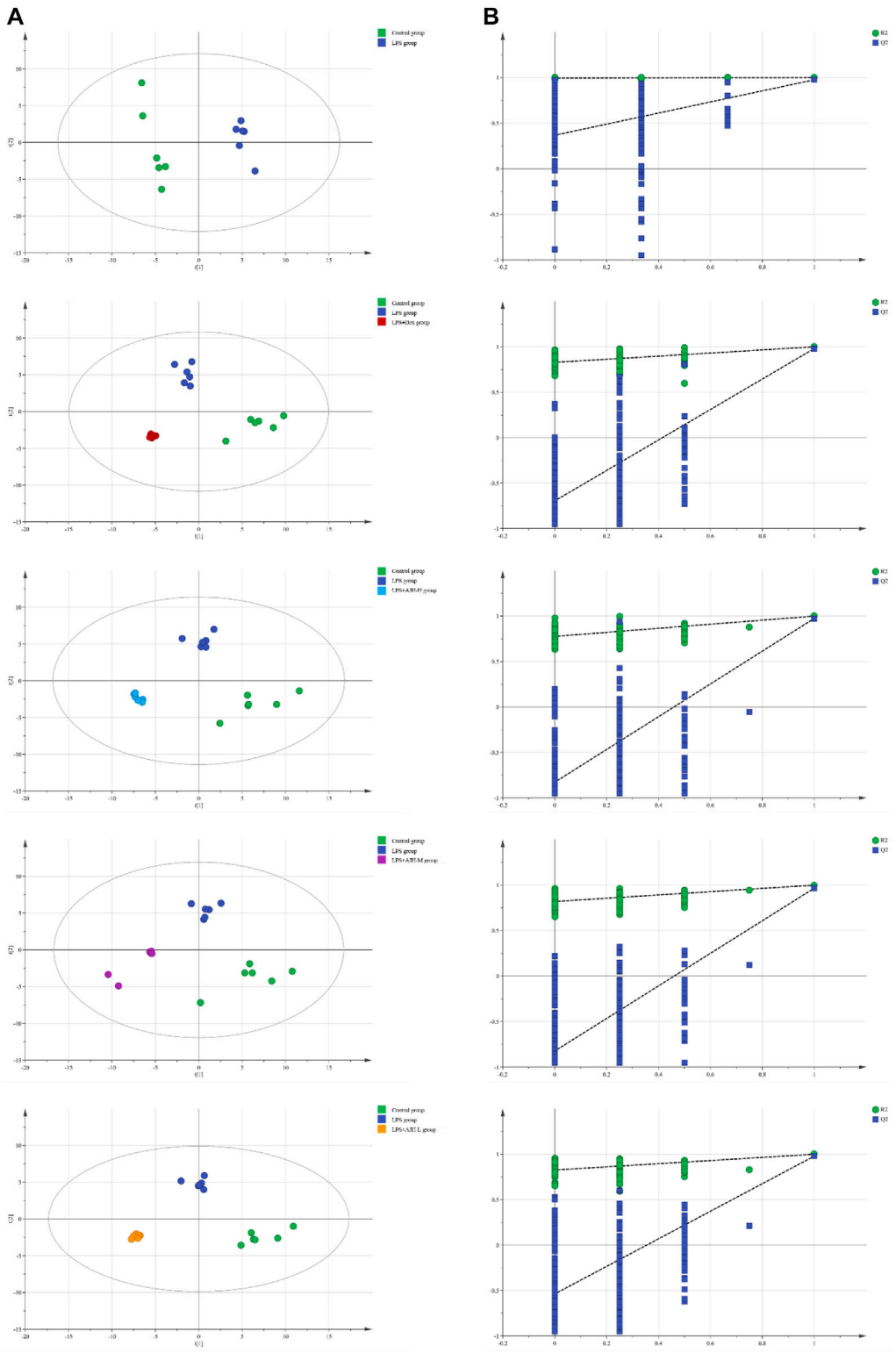

FIGURE 7
Metabolomics analysis between control and LPS groups, between control, LPS, and LPS + Dex groups, between control, LPS, and LPS + AJH-H groups, between control, LPS, and LPS + AJH-M groups, and between control, LPS, and LPS + AJH-L groups. **(A)** PLS-DA score plot; **(B)** permutation test of the PLS-DA model.

identified biomarkers in each group, as shown in Figures 8A, B. Compared with the control group, the levels of L-phenylalanine, linoleic acid, L-tyrosine, methyl indole-3-acetate, propionylcarnitine, 2-methylhippuric acid, DL-carnitine, corticosterone, creatine, neosaxitoxin, 5-HEPE, 3-hydroxydecanoic acid, 3-phenyllactic acid, iloprost, quinoline,

10.3389/fphar.2023.1131479

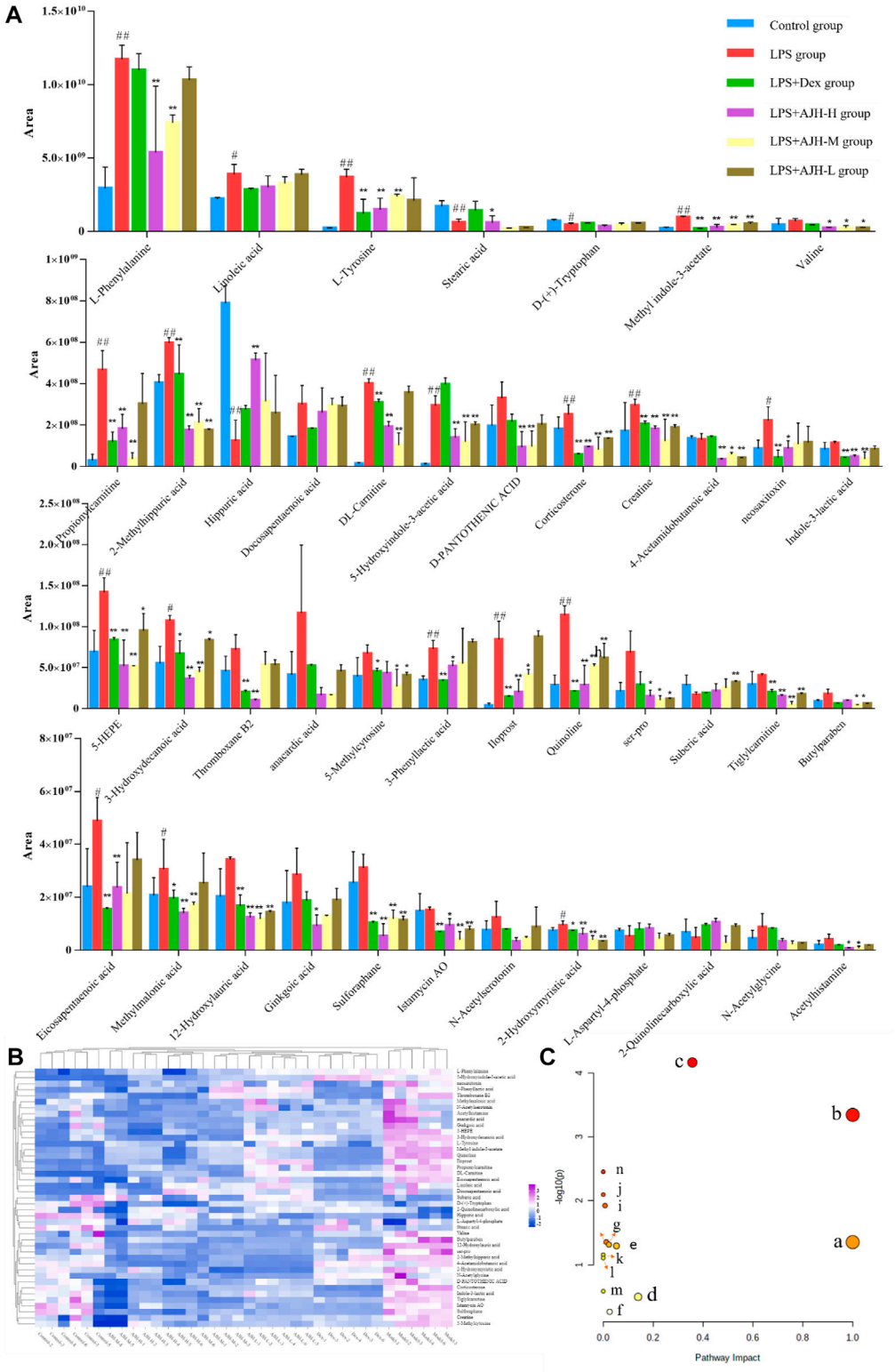

FIGURE 8
Systems analysis of potential metabolomic biomarkers in each group. **(A)** Histogram of the relative content of potential metabolomic biomarkers ($^{\#}p < 0.05$, $^{\#\#}p < 0.01$ vs the control group; $^{*}p < 0.05$, $^{**}p < 0.01$ vs the LPS group). **(B)** Heatmap of potential metabolomic biomarkers in control, LPS, LPS + Dex, LPS + AJH-H, LPS + AJH-M, and LPS + AJH-L groups. **(C)** Metabolic pathway analysis associated with the pathogenesis of ALI using MetaboAnalyst 5.0 (a. linoleic acid metabolism; b. phenylalanine, tyrosine, and tryptophan biosynthesis; c. phenylalanine metabolism; d. tyrosine metabolism; e. tryptophan metabolism; f. steroid hormone biosynthesis; g. valine, leucine, and isoleucine degradation; h. arginine and proline metabolism; i. pantothenate and CoA biosynthesis; j. aminoacyl-tRNA biosynthesis; k. valine, leucine, and isoleucine biosynthesis; l. ubiquinone and other terpenoid–quinone biosynthesis; m. glycine, serine, and threonine metabolism; n. biosynthesis of unsaturated fatty acids).

TABLE 4 Details about 14 metabolic pathways.

No.	Pathway name	Match status	P	-log(p)	Holmp	Impact	Biomarkers
a	Linoleic acid metabolism	1/5	0.044409	1.3525	1	1	Linoleate
b	Phenylalanine, tyrosine, and tryptophan biosynthesis	2/4	0.0004501	3.3467	0.03736	1	L-Phenylalanine and L-tyrosine
c	Phenylalanine metabolism	3/10	0.0000679	4.168	0.00571	0.35714	L-Tyrosine, hippurate, and L-phenylalanine
d	Tyrosine metabolism	1/42	0.32039	0.49432	1	0.13972	L-Tyrosine
e	Tryptophan metabolism	2/41	0.050822	1.2939	1	0.05291	N-Acetylserotonin and 5-hydroxyindoleacetate
f	Steroid hormone biosynthesis	1/85	0.54752	0.2616	1	0.02562	Corticosterone
g	Valine, leucine, and isoleucine degradation	2/40	0.048593	1.3134	1	0.02264	L-Valine and methylmalonate
h	Arginine and proline metabolism	2/38	0.044248	1.3541	1	0.01212	Creatine and 4-acetamidobutanoate
i	Pantothenate and CoA biosynthesis	2/19	0.011871	1.9255	0.94967	0.00714	Pantothenate and L-valine
j	Aminoacyl-tRNA biosynthesis	3/48	0.0079837	2.0978	0.64668	0	L-Phenylalanine, L-valine, and L-tyrosine
k	Valine, leucine, and isoleucine biosynthesis	1/8	0.070168	1.1539	1	0	L-Valine
l	Ubiquinone and other terpenoid–quinone biosynthesis	1/9	0.07861	1.1045	1	0	L-Tyrosine
m	Glycine, serine, and threonine metabolism	1/33	0.26108	0.58322	1	0	Creatine
n	Biosynthesis of unsaturated fatty acids	3/36	0.0035154	2.454	0.28826	0	Octadecanoic acid, linoleate, and (5Z,8Z,11Z,14Z,17Z)-icosapentaenoic acid

eicosapentaenoic acid, methylmalonic acid, and 2-hydroxymyristic acid were significantly upregulated in the LPS group ($p < 0.05/p < 0.01$). The levels of stearic acid, D-(+)-tryptophan, and hippuric acid were downregulated in the LPS group ($p < 0.05/p < 0.01$). We found that the LPS + AJH-treated groups had a callback effect on the aforementioned potential biomarkers ($p < 0.05$ and $p < 0.01$). Once again, the therapeutic effects of LPS + AJH-M and LPS + AJH-H groups were better than those of the LPS + AJH-L group.

To further classify the metabolic pathways related to ALI, the 43 identified metabolic biomarkers were introduced into MetaboAnalyst 5.0 software to obtain 14 metabolic pathways, as shown in Figure 8C and Table 4. Based on the screening criteria of the pathway impact value greater than 0.1 and literature reports (Hu et al., 2020), four metabolic pathways closely associated with AJH intervention in ALI were obtained: linoleic acid metabolism, phenylalanine, tyrosine, and tryptophan biosynthesis, phenylalanine metabolism, and tyrosine metabolism.

4 Discussion

ALI is caused by the excessive release of the inflammatory cytokines to break the balance of inflammatory and anti-inflammatory cytokines, which can further develop into the systemic inflammatory response syndrome (SIRS), acute respiratory distress syndrome (ARDS), and eventually to multiple organ failure (MOF) (Liu and Chen, 2016). Therefore, inflammation is of great significance in ALI, especially chronic obstructive pulmonary disease and acute exacerbation of chronic obstructive pulmonary disease. Inflammation causes the infiltration of inflammatory cells and can release the chemokines and pro-inflammatory cytokines (Han et al., 2022; Yuan et al., 2022). The related study has demonstrated that TNF-α, IL-1β, IL-6, IL-8, and IL-18 are most closely associated with the outcome of ALI and are the current diagnosis and prognosis method (Parsons et al., 2005). Lv et al. (2021) indicated that fluorofenidone has a therapeutic effect on ALI by alleviating the lung tissue structure and decreasing the levels of IL-1β, IL-6, and TNF-α in the BALF. In our study, the level of IL-6 and IL-10 in serum and BALF were significantly upregulated or downregulated in ALI model rats compared with the control group, which might imply that AJH had anti-inflammatory capability. In addition, the lung wet/dry (W/D) ratio and indexes of the thymus and spleen in the LPS group were markedly elevated. The aforementioned indexes were also improved in the AJH-treated groups at different levels. Therefore, our study proved that AJH improved lung function and decreased systemic inflammation and provided evidence of an anti-inflammatory role of AJH at multiple levels. In our histopathological study, marked inflammatory cell infiltration, alveolar ectasia and fusion, and bronchiolar stenosis were improved in the AJH-treated groups at different levels.

In our previous study, we identified 236 components in AJH. Network analysis indicated that 41 core components could regulate the inflammation-related pathways, and the core components have anti-inflammatory effects (Feng et al., 2022). According to Bencao Shiyi, AJH is effective in reducing swelling, resolving phlegm, and relieving cough, which is widely used for treating cough, wheezing,

blood in sputum, chronic bronchitis, and damp heat jaundice. Zhou et al. (2012) investigated and found that AJH is effective in preventing respiratory diseases, which can relieve symptoms and improve the pulmonary function in chronic obstructive pulmonary disease. Recently, network analysis illustrates the complex interactions among the biological systems, drugs, and disease from a network perspective, which opens avenues for new research ideas and technical means to study the action mechanisms of the CM formulae (Li, 2021). In our study, we further identified the serum components in ALI rats and used integrated network analysis and metabolomics to study the therapeutic effects of AJH in the ALI treatment. We identified a total of 71 serum components and 18 related metabolites in the ALI rat model, mainly including flavonoids, phenylpropanoids, and terpenes.

Because serum components in AJH might act on the diverse potential targets, we collected targets of serum components and targets associated with ALI to further explore the mechanisms underlying AJH against ALI by network analysis. According to degree values in the AJH–component–target–ALI network, we selected the five core serum components, including hydroxygenkwanin, luteolin, apigenin, kaempferol, and quercetin. The aforementioned core serum components of AJH belonged to flavonoids. Flavonoids are ubiquitous in all vascular plants and have been recognized to possess anti-inflammatory, anti-atherogenic, anti-allergic, and anti-cancer activities *in vitro* and *in vivo* (Ana et al., 2008; Chagas et al., 2022). Jiang et al. (2014) indicated that hydroxygenkwanin, luteolin, and apigenin possess immunoregulatory functions in LPS-activated RAW264.7 cells by suppressing the production of NO, which shows significant anti-inflammatory and antioxidant activities. In our previous study, luteolin, kaempferol, and quercetin showed an anti-inflammatory effect by regulating the IL-6 and MMP9 levels in the TNF-α-induced A549 cell model (Han et al., 2021; Feng et al., 2022). In addition, the PPI network was constructed to select the key targets among 81 overlapping targets, including TNF, TP53, ALB, IL-6, AKT1, VEGFA, EGFR, MAPK, and TLR4. The related studies revealed that IL-6, VEGFA, EGFR, and MAPK are linked to inflammatory pathogenesis of ALI (Chu et al., 2016; Ying et al., 2022). These key targets might be regulated to achieve anti-inflammatory activity of AJH against ALI. According to GO and KEGG analysis, some targets among the 81 overlapping targets are highly enriched inflammatory-related pathways, including the PI3K-Akt, AGE-RAGE, and JAK-STAT signaling pathways. Yu et al. (2022) suggested that the AGE-RAGE signaling pathway is activated to further increase the levels of pro-inflammatory cytokines, including IL-1β and TNF. The relevant studies illustrated that the PI3K-AKT could regulate downstream inflammatory cytokines, which plays a crucial role in inflammatory response (Schaper and Rose-John, 2015; Nazanin et al., 2020). Therefore, the serum components of AJH might act on 81 overlapping targets to regulate inflammatory-related pathways.

The metabolomics analysis revealed some potential biomarkers related with the therapeutic effects of AJH for LPS-induced ALI. Upregulation of L-Phenylalanine and downregulation of L-tyrosine in the ALI rat model were the intermediates of phenylalanine, tyrosine, and tryptophan biosynthesis. Capuron et al. (2011) illustrated that increased inflammation is linked to reduced tryptophan levels to improve tryptophan catabolism, and the inflammation was associated with increasing phenylalanine levels at the expense of tyrosine. We found that L-phenylalanine and L-tyrosine concentrations were called back in the LPS + AJH-treated groups, indicating the therapeutic effects of AJH on LPS-induced ALI rats. In addition, due to mitochondria being vulnerable to oxidation stress and pro-inflammatory mediators (Liu and Chen, 2016). Ji (2020), a LPS-induced macrophage inflammatory environment reduces the core enzyme levels of mitochondria and affects mitochondrial function that is closely related to the stability of the citrate cycle. In our study, the creatine levels associated with the citrate cycle were significantly downregulated in the LPS + AJH-treated groups, which revealed that AJH could protect LPS-induced ALI rats by restoring the disordered metabolism. Furthermore, the relative study suggested that fatty acids and derivatives play essential roles in various physiological processes, which have endogenous anti-inflammatory, antibacterial, antifungal, antiviral, and immunomodulatory agents (Das, 2018) and were considered clinical diagnosis indexes associated with inflammation (Does et al., 2018). Linoleic acid, as typical essential fatty acids, is a precursor and generates dihomo-gamma-linolenic acid and arachidonic acid (Evans et al., 2014). According to our results, the levels of linoleic acid in ALI rats were increased, but its concentration was called back in the LPS + AJH-treated groups. The previous study showed that arachidonic acid, as an important precursor of inflammatory mediators (eicosanoids), can regulate inflammatory and immune responses (Chandrasekharan et al., 2016). Meanwhile, arachidonic acid was related to inflammatory pathways including TLR4 and MAPK (Mateu et al., 2016), which could be evidenced from our network analysis results. Moreover, the level of arachidonic acid among 102 metabolites was decreased in ALI rats in our study, which may be converted into pro-inflammatory products and is consistent with the previous results (Wang et al., 2020).

Therefore, AJH modulation on potential biomarker metabolism might be related to the regulation of inflammatory-related pathways selected by network analysis of serum components. In addition, we further hypothesized that AJH exerts anti-inflammatory activity in the LPS-induced ALI model by regulating potential biomarkers, including L-phenylalanine, L-tyrosine, and linoleic acid levels in phenylalanine, tyrosine, and tryptophan biosynthesis and linoleic acid metabolism. Thus, the regulation of AJH on phenylalanine, tyrosine, and tryptophan biosynthesis and linoleic acid metabolism may be associated with its alleviatory effects on inflammation responses *in vivo* to improve LPS-induced ALI. Our study initially elucidated serum material basis and effective mechanism of AJH in the ALI treatment by network analysis and untargeted metabolomics. For a better understanding of the molecular mechanism of potential biomarkers and related metabolism pathways, targeted metabolomics, proteomics, and genomics need to be studied further.

5 Conclusion

In our study, we integrated metabolomics and network analysis of serum pharmacochemistry and systematically unrevealed the material basis and molecular mechanism of AJH in the ALI

treatment. A total of 71 serum components and 18 related metabolites were identified by UPLC-Orbitrap Fusion MS. After network analysis of the aforementioned serum components, five core flavonoid components were selected. Preliminarily, AJH was hypothesized to treat ALI by modulating the core targets, including TNF, TP53, ALB, IL-6, AKT1, MAPK, and TLR4, and related signaling pathways (PI3K-Akt, AGE-RAGE, and JAK-STAT), which laid the foundation for the specific molecular mechanism of ALI treatment by AJH. Meanwhile, metabolomics results showed that AJH was effective in treating ALI by alleviating infiltration of inflammatory cells in alveolar spaces and regulating the expression of inflammatory cytokines. AJH might link to reverse the abnormality of phenylalanine, tyrosine, and tryptophan biosynthesis and linoleic acid metabolism pathways to regulate the concentrations of potential biomarkers to normal levels. Therefore, AJH could alleviate inflammation responses in the ALI treatment.

Data availability statement

The original contributions presented in the study are included in the article/Supplementary Material; further inquiries can be directed to the corresponding authors.

Ethics statement

The experimental protocol was reviewed and approved by the Experimental Animal Care and Ethics Committee of Henan University of Chinese Medicine.

Author contributions

X-XH and Y-GT designed the study, analyzed the data, and drafted the manuscript. Y-GT and Y-PH performed animal experiments. W-JL, DZ, X-FL, and Y-PH designed this study and analyzed the corresponding data. S-XF and J-SL designed, supervised, and reviewed the manuscript. All authors contributed to the article and approved the submitted version.

Funding

This work was supported by the Henan Province Science and Technology Key Projects Fund (222102310375), Henan University of Chinese Medicine In-school Support Projects Fund (MP 2021–14), and Collaborative Innovation Center for Chinese Medicine and Respiratory Diseases co-constructed by Henan Province and Education Ministry of P.R. of China [(2022)002].

Conflict of interest

The authors declare that the research was conducted in the absence of any commercial or financial relationships that could be construed as a potential conflict of interest.

Publisher's note

All claims expressed in this article are solely those of the authors and do not necessarily represent those of their affiliated organizations, or those of the publisher, the editors, and the reviewers. Any product that may be evaluated in this article, or claim that may be made by its manufacturer, is not guaranteed or endorsed by the publisher.

Supplementary material

The Supplementary Material for this article can be found online at: https://www.frontiersin.org/articles/10.3389/fphar.2023.1131479/full#supplementary-material

References

Ana, G., Eduarda, F., Lima, L. J, Lurdes, M., and Luísa, C. M. (2008). Molecular mechanisms of anti-inflammatory activity mediated by flavonoids. *Curr. Med. Chem.* 15 (16), 1586–1605. doi:10.2174/092986708784911579

Bin, Y., Wenzheng, B., and Jinglong, W. (2022). Active disease-related compound identification based on capsule network. *Briefings Bioinforma.* 23 (1), bbab462. doi:10.1093/BIB/BBAB462

Cao, Q. S., Li, Z. C., Han, L. W., Zhang, Y. H., Zhang, Y. L., Hu, Y. J., et al. (2021). Effect of flavonoids of Ardisia japonica on levels of TNF-α and IL-1β of immune cytokines in hepatic fibrosis rats. *Laboratory Med. Clin.* 18 (07), 904–908.

Capuron, L., Schroecksnadel, S., Féart, C., Aubert, A., Higueret, D., Barberger-Gateau, P., et al. (2011). Chronic low-grade inflammation in elderly persons is associated with altered tryptophan and tyrosine metabolism: Role in neuropsychiatric symptoms. *Biol. Psychiatry* 70 (2), 175–182. doi:10.1016/j.biopsych.2010.12.006

Chagas, M. D. S. S., Behrens, M. D., Moragas-Tellis, C. J., Penedo, G. X. M., Silva, A. R., and Gonçalves-de-Albuquerque, C. F. (2022). Flavonols and flavones as potential anti-inflammatory, antioxidant, and antibacterial compounds. *Oxidative Med. Cell. Longev.* 2022, 9966750. doi:10.1155/2022/9966750

Chandrasekharan, J. A., Marginean, A., and Sharma-Walia, N. (2016). An insight into the role of arachidonic acid derived lipid mediators in virus associated pathogenesis and malignancies. *Prostagl. Other Lipid Mediat.* 126, 46–54. doi:10.1016/j.prostaglandins.2016.07.009

Chang, X. L., Li, W., Jia, Z. H., Tadaaki, S., Shinji, F., and Kazuo, K. (2007). Biologically active triterpenoid saponins from Ardisia japonica. *J. Nat. Prod.* 70 (2), 179–187. doi:10.1021/np0604681

Chu, C., Yao, S., Chen, J., Wei, X., Xia, L., Chen, D., et al. (2016). Eupatorium lindleyanum DC. flavonoids fraction attenuates lipopolysaccharide-induced acute lung injury in mice. *Int. Immunopharmacol.* 39, 23–33. doi:10.1016/j.intimp.2016.06.032

Das, U. N. (2018). Arachidonic acid and other unsaturated fatty acids and some of their metabolites function as endogenous antimicrobial molecules: A review. *J. Adv. Res.* 11, 57–66. doi:10.1016/j.jare.2018.01.001

Does, A. M. v. d., Heijink, M., Mayboroda, O. A., Persson, L. J., Aanerud, M., Bakke, P., et al. (2018). Dynamic differences in dietary polyunsaturated fatty acid metabolism in sputum of COPD patients and controls. *BBA - Mol. Cell. Biol. Lipids* 1864 (3). doi:10.1016/j.bbalip.2018.11.012

Evans, S. J., Ringrose, R. N., Harrington, G. J., Mancuso, P., Burant, C. F., and McInnis, M. G. (2014). Dietary intake and plasma metabolomic analysis of polyunsaturated fatty acids in bipolar subjects reveal dysregulation of linoleic acid metabolism. *J. Psychiatric Res.* 57, 58–64. doi:10.1016/j.jpsychires.2014.06.001

Feng, S. X., Yuan, J., Zhao, D., Li, R. R., Liu, X. F., Tian, Y. G., et al. (2022). Systematic characterization of the effective constituents and molecular mechanisms of Ardisiae Japonicae Herba using UPLC-Orbitrap Fusion MS and network pharmacology. *PloS one* 17 (6), e0269087. doi:10.1371/journal.pone.0269087

Gong, X., Cui, H. T., Bian, Y. H., Li, Y. T., Wang, Y. X., Peng, Y. F., et al. (2021). Ethanol extract of Ardisiae Japonicae Herba inhibits hepatoma carcinoma cell proliferation *in vitro* through regulating lipid metabolism. *Chin. Herb. Med.* 13 (3), 410–415. doi:10.1016/j.chmed.2021.06.003

Han, X. X., Tian, Y. G., Liu, X. F., Zhao, D., Du, X. H., Dong, H. R., et al. (2022). Network pharmacology combined with pharmacodynamics revealed the anti-inflammatory mechanism of Tanreqing capsule against acute-exacerbation chronic obstructive pulmonary disease. *Sci. Rep.* 12 (1), 13967. doi:10.1038/S41598-022-18326-1

Han, X. X., Zhao, D., Liu, X. F., Dong, H. R., and Feng, S. X. (2021). Study on the mechanism of radix astragali seu hedysari-fructus perillae combination in the treatment of chronic obstructive pulmonary disease based on network pharmacology and molecular docking. *Mod. Traditional Chin. Med. Materia Medica-World Sci. Technol.* 23 (09), 3147–3159.

Hu, L., Wang, Y., Sun, H., Xiong, Y., Zhong, L., Wu, Z., et al. (2020). An untargeted metabolomics approach to investigate the wine-processed mechanism of Scutellariae radix in acute lung injury. *J. Ethnopharmacol.* 253 (C), 112665. doi:10.1016/j.jep.2020.112665

Huang, B. M., Zha, Q. L., Chen, T. B., Xiao, S. Y., Xie, Y., Luo, P., et al. (2018a). Discovery of markers for discriminating the age of cultivated ginseng by using UHPLC-QTOF/MS coupled with OPLS-DA. *Phytomedicine* 45, 8–17. doi:10.1016/j.phymed.2018.03.011

Huang, X. F., Xiu, H. Q., Zhang, S. F., and Zhang, G. S. (2018b). The role of macrophages in the pathogenesis of ALI/ARDS. *Mediat. Inflamm.* 2018, 1264913. doi:10.1155/2018/1264913

Ji, D. (2020). *Effects of tricarboxylic acid cycle on mitochondrial function in imflammatory and anti-inflammatory environments*. Shanghai, China: Shanghai Ocean University.

Jiang, C. P., He, X., Yang, X. L., Zhang, S. L., Li, H., Song, Z. J., et al. (2014). Anti-rheumatoid arthritic activity of flavonoids from Daphne genkwa. *Phytomedicine* 21 (6), 830–837. doi:10.1016/j.phymed.2014.01.009

Jiang, Z. F., Zhang, L., and Shen, J. (2020). MicroRNA: Potential biomarker and target of therapy in acute lung injury. *Hum. Exp. Toxicol.* 39 (11), 1429–1442. doi:10.1177/0960327120926254

Levitt, J. E., Calfee, C. S., Goldstein, B. A., Vojnik, R., and Matthay, M. A. (2013). Early acute lung injury: Criteria for identifying lung injury prior to the need for positive pressure ventilation. *Crit. care Med.* 41 (8), 1929–1937. doi:10.1097/CCM.0b013e31828a3d99

Li, S. 2021. Network pharmacology evaluation method guidance-draft. *World J. Traditional Chin. Med.* 7(01), 148–154. doi:10.4103/wjtcm.wjtcm_11_21

Li, Y., Li, S. Y., Li, J. S., Deng, L., Tian, Y. G., Jiang, S. L., et al. (2012). A rat model for stable chronic obstructive pulmonary disease induced by cigarette smoke inhalation and repetitive bacterial infection. *Biol. Pharm. Bull.* 35 (10), 1752–1760. doi:10.1248/bpb.b12-00407

Liu, C., Yin, Z., Feng, T., Zhang, M., Zhou, Z., and Zhou, Y. (2021). An integrated network pharmacology and RNA-Seq approach for exploring the preventive effect of Lonicerae japonicae flos on LPS-induced acute lung injury. *J. Ethnopharmacol.* 264, 113364. doi:10.1016/j.jep.2020.113364

Liu, T. Y., and Chen, S. B. (2016). Sarcandra glabra combined with lycopene protect rats from lipopolysaccharide induced acute lung injury via reducing inflammatory response. *Biomed. Pharmacother.* 84, 34–41. doi:10.1016/j.biopha.2016.09.009

Liu, W. L., Yang, D. G., Yu, S. M., Huang, L. Y., Chen, S. F., and Guo, L. C. (2009). Studies on pharmacological action of aidicha. *Lishizhen Med. Materia Medica Res.* 20 (12), 3002–3003.

Lv, X., Yao, T., He, R., He, Y., Li, M., Han, Y., et al. (2021). Protective effect of fluorofenidone against acute lung injury through suppressing the MAPK/NF-κB pathway. *Front. Pharmacol.* 12 (null), 772031. doi:10.3389/fphar.2021.772031

Mateu, A., Ramudo, L., Manso, M. A., and Dios, I. D. (2016). Cross-talk between TLR4 and PPAR gamma pathways in the arachidonic acid-induced inflammatory response in pancreatic acini. *Chem. Chem.* 69, 132–141. doi:10.1016/j.biocel.2015.10.022

Nazanin, Z. S., Sajad, F., Hosein, F. M., Haroon, K., and Luciano, S. (2020). Astaxanthin targets PI3K/Akt signaling pathway toward potential therapeutic applications. *Food Chem. Toxicol.* 145, 111714. doi:10.1016/j.fct.2020.111714

Parsons, P. E., Eisner, M. D., Thompson, B. T., Matthay, M. A., Ancukiewicz, M., Bernard, G. R., et al. (2005). Lower tidal volume ventilation and plasma cytokine markers of inflammation in patients with acute lung injury. *Crit. care Med.* 33 (1), 1–6. doi:10.1097/01.ccm.0000149854.61192.dc

Savino, S., Mirae, P., Cecilia, T., Tanushree, T., Ryan, T., Tommaso, M., et al. (2019). Biomarkers for Acute Respiratory Distress syndrome and prospects for personalised medicine. J. Inflamm. *Lond. Engl.* 16 (1), 1. doi:10.1186/s12950-018-0202-y

Schaper, F., and Rose-John, S. (2015). Interleukin-6: Biology, signaling and strategies of blockade. *Cytokine Growth Factor Rev.* 26 (5), 475–487. doi:10.1016/j.cytogfr.2015.07.004

SeungHye, H., and Mallampalli, R. K. (2015). The acute respiratory distress syndrome: From mechanism to translation. *J. Immunol.* 194 (3), 855–860. doi:10.4049/jimmunol.1402513

Societies, W. F. o. C. M. (2021). Network pharmacology evaluation methodology guidance. *World J. Traditional Chin. Med.* 16 (04), 527–532.

Tien, D. N., KiHwan, B., Antony, W., B, M. J., J, L. G. S. F., Marion, B., et al. (2007). A dimeric lactone from Ardisia japonica with inhibitory activity for HIV-1 and HIV-2 ribonuclease H. *J. Nat. Prod.* 70 (5), 839–841. doi:10.1021/np060359m

Wang, T., Lin, S., Liu, R., Li, H., Liu, Z., Xu, H., et al. (2020). Acute lung injury therapeutic mechanism exploration for Chinese classic prescription Qingzao Jiufei Decoction by UFLC-MS/MS quantification of bile acids, fatty acids and eicosanoids in rats. *J. Pharm. Biomed. Analysis* 189, 113463. doi:10.1016/j.jpba.2020.113463

Wu, Y. Z., Zhang, Q., Wei, X. H., Jiang, C. X., Li, X. K., Shang, H. C., et al. (2022). Multiple anti-inflammatory mechanisms of Zedoary Turmeric Oil Injection against lipopolysaccharides-induced acute lung injury in rats elucidated by network pharmacology combined with transcriptomics. *Phytomedicine Int. J. phytotherapy Phytopharm.* 106, 154418. doi:10.1016/j.phymed.2022.154418

Xi, S. Y. (2006). "Experimental study on the effects of dicha kechuan oral liquid on the antioxidative enzymes' activity and maleic dialdehyde contents," in *Serum and lung tissues of mice with smoking induced chronic bronchitis master* (Tianjin, China: Hebei University of Chinese Medicine).

Xiong, H., Li, N., Zhao, L. Q., Li, Z., Yu, Y. Z., Cui, X. Y., et al. (2022). Integrated serum pharmacochemistry, metabolomics, and network pharmacology to reveal the material basis and mechanism of danggui shaoyao san in the treatment of primary dysmenorrhea. *Front. Pharmacol.* 13, 942955. doi:10.3389/fphar.2022.942955

Ying, W., Yuan, Y., Wenting, W., Ying, H., Hong, Z., Xiaoxia, Z., et al. (2022). Mechanisms underlying the therapeutic effects of Qingfeiyin in treating acute lung injury based on GEO datasets, network pharmacology and molecular docking. *Comput. Biol. Med.* 145, 105454. doi:10.1016/j.compbiomed.2022.105454

Yu, X. D., Zhang, D., Xiao, C. L., Zhou, Y., Li, X., Wang, L., et al. (2022). P-coumaric acid reverses depression-like behavior and memory deficit via inhibiting AGE-RAGE-mediated neuroinflammation. *Cells* 11 (10), 1594. doi:10.3390/cells11101594

Yuan, J., Zhao, D., Liu, X. F., Tian, Y. G., Zhang, H. J., Feng, S. X., et al. (2022). Systematic characterization of the components and molecular mechanisms of Jinshui Huanxian granules using UPLC-Orbitrap Fusion MS integrated with network pharmacology. *Sci. Rep.* 12 (1), 12476. doi:10.1038/s41598-022-16711-4

Zhang, H. Y., Sha, J. C., Feng, X. J., Hu, X. Y., Chen, Y. P., Li, B., et al. (2019). Dexmedetomidine ameliorates LPS induced acute lung injury via GSK-3β/STAT3-NF-κB signaling pathway in rats. *Int. Immunopharmacol.* 74, 105717. doi:10.1016/j.intimp.2019.105717

Zhang, J., Zhang, M., Zhang, W. H., Zhu, Q. M., Huo, X. K., Sun, C. P., et al. (2022). Total flavonoids of Inula japonica alleviated the inflammatory response and oxidative stress in LPS-induced acute lung injury via inhibiting the sEH activity: Insights from lipid metabolomics. *Phytomedicine* 107, 154380. doi:10.1016/J.PHYMED.2022.154380

Zhou, X., Ge, Z. X., and Bi, P. (2012). Miao medicine lung frame with warm air fried western medicine treatment chronic obstructive pulmonary disease at stable phrase effect analysis. *Chin. J. Exp. Traditional Med. Formulae* 18 (15), 305–307. doi:10.13422/j.cnki.syfjx.2012.15.013

Glossary

ALI	Acute lung injury
AJH	Ardisiae Japonicae Herba
LPS	Lipopolysaccharide
Dex	Dexamethasone
BALF	Bronchoalveolar lavage fluid
AGE-RAGE	Advanced glycation end product–receptor for advanced glycation end product
PI3K-AKT	Phosphatidylinositol-3-kinase/protein kinase B
JAK-STAT	Tyrosine kinase/signal transducer and transcription activator
IL	Interleukin
CM	Chinese medicine
ELISA	Enzyme-linked immunosorbent assay
ARRIVE	Animal Research: Reporting of *in vivo* Experiments
H&E	Hematoxylin and eosin
W/D	Wet/dry
QC	Quality control
OMIM	Online Mendelian Inheritance in Man
BP	Biological processes
CC	Cellular components
MF	Molecular functions
TIC	Total ion chromatogram
PCA	Principal component analysis
PLS-DA	Partial least squares-discriminant analysis
VIP	Variable importance
TNF	Tumor necrosis factor
TP	Tumor protein
ALB	Albumin
AKT	AKT serine/threonine kinase
MAPK	Mitogen-activated protein kinase
TLR	Toll-like receptor
SIRS	Systemic inflammatory response syndrome
ARDS	Acute respiratory distress syndrome
MOF	Multiple organ failure

frontiers | Frontiers in Pharmacology

TYPE Review
PUBLISHED 23 August 2023
DOI 10.3389/fphar.2023.1242318

OPEN ACCESS

EDITED BY
Bey Hing Goh,
Monash University Malaysia, Malaysia

REVIEWED BY
Hong-Hua Wu,
Tianjin University of Traditional Chinese Medicine, China
Junfei Gu,
Nanjing University of Chinese Medicine, China
Zhong-Yan Zhou,
Shanghai University of Traditional Chinese Medicine, China
Jinghui Zhai,
First Affiliated Hospital of Jilin University, China

*CORRESPONDENCE
Wei Ma,
mawei@hljucm.net
Weichao Ren,
lzyrenweichao@126.com

†These authors have contributed equally to this work

RECEIVED 19 June 2023
ACCEPTED 07 August 2023
PUBLISHED 23 August 2023

CITATION
Wang P, Wang Z, Zhang Z, Cao H, Kong L, Ma W and Ren W (2023), A review of the botany, phytochemistry, traditional uses, pharmacology, toxicology, and quality control of the *Astragalus memeranaceus*. *Front. Pharmacol.* 14:1242318. doi: 10.3389/fphar.2023.1242318

A review of the botany, phytochemistry, traditional uses, pharmacology, toxicology, and quality control of the *Astragalus memeranaceus*

Panpan Wang†, Zhen Wang†, Zhanping Zhang, Huiyan Cao, Lingyang Kong, Wei Ma* and Weichao Ren*

School of Pharmacy, Heilongjiang University of Chinese Medicine, Harbin, China

Astragali Radix (Huangqi) is mainly distributed in the Northern Hemisphere, South America, and Africa and rarely in North America and Oceania. It has long been used as an ethnomedicine in the Russian Federation, Mongolia, Korea, Kazakhstan, and China. It was first recorded in the Shennong Ben Cao Jing and includes the effects of reinforcing healthy qi, dispelling pathogenic factors, promoting diuresis, reducing swelling, activating blood circulation, and dredging collaterals. This review systematically summarizes the botanical characteristics, phytochemistry, traditional uses, pharmacology, and toxicology of Astrag*alus* to explore the potential of Huangqi and expand its applications. Data were obtained from databases such as PubMed, CNKI, Wan Fang Data, Baidu Scholar, and Google Scholar. The collected material also includes classic works of Chinese herbal medicine, Chinese Pharmacopoeia, Chinese Medicine Dictionary, and PhD and Master's theses. The pharmacological effects of the isoflavone fraction in Huangqi have been studied extensively; The pharmacological effects of Huangqi isoflavone are mainly reflected in its anti-inflammatory, anti-tumor, anti-oxidant, anti-allergic, and anti-diabetic properties and its ability to treat several related diseases. Additionally, the medicinal uses, chemical composition, pharmacological activity, toxicology, and quality control of Huangqi require further elucidation. Here, we provide a comprehensive review of the botany, phytochemistry, traditional uses, pharmacology, toxicology, and quality control of Astragalus to assist future innovative research and to identify and develop new drugs involving Huangqi.

KEYWORDS

***Astragalus memeranaceus*, ethnopharmacology, botany, traditional uses, phytochemistry, pharmacology, toxicology**

Introduction

Astragalus L. is the largest genus in the family Leguminosae comprising approximately 2,900 species. *Astragalus membranaceus* (Fisch.) Bunge and *Astragalus membranaceus* (Fisch.) Bge. Var. *mongholicus* (Bge) Hsiao are used worldwide because of their high medicinal and nutritional value (Wu et al., 2018). Astragali Radix (Huangqi), the dried roots of *A. membranaceus* or *Astragalus mongholicus*, is commonly used as a herbal ethnopharmacological herb in China. Huangqi is mainly distributed in the Russian

Federation, Mongolia, and China (Li et al., 2017a). The application of Huangqi can be traced back to the Han Dynasty and was first recorded in Shennong Ben Cao Jing (Han Dynasty, BCE 202–220), where it was categorized as a high-quality product. Li Shizhen's "Compendium of the Materia Medica" (Ming Dynasty, AD 1552–1578) lists Huangqi as the first tonic herb, which mainly reinforced healthy qi, dispelling pathogenic factors, promoting diuresis, and reducing swelling. Huangqi has been prevalent for more than 2,000 years with over 200 types of herbal decoctions and has experienced extensive clinical application in Chinese medicine (Yuan et al., 2012).

The chemical composition of *Astragalus* is complex and mainly includes flavonoids, saponins, and polysaccharide compounds, as well as amino acids and trace elements (Wang et al., 2021a). To date, more than 200 compounds have been isolated from Astragalus species, among which isoflavones such as calycosin (CAL), calycosin-7-glucoside (CG), formononetin (FMN), and ononin (ON) have significant value because of their significant antioxidant, anticancer, anti-inflammatory, and neuroprotective pharmacological effects (Jin et al., 2014; Yu et al., 2018b). Modern pharmacological studies have verified that Huangqi has various pharmacological activities, which can improve the body's immunity; scavenge free radicals; and exert anti-inflammatory, anti-tumor, anti-diabetic, and antioxidant effects (Wu et al., 2016). The aqueous extracts of Huangqi are often used separately or in combination with other drugs to expand the range of its medicinal effects. For example, the combined use of *Astragalus* and *Angelica* in Angelica blood tonic soup can improve the deficiency of both qi and blood (Ning et al., 2002). In addition, Huangqi is rich in Astragalus polysaccharides (Shi et al., 2014; Xue et al., 2015), which can treat severe acute respiratory syndrome coronavirus-2 (SARS-CoV2) infection. The combination of Huangqi and *Lonicera japonica* Thunb. has exhibited significant anti-SARS-CoV2 activity (Yeh et al., 2021). Safety evaluation studies on the toxicological effects of Huangqi have also received extensive attention. The main factors responsible for its pharmacological effects are closely related to its complex chemical composition and chemical-component interactions. Moreover, its wide range of biological activities makes Huangqi an extremely valuable medicinal resource.

As a rare botanical, Huangqi has attracted much attention because of its unique medicinal value and health effects. At present, the research on Huangqi mainly focuses on its chemical composition and pharmacological activity. However, there is a lack of comprehensive and up-to-date information about Huangqi. In this study, the literature on Huangqi since 1983 was collected, and the duplicated and irrelevant literature was removed. This review systematically summarized the literature on the botany, phytochemistry, traditional uses, pharmacology, toxicology, and quality control of Huangqi. This review aims to comprehensively and objectively understand Huangqi, solve the problems in its application, explore its inherent potential, and provide new ideas for future innovative research and the search for new drugs.

Botany

Astragalus is widely distributed in the Northern Hemisphere, South America, and Africa; is rare in North America and Oceania; and is used as an ethnomedicine in the Russian Federation, Korea, Mongolia, Kazakhstan, and China (Figure 1). *Astragalus membranaceus* has the following morphological features: stems 60–150 cm tall, villous; leaves pinnately compound; leaflets 21–31 mm, ovate-lanceolate or elliptic, 7–30 mm long, 4–10 mm wide, white villous on both surfaces; leaf rachis villous; stipules narrowly lanceolate, 4–6 mm white villous; racemes axillary; flowers with striated bracts below; ovary hairy with an ovary stalk; pods membranous, swollen, ovate-tortuous, long-stalked, black pubescent (Figures 2B, D).

Red indicates the use and distribution areas of Huang Q in the world, and blue indicates no distribution

Astragalus mongholicus is smaller than the original variety, with smaller leaflets (5–10 mm long and 3–5 mm wide) and glabrous pods and grows in an environment similar to that of *A. membranaceus*, such as sunny grasslands, thickets, and mountain slopes. The roots of these species can be used as a medicine and make a strong tonic that nourishes the kidneys, tonifies the spleen, prevents sweating, expels excess water, and eliminates swelling and pus. *A. mongholicus* grows on forest edges, thickets, sparse forests, meadows, and mountain slopes and is one of the most commonly used Chinese herbs (Figure 2A, C). *Astragalus* flowers in June–August and produces fruits in July–September. Good quality *Astragalus* plants are harvested at 4–5 years of age; transplanted seedlings can be harvested after 3 years. Plants can be harvested in autumn (August–September), after the branches and leaves wither, or in spring (March–April), before the plant sprouts. Plants are dug out after removing the soil and the stems, seedlings, and roots are cut off and dried in the Sun until they have dried by 60% or 70%. Then, they are arranged into small bundles stacked up together, natural pan sugar is added, sundried until soft, rubbed by hand, and then sundried completely (Sun, 2015). Research has revealed that the best harvesting period for *Astragalus* is from late October to mid-November when it has the highest yield, the best traits, and the best quality. The best time to harvest Huangqi is on a sunny day, and the entire root should be dug deeply to prevent the quality from being reduced through the breakage of the main root. The cleaning method of Huangqi greatly influences the content of the active ingredients, such as astragaloside IV and GC (Tang, 2022).

Phytochemistry

To date, more than 200 compounds have been isolated from *Astragalus* species, including flavonoids, triterpenoids, polysaccharides, amino acids, alkaloids, *β*-sitosterol, metalloids, and anthraquinones Supplementary Tables S1, S2. Among these, flavonoids and triterpenoids are the most abundant and polysaccharides, isoflavonoids, and triterpenoid saponins are the main active compounds of Huangqi responsible for its various pharmacological properties; these chemical components have been extensively studied (Song et al., 2007).

Flavonoids

More than 100 flavonoid compounds have been isolated from *A. membranaceus*, with isoflavones, flavonoids, isoflavanes, and pterocarpans as the four major groups (Zhang et al., 2021a).

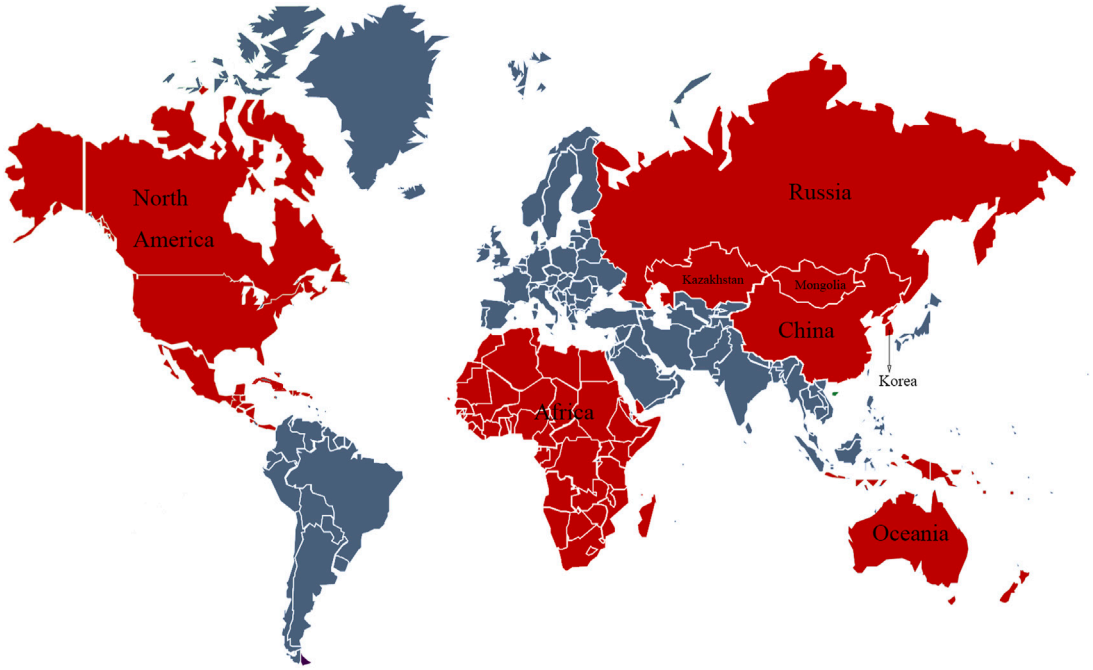

FIGURE 1
World map of Huangqi distribution.

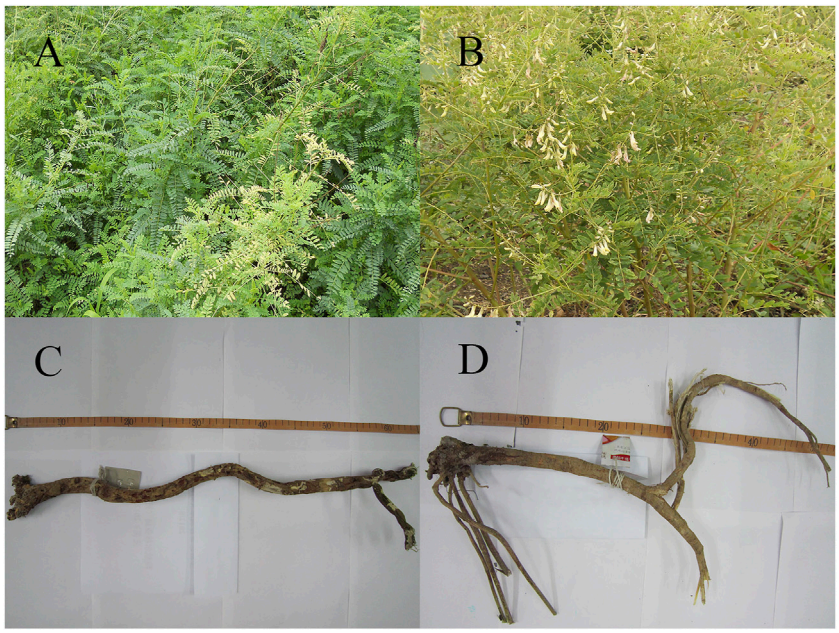

FIGURE 2
(A) *A. mongholicu* above ground parts; **(B)** *A. membranaceus* above ground parts; **(C)** *A. mongholicus* dry roots; **(D)** *A. membranaceus* dry roots.

Based on their structures, flavonoids can be divided into flavonols, flavones, flavanones, flavanols, anthocyanins, isoflavones, dihydro flavonols, and chalcones. Isoflavones are the most abundant among them, accounting for 80% of the total flavonoid content and are the signature Huangqi flavonoid compound (Huang et al., 2009). FMN and CAL, two important isoflavones in Huangqi, have been widely studied for their multiple pharmacological functions (Gao et al., 2014). CG has been demonstrated to possess various pharmacological activities, including antioxidant, anti-inflammatory, and neuroprotective activities (Choi et al., 2007;

Jian et al., 2015). More importantly, CG has been described as a chemical indicator for the quality control of Huangqi in the Chinese Pharmacopoeia (2020).

Saponins

Astragalus is rich in saponins, with triterpene saponins being the unique bioactive compounds. Saponins such as astragaloside I-VIII, isoastragaloside I-II, acetyl astragaloside, and soy saponin l and more than 100 triterpenoids have been isolated from *Astragalus* (Kitagawa et al., 1983a; Kitagawa et al., 1983b; Wang et al., 1983; Guo et al., 2019). Further, several cyclohexane-type tetracyclic triterpenes and oleanolane-type pentacyclic triterpenes, which are triterpene glycosides that contain a 30 carbon-atom skeleton, have been isolated from *Astragalus*. Astragalosides I, II, and IV are the most abundant saponins isolated from *Astragalus* roots. Astragaloside IV, which has significant pharmacological activities, has been studied extensively and described as one of the important indicators for the quality control of Huangqi in the Chinese Pharmacopoeia (Choi et al., 2007; Qi et al., 2008).

Polysaccharides

More than 30 types of Astragalus polysaccharide, one of the main components in Huangqi, have been isolated from *Astragalus*, which are mainly divided into dextrans and heteropolysaccharides (Guo et al., 2019). Additionally, rhamnose, xylose, glucose, galactose, mannose, and alcohol-soluble polysaccharide (ASP) have been isolated from *Astragalus*. Alcohol-soluble polysaccharide is a neutral polysaccharide composed of mannose, glucose, galactose, and arabinose with pyranose rings and α-glycosidic bonds (Yu et al., 2018a). Recently, a new soluble sugar named APS4 has been isolated from *Astragalus*. The average molecular weight of APS4, composed of rhamnose, arabinose, xylose, mannose, and galactose, is approximately 1.5×10^3 kDa, as revealed using high-performance gel permeation chromatography. APS4 has been demonstrated to have potential applications in cancer therapy (Yu et al., 2019).

Others

Astragalus species also contain molybdenum, copper, manganese, scandium, rubidium, selenium, chromium, cobalt, cesium, iron, zinc, and more than 20 trace elements; however, the iron, manganese, zinc, and aluminum contents are higher than those of the others (Fu et al., 2014). In addition, *Astragalus* species contains 20 amino acids, including arginine, aspartic acid, asparagine, proline, and alanine (Shao et al., 2004). Further, other compounds such as folic acid, palmitic acid, bitter elements, coumarin, chloric acid, coumaric acid, choline, linolenic acid, legume sterols, ferulic acid, isoferulic acid, hydroxyphenyl acrylic acid, deerskinol, betaine, caffeic acid, linoleic acid, and β-sitosterol have also been identified from *Astragalus* species.

Traditional uses

Huangqi is named so because of its yellow color and significant tonic potential. Huangqi contains various active ingredients and thus has a wide range of pharmacological effects, playing an important role in traditional Chinese medicine. Huangqi supplements the qi, solidifies the surface, benefits water, supports toxins, and generates muscles. As a traditional Chinese medicine, it is mainly used for treating spleen and stomach weakness, qi deficiency and blood withdrawal, qi deficiency and edema, chronic nephritis, ulcers, or ulcers that remain uncured. In China, it is known as the "Little Ginseng of Northeast China" (Napolitano et al., 2013). The Dictionary of Traditional Chinese Medicine records that Huangqi is taken in a decoction of 9–15 g. Large doses include 30–60 g (Li, 2005). It is suitable for stir-baking with an adjuvant to tonify and replenish the middle qi and used raw to secure the exterior, induce diuresis, and expel toxins. Huangqi has been used clinically in a variety of classical prescriptions. Related formulations of Huangqi with other herbs are shown in Table 1.

Huangqi has a long history and is widely used in classical formulations. Huangqi was first recorded as a high grade herb in the Shennong Ben Cao Jing《神农本草经》(Han Dynasty, BCE 202–220), and Li Shizhen's Compendium of Materia Medica《本草纲目》(Ming Dynasty, AD 1552–1578) lists Huangqi as the leading tonic medicine. In Zhang Zhongjing's the Golden Chamber《金匮要略》(Eastern Han Dynasty, AD 200–210), the dosage and preparation of different medicinal formulations are described in detail, and Huangqi is mentioned in eight of these formulations: Huangqi Gui Zhi Wuwu Tang, Huangqi Jianzhong Tang, Fangji Huangqi Tang, Fangji Gui Zhi Tang, Wutou Tang, Gui Zhi Tang, Huangqi Peony Bitter Wine Tang, and Qianjin Sanhuang Tang.However, there are no records of prescribing Huangqi for febrile diseases《伤寒论》(Dong Han Dynasty, AD 25–220). In the Secret Record of the Chamber of Orchids《兰室秘藏》(Yuan Dynasty, AD 1115–1368), written by Li Dong Yuan, Huangqi is mentioned 19 times as a tonifying agent of the spleen (Liu et al., 2022). In Nei Wai Shang Bian Huo Lun《内外伤辩惑论》(Yuan Dynasty, AD 1232–1247), Huangqi is mentioned 11 times in grouping frequency and nine times in combination with ginseng for its effectiveness in benefiting the qi and strengthening the spleen. Huangqi is mentioned 15 times in the Treatise on the Spleen and Stomach《脾胃论》(Yuan Dynasty, AD 1249) as an agent widely used to tonify the deficiencies of the spleen and stomach. Wu Jutong wrote Warm Disease Argument《温病条辩》(Qing Dynasty, A.D. 1644–1911), where in addition to borrowing Qingshu Yiqi Tang and Buzhong Yiqi Tang and formulating his own formula, he only used the addition and subtraction of Buzhong Yiqi Tang to treat "Qi deficiency and lower trapping, the portal does not hide." According to Wang Qingren, Huangqi is the preferred qi tonic for treating Yuan Qi deficiency. In 11 of the 33 prescriptions in the Medical Forest Correction《医林改错》(Qing Dynasty, AD 1830), Huangqi has been mentioned as the most abundant agent (Sha, 2014). Jing Yue advocated warm tonicity and proposed the idea of "Yang Fei You Yu." He used qi tonicity in several formulas, including Huangqi in 42 of the 132 formulas (Yi, 2013). In the Orthodox Manual of External Medicine《外科正宗》(Ming Dynasty, AD 1617), Huangqi appears 10 times among 32 main treatment formulas for swollen ulcers. Chen Yuren believed that swollen ulcers were caused by "weakness of the spleen and stomach and weakened Yang Qi," and Huangqi was used in the formulas to nourish qi deficiency and

TABLE 1 Traditional and clinical uses of Huangqi in China.

NO.	Prescription name	Major component	Formulation	Traditional and clinical uses	Ref
1	Bu-zhong-yi-qi-tang	Huangqi, Renshen, Zhigancao, Baizhu, Chenpi, Shenma, Chaihu	Decoction	Chronic gastritis, gastroptosis, myasthenia gravis, uterine prolapse	Treatise on the Spleen and Stomach《脾胃论》
2	Yiqi congming tang	Huangqi, Renshen, Gancao, Shenma, Gegen, Manjingzi, Baishao, Huangbai	Decoction	Vertigo, cervical spondylosis, cerebral arteriosclerosis, hypertension, tinnitus, dementia	Treatise on the Spleen and Stomach《脾胃论》
3	Shengxian tang	Huangqi, Zhimu, Chaihu, Shenma, Gegen	Decoction	Sick sinus syndrome, chronic fatigue syndrome, gastroptosis, coronary heart disease, diarrhea	A Record of Medieval References to the West in Medicine《医学衷中参西录》
4	Danggui buxue tang	Huangqi, Danggui	Decoction	Leukopenia, functional uterine bleeding, diabetic nephropathy, nephrotic syndrome	Treatise on the Confusion of Internal and External Injuries《内外伤辨惑论》
5	Guipi tang	Huangqi, Renshen, Baizhu, Zhigancao, Fuling, Danggui,Longyanrou, Suanzaoren, Yuanzhi, Muxiang	Decoction	Insomnia, palpitations, depression, facial spasm	Ji Sheng Fang《济生方》
6	Danggui liuhuang tang	Huangqi, Shengdihuang, Shudihuang, Huangqin, Huangbai, Huanglian	Decoction	Night sweats, perimenopausal syndrome, hyperthyroidism, chronic prostatitis, viral myocarditis	Secret Record of the Chamber of Orchids《兰室秘藏》
7	Huangqi guizhi wuwu tang	Huangqi, Baishao, Guizhi, Shengjiang, Dazao	Decoction	Diabetes mellitus, cervical spondylosis	The Golden Chamber《金匮要略》
8	Huangqi jianzhong tang	Huangqi, Shaoyao, Guizhi, Zhigancao, Shengjiang, Dazao, Maltose	Decoction	Reflux esophagitis, chronic atrophic gastritis, gastric ulcer, stable chronic obstructive pulmonary disease, gastric cancer	The Golden Chamber《金匮要略》
9	Buyang huanwu tang	Huangqi, Danggui, Chishao, Dilong, Chuanxiong, Taoren, Honghua	Decoction	Hemiplegia, mouth and eye deviation, frequent urination	Yilin Correcting Mistakes《医林改错》
10	Fangji Huangqi tang	Fangji, Huangqi, Baizhu, Gancao, Shengjiang, Dazao	Decoction	Rheumatism	The Golden Chamber《金匮要略》
11	Taishan panshi san	ZhiHuangqi, Renshen, Danggui, Chuangxiong, Baishao, Dihuang, Baizhu, Duanxu, Sharen, Huangqin, Zhigancao, Glutinous rice	Powder	Shortness of breath and fatigue, palpitations and insomnia, dizziness in the head, and pale tongue	Jingyue's Complete Works《景岳全书》
12	Shengyu tang	Huangqi, Dangshen, Danggui, Chuanxiong, Baishao, Shudihuang	Decoction	Menorrhagia, oligomenorrhea, bleeding, prolonged menstrual period, infertility, coronary heart disease, angina pectoris, cervical spondylosis	Secret Record of the Chamber of Orchids《兰室秘藏》
13	Neibu Huangqi tang	Huangqi, Renshen, Fuling, Danggui, Chuanxiong, Baishao, Shudihuang, Rougui, Maidong, Yuanzhi, Gancao	Decoction	Non-infectious fever, duodenal ulcer, chronic suppurative osteomyelitis, diabetes mellitus after orthopedic surgery	Surgical Masamune《外科正宗》
14	Yupingfeng san	Huangqi, Baizhu, Fangfeng	Pill	Cold, night sweats, allergic rhinitis	Effective Formulae Handed Down for Generations《世医得效方》
15	Duli san	Calcinated oyster, Huangqi, Mahuang root	Powder	Spontaneous sweating and night sweating caused by postpartum, postoperative, pulmonary tuberculosis, and autonomic dysfunction	Prescription of Peaceful Benevolent Dispensary《太平惠民和剂局方》

strengthen the spleen (Zhao et al., 2018). Huangqi appears 25 times as a tonic for deficiency, thirst, sores, and fractures in the Prescription of Peaceful Benevolent Dispensary《太平惠民和剂局方》(Ming Dynasty, A.D. 1078–1085), written by the Song Dynasty Hodong Bureau (Wang, 2021).

In addition to the studies on Huangqi in classical medicine, it has been extensively studied recently. In Records of Chinese Medicine with Reference to Western Medicine《医学衷中参西录》, Zhang Xichun mentioned Huangqi 35 times for its tonic power that promotes myogenesis, solid qi, diuresis and prevents the collapse of the belt. He also created four formulas of Shengxian Tang, all with Huangqi as the leading substance, that tonify and increase the qi and treat qi trapped in the chest. Zhang Xichun believed that some drugs need to be used raw to obtain the complete benefits of the medicine, and heating weakens concoctions, making them ineffective or may even cause them to have the opposite effect.

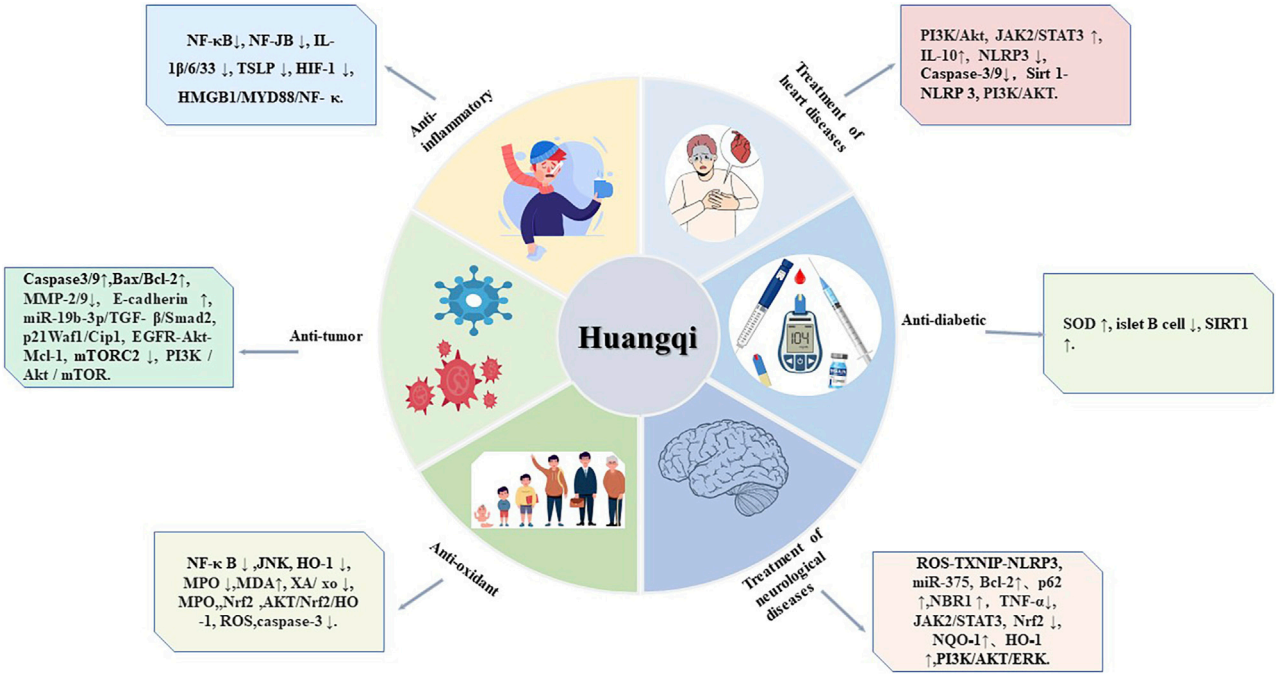

FIGURE 3
Six pharmacological effects of Huangqi. This figure shows the most highlighted six effects in studies on Huangqi.

Thus, we believe that with the increased understanding of the pharmacology and pharmacological effects of Huangqi, its therapeutic effects have also enriched and improved.

Pharmacology

The medicinal component of *Astragalus* is its dried root. Modern pharmacological studies have shown that Huangqi has a wide range of immunological activities and is widely used as an immunostimulant, antioxidant, hepatoprotectant, diuretic, and expectorant. In recent years, astragalus isoflavones have been widely used because of their anti-inflammatory, anti-tumor, treatment of heart diseases, treatment of neurological diseases, anti-diabetic, and Anti-oxidant effects This review discusses the pharmacological effects of the isoflavone compounds in *Astragalus* Figure 3 and Table 2 to assist further scientific research.

Anti-inflammatory

Inflammation is a defensive response of the body to the external stimuli and is characterized by redness, swelling, fever, pain, and dysfunction. Bacteria such as rickettsiae, mycoplasmas, spirochetes, fungi, and parasites are the most common causes of inflammation (Yang et al., 2021). Modern pharmacology has demonstrated that *Astragalus* isoflavones have anti-inflammatory effects, the main substances of which are FMN and CAL. Yu Ping Feng San (YPFS) is a traditional Chinese medicinal decoction widely used to treat atopic dermatitis (AD). The active ingredients CAL and FMN extracted from YPFS can reduce epidermal thickening at the initial stage of sensitization alone, and they inhibit thymic stromal lymphopoietin (TSLP) by regulating nuclear factor kappa B (NF-κB) activation and translocation, thereby reducing allergic inflammation. This confirms the anti-inflammatory activity of FMN and CAL(Shen et al., 2014).

Numerous anti-inflammatory studies have demonstrated that drugs usually exert their anti-inflammatory effects by modulating the expression of nuclear factors and κB inhibitors such as NF-κB, Interleukin (IL-1β/6/33), tumor necrosis factor (TNF), Mitogen-activated protein kinase (MAPK), thymic stromal lymphopoietin (TSLP), and hypoxia inducible factor-1 (HIF-1α). A study administered FMN to fluorescein isothiocyanate (FITC)-induced AD mice and FITC-treated HaCaT cells followed by polyinosinic: polycytidylic acid or lipopolysaccharide treatment and reported that TSLP/IL-33 levels were reduced *in vitro* and *in vivo* whereas E-calcine mucin levels were increased *in vitro* (Li et al., 2018). This may be because FMN reduces TSLP/IL-33 production while alleviating the inflammatory response by regulating E-calcine mucin. Moreover, FMN can alleviate AD by promoting the upregulation of tumor necrosis factor alpha-inducible protein 3 (A20) expression by siGPER. FMN significantly increases the expression of A20 protein and mRNA while suppressing the expression of TSLP protein and mRNA (Yuan et al., 2021). FMN inhibits the production of inflammatory mediators and cytokines in osteoarthritis (AO), as well as the expression of cyclooxygenase-2 and nitric oxide synthase, thereby inhibiting the synthesis of matrix metalloproteinases (MMPs) and thrombomodulin. This mechanism involves the activation of phosphatases and the inhibition of IL-1β-induced activation of NF-κB and protein kinase B (AKT) (Jia et al., 2022). CAL has been found to ameliorate lung injury and inflammatory response in mice with pneumonia caused by

TABLE 2 The pharmacological effects of Astragalus isoflavones.

Pharmacological effects	Extracts/Compounds	Types	Animal/cell	Dosage	Effects	Ref
anti-inflammatory action	Claycosin, Formononetin	*In vivo*	BALB/c mice	FMN (5 mg/kg) CAL (0.5, 5, 10 mg/kg)	Inhibition of TSLP production through regulation of NF-kB activation and translocation	Shen et al. (2014)
	Formononetin	*In vivo*	BALB/c mice	0,2,4,10 mg/kg	Decreased TSLP/IL-33 levels and increased E-calcineurin	Li et al. (2018)
	Claycosin	*In vitro*	Chondrocyte	1, 5, 10, 20 μg/mL	Blocking IL-1 by inhibiting the PI3K/AKT/FOXO1 pathway ß Induced chondrocyte apoptosis, inflammation, and ECM degradation	Guo et al. (2022)
	Claycosin	*In vivo*	C57BL/6J mice	5, 10, 20 mg/kg	Organization of κB-α, increased protein expression of p κB-α and NF-Bκ. The expression of B and p65 proteins is inhibited	Yujun et al. (2022)
	Formononetin	*In vivo*	SD mice	25, 50, 100 mg/kg	Inhibiting the NF-JB pathway reduces inflammation and promotes gastric mucosal angiogenesis	Yi et al. (2022)
	calycosin	*In vivo*	BALB/c mice	2, 10, 50 mg/kg	Adjusting HIF-1 in AD α, used as a potential anti allergic and barrier repair agent. Significantly reduce HIF-1 α Express and repair TJs	Jia et al. (2018)
	Formononetin	*In vitro*	BALB/c mice/HaCaT cell	10 mg/kg	Significantly promotes the expression of A20 protein and its mRNA, while suppressing the expression of TSLP protein and its mRNA.	Yuan et al. (2021)

(Continued on following page)

10.3389/fphar.2023.1242318

TABLE 2 (*Continued*) The pharmacological effects of Astragalus isoflavones.

Pharmacological effects	Extracts/Compounds	Types	Animal/cell	Dosage	Effects	Ref
	Formononetin	*In vivo*	Chondrocytes	10 mg/kg	Inhibiting the production of inflammatory mediators and cytokines, inhibiting the expression of cyclooxygenase-2 and inducing nitric oxide synthase, inhibiting the synthesis of metabolic factors such as MMPs and thrombospondin-5	Jia et al. (2022)
	Calycosin	*In vivo/in vitro*	SD rats	7.5, 15, 30 μg/mL	Inhibited inflammation and oxidative stress, improved damage to AEC-II cells, LPS or CLP induced HMGB1/MYD88/NF- κ; activation of B pathway and NLRP inflammatory tissue	Chen et al. (2021)
anti-tumor effect	Formononetin	*In vitro*	A2780 cell	0, 80, 160, 240 μg/mL	The ratio of Caspase3/9 and Bax/Bcl-2 protein expression was increased; reduced MMP-2/9 protein expression and ERK phosphorylation levels	Zhang et al. (2018)
	Formononetin	*In vitro*	SK-OV3 cell	35, 70, 140 μmol/L	Increasing E-cadherin and decreasing MMP-9 expression to inhibit migration and invasion of ovarian cancer SKOV-3 cells	Gu et al. (2020)
	Formononetin	*In vitro*	SK-OV3 cell	35, 70, 140 μmol/L	Acting on miR-19b-3p/TGF- β/The Smad2 signaling pathway inhibits the proliferation, migration, and invasion of SKOV3 in ovarian cancer cells, inducing their apoptosis	Niu et al. (2021)

(Continued on following page)

10.3389/fphar.2023.1242318

TABLE 2 (*Continued*) The pharmacological effects of Astragalus isoflavones.

Pharmacological effects	Extracts/Compounds	Types	Animal/cell	Dosage	Effects	Ref
	Calycosin	*In vitro*	PDACcell	50 μg/mL	Inhibition of cell growth by inducing cell cycle arrest and caspase-dependent apoptosis induced by p21Waf1/Cip1	Zhang et al. (2020)
	Formononetin	*In vivo/in vitro*	HeLa, SK-Hep1, HCT116 HuVECs cell	0, 10, 30, 50, 100 μg/mL	Inhibit PD-L1 cell proliferation and cell migration and promote apoptosis of tumor cells	Wang et al. (2022)
	Formononetin	*In vivo/in vitro*	NSCLC cell	0.5, 1.5, 3, 10 μg/mL	Inhibition of EGFR-Akt-Mcl-1 axis to suppress tumor growth in non-small cell lung cancer	Yu et al. (2020)
	Formononetin	*In vitro*	MDA-MB-468 cell	50 mg/kg	Inhibition of mTORC2 enhances the inhibitory effect of everolimus on the mTOR pathway	Zhou et al. (2019)
	campanulin, ononin, calycosin formononetin	*In vitro*	MCF-7, SK-BR-3, MDA-MB-231 cell	25, 50, 100 μg/mL	Inhibition of cell proliferation and induction of apoptosis via PI3K/Akt/mTOR pathway	Zhou et al. (2018)
	Calycosin	*In vitro*	A549, H1299, BEAS-2B cell	25, 50, 100 μg/mL	Inhibition of LUAD cell colony formation, invasion, migration and EMT process by regulating circ_0001946/miR-21/GPD1L/HIF-1 alpha pathway	Huang et al. (2013)
	Formononetin	*In vitro*, *in vivo*	U2OS cell	25, 50, 100 mg/kg	Promotes apoptosis by inactivating the intracellular miR-375/ERα-PI3K/Akt cascade pathway	Hu et al. (2019)

(Continued on following page)

10.3389/fphar.2023.1242318

TABLE 2 (*Continued*) The pharmacological effects of Astragalus isoflavones.

Pharmacological effects	Extracts/Compounds	Types	Animal/cell	Dosage	Effects	Ref
cardioprotection	campanulin	*In vivo*	Male Wistar rats	15, 30 mg/kg	Mitigating I/R damage by activating PI3K/Akt signaling pathway	Ren et al. (2016)
	campanulin	*In vivo*	H9C2 cell	30 mg/kg	Activation of the JAK2/STAT3 signaling pathway through upregulation of IL-10 secretion to attenuate myocardial I/R injury	Liu et al. (2020)
	Formononetin	*In vitro*	Senescent tissue, H9C2 cell	5 μM	Mitigating I/R-induced apoptosis in senescent cells by promoting autophagy	Huang et al. (2018b)
	Formononetin	*In vivo*	Rat MIRI model	10, 30 mg/kg	Improved MIRI in rats and inhibited NLRP3 inflammasome activation	Wang et al. (2020a)
	Calycosin	*In vivo*	SD rats	30 mg/kg	Reversed histopathological changes, significantly reduced serum levels of myocardial markers, inhibited inflammatory factors, apoptosis, and oxidative stress	Huang et al. (2020)
	Calycosin	*In vivo/in vitro*	H9C2 cell	50, 100, 200 μM	The reduction of apoptosis in H9C2 cells is through regulating Sirt 1-NLRP 3 pathway to cope with DOX-induced cardiotoxicity	Zhai et al. (2020)
	Calycosin	*In vivo*	AIC model	1,10, 50 μmol/L	The formation of autophagic vesicles was promoted by atg7, which improved cardiac function and restored autophagy	Lu et al. (2021)

(Continued on following page)

10.3389/fphar.2023.1242318

TABLE 2 (*Continued*) The pharmacological effects of Astragalus isoflavones.

Pharmacological effects	Extracts/Compounds	Types	Animal/cell	Dosage	Effects	Ref
	Calycosin	*In vivo/in vitro*	C57 BL/6 J mice cell	5, 10, 20, 40, 80, 160 μg/mL	It improved DOX-induced myocardial function, inhibited brain natriuretic peptide and improved histomorphological changes in mice	Zhang et al. (2022)
neuroprotection	Formononetin, Calycosin,Campanulin	*In vitro*	PC 12 cell	0.01, 0.05,0.1, 0.5, 1 μg/mL	Addition of endogenous antioxidants decreased the activities of antioxidant enzymes, superoxide dismutase (SOD) and glutathione peroxidase (GSH-PX)	Yu et al. (2009)
	Formononetin	*In vitro*	SD rats	30 mg/kg	The number of dendritic spines and the expressions of NGF, p-AKT, GAP-43, BDNF, p-Trk A, p-Trk B and p-ERK1/2 were significantly increased	Wu et al. (2020)
	Calycosin	*In vivo*	SD rats	5, 10, 20 mg/kg	Estrogen receptor activation, positive feedback regulation of miR-375, dysregulation of RASD1, and upregulation of Bcl-2 leads can reduce brain water content and improve neurological deficits	Hsu et al. (2020)
	Calycosin	*In vivo*	SD rats	5, 10, 20 mg/kg	The levels of P62, NBR1 and Bcl-2 were significantly decreased, and the level of TNF-α was significantly increased	Wang et al. (2014b)
	Formononetin	*In vivo*	SD rats	30, 60 mg/kg	By activating Nrf2/ARE signaling pathway, it inhibits oxidative stress and reduces hippocampal neuronal injury	Yu et al. (2022)

(Continued on following page)

10.3389/fphar.2023.1242318

TABLE 2 (*Continued*) The pharmacological effects of Astragalus isoflavones.

Pharmacological effects	Extracts/Compounds	Types	Animal/cell	Dosage	Effects	Ref
	Calycosin	*In vivo*	SD rats	50 mg/kg	It can inhibit oxidative stress by enhancing the NRF2 antioxidant pathway and inhibit inflammatory response by blocking NACHT, NALP3 and NF-κB pathways	Yao et al. (2022)
	Formononetin, Calycosin,Daidzein	*In vivo/in vitro*	Cortical neuronal cells	1, 5, 25 μM	Synergistic activation of estrogen receptor-PI3K-Akt signaling pathway improved neurological deficits and significantly attenuated L-glutamate and OGD/Ro-induced neuronal death	Gu et al. (2021)
antidiabetic	Calycosin	*In vitro*	BRL-3A cells	10^{-8} to 10^{-4} M	Improves AGEs-induced impairment of hepatocyte viability, thereby significantly reducing basal glucose uptake by hepatocytes	Xu et al. (2015)
	Formononetin, Calycosin	*In vivo*	Male mice	0.03–0.1 mg/kg	Enhances the hypoglycemic effect of antifolin in diabetic mice, while relying on antifolin-induced insulin release	Ma et al. (2007)
	Formononetin	*In vivo*	KM mice	5, 10, 20 mg/kg	By inhibiting apoptosis of islet B Cells, promoting regeneration of islet B Cells, promoting insulin secretion, hepatic glycogen synthesis and hepatic glycolysis	Qiu et al. (2016)

(Continued on following page)

10.3389/fphar.2023.1242318

TABLE 2 (*Continued*) The pharmacological effects of Astragalus isoflavones.

Pharmacological effects	Extracts/Compounds	Types	Animal/cell	Dosage	Effects	Ref
	Formononetin	*In vivo*	SD rats	10, 20, 40 mg/kg	Improvements in glucose tolerance, insulin sensitivity, and reduction in lipid levels and glycated hemoglobin levels in blood and significantly increased SIRT-1 expression in pancreatic tissue	Oza and Kulkarni (2018)
anti-oxidant	Formononetin	*In vivo*	BALB/c mice	10, 20, 40 mg/kg	Significantly inhibited the activation of NF-κB and JNK, and significantly increased the expression of heme oxygenase 1 (HO-1)	Cheng et al. (2015)
	Calycosin	*In vitro*	HepG2 cell	8 μg/mL	It significantly inhibited the isoproterenol-induced increase in myeloperoxidase (MPO) activity and malondialdehyde (MDA) levels	Cheng et al. (2015)
	Formononetin	*In vivo*	BALB/c mice	10, 20, 40 mg/kg	Significantly inhibited NF-kB and J n K and increased the expression of heme oxygenase 1 (HO-1)	Yi et al. (2020)
	Calycosin	*in vitro*	Rat brain astrocytes	2.5, 25, 50, 100 μM	Activates signaling pathway, effectively inhibits excessive ROS production and inflammatory factor expression, increases SOD activity, and reduces astrocyte damage	Lu et al. (2022)

10.3389/fphar.2023.1242318

respiratory syncytial virus infection. The mechanism may be related to the inhibition of NF-κB signaling pathway activation. CAL acts on AO by inhibiting IL-1β protein-induced activation of PI3K/AKT/FoxO1 signaling (Guo et al., 2022); it can mitigate sepsis-induced acute lung injury through the HMGB1/MyD88/NF-κB pathway and activation of NLRP3 inflammatory vesicles (Chen et al., 2021). HIF-1α may be a therapeutic target in AD when CAL is used to treat AD. CAL can inhibit HIF-1 α expression both *in vivo* and *in vitro*; it downregulates HIF-1 α expression in HaCaT cells to repair tight junctions and reduce allergic inflammation (Jia et al., 2018).

Anti-tumor

Tumors arise from the proliferation of local tissue cells affected by various tumorigenic factors in the body. Tumors are classified as benign and malignant, and cancer is a type of malignant tumor that originates from epithelial tissue. According to the studies conducted in the last decade, FMN and CAL can treat oncological diseases, including lung (Yang et al., 2014), breast (Yu et al., 2017), colorectal (Hu et al., 2023), ovarian (Yao et al., 2019), and gastric cancers (Zhou et al., 2015), via various molecular pathways. Their mechanism of anti-tumor action includes inhibition of cell proliferation, influence on the cell cycle, and induction of apoptosis.

Multiple pathways to inhibit tumor cell proliferation

The four isoflavone extracts of Huangqi, GC, CAL, FMN, and ON, have been found to inhibit the proliferation of SK-BR-3, MCF-7, and MDA-MB-231 cells in a dose-dependent manner, as well as to decrease the levels of p-GS3K β, p-PI3K, p-Akt, and p-mTOR and substantial increase total mTOR levels (Zhou et al., 2018). Additionally, CAL can regulate the circ_0001946/miR-21/GPD1L/HIF-1α signaling axis in a dose-dependent manner. miR-21 is the most recognized and significant miRNA associated with carcinogenesis and is involved in the pathogenesis of many cancers (Huang et al., 2013). CAL downregulates miR-21 at circ_0001946 and GPD1L levels and upregulates HIF-1α levels in lung adenocarcinoma cells, thereby inhibiting cell proliferation, invasion, migration, and epithelial-mesenchymal transitions (EMT) processes (Zhou et al., 2018). Extracellular regulatory protein kinase 1/2 (ERK1/2) can enter the nucleus to promote the transcription and expression of certain genes and is closely related to cell proliferation and differentiation. FMN can act by inhibiting the ERK1/2 pathway and inactivating laminin A/C in nasopharyngeal carcinoma (NPC) cells. Further, B-cell lymphoma-2 (Bcl-2), ERK1/2, laminin A/C, and CK19 expressions have been found to be downregulated in FMN-treated NPC CNE2 cells, whereas intracellular Bax expression is elevated, indicating an inhibition of cell proliferation (Ying et al., 2019).

Influence on the cell cycle through multiple pathways

CAL can inhibit breast cancer cell growth by regulating AKT signaling pathway, inducing the activation of MAPK, STAT3, NF-κB, and related apoptotic proteins and reducing the expression levels of TGF-β1, SMAD2/3, and SLUG to arrest the cell cycle in G0/G1 phase (Zhou et al., 2018). CAL inhibits Bcl-2 expression and promotes Bax, caspase-3, PARP, TGF-β1, SMAD2/3, and SLUG expressions by blocking the growth of hepatocellular carcinoma BEL-7402 cell line in G0/G1 phase. In addition, CAL induces MAPK, STAT3, NF-κB, and related apoptotic proteins in HepG2 hepatocellular carcinoma cells by regulating AKT pathway protein activation to induce G0/G1 phase cell cycle arrest (Liu et al., 2021b). Furthermore, FMN inhibits colon cancer (SW1116 and HCT116) cell growth through miR-149-induced downregulation of EphB3 and inhibition of PI3K/AKT and STAT3 signaling pathways to downregulate cell cycle-associated protein Cyclin D1 expression and block the cell cycle at the G0/G1 point (Wang et al., 2018a). FMN induces G1 phase arrest in MCF-7, SK-BR-3, and MDAMB-231 breast cancer cells by downregulating the expression of Cyclin D1 and Cyclin E and negatively regulating the expression of P21 and P27 (Zhou et al., 2016).

Induction of apoptosis through multiple pathways

FMN has been shown to alleviate ovarian cancer in SKOV-3 cells by increasing E-cadherin expression and decreasing MMP-9 expression, which inhibits the cancer cell proliferation, migration, and invasion (Gu et al., 2020). Further studies have demonstrated that FMN causes apoptosis in SKOV-3 cells. The anti-tumor effect of FMN is achieved by regulating the miR-19b-3p/TGF-β/Smad2 signaling pathway (Niu et al., 2021). The Bcl-2 protein family significantly inhibits apoptosis, and FMN shows a dose-dependent inhibition of Bax/Bcl-2 and caspase-3/9 protein expressions in ovarian cancer cells, thereby exhibiting anti-proliferative, anti-migratory, and invasive effects. The Bax/Bcl-2 ratio has been found to increase after FMN treatment, whereas caspase-3 and caspase-9 levels are elevated (Lee et al., 2018). CAL induces p21Waf1/Cip1 cycle arrest and promotes caspase apoptosis and MIA PaCa-2 cell migration in macrophages RAW 264.7, which occurs through the induction of the Raf/MEK/ERK pathway and promotion of M2 tumor-associated macrophages acting in the tumor microenvironment (Zhang et al., 2020). CAL can reduce the viability of colorectal cancer (CRC) cells through targeted inhibition of PI3K/Akt signaling pathway and upregulation of Phosphatase gene (PTEN) protein and estrogen receptor *β* (Erβ), thereby inducing CRC cell apoptosis. PTEN and ERβ protein expressions are significantly upregulated in CRC cells subjected to CAL, whereas p-AKT/AKT ratio and Bcl-2 levels are downregulated, confirming the anti-tumor effect of CAL(Zhang et al., 2021b). FMN induces apoptosis in OGS cells and inhibits the growth of solid tumors, resulting in an increase in intracellular Apaf-1 positive cells and a decrease in endogenous Ki-67, p-PI3KCATyr317, and p-AKTSer473 immune cells. The mechanism of action is related to the inactivation of miR-375/ERα-PI3K/AKT signaling pathway in cells (Hu et al., 2019).

Treatment of heart diseases

Cardiovascular diseases account for approximately 17.5 million deaths worldwide annually, it is crucial to screen for effective therapeutic agents against these diseases (Xin et al., 2013). The most common and critical heart diseases include hypertension, coronary artery disease, and arrhythmia, which can occur independently or in combination with other heart diseases. *Astragalus* isoflavones have anti-apoptotic, autophagy-

promoting, anti-inflammatory, and antioxidant roles in heart diseases.

CAL can inhibit cardiomyocyte apoptosis by promoting the activation of the PI3K/AKT signaling pathway, thereby reducing myocardial injury. High-dose CG pretreatment has been shown to significantly improve cardiac function in rats, with the upregulation of superoxide dismutase (SOD), Ejection Fraction (EF), fractional shortening (FS), and left ventricular end-systolic pressure and downregulation of left ventricular end-diastolic pressure and malonaldehyde (MDA). Caspase-3 and caspase-9 activities were also inhibited (Ren et al., 2016). Further studies revealed that CG may mitigate ischemia/reperfusion (I/R) injury by upregulating IL-10 to activate the JAK2/STAT3 signaling pathway (Liu et al., 2020). Using isolated heart tissues from senescent mice and chemically induced senescent H9C2 cells as experimental subjects, a study demonstrated that FMN can attenuate I/R-induced apoptosis in cells or tissues (Huang et al., 2018b). Additionally, FMN can inhibit the activation of nod-like receptor protein 3 (NLRP3) inflammasome in rats and improve IR in rats via the reactive oxygen species (ROS)-TXNIP-NLRP3 signaling pathway (Wang et al., 2020a). CAL protects the heart by eliminating histopathological changes owing to its anti-inflammatory, anti-apoptotic, antioxidant, and anti-lipid peroxidation activities. CAL may exert cardioprotective effects by modulating the Sirt1-NLRP3 pathway, thereby ameliorating adriamycin/adriamycin (DOX)-induced cardiotoxicity, reducing apoptosis and inhibiting oxidative stress. CAL may also be useful in the treatment of myocardial infarction to reduce cardiac dysfunction and its associated complications (Huang et al., 2020). CAL induces apoptosis through the Bcl-2, Bax, and PI3K-Akt signaling pathways and increases H9C2 cell viability. In addition, CAL has been shown to improve Sirt1-NLRP3 levels in cells and mouse hearts. CAL can improve cardiac function in adult zebrafish and restore autophagy through atg7 autophagy-mediated production of protection against DOX-induced cardiotoxicity (Lu et al., 2021). Zhang et al. established a cardiotoxicity model using DOX stimulation in H9C2 cells and C57BL/6J mice. The cardioprotective mechanism was confirmed using *in vivo* and *ex vivo* experiments, which showed that CAL alleviated DOX-induced cardiotoxicity by inhibiting the activation of NLRP3 inflammatory vesicles (Zhang et al., 2022).

Treatment of neurological diseases

Neurological diseases are pathological conditions that negatively affect the peripheral nervous system, spinal cord, and/or brain, ultimately leading to functional disorders (Gunata et al., 2020; Cao et al., 2023). Its etiology is complex and includes trauma, infection, genetics, tumors, immunology, and several other factors that can lead to neurological dysfunction, resulting in neurological diseases. Several studies have demonstrated the neuroprotective properties of FMN and CAL against cerebral ischemia, dementia, traumatic brain injury, Alzheimer's disease, anxiety, and depression. The pathways involved in these neuroprotective mechanisms are ERPI3K-Akt, PI3K/AKT/ERK, and ROS-TXNIP-NLRP3 pathways. The neuroprotective effect of five *Astragalus* isoflavone compounds on xanthine (XA)/xanthine oxidase (XO)-induced damage in PC12 cells has been investigated. The reduction of SOD, antioxidant glutathione peroxidase, and enzymatic activities is prevented in isoflavone-treated cells; these neuroprotective effects may be produced by increasing endogenous antioxidants (Yu et al., 2009). FMN can promote the expression of NGF, GAP-43, BDNF, p-Trk A, p-Trk B, p-ERK 1/2, and p-AKT by increasing the number of neuronal dendritic spines and ß III-microtubulin, with the best effect at 30 mg/kg (Wu et al., 2020). CAL treatment in stroke patients increases brain BDNF/TrkB expression, ameliorates neurological damage, and transforms microglia from an activated amoeboid state to a resting branching state. BDNF/TrkB -mediated CAL ameliorates ischemic stroke injury in rats by switching microglia from an activated to a resting branching state (Hsu et al., 2020). The pathogenic mechanisms underlying I/R include elevated intracellular Ca^{2+} levels, excitatory neurotransmitter release, oxidative stress, inflammation, and apoptosis (Durukan and Tatlisumak, 2007). CAL has neuroprotective effects in I/R rats, significantly reducing the brain water content and improving neurological deficits. The mechanism of action may be related to the positive feedback regulation of miR-375 through ER-α (Wang et al., 2014b). The effect of CAL on I/R may be related to its anti-autophagic, anti-apoptotic, and anti-inflammatory activities. A study established an I/R rat model with middle cerebral artery occlusion and reported that CAL pretreatment for 14 days significantly reduced brain edema and improved neurological function in I/R rats, as well as significantly upregulated the expression of Bcl-2, p62, and NBR1 and downregulated the level of tumor necrosis factor alpha (TNF-α) (Wang et al., 2018b). FMN action in I/R rats reduces ASC, p-STAT3, p-JAK2, NLRP3, cl-IL-1β, and cl-caspase-1 protein levels in the brain tissue of rats with infarct volume. The neuroprotective effect of FMN is achieved through the inhibition of the JAK2/STAT3 signaling pathway (Yu et al., 2022). FMN reduces hippocampal neuronal damage and oxidative stress in rats, improves depression-like behavior in rats with mild stress (CUMS)-induced depression, and reverses the CUMS-induced decrease in nuclear factor erythroid-2-related factor 2 (Nrf2) protein and increase in NQO-1 and HO-1 proteins in the nucleus (Yao et al., 2022). CAL may also be effective against cerebral hemorrhage-induced injury by inhibiting oxidative damage and inflammatory responses, and 50 mg/kg CAL has been shown to significantly inhibit ischemic brain injury. Lesion volume, blood volume, and hemispheric enlargement are significantly reduced after CAL treatment. CAL likely inhibits oxidative stress by enhancing the Nrf2 antioxidant pathway and suppresses the inflammatory response by blocking the activation of NACHT, NALP3 inflammatory vesicles, and NF-κB pathway (Chen et al., 2020). *Astragalus* isoflavones alleviate I/R by activating the ER-PI3K-Akt pathway, which may be a molecular target for synergistic neuroprotection by Astragalus isoflavones (Gu et al., 2021).

Anti-diabetic

Diabetes is a chronic endocrine disease characterized by glucose, fat, and protein metabolism disorders caused by insulin deficiency, insulin insensitivity, or both, which can lead to the damage and dysfunction of various organs in the body (Krasteva et al., 2014). Type 1 diabetes is characterized by absolute insulin deficiency, whereas type 2 diabetes is characterized by relative insulin deficiency and insulin resistance. CAL ameliorates advanced

glycation end products (AGEs)-induced impairment of hepatocyte viability and AGEs-induced dysfunction of hepatocyte glucose uptake in a dose-dependent manner (Xu et al., 2015). The combined application of FMN, CAL, and Tetrandrine has been demonstrated to be effective against hyperglycemia and hypoinsulinemia in streptozotocin (STZ)-induced diabetic mice (Ma et al., 2007); this is because FMN and CAL can enhance the hypoglycemic effect of Tetrandrine. In another study, FMN significantly reduced the fasting blood glucose levels at doses of 5, 10, and 20 mg/kg in alloxan-induced type 1 diabetes mice, indicating that FMN promotes islet B cell regeneration, insulin secretion, and liver glycogen synthesis by inhibiting islet B cell apoptosis (Qiu et al., 2016). FMN can also treat STZ-induced type 2 diabetes. Significant improvement in the fasting blood glucose levels has been observed after 40 mg/kg FMN treatment of rats, and FMN at doses of 10, 20, and 40 mg/kg can significantly reduce serum urea nitrogen, glucose, albumin, and creatinine levels. Further, FMN can significantly increase lipid peroxidation and SOD levels and reduce renal peroxidase activity, cytokine levels, inflammatory changes, and renal cell necrosis, thereby protecting pancreatic *ß*-cells from necrosis and degeneration (Jain et al., 2020).

Anti-oxidant

Recent studies have reported that Huangqi extract has strong antioxidant activity and may act as a free radical scavenger, thereby alleviating the symptoms of oxidative stress in the early stages of diabetic nephropathy. Some studies have discovered that CAL and GC have significant anti-lipid peroxidation activity (Kim et al., 2003). FMN, CAL, and CA, isolated from Huangqi, have been found to significantly inhibit XA/XO-induced cell damage; they have significant superoxide anion and free radical (DPPH) radical scavenging abilities, which can effectively inhibit cell damage caused by XA and XO. Among these compounds, CAL has the most prominent antioxidant activity (Yu et al., 2005). Studies have reported that Huangqi extract can improve blood lipid levels, inhibit lipid peroxidation, increase the activity of antioxidant enzymes, and reduce the risk of hyperlipidemia and oxidative stress-related coronary heart disease in humans (Ma et al., 2011). In addition, the combination of CAL with gallic acid can significantly inhibit increased myeloperoxidase (MPO) activity due to isoproterenol (ISO) (Cheng et al., 2015). Oxidative stress-induced brain cell damage is an important factor in the pathogenesis of ROS-related nervous system diseases. Astrocytes are important immunocompetent brain cells that play a role in various nervous system diseases. CAL regulates oxidative stress through the AKT/Nrf2/HO-1 pathway, thereby preventing oxidative damage in brain astrocytes. CAL-treated cells exhibit enhanced viability, inhibition of ROS and inflammatory factor production, increased SOD expression, and dose-dependent inhibition of H_2O_2-induced damage (Lu et al., 2022). CAL was found to exert antioxidant effects by restoring SOD/CAT activity and reducing ROS content and caspase-3 activity in a Parkinson's disease model, thereby altering α-syn amyloid-induced neurotoxicity (Pan et al., 2021). In an allergic asthma model, treatment with FMN (10, 20, and 40 mg/kg) and the positive control drug dexamethasone (2 mg/kg) decreased ROS activity and increased SOD activity increased. The oxidation-related signaling molecules involved in this action are c-Jun N-terminal kinase (JNK), NF-κB, and the transcription factor Nrf2(Yi et al., 2020).

Other pharmacological effects

Astragalus isoflavones also exhibit antiviral, estrogen-like, antibacterial, hepatoprotective, and immune-enhancing effects. Isoflavones have a molecular structure similar to that of estrogen and can therefore bind to estrogen receptors; hence, they are classified as phytoestrogens. CAL has a protective effect on the liver of mice with acute immune liver injury caused by concanavalin A (ConA) (Liang et al., 2018), likely because of its antioxidant effect on free radicals and the enhancement of estrogen-like effects by promoting hepatic ER expression. FMN may enhance estrogen-like effects by promoting estrogen receptor protein expression (El-Bakoush and Olajide, 2018) and exert antimicrobial effects by attenuating the cytotoxic and inflammatory response of *Streptococcus suis in vitro*; lysozyme could be an ideal target against this pathogen (Wang et al., 2020b). Further, FMN has anti-apoptotic and anti-inflammatory effects on the liver mainly by inhibiting the expression of TNF-α, NF-κB-p65, TLR3, and NLRP3 and upregulating Bcl-2. It also exerts anti-metabolism-related effects on fatty liver disease through lipophagy (Liu et al., 2021a). CAL exhibits hepatoprotective functions mainly by affecting the expression of STAT3, FXR, a-SMA, and ERβ5, which in turn regulates free fatty acid *ß*-oxidation, gluconeogenesis, triglyceride synthesis, glucose metabolism, collagen deposition, and hydroxyproline content (Duan et al., 2017; Duan et al., 2018).

Toxicology

Although *Astragalus* has been widely used in clinical practice for several years, comprehensive safety and toxicity assessments have not yet been conducted. Studies on the toxicology of *Ast*ragalus have long been of interest to researchers, especially those focusing on the therapeutic toxicity of secondary metabolites of *Astragalus*. *Astragalus* species can be classified into three main categories based on their toxic effects on animals: species that can synthesize aliphatic nitro compounds, species that can cause madder poisoning, and species that can accumulate selenium (Rios and Waterman, 1997). Toxicological studies on astragaloside have shown that it is toxic above a dose of 1.0 mL/kg to some embryos as well as mothers. However, no specific toxicities such as acute toxicity, subacute or subchronic toxicity, genotoxicity, or immunotoxicity have been observed (Jiangbo et al., 2009). The extract of *Astragalus*, historically recognized as a traditional medicine and food, has now been evaluated for its subchronic toxicity and genotoxic safety as a modern dietary ingredient, along with the triterpene glycosidic cyclic element astragalinol (Szabo, 2014). Rats were administered astragalol at 0, 40, 80, and 150 mg/kg/day for 91 consecutive days, but no treatment-related deaths or cardiac effects were observed. In a toxicity study on Huangqi extract, acute and subchronic oral toxicity tests were performed on rats. In acute toxicity studies, a single dose can reach up to 5,000 mg/kg. In a 13-week subchronic

toxicity study based on clinical symptoms, body weight, and autopsy results, there were no deaths or toxic reactions (Song et al., 2017). Huangqi can be used for food health and consumed for a long time at standard doses. Because *Astragalus* species may be contaminated with pesticides or heavy metals during cultivation, leading to increased safety concerns (Jiaojiao et al., 2019) and reducing its value, it is important to control the use of pesticides and conduct soil quality testing.

In addition, the combination of Huangqi can achieve the effect of increasing efficiency and reducing toxicity. Apatinib mesylate combined with astragaloside can significantly inhibit the growth of hepatocellular carcinoma transplantation tumors in nude mice, promote the apoptosis of transplantation tumor cells, and cause inhibitory effects on the proliferation, migration, and invasion of HCC cells (Sun et al., 2023). Astragaloside (Peng et al., 2017), astragaloside (Lina et al., 2022) and doxorubicin can alleviate cardiotoxicity and improve anti-tumor effect. The combination of astragaloside and angiotensin-converting enzyme inhibitors (ACEi) can reduce the degree of proteinuria and delay the progression of diabetic kidney injury in mice (Li et al., 2021). The above experimental results indicate that the combination of Huangqi active ingredients with other drugs has shown certain advantages in basic research, but the mechanism of its efficiency and toxicity reduction needs to continue to be explored. Although the safety of Huangqi has been heavily formalized, independent studies on Huangqi are still lacking, and further *in vitro* and clinical trials are required for confirmation.

Quality control

Analysis methods

Misidentification and adulteration of varieties are the main problems in the identification of herbal medicines (Zhu et al., 2022). Due to non-standard market systems and market supervision and control, counterfeit and inferior Huangqi products often appear. The quality of Huangqi medicinal herbs is also influenced by different geographical locations, cultivation techniques, and climatic environments (Yang et al., 2020). Therefore, the key to the quality control of Active ingredients in Huangqi lies in the establishment of quality analysis methods.

At present, the 2020 edition of the Chinese Pharmacopoeia controls the quality of Huangqi from three aspects: morphology, microscopy, and thin-layer chromatography. It is required that the moisture content shall not exceed 10.0%, the total ash content shall not exceed 5.0%, and the leaching content shall not be less than 17.0% (Gong et al., 2018). The content of astragaloside A determined by High-performance liquid chromatography shall not be less than 0.080%, and the content of calyx Isoflavone glucoside shall not be less than 0.020%. Traditionally, High-performance liquid chromatography was used to determine the content of Huangqi. However, these methods may not be sufficient to evaluate the quality of Huangqi medicinal herbs. With the improvement of analytical technology, people have adopted other methods to determine the chemical composition of Huangqi and control its quality. For example, chromatography-mass spectrometry (LC-MS), external spectroscopy (IR), and ultraviolet spectroscopy (UV) provide effective means for quantitative analysis of the Active ingredients of Huangqi (Huang et al., 2018a).

Chemical fingerprint

Traditional Chinese medicine fingerprint is a comprehensive and quantifiable identification method established based on systematic research on the chemical composition of traditional Chinese medicine, used to evaluate the authenticity, stability, consistency, and effectiveness of traditional Chinese medicine. The fingerprint of traditional Chinese medicine, as a standard for quality control, has also been included in the Chinese Pharmacopoeia. Currently, the Chinese Pharmacopoeia does not include the fingerprint of Huangqi. Scholars (Wang et al., 2023) have established a UPLC fingerprint and content determination method for the stem and leaf of Mongolian Huangqi, and compared and analyzed 15 batches of Mongolian Huangqi stem and leaf samples from different regions. A rapid and effective method for evaluating the quality of *Astragalus mongholicu* stem and leaf has been established. DNA barcoding technology also shows broad application prospects in the identification of astragalus medicinal materials. The fingerprint determined by LC-MS combined with the ITS interval domain DNA map uses the astragalus plant genome region as the barcode, which can quickly and accurately classify the source plants, and can be used as the barcode mark for quality control of astragalus (Xiao et al., 2011). With the development of technology, quality marker (Q-marker) was proposed in 2016 (Changxiao et al., 2016), and the idea of an "effect component target fingerprint" was discovered (Liao et al., 2018) to predict and identify the quality of Chinese medicine Q-marker through network pharmacology and high-performance liquid chromatography fingerprint. Li et al. (Li et al., 2022) established a reliable analytical method combined with network pharmacology, established fingerprint spectra of 23 batches of Huangqi, successfully isolated and quantified 8 compounds, and is expected to become a new approach for quality control of Huangqi (Huang et al., 2018a). At present, the HPLC-ELSD method is mainly used for the development of fingerprints of saponins and polysaccharides; The HPLC-DAD/HPLC-UV method can be used to establish the fingerprint of flavonoids and polysaccharides.; The PLC-CAD method can be used to develop fingerprints of flavonoids and saponins (Zhen et al., 2023).

With the continuous development of technology, the quality control methods of medicinal materials are also constantly innovating. With the discovery of the pharmacological effects of the Active ingredient of Astragalus, the innovation of quality control methods and technologies of Astragalus is becoming more and more important. These methods and technologies are convenient for people to understand Chinese medicinal materials truly, quickly, and accurately, and provide a reference and basis for the quality control of the Active ingredient of Huangqi.

Conclusion and future perspectives

This review discusses the recent advances in botany, phytochemistry, traditional uses, pharmacology, toxicology, and

quality control of *Astragalus*. Presently, several pharmacological studies have been conducted on *Astragalus* isoflavones, including FMN and CAL. Therefore, this review mainly focused on the pharmacological effects of isoflavones. Pharmacological studies have shown that isoflavones possess many pharmacological activities, including anti-inflammatory, anti-tumor, anti-diabetic, cardioprotective, neuroprotective, and antioxidant effects. They are also used in many other applications aspects to their diverse activities. However, despite extensive pharmacological research on *Astragalus* isoflavones, some problems require further discussion.

First, *Astragalus* has a large demand as a medicine as well food; therefore, its clinical application should be extensively investigated to avoid excessive dosage and incompatibility. Meanwhile, herbs such as Huangqi are highly popular in both China and abroad. Tea, soup, and congee have become important media for healthcare, with the research and production of healthcare products increasing. Additionally, it has been established that Huangqi has a wide range of applications in herbal healthcare, particularly in immunomodulation and regulation of blood glucose. According to the clinical pharmacological effects of Huangqi, the use of Huangqi in combination with other herbal medicines in healthcare products should not be limited to the above functions but can also be studied in the areas of auxiliary improvement of memory, sleep, growth, and development, promotion of digestion, and auxiliary protection against gastric mucosa damage.

Second, more than 200 compounds have been isolated from *Astragalus* species; although flavonoids and saponins have been comprehensively studied, the study of polysaccharide components of *Astragalus* remains limited. Some studies show that highly valuable the field of pharmacology is; in fact, pharmacological research and clinical applications are inseparable; therefore, combining pharmacological and clinical studies makes the application of Huangqi possible in many fields.

Third, in terms of pharmacological effects, recent studies on the active ingredients of *Astragalus* have mainly focused on FMN and CA, and studies on other active compounds and their effects are limited. In addition, most of these studies have focused on the anti-tumor and anti-inflammatory effects of FMN and CAL; however, the mechanism and target of action of the main pharmacological effects, such as anti-tumor and anti-inflammatory effects, are not fully understood. The number of samples was small, the type was single, and the pathological characteristics of different clinical patients were considered and studied. Future pharmacological research should focus on exploring active ingredients and their mechanisms of interaction with specific target ingredients, which can lay the foundation for expanding clinical applications in the future while also providing modern pharmacological interpretations of traditional applications.

Fourth, embryotoxicity and maternal toxicity have been observed above 1.0 mL/kg *Astragalus* methoside administration. However, the dose–effect relationship between the safety and toxicity of isoflavones, a phytoestrogen of *Astragalus*, has not been studied. Thus, the mechanism of action and toxicological properties of *Astragalus* require further investigation. *Astragalus* may be contaminated by pesticides and heavy metals during cultivation, leading to increased safety problems and reduced value; therefore, there is a need to control the use of pesticides and conduct soil quality tests.

In conclusion, traditional Chinese medicine, Huangqi, has a wide range of medicinal properties. In this review, we discuss the research progress on the botanical features, phytochemistry, traditional applications, pharmacology, toxicology, and quality control of *Astragalus*. This information can lay a theoretical foundation for the future development and new clinical applications of Huangqi.

Author contributions

PW wrote this paper; ZW checked the chemical structure and formula, and reviewed and edited the manuscript; ZZ, HC, and LK searched for literature, downloaded it, and classified it; WM and WR conceived and designed this review. All authors contributed to the article and approved the submitted version.

Funding

This work was supported by National Key Research and Development Program of China (2021YFD1600902), Talent training project supported by the central government for the reform and development of local colleges and Universities (ZYRCB2021008), Heilongjiang Tou yan Innovation Team Program (HLJTYTP2019001).

Conflict of interest

The authors declare that the research was conducted in the absence of any commercial or financial relationships that could be construed as a potential conflict of interest.

Publisher's note

Supplementary material

The Supplementary Material for this article can be found online at: https://www.frontiersin.org/articles/10.3389/fphar.2023.1242318/full#supplementary-material

References

Aslanipour, B., Gulcemal, D., Nalbantsoy, A., Yusufoglu, H., and Bedir, E. (2017). Secondary metabolites from Astragalus karjaginii BORISS and the evaluation of their effects on cytokine release and hemolysis. *Fitoterapia* 122, 26–33. doi:10.1016/j.fitote.2017.08.008

Bi, Z., Yu, Q., Li, P., Lin, Y., and Gao, X. (2007). Flavonoids from the aerial parts of Astragalus mongholicus. *Chin. J. Biochem. Pharm.* 5 (04), 263–265.

Bian, Y., Jia, G., Bi, Z., Yue, S., and Li, P. (2006). Studies on chemical constituents of Astragalus membranaceus (fisch) Bge. Var. mongholicus (Bge) Hsiao. *Chin. Pharm. J.* 16, 1217–1221.

Bian, Y., and Li, P. (2008). Studies on chemical constituents of Astragalus membranaceus (fisch) Bge. Var. mongholicus (Bge) Hsiao. *Chin. Pharm. J.* 5 (04), 256–259.

Cao, M., Wu, J., Peng, Y., Dong, B., Jiang, Y., Hu, C., et al. (2023). Ligustri Lucidi Fructus, a traditional Chinese Medicine: comprehensive review of botany, traditional uses, chemical composition, pharmacology, and toxicity. *J. Ethnopharmacol.* 301, 115789. doi:10.1016/j.jep.2022.115789

Changxiao, L., Shilin, C., Xiaohe, X., Tiejun, Z., Wenbin, H., and Maoliang, L. (2016). A new concept on quality marker of Chinese materia medica: quality control forChinese medicinal products. *China Tradit. Herb. Drugs* 47 (09), 1443–1457.

Chen, C., Cui, J., Ji, X., and Yao, L. (2020). Neuroprotective functions of calycosin against intracerebral hemorrhage-induced oxidative stress and neuroinflammation. *Future Med. Chem.* 12 (7), 583–592. doi:10.4155/fmc-2019-0311

Chen, G., Hou, Y., Li, X., Pan, R., and Zhao, D. (2021). Sepsis-induced acute lung injury in young rats is relieved by calycosin through inactivating the HMGB1/MyD88/NF-κB pathway and NLRP3 inflammasome. *Int. Immunopharmacol.* 96, 107623. doi:10.1016/j.intimp.2021.107623

Cheng, Y., Zhao, J., Tse, H. F., Le, X. C., and Rong, J. (2015). Plant natural products calycosin and gallic acid synergistically attenuate neutrophil infiltration and subsequent injury in isoproterenol-induced myocardial infarction: a possible role for leukotriene B4 12-hydroxydehydrogenase? *Oxid. Med. Cell Longev.* 2015, 434052. doi:10.1155/2015/434052

Choi, S. I., Heo, T. R., Min, B. H., Cui, J. H., Choi, B. H., and Park, S. R. (2007). Alleviation of osteoarthritis by calycosin-7-O-beta-D-glucopyranoside (CG) isolated from Astragali radix (AR) in rabbit osteoarthritis (OA) model. *Osteoarthr. Cartil.* 15 (9), 1086–1092. doi:10.1016/j.joca.2007.02.015

Duan, X., Meng, Q., Wang, C., Liu, Z., Liu, Q., Sun, H., et al. (2017). Calycosin attenuates triglyceride accumulation and hepatic fibrosis in murine model of non-alcoholic steatohepatitis via activating farnesoid X receptor. *Phytomedicine* 25, 83–92. doi:10.1016/j.phymed.2016.12.006

Duan, X., Meng, Q., Wang, C., Liu, Z., Sun, H., Huo, X., et al. (2018). Effects of calycosin against high-fat diet-induced nonalcoholic fatty liver disease in mice. *J. Gastroenterol. Hepatol.* 33 (2), 533–542. doi:10.1111/jgh.13884

Durukan, A., and Tatlisumak, T. (2007). Acute ischemic stroke: overview of major experimental rodent models, pathophysiology, and therapy of focal cerebral ischemia. *Pharmacol. Biochem. Be* 87 (1), 179–197. doi:10.1016/j.pbb.2007.04.015

El Dib, R. A., Soliman, H. S., Hussein, M. H., and Attia, H. G. (2015). Two new flavonoids and biological activity of Astragalus abyssinicus (hochst) steud. Ex A. Rich. Aerial parts. *Drug Res.* 65 (5), 259–265. doi:10.1055/s-0034-1377003

El-Bakoush, A., and Olajide, O. A. (2018). Formononetin inhibits neuroinflammation and increases estrogen receptor beta (ERβ) protein expression in BV2 microglia. *Int. Immunopharmacol.* 61, 325–337. doi:10.1016/j.intimp.2018.06.016

Fu, J., Wang, Z., Huang, L., Zheng, S., Wang, D., Chen, S., et al. (2014). Review of the botanical characteristics, phytochemistry, and pharmacology of Astragalus membranaceus (Huangqi). *Phytother. Res.* 28 (9), 1275–1283. doi:10.1002/ptr.5188

Gao, J., Liu, Z. J., Chen, T., and Zhao, D. (2014). Pharmaceutical properties of calycosin, the major bioactive isoflavonoid in the dry root extract of Radix astragali. *Pharm. Biol.* 52 (9), 1217–1222. doi:10.3109/13880209.2013.879188

Gong, A., Duan, R., Wang, H., Kong, X., Dong, T., Tsim, K., et al. (2018). Evaluation of the pharmaceutical properties and value of astragali radix. *Medicines* 5 (2), 46. doi:10.3390/medicines5020046

Gu, C., Yuan, L., and Meng, L. (2020). Effect of formononetin on the viability, migration and invasion of ovarian cancer cells *in vitro*. *Chin. J. Pathophysiol.* 36 (08), 1434–1438.

Gu, Y., Chen, X., Fu, S., Liu, W., Wang, Q., Liu, K. J., et al. (2021). Astragali radix isoflavones synergistically alleviate cerebral ischemia and reperfusion injury via activating estrogen receptor-PI3K-akt signaling pathway. *Front. Pharmacol.* 12, 533028. doi:10.3389/fphar.2021.533028

Gunata, M., Parlakpinar, H., and Acet, H. A. (2020). Melatonin: a review of its potential functions and effects on neurological diseases. *Rev. Neurol-France.* 176 (3), 148–165. doi:10.1016/j.neurol.2019.07.025

Guo, K., He, X., Zhang, Y., Li, X., Yan, Z., Pan, L., et al. (2016). Flavoniods from aerial parts of Astragalus hoantchy. *Fitoterapia* 114, 34–39. doi:10.1016/j.fitote.2016.08.009

Guo, X., Pan, X., Wu, J., Li, Y., and Nie, N. (2022). Calycosin prevents IL-1β-induced articular chondrocyte damage in osteoarthritis through regulating the PI3K/AKT/FoxO1 pathway. *Vitro Cell Dev-An.* 58 (6), 491–502. doi:10.1007/s11626-022-00694-7

Guo, Z., Lou, Y., Kong, M., Luo, Q., Liu, Z., and Wu, J. (2019). A systematic review of phytochemistry, pharmacology and pharmacokinetics on astragali radix: implications for astragali radix as a personalized medicine. *Int. J. Mol. Sci.* 20 (6), 1463. doi:10.3390/ijms20061463

Hao, J., Li, J., Li, X., Liu, Y., Ruan, J., Dong, Y., et al. (2016). Aromatic constituents from the stems of Astragalus membranaceus (fisch) Bge. Var. Mongholicus (Bge) Hsiao. *Molecules* 21 (3), 354. doi:10.3390/molecules21030354

He, Z. Q., and Wang, B. Q. (1990). Isolation and identification of chemical constituents of Astragalus root. *Acta Pharm. Sin.* 25 (9), 694–698.

Hsu, C. C., Kuo, T. W., Liu, W. P., Chang, C. P., and Lin, H. J. (2020). Calycosin preserves BDNF/TrkB signaling and reduces post-stroke neurological injury after cerebral ischemia by reducing accumulation of hypertrophic and TNF-alpha-containing microglia in rats. *J. Neuroimmune Pharm.* 15 (2), 326–339. doi:10.1007/s11481-019-09903-9

Hu, W., Wu, X., Tang, J., Xiao, N., Zhao, G., Zhang, L., et al. (2019). *In vitro* and *in vivo* studies of antiosteosarcoma activities of formononetin. *J. Cell Physiol.* 234 (10), 17305–17313. doi:10.1002/jcp.28349

Hu, Y., Zhai, W., Tan, D., Chen, H., Zhang, G., Tan, X., et al. (2023). Uncovering the effects and molecular mechanism of Astragalus membranaceus (Fisch) Bunge and its bioactive ingredients formononetin and calycosin against colon cancer: an integrated approach based on network pharmacology analysis coupled with experimental validation and molecular docking. *Front. Pharmacol.* 14, 1111912. doi:10.3389/fphar.2023.1111912

Hua, T., Yanru, D., Kun, Z., and Huiyuan, C. (2016). Chemical Constituents of Astragalus membranaceus var.mongholicus. *Chin. J. Exp. Tradit. Med. Form.* 22 (07), 70–73. doi:10.13422/j.cnki.syfjx.2016070070

Huang, J., Liu, Y., and Huang, X. (2018b). Formononetin may protect aged hearts from ischemia/reperfusion damage by enhancing autophagic degradation. *Mol. Med. Rep.* 18 (6), 4821–4830. doi:10.3892/mmr.2018.9544

Huang, J., Shen, H., Mi Jiang, L. H., Yuan, Y., and Wang, Q. (2020). Calycosin reduces infarct size, oxidative stress and preserve heart function in isoproterenol-induced myocardial infarction model. *Pak J. Pharm. Sci.* 33 (3), 1341–1347. doi:10.36721/pjps.2020.33.3.Sp.1341-1347.1

Huang, J., Yin, L., Dong, L., Quan, H., Chen, R., Hua, S., et al. (2018a). Quality evaluation for Radix Astragali based on fingerprint, indicative components selection and QAMS. *Biomed. Chromatogr.* 32 (11), e4343. doi:10.1002/bmc.4343

Huang, X., Liu, Y., Song, F., Liu, Z., and Liu, S. (2009). Studies on principal components and antioxidant activity of different Radix Astragali samples using high-performance liquid chromatography/electrospray ionization multiple-stage tandem mass spectrometry. *Talanta* 78 (3), 1090–1101. doi:10.1016/j.talanta.2009.01.021

Huang, Y., Yang, Y. B., Zhang, X. H., Yu, X. L., Wang, Z. B., and Cheng, X. C. (2013). MicroRNA-21 gene and cancer. *Med. Oncol.* 30 (1), 376. doi:10.1007/s12032-012-0376-8

Jain, P. G., Nayse, P. G., Patil, D. J., Shinde, S. D., and Surana, S. J. (2020). The possible antioxidant capabilities of formononetin in guarding against streptozotocin-induced diabetic nephropathy in rats. *Futur J. Pharm. Sci.* 6 (1), 53. doi:10.1186/s43094-020-00071-9

Janibekov, A. A., Youssef, F. S., Ashour, M. L., and Mamadalieva, N. Z. (2018). New flavonoid glycosides from two Astragalus species (Fabaceae) and validation of their antihyperglycaemic activity using molecular modelling and *in vitro* studies. *Ind. Crop Prod.* 118, 142–148. doi:10.1016/j.indcrop.2018.03.034

Jia, C., Hu, F., Lu, D., Jin, H., Lu, H., Xue, E., et al. (2022). Formononetin inhibits IL-1β-induced inflammation in human chondrocytes and slows the progression of osteoarthritis in rat model via the regulation of PTEN/AKT/NF-κB pathway. *Int. Immunopharmacol.* 113, 109309. doi:10.1016/j.intimp.2022.109309

Jia, Z., Wang, X., Wang, X., Wei, P., Li, L., Wu, P., et al. (2018). Calycosin alleviates allergic contact dermatitis by repairing epithelial tight junctions via down-regulating HIF-1α. *J. Cell Mol. Med.* 22 (9), 4507–4521. doi:10.1111/jcmm.13763

Jian, L., Xin, L., Yufang, M., and Yifan, H. (2015). Protective effect of calycosin-7-O-β-D-glucopyranoside against oxidative stress of BRL-3A cells induced by thioacetamide. *Pharmacogn. Mag.* 11 (43), 524–532. doi:10.4103/0973-1296.160461

Jiangbo, Z., Xuying, W., Yuping, Z., Xili, M., Yiwen, Z., and Tianbao, Z. (2009). Effect of astragaloside IV on the embryo-fetal development of Sprague-Dawley rats and New Zealand White rabbits. *J. Appl. Toxicol.* 29 (5), 381–385. doi:10.1002/jat.1422

Jiaojiao, Y., Dandan, K., Jiaoyang, L., Wenjie, Q., Xuemei, Q., Zhuowen, F., et al. (2019). Analysis of heavy metal pollution in Astragalus membranaceus and its health risk assessment. *Chin. J. Chin. Mater Med.* 44 (14), 3094–3099. doi:10.19540/j.cnki.cjcmm.20190517.201

Jin, Y. M., Xu, T. M., Zhao, Y. H., Wang, Y. C., and Cui, M. H. (2014). *In vitro* and *in vivo* anti-cancer activity of formononetin on human cervical cancer cell line HeLa. *Tumour Biol.* 35 (3), 2279–2284. doi:10.1007/s13277-013-1302-1

Kavtaradze, N., Alaniya, M., Masullo, M., Cerulli, A., and Piacente, S. (2020). New flavone glycosides from Astragalus tanae endemic to Georgia. *Chem. Nat. Compd+* 56 (1), 70–74. doi:10.1007/s10600-020-02946-y

Kim, C., Ha, H., Kim, J. S., Kim, Y. T., Kwon, S. C., and Park, S. W. (2003). Induction of growth hormone by the roots of Astragalus membranaceus in pituitary cell culture. *Arch. Pharm. Res.* 26 (1), 34–39. doi:10.1007/bf03179928

Kitagawa, I., Saito, M., Takagi, A., and Yoshikawa, M. (1983b). Saponin and sapogenol. XXXVII. Chemical constituents of astragali radix, the root of Astragalus

membranaceus Bunge. (4). Astragalosides VII and VIII. *Chem. Pharm. Bull.* 31 (2), 716–722. doi:10.1248/cpb.31.716

Kitagawa, I., Wang, H., Saito, M., Takagi, A., and Yoshikawa, M. (1983a). Saponin and sapogenol. XXXV. Chemical constituents of Astragali Radix, the root of Astragalus membranaceus Bunge. (2). Astragalosides I,II and IV, acetylastragaloside I and isoastragalosides I and II. *Chem. Pharm. Bull.* 31 (2), 698–708. doi:10.1248/cpb.31.698

Krasteva, A., Panov, V., Krasteva, A., Kisselova, A., and Krastev, Z. (2014). Oral cavity and systemic diseases—diabetes mellitus. *Biotechnol. Biotec Eq* 25 (1), 2183–2186. doi:10.5504/bbeq.2011.0022

Krasteva, I., Bratkov, V., Bucar, F., Kunert, O., Kollroser, M., Kondeva-Burdina, M., et al. (2015). Flavoalkaloids and flavonoids from *Astragalus monspessulanus*. *J. Nat. Prod.* 78 (11), 2565–2571. doi:10.1021/acs.jnatprod.5b00502

Lee, H., Lee, D., Kang, K. S., Song, J. H., and Choi, Y. K. (2018). Inhibition of intracellular ROS accumulation by formononetin attenuates cisplatin-mediated apoptosis in LLC-PK1 cells. *Int. J. Mol. Sci.* 19 (3), 813. doi:10.3390/ijms19030813

Li, G., Ai, B., Zhang, W., Feng, X., and Jiang, M. (2021). Efficacy and safety of astragalus injection combined with western medicine in the treatment of early diabetic nephropathy: a protocol for systematic review and meta-analysis. *Med. Baltim.* 100 (12), e25096. doi:10.1097/md.0000000000025096

Li, L., Li, Z., Yan, S., and Su, Y. (2017b). Chemical constituents in roots of Astragalus membranaceus. *China Tradit. Herb. Drugs* 48 (13), 2601–2607.

Li, L., Wang, Y., Wang, X., Tao, Y., Bao, K., Hua, Y., et al. (2018). Formononetin attenuated allergic diseases through inhibition of epithelial-derived cytokines by regulating E-cadherin. *Clin. Immunol.* 195, 67–76. doi:10.1016/j.clim.2018.07.018

Li, L., Zheng, S., Brinckmann, J. A., Fu, J., Zeng, R., Huang, L., et al. (2017a). Chemical and genetic diversity of Astragalus mongholicus grown in different eco-climatic regions. *PLoS One* 12 (9), e0184791. doi:10.1371/journal.pone.0184791

Li, W. (2005). *Dictionary of traditional Chinese medicine*. Beijing: The peoples medical publishing house.

Li, X., Guo, X., Sha, M., Gao, W., and Li, X. (2022). Combining network pharmacology with chromatographic fingerprinting and multicomponent quantitative analysis for the quality evaluation of Astragali Radix. *Biomed. Chromatogr.* 36 (4), e5319. doi:10.1002/bmc.5319

Li, X., Qu, L., Dong, Y., Han, L., Liu, E., Fang, S., et al. (2014). A review of recent research progress on the astragalus genus. *Molecules* 19 (11), 18850–18880. doi:10.3390/molecules191118850

Liang, C., Zhou, A., Sui, C., and Huang, Z. (2018). The effect of formononetin on the proliferation and migration of human umbilical vein endothelial cells and its mechanism. *Biomed. Pharmacother.* 111, 86–90. doi:10.1016/j.biopha.2018.12.049

Liao, M., Shang, H., Li, Y., Li, T., Wang, M., Zheng, Y., et al. (2018). An integrated approach to uncover quality marker underlying the effects of Alisma orientale on lipid metabolism, using chemical analysis and network pharmacology. *Phytomedicine* 45, 93–104. doi:10.1016/j.phymed.2018.04.006

Lina, L., Peiqin, Z., Zhu, H., and Zhang, Y. (2022). Astragaloside - alleviates epirubicin-induced cardiotoxicity in rats. *Chin. J. Clin. Med.* 29 (6), 1006–1011. doi:10.12025/j.issn.1008-6358.2022.20221746

Liu, G., Piao, X. J., Xu, W. T., Zhang, Y., Zhang, T., Xue, H., et al. (2021b). Calycosin induces mitochondrial-dependent apoptosis and cell cycle arrest, and inhibits cell migration through a ROS-mediated signaling pathway in HepG2 hepatocellular carcinoma cells. *Toxicol Vitro* 70, 105052. doi:10.1016/j.tiv.2020.105052

Liu, G., Zhao, W., Bai, J., Cui, J., Liang, H., and Lu, B. (2021a). Formononetin protects against concanavalin-A-induced autoimmune hepatitis in mice through its anti-apoptotic and anti-inflammatory properties. *Biochem. Cell Biol.* 99 (2), 231–240. doi:10.1139/bcb-2020-0197

Liu, W. N., Zhou, S. l., Guan, X., and Li, D. X. (2022). Study on the rules of medication in LAN shi Mi Zang (Lanshi Mi Zang) for the treatment of spleen and stomach diseases. *Hunan TCM J.* 38 (9), 1–10. doi:10.16808/j.cnki.issn1003-7705.2022.09.008

Liu, Y., Che, G., Di, Z., Sun, W., Tian, J., and Ren, M. (2020). Calycosin-7-O-beta-D-glucoside attenuates myocardial ischemia-reperfusion injury by activating JAK2/STAT3 signaling pathway via the regulation of IL-10 secretion in mice. *Mol. Cell Biochem.* 463 (1-2), 175–187. doi:10.1007/s11010-019-03639-z

Lu, C. Y., Day, C. H., Kuo, C. H., Wang, T. F., Ho, T. J., Lai, P. F., et al. (2022). Calycosin alleviates H2O2-induced astrocyte injury by restricting oxidative stress through the Akt/Nrf2/HO-1 signaling pathway. *Environ. Toxicol.* 37 (4), 858–867. doi:10.1002/tox.23449

Lu, X., Lu, L., Gao, L., Wang, Y., and Wang, W. (2021). Calycosin attenuates doxorubicin-induced cardiotoxicity via autophagy regulation in zebrafish models. *Biomed. Pharmacother.* 137, 111375. doi:10.1016/j.biopha.2021.111375

Ma, J., Qiao, Z., and Xiang, X. (2011). Aqueous extract of Astragalus mongholicus. *J. Med. Plants Res.* 5 (5), 855–858.

Ma, W., Nomura, M., Takahashi-Nishioka, T., and Kobayashi, S. (2007). Combined effects of fangchinoline from stephania tetrandra radix and formononetin and calycosin from Astragalus membranaceus radix on hyperglycemia and hypoinsulinemia in streptozotocin-diabetic mice. *Biol. Pharm. Bull.* 30 (11), 2079–2083. doi:10.1248/bpb.30.2079

Maamria, L., Long, C., Haba, H., Lavaud, C., Cannac, A., and Benkhaled, M. (2015). Cycloartane glycosides from Astragalus gombo. *Phytochem. Lett.* 11, 286–291. doi:10.1016/j.phytol.2015.01.014

Napolitano, A., Akay, S., Mari, A., Bedir, E., Pizza, C., and Piacente, S. (2013). An analytical approach based on ESI-MS, LC-MS and PCA for the quali-quantitative analysis of cycloartane derivatives in Astragalus spp. *J. Pharm. Biomed. Anal.* 85, 46–54. doi:10.1016/j.jpba.2013.06.021

Ning, L., Chen, C., Jin, R., Wu, Y., Zhang, H., Sun, C., et al. (2002). Effect of components of dang-gui-bu-xue decoction on hematopenia. *Zhongguo Zhong Yao Za* 27, 50–53.

Niu, Y., Jia, X., and Wang, Y. (2021). Formononetin regulates the proliferation, migration, invasion and apoptosis of ovarian cancer cells by regulating miR-19b-3p/TGF-β/Smad2 signaling pathway. *J. Shenyang Pharm. Univ.* 38 (10), 1068–1075. doi:10.14066/j.cnki.cn21-1349/r.2020.1202

Oza, M. J., and Kulkarni, Y. A. (2018). Formononetin treatment in type 2 diabetic rats reduces insulin resistance and hyperglycemia. *Front. Pharmacol.* 9, 739. doi:10.3389/fphar.2018.00739

Pan, Q., Ban, Y., and S, K. (2021). Antioxidant activity of calycosin against α-synuclein amyloid fibrils-induced oxidative stress in neural-like cells as a model of preventive care studies in Parkinson's disease. *Int. J. Biol. Macromol.* 182, 91–97. doi:10.1016/j.ijbiomac.2021.03.186

Peng, H., Zhang, X., and Li, F. (2017). Mechanisms of Astragalus polysaccharids synergized with doxorubicin against drug resistance in HL-60/A cells. *J. Exp. Hemat* 25, 743–748. doi:10.7534/j.issn.1009-2137.2017.03.019

Qi, L. W., Yu, Q. T., Yi, L., Ren, M. T., Wen, X. D., Wang, Y. X., et al. (2008). Simultaneous determination of 15 marker constituents in various radix Astragali preparations by solid-phase extraction and high-performance liquid chromatography. *J. Sep. Sci.* 31 (1), 97–106. doi:10.1002/jssc.200700286

Qiu, G., Tian, W., Huan, M., Chen, J., and Fu, H. (2016). Formononetin exhibits anti-hyperglycemic activity in alloxan-induced type 1 diabetic mice. *Exp. Biol. Med.* 242 (2), 223–230. doi:10.1177/1535370216657445

Ren, M., Wang, X., Du, G., Tian, J., and Liu, Y. (2016). Calycosin-7-O-beta-D-glucoside attenuates ischemia-reperfusion injury *in vivo* via activation of the PI3K/Akt pathway. *Mol. Med. Rep.* 13 (1), 633–640. doi:10.3892/mmr.2015.4611

Rios, J. L., and Waterman, P. G. (1997). A review of the pharmacology and toxicology of Astragalus. *Phytother. Res.* 11, 411–418. doi:10.1002/(sici)1099-1573(199709)11:6<411::aid-ptr132>3.0.co;2-6

Sha, W. J. (2014). *Research on prescription compatibility rules in Wang qing-ren's yi lin qian cuo*. China: Hebei Med Univ.

Shao, B. M., Xu, W., Dai, H., Tu, P., Li, Z., and Gao, X. M. (2004). A study on the immune receptors for polysaccharides from the roots of Astragalus membranaceus, a Chinese medicinal herb. *Biochem. Bioph Res. Co.* 320 (4), 1103–1111. doi:10.1016/j.bbrc.2004.06.065

Shen, D., Xie, X., Zhu, Z., Yu, X., Liu, H., Wang, H., et al. (2014). Screening active components from Yu-ping-feng-san for regulating initiative key factors in allergic sensitization. *PLoS One* 9 (9), e107279. doi:10.1371/journal.pone.0107279

Shi, L., Yin, F., Xin, X., Mao, S., Hu, P., Zhao, C., et al. (2014). Astragalus polysaccharide protects astrocytes from being infected by HSV-1 through TLR3/NF-κB signaling pathway. *Evid-Based Compl Alt.* 2014, 285356. doi:10.1155/2014/285356

Song, J., Lee, D., Min, B., Bae, J. S., Chang, G. T., and Kim, H. (2017). Safety evaluation of Astragalus extract mixture HT042 and its constituent herbs in Sprague-Dawley rats. *Phytomedicine* 32, 59–67. doi:10.1016/j.phymed.2017.03.005

Song, J. Z., Mo, S. F., Yip, Y. K., Qiao, C. F., Han, Q. B., and Xu, H. X. (2007). Development of microwave assisted extraction for the simultaneous determination of isoflavonoids and saponins in radix astragali by high performance liquid chromatography. *J. Sep. Sci.* 30 (6), 819–824. doi:10.1002/jssc.200600340

Su, H. F., Shaker, S., Kuang, Y., Zhang, M., Ye, M., and Qiao, X. (2021). Phytochemistry and cardiovascular protective effects of huang-qi (astragali radix). *Med. Res. Rev.* 41 (4), 1999–2038. doi:10.1002/med.21785

Subarnas, A., Sun, O. Y., and Hikino, H. (1991). Isoflavans and a pterocarpan from Astagalus mongholicus. *Phytochemistry* 30 (8), 2777–2780.

Sun, L. (2015). Investigation on main cultivation of Astragalus membranaceus var. mongholicus and commercial specifications grades. *Zhong Yo Cai* 38 (12), 2487–2492. doi:10.15979/j.cnki.cn62-1104/f.2015.12.029

Sun, M., Wang, J., and Shi, Z. (2023). Effects of apatinib mesylate combined with astragaloside IV on proliferation, migration and invasion of primary hepatocellular carcinoma cells. *Prog. Anat. Sci.* 29, 1. doi:10.16695/j.cnki.1006-2947.2023.01.015

Szabo, N. J. (2014). Dietary safety of cycloastragenol from Astragalus spp: subchronic toxicity and genotoxicity studies. *Food Chem. Toxicol.* 64, 322–334. doi:10.1016/j.fct.2013.11.041

Tang, Z. X. (2022). Effects of different harvesting periods and different cleaning methods on the quality of Astragalus membranaceus. *Agric. Tech. Inf.* 633 (04), 57–60+67. doi:10.15979/j.cnki.cn62-1057/s.2022.04.026

Un, R., Horo, I., Masullo, M., Falco, A., Senol, S. G., Piacente, S., et al. (2016). Cycloartane and oleanane-type glycosides from Astragalus pennatulus. *Fitoterapia* 109, 254–260. doi:10.1016/j.fitote.2016.01.015

Vasilev, H., Ross, S., Smejkal, K., Marsik, P., Jankovska, D., Havlik, J., et al. (2019). Flavonoid glycosides from endemic Bulgarian *Astragalus aitosensis* (ivanisch). *Molecules* 24 (7), 1419. doi:10.3390/molecules24071419

Wang, Y., Dong, X., Li, Z., Wang, W., Tian, J., and Chen, J. (2014b). Downregulated RASD1 and upregulated miR-375 are involved in protective effects of calycosin on cerebral ischemia/reperfusion rats. *J. Neurol. Sci.* 339 (1-2), 144–148. doi:10.1016/j.jns.2014.02.002

Wang, A. L., Li, Y., Zhao, Q., and Fan, L. Q. (2018a). Formononetin inhibits colon carcinoma cell growth and invasion by microRNA-149-mediated EphB3 downregulation and inhibition of PI3K/AKT and STAT3 signaling pathways. *Mol. Med. Rep.* 17 (6), 7721–7729. doi:10.3892/mmr.2018.8857

Wang, A. L., Ren, Q., Zhang, X., Lu, H., and Chen, J. (2018b). Neuroprotective mechanisms of calycosin against focal cerebral ischemia and reperfusion injury in rats. *Cell Physiol. Biochem.* 45 (2), 537–546. doi:10.1159/000487031

Wang, D. S., Liu, H., Liu, Y., Li, H., Li, Z., Shao, G., et al. (2020b). Formononetin alleviates Streptococcus suis infection by targeting suilysin. *Microb. Pathog.* 147, 104388. doi:10.1016/j.micpath.2020.104388

Wang, D. S., Yan, L. Y., Yang, D. Z., Lyu, Y., Fang, L. H., Wang, S. B., et al. (2020a). Formononetin ameliorates myocardial ischemia/reperfusion injury in rats by suppressing the ROS-TXNIP-NLRP3 pathway. *Biochem. Bioph Res. Co.* 525 (3), 759–766. doi:10.1016/j.bbrc.2020.02.147

Wang, D. W. (2021). *Research on the characteristics of Taiping Huimin he Yao Fang from the perspective of the theoretical framework of prescription science*. China: CDUTCM.

Wang, D. W., Xiao, C. J., Qiu, L., Tian, X. Y., Dong, X., and Jiang, B. (2021a). Two new 8-isopentenyl isoflavane derivatives from Astragalus dolichochaete diels. *Nat. Prod. Res.* 35 (8), 1323–1330. doi:10.1080/14786419.2019.1647426

Wang, D. W., Xiong, F., Yang, L., Xiao, Y., and Zhou, G. (2021b). A seasonal change of active ingredients and mineral elements in root of Astragalus membranaceus in the qinghai-tibet plateau. *Biol. Trace Elem. Res.* 199 (10), 3950–3959. doi:10.1007/s12011-020-02486-0

Wang, J. Y., Jiang, M. W., Li, M. Y., Zhang, Z. H., Xing, Y., Ri, M., et al. (2022). Formononetin represses cervical tumorigenesis by interfering with the activation of PD-L1 through MYC and STAT3 downregulation. *J. Nutr. Biochem.* 100, 108899. doi:10.1016/j.jnutbio.2021.108899

Wang, Q., Guo, S., Li, H.-w., Xie, Y., and Shang, E. (2023). Study on establishment of UPLC fingerprints and chemical pattern recognition of the stems and leaves of Astragalus membranaceus var. mongholicus (Bge) Hsiao from different regions. *China Tradit. Herb. Drugs* 54 (13), 4312–4320.

Wang, Y., Wang, X., and Ulij, O. (2014a). Chemical constituents of roots of Astragalus membranaceus(fisch) Bge. Var. mongholicus (Bge) Hsiao. *Chin. Pharm. J.* 49 (05), 357–359.

Wang, Z. B., Zhai, Y. D., Ma, Z. P., Yang, C. J., Pan, R., Yu, J. L., et al. (2015). Triterpenoids and flavonoids from the leaves of Astragalus membranaceus and their inhibitory effects on nitric oxide production. *Chem. Biodivers.* 12 (10), 1575–1584. doi:10.1002/cbdv.201400371

Wang, Z., Wenbo, Z., Yajun, C., Yu, J., Zhenping, M., Gaosong, W., et al. (2017). Flavonoids from the leaves of Astragalus membranaceus. *Chin. Tradit. Pat. Med.* 39 (08), 1634–1638.

Wang, Z. X., Cheng, M. Q., He, Q., and Guo, J. S. (1983). Study on chemical composition of astragali radix. *Chin. Tradit. Herb. Drugs* 1 (8), 1–15.

Wen, Y., Liang, C., Dan, Z., Huang, X., and Li, H. (2010). Studies on chemical constituents of Astragalus mongolicus. *Chin. Tradit. Pat. Med.* 13 (02), 115–119. doi:10.14053/j.cnki.ppcr.2010.02.007

Wu, B., Guo, Q. S., Shi, H. Z., Shi, G. W., Yan, S. M., Wu, M. J., et al. (2018). Effect of Astragali Radix on growth, immunity and related gene expression of Whitmania pigra. *Chin. J. Chin. Mater Med.* 43 (18), 3611–3617. doi:10.19540/j.cnki.cjcmm.20180703.006

Wu, J., Ke, X., Ma, N., Wang, W., Fu, W., Zhang, H., et al. (2016). Formononetin, an active compound of Astragalus membranaceus (Fisch) Bunge, inhibits hypoxia-induced retinal neovascularization via the HIF-1α/VEGF signaling pathway. *Drug Des. Devel Ther.* 10, 3071–3081. doi:10.2147/dddt.S114022

Wu, Q. L., Cheng, Y. Q., Liu, A. J., and Zhang, W. D. (2020). Formononetin recovered injured nerve functions by enhancing synaptic plasticity in ischemic stroke rats. *Biochem. Bioph Res. Co.* 525 (2), 67–72. doi:10.1016/j.bbrc.2020.02.015

Wu, R., Wang, Q., Wu, X., Tai, W., Dai, N., Wu, J., et al. (2015). Three flavonoids from the leaves of Astragalus membranaceus and their antifungal activity. *Monatsh Chem.* 146 (10), 1771–1775. doi:10.1007/s00706-015-1473-0

Xiao, C. J., Zhang, Y., Qiu, L., Dong, X., and Jiang, B. (2014). Schistosomicidal and antioxidant flavonoids from Astragalus englerianus. *Planta Med.* 80 (18), 1727–1731. doi:10.1055/s-0034-1383219

Xiao, W. L., Motley, T. J., Unachukwu, U. J., Lau, C. B., Jiang, B., Hong, F., et al. (2011). Chemical and genetic assessment of variability in commercial Radix Astragali (Astragalus spp) by ion trap LC-MS and nuclear ribosomal DNA barcoding sequence analyses. *J. Agric. Food Chem.* 59 (5), 1548–1556. doi:10.1021/jf1028174

Xin, M., Olson, E. N., and Bassel-Duby, R. (2013). Mending broken hearts: cardiac development as a basis for adult heart regeneration and repair. *Nat. Rev. Mol. Cell Biol.* 14 (8), 529–541. doi:10.1038/nrm3619

Xu, Y., Xiong, J., Zhao, Y., He, B., Zheng, Z., Chu, G., et al. (2015). Calycosin rebalances advanced glycation end products-induced glucose uptake dysfunction of hepatocyte *in vitro*. *Am. J. Chin. Med.* 43 (6), 1191–1210. doi:10.1142/s0192415x15500688

Xue, H., Gan, F., Zhang, Z., Hu, J., Chen, X., and Huang, K. (2015). Astragalus polysaccharides inhibits PCV2 replication by inhibiting oxidative stress and blocking NF-κB pathway. *Int. J. Biol. Macromol.* 81, 22–30. doi:10.1016/j.ijbiomac.2015.07.050

Yang, L., Wang, X., Hou, A., Zhang, J., Wang, S., Man, W., et al. (2021). A review of the botany, traditional uses, phytochemistry, and pharmacology of the Flos Inulae. *J. Ethnopharmacol.* 276, 114125. doi:10.1016/j.jep.2021.114125

Yang, M., Li, Z., Liu, L., Bo, A., Zhang, C., and Li, M. (2020). Ecological niche modeling of Astragalus membranaceus var. mongholicus medicinal plants in Inner Mongolia, China. *Sci. Rep.* 10 (1), 12482. doi:10.1038/s41598-020-69391-3

Yang, Y., Zhao, Y., Ai, X., Cheng, B., and Lu, S. (2014). Formononetin suppresses the proliferation of human non-small cell lung cancer through induction of cell cycle arrest and apoptosis. *Int. J. Clin. Exp. Pathol.* 7 (12), 8453–8461. doi:10.1002/3527603344.ch16

Yao, C., Zhao, G., Wang, C., and Qiang, L. (2022). Effect and mechanism of formononetin on depression in rats by activating Nrf2/ARE signaling pathway. *J. Trop. Med-Us.* 22 (11), 1467–1472+1486+1611. doi:10.3969/j.issn.1672-3619.2022.11.002

Yao, J. N., Zhang, X. X., Zhang, Y. Z., Li, J. H., Zhao, D. Y., Gao, B., et al. (2019). Discovery and anticancer evaluation of a formononetin derivative against gastric cancer SGC7901 cells. *Invest. New Drug* 37 (6), 1300–1308. doi:10.1007/s10637-019-00767-7

Yazhou, Z., Feng, X., Liang, J., Jingshu, T., Ming-ying, S., Xuan, W., et al. (2012). Isoflavonoids from roots of Astragalus membranaceus var. mongholicus. *Zhongguo Zhong yao za zhi* 37 (21), 3243–3248.

Yeh, Y. C., Doan, L. H., Huang, Z. Y., Chu, L. W., Shi, T. H., Lee, Y. R., et al. (2021). Honeysuckle (*Lonicera japonica*) and Huangqi (Astragalus membranaceus) suppress SARS-CoV-2 entry and COVID-19 related cytokine storm *in vitro*. *Front. Pharmacol.* 12, 765553. doi:10.3389/fphar.2021.765553

Yi, J. Z. (2013). *Study on the compatibility rules of tonic prescriptions in Jing Yue Quan Shu (Jingyue's Complete Works) for treating miscellaneous diseases of internal medicine*. Heilongjiang: Heilongjiang Univ TCM.

Yi, L., Cui, J., Wang, W., Tang, W., Teng, F., Zhu, X., et al. (2020). Formononetin attenuates airway inflammation and oxidative stress in murine allergic asthma. *Front. Pharmacol.* 11, 533841. doi:10.3389/fphar.2020.533841

Yi, L., Lu, Y., Yu, S., Cheng, Q., and Yi, L. (2022). Formononetin inhibits inflammation and promotes gastric mucosal angiogenesis in gastric ulcer rats through regulating NF-κB signaling pathway. *J. Recept Signal Transduct. Res.* 42 (1), 16–22. doi:10.1080/10799893.2020.1837873

Ying, K., Liu, Y., Zhang, C., and Shangguan, M. (2019). Medical findings of nasopharyngeal carcinoma patients and anti-tumor benefits of formononetin. *Eur. J. Pharmacol.* 861, 172619. doi:10.1016/j.ejphar.2019.172619

Yu, D.-H., Bao, Y.-M., Wei, C.-L., and An, L.-J. (2005). Studies of chemical constituents and their antioxidant activities from Astragalus mongholicus Bunge. *Biomed. Environ. Sci.* 18 (5), 297–301.

Yu, D., Bao, Y., An, l. J., and Yang, M. (2009). Protection of PC12 cells against superoxide-induced damage by isoflavonoids from Astragalus mongholicus. *Biomed. Environ. Sci.* 22 (1), 50–54. doi:10.1016/S0895-3988(09)60022-2

Yu, J., Ji, H., Dong, X., Feng, Y., and Liu, A. (2019). Apoptosis of human gastric carcinoma MGC-803 cells induced by a novel Astragalus membranaceus polysaccharide via intrinsic mitochondrial pathways. *Int. J. Biol. Macromol.* 126, 811–819. doi:10.1016/j.ijbiomac.2018.12.268

Yu, J., Ji, H. Y., and Liu, A. J. (2018a). Alcohol-soluble polysaccharide from Astragalus membranaceus: preparation, characteristics and antitumor activity. *Int. J. Biol. Macromol.* 118, 2057–2064. doi:10.1016/j.ijbiomac.2018.07.073

Yu, J., Wang, Z., Wang, Q., and Kuang, H. X. (2018b). Research progress on pharmacological effects of flavonoids in Astragalus membranaceus. *Tradit. Chin. Med. Inf.* 35 (02), 104–108. doi:10.19656/j.cnki.1002-2406.180065

Yu, J., Zhu, L., Zheng, H., Gong, X., Jiang, H., Chen, J., et al. (2017). Sulfotransferases and breast cancer resistance protein determine the disposition of calycosin *in vitro* and *in vivo*. *Mol. Pharm.* 14 (9), 2917–2929. doi:10.1021/acs.molpharmaceut.7b00042

Yu, L., Zhang, Y., Chen, Q., He, Y., Zhou, H., Wan, H., et al. (2022). Formononetin protects against inflammation associated with cerebral ischemia-reperfusion injury in rats by targeting the JAK2/STAT3 signaling pathway. *Biomed. Pharmacother.* 149, 112836. doi:10.1016/j.biopha.2022.112836

Yu, X., Gao, F., Li, W., Zhou, L., Liu, W., and Li, M. (2020). Formononetin inhibits tumor growth by suppression of EGFR-Akt-Mcl-1 axis in non-small cell lung cancer. *J. Exp. Clin. Cancer Res.* 39 (1), 62. doi:10.1186/s13046-020-01566-2

Yuan, W., Chen, Y., Zhou, Y., Bao, K., Yu, X., Xu, Y., et al. (2021). Formononetin attenuates atopic dermatitis by upregulating A20 expression via activation of G protein-coupled estrogen receptor. *J. Ethnopharmacol.* 266, 113397. doi:10.1016/j.jep.2020.113397

Yuan, Y. M., Gao, J. W., Shi, Z., Huang, P., Lu, Y. S., Yao, M. C., et al. (2012). Herb-drug pharmacokinetic interaction between radix astragali and pioglitazone in rats. *J. Ethnopharmacol.* 144 (2), 300–304. doi:10.1016/j.jep.2012.09.012

Yujun, W., Hambonny, B., Yanping, S., Hui, J., and Ling, C. (2022). To study the protective effect of calycosin on respiratory syncytial virus (RSV) -induced pneumonia in mice and its mechanism. *Zhongguo Zhong yao za zhi* 45 (3), 715–719. doi:10.13863/j.issn1001-4454.2022.03.035

Zhai, J., Tao, L., Zhang, S., Gao, H., Zhang, Y., Sun, J., et al. (2020). Calycosin ameliorates doxorubicin-induced cardiotoxicity by suppressing oxidative stress and inflammation via the sirtuin 1-NOD-like receptor protein 3 pathway. *Phytother. Res.* 34 (3), 649–659. doi:10.1002/ptr.6557

Zhang, C. H., Yang, X., Wei, J. R., Chen, N. M., Xu, J. P., Bi, Y. Q., et al. (2021a). Ethnopharmacology, phytochemistry, pharmacology, toxicology and clinical applications of radix astragali. *Chin. J. Integr. Med.* 27 (3), 229–240. doi:10.1007/s11655-019-3032-8

Zhang, C. H., Zhang, J. Q., Zhang, T., Xue, H., Zuo, W. B., Li, Y. N., et al. (2021b). Calycosin induces gastric cancer cell apoptosis via the ROS-mediated MAPK/STAT3/NF-κB pathway. *OncoTargets Ther.* 14, 2505–2517. doi:10.2147/OTT.S292388

Zhang, J., Liu, L., Wang, J., Ren, B., Zhang, L., and Li, W. (2018). Formononetin, an isoflavone from Astragalus membranaceus inhibits proliferation and metastasis of ovarian cancer cells. *J. Ethnopharmacol.* 221, 91–99. doi:10.1016/j.jep.2018.04.014

Zhang, L., Fan, C., Jiao, H. C., Zhang, Q., Jiang, Y. H., Cui, J., et al. (2022). Calycosin alleviates doxorubicin-induced cardiotoxicity and pyroptosis by inhibiting NLRP3 inflammasome activation. *Oxid. Med. Cell Longev.* 2022, 1733834. doi:10.1155/2022/1733834

Zhang, L. J., Liu, H. K., Hsiao, P. C., Kuo, L. M., Lee, I. J., Wu, T. S., et al. (2011). New isoflavonoid glycosides and related constituents from astragali radix (Astragalus membranaceus) and their inhibitory activity on nitric oxide production. *J. Agric. Food Chem.* 59 (4), 1131–1137. doi:10.1021/jf103610j

Zhang, Y., Li, X., Ruan, J., Wang, T., Dong, Y., Hao, J., et al. (2016). Oleanane type saponins from the stems of Astragalus membranaceus (Fisch) Bge. var. mongholicus (Bge) Hsiao. *Fitoterapia* 109, 99–105. doi:10.1016/j.fitote.2015.12.006

Zhang, Z., Auyeung, K. K., Sze, S. C., Zhang, S., Yung, K. K., and Ko, J. K. (2020). The dual roles of calycosin in growth inhibition and metastatic progression during pancreatic cancer development: a "TGF-β paradox". *Phytomedicine* 68, 153177. doi:10.1016/j.phymed.2020.153177

Zhao, Z., Mu, C. C., and Zhang, H. (2018). To explore the rules of medication in the book "Zhengzong of Surgery Attending Prescription for Cancer" based on data mining. *Chin. J. Basic Med. Tradit. Chin. Med.* 35 (6), 832–834+859. doi:10.19945/j.cnki.issn.1006-3250.2018.06.041

Zhen, W., Zhang, J., Jiao, H., Liu, J., and Wang, J. (2023). Research progress on pharmacological action and quality control of effective components of Astragali Radix. *Drug Eval. Stud.* 46 (04), 917–924.

Zhou, J., Zejing, M., Guoyue, Z., and Gang, R. (2021). Advances in chemical constituents and biological activities of Astragalus SPP. *Chin. Tradit. Pat. Med.* 43 (07), 1845–1851.

Zhou, Q., Zhang, W., Li, T., Tang, R., Li, C., Yuan, S., et al. (2019). Formononetin enhances the tumoricidal effect of everolimus in breast cancer MDA-MB-468 cells by suppressing the mTOR pathway. *Evid. Based Complement. Altern. Med.* 2019, 9610629. doi:10.1155/2019/9610629

Zhou, R., Chen, H., Chen, J., Chen, X., Wen, Y., and Xu, L. (2018). Extract from Astragalus membranaceus inhibit breast cancer cells proliferation via PI3K/AKT/mTOR signaling pathway. *Bmc Complem Altern. M.* 18 (1), 83. doi:10.1186/s12906-018-2148-2

Zhou, R., Chen, H., Ye, M., and Xu, L. (2016). Effect of formononetin on cell cycle gene and protein expression in different subtypes of breast cancer. *Drug Eval. Stud.* 39 (3), 362–366. doi:10.7501/j.issn.1674-6376.2016.03.006

Zhou, Y., Liu, Q. H., Liu, C. L., and Lin, L. (2015). Calycosin induces apoptosis in human ovarian cancer SKOV3 cells by activating caspases and Bcl-2 family proteins. *Tumour Biol.* 36 (7), 5333–5339. doi:10.1007/s13277-015-3194-8

Zhu, S., Liu, Q., Qiu, S., Dai, J., and Gao, X. (2022). DNA barcoding: an efficient technology to authenticate plant species of traditional Chinese medicine and recent advances. *Chin. Med.* 17 (1), 112. doi:10.1186/s13020-022-00655-y

Glossary

Huangqi	**A**stragali Radix
FMN	**f**ormononetin
CAL	**c**alycosin
CG	**c**alycosin-7-glucoside
ON	**o**nonin
ASP	**p**olysaccharide
A20	**t**umor necrosis factor alpha-inducible protein 3
AD	**a**topic dermatitis
ER	**e**strogen receptor
ER α	**e**strogen receptor alpha
ER β	**e**strogen receptor β
FITC	**f**luorescein isothiocyanate
HIF-1 alpha	**h**ypoxia-inducible factor alpha
IL-1β/6/33	**i**nterleukin
siRNA	**s**mall interfering RNA
siA20	**s**mall interfering RNA
siGPER	**s**mall interfering RNA
TNF-α	**t**umor necrosis factor alpha
TNF	**t**umor necrosis factor
TSLP	**t**hymic stromal lymphopoietin
YPFS	**Y**u Ping Feng San
EMT	**e**pithelial-mesenchymal transitions
MAPK	**m**itogen-activated protein kinase
PTEN	**p**hosphatase gene
EF	**E**jection Fraction
AGEs	**a**dvanced glycation end products
ROS	**r**eactive oxygen species
anti-SARS-CoV2	**n**ovel coronavirus
MMPs	**m**atrix metalloproteinases
IL-1β	**I**nterleukin
LPS	**l**ipopolysaccharide
Bcl-2	**B**-cell lymphoma-2
ERK1/2	**e**xtracellular regulatory protein kinase 1/2
SOD	**s**uperoxide dismutase
LVESP	**l**eft ventricular end-systolic pressure
ISO	**i**soproterenol
DOX	**a**driamycin
MDA	**m**alondialdehyde
CUMS	**m**ild stress
AGEs	**g**lycation end products
INS	**i**nsulin
STZ	**s**treptozotocin
α-SYN	**α**-synuclein
I/R	**i**schemia/reperfusion
RSV	**r**espiratory syncytial virus
AO	**o**steoarthritis
CLP	**a**ppendiceal ligation puncture
ALI	**a**cute lung injury
NPC	**n**asopharyngeal carcinoma
HIF-1α	**h**ypoxia inducible factor-1
MDA	**m**alonaldehyde
FS	**f**ractional shortening
DPPH	**f**ree radical
ConA	**c**oncanavalin A
Q-maker	**q**uality markers

frontiers | Frontiers in Pharmacology

TYPE Review
PUBLISHED 24 August 2023
DOI 10.3389/fphar.2023.1208055

OPEN ACCESS

EDITED BY
Aiping Lyu,
Hong Kong Baptist University, Hong Kong SAR, China

REVIEWED BY
Li Peng,
Shanxi Agricultural University, China
Jung Chao,
China Medical University, Taiwan

*CORRESPONDENCE
Chen Chen,
chen.chen@uq.edu.au
Ming Yang,
20050858@jxutcm.edu.cn
Lingyun Zhong,
ly1638163@163.com

†These authors have contributed equally to this work and share first authorship

RECEIVED 18 April 2023
ACCEPTED 10 August 2023
PUBLISHED 24 August 2023

CITATION
Zhang W, Zhang C, Cao L, Liang F, Xie W, Tao L, Chen C, Yang M and Zhong L (2023), Application of digital-intelligence technology in the processing of Chinese materia medica.
Front. Pharmacol. 14:1208055.
doi: 10.3389/fphar.2023.1208055

Application of digital-intelligence technology in the processing of Chinese materia medica

Wanlong Zhang[1†], Changhua Zhang[1,2†], Lan Cao[1], Fang Liang[3], Weihua Xie[1], Liang Tao[2], Chen Chen[4*], Ming Yang[5*] and Lingyun Zhong[1*]

[1]College of Pharmacy, Jiangxi University of Chinese Medicine, Nanchang, Jiangxi, China, [2]Nanchang Research Institute, Sun Yat-sen University, Nanchang, Jiangxi, China, [3]College of Physical Culture, Yuzhang Normal University, Nanchang, Jiangxi, China, [4]School of Biomedical Sciences, University of Queensland, Brisbane, QLD, Australia, [5]Key Laboratory of Modern Chinese Medicine Preparation of Ministry of Education, Jiangxi University of Chinese Medicine, Nanchang, Jiangxi, China

Processing of Chinese Materia Medica (PCMM) is the concentrated embodiment, which is the core of Chinese unique traditional pharmaceutical technology. The processing includes the preparation steps such as cleansing, cutting and stir-frying, to make certain impacts on the quality and efficacy of Chinese botanical drugs. The rapid development of new computer digital technologies, such as big data analysis, Internet of Things (IoT), blockchain and cloud computing artificial intelligence, has promoted the rapid development of traditional pharmaceutical manufacturing industry with digitalization and intellectualization. In this review, the application of digital intelligence technology in the PCMM was analyzed and discussed, which hopefully promoted the standardization of the process and secured the quality of botanical drugs decoction pieces. Through the intellectualization and the digitization of production, safety and effectiveness of clinical use of traditional Chinese medicine (TCM) decoction pieces were ensured. This review also provided a theoretical basis for further technical upgrading and high-quality development of TCM industry.

KEYWORDS

digital and intelligent technologies, Chinese medicine processing, industrialization, standardization, application progress

Abbreviations: ANN, artificial neural network; BPNN, backpropagation neural network; ChP, Pharmacopoeia of the People's Republic of China; CNN, convolutional neural networks; DESI-MSI, desorption electrospray ionization mass spectrometry Imaging; DM, data mining; DSS, decision support system; DT, digital twins; FT-NIR, fourier-transform near infrared; GA, genetic algorithm; GC-IMS, gas chromatography-ion migration spectrometry; GCN, Graph Convolutional Networks; 5-HMF, 5-hydroxymethylfurfural; IoT, internet of things; LS-SVM, least squares support vector machine; MIR, middle infrared; ML, machine learning; NIR, near infrared; PAT, process analysis technology; PCA, principal component analysis; PCMM, Processing of Chinese Materia Medica; PDA, photo-diode array; PLS-DA, partial least squares discriminant analysis; RFID, radio frequency identification; RTRT, real-time release test; TCM, traditional Chinese medicine; UHPLC-Q-TOF-MS/MS, ultra-high pressure liquid chromatography quadrupole time of flight tandem mass spectrometry; WSN, wireless sensor networks.

1 Introduction

Processing of Chinese Materia Medica (PCMM) refers to the processing Chinese botanical drugs by roasting, firing, frying, washing, soaking, bleaching, steaming, boiling and other methods. The purpose of processing is to eliminate or reduce the toxicity of the drug, to enhance the efficacy, to facilitate medicine preparation and storage, and to purify the botanical drugs. Under the guidance of the traditional Chinese medicine (TCM) theory, the proper processing is designed along the therapeutic nature of the drug and eliminates or balances the bias and toxicity, the effects of ascending, descending, floating and sinking, and the meridian tropism of drug, *etc.* So the corresponding changes of drug processing will improve the efficacy and indications, reduce the toxicity, enhance the clinical efficacy, and increase the clinical use. The theory of processing medicine and the theory of differential usage of the raw and cooked medicine were reported (Zhong et al., 2019; Zhai et al., 2020). For example, toxicity of *Aconitum carmichaelii* Debeaux [Ranunculaceae; *Aconite lateralis* radix praeparata] was reduced by heating with hydrolysis of toxic ingredients (Wang et al., 2023). After the dried *Rehmannia glutinosa* (Gaertn.) DC. [Orobanchaceae; *Rehmannia* radix] was made into *Rehmanniae* radix praeparata by multiple steaming and drying with yellow rice wine, its property changed from cold to warm, and its efficacy changed from clearing to tonifying. The steaming and drying repeats created the medicinal components with antioxidant activity of *rehmannia* radix (Kim et al., 2019; Xia et al., 2020; Li et al., 2022). After steaming with black bean juice, the efficacy of *Reynoutria* multiflora (Thunb.) Moldenke [Polygonaceae; *Polygoni multiflora* radix] was changed from diarrhea to tonifying (Gu et al., 2022; Song et al., 2022). The analgesic effect was enhanced by vinegar-processing *Corydalis* yanhusuo (Y.H.Chou and Chun C.Hsu) W.T.Wang ex Z.Y.Su and C.Y.Wu [Papaveraceae; *Corydalis* rhizoma] (Wu et al., 2021). These are typical and widely used examples in the PCMM.

However, the processing traditional Chinese decoction is generally empirical, and there are obvious problems in the PCMM decoction pieces, such as backward or old equipment, low efficiency, no or very few digitalization and intelligence, and insufficient standardization (Yang et al., 2016; Sun et al., 2018). The development of digitalization, networking and intelligence in medicine manufacturing (Wang et al., 2020), and applying intelligent digital technologies such as intelligent sensors, real-time analysis technology and artificial intelligence to drug processing, will promote the high-quality products in TCM industry (Oztemel and Gursev, 2020).

In this review, the application of digital intelligence technology in the PCMM was reviewed on three major aspects: overview of process of PCMM, application of digital-intellectualization technology in PCMM, and digital-intellectualization industrial transformation of PCMM. The shortcomings of traditional methods in the processing of PCMM and the application significance of digital intelligence technology are shown in Table 1.

2 Overview of process of PCMM

PCMM is a key factor affecting the quality and efficacy of decoction pieces. Usually, the botanical drugs are processed by fire after cleansing and cutting, so they are also called stir-frying. The commonly used stir-frying methods include stir-baking, steaming, boiling, and calcining. At present, in the general rules of the appendix of the 2020 edition of Pharmacopoeia of the People's Republic of China (ChP), the processing methods are systematically,

TABLE 1 The shortcomings of traditional processing of PCMM and the benefit of modern processing with digital intelligence technology.

Process of PCMM	The main problems in the traditional way	Digital and intelligent technologies	Significance of technology applications	References
Cleansing processing	low accuracy; low efficiency	the machine vision system; CNN; BPNN	Automatic detection and classification of medicinal materials	Shen et al. (2019); Steinbrener et al. (2019); Singh and Chaudhury (2020); Kazi and Panda (2022)
Cutting processing	Demulcent: difficult to control the process parameters during moistening	the fuzzy neural network; an intelligent vacuum gas phase displacement moistening machine	make a better control of the moistening process; maximize the retention of medicinal ingredients	Li et al. (2021); He et al. (2022)
	Cutting: facing the lost craft; empirical; significant differences in tools	deep learning architecture; computer vision technology; three-dimensional point cloud dual robot system	individualized cutting of different kinds of medicinal materials	Azarmdel et al. (2019); Chen et al. (2021); Bao et al. (2022); Liu et al. (2022); Wei et al. (2022); Yu et al. (2023)
	Drying: drying degree that cannot be controlled in real time	The delay mean rule; GA; ANN	real-time monitoring and controlling of drying	Fabani et al. (2021); Ke et al. (2022)
Stir-frying processing	outdated equipment; low degree of intelligence; empirical; fuzzy processing end point; different quality of excipients; uncontrollable heat	electronic nose; electronic tongue; cluster analysis; ANN; combining bionic sensors with chemometrics	accurately determine the end point of processing; Intelligently adjust the fire, time and temperature in the processing process	Niquet-Leridon et al. (2015); Xu et al. (2015); Huang et al. (2019); Lin et al. (2021); Zheng et al. (2022)
Quality control of decoction pieces	lack of standardization and standardization; varies in quality; low efficiency and high consumption	NIR spectroscopy combined with real-time release test and chemometrics; ANN; LS-SVM; deconvolution software; DNA metabarcoding	monitor key quality parameters of PCMM in real time; rapid qualitative and quantitative analysis of medicinal materials; accurately distinguish between genuine and counterfeit	Wang et al. (2015); Guo et al. (2019); Liu et al. (2020); Wang et al. (2020); Zuo et al. (2020); Qiu et al. (2021); Jin et al. (2022); Noroozi et al. (2022); Vecchietti et al. (2022)

completely and scientifically classified as cleansing processing, cutting processing, stir-frying and other processing (Chinese Pharmacopoeia Commission, 2020). The processing of Chinese medicine is a dynamic process, in addition to the physical structure changes, its chemical composition may also change with different processing parameters. As mentioned above, processing PCMM is briefly divided into cleansing, cutting, stir-frying and quality control of decoction pieces. The conditions and raw materials required in different preparation methods are different, and the influencing factors are also different. Therefore, it is necessary to classify and discuss the processing.

2.1 Cleansing processing

Cleansing, also known as pure selection, is the first step in the processing PCMM. Generally, the purpose of removing impurities, size grading, removing non-medicinal parts and separating medicinal portions is achieved by selecting, screening, selection in wind (separating impurities from drugs by wind according to different specific gravity of drugs and impurities) and magnetic separation (using strong magnetic materials to absorb magnetic impurities in botanical drugs) to ensure the accuracy of each medicinal amount in the prescription.

2.2 Cutting processing

Cutting processing refers to the processing softening the purified medicinal materials with cutting them into slices, filaments, segments, blocks or other shapes with appropriate cutting tools. After cutting, it is easier to crush process, extract the effective components, and facilitate the preparation of decoctions and other preparations. In addition to fresh and dry cutting, the cutting methods may soften the medicinal materials. Generally, according to the characteristics of medicinal materials and the conditions of season and temperature, different methods such as leaching, washing, soaking, bleaching, and moistening are adopted to soften dry medicinal materials by absorbing a certain amount of moisture. The soften degree is checked by the bending method, finger pinch method, puncture method, and others in order to have a better cutting. However, at present, it is difficult to control the processing parameters during soaking and moistening. Long-term soaking may cause a significant loss of effective components. If the moistening is not appropriate, successful cutting may not be achieved (Qin et al., 2018).

The cut medicinal materials contain more water and must be dried in time to maintain the quality for decoction pieces. During the drying process, temperature, time, and drying methods affect the degree of drying, and sometimes lead to changes in metabolites or content, and biological activity (Qiao et al., 2022). The size, thickness and texture of the decoction pieces affect the drying uniformity of the decoction pieces, resulting in a large difference in the moisture content of a batch of decoction pieces. It may significantly affect the quality of the decoction medicine. However, the current moisture measurement method usually refers to the samples at a certain time interval of drying treatment, which may not actually represent the continuity of the drying process, especially during the vacuum drying process (Wang et al., 2021). Therefore, finding an online intelligent drying method to prepare decoction pieces will provide a scientific and accurate basic data for the quality control of traditional Chinese botanical drugs and the strong rational application of medicines in clinical practice.

2.3 Stir-frying processing

Stir-frying generally refers to a processing method of Chinese botanical drugs by fire. The heat, temperature, time, acid and alkali environment, varieties or amount of excipients, applied in the stir-frying processing affect the efficacy of processed products. It is necessary to standardize the processing, so that the effective components and botanical drugs of medicinal materials are fully retained, for ensuring the effectiveness of medicinal materials. The heat may be different with the mild fire, medium fire and martial fire. The commonly used heating methods are stir-baking, steaming, boiling and calcining. Adding different varieties or amount of excipients, the stir-frying processing may change the “four properties and five flavors” (four properties of cold, hot, warm, cool and five flavors of sour, bitter, sweet, spicy and salty) in the drug, thus may alter the therapeutic effect. Obtaining a variety of processed products of a drug may be appropriate for specific clinical treatment. Excipients are mainly divided into liquid excipients and solid excipients. The input of excipients may have an effect on the contents of botanical drugs of drugs, so as to achieve the purpose of reducing toxicity and increasing efficiency (Li et al., 2021).

Other methods include duplication, making frost-like powder, levigating, sprouting and fermentation (Chinese Pharmacopoeia Commission, 2010). *Pinellia ternata* (Thunb.) Makino [Araceae; *Pinelliae* rhizoma], *Arisaema erubescens* (Wall.) Schott [Araceae; *Arisaematis* rhizoma], *Sauromatum giganteum* (Engl.) Cusimano and Hett. [Araceae; *Typhonii* rhizoma] and other Araceae botanical drugs are often processed by duplication method.

Fermentation method requires controlled environment of temperature, humidity, moisture, *etc.*, and the fermentation processing must be completed in one processing step without interruption. The temperature and humidity, pH value and medium substrate should be checked and monitored in real time to avoid unwanted bacterial growing, mildew and rancidity caused by environmental factors. In addition, making frost-like powder, levigating and dry distillation are also the characteristics of PCMM. In these processing methods, firepower, temperature, time, water addition and excipients may also affect the quality of decoction pieces to a certain degree.

2.4 The main problems of quality control of decoction pieces

The processing is a key factor to ensure the safety and effectiveness of Chinese botanical drugs. At present, the PCMM has a good science and technology foundation and careful scale measurement. There are, however, still some difficulties, such as the characteristic processing technology on the verge of being lost, the lack of innovation, the lack of brand quality, and the lack of precise clinical application, *etc.* The quality of Chinese medicine decoction

piece is still difficult to quantify, to evaluate, to control, and to maintain efficiency, through the extensive processing steps. These difficulties become the key scientific limitation restricting the development of Chinese botanical drugs industry.

3 Applications of digital and intelligent technologies in process of PCMM

Digitization is the basic process of converting many complex and changeable information into measurable numbers, and then establishing appropriate digital models based on these numbers, transforming them into a series of binary codes, and introducing them into the computer for unified digital processing. Intelligence refers to the attributes of things that may meet various needs under the support of computer network, big data, internet, and artificial intelligence. The initial definition of digital and intelligent technologies is ***the combination of digital intelligence and intelligent digitalization***. At present, the main branches of artificial intelligence applications include machine learning (ML), machine vision, Internet of Things (IoT), artificial neural network (ANN), robotics and expert system, *etc.* (Kutyauripo et al., 2023). Digital technology, artificial intelligence and other technologies continue to grow, and digital intelligent technology has been widely used in the daily life. For example, self-driving cars use the most reasonable autonomous driving scheme according to the information of the surrounding scene, identified driving intention, and intelligently responsive emergencies (Shi et al., 2022).

Due to the objectivity and intelligence of digital intelligence technology, researchers in the medical field use them to automatically detect and identify organ dysfunction to optimize disease diagnosis and treatment (Ehrenreich et al., 2020; Hatanaka, 2020). As an important part of improving clinical efficacy, the PCMM processing is a cumbersome, complex, diversed and influencing factor. Moreover, the whole processing is decided by pharmacists based on experience, which may have obvious limitations. The lack of accurate processing quality control technology is likely to greatly impact the efficacy of drug. At the same time, due to the complex chemical reactions along the processing, the unforeseeable degree of effective variation, the lack of reliable online instruments, the complex modeling, the lack of visualization technology, the lack of efficiency, the low sensitive detection, and the lack of real-time monitoring technology, the most optimized processing is still hard to achieve. Therefore, it is necessary to introduce digital intelligence technology into the processing control of traditional Chinese medicine using objective quantitative indicators to accurately regulate the processing steps.

3.1 The application of digital intelligence technology in cleansing processing

The machine vision system may quickly obtain a large amount of information, which is more efficient and accurate than manual selection. It is easy to process automatically and integrate with designed and processing-controlled information; which is highly suitable for modern automated production processes. Convolutional neural networks (CNN) has powerful visual information on processing capabilities and may achieve efficient hierarchical feature expression of data. CNN plays an important role in applications such as image classification and detection in processing control (Kazi and Panda, 2022). Therefore, based on the CNN recognition method, the data sets of different medicament portions and various impurities may be constructed. The Wiener filtering algorithm and multi-scale enhancement algorithm are used for image preprocessing to identify different medicinal parts and impurities (Shen et al., 2019; Steinbrener et al., 2019). The local texture feature extraction technology is used to form texture features. The performance of the proposed feature set is compared with the existing techniques based on running length matrix, co-occurrence matrix, size region matrix, neighborhood gray tone difference matrix and wavelet decomposition. The backpropagation neural network (BPNN) may also classify the same medicinal materials of different origin and species (Singh and Chaudhury, 2020). In addition to screening the image features of medicinal materials, it may also be combined with various sensors to quantify the shape, color, taste and other indicators of Chinese medicinal materials, so as to select impurities, non-medicinal parts and different medicinal portions respectively (Yin et al., 2021; Wang et al., 2022).

3.2 The application of digital intelligence technology in cutting processing

In the process of softening, many water-soluble active ingredients may be lost or destroyed to varying degrees. Li et al. (2021) developed an intelligent vacuum gas phase displacement moistening machine. By controlling the vacuum degree and infiltration time, the medicinal materials were softened quickly and evenly with low water content, and reduced loss of active ingredients during the process of infiltration. At the same time, this improved vacuum played an important role in reducing the energy consumption of subsequent drying, improving work efficiency, and reducing production costs. He et al. (2022) designed a predictive control method of the processing temperature of Chinese medicine decoction pieces based on the fuzzy neural network, in order to solve the problem that the temperature of Chinese medicine decoction pieces was difficult to control during gas phase replacement wetting. This method realized the optimal automatic control of the temperature tracking set value of Chinese medicine decoction pieces in the processing step of gas phase replacement wetting. All these new intelligent technologies make a better control of the moistening processing of Chinese medicine decoction pieces, maximize the retention of medicinal ingredients, and improve clinical efficacy of the drugs.

As for cutting, different kinds of medicinal materials may be discussed separately. Combining advanced computer vision technology with deep learning architecture, the image data sets of different kinds of plant medicinal materials are constructed. The mathematical model of rhizome cutting specification is established; and the cutting of different specifications and tablets is designed by intelligent conversion of blade position (Yu et al., 2023). The circular mask large template was used to detect the seed morphology, the data distribution was used to locate the spindle and distinguish the

different parts of the seed to obtain the slices of the seed medicinal materials (Wei et al., 2022). Through the cutting and coring mechanism of flower medicinal materials, the cutting and coring processes at different positions are realized to obtain flower medicinal materials such as pollen, stigma and inflorescence (Chen et al., 2021). Animal medicinal materials may be analyzed by machine vision and three-dimensional point cloud dual robot system, using 3D scanning system, corpse fixing device and laser-guided efficient cutting robot, to develop a system that may intelligently grab, clean and cut various animal tissues of different sizes and shapes (Azarmdel et al., 2019; Bao et al., 2022; Liu et al., 2022). The delay-mean-rule is designed by simulated annealing algorithm and time window variable optimization method. Such rule is used for real-time monitoring and controlling of drying of medicinal materials by dryer equipment (Ke et al., 2022). The genetic algorithm (GA) was used to optimize the ANN to simulate the drying processing, the best drying curves was obtained, and green drying method was selected (Fabani et al., 2021).

3.3 The application of digital intelligence technology in stir-frying processing

In the PCMM, heat refers to the size and duration of fire when the drug is heated, which is a key factor affecting the quality of decoction pieces. Studies have shown that with the change of fire degree, the content of volatile components, amino acids and reduced sugars in drugs have changed significantly (Chen et al., 2016; Hu et al., 2016). Therefore, through the digital technology, the various influencing factors in the processing are objectively quantified, and then the artificial intelligence technology is used to adjust and control the fire, time, temperature and processing end point, which is conducive to the standardization of processing technology and the quality of decoction pieces. As such, it realizes the intelligent and modern production of decoction pieces.

The contents of chemical components and biological activity of drugs may be changed by steaming, boiling, and frying under different air pressures (Trakoontivakorn et al., 2012; Guo et al., 2022). Maillard reaction often occurs in the heat treatment process of food and pharmaceutical, which is the main chemical reaction to produce new flavor and new color in the processing food and Chinese botanical drugs. With the increase in temperature, Maillard reaction often shows an increasing trend too (Gerrard, 2006; Zhang, 2020). Xu et al. (2015) compared the raw betel nut with its processed products of stir-frying yellow, stir-frying coke and stir-frying charcoal, and found that the contents of 5-HMF and arecoline in the three processed products were significantly different and closely related to the levels obtained by electronic nose and electronic tongue. Zheng et al. (2022) used cluster analysis and Artificial neural network analysis (ANN) to better identify gardenia with various processing degrees. For the determination of the end point of processing, the color difference and distribution in the image may be used to determine the degree of stir-frying and cooking of the drug, so that the processing system may determine whether to use partial tumbling, or to end the processing when the decoction pieces reach the optimal efficacy; such processing system may avoid improper or excessive processing (Lin et al., 2021). By combining bionic sensors with chemometrics, the overall quality evaluation system of decoction pieces was established and used to determine whether the processing time of decoction pieces reached sufficient with the most optimized quality (Zhang et al., 2023). In addition, fermentation drugs were processed within antibacterial biomolecules-covalent organic frameworks through a combination of artificial intelligence technologies, such as low-cost sensors, machine learning (ML), and intelligently release antibacterial substances according to pH values, to intelligently regulate and evaluate the drug fermentation processing (Viejo and Fuentes, 2020; Qiao et al., 2021).

3.4 Application of digital intelligence technology in quality control of decoction pieces

Due to the particularity of Chinese medicine decoction pieces, it is not only necessary to control the process of PCMM but also to test the quality of the final pieces to ensure the safety and effectiveness of the drug. At present, many scholars have achieved stable and rapid qualitative and quantitative analysis through new technical methods such as electronic sensors, Fourier transform near-infrared technology (Lan et al., 2020), Desorption electrospray Ionization mass spectrometry (DESI-MSI) combined with metabolomics (Liu et al., 2022), Static headspace-multi-capillary column with gas chromatography coupled to ion mobility spectrometry (Cao et al., 2014) and Process Analysis Technique (PAT) based on chemometrics (Korasa and Vrečer, 2018; Kamyar et al., 2021). Near Infrared Spectrum (NIR) spectroscopy has become the most commonly used PAT process analyzer in pharmaceutical technology because of its advantages of non-destructive measurement and real-time monitoring in the process, and is particularly suitable for complex production that requires process quality control (Lee et al., 2019). Therefore, it is urgent to find technical methods that may monitor key quality parameters in real time in the processing, and obtain high quality slices through continuous monitoring the process, so as to eliminate the unqualified final quality of slices that may be caused by improper processing.

Jin et al. (2022) and Zuo et al. (2020) monitored, in real-time, the online quality of industrial concentration processing of *Lonicera japonica* Thunb. [Caprifoliaceae; *Lonicerae japonicae* flos] and the steaming processing of *Gastrodia elata* Blume [Orchidaceae; *Gastrodiae* rhizoma] by NIR spectroscopy as a processing analysis tool combined with real-time release sensor and chemometrics. Thus, the quality of drugs and therapeutic effect were significantly improved. Qiu et al. (2021) reported that enzymatic browning was the main factor of metabolic changes during the processing of *Salvia miltiorrhiza* Bunge [Lamiaceae; *Salviae miltiorrhizae* radix et rhizoma] using metabolomic data, which was helpful to select the best processing technology of *Salviae miltiorrhizae* radix et rhizoma according to the actual needs. Therefore, a combination of NIR spectroscopy, metabolomics, Gas Chromatography-ion Migration Spectrometry (GC-IMS) (Xu et al., 2022), online stepwise background subtraction-based Ultra

high performance Liquid chromatography-Quadrupole-time-of-Flight Tandem Mass Spectrometry (UHPLC-Q-TOF-MS/MS) dynamic detection (Guo et al., 2022) and other digital intelligence techniques should be considered to monitor the odor, metabolic components and chemical components during the PCMM processing, and to provide real-time and data-based test results to the cloud, with reduced falsification of testing and optimized drug quality. The content of active ingredients in Chinese medicinal materials, intermediate products and processed products may be rapidly determined by ANN and Least squares support vector machine (LS-SVM) combined with spectrophotometry or Fourier-Transform near infrared (FT-NIR). The deconvolution software may be used to qualitatively and quantitatively analyze the impurities of medicinal materials by HPLC and HPLC-Photodiode array detector (PDA) systems (Wang et al., 2020; Qiu et al., 2021; Noroozi et al., 2022; Vecchietti et al., 2022). For some new chemical components of processed products, the influence of their chemical characteristics on performance is used to predict their effects in the patients through machine learning (ML) models to prevent drug-induced damage (Mcloughlin et al., 2021). DNA barcoding may quickly detect the quality of Chinese medicine decoction pieces at the molecular level, which is efficient, reliable, sensitive and repeatable, and may ensure the safety of clinical medication (Wang et al., 2015; Xin et al., 2018). In addition, for some valuable medicinal materials that are easily adulterated, UHPLC-Q-TOF-MS, PCA methods may be combined with Progenesis QI, Makerlynx XS and other software to identify medicinal materials according to specific characteristic markers, and to accurately distinguish between genuine and counterfeit (Guo et al., 2019; Liu et al., 2020).

4 Digital intelligent research and industrial transformation of PCMM

Örs et al. (2020) proposed operational digital twin (DT) for chemical processes, aiming at data management, processing detection, processing modeling, processing optimization, production scheduling, and advanced processing control. A system based on DT was proposed to regulate the processing. Sensors were used to collect data, and the medicinal materials were identified and classified by machine vision, smell and CNN. Personalized or optimized processing was carried out according to the characteristics of each batch of medicinal materials. At the same time, a system designed by the concept, may analyze and control the processing through real-time measurements to ensure the processing moderation and the quality of final decoction pieces, so as to transform the PCMM to the digital intelligence environment. Through the intelligent control of each step of the processing, each processing is fully executed throughout every step, with strictly controlled quality of decoction pieces, carefully monitored digital characterization of PCMM, and using novel intelligent control of traditional Chinese medicine processing. This section will progress from the research and development of TCM processing laboratory and the processing line of factory, to the digital intelligence technology not only to the processing trial, but also to the industrial production lines.

4.1 Lab test

Through data mining (DM), the database of raw and processed products of traditional Chinese medicinal materials was established; the internal relationship between raw and processed products of traditional Chinese medicine and processing steps was analyzed; the related model of processing and quality of decoction pieces was constructed; and the conditions and regulation of processing steps were established (Fusheng et al., 2009). Based on the model of the efficacy of traditional Chinese medicine formula (Liu et al., 2022), a weighted calculation method related to the processing conditions such as temperature, types and methods of excipients, may be constructed. The graph convolutional network (GCN) is combined with the conditions in the processing steps to predict the efficacy of processed products.

The research on the technology in producing PCMM is an important link to realize the standardization of the traditional Chinese medicine processing. ML is the core of artificial intelligence, which may predict new and invisible data based on previous observed results and data, so that the computer may automatically learn without manual intervention, to adjust the operation accordingly, and to make decisions automatically. It is often divided into three categories: supervised learning, unsupervised learning and reinforcement learning (Kersting, 2018; Lins and Givigi, 2021). The lab test may discover the changing components during the processing by CNN and deep learning (DL), so that the quality markers of decoction pieces, standardizing the PCMM technologies, controlling the quality of decoction pieces, and formulating the standard of decoction pieces may be achieved (Skrede et al., 2020). In addition, the fuzzy logic method may be used to explore the effects of different processing methods on the sensory properties of decoction pieces without reducing the efficacy, and appropriate processing methods may be selected to improve the appearance and taste of decoction pieces (Sasikumar et al., 2019; Deba-Rementeria et al., 2023).

4.2 Intelligent industrial production of traditional Chinese medicine decoction pieces

With the advent of the fourth industrial revolution, the future factory will be highly digital and intelligent to meet the needs of real-time, flexible, personalized and automated monitoring of traditional Chinese medicine processing, and will realize the intelligent production of 'Internet + manufacturing' (Zunino et al., 2020). The online detection technology, Internet digital technology and artificial intelligence control technology are running through the automatic processing equipment and production line. The computer information management system of drug processing and the digital intelligent production line of Chinese medicine decoction pieces can be established (Shi et al., 2022). The establishment of a standardized system of processing equipment and processing parameters is the key factor to promote the modernization of Chinese medicine decoction pieces. The combination of digital intelligence technology and the equipment system of purification, cutting and processing, including washing machine, screening machine, cutting machine, stir-frying machine, and boiling pot, gradually establish a

production line of Chinese medicine processing equipment in line with the characteristics of produced Chinese medicine with appropriate integration and automation. Follow the ancient processing technology, combined with modern digital intelligence technology and new intelligent processing equipment, a production line with high efficiency, energy saving, continuous production and controllable quality may be created to improve the manufacturing level of Chinese botanical drugs industry, and to accelerate the transformation of traditional Chinese decoction pieces industry to digital intelligence (Shi et al., 2022; Zhu et al., 2022).

4.2.1 Digital and intelligent equipment of PCMM

Hardware equipment is the infrastructure of the industrial production. With the acceleration of the modernization of TCM, the processing equipment needs to be constantly innovated. The standardization of traditional Chinese medicine processing equipment is the premise of the standardization of processing parameters. The development of digital intelligent processing equipment is helpful to solve the modernization problem of TCM decoction piece industry.

The sensor can objectively show the shape, color and taste of the drug through the digital form of the sensitive element, which is the first link to realize automatic detection and control. New sensors are added to the processing equipment, and the corresponding mathematical model is established. The artificial intelligence system is used for automatic control, and the technological innovation is achieved to promote the new equipment creation. The traditional processing technologies such as levigating, dry distillation, duplication, and roasting are combined with modern microwave technology, cyclone and foam separation, mass transfer and heat transfer, and biotransformation to develop new processing equipment.

The stir-frying equipment is the most characteristic pharmaceutical equipment of traditional Chinese medicine. Taking the stir-baking equipment as an example, the stir-frying machine is transformed into a fuel gas heat source supply and automatic temperature control system, which may not only achieve rapid heating, but also use the real-time, continuous and non-contact measurement of the temperature in the pot by a temperature sensor. It is truly the digital monitored and managed PCMM processing (Yang et al., 2022). Non-contact infrared temperature measurement uses infrared thermal imaging technology and ANN-based data-driven algorithm to estimate the temperature of medicinal materials. This system realizes dynamic continuous non-contact temperature measurement, and monitors the temperature parameters during processing (Liu et al., 2022). The online detection system of traditional Chinese medicine processing equipment combines the intelligent sensory technology and online monitoring technology to digitally express the processing steps and realize the objectification of the PCMM. The application of internet, internet of things (IoT), big data and computer technology improves the traditional Chinese medicine processing equipment, promotes the informatization and automation of processing, optimizes the quality of decoction pieces, accelerates the transformation, and upgrades the traditional Chinese medicine decoction pieces industry.

4.2.2 Digital and intelligent production line

Based on the application of the above-mentioned digital intelligent technology in the processing and the digital intelligent processing equipment, an efficient digital intelligent production line of Chinese medicine decoction pieces may be designed (Figure 1). By automating the processing of large quantities of medicinal materials while making the processing digital and intelligent, high-quality, and effective decoction pieces may be produced. Digital intelligent processing factory may use the IoT technology combined with the other advanced technologies, such as industrial big data, Wireless Sensor network (WSN), Radio Frequency Identification (RFID), and cloud computing platforms, to achieve intelligent management by monitoring the use of materials in the production line and maximizing the efficiency of optimized production (Liu et al., 2020). This digital intelligent processing factory may integrate all medicinal materials, processing techniques, processing equipment and pharmaceutical operations into digital data through big data, deep learning, case analysis and simulation modeling technologies. Through RGB image data, convolutional neural network and discriminant function, each medicinal material is classified, and transported to different processing workshops by transportation robots. Appropriate processing is carried out according to the nature of the drug itself and the medicinal needs. The corresponding mathematical model is established to ensure that the key processing parameters are optimized to maintain a high product quality (Mears et al., 2017). The decoction pieces produced in each processing workshop are sent to the laboratory for rapid, accurate and non-destructive quality testing. The qualified decoction pieces are classified and packaged with suitable multifunctional biodegradable intelligent packaging materials. The processing steps may be traced through the intelligent functions of microbial spoilage biosensor, detection, recording, tracing and communication (He and Shi, 2021; Khan et al., 2023; Kong et al., 2023; Palazzo et al., 2023). Subsequently, the decoction pieces are transported to a number of intelligent warehouses with different storage conditions. The system analyzes the quantity of ordered products according to the collection, monitors the real-time inventory in the warehouse, intelligently adjusts the processing variety and quantity, rationally saves the storage space in the warehouse, and reduces the risk and cost of expired products (Ahmadi et al., 2022). Through integrated software such as cloud computing and big data, with automatic data collection and decision-making, dynamical regulation between departments may be achieved (Coito et al., 2020).

Take Fuzi (*Aconite lateralis* radix praeparata), an important medicine for restoring "Yang" and rescuing patient from collapse, as an example (Figure 2). Aconitum carmichaeli contains a large number of diester alkaloids, which have strong toxicity. The processed products from it are generally used in clinic with reduced toxicity, and there are many kinds of processed products (He et al., 2023). Herbon mass spectrometry, and the appropriate fitting function was selected intelligently to reduce the toxicity of aconite (Qiu et al., 2020). Finally, machine vision, intelligent cutting robot, and real-time drying monitoring technology were used to cut aconite into appropriate thickness and dried for clinic use.

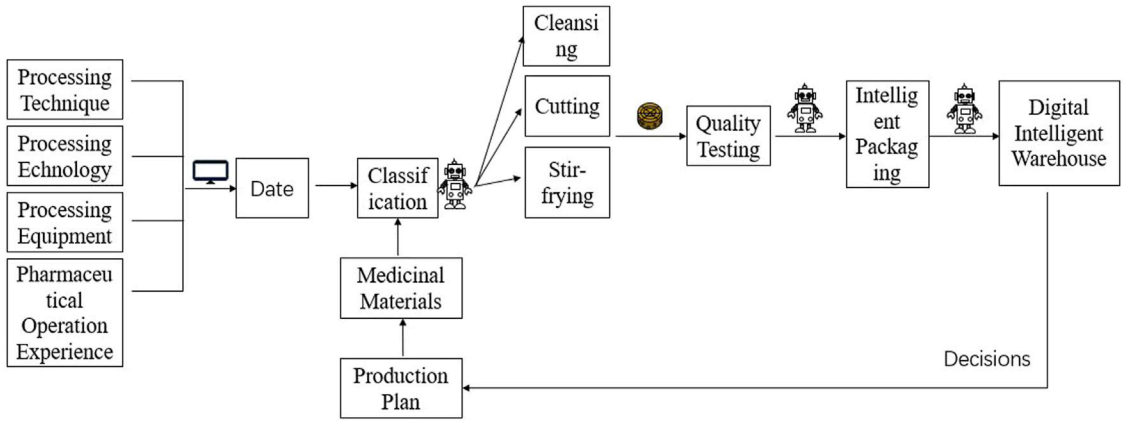

FIGURE 1
Schematic diagram of digital intelligent production line of Chinese decoction pieces.

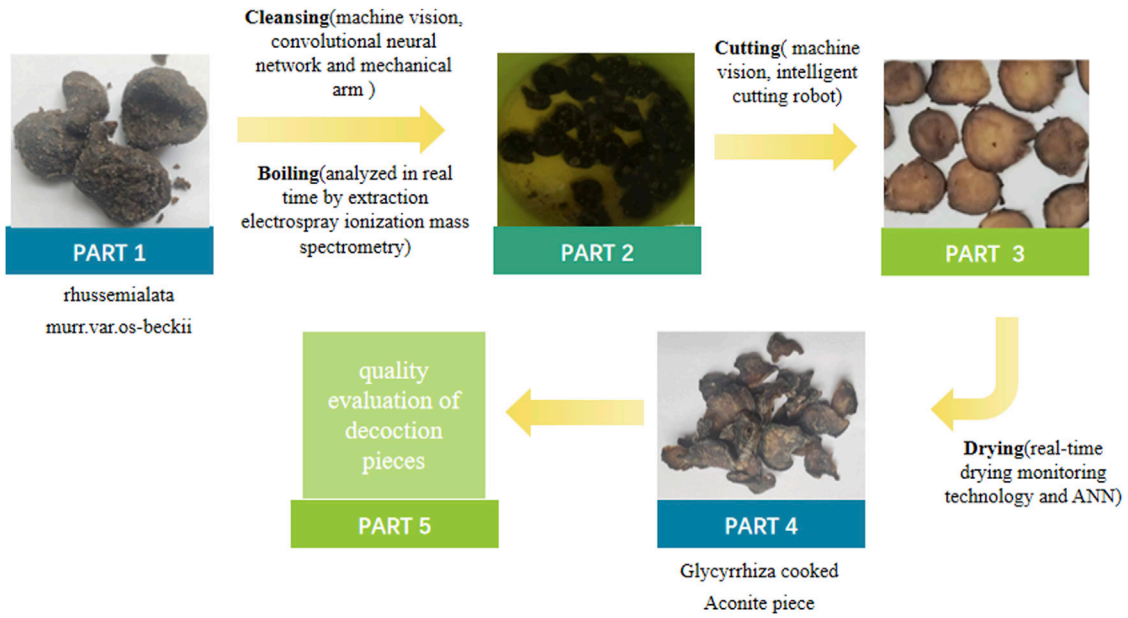

FIGURE 2
Processing flow chart of aconite.

4.2.3 Other auxiliary systems

In addition to the equipment and technology required for processing, the digital intelligent processing factory also needs to detect faults and abnormalities in real time, and applies the intelligent alarm system to provide detection and diagnosis of abnormal events and solutions to minimize emergency closure during processing and to maintain efficient and continuous production (Gupta et al., 2013; Velasquez et al., 2022). Under the digital monitoring and intelligent control, the actual production processing is constantly monitored and right decision is rapidly achieved to maintain the production line at the most optimal level. This result promotes the intelligent control of the workshop, creates a machine automation workflow, and pursues robust and adaptive decision in the workflow through artificial intelligence thinking and learning (Fu et al., 2019; Ng et al., 2021). By using the auxiliary technology of brain-computer interface to enhance and develop novel technology, by sensing the temperature and imagine of the environment, and by monitoring the water use of the factory to intelligently control the lighting, temperature and water valve switch of the factory, the factory is running at the most optimized condition with saved resources (Al-Hudhud et al., 2019; Uysal and Mergen, 2021). The intelligent system is developed to detect the content of drugs in the sewage of the processing plant, to predict the drug contents and the influence by re-irrigated plants after treatment, to reasonably control the drug content in the

sewage, and to realize the green and sustainable production mode (González García et al., 2019).

5 Conclusion

Chinese medicine processing is very important to the preparation and use of Chinese medicine. Many countries in the world have taken the green and sustainable development as an important direction of scientific and technological revolution and industrial transformation. The new generation of information technology is rapidly progressing and the digital economy is expanding in scale. In this context, grasping the opportunity of technological iteration, accelerating the digitalization and intelligent transformation, and upgrading of the TCM industry have become an important starting point to promote the high-quality sustainable development of the TCM industry. Digital intelligent transformation is the combination of digital transformation and intelligent elements (such as artificial intelligence, Internet of Things and other technologies). Numeral intelligent processing makes all traditional experience objective and information, production processing and quality control, into digital and intelligent controlled processing. New technology aims to improve the problems of distinguishing, evaluating and controlling the quality of traditional Chinese medicine decoction pieces through extensive processing with low efficiency. Through the multi-dimensional holographic processing property characterization, the electronic rapid identification of the shape and taste quality of decoction pieces, and the intelligent control of fire temperature and other technologies, the traditional processing technology may be thoroughly innovated and improved. The scientific content of TCM may be improved. The modern development needs may be met. The clinical application of characteristic decoction pieces may be expanded. The high-quality industrial benefits may be achieved. The intelligent manufacturing of a number of traditional Chinese medicine decoction pieces may be achieved. This paper reviewed the application of digital intellectualization technology in the processing of TCM, which promoted the standardization of the processing, the standardization of the quality of decoction pieces, the digitalization and intellectualization of production, and the safety and effectiveness of clinical use of TCM decoction pieces. At the same time, this review also provided a theoretical basis for the technical progress and high-quality development of TCM industry in the future.

Author contributions

Conceived and designed the paper: CZ, MY, LZ; Wrote the paper: WZ, CZ, LC, FL, WX, LT; Proof reading and edited the paper: CZ, CC, MY, LZ. All authors contributed to the article and approved the submitted version.

Funding

This work was funded by Key laboratory of TCM Processing Technology, Jiangxi Traditional Chinese Medicine Science and Education No.8 (2022); TCM processing technology inheritance and innovation team (No. CXTD22003); Jiangxi Province Shuangqian Talent Plan Project [Gancaiban No.9 (2019)]; Chinese Medicine Standardization Project of Jiangxi Province (No. 2020B01 and No. 2020B04); Gan Po Talent Support Program - Academic and technical leaders training program in major disciplines for Zhang CH (Academic - Leading talent); the Nanchang Key Laboratory of Drug Development and Transformation for Prevention and Treatment of Cancer and Endocrine Metabolic Diseases [Hongkezi No.165 (2023)]; Horizontal project of Nanchang Research Institute of Sun Yat-sen University (H20221206); Science and Technology Project of Education Department of Jiangxi Province (GJJ213111); CC was supported by Australian NHMRC and The University of Queensland.

Conflict of interest

The authors declare that the research was conducted in the absence of any commercial or financial relationships that could be construed as a potential conflict of interest.

Publisher's note

References

Ahmadi, E., Mosadegh, H., Maihami, R., Ghalehkhondabi, I., Sun, M., and Süer, G. A. (2022). Intelligent inventory management approaches for perishable pharmaceutical products in a healthcare supply chain. *Comput. Oper. Res.* 147, 105968. doi:10.1016/j.cor.2022.105968

Al-Hudhud, G., Alqahtani, L., Albaity, H., Alsaeed, D., and Al-Turaiki, I. (2019). Analyzing passive BCI signals to control adaptive automation devices. *Sensors (Basel, Switz.* 19 (14), 3042. doi:10.3390/s19143042

Azarmdel, H., Mohtasebi, S. S., Jafari, A., and Rosado Muñoz, A. (2019). Developing an orientation and cutting point determination algorithm for a trout fish processing system using machine vision. *Comput. Electron. Agric.* 162, 613–629. doi:10.1016/j.compag.2019.05.005

Bao, X. L., Leng, J. S., Mao, J. C., and Chen, B. Y. (2022). Cutting of sheep carcass using 3D point cloud with dual-robot system. *Int. J. Agric. Biol. Eng.* 15 (5), 163–171. doi:10.25165/j.ijabe.20221505.7161

Cao, G., Shou, Q. Y., Li, Q. L., Jiang, J. P., and Chen, X. C. (2014). Static headspace-multicapillary column with gas chromatography coupled to ion mobility spectrometry as a simple approach for the discrimination of crude and processed traditional Chinese medicines. *J. Sep. Sci.* 37 (21), 3090–3093. doi:10.1002/jssc.201400627

Chen, H., Pan, H., Zhang, X., Liu, F., Chen, M., Luo, G., et al. (2016). GC-MS combined with AMDIS and Kovats retention index to investigate dynamic change rules of volatile components from Atractylodis Macrocephalae Rhizoma with different stir-baking degrees. *Zhongguo Zhong yao za zhi = Zhongguo zhongyao zazhi = China J. Chin. materia medica* 41 (14), 2646–2651. doi:10.4268/cjcmm20161413

Chen, J., Bian, X., Chen, L., Chen, T., Chen, Z., and Yu, C. (2021). Design and testing of a production line mechanism for continuous cutting and coring of broccoli. *Comput. Electron. Agric.* 191, 106505. doi:10.1016/j.compag.2021.106505

Chinese Pharmacopoeia Commission (2010). *Pharmacopoeia of the People's Republic of China-volume IV*. China: China Medical Science Press.

Chinese Pharmacopoeia Commission (2020). *Pharmacopoeia of the People's Republic of China-volume IV*. China: China Medical Science Press.

Coito, T., Martins, M. S. E., Viegas, J. L., Firme, B., Figueiredo, J., Vieira, S. M., et al. (2020). A middleware platform for intelligent automation: an industrial prototype implementation. *Comput. Ind.* 123, 103329. doi:10.1016/j.compind.2020.103329

Deba-Rementeria, S., Paz, A., Estrada, O., and Vázquez-Araújo, L. (2023). Consumer perception and physicochemical characterization of a new product made from lactic acid fermented orange peels. *Int. J. Gastron. Food Sci.* 31, 100647. doi:10.1016/j.ijgfs.2022.100647

Ehrenreich, J., Bette, M., Schmidt, A., Roessler, M., Bakowsky, U., Geisthoff, U. W., et al. (2020). Evaluation of digital image analysis as a supportive tool for the stratification of head and neck vascular anomalies. *Eur. Arch. Otorhinolaryngol.* 277 (10), 2893–2906. doi:10.1007/s00405-020-06097-2

Fabani, M. P., Capossio, J. P., Roman, M. C., Zhu, W. L., Rodriguez, R., and Mazza, G. (2021). Producing non-traditional flour from watermelon rind pomace: artificial neural network (ANN) modeling of the drying process. *J. Environ. Manage.* 281, 111915. doi:10.1016/j.jenvman.2020.111915

Fu, Y., Zhou, M., Guo, X., and Qi, L. (2019). Artificial-Molecule-based chemical reaction optimization for flow shop scheduling problem with deteriorating and learning effects. *IEEE Access* 7, 53429–53440. doi:10.1109/ACCESS.2019.2911028

Fusheng, Z., Xiaoping, L., Xushijie, C., Jiannan, C., and Chen, Q. (2009). Methodology for modeling on Chinese herbal property theory. *World Sci. Technol.* 11 (2), 229–233. doi:10.1016/S1876-3553(10)60015-4

Gerrard, J. A. (2006). The maillard reaction in food: progress made, challenges ahead—conference report from the eighth international symposium on the maillard reaction. *Trends Food Sci. Technol.* 17 (6), 324–330. doi:10.1016/j.tifs.2005.11.011

González García, M., Fernández-López, C., Bueno-Crespo, A., and Martínez-España, R. (2019). Extreme learning machine-based prediction of uptake of pharmaceuticals in reclaimed water-irrigated lettuces in the Region of Murcia, Spain. *Biosyst. Eng.* 177, 78–89. doi:10.1016/j.biosystemseng.2018.09.006

Gu, D., Wang, Y., Jin, H., Kang, S., Liu, Y., Zan, K., et al. (2022). Changes of physicochemical properties and immunomodulatory activity of polysaccharides during processing of polygonum multiflorum Thunb. *Front. Pharmacol.* 13, 934710. doi:10.3389/fphar.2022.934710

Guo, J., Shang, Y., Yang, X., Li, J., He, J., Gao, X., et al. (2022). An online stepwise background subtraction-based ultra-high pressure liquid chromatography quadrupole time of flight tandem mass spectrometry dynamic detection integrated with metabolic molecular network strategy for intelligent characterization of the absorbed chemical-fingerprint of QiangHuoShengShi decoction *in vivo*. *J. Chromatogr. A* 1675, 463172. doi:10.1016/j.chroma.2022.463172

Guo, W. Y., Bai, J., Zhang, Q. N., Duan, K. F., Zhang, P. P., Zhang, J. H., et al. (2022). Influence of thermal processing on the quality of hawthorn: quality markers of heat-processed hawthorn. *J. Sep. Sci.* 45 (19), 3774–3785. doi:10.1002/jssc.202200222

Guo, X., Cheng, X., Liu, W., Li, M., Wei, F., and Ma, S. (2019). Identification of velvet antler and its mixed varieties by UPLC-QTOF-MS combined with principal component analysis. *J. Pharm. Biomed. Anal.* 165, 18–23. doi:10.1016/j.jpba.2018.10.009

Gupta, A., Giridhar, A., Reklaitis, G. V., and Venkatasubramanian, V. (2013). "Intelligent alarm system applied to continuous pharmaceutical manufacturing," in *Computer aided chemical engineering, computer aided chemical engineering*. Editors A. Kraslawski and I. Turunen (Amsterdam, Netherlands: Elsevier), 499–504.

Hatanaka, Y. (2020). Retinopathy analysis based on deep convolution neural network. *Adv. Exp. Med. Biol.* 1213, 107–120. doi:10.1007/978-3-030-33128-3_7

He, D. F., Cen, J. H., Zhu, W., Li, X. N., and Yang, Y. X. (2022). *A predictive control method for the temperature of Chinese herbal medicine based on fuzzy neural network*. Amsterdam, Netherlands: Elsevier, 15.

He, G., Wang, X., Liu, W., Li, Y., Shao, Y., Liu, W., et al. (2023). Chemical constituents, pharmacological effects, toxicology, processing and compatibility of Fuzi (lateral root of Aconitum carmichaelii debx): a review. *J. Ethnopharmacol.* 307, 116160. doi:10.1016/j.jep.2023.116160

He, M., and Shi, J. (2021). Circulation traceability system of Chinese herbal medicine supply chain based on internet of things agricultural sensor. *Sustain. Comput. Inf. Syst.* 30, 100518. doi:10.1016/j.suscom.2021.100518

Hu, M. B., Peng, W., Liu, Y. J., Yan, D., Chen, X., and Wu, C. J. (2016). Maillard reaction induces changes in saccharides and amino acids during stir-baking of areca nuts. *Trop. J. Pharm. Res.* 15 (10), 2107–2112. doi:10.4314/tjpr.v15i10.8

Huang, Y. S., Li, C., Hu, H. Y., Wang, Y. T., Shen, M. Y., Nie, S. P., et al. (2019). Simultaneous determination of acrylamide and 5-hydroxymethylfurfural in heat-processed foods employing enhanced matrix removal-lipid as a new dispersive solid-phase extraction sorbent followed by liquid chromatography-tandem mass spectrometry. *J. Agric. Food. Chem.* 67 (17), 5017–5025. doi:10.1021/acs.jafc.8b05703

Jin, Y., Du, W., Liu, X., and Wu, Y. (2022). Application of near infrared spectroscopy and real time release testing combined with statistical process control charts for on-line quality control of industrial concentrating process of traditional Chinese medicine "Jinyinhua". *Infrared Phys. Technol.* 123, 104135. doi:10.1016/j.infrared.2022.104135

Kamyar, R., Lauri Pla, D., Husain, A., Cogoni, G., and Wang, Z. (2021). Soft sensor for real-time estimation of tablet potency in continuous direct compression manufacturing operation. *Int. J. Pharm.* 602, 120624. doi:10.1016/j.ijpharm.2021.120624

Kazi, A., and Panda, S. P. (2022). Determining the freshness of fruits in the food industry by image classification using transfer learning. *Multimed. Tools Appl.* 81 (6), 7611–7624. doi:10.1007/s11042-022-12150-5

Ke, C., Zhang, M., Zuo, Y., Xiang, F., Zhang, D., and Tao, F. (2022). Data-driven real-time control method for process equipment in flow shop towards product quality improvement. *Procedia CIRP* 107, 908–913. doi:10.1016/j.procir.2022.05.083

Kersting, K. (2018). Machine learning and artificial intelligence: two fellow travelers on the quest for intelligent behavior in machines. *Front. Big Data*. 1, 6. doi:10.3389/fdata.2018.00006

Khan, A., Ezati, P., Kim, J. T., and Rhim, J. W. (2023). Biocompatible carbon quantum dots for intelligent sensing in food safety applications: opportunities and sustainability. *Mat. Today sustain.* 21, 100306. doi:10.1016/j.mtsust.2022.100306

Kim, Y. J., Hong, C. O., Han, J. W., Lee, S. H., Chang, J. K., Ma, K., et al. (2019). Chemical composition and antioxidant compounds of Rehmannia glutinosa during steaming process. *Planta Med.* 85 (18), 1568. doi:10.1055/s-0039-3400150

Kong, J., Ge, X., Sun, Y., Mao, M., Yu, H., Chu, R., et al. (2023). Multi-functional pH-sensitive active and intelligent packaging based on highly cross-linked zein for the monitoring of pork freshness. *Food Chem.* 404, 134754. doi:10.1016/j.foodchem.2022.134754

Korasa, K., and Vrečer, F. (2018). Overview of PAT process analysers applicable in monitoring of film coating unit operations for manufacturing of solid oral dosage forms. *Eur. J. Pharm. Sci.* 111, 278–292. doi:10.1016/j.ejps.2017.10.010

Kutyauripo, I., Rushambwa, M., and Chiwazi, L. (2023). Artificial intelligence applications in the agrifood sectors. *J. Agric. Food Res.* 11, 100502. doi:10.1016/j.jafr.2023.100502

Lan, Z., Zhang, Y., Sun, Y., Ji, D., Wang, S., Lu, T., et al. (2020). A mid-level data fusion approach for evaluating the internal and external changes determined by FT-NIR, electronic nose and colorimeter in Curcumae Rhizoma processing. *J. Pharm. Biomed. Anal.* 188, 113387. doi:10.1016/j.jpba.2020.113387

Lee, Y., Zhou, G., Ikeda, C., Chouzouri, G., and Howell, L. (2019). Application of online near infrared for process understanding of spray-drying solution preparation. *J. Pharm. Sci.* 108 (3), 1203–1210. doi:10.1016/j.xphs.2018.10.022

Li, H. W., Zhang, M. Q., Liu, C. M., Li, Y., and Liu, A. G. (2021). *An intelligent vacuum gas phase displacement moistening machine*, 11. China: State Intellectual Property Office of the People's Republic of China. Patent No ZL202020309810.6.

Li, M., Jiang, H., Hao, Y., Du, K., Du, H., Ma, C., et al. (2022). A systematic review on botany, processing, application, phytochemistry and pharmacological action of Radix Rehmnniae. *J. Ethnopharmacol.* 285, 114820. doi:10.1016/j.jep.2021.114820

Li, Y., Wang, X., Chen, H., Yuan, J., Meng, Y., and Yang, W. (2021). Comparison of the chemical constituents of raw Fructus Aurantii and Fructus Aurantii stir-baked with bran, and the biological effects of auraptene. *J. Ethnopharmacol.* 269, 113721. doi:10.1016/j.jep.2020.113721

Lin, C. S., Pan, Y. C., Kuo, Y. X., Chen, C. K., and Tien, C. L. (2021). A study of automatic judgment of food color and cooking conditions with artificial intelligence technology. *Processes* 9 (7), 1128. doi:10.3390/pr9071128

Lins, R. G., and Givigi, S. N. (2021). Cooperative robotics and machine learning for smart manufacturing: platform design and trends within the context of industrial internet of things. *IEEE Access* 9, 95444–95455. doi:10.1109/ACCESS.2021.3094374

Liu, J., Huang, Q., Yang, X., and Ding, C. (2022). HPE-GCN: predicting efficacy of tonic formulae via graph convolutional networks integrating traditionally defined herbal properties. *Methods* 204, 101–109. doi:10.1016/j.ymeth.2022.05.003

Liu, W., Cheng, X., Guo, X., Hu, X., Wei, F., and Ma, S. (2020). Identification of Calculus Bovis and its mixed varieties by ultra-high-performance liquid chromatography/quadrupole time-of-flight mass spectrometry (UHPLC-Q/TOF-MS) combined with the principal component analysis (PCA) method. *J. Pharm. Biomed. Anal.* 179, 112979. doi:10.1016/j.jpba.2019.112979

Liu, Y., Guo, C., and Er, M. J. (2022). Robotic 3-D laser-guided approach for efficient cutting of porcine belly. *IEEE-ASME Trans. Mechatron.* 27 (5), 2963–2972. doi:10.1109/TMECH.2021.3129911

Liu, Y., Tong, K. D., Mao, F., and Yang, J. (2020). Survey of natural products reported by Asian research groups in 2019. *Int. J. Adv. Manuf. Technol.* 107 (3-4), 1101–1120. doi:10.1080/10286020.2020.1844675

Liu, Y., Yang, X., Zhou, C., Wang, Z., Kuang, T., Sun, J., et al. (2022). Unveiling dynamic changes of chemical constituents in raw and processed Fuzi with different steaming time points using desorption electrospray ionization mass spectrometry imaging combined with metabolomics. *Front. Pharmacol.* 13, 842890. doi:10.3389/fphar.2022.842890

Liu, Z. F., Cascioli, V., and Mccarthy, P. W. (2022). A single subject, feasibility study of using a non-contact measurement to "visualize" temperature at body-seat interface. *Sensors* 22 (10), 3941. doi:10.3390/s22103941

Mcloughlin, K. S., Jeong, C. G., Sweitzer, T. D., Minnich, A. J., Tse, M. J., Bennion, B. J., et al. (2021). Machine learning models to predict inhibition of the bile salt export pump. *J. Chem. Inf. Model.* 61 (2), 587–602. doi:10.1021/acs.jcim.0c00950

Mears, L., Stocks, S. M., Albaek, M. O., Sin, G., and Gernaey, K. V. (2017). Mechanistic fermentation models for process design, monitoring, and control. *Trends. Biotechnol.* 35 (10), 914–924. doi:10.1016/j.tibtech.2017.07.002

Ng, K. K. H., Chen, C., Lee, C. K. M., Jiao, J. R., and Yang, Z. (2021). A systematic literature review on intelligent automation: aligning concepts from theory, practice, and future perspectives. *Adv. Eng. Inf.* 47, 101246. doi:10.1016/j.aei.2021.101246

Niquet-Leridon, C., Jacolot, P., Niamba, C. N., Grossin, N., Boulanger, E., and Tessier, F. J. (2015). The rehabilitation of raw and brown butters by the measurement of two of the major Mail lard products, N-epsilon-carboxymethyl-lysine and 5-hydroxymethylfurfural, with validated chromatographic methods. *Food Chem.* 177, 361–368. doi:10.1016/j.foodchem.2015.01.011

Noroozi, R., Sohrabi, M. R., and Davallo, M. (2022). A simple and rapid spectrophotometric method coupled with intelligent approaches for the simultaneous determination of antiepileptic drugs in pharmaceutical formulations, biological, serological, and breast milk samples. *Chemom. Intell. Lab. Syst.* 228, 104633. doi:10.1016/j.chemolab.2022.104633

Örs, E., Schmidt, R., Mighani, M., and Shalaby, M. (2020). "A conceptual framework for AI-based operational digital twin in chemical process engineering," in 2020 IEEE International Conference on Engineering, Technology and Innovation (ICE/ITMC). 2020 IEEE International Conference on Engineering, Technology and Innovation (ICE/ITMC), Cardiff, United Kingdom, 15-17 June 2020, 1–8.

Oztemel, E., and Gursev, S. (2020). Literature review of Industry 4.0 and related technologies. *J. Intell. Manuf.* 31 (1), 127–182. doi:10.1007/s10845-018-1433-8

Palazzo, M., Vollero, A., and Siano, A. (2023). Intelligent packaging in the transition from linear to circular economy: driving research in practice. *J. Clean. Prod.* 388, 135984. doi:10.1016/j.jclepro.2023.135984

Qiao, J., Lu, G., Wu, G., Liu, H., Wang, W., Zhang, T., et al. (2022). Influence of different pretreatments and drying methods on the chemical compositions and bioactivities of Smilacis Glabrae Rhizoma. *Chin. Med.* 17 (1), 54. doi:10.1186/s13020-022-00614-7

Qiao, S., Duan, W., Yu, J., Zheng, Y., Yan, D., Jin, F., et al. (2021). Fabrication of biomolecule–covalent-organic-framework composites as responsive platforms for smart regulation of fermentation application. *ACS Appl. Mat. Interfaces* 13 (27), 32058–32066. doi:10.1021/acsami.1c02120

Qin, K., Cao, G., Jin, J., Li, W., Liu, X., Cai, H., et al. (2018). Problems and solutions in modern research of traditional Chinese herbal pieces processing technology. *Zhongguo Zhong yao za zhi = Zhongguo zhongyao zazhi = China J. Chin. materia medica* 43 (18), 3795–3800. doi:10.19540/j.cnki.cjcmm.20180702.008

Qiu, S., Tu, Y., Huang, D., Dong, Z., Huang, M., Cheng, J., et al. (2021). Selection of appropriate post-harvest processing methods based on the metabolomics analysis of Salvia miltiorrhiza Bunge. *Food Res. Int.* 144, 110366. doi:10.1016/j.foodres.2021.110366

Qiu, T., Yang, Y., Sun, H., Hu, T., Wang, X., Wang, Y., et al. (2021). Rapid discrimination and quantification of kudzu root with its adulterant part using FT-NIR and a machine learning algorithm. *Vib. Spectrosc.* 116, 103289. doi:10.1016/j.vibspec.2021.103289

Qiu, Z. D., Chen, J. L., Zeng, W., Ma, Y., Chen, T., Tang, J. F., et al. (2020). Real-time toxicity prediction of Aconitum stewing system using extractive electrospray ionization mass spectrometry. *Acta Pharm. Sin. B* 10 (5), 903–912. doi:10.1016/j.apsb.2019.08.012

Sasikumar, R., Vivek, K., and Deka, S. C. (2019). Sensory evaluation of ultrasound assisted microwave treated fruit (Haematocarpus validus) juice through fuzzy logic approach. *Int. Food Res. J.* 26 (4), 1229–1236.

Shen, Y., Yin, Y. X., Zhao, C. J., Li, B., Wang, J., Li, G. L., et al. (2019). Image recognition method based on an improved convolutional neural network to detect impurities in wheat. *IEEE Access* 7, 162206–162218. doi:10.1109/ACCESS.2019.2946589

Shi, H., Cao, G. H., Ma, G. Q., Duan, J. S., Bai, J. M., and Meng, X. Y. (2022). New progress in artificial intelligence algorithm research based on big data processing of IOT systems on intelligent production lines. *Comput. Intell. Neurosci.* 2022, 3283165. doi:10.1155/2022/3283165

Shi, Z. N., Zhai, Y., Zhang, Y. T., and Wei, H. Q. (2022). SNAL: sensitive non-associative learning network configuration for the automatic driving strategy. *Sci. Rep.* 12 (1), 20045. doi:10.1038/s41598-022-24674-9

Singh, K. R., and Chaudhury, S. (2020). Comparative analysis of texture feature extraction techniques for rice grain classification. *IET Image Process* 14 (11), 2532–2540. doi:10.1049/iet-ipr.2019.1055

Skrede, O., De Raedt, S., Kleppe, A., Hveem, T. S., Liestøl, K., Maddison, J., et al. (2020). Deep learning for prediction of colorectal cancer outcome: a discovery and validation study. *Lancet* 395 (10221), 350–360. doi:10.1016/S0140-6736(19)32998-8

Song, Y., Yang, J., Hu, X., Gao, H., Wang, P., Wang, X., et al. (2022). A stepwise strategy integrating metabolomics and pseudotargeted spectrum–effect relationship to elucidate the potential hepatotoxic components in Polygonum multiflorum. *Front. Pharmacol.* 13, 935336. doi:10.3389/fphar.2022.935336

Steinbrener, J., Posch, K., and Leitner, R. (2019). Hyperspectral fruit and vegetable classification using convolutional neural networks. *Comput. Electron. Agric.* 162, 364–372. doi:10.1016/j.compag.2019.04.019

Sun, M., Chang, W., Van Wijk, E., He, M., Van Wijk, R., and Wang, M. (2018). Application of delayed luminescence method on measuring of the processing of Chinese herbal materials. *Chin. Med.* 13 (1), 43. doi:10.1186/s13020-018-0202-0

Trakoontivakorn, G., Tangkanakul, P., and Nakahara, K. (2012). Changes of antioxidant capacity and phenolics in ocimum herbs after various cooking methods. *Jarq - Jpn. Agric. Res. Q.* 46 (4), 347–353. doi:10.6090/jarq.46.347

Uysal, M. P., and Mergen, A. E. (2021). Smart manufacturing in intelligent digital mesh: integration of enterprise architecture and software product line engineering. *J. Ind. Inf. Integr.* 22, 100202. doi:10.1016/j.jii.2021.100202

Vecchietti, D., Nishio, A., Fujita, Y., Yoshida, T., Yanagisawa, T., and Kou, D. (2022). Liquid chromatography coupled with photodiode array and a multivariate curve resolution – alternating least square algorithm for identification and quantification of co-eluting impurities in pharmaceutical analysis. *J. Chromatogr. A* 1678, 463364. doi:10.1016/j.chroma.2022.463364

Velasquez, D., Perez, E., Oregui, X., Artetxe, A., Manteca, J., Mansilla, J. E., et al. (2022). A hybrid machine-learning ensemble for anomaly detection in real-time industry 4.0 systems. *IEEE Access* 10, 72024–72036. doi:10.1109/ACCESS.2022.3188102

Viejo, C. G., and Fuentes, S. (2020). Low-cost methods to assess beer quality using artificial intelligence involving robotics, an electronic nose, and machine learning. *FERMENTATION* 6 (4), 104. doi:10.3390/fermentation6040104

Wang, J., Wu, H., and Chen, Y. (2020). Made in China 2025 and manufacturing strategy decisions with reverse QFD. *Int. J. Prod. Econ.* 224, 107539. doi:10.1016/j.ijpe.2019.107539

Wang, L., Kong, W., Yang, M., Han, J., and Chen, S. (2015). Safety issues and new rapid detection methods in traditional Chinese medicinal materials. *Acta Pharm. Sin. B* 5 (1), 38–46. doi:10.1016/j.apsb.2014.12.005

Wang, M., Hu, W., Zhou, X., Yu, K., Wang, Y., Yang, B., et al. (2023). Ethnopharmacological use, pharmacology, toxicology, phytochemistry, and progress in Chinese crude drug processing of the lateral root of Aconitum carmichaelii Debeaux. (Fuzi): a review. *J. Ethnopharmacol.* 301, 115838. doi:10.1016/j.jep.2022.115838

Wang, X., Wang, Y., Li, Y., Xu, S., Shao, F., Zeng, Y., et al. (2021). Colorimetric determination of Listeria monocytogenes using aptamer and urease dual-labeled magnetic nanoparticles and cucurbit[7]uril-mediated supramolecular assembly of gold nanoparticle. *Zhongguo Zhong yao za zhi = Zhongguo zhongyao zazhi = China J. Chin. materia medica* 46 (1), 41–45. doi:10.1007/s00604-021-05130-3

Wang, Y. D., Ren, X. D., Huang, Y., Mustafa, M., Sun, D. B., Xue, F., et al. (2022). The recognition of different odor using convolutional neural networks extracted from time and temperature features. *IEEE Sens. J.* 22 (16), 16234–16243. doi:10.1109/JSEN.2022.3188464

Wang, Y. Q., Yang, Y. Z., Sun, H. J., Dai, J. P., Zhao, M. X., Teng, C. Z., et al. (2020). Application of a data fusion strategy combined with multivariate statistical analysis for quantification of puerarin in Radix puerariae. *Vib. Spectrosc.* 108, 103057. doi:10.1016/j.vibspec.2020.103057

Wei, Y., Gu, K., and Tan, L. (2022). A positioning method for maize seed laser-cutting slice using linear discriminant analysis based on isometric distance measurement. *Inf. Process. Agric.* 9 (2), 224–232. doi:10.1016/j.inpa.2021.05.002

Wu, L., Yang, Y., Mao, Z., Wu, J., Ren, D., Zhu, B., et al. (2021). Processing and compatibility of Corydalis yanhusuo: phytochemistry, pharmacology, pharmacokinetics, and safety. *Evid.-based Complement. Altern. Med.* 2021, 1271953–1271959. doi:10.1155/2021/1271953

Xia, F., Liu, C., and Wan, J. (2020). Characterization of the cold and hot natures of raw and processed Rehmanniae Radix by integrated metabolomics and network pharmacology. *Phytomedicine* 74, 153071. doi:10.1016/j.phymed.2019.153071

Xin, T., Xu, Z., Jia, J., Leon, C., Hu, S., Lin, Y., et al. (2018). Biomonitoring for traditional herbal medicinal products using DNA metabarcoding and single molecule, real-time sequencing. *Acta Pharm. Sin. B* 8 (3), 488–497. doi:10.1016/j.apsb.2017.10.001

Xu, M., Yang, S. L., Peng, W., Liu, Y. J., Xie, D. S., Li, X. Y., et al. (2015). A novel method for the discrimination of semen arecae and its processed products by using computer vision, electronic nose, and electronic tongue. *Evid.-based Complement. Altern. Med.* 2015, 753942. doi:10.1155/2015/753942

Xu, X. D., Sun, C. X., Liu, B., Zhou, Q. L., Xu, P., Liu, M. Y., et al. (2022). Flesh flavor of red swamp crayfish (*Procambarus clarkii* Girard, 1852) processing by GS-IMS and electronic tongue is changed by dietary animal and plant protein. *Food Chem.* 373, 131453. doi:10.1016/j.foodchem.2021.131453

Yang, B., Yang, L., Yang, J., Lu, G., Feng, L., and Jia, X. (2022). Twenty years in the 21st century: temporal and spatial evolution of Chinese medicinal processing equipment. *Zhongguo Zhong yao za zhi = Zhongguo zhongyao zazhi = China J. Chin. materia medica* 47 (5), 1177–1183. doi:10.19540/j.cnki.cjcmm.20210813.601

Yang, M., Zhong, L. Y., Xue, X., Liu, R. H., and Gong, Q. F. (2016). Inheritance and innovation of traditional processing technology of Chinese medicine. *China J. Chin. Materia Medica* 41 (03), 357–361. doi:10.4268/cjcmm20160301

Yin, T. J., Yang, Z. W., Miao, N., Zhang, X., Li, Q. S., Wang, Z. Q., et al. (2021). Development of a remote electronic tongue system combined with the VMD-HT feature extraction method for honey botanical origin authentication. *Measurement* 171, 108555. doi:10.1016/j.measurement.2020.108555

Yu, Z., Yang, K., Hu, Z., Peng, B., Gu, F., Yang, L., et al. (2023). Parameter optimization and simulation analysis of floating root cutting mechanism for garlic harvester. *Comput. Electron. Agric.* 204, 107521. doi:10.1016/j.compag.2022.107521

Zhai, C., Zhao, J., Chittiboyina, A. G., Meng, Y., Wang, M., and Khan, I. A. (2020). Newly generated atractylon derivatives in processed rhizomes of atractylodes macrocephala koidz. *Molecules* 25 (24), 5904. doi:10.3390/molecules25245904

Zhang, P., Xu, Y. D., Qu, F. N., Zhou, P., Zhang, J., Bi, X. Y., et al. (2023). Rapid quality evaluation of four kinds of Polygoni Multiflori Radix Praeparata by electronic eye combined with chemometrics. *Phytochem. Anal.* 34, 301–316. doi:10.1002/pca.3208

Zhang, S. F. (2020). Influence of different cooking methods on the maillard reactions of marine products. *J. Coast. Res.* 110, 197–200. doi:10.2112/JCR-SI110-047.1

Zheng, Y. H., Wang, Y., Zhang, Q., Liu, W. H., Li, K., Xia, M. Y., et al. (2022). A novel method for quality evaluation of gardeniae fructus praeparatus during heat processing based on sensory characteristics and chemical compositions. *Molecules* 27 (11), 3369. doi:10.3390/molecules27113369

Zhong, L., Cui, M., Yang, M., and Gong, Q. (2019). Modern researches on effect of processing of Chinese herb medicine on Chinese medical properties. *Zhongguo Zhong yao za zhi = Zhongguo zhongyao zazhi = China J. Chin. materia medica* 44 (23), 5109–5113. doi:10.19540/j.cnki.cjcmm.20190916.301

Zhu, J., Zhong, L. Y., Yang, M., Gong, Q. F., Yu, H., Huang, Y., et al. (2022). Analysis of current status of traditional Chinese medicine processing technology inheritance and thinking of innovative development. *China Joumal Traditional Chin. Med. Pharm.* 37 (09), 4919–4923.

Zunino, C., Valenzano, A., Obermaisser, R., and Petersen, S. (2020). Factory communications at the dawn of the fourth industrial revolution. *Comput. Stand. Interfaces*. 71, 103433. doi:10.1016/j.csi.2020.103433

Zuo, Y. M., Yang, J., Li, C., Deng, X. H., Zhang, S. S., and Wu, Q. (2020). Near-infrared spectroscopy as a process analytical technology tool for monitoring the steaming process of Gastrodiae rhizoma with multiparameters and chemometrics. *J. Anal. Methods Chem.* 2020, 8847277. doi:10.1155/2020/8847277

frontiers | Frontiers in Pharmacology

TYPE Original Research
PUBLISHED 31 August 2023
DOI 10.3389/fphar.2023.1217599

OPEN ACCESS

EDITED BY
Uraiwan Panich,
Mahidol University, Thailand

REVIEWED BY
Vikram Kumar,
Amity University Jaipur, India
Delin Zhang,
Chengdu University of Traditional Chinese Medicine, China
Liang Peng,
Shaanxi University of Chinese Medicine, China

*CORRESPONDENCE
Faming Wu,
wufaming@zmu.edu.cn
Jian Xie,
xiejian@zmu.edu.cn

†These authors have contributed equally to this work

RECEIVED 05 May 2023
ACCEPTED 15 August 2023
PUBLISHED 31 August 2023

CITATION
Liu F, Peng J, Feng Y, Ma Y, Ren Y, Sun P, Zhao Y, Liu S, Wu F and Xie J (2023), An ethnobotanical study on the medicinal herb practices of the gelao ethnic minority in North Guizhou, China: an exploration of traditional knowledge. *Front. Pharmacol.* 14:1217599. doi: 10.3389/fphar.2023.1217599

An ethnobotanical study on the medicinal herb practices of the gelao ethnic minority in North Guizhou, China: an exploration of traditional knowledge

Fusong Liu[1†], Jie Peng[1†], Yi Feng[1], Yuhan Ma[1], Yan Ren[2], Pei Sun[3], Yongxia Zhao[1], Sha Liu[1], Faming Wu[1,4*] and Jian Xie[1,4*]

[1]School of Pharmacy, Zunyi Medical University, Zunyi, China, [2]School of Pharmacy, Southwest Minzu University, Chengdu, China, [3]Industrial Crop Research Institute, Sichuan Academy of Agriculture Sciences, Chengdu, China, [4]Guizhou Medical and Health Industry Research Institute, Zunyi Medical University, Zunyi, China

Introduction: The Gelao ethnic minority of northern Guizhou, China have long possessed extensive traditional knowledge of medicinal herbs. This ethnobotanical study aimed to document and evaluate wild plants used medicinally by the Gelao people, providing insights into their traditional medicine and knowledge systems.

Methods: Field research was conducted in Gelao communities of Daozhen, Wuchuan and Zheng'an counties using interviews, surveys and participatory rural appraisal.

Results: Quantitative ethnobotanical indices were utilized to assess the cultural significance of 187 herbs identified. The herbs belonged to 84 families, primarily Compositae, and were mostly roots, rhizomes and whole plants. They were used to treat digestive, respiratory and inflammatory disorders, gynecological diseases, bites and other conditions, mainly through decoctions. 25 highly significant herbs (national plant cultural significance index > 1000) were known to protect health. Some function as food and are considered safe. However, the study revealed issues including a declining number of knowledgeable elders and inadequate hygiene controls.

Conclusion: Our findings demonstrate the Gelao's extensive medicinal plant knowledge and highlight the need for further ethnobotanical research to document and preserve this culturally important tradition. The identified herbs also represent an alternative medicinal resource with potential modern applications pending further investigation of their pharmacology and sustainable use. Overall, this study provides valuable insights into Gelao ethnobotanical knowledge and the potential of indigenous medicine for modern healthcare.

KEYWORDS

gelao ethnic minority, traditional medicinal herbs, ethnobotany, wild plants, NCSI

Abbreviations: PRA, participatory rural appraisal; 5W + 1H, Why What Where When Who How; FQI, frequency of quotation index; AI, availability index; FUI, frequency of utilization index; PUI, parts used index; MFI, multifunctional use index; CEI, curative effect index; DSI, drug safety index; NCSI, national plant cultural significance index.

Introduction

Throughout history, the human species has harnessed the bounty of natural resources to combat diseases, leading to the evolution of diverse traditional medicinal cultures, each with distinct regional characteristics (Jia et al., 2015). However, the swift advancement of modern medicine has precipitated the decline, and in some cases, the extinction of these traditional medicinal cultures, thereby dealing a significant blow to our collective human heritage (Li et al., 2015; Yang et al., 2021). China is a country with one of the best-preserved traditional medicinal cultures, with traditional Chinese medicine being fully inherited and developed to play an unimaginable role in disease prevention, treatment, and daily healthcare (Wang, 2013). In addition, other traditional medicinal cultures, such as Tibetan medicine, Mongolian medicine, Uyghur medicine, Dai medicine, and Miao medicine, have also been well-preserved and developed (Sun et al., 2020). Almost every ethnic minority in China boasts a unique medicinal culture, contributing significantly to their ethnic inheritance (Kang et al., 2016; Li et al., 2020; Zi and Zeng, 2023).

Guizhou, a province populated by a tapestry of ethnic groups, is home to the Gelao ethnic minority, an indigenous community with a rich and unique cultural heritage. Over 90% of the global Gelao population resides in the Zunyi region of northern Guizhou, notably in Wuchuan County and Daozhen County—Gelao autonomous counties where approximately half of the inhabitants are of Gelao descent. The Gelao people, steeped in history, have crafted a vibrant and unique culture, with traditional Gelao medicine serving as a key pillar. This ancient and enigmatic community has a wealth of knowledge and practices concerning medicinal plants, utilizing at least 61 species known for their edibility and medicinal properties. The book "Gelao Medicine" records 200 types of therapeutic agents commonly harnessed by the Gelao community, including 174 plant-based, 23 animal-based, and 3 mineral-based remedies. The roots of Gelao traditional medicine stretch back to at least 2200 years ago, the Han dynasty era, as evidenced by 63 of their commonly used remedies being recorded in the ancient Chinese pharmacopoeia, "Shennong Bencaojing" (The Classic of Herbal Medicine). While it is impossible to ascertain who first utilized these substances medicinally, Gelao medicine exhibits distinct characteristics when compared to traditional Chinese medicine and other ethnic traditional medicines, especially in the application of the same remedy for different ailments, and the combination and compatibility of remedies. The Gelao traditional medicine philosophy is grounded in the concept of yin-yang balance, which posits the existence of a life force called 'qi' flowing through invisible meridians in the body. Disruptions in the flow and distribution of qi are believed to result in disease, and treatments aim to restore the balance and harmony of qi through various methods. The therapeutic repertoire of Gelao traditional medicine is diverse, encompassing external therapies like acupuncture, moxibustion, cupping, and massage, and internal therapies involving decoctions, wines, powders, and pills made from various plant or animal materials.

However, the Gelao people have not formed a systematic script, and their traditional culture has primarily been preserved through oral transmission, inscriptions, and documents, which continue to be passed down to this day. Unfortunately, the traditional Gelao medicine culture is rapidly disappearing due to the influence of modern medicine, traditional Chinese medicine, as well as factors such as ethnic Hanization, relocation, and poverty alleviation. In terms of ethnic ethnobotanical research in Guizhou, most studies have focused on investigation and classification of edible, tea-like, and dyeing ethnic plants, such as He's research on the edible plants of the Dong ethnic group (He et al., 2019), Hong's research on the Shui ethnic group (Hong et al., 2015a), and Hu's research on the Baiku Yao ethnic group (Hu et al., 2022). These studies have found that different ethnic groups have rich and diverse plants with unique cultural characteristics, providing valuable information for the research and development of ethnic plants in Guizhou. Our previous study also found that the Gelao people have rich traditional knowledge of wild edible plants (Xie et al., 2022). There is a lack of research focusing on traditional medicinal knowledge of ethnic herbs in Guizhou, particularly concerning traditional Gelao medicinal herbs. This study aims to address this gap.

Therefore, this study employed ethnobotanical research methods (Wang, 2017) to investigate the traditional medicinal herbs of the Gelao ethnic minority. Our objective is to understand their traditional knowledge of herb usage in specific regions and groups, the relationship between their villages and natural environments, and the use of traditional medicinal herbs in local community health practices. This study represents the first comprehensive ethnobotanical investigation and documentation of the traditional medicinal plants used by the Gelao ethnic minority in northern Guizhou, China, filling a significant research gap in this field. We utilized various quantitative and qualitative methods to conduct in-depth analysis of the diversity, selection, conservation value, and other aspects of the Gelao traditional medicinal plants, revealing the characteristics and patterns of the Gelao traditional medicinal plant knowledge. Furthermore, we combined the historical, cultural, and ecological background of the Gelao ethnic group, and explored the formation, development, and changes of the Gelao traditional medicinal plant knowledge, providing a new perspective for understanding and protecting the Gelao ethnobotany and ethnic culture. This study will also offer appropriate suggestions for the sustainable use of plant resources for traditional Gelao medicine.

Materials and methods

Study area

The present study was conducted in the northern part of Guizhou province, specifically in Daozhen, Wuchuan, and Zheng'an counties. These counties are situated between 28°9′-29°13′N and 107°4′-108°13′E, encompassing the Dalou Mountains, southeastern foothills, and the branch and sub-branches of the Dalou Mountain Range, as well as the upper reaches of the Furong River. The region experiences a subtropical humid monsoon climate and a mid-subtropical humid monsoon climate, with an average annual temperature of 8°C–16.14°C and an annual precipitation of 800–1400 mm (Figure 1) (Yang et al., 2002). The local economy primarily relies on agriculture, with crops such as rice, corn, vegetables, and tea oil being the main agricultural

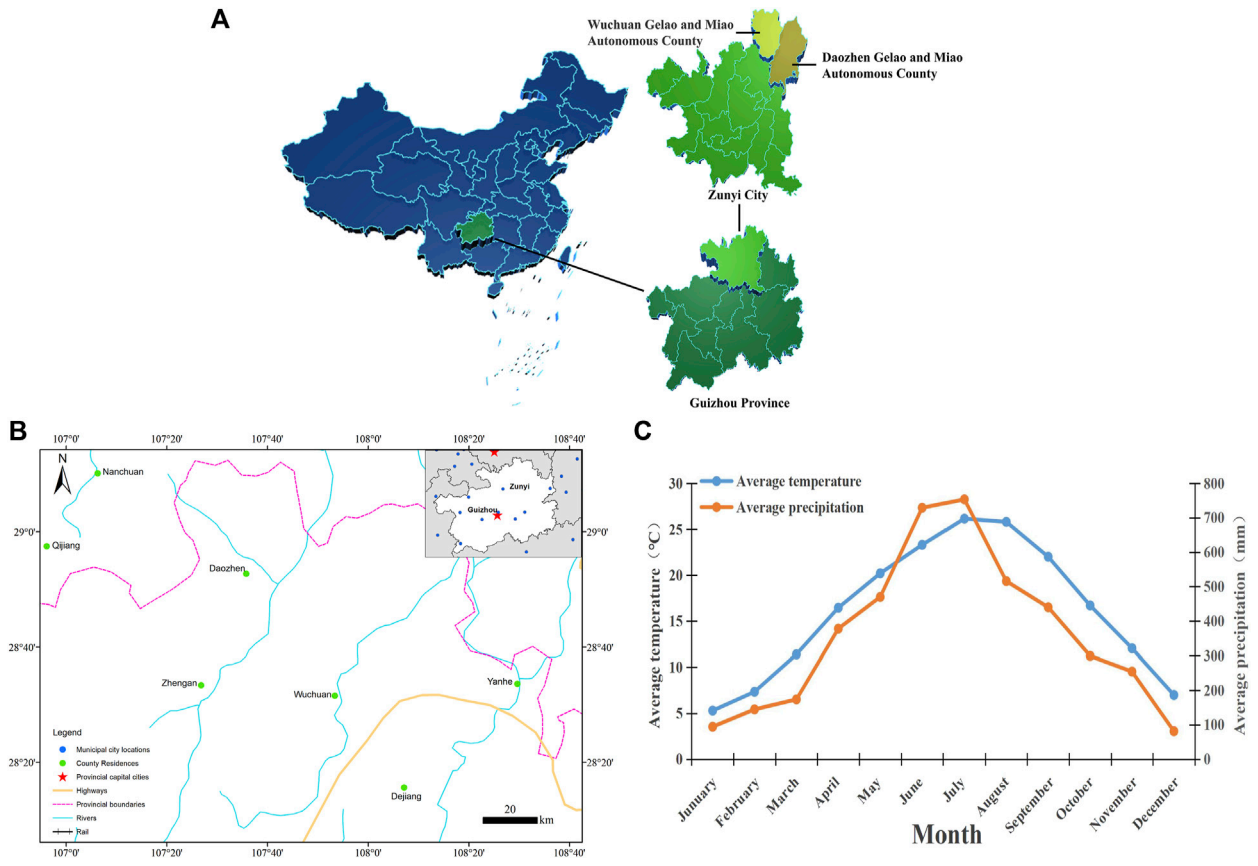

FIGURE 1
Survey area. **(A)** Daozhen County, Wuchuan County and Zheng'an County belong to a minority autonomous county in the northeastern mountainous area of Guizhou Province. **(B)** The traffic situation in the study area. **(C)** The annual average temperature and precipitation.

products. Additionally, tourism plays a significant role in the region, attracting a large number of visitors.

The study area is a diverse settlement comprising multiple ethnic groups, including the Gelao, Miao, and Han ethnic groups. Daozhen and Wuchuan serve as the birthplace and main settlement area of the Gelao people, with a population of 310,000 (Xiao et al., 2022). The Gelao people have created various spiritual and cultural heritages throughout their historical practice and passed them down from generation to generation, forming the unique intangible cultural heritage of the Gelao people. The "Nuo" culture represents a typical aspect of their culture, originating from the totem worship of primitive society and belonging to the category of shamanism culture. The ancestors of the Gelao people held primitive religious beliefs that "all things have spirits" and developed shamanic activities that revolved around daily life. This gave rise to figures such as the "Duan Gong" and "witch," who served as intermediaries between humans and gods, driving away evil forces and protecting human beings. Additionally, the Gelao people celebrate various traditional festivals that showcase their unique characteristics. These include the Mountain Worship Festival, the New Rice Festival, and the Cattle Worship Festival. The Mountain Worship Festival takes place on the third day of the third lunar month each year, during which people worship mountains or trees. The New Rice Festival, held in July or August depending on the maturity of early rice, commemorates the contributions of ancestors in opening up new farmland and celebrates the upcoming harvest. The traditional Cattle Worship Festival, celebrated on the first day of October in the lunar calendar, originated from the Gelao people's domestication of wild buffaloes, which eventually became domestic cattle, and their subsequent worship of these animals (Shang, 2017). These traditional cultures and festivals highlight the Gelao people's traditional way of life and unique cultural characteristics.

Ethnobotanical information collection

During the survey, we employed various methods to collect ethnobotanical information. Key informant interviews, semi-structured interviews, and participatory observation were utilized (Cheng et al., 2020), with interviews based on the "5W+1H" framework, which includes questions about who, what, where, when, why, and how (Pei and Long, 1998).

Key informant interview is a qualitative research method used to collect traditional knowledge from local residents who possess expertise and experience, such as barefoot doctors and professional herbalists. In this study, we conducted in-depth interviews with representative individuals from three generations of the Gelao ethnic group, including elders with herbal knowledge, middle-aged people, and young individuals with some experience in

FIGURE 2
Ethnobotanical investigation of Gelao Nationality. **(A–C)** Surveys at the local herbal shop. **(D)** A doctor of Gelao nationality is diagnosing the patient. **(E, F)** Surveys in local temporary markets. **(G, H)** Collect medicinal specimens under the guidance of local people. **(I)** Making medicinal specimens.

herbal use. We collected information on medicinal plants and recorded, organized, and analyzed the traditional knowledge of herbal medicine used by the Gelao people. This included information such as local names, medicinal parts, processing methods, efficacy, safety, and other basic details.

Semi-structured interviews, on the other hand, involve a predetermined list of questions to gather qualitative data. This approach can provide more specific and detailed information (Supplementary Table S1). We conducted surveys on herbal medicine in herbal shops and temporary markets in the local area. Temporary markets are organized by local residents every 5 days, with different towns staggering their market days. For example, town A holds markets on the first, sixth, 11th, 16th, 21st, and 26th days of each month, while town B holds markets on the second, seventh, 12th, 17th, 22nd, and 27th days of each month. These temporary markets effectively bring together local herbal doctors and Gelao residents who purchase herbs. To gather a large amount of information in a limited time, we distributed survey documents (Figures 2A–F).

Participatory Rural Appraisal (PRA) is a widely used method in ethnobotanical research, in which researchers and local experts with abundant knowledge of local plants, such as doctors or farmers, investigate the overall situation of medicinal plants and related issues to explore and solve problems. We learned how Gelao people identify and distinguish medicinal plants from local herbal doctors or farmers, and we acquired knowledge about the methods of collecting, processing, and preserving herbs. With the guidance of these experts, we collected local herbs, made herbal specimens, and recorded information such as the growth environment, collection location, and time of the herbs (Figures 2G,H). Combining literature and professional knowledge, we classified and identified the herbs, determined their plant sources,

recorded their medicinal value, usage, and dosage, and brought plant specimens back to the laboratory for further analysis (Figure 2I).

Ethnobotanical quantitative evaluation method

The national plant cultural significance index (NCSI) was used to quantitatively evaluate the wild medicinal plants in the surveyed area. The evaluation was based on the following formula:

$$NCSI = FQI \times AI \times FUI \times PUI \times MFI \times CEI \times DSI \times 10^{-2}$$

where FQI represents the frequency of quotation index, AI represents the availability index, FUI represents the frequency of utilization index, PUI represents the parts used index, MFI represents the multifunctional use index, CEI represents the curative effect index, and DSI represents the drug safety index (Pieroni, 2000).

The values for each index were established and assigned levels based on the guidelines outlined in "Research Methods in Ethnic Botany" (Wang, 2017). The frequency of quotation index (FQI) refers to the number of individuals who mention a particular plant among all information sources. The availability index (AI) is divided into very common (4.0), common (3.0), ordinary (2.0), and uncommon (1.0). The frequency of utilization index (FUI) is categorized as more than 10 times per year (5.0), 6–10 times per year (4.0), 2–5 times per year (3.0), at least once per year (2.0), once every 2–3 years (1.0), and not used in the past 5 years (0.5). The parts used index (PUI) is classified as whole plant (5.0), aboveground or underground parts (4.0), stems, leaves, flowers, fruits, seeds (3.0), bark, kernels (2.0), special parts, processed products (1.0). The multifunctional use index (MFI) has a base value of 0 and increases by 1 for each additional use, with a score of 1 for only one use and 5 for five uses. The curative effect index (CEI) is divided into excellent (5.0), very good (4.0), good (3.0), fair (2.0), and poor (1.0). The drug safety index (DSI) is categorized as very high (medicinal and edible: 5.0), high (safe and non-toxic: 4.0), moderately high (has some side effects: 3.0), moderate (slightly toxic: 2.0), and low (highly toxic: 1.0).

Specimen identification

During the course of this survey, we identified the plant species by referring to various botanical literature, including the electronic version of the "Flora of China" (http://www.iplant.cn/frps) (Qian, 1963), the "Illustrated Handbook of Flowers in Hengduan Mountains" (Niu and Sun, 2021), and the "Field Identification Handbook of Common Plants in China: Hengshan Volume" (Ma and He, 2016). The identification process involved observing morphological characteristics, leaves, flowers, fruits, and other parts of the plants, and comparing them with relevant botanical literature to determine their species classification. We then prepared herbarium specimens, organized and analyzed all collected information according to the research objectives, and created tables and charts. The relevant specimens collected during the survey have been deposited in the Chinese Medicinal Herbarium at the School of Pharmacy, Zunyi Medical University.

Results

Basic information of informants

The basic information of the 68 informants was statistically analyzed. The results showed that the ages of all informants ranged from 24 to 89 years, with 6 informants under 30 years old, 11 between 30 to 35 years old, 9 between 36 to 45 years old, 13 between 46 to 55 years old, 14 between 56 to 65 years old, and 15 over 65 years old. Of the total informants, 35 were male and 33 were female, resulting in an almost equal gender ratio. Among them, 54 were from the Gelao ethnic group, accounting for 79.41% of the total, while 11 were from the Miao ethnic group and 3 were from the Han ethnic group. The survey results indicated that informants over the age of 50 were more likely to provide effective information, especially as young people below the age of 35 were unable to provide much useful information (Figure 3).

History and cultural background of herbal use among the gelao ethnic group

The Gelao ethnic group, residing primarily in the mountainous areas of northern Guizhou in southern China, possesses a rich cultural heritage and traditional medicinal knowledge, with herbal medicine playing a significant role in their daily lives. Herbal medicine serves as a traditional healing method and is deeply rooted in their cultural practices. Existing literature indicates that the Gelao people have a long history of herbal medicine use, with their knowledge, utilization, and transmission of herbal medicine intertwined within their social fabric (A, 2006). Within the Gelao's traditional medical system, herbal medicine holds paramount importance, believed to treat physical illnesses, regulate health, and even ward off malevolent spirits.

Survey results show that the Gelao people's knowledge of traditional medicine is passed down through oral transmission of experience and practice, resulting in unique regional and familial inheritance characteristics in the use and dissemination of herbal medicine (Wei et al., 2002). The Gelao employ various forms of herbal medicine preparations, including decoctions, tinctures, powders, external applications, fumigants, and more. Specific rules govern the combination and compatibility of different herbal medicines for different ailments (Zhao, 2003). For example, *Taraxacum mongolicum* Hand.-Mazz., *Paris polyphylla* Sm., and *Rostellularia mollissima* (Nees) Nees are widely used herbal medicines among the Gelao, known for their heat-clearing, detoxifying, anti-inflammatory, and analgesic properties. Apart from their medical applications, the Gelao incorporate herbal medicine into various aspects of their daily lives. In food preparation, herbs such as *Jasminum sambac* (L.) Aiton, *Capsicum annuum* L., and *Zingiber officinale* Roscoe are used to add flavor and medicinal value to their cuisine. Adding herbal medicine to soups enhances their medicinal properties. Herbal medicine is also utilized for dye-making (*Rubia cordifolia* L.), spices (*Cinnamomum cassia* (L.) J.Presl), skincare products (*Z. officinale* Roscoe, *Litsea coreana* var. *lanuginosa* (Migo) Yen C.Yang & P.H.Huang).

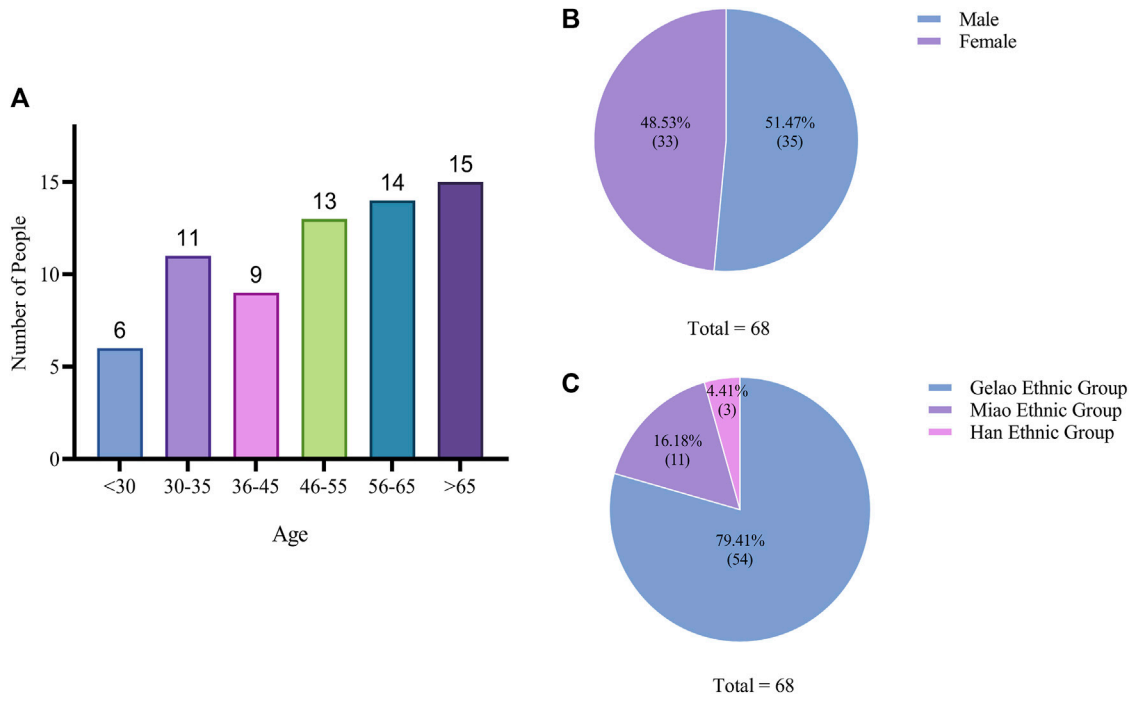

FIGURE 3
Demographic profile of informants.

Furthermore, many of the Gelao's festivals are closely connected to the use of herbal medicine. The application and utilization of herbal medicine among the Gelao people often intertwine with their religious beliefs, which are rooted in shamanism. According to their beliefs, various supernatural forces, including gods, ghosts, and ancestral spirits, exist in nature and can influence people's lives and health. Therefore, during the process of using herbal medicine, the Gelao people often engage in communication and prayers with these deities, seeking blessings and protection. For example, during the annual "Respectful Sparrow Festival", herbs are collected to create sacrificial objects for ancestor worship and to ward off evil spirits (Luo, 2018). Legend has it that a severe epidemic once broke out in a Gelao village, and the ancestors searched everywhere for a cure, but to no avail. Many people fell ill and died. At this critical juncture, a divine eagle brought a divine herb, saving the lives of the entire village. This is the origin of the "Respectful Sparrow Festival", which has been passed down for 300 years (Figure 4). This traditional festival is the only mountain king sacrifice and blessing ceremony in the southwestern region, where Gelao people gather together to drink herbal medicine to dispel poison (Zhou and Zhang, 2006).

Sources of traditional medicinal plants used by the gelao ethnic group

The sources of traditional Gelao medicinal plants are abundant. Our survey identified 142 species of wild medicinal plants and 45 species of cultivated plants, some of which can also be found in the wild (Figure 5A). Although cultivated plants contribute to the availability of medicinal materials, the Gelao primarily rely on collecting wild plants. The collected specimens were mainly found between altitudes of 800–2000 m in areas such as front and backyards, roadsides, nearby mountains, valleys, and farmlands.

In terms of plant taxonomy, we collected a total of 187 species of Gelao medicinal plants from 84 families. The most prominent families were Compositae, Rosaceae, Liliaceae, and Leguminosae, with 17, 10, 9, and 9 species, respectively. Additionally, the Gramineae, Umbelliferae, and Rutaceae families also had a significant presence. The Polygonaceae and Araceae families were relatively special, each with 5 species of medicinal plants (Figure 5B). In reality, there may be more species of Araceae plants, but they were difficult to distinguish during the investigation (Supplementary Table S1).

We also analyzed the botanical characteristics of the medicinal plants we surveyed. Out of the medicinal plants, 111 species were herbaceous, accounting for 59.36% of the total, 49 species were woody, accounting for 26.20% of the total, 21 species were vines, accounting for 11.23% of the total, and 6 species were ferns, algae, and other plants, accounting for 3.21% of the total (Figure 5C).

Approximately One-fourth of these medicinal plants are shade-tolerant, indicating that the selection of medicinal plant types by the Gelao people is influenced by their living environment. Some plants can yield two types of medicinal materials, such as *Reynoutria multiflora* (Thunb.) Moldenke and *Eriobotrya japonica* (Thunb.) Lindl.

Parts used and processing methods of traditional medicinal plants used by the gelao ethnic group

In this study, we collected 187 traditional medicinal plants used by the Gelao ethnic group, categorized based on the plant parts utilized, including Herba (the entire plant or aboveground parts),

FIGURE 4
The Gelao ethnic group celebrates the "Respectful Sparrow Festival". **(A)** A ceremony where they pay homage to their totem. **(B)** During this festival, the Gelao people perform a local exorcism dance. **(C)** People consume herbal decoction at the "Respectful Sparrow Festival". (The pictures come from https://www.baidu.com/).

Radix et Rhizoma (roots, rhizomes, Bulbs, and other underground parts), Fructus (fruits), Folium (leaves), and Flos (flowers). Radix-based medicinal plants were the most prevalent, with 74 species, followed by Herba-based plants (52 species). Some medicinal plants that are specified to use a particular part in the Chinese Pharmacopoeia are traditionally used by the Gelao ethnic group as Herba, such as *Lygodium japonicum* (Thunb.) Sw. There were 17 species of Folium-based medicinal plants, 16 species of Fructus-based ones, 11 species of Flos-based ones, 7 species of Semen-based ones, 4 species of Cortex-based ones, and 8 species of other parts (Figure 6A). Some of these plants have multiple parts that can be used medicinally, such as *Taxus chinensis* (Pilg.) Rehder and *Talinum paniculatum* (Jacq.) Gaertn.

Regarding processing methods, the Gelao ethnic group primarily employed simple sun-drying, which was used for 161 species. After sun-drying, some medicinal plants were cut into sections (mainly for herbal medicinal materials), while others were sliced (mainly for Radix, Caulis, and Tendrillus medicinal materials). The second most common processing method involved using fresh materials directly (36 species). The emphasis on using fresh materials is an important characteristic of the Gelao ethnic group's traditional medicinal plants use. Shade-drying (10 species) was mainly used for certain aromatic medicinal plants, and other methods such as oven-drying and drying after boiling were also utilized (Figure 6B). The choice of processing method varied depending on the plant part used and the desired medicinal properties.

Functions and applications of traditional medicinal plants used by the gelao ethnic group

The traditional medicinal plants used by the Gelao ethnic group serve various functions and applications in treating a range of diseases. Among the 187 recorded plant species, the most common applications were for treating digestive system diseases (28 species) and cold-related diseases (26 species). Additionally, there were 16 species for treating inflammation, 14 species for gynecological diseases, 11 species for snake bites, 10 species for rheumatic diseases, 8 species for urinary system diseases, 5 species for liver diseases, 4 species for tuberculosis, 4 species for cardiovascular diseases, 3 species for hemorrhoids, 3 species for burns, and 1 species for enuresis. Furthermore, there were 12 species for nourishing, 10 species for pain relief, 4 species for detoxification, 3 species for calming, and 3 species for heat relief. There were also 39 species that could not be classified into specific categories (Figure 7A).

During the investigation, it was observed that Gelao medicinal practitioners primarily prescribed treatments for digestive system

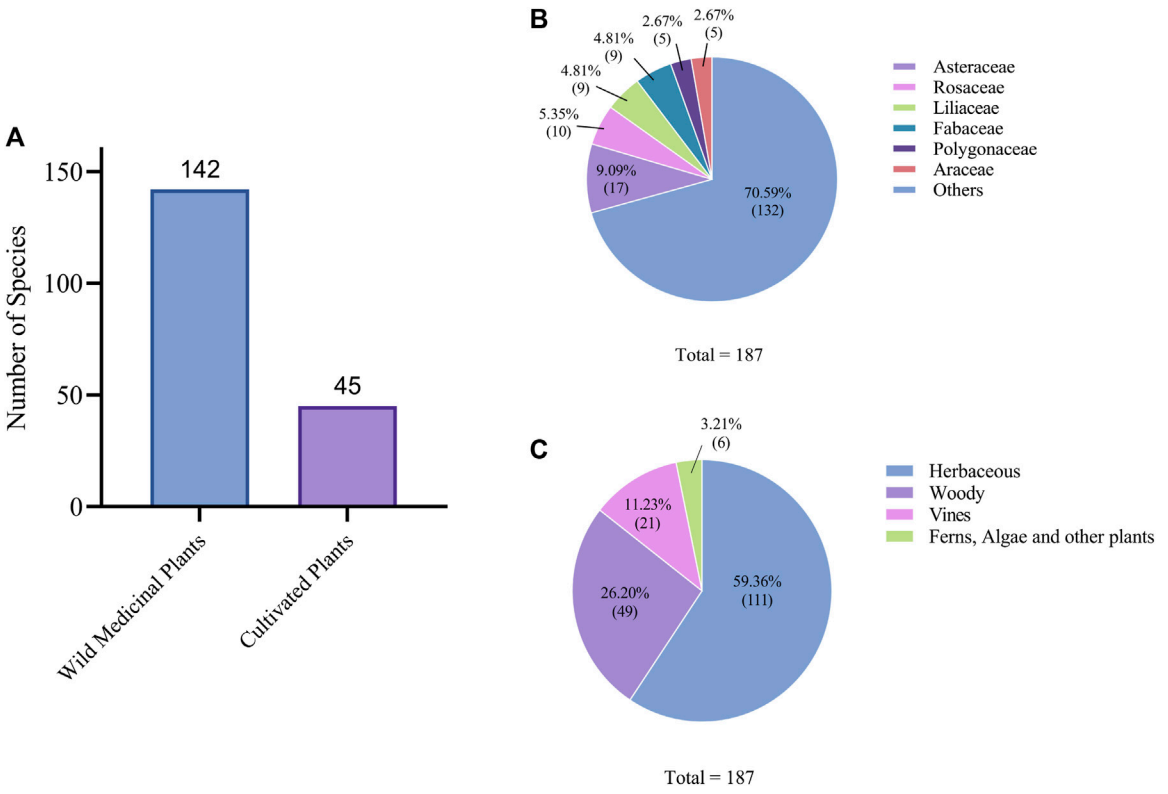

FIGURE 5
Frequency of use of the medicinal plants in the study area. **(A)** Wild medicinal plants and cultivated medicinal plants were found in the survey area. **(B)** Taxonomic diversity of medicinal plants in the study area. **(C)** Life forms of medicinal plants in the study area.

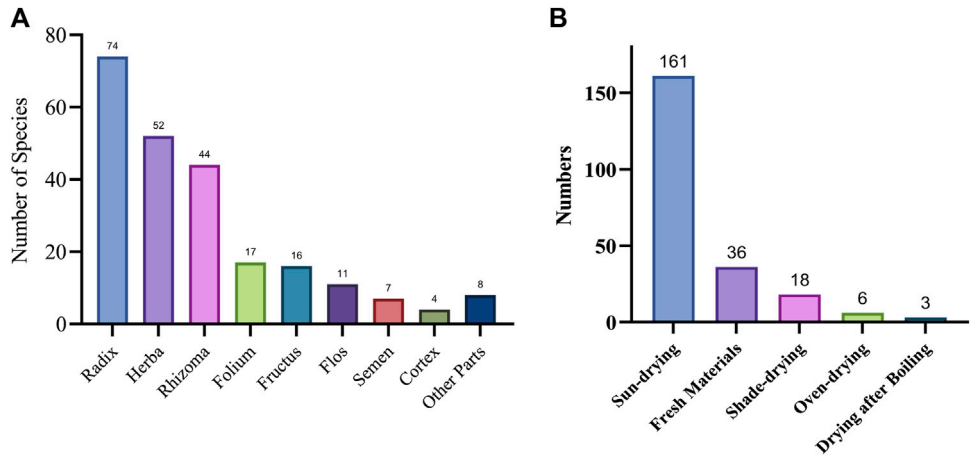

FIGURE 6
Use parts and processing methods of medicinal plants. **(A)** Plant parts used for the treatment of human ailments. **(B)** processing methods of medicinal plants.

diseases, particularly intestinal diseases, and rheumatic diseases, which accounted for approximately half of all prescriptions. However, the use of traditional medicine has declined. Although we found many medicinal plants that were effective for treating snake bites, they are not commonly used today. The reasons for this are twofold. Firstly, after the relocation and poverty alleviation efforts in Guizhou Province, most Gelao people have moved away from their traditional living environment, and such cases have become less frequent. Secondly, in cases of emergency and serious illnesses, people no longer seek treatment from traditional medicinal practitioners, but instead prioritize seeking advanced medical treatment.

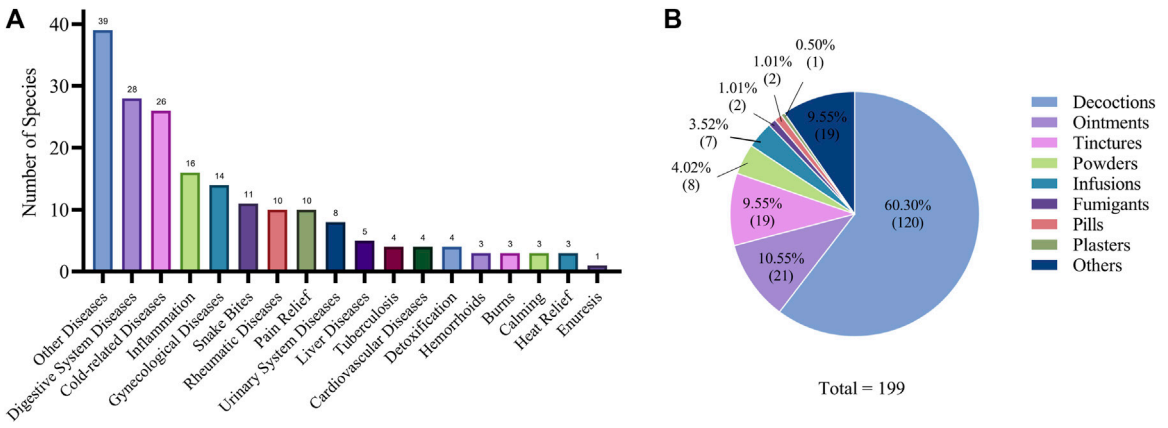

FIGURE 7
Functions and applications of traditional medicinal plants used by the gelao ethnic group. **(A)** diseases treated by Gelao medicinal plants. **(B)** The methods of using traditional medicines of the Gelao ethnic group.

Gelao medicinal practitioners primarily focus on treating chronic diseases, but they still play an irreplaceable role in the region during special periods. For instance, certain Gelao traditional medicinal plants were widely applied in combating COVID-19, especially for treating cough, sore throat, and diarrhea. Plants like *Stemona japonica* (Bl.) Miq, *Reineckea carnea* (Andrews) Kunth, and *Ainsliaea glabra* Hemsl. were used for cough treatment, while the root bark of *Ardisia crenata* Sims and *Ardisia crispa* (Thunb.) A. DC. were employed for treat sore throat treatment. Apricot leaves and Saposhnikovia divaricata were used to treat diarrhea, with local residents believing in their high efficacy.

There are eight types of traditional medicinal formulations made from the 187 medicinal plants used by the Gelao people. Among them, decoctions are the most commonly used form, with 120 different types of decoctions that can be prepared by boiling in water or brewing as tea. Other formulations include ointments (21), tinctures (19), powders (8), infusions (7), fumigants (2), pills (2), plasters (1), and 19 others that could not be classified (Figure 7B).

Functions and applications of traditional medicinal plants used by the gelao ethnic group

We employed quantitative ethnobotanical methods to assess the significance of 187 traditional medicinal plants used by the Gelao ethnic group. The results, comparing the importance index (NCSI) of Gelao traditional medicinal plants, are presented in Supplementary Table S2. Based on the NCSI, we categorized the Gelao traditional medicinal plants into clusters and identified those that are widely utilized, highly valued, and play significant roles in Gelao traditional healthcare. The first cluster (NCSI >1000) consists of 25 traditional medicinal plants, including *Artemisia argyi* H.Lév. & Vaniot, *T. mongolicum* Hand.-Mazz., *Mentha canadensis* L., *Houttuynia cordata* Thunb. and *Prunella laciniata* L., which are commonly encountered in daily life and are well-known among local residents. Moreover, many of them serve as both medicinal and edible resources. The second cluster (1000 > NCSI ≥500) comprises 34 traditional medicinal plants such as *Epimedium brevicornu* Maxim., *A. crenata* Sims, *Portulaca oleracea* L., and *T. paniculatum* (Jacq.) Gaertn. This cluster is important for daily healthcare among local residents and has unique usage methods with high development potential. The third cluster (500 > NCSI ≥100) includes 88 traditional medicinal plants, which exhibit a diverse range of species and are mainly employed to treat common and special diseases in the local area. Although this cluster has relatively lower levels of development, it holds promising prospects for further exploration. The fourth cluster (100 > NCSI) encompasses 40 traditional medicinal plants, which obtain lower importance indices not due to their therapeutic effects or application value, but because they are mainly utilized for treating rare diseases among the Gelao population or possess certain toxic side effects (Figure 8).

Discussion

In rural areas of China, traditional herbal doctors serve as the first line of defense for residents' health, and even in modern times with highly developed medicine, they still play a vital role (Wei et al., 2017). While influenced by traditional Chinese medicine, most ethnic herbal doctors have incorporated their own theories and experiences, gradually blending their unique characteristics with the broader medical practices. This integration has not only preserved their traditional knowledge but also improved their medical skills.

Application characteristics of traditional gelao herbal medicine

The Gelao ethnic group resides in a mountainous region with complex geological structures (Liu, 2007; Zheng, 2007). The area experiences a subtropical humid climate with warm and moist conditions, along with abundant rainfall. However, scarcity of

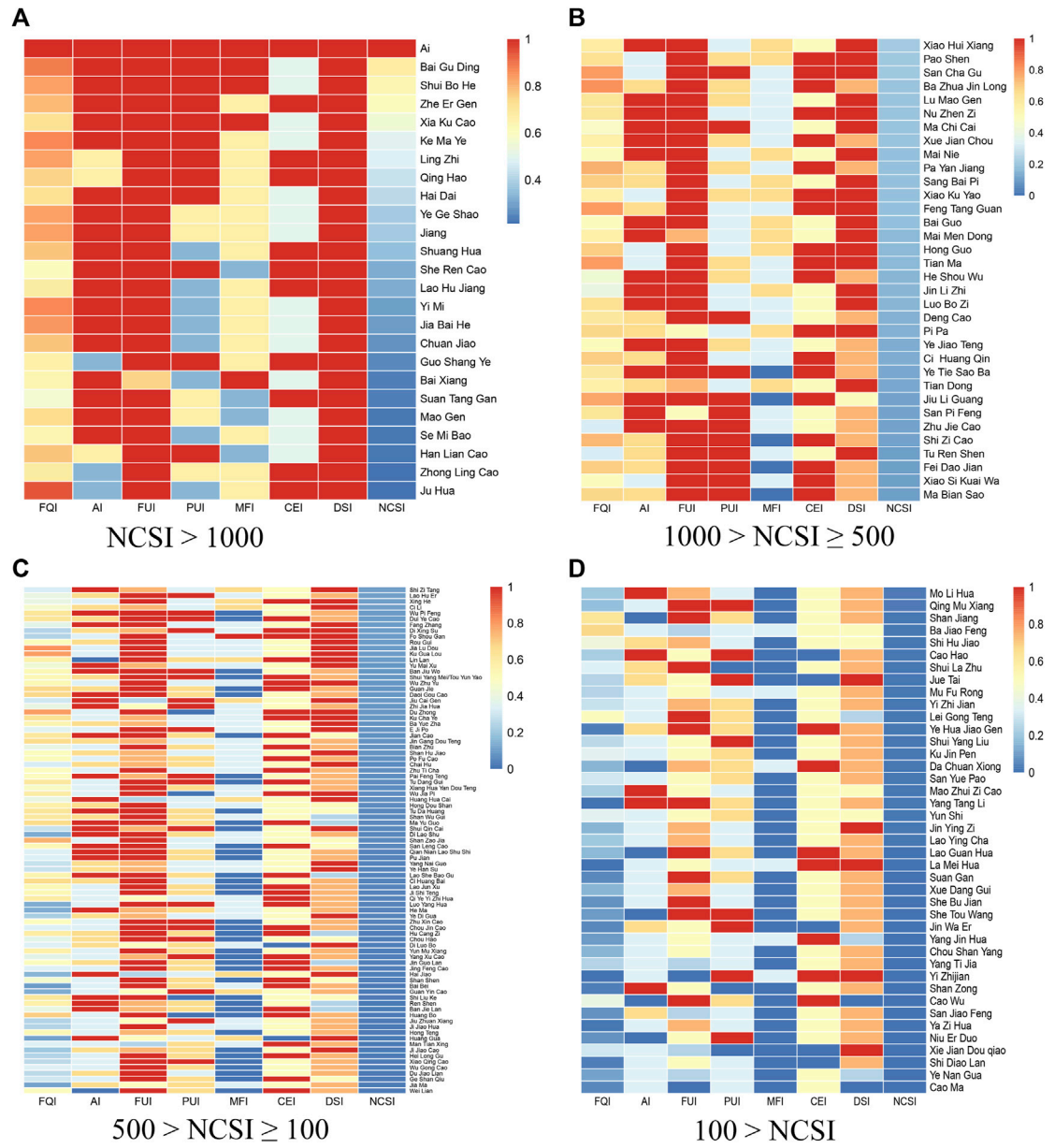

FIGURE 8
Quantitative evaluation of traditional Gelao medicinal plants. **(A)** NCSI >1000. **(B)** 1000 > NCSI ≥500. **(C)** 500 > NCSI ≥100. **(D)** 100 > NCSI.

agricultural resources, outdated traditional farming practices, and various environment, climate, geology, resources, and cultural factors have contributed to the development of distinct applications for preventing and treating common diseases among the Gelao people. Due to the high acidity of the soil in the region, as well as the tendency towards oily, greasy, raw and cold foods, and the humid and rainy climate, gastrointestinal disorders, rheumatism, and traumatic injuries are the most common diseases among the Gelao people.

The Gelao people often use *Pimpinella candolleana* Wight et Arn. To treat various gastrointestinal diseases. They mash the fresh *Pimpinella candolleana* Wight et Arn together with rice water and consume the juice. We have conducted pharmacological experiments to validate its significant therapeutic effects on gastrointestinal disorders. Although the Chinese Pharmacopoeia stipulates that the medicinal part of *A. crenata* Sims is dry root, the Gelao people use fresh or dried root bark to treat various inflammations (such as gingivitis and tonsillitis). To investigate this characteristic usage, we tested the content of the main effective active ingredient, bergenin, in the root and bark of *A. crenata* Sims, and found that it mainly exists in the bark, with a very low content in the wood part (these results will be reported in other articles).

Due to the damp climate and living conditions, the Gelao people have a relatively high incidence of rheumatic diseases, especially among the elderly. To alleviate rheumatic problems, they frequently use spicy condiments like *Capsicum annuum* L. and *Zanthoxylum bungeanum* Maxim., known for their moisture-removing properties.

In terms of medicinal treatment, they use various vine-based herbs and animal-based medicines, either externally as poultices or by preparing wines with snake medicines. Regarding respiratory diseases, due to the high humidity and low temperature in the region during winter, people generally use coal or wood for heating, leading to poor indoor air circulation and making them susceptible to respiratory ailments such as colds, coughs, and asthma. To address these issues, the Gelao people utilize specific herbs like *S. japonica* (Blume) Miq., *R. carnea* (Andrews) Kunth, *Ophiopogon japonicus* (Thunb.) Ker Gawl., and *Adenophora stricta* Miq. To make tea or mix with egg whites to alleviate symptoms. In the case of skin diseases, as people generally live in mountainous areas where mosquito bites are common, they rely on various herbs such as *Senecio scandens* Buch.-Ham. ex D. Don, *Verbena officinalis* L., and *A. argyi* H.Lév. & Vaniot to create herbal baths for treating skin diseases such as eczema, scabies, and acne.

The Gelao people highly value fresh herbal medicine. Traditional Gelao herbal doctors typically collect herbs themselves from the mountains, with only a few herbs purchased from the market. These herbal doctors also cultivate commonly used herbs around their clinics, often within their own courtyards, resulting in up to thirty different species being present. This practice is not solely for convenience but primarily driven by the Gelao herbal doctors' strong sense of preserving precious herbal resources. In fact, the traditional Gelao herbal medicine also includes abundant animal and mineral medicines, such as cinnabar in mineral medicine, and *Passer montanus*, Pheretima, Elephant Leather in animal medicine (Wang, 2017). However, due to various factors, the Gelao people mainly use herbal medicines. Overall, the distinctive applications of these herbal medicines reflect the Gelao people's wisdom and their long-standing tradition of utilizing traditional herbal medicine.

Comparison of traditional medicinal plants of the gelao ethnic group with other ethnic groups

Firstly, the sources of plants are different. Traditional healers often use readily available medicinal plants in their surroundings to treat diseases (Hong et al., 2015b). This phenomenon is influenced by the specific environment in which these groups reside (Liu et al., 2016). For example, the Tibetan people inhabit high-altitude areas, resulting in the utilization of medicinal plants with characteristics specific to plateau regions (Li et al., 2016). Previous research conducted in the multi-ethnic regions of Gansu, Inner Mongolia, and Ningxia in northwest China showed that the significant drought and cold resistance of the traditional medicinal plants utilized in those areas (Jia et al., 2022). In contrast, The Gelao people predominantly inhabit the northern part of Guizhou Province, southwestern China, characterized by abundant rainfall, a mild climate, and diverse topography. This unique geographical environment provides a favorable living environment for plants and serves as a rich source of medicinal resources for Gelao traditional healers (Zeng et al., 2013). However, these medicinal plants obviously have a "southern China" characteristic, and traditional Chinese medicines such as ephedra, astragalus, and dried hay are rarely used by Gelao healers. Furthermore, there is limited overlap between the medicinal plants used by Gelao people and those employed by other ethnic groups, such as the Tibetan, Hui, Mongolian, and Uyghur people residing in the arid regions of northern China (Guo et al., 2022). For example, our survey of traditional medicinal plants in the multi-ethnic areas at the junction of Gansu, Ningxia, and Inner Mongolia revealed minimal similarities with those employed by the Gelao people.

Secondly, the way of inheritance is different. Compared with ethnic groups such as the Han, Tibetan, Mongolian, Zhuang, and Uyghur people, who have established complete medical education systems (Liang et al., 2016), Gelao healers are mainly engaged in agricultural production, with medical treatment as a secondary profession. This "agricultural-medical integration" mobile diagnosis and treatment population greatly limits the inheritance of Gelao medicine. Gelao traditional medicine is mainly passed down through family and apprenticeship, through methods such as "oral transmission and heart-to-heart teaching," "Hands-on guidance," and "exchange of medicinal formulas". However, these practices have hindered the development and formalization of Gelao traditional medicine.

Thirdly, the theoretical system is different. Traditional medicine among ethnic groups such as the Han, Tibetan, Mongolian, Zhuang, and Uyghur people has formed a systematic theoretical system. In contrast, Gelao healers are still in the stage of empirical use of medicine. Therefore, the medicinal plants they use are often based on specific diseases, while they lack understanding of disease etiology and pathogenesis. Although they also emphasize treating the root cause of the disease, they primarily focus on treating specific symptoms, and their treatment of mental illness is closer to witchcraft. On the other hand, Gelao people also emphasize balancing the body's energy. Some Gelao healers believe that most diseases can be treated by regulating the body's energy, and they believe that the medicinal plants they use can provide useful energy to patients. When the body's energy is balanced, the disease will naturally disappear. Similarly, traditional medicine in other regions or ethnic groups in China also emphasizes the balance of the body's "yin" and "yang", and the five elements to achieve therapeutic outcomes (Wang et al., 2022).

Challenges and threats to the use of traditional medicinal plants among the gelao ethnic group

Traditional medicinal plants used by the Gelao ethnic group have demonstrated significant therapeutic effects in certain unique diseases within their local region. However, they also face numerous challenges, including imprecise dosages, unregulated use, and hygiene and safety issues. Our research revealed that traditional Gelao herbalists lack accurate measuring tools when preparing herbal remedies, often relying on subjective estimation. Hygiene issues arise from the rudimentary conditions of their "pharmacies", which frequently result in mold growth on the medicinal plants. Furthermore, the processing of toxic herbs is often insufficiently regulated, posing significant risks to patient safety. Although Gelao herbalists possess extensive knowledge of the properties and side effects of toxic herbs, they often use these remedies externally or prescribe them for long-term consumption with explicit instructions

for preparation. Additionally, most Gelao herbalists have unique formulas and primarily treat two to five specific diseases.

Based on the challenges and limitations of the Gelao traditional medicinal plants. We believe that the Gelao traditional medicinal plant resources are threatened by ecological environmental changes, human destruction, alien invasion, and other factors, resulting in some plant species becoming rare or extinct. The traditional medicinal plant knowledge is affected by cultural inheritance gaps, education deficiencies, market competition, and other factors, resulting in some knowledge being forgotten or lost. The scientific value and social value of the Gelao traditional medicinal plants have not been fully recognized and utilized, resulting in some plants and knowledge being inefficiently or excessively used. The local government has also made some efforts based on this. The government has strengthened the protection and management of the Gelao traditional medicinal plant resources, established some facilities such as nature reserves, botanical gardens, seed banks, etc., implemented some policies such as returning farmland to forest, ecological compensation, green development, etc. It has strengthened the inheritance and popularization of the Gelao traditional medicinal plant knowledge, carried out some activities such as ethnic education, cultural heritage, science popularization, etc., and cultivated some talents such as ethnic pharmacists, ethnic scholars, ethnographers, etc. It has strengthened the research and development of the Gelao traditional medicinal plants, supported some work such as scientific research projects, technology transfer, product innovation, etc., and promoted some industries such as ethnic medicines, ethnic foods, ethnic tourism, etc.

The current status of traditional medicinal knowledge among the gelao ethnic group and the importance of preserving traditional herbal knowledge

Our research on traditional consumption of wild plants by the Gelao ethnic group revealed that their traditional cultural knowledge is gradually being eroded by Han culture and globalized digital culture (Guo, 2018). Traditional medicinal knowledge among the Gelao ethnic group is particularly vulnerable in this regard (Xie et al., 2022). The valuable information provided by our interviewees mostly came from elderly and middle-aged individuals, with the latter representing the newest generation of Gelao herbalists, most of whom are over 45 years old. Younger Gelao herbalists have become almost extinct, and the few remaining young practitioners have typically received systematic training in traditional Chinese medicine and lack the distinct characteristics of traditional Gelao herbalists. They mostly rely on purchased Chinese medicine pills rather than gathering their own herbs. While they have abandoned some of their ancestors' negative practices, they have also lost some of their ethnic characteristics. Additionally, male interviewees were more likely to provide valuable information than females, who provided fewer details about the types of herbs, processing methods, and usage techniques. This may be related to the traditional Gelao custom of passing herbal knowledge down to males but not to females.

The unique characteristics of traditional Gelao medicine are being gradually absorbed by Chinese and modern medicine cultures, with much of the mystical knowledge of traditional Gelao medicine now relegated to folklore. This cultural erosion is accelerating, and many traditional cultural practices now only exist in museums and ancient texts. Without proper documentation, the accumulated knowledge of generations of traditional medicine practitioners will be lost forever (Mohammed et al., 2019; Xiong et al., 2020; Shu et al., 2022).

Limitation and prospect of this study

This study also has some limitations. It only involves the ethnobotanical aspect of the Gelao traditional medicinal plants, without involving the ethnopharmacological aspect, that is, it did not conduct chemical and pharmacological analysis of these plants to verify their active ingredients and mechanisms of action. The study only relies on the subjective reports of the Gelao people on plant use and knowledge, and the number of informants is also small. Since this study only focuses on the use of medicinal herbs by the Gelao ethnic group, it is biased towards the field of ethnobotany. We will also conduct more in-depth chemical and pharmacological studies in our future research, in order to provide valuable clues for further development and utilization of new and valuable Gelao medicines, as well as more scientific support for Gelao traditional medicine.

Conclusion

The Gelao community have accumulated wealth of experience in utilizing herbal medicine to combat diseases. We have collected important information on 187 medicinal plants, including their botanical names, sources, processing methods, primary therapeutic uses, and administration techniques. However, we have also observed a rapid decline in this valuable knowledge. Our mission is to document, systematize, and safeguard these clinically validated medicinal practices. This undertaking opens up avenues for the preservation of traditional herbal medicine knowledge among the Gelao people while offering firsthand insights for the development and utilization of herbal remedies with notable therapeutic effects against specific ailments. Nevertheless, it is important to acknowledge the potential bias in the information we have obtained, as well as the presence of unverifiable or inaccurate data from our sources, which may introduce certain inaccuracies into our analysis.

Furthermore, the information we have gathered is derived from the medication experience of local residents, and further research is necessary to verify the reliability, safety, and efficacy of these medicines in clinical applications. In the future, we plan to conduct comprehensive and systematic investigations into Gelao traditional medicine and culture, establish appropriate protective measures, and develop high-value pharmaceutical products.

Data availability statement

The original contributions presented in the study are included in the article/Supplementary Material, further inquiries can be directed to the corresponding authors.

Ethics statement

Ethical review and approval was not required for the study on human participants in accordance with the local legislation and institutional requirements. Written informed consent from the patients/participants was not required to participate in this study in accordance with the national legislation and the institutional requirements.

Author contributions

Conceptualization, JX and FW; Data curation, FL and JP; Formal analysis, YF, YM, YR, PS, YZ and SL; Methodology, JX; Resources, JX; Software, JX; Supervision, FW and JX; Validation, FL; Writing–original draft, FuL; Writing–review and editing, JX; project administration, FW; funding acquisition, JX and FW. All authors contributed to the article and approved the submitted version.

Funding

This research was funded by the National Natural Science Foundation of China (82060687); Doctor science foundation of Zunyi Medical University (F-941); Science and Technology Fund of Guizhou Provincial Health Commission (gzwkj 2021-539); Innovation and Entrepreneurship Training program for Students of Zunyi Medical University (ZYDC2022040, ZYDC2021028, ZYDC2021134, ZYDC2021146, ZYDC2021144, ZYDC202202210).

Acknowledgments

All the authors are grateful for the help of the School of Pharmacy and the platform of the Department of Medical Genetics of Zunyi Medical University.

Conflict of interest

The authors declare that the research was conducted in the absence of any commercial or financial relationships that could be construed as a potential conflict of interest.

Publisher's note

Supplementary material

The Supplementary Material for this article can be found online at: https://www.frontiersin.org/articles/10.3389/fphar.2023.1217599/full#supplementary-material

References

Authors AnonymousTu, A. (2006). *Traditional medicine of the gelao ethnic group*. Guizhou Ethnic Stu.

Cheng, Z., Luo, B. S., Fang, Q., and Long, C. L. (2020). Ethnobotanical study on plants used for traditional beekeeping by Dulong people in Yunnan, China. *J. Ethnobiol. Ethnomed* 16, 61. doi:10.1186/s13002-020-00414-z

Guo, C. A., Ding, X. Y., Hu, H. B., Zhang, Y., Yang, H. Z., and Wang, Y. H. (2022). An ethnobotanical study on wild plants used by Tibetan people in Gyirong Valley, Tibet, China. *J. Ethnobiol. Ethnomed* 18, 67. doi:10.1186/s13002-022-00565-1

Guo, J. H. (2018). Study on the protection and lnheritance of national language and culture under lnternational cultural competition. *Guizhou Ethn. Stu* 39, 215–218. doi:10.13965/j.cnki.gzmzyj10026959.2018.11.047

He, J. W., Zhang, R. F., Lei, Q. Y., Chen, G. X., Li, K. G., Ahmed, S., et al. (2019). Diversity, knowledge, and valuation of plants used as fermentation starters for traditional glutinous rice wine by Dong communities in Southeast Guizhou, China. *J. Ethnobiol. Ethnomed* 15, 20. doi:10.1186/s13002-019-0299-y

Hong, L. Y., Guo, Z. Y., Huang, K. H., Wei, S. J., Liu, B., Meng, S. W., et al. (2015a). Ethnobotanical study on medicinal plants used by Maonan people in China. *J. Ethnobiol. Ethnomed* 11, 32. doi:10.1186/s13002-015-0019-1

Hong, L. Y., Zhuo, J. X., Lei, Q. Y., Zhou, J. G., Ahmed, S., Wang, C. Y., et al. (2015b). Ethnobotany of wild plants used for starting fermented beverages in Shui communities of southwest China. *J. Ethnobiol. Ethnomed* 11, 42. doi:10.1186/s13002-015-0028-0

Hu, R. C., Li, T. T., Qin, Y. R., Liu, Y. J., and Huang, Y. F. (2022). Ethnobotanical study on plants used to dye traditional costumes by the Baiku Yao nationality of China. *J. Ethnobiol. Ethnomed* 18, 2. doi:10.1186/s13002-021-00497-2

Jia, M. R., Zhang, Y., Yan, Z. Y., Ma, C. Y., Lai, X. R., and Wang, Z. (2015). Species and use of current Chinese minority medicine. *Mod. Tradi Chin. Med. Mater. Med-World Sci. Technol.* 17, 1546–1550. doi:10.11842/wst.2015.07.035

Jia, X. H., Zhao, Y. X., Zhu, Y. Y., Zeng, X., Liang, X. H., Xie, J., et al. (2022). Ethnobotany of wild edible plants in multiethnic areas of the Gansu–Ningxia–Inner Mongolia junction zone. *J. Ethnobiol. Ethnomed* 18, 53. doi:10.1186/s13002-022-00549-1

Kang, L., Zhu, H., Dai, Z. H., Li, L., and Da, F. F. (2016). Medicine culture of minority nationality in guangxi. *Chin. Arch. Tradi Chin. Med.* 34, 1434–1437. doi:10.13193/j.issn.1673-7717.2016.06.044

Li, F., Zhuo, J., Liu, B., Jarvis, D., and Long, C. (2015). Ethnobotanical study on wild plants used by Lhoba people in Milin County, Tibet. *J. Ethnobiol. Ethnomed* 11, 23. doi:10.1186/s13002-015-0009-3

Li, X. H., Zhao, C. Y., Liu, Y., Wan, L., Jia, M. R., Xie, C. X., et al. (2016). Research progress on resources and quality evaluation of Tibetan medicine in Qinghai-Tibet Plateau. *China J. Chin. Mater. Med.* 41, 562–566. doi:10.4268/cjcmm20160402

Li, Z. Y., Li, C. F., Zhang, X. B., Tang, S. H., Yang, H. J., Cui, X. M., et al. (2020). Policies and problems of modernizing ethnomedicine in China: A focus on the Yi and Dai traditional medicines of yunnan province. *Evid. Based Complement. Altern. Med.* 2020, 1023297. doi:10.1155/2020/1023297

Liang, Z. H., Ma, J., and Liu, J. (2016). On the change of minority traditional medicine knowledge inheritance and protection policy. *Guizhou Ethn. Stu* 37, 79–83. doi:10.13965/j.cnki.gzmzyj10026959.2016.12.017

Liu, B., Guo, Z. Y., Bussmann, R., Li, F. F., Li, J. Q., Hong, L. Y., et al. (2016). Ethnobotanical approaches of traditional medicine studies in southwest China: A literature review. *J. Ethnopharmacol.* 186, 343–350. doi:10.1016/j.jep.2016.02.040

Liu, J. N. (2007). *Overview of daozhen gelao and Miao autonomous county*. Guiyang: Nationalities Pub House.

Luo, S. G. (2018). *Chinese festival log - gelao ethnic group eating new festival*. Beijing: Guangming Daily Pub House.

Ma, K. P., and He, Z. X. (2016). *Field guide to wild plants of China, hengshan mountain*. Beijing: The Commercial Press.

Mohammed, B., Abdelaaty, A. S., Omer, M. A., Fahd, A. N., Wail, M. A., Amal, A. H. S., et al. (2019). Ethnopharmacological survey of herbal remedies used for the treatment of cancer in the greater casablanca-Morocco. *Evidence-based Complementary Altern. Med.* 2019, 1613457. doi:10.1155/2019/1613457

Niu, Y., and Sun, H. (2021). *Flowering plants of hengduan mountains*. Kunming: Yunnan Tech Pub House.

Pei, S. J., and Long, C. L. (1998). *Applied ethnobotany*. Kunming: Yunnan National Pub House.

Pieroni, A. (2000). Medicinal plants and food medicines in the folk traditions of the upper Lucca Province, Italy. *J. Ethnopharmacol.* 70, 235–273. doi:10.1016/s0378-8741(99)00207-x

Qian, C. S. (1963). *Flora of China*. Beijing: Sci Press.

Shang, W. L., S. (2017). On the development of ethnic culture tourism case study—a gelao community in the north of Guizhou province. *J. Shaanxi Xueqian Norm. Univ.* 33, 76–80. doi:10.11995/j.issn.2095-770X.2017.12.01

Shu, H., Yang, H. P., and Li, M. (2022). Survey on the awareness and development attitude of villagers towards Li medicine in Ledong Li Autonomous County. *Chin. J. Rural. Med. Phar* 29, 55–56. doi:10.19542/j.cnki.1006-5180.006555

Sun, X. M., Zhang, X. H., Wang, H. F., and Zhu, G. W. (2020). Industry Status and development strategies of Chinese ethnic medicine. *Chin. J. Exp. Tradi Med. Formulae* 26, 195–202. doi:10.13422/j.cnki.syfjx.20201058

Wang, D. C., Ma, Y. C., Sun, R. Q., Lu, C. H., and Li, L. S. (2022). Brief dicussion on the treatment method of yin and yang and five elements diagnosis and treatment system in traditonal Chinese medicine. *Chin. J. Tradit. Chin. Med. Pharm.* 37, 6228–6233.

Wang, H. N. (2017a). *Color spectrum of Gelao ethnic medicine*. Guiyang: Guizhou Sci Technol Pub House.

Wang, W. J. (2013). Research on the classification of intangible cultural heritage of traditional Chinese medicine. *Jiangxi Soc. Sci.* 33, 206–211.

Wang, Y. H. (2017b). *Common research methods in ethnobotany*. Hangzhou: ZheJiang Edu Pub Group.

Wei, B., Hu, C. G., Yang, L. Y., Zhao, J. H., Pan, L. T., and Du, J. (2002). Overview of gelao medicine in Guizhou. *Chin. J. Ethnomed Ethnopharm* 2002, 252–253.

Wei, X., Nong, Z. F., Mei, X. P., Zou, M., Shu, J. L., Li, R. H., et al. (2017). Serum uric acid as a simple risk factor in patients with rheumatic heart disease undergoing valve replacement surgery. *J Med Pharm. Chin Minorities* 23, 69–74. doi:10.1016/j.cca.2017.07.019

Xiao, H., Liu, F. S., Xie, J., Wu, F. M., and Liu, S. (2022). Study on the seed characteristics and germination of traditional Gelao medicine Pimpinella Candolleana. *J. Zunyi Med. Univ.* 45, 743–747. doi:10.14169/j.cnki.zunyixuebao.2022.0126

Xie, J., Liu, F. S., Jia, X. H., Zhao, Y. X., Liu, X. Q., Luo, M. X., et al. (2022). Ethnobotanical study of the wild edible and healthy functional plant resources of the Gelao people in northern Guizhou, China. *J. Ethnobiol. Ethnomed* 18, 72. doi:10.1186/s13002-022-00572-2

Xiong, Y., Sui, X. Y., Ahmed, S., Wang, Z., and Long, C. L. (2020). Ethnobotany and diversity of medicinal plants used by the Buyi in eastern Yunnan, China. *Plant divers.* 42, 401–414. doi:10.1016/j.pld.2020.09.004

Yang, M. H., Liang, Z. T., and Sheng, P. (2021). Xinjiang ethnic medicines: A review. *Chin. J. Exp. Tradi Med. Formulae* 27, 227–236. doi:10.13422/j.cnki.syfjx.20211117

Yang, X. Y., Wang, J. G., and Liu, F. C. (2002). *Natural conditions and sustainable agricultural development in Guizhou*. Guiyang: Guizhou Sci Technol Pub House.

Zeng, H., Zhang, G. H., and Pu, Y. C. (2013). *General situation and protection of biodiversity in Guizhou province*. Beijing: Forest Science and Technology, 124–126. doi:10.13456/j.cnki.lykt.2013.09.003

Zhao, J. H. (2003). *Gelao ethnic medicine*. Guiyang: Guizhou Ethnic Pub House.

Zheng, J. Y. (2007). *Overview of wuchuan gelao and Miao autonomous county*. Nationalities Pub House.

Zhou, J. Y., and Zhang, Y. (2006). *Festival and society: The cultural symbol of the gelao people's "Bird-Respecting festival*. Guiyang: J Guizhou Minzu Univ Phi Soc Sci, 66–69.

Zi, H., and Zheng, H. X. (2023). Development history of Manchu medicine culture and classical representative famous prescriptions. *Chin. Arch. Tradi Chin. Med.* 41, 137–140. doi:10.13193/j.issn.1673-7717.2023.02.030

frontiers | Frontiers in Pharmacology

TYPE Original Research
PUBLISHED 25 September 2023
DOI 10.3389/fphar.2023.1221046

OPEN ACCESS

EDITED BY
Somasundaram Arumugam,
National Institute of Pharmaceutical Education and Research, Kolkata, India

REVIEWED BY
Vikram Kumar,
Amity University Jaipur, India
Chunyu Li,
Chinese Academy of Medical Sciences and Peking Union Medical College, China
Mahendran Sekar,
Monash University Malaysia, Malaysia

*CORRESPONDENCE
Qiuhong Xie,
qhxie@jlu.edu.cn
Hongyu Xiang,
hyxiang@jlu.edu.cn

RECEIVED 11 May 2023
ACCEPTED 11 September 2023
PUBLISHED 25 September 2023

CITATION
Zheng W, Shi C, Meng Y, Peng J, Zhou Y, Pan T, Ning K, Xie Q and Xiang H (2023), Integrated network analysis and metabolomics reveal the molecular mechanism of Yinchen Sini decoction in CCl_4-induced acute liver injury. *Front. Pharmacol.* 14:1221046. doi: 10.3389/fphar.2023.1221046

Integrated network analysis and metabolomics reveal the molecular mechanism of Yinchen Sini decoction in CCl_4-induced acute liver injury

Weiwei Zheng[1], Chao Shi[1], Yao Meng[1], Jian Peng[1], Yongfei Zhou[1], Tong Pan[1], Ke Ning[1], Qiuhong Xie[1,2,3]* and Hongyu Xiang[1,2,3]*

[1]Key Laboratory for Molecular Enzymology and Engineering of Ministry of Education, School of Life Sciences, Jilin University, Changchun, Jilin, China, [2]National Engineering Laboratory for AIDS Vaccine, School of Life Sciences, Jilin University, Changchun, Jilin, China, [3]Institute of Changbai Mountain Resource and Health, Jilin University, Fusong, Jilin, China

Objective: Yinchen Sini decoction (YCSND), a traditional Chinese medicine (TCM) formula, plays a crucial role in the treatment of liver disease. However, the bioactive constituents and pharmacological mechanisms of action remain unclear. The present study aimed to reveal the molecular mechanism of YCSND in the treatment of acute liver injury (ALI) using integrated network analysis and metabolomics.

Methods: Ultra-high-performance liquid chromatography coupled with Q-Exactive focus mass spectrum (UHPLC-QE-MS) was utilized to identify metabolites in YCSND, and high-performance liquid chromatography (HPLC) was applied to evaluate the quality of four botanical drugs in YCSND. Cell damage and ALI models in mice were established using CCl_4. ^{1}H-NMR metabolomics approach, along with histopathological observation using hematoxylin and eosin (H&E), biochemical measurements, and reverse transcription quantitative real-time PCR (RT-qPCR), was applied to evaluate the effect of YCSND on CCl_4- induced ALI. Network analysis was conducted to predict the potential targets of YCSND in ALI.

Result: Our results showed that 89 metabolites in YCSND were identified using UHPLC-QE-MS. YCSND protected against ALI by reducing the levels of alanine aminotransferase (ALT), aspartate aminotransferase (AST), and malondialdehyde (MDA) contents and increasing those of superoxide dismutase (SOD), and glutathione (GSH) both in vivo and in vitro. The ^{1}H-NMRmetabolic pattern revealed that YCSND reversed CCl_4-induced metabolic abnormalities in the liver. Additionally, the Kyoto Encyclopedia of Genes and Genome (KEGG) pathway enrichment analysis identified five pathways related to liver injury, including the PI3K-AKT, MAPK, HIF-1, apoptosis, and TNF signaling pathways. Moreover, RT-qPCR showed YCSND regulated the inflammatory response (*Tlr4*, *Il6*, *Tnfα*, *Nfκb1*, *Ptgs2*, and *Mmp9*) and apoptosis (*Bcl2*, *Caspase3*, *Bax*, and *Mapk3*), and inhibited PI3K-AKT signaling pathway (*Pi3k* and *Akt1*). Combined network analysis and metabolomics showed a link between the key targets (*Tlr4*, *Ptgs2*, and *Mmp9*) and vital metabolites (choline, xanthine, lactate, and 3-hydroxybutyric acid) of YCSND in ALI.

Conclusion: Overall, the results contribute to the understanding of the therapeutic effects of YCSND on ALI, and indicate that the integrated network analysis and metabolomics could be a powerful strategy to reveal the pharmacological effects of TCM.

KEYWORDS

Yinchen Sini decoction, acute liver injury, network analysis, 1 H-NMR, PI3K-AKT

1 Introduction

Acute liver injury (ALI) is a reversible wound-healing process caused by several xenobiotic and toxic metabolites in the liver, particularly chemical toxins, drugs, alcohol, and viruses (Ren et al., 2019). CCl_4 is a powerful hepatoxic and nephrotoxic agent that is widely used to induce hepatotoxicity in experimental animals and to establish models of acute/chronic liver injury, hepatic fibrosis/cirrhosis, hepatic failure and nephrotoxicity (Unsal et al., 2021). CCl_4-induced ALI possesses similar molecular mechanisms with human ALI, making it a suitable model for ALI research. CCl_4 is metabolized by hepatic cytochrome P450 enzymes (CYP450), producing reactive oxygen species (ROS), and excessive ROS production can induce oxidative stress, inflammatory response, and hepatocyte apoptosis, all of which play a pivotal role in ALI pathogenesis. (Xie et al., 2018). In the absence of effective treatment, ALI can evolve into more severe liver diseases, such as chronic liver injury, liver fibrosis, and even irreversible liver cirrhosis and cancer. Currently, there is no safe and effective therapeutic drug for ALI owning to its multiple pathogenic factors and complicated pathological processes. In China, some common hepatoprotective drugs used to treat ALI include silymarin and magnesium isoglycyrrhizinate (Li M. et al., 2022; Liu et al., 2022). However, the use of these drugs is associated with several issues, including limited therapeutic efficacy and severe side effects (Xie et al., 2018; Ren et al., 2019), indicating the need to develop more effective and safer drugs for ALI treatment.

Traditional Chinese medicine (TCM) formulas are commonly used to treat ALI, with the advantages of fewer side effects and multiple metabolites with several targets (Zhang et al., 2018). Several TCM formulas have been successfully used to treat CCl_4-induced ALI (Lee et al., 2020; Wei et al., 2021; Zhao Q. et al., 2022). Yinchen Sini decoction (YCSND), a TCM formula from the Song dynasty, is composed of four Chinese botanical drugs, *Artemisia capillaris* Thunb. [Asteraceae; Artemisiae scopariae herba], *Aconitum carmichaelii* Debeaux [Ranunculaceae, Aconiti lateralis radix praeparata], *Zingiber officinale* Roscoe [Zingiberaceae, Zingiberis rhizoma], and honey-fried *Glycyrrhiza glabra* L. [Fabaceae, Glycyrrhizae radix et rhizoma praeparata cum melle]. Among the four botanical drugs, *Artemisia capillaris* Thunb. [Asteraceae; Artemisiae scopariae herba] and *Aconitum carmichaelii* Debeaux [Ranunculaceae, Aconiti lateralis radix praeparata] possess antioxidant, anti-inflammatory, and anti-apoptotic effects; *Zingiber officinale* Roscoe [Zingiberaceae, Zingiberis rhizoma] and honey-fried *Glycyrrhiza glabra* L. [Fabaceae, Glycyrrhizae radix et rhizoma praeparata cum melle] mainly play harmonic roles in detoxifying *Aconitum carmichaelii* Debeaux [Ranunculaceae, Aconiti lateralis radix praeparata], and these metabolites of YCSND synergistically exert positive effects in the body (Wang M. F. et al., 2021; Wang Y. et al., 2021; Huang et al., 2021). Recent pharmacological studies have shown that YCSND has hepatoprotective properties, and some metabolites occurring in YCSND, including scoparone (Hsueh et al., 2021), glycyrrhizic acid (Huo et al., 2020), and chlorogenic acid (Merzouk et al., 2017) have been reported to exert hepatoprotective effects. YCSND has been clinically used to treat hepatobiliary disease (Wang et al., 2008; Chen et al., 2019) and was effective against hepatic inflammation in a mouse model of intrahepatic cholestasis (Wang Q. et al., 2020). However, studies on the effect of YCSND in CCl_4-induced liver injury are limited. For instance, Li et al. (2016a; 2016b) revealed that combined treatment with YCSND and *Conioselinum anthriscoides* [Apiaceae; Ligusticum Chuanxiong rhizoma] may potentially prevent CCl_4-induced chronic liver injury by significantly reducing alanine aminotransferase (ALT) and aspartate aminotransferase (AST) levels, *Smad3* and *Smad7* mRNA expression, and collagen I and III expressions in the liver. However, the effectiveness of only YCSND in ALI treatment, and its molecular mechanism are yet to be elucidated.

Traditional network analysis is typically used to predict potential targets and molecular mechanisms of TCM in disease treatment, using data mining and scientific computing techniques based on public databases (Yang et al., 2023). Network analysis can reveal the patterns and rules that govern the associations between drugs and diseases, enabling efficient screening of potential drug targets and pathways with therapeutic effects. However, the accuracy and reliability of the predictions may be skewed owing to limitations in the quality of the database information, such as errors, noise, and biases (Li Z. et al., 2022). Moverover, the composition of a TCM formula may not be a simple superposition of individual plant-derived metabolites. During the processing of TCM formulas, botanical drugs may exhibit synergistic, cooperative, or inhibitory effects, potentially accompanied by changes in their metabolites (Li Z. et al., 2022). Due to these complexities, the conventional network analysis approach, which relies on public databases to screen plant-derived ingredients, appears to be unreliable for studying TCM formulations. Network predictions using actual constituents of plant-derived formulations appear to be more dependable than conventional databases. Therefore, it is urgent and necessary to develop a new method of network analysis for the study of TCM metabolites to improve the accuracy of network prediction.

^{1}H-NMR technology is a beneficial tool for analyzing metabolites and has several advantages, such as reliable results, nondestructive sampling, and minimal sample preparation (Borém et al., 2023). Integrated of network analysis and metabolomics has unique advantages in the study of TCM formulas, as it can reveal the intricate mechanisms of action within the body from multiple perspectives, including metabolites of botanical drug, targets, pathways, and metabolites *in vivo* (Zhao Q. et al., 2022). Network analysis and metabolomics have successfully been applied to uncover the mechanisms of several TCM formulas in liver disease treatment (Yu et al., 2019; Wang et al., 2022; Yang et al., 2023).

In this study, a novel network prediction method based on the actual metabolites of YCSND was employed. This approach

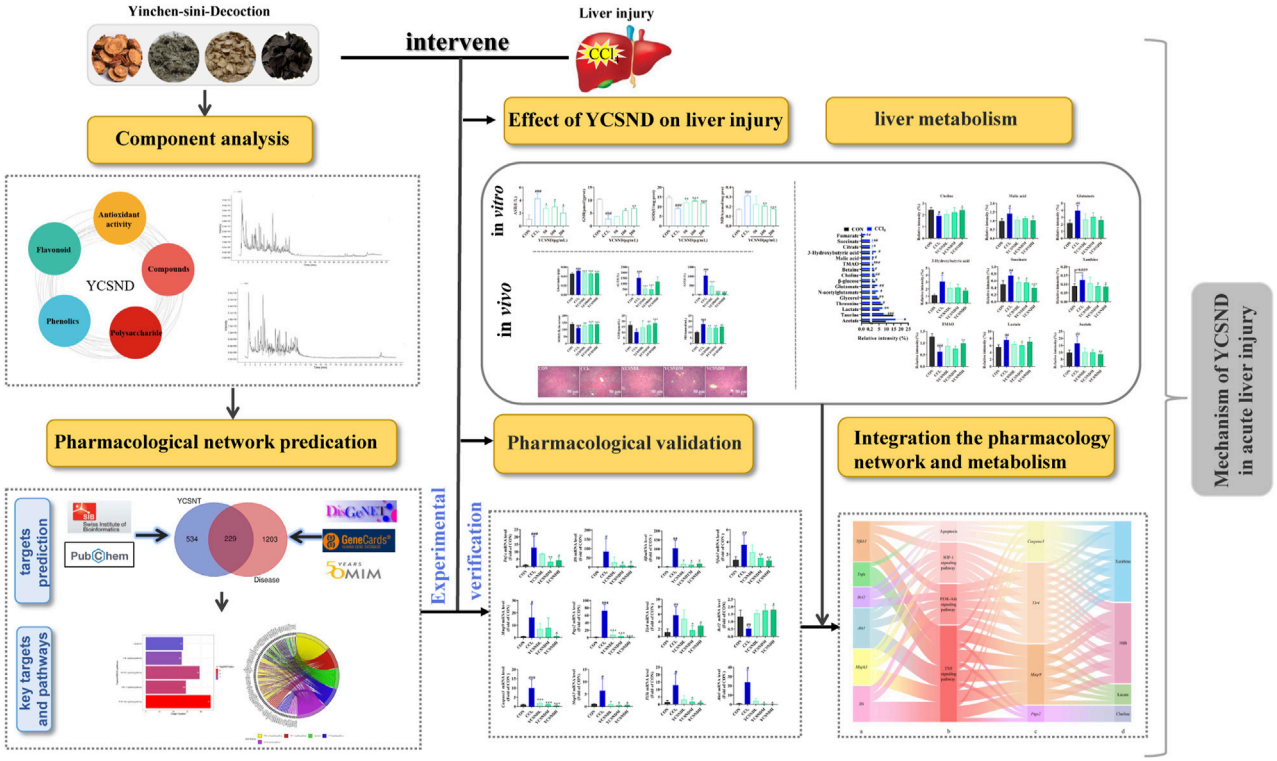

FIGURE 1
Graphic abstract.

improves upon traditional blind screening by enhancing the accuracy of network predictions and it also enables faster and more precise identification of effective targets and pathways facilitating a more efficient exploration of underlying mechanisms. Additionally, the predicted targets and pathways were validated using reverse transcription quantitative real-time PCR (RT-qPCR). Moreover, network predictions and metabolomics were integrated to elucidate the molecular mechanisms of YCSND in liver injury from multiple perspectives. The present study serves as a theoretical basis for the therapeutic use of YCSND in liver diseases, offering novel insights into the study of TCM formulations. The graphic abstract of this study is shown in Figure 1.

2 Materials and methods

2.1 Preparation of YCSND

Botanical drugs for YCSND, including *Artemisia capillaris* Thunb. [Asteraceae; Artemisiae scopariae herba], *Aconitum carmichaelii* Debeaux [Ranunculaceae, Aconiti lateralis radix praeparata], *Zingiber officinale* Roscoe [Zingiberaceae, Zingiberis rhizoma], and honey-fried *Glycyrrhiza glabra* L. [Fabaceae, Glycyrrhizae radix et rhizoma praeparata cum melle] were purchased from the drug department of Yunling grass bouquet (Yunnan, China) and were authenticated by Prof. Yuguang Chen (Changchun traditional Chinese medicine hospital). YCSND was prepared using 10 g each of *Artemisia capillaris* Thunb. [Asteraceae; Artemisiae scopariae herba], *Aconitum carmichaelii* Debeaux [Ranunculaceae, Aconiti lateralis radix praeparata], *Zingiber officinale* Roscoe [Zingiberaceae, Zingiberis rhizoma], and honey-fried *Glycyrrhiza glabra* L. [Fabaceae, Glycyrrhizae radix et rhizoma praeparata cum melle]. Quality control for the four botanical drugs for YCSND met the standards of the Chinese Pharmacopoeia (Table 1). The botanical drug mixture (40 g) was soaked and decocted with 400 mL of distilled water for 45 min. The first liquid was obtained by centrifuging at 4,000 rpm for 10 min, and the residues were sequentially extracted twice with an equal volume of water for another 45 min. The supernatants were then mixed and concentrated in a rotary evaporator. Finally, the concentrated liquid was stored at −80°C for 24 h and dried in a freeze dryer for another 36 h, and the freeze-dried YCSND powder (with an extraction rate of 35.6%) was stored at 4°C for further experiments.

2.2 Metabolite analysis of YCSND

Total phenolic, total flavonoid and polysaccharide contents were determined using previously described methods (Sahayarayan et al., 2020; Wu et al., 2021; Mogadem et al., 2022). 2,2-diphenyl-1-picrylhydrazyl radical (DPPH), 2,2′-azino-bis (3-ethylbenzothiazoline-6-sulphonic acid) radical (ABTS), superoxide radical (O_2^-), and hydroxyl radical (·OH) scavenging

TABLE 1 Contents of the main identified metabolites in YCSND extract.

Plant Name	Metabolites	Retention time (min)	Wavelength (nm)	Contents (mg/g)
Artemisia capillaris Thunb. [Asteraceae; Artemisiae scopariae herba]	chlorogenic acid	11.442	325	7.602
Zingiber officinale Roscoe [Zingiberaceae, Zingiberis rhizoma]	6-gingerol	18.749	230	6.520
Aconitum carmichaelii Debeaux [Ranunculaceae, Aconiti lateralis radix praeparata]	benzoylmesaconine	19.154	235	0.089
	benzoylaconine	25.753		0.005
	benzoylhypacoitine	55.053		0.147
honey-fried *Glycyrrhiza glabra* L. [Fabaceae, Glycyrrhizae radix et rhizoma praeparata cum melle]	liquiritin	8.561	254	5.311
	glycyrrhizic acid	34.542		25.348
YCSND	chlorogenic acid	11.442	325	2.029
	scoparone	40.563		1.441
	caffeic acid	14.861		0.092
	isochlorogenic acid B	40.563		0.023
	6-gingerol	18.749	230	1.416
	6-shogaol	31.227		1.860
	liquiritin	8.561	325	1.024
	glycyrrhizic acid	34.542		7.333
	benzoylmesaconine	19.154	235	0.051
	benzoylaconine	25.753		0.005
	benzoylhypacoitine	55.053		0.052
	neoaconitine	39.922		0.007
	hypaconitine	45.690		0.001
	aconine	50.180		No detected

activities were determined using previously described methods (Siddhuraju and Manian, 2007), Vitamin C as the positive control. Metabolite analysis of YCSND was performed using ultra-high-performance liquid chromatography coupled with Q-Exactive focus mass spectrum (UHPLC-QE-MS) at Biotree Biomedical Technology CO., Ltd (Shanghai, China). High-performance liquid chromatography (HPLC) was used to analyze for chemical fingerprints and quantification of metabolites of YCSND. Detailed procedures of UHPLC-QE-MS and HPLC are described in the Supplementary Materials (Supplementary Table S1).

2.3 Cell pretreatment

HepG2 cells in the exponential growth phase were seeded into cell plates for 24 h, followed by treatment with YCSND (50, 100, and 200 μg/mL) for another 12 h. Cells in the normal and model groups were treated with equal volumes of DMEM instead of YCSND. Subsequently, the cells were treated with CCl_4 (final concentration 0.05%, diluted with DMSO) for 12 h, except those in the normal group. Finally, the prepared cells were used for subsequent analyses.

2.4 Cell viability assay

Cell viability was determined using the MTT assay method (Bilkan et al., 2022). Briefly, MTT (5 mg/mL, 20 μL/per well) was added to the cells and incubated at 37°C for 4 h. Subsequently, the solutions were removed, DMSO (100 μL/well) was added to the wells, and absorbance was measured at 490 nm using a microplate reader (BioTek, USA).

2.5 Animal experiment design

Male Kunming mice (4-5 weeks old; 18–22 g) were purchased from Liaoning Changsheng Biotechnology. All animal experimentation procedures were approved by the Animal Care and Use Committee of Jinlin University (approval no.: 2021SY0715). The mice were housed under standard conditions at 23°C ± 2°C in a 12-h light/dark cycle and fed standard mice chow and water. After adaptive feeding for 7 d, the mice were randomly assigned to five groups (six mice per group): control (CON), CCl_4-treated (CCl_4), low-dose YCSND (YCSNDL), medium-dose YCSND (YCSNDM), and high-dose YCSND groups

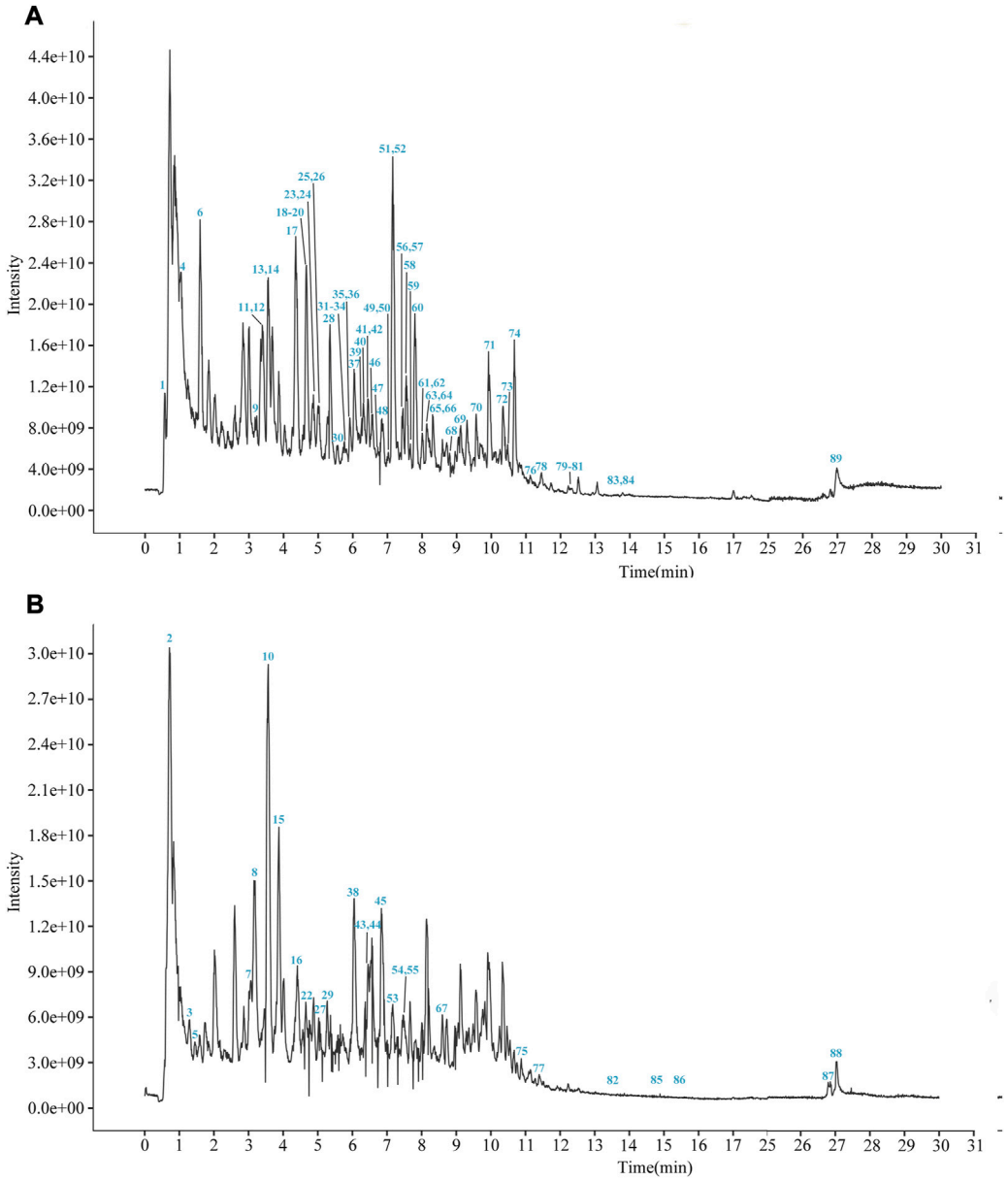

FIGURE 2
The total ion current chromatogram of YCSND in positive mode **(A)** and negative mode **(B)**.

(YCSNDH). Mice in the CON and CCl_4 groups were treated with physiological saline, whereas those in the three YCSND groups were treated with 400, 800, and 1,600 mg/kg body weight of YCSND powders per day, respectively. According to the description of the body surface area normalization method between humans and animals (Reagan-Shaw et al., 2008), the dose of humans was converted into the dose of mice: 40 g raw drugs of YCSND per day for a 70 kg person is equivalent to 1,600 mg/kg YCNSD extract as the high dose. The intragastric administration was continued for 21 d. All mice were intraperitoneally injected with 0.3% CCl_4 (v/v, 10 mL/kg, diluted in olive oil) 2 h after the last administration, except for mice in the CON group, which were injected with an equal volume of olive oil. After 24 h, all mice were euthanized by carbon dioxide inhalation (Supplementary Figure S1), and liver samples and serum were collected for further analyses.

2.6 Determination of physiological index

ALT and AST levels in cell culture supernatants and serum were determined using standardized kits (Jiancheng, Nanjing, China), according to the manufacturer's instructions. Superoxide dismutase (SOD) and glutathione (GSH) activities and malondialdehyde (MDA) contents of HepG2 cells and serum were determined using standardized kits (Jiancheng, Nanjing, China), according to the manufacturer's instructions. Cell protein contents were measured using a bicinchoninic acid (BCA) protein assay kit (Bioss, Beijing, China).

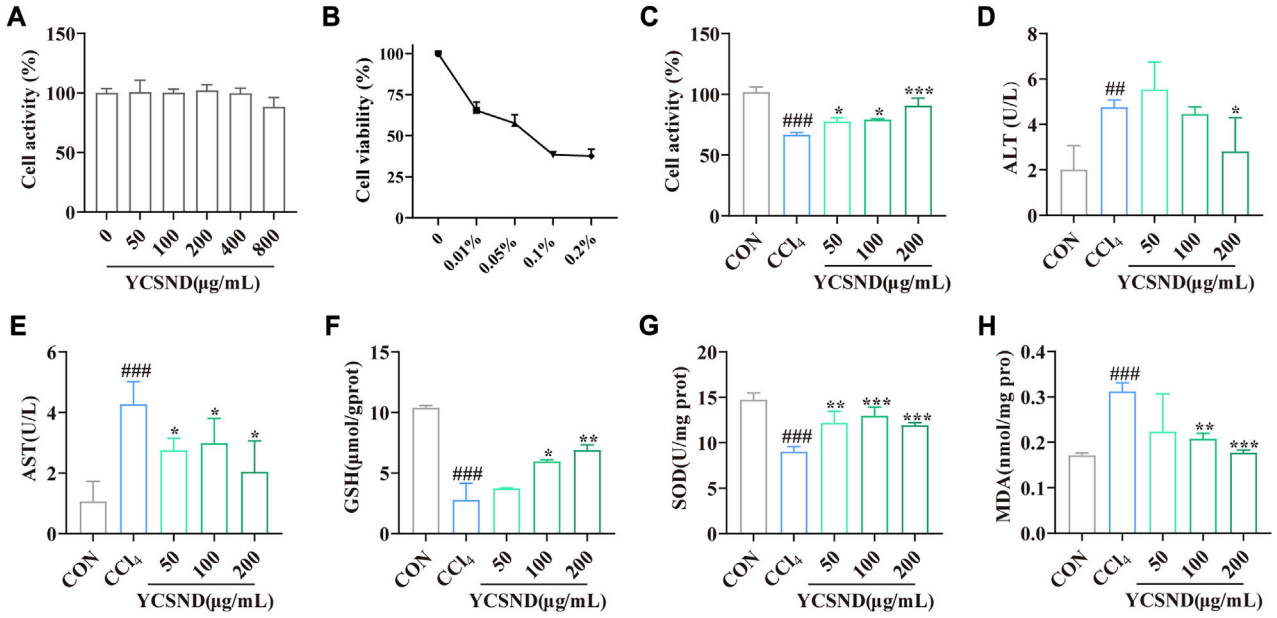

FIGURE 3
Effect of Yinchen sini decoction (YCSND) on CCl_4-treated HepG2 cells. **(A)** HepG2 cell viability after YCSND treatment. **(B)** Effect of CCl_4 treatment at different concentrations on HepG2 cell viability. **(C)** HepG2 cell viability following treatment with YCSND and 0.05% CCl_4. **(D–H)** Effect of YCSND pretreatment on ALT, AST, GSH, SOD, and MDA contents in CCl_4-treated HepG2 cells. $^{\#}p < 0.05$, $^{\#\#}p < 0.01$, $^{\#\#\#}p < 0.001$ vs. CON group; $^{*}p < 0.05$, $^{**}p < 0.01$, $^{***}p < 0.001$ vs. CCl_4 group.

2.7 Liver histopathology assay

A small piece of the cut right lobe of the liver was fixed in a 10% formalin solution, dehydrated, made transparent, paraffin-embedded, and cut into 2-mm thick sections. Thereafter, the liver tissue was stained with hematoxylin and eosin (H&E) and viewed using a light microscope (Shrestha et al., 2016).

2.8 RNA extraction and RT-qPCR

Total RNA extraction of the liver tissue, cDNA synthesis, and qPCR were performed according to previously described procedures (Wang Y. et al., 2020) RT-qPCR was performed using the RealStar Green Fast Mixture (Genstar, Beijing, China). Glyceraldehyde-3-phosphate dehydrogenase (*Gapdh*) was selected as the internal control for RT-qPCR and subsequent normalization. The relative expression levels of target genes were calculated using the comparative CT method ($2^{-\Delta\Delta CT}$). The primer sequences of the genes are listed in Supplementary Table S2.

2.9 ^{1}H-NMR metabonomic analysis of the liver

Sample preparation for ^{1}H-NMR was performed according to previously described methods with slight modifications (Liu et al., 2021). Briefly, approximately 200 mg of frozen liver samples were homogenized with 600 μL of methanol and ultra-water mixture (v/v, the ratio of 2:1) for 30 s, and the treated samples were centrifuged at 12,000 rpm for 10 min at 4°C. Thereafter, the above procedure was repeated twice. Cell supernatant from the three extraction were mixed in a 2 mL tube and methanol was removed by evaporation. Subsequently, the treated samples were resuspended and vortexed uniformly in 750 μL of 0.1 M phosphate buffer (pH = 7.4) with 0.01% TSP and 10% D_2O. To remove insoluble ingredients, the extracts were centrifuged at 12,000 rpm for 10 min at 4°C. Finally, 550 μL of the supernatant was transferred to an NMR tube for ^{1}H NMR detection. ^{1}H-NMR detection and spectral processing were performed according to previously described methods (Ruiz-Rodado et al., 2016). Orthogonal partial least squares-discriminant analysis (OPLS-DA) was applied to multivariate pattern recognition analysis using SIMCA (version 14.0, UMETRICS, Umeå, Sweden). Metabolites with variable importance for projection (VIP) > 1 and $p < 0.05$ were identified as differentially expressed metabolites between the two groups based on *t*-test. Metabolites were assigned using the Human Metabolome Database (http://www.hmdb.ca), and metabolomics pathway analysis was performed using MetaboAnalyst (https://www.metaboanalyst.ca).

2.10 Network analysis

Network analysis was used to predict the potential molecular mechanism of YCSND in liver injury. The targets of the active metabolites in YCSND were determined following previously described method (Guo et al., 2021). The candidate targets of ALI were screened by searching the keywords “liver injury” in the OMIM database (https://www.omim.org/), DisGeNET database

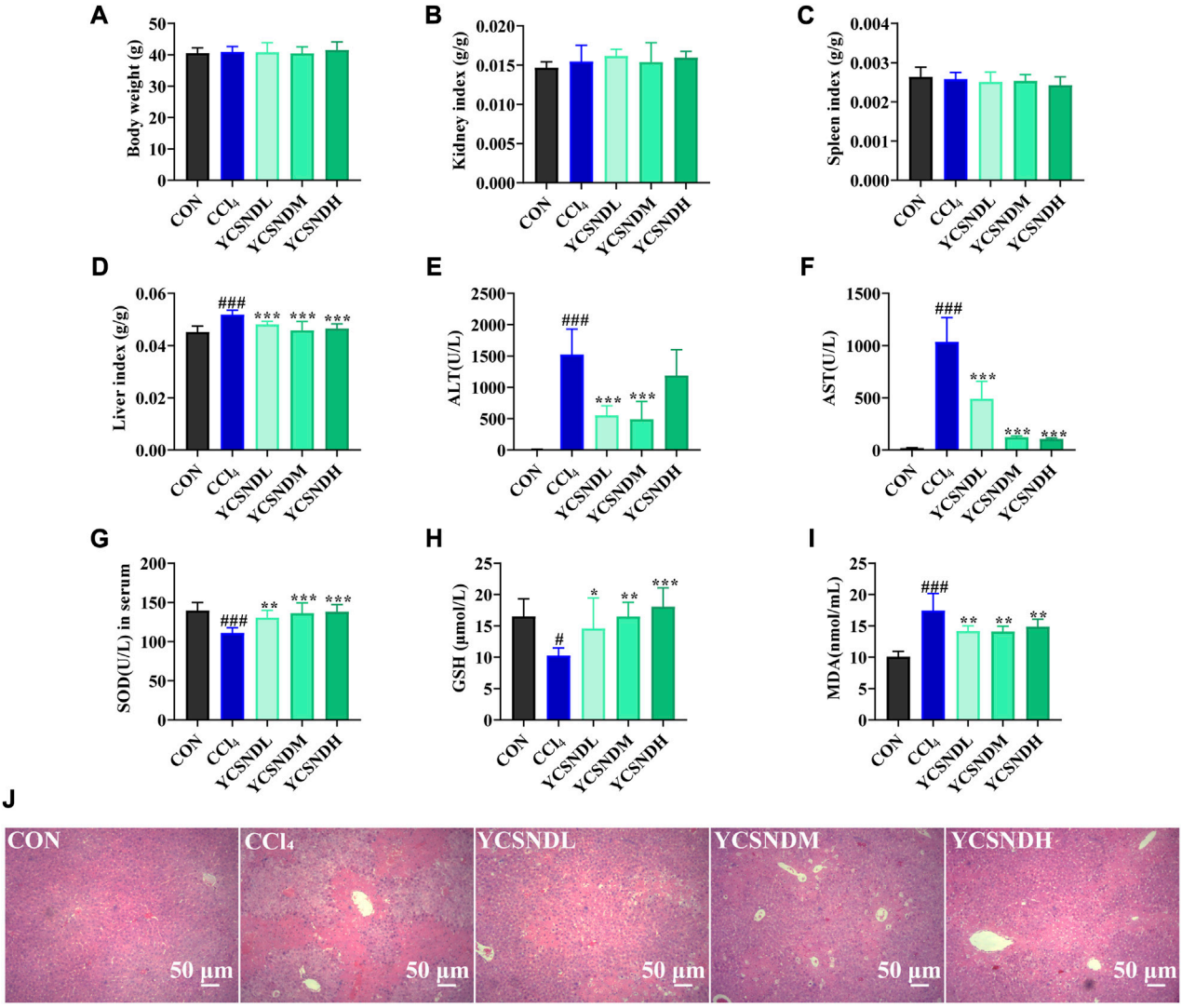

FIGURE 4
Effects of Yinchen sini decoction (YCSND) on CCl_4-induced acute liver injury (ALI) mice. **(A-D)** The body weight, kidney index, spleen index and liver index. **(E-I)** The serum of ALT, AST, SOD and GSH levels, and MDA contents. **(J)** H&E staining of liver tissue sections. #$p < 0.05$, ##$p < 0.01$, ###$p < 0.001$ vs. CON group; *$p < 0.05$, **$p < 0.01$, ***$p < 0.001$ vs. CCl_4 group.

(https://www.disgenet.org/), and GeneCard database (https://www.genecards.org/). The species "*Homo sapiens*" was selected, and the target gene information related to liver injury was collected and integrated. Venn diagram was used to obtain intersecting targets from the active ingredient targets of YCSND and the liver-injury targets. An intersecting target network between the metabolites of YCSND and targets was constructed using Cytoscape 3.8.2. Gene ontology (GO) and Kyoto Encyclopedia of Genes and Genomes (KEGG) pathways enrichment analyses were performed using the Metascape database (https://metascape.org/). The top 20 predicted KEGG pathways, related metabolites, and targets of YCSND for the treatment of liver injury were screened to construct a metabolites-target-pathway (M-T-P) network using Cytoscape 3.8.2. Furthermore, we screened five typical KEGG pathways to construct a target-pathway (T-P) network using an online website (https://www.bioinformatics.com.cn).

2.11 Integrated metabonomics and network analysis

Targets of the metabolites *in vivo* affected by YCSND were predicted using the SWISS database (http://www.swisstargetprediction.ch/). Overlapping targets were obtained among those from the metabolites and network prediction. These targets played a key role in YCSND against ALI.

2.12 Data analysis

Each experiment was performed independently at least three times, and data are expressed as mean ± standard deviation (SD). Statistical analysis was performed using GraphPad Prism (version 8.0) and SPSS 22.0. Statistical significance of differences was assessed with Student's *t*-test for two groups or one-way ANOVA for

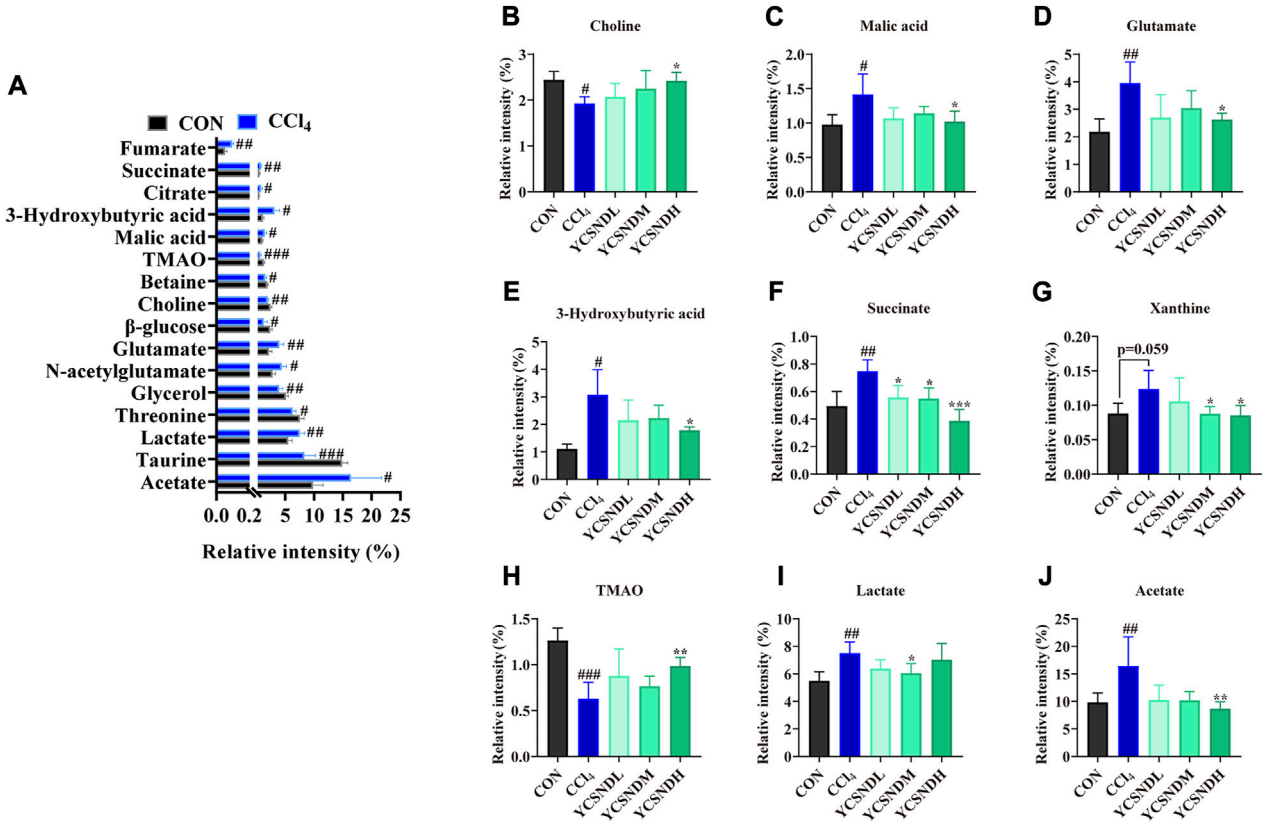

FIGURE 5
Differential metabolites between the CCl_4 group and CON group or YCSND group, based on ^{1}H-NMR. **(A)** The trend of differential metabolites between CCl_4 and CON groups. **(B–J)** The relative contents of choline, malic acid, glutamate, 3-hydroxybutyric acid, succinate, xanthine, TMAO, lactate, and acetate, based on ^{1}H-NMR analysis. #$p < 0.05$, ##$p < 0.01$, ###$p < 0.001$ vs. CON group; *$p < 0.05$, **$p < 0.01$, ***$p < 0.001$ vs. CCl_4 group.

multiple groups. Differences were considered significant when $p < 0.05$.

3 Results

3.1 Compositions and antioxidant activity of YCSND

YCSND contained polysaccharides (408.55 ± 15.04 mg Glu/g), flavonoids (92.70 ± 3.37 mg RE/g), and polyphenols (39.76 ± 0.83 mg GAE/g) (Supplementary Table S3). Additionally, YCSND showed excellent antioxidant activity against several free radicals, including DPPH, ABTS, O^{2-} and ·OH (Supplementary Table S3), which was partly attributed to its polysaccharide, flavonoid, and polyphenol contents (Zhang Q. et al., 2022; Ziyatdinova and Kalmykova, 2023). Moreover, UHPLC-QE-MS identified 89 metabolites, including 20 flavonoids, 18 terpenoids, 14 phenols, 11 phenylpropanoids, 11 alkaloids, three chalcones, and four coumarin derivatives (Supplementary Table S4; Figure 2). Furthermore, key metabolites in YCSND were identified and quantified using HPLC. Supplementary Figure S2 shows the chromatograms of the primarily identified and quantified metabolites of YCSND, and Table 1 lists their specific contents. The main metabolites of YCSND include chlorogenic acid, scoparone, 6-gingerol, 6-shogaol, liquiritin and glycyrrhizic acid. The content of diester alkaloids (neoaconitine, hypaconitine, and aconine) in YCSND is 0.008 mg/g, which is significantly below the pharmacopeia standard of 0.01%. This indicates that YCSND has minimal toxicity. Notably, the metabolites of YCSND included glycyrrhizic acid, chlorogenic acid, 6-gingerol and scoparone, which have been reported to possess antioxidant activity (Merzouk et al., 2017; Huo et al., 2020; Hsueh et al., 2021; Liu et al., 2023). Overall, it could be speculated that these abundant metabolites may contribute to the antioxidant activity of YCSND.

3.2 Effects of YCSND on CCl_4-induced HepG2 cell damage

YCSND at concentrations of 0–800 μg/mL had no significant ($p > 0.05$) cytotoxic effect on HepG2 cells (Figure 3A); therefore, subsequent experiments were performed using 50, 100, and 200 μg/mL of YCSND. Additionally, an appropriate CCl_4 concentration of 0.05% was selected to induce cell damage, which reduced cell viability to approximately 50% (Figure 3B). Expectedly, pretreatment with 50, 100, and 200 μg/mL of YCSND reversed CCl_4-induced cell damage by significantly improving cell viability by 10.87, 12.84, and 24.10%, respectively, compared with the CCl_4 group (Figure 3C). Additionally, we examined the protective effects of YCSND against CCl_4-induced cell damage

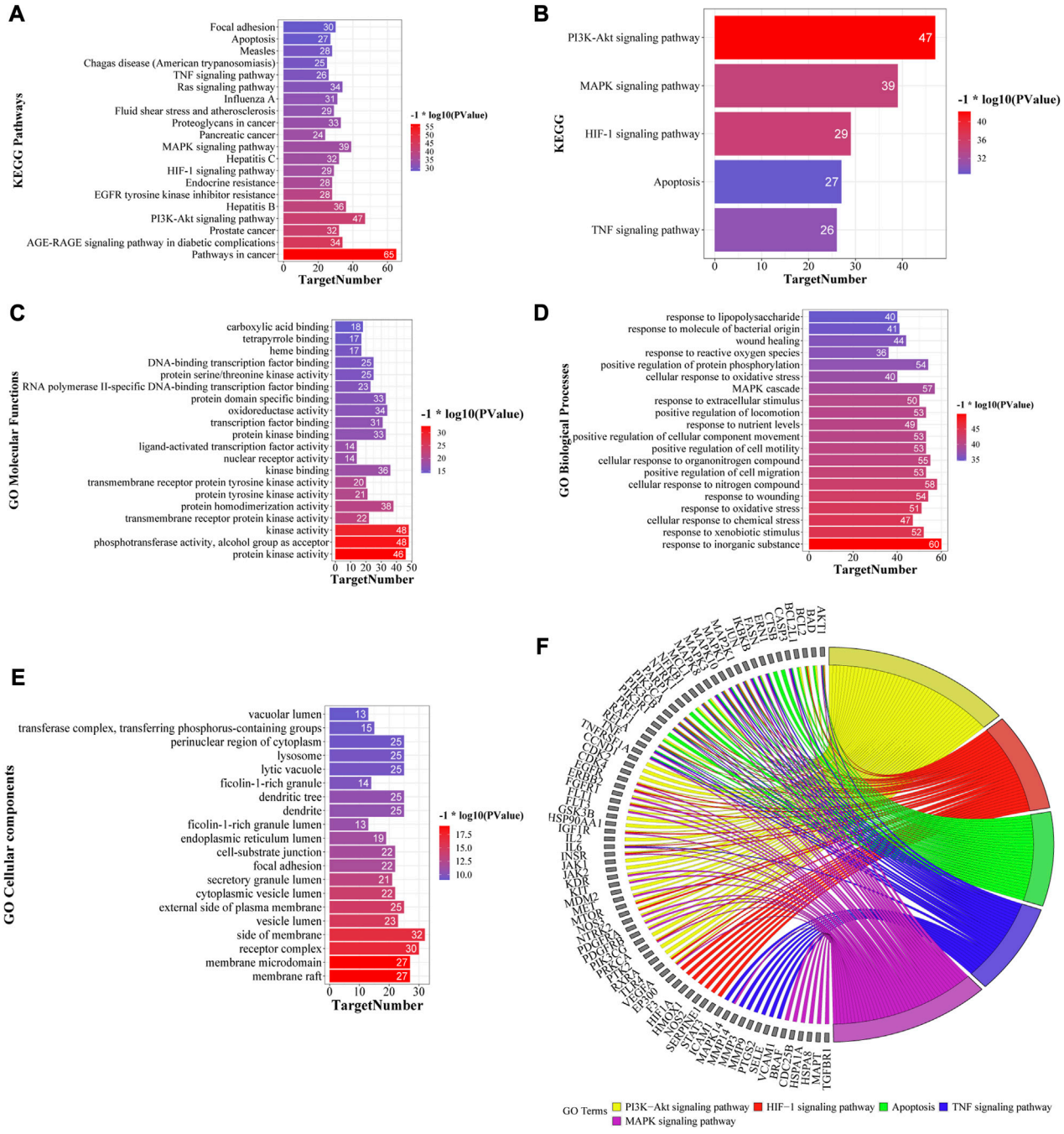

FIGURE 6
Top 20 KEGG pathways **(A)** and five key KEGG pathways **(B)** of Yinchen sini decoction (YCSND) in liver injury. **(C–E)** Go enrichments including the top 20 of cellular component (CC), molecular Function (MF) and biological process, (BP). **(F)** Target-pathway network of five key KEGG pathways, including PI3K-AKT and HIF-1 signaling pathways, apoptosis, and TNF and MAPK signaling pathways.

using biochemical indices. CCl_4-treated cells had significantly higher extracellular AST and AST, and MDA contents but lower intracellular GSH and SOD levels (Figures 3D–H). However, pretreatment with 50, 100, and 200 μg/mL of YCSND reversed the changes in these indices, especially at a dose of 200 μg/mL (Figures 3D–H), indicating that YCSND could reduce CCl_4-induced HepG2 cell damage.

3.3 Effects of YCSND on ALI in mice *in vivo*

To study the effects of YCSND on ALI *in vivo*, a mouse model of CCl_4-induced ALI was generated. Physiological assessment showed that there were no significant differences in body weight, spleen index and kidney index among the groups (Figures 4A–C). However, liver index was significantly

10.3389/fphar.2023.1221046

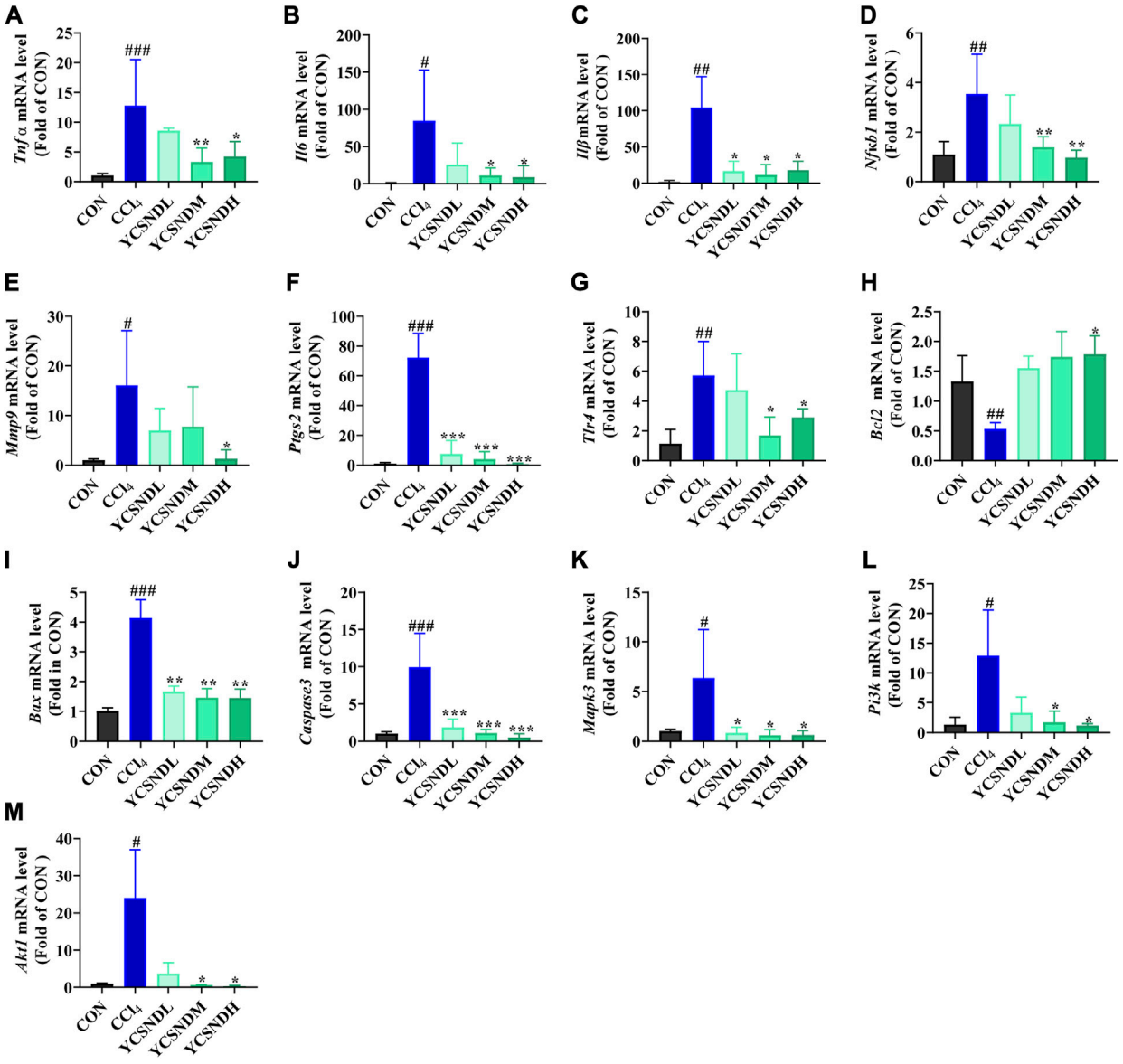

FIGURE 7
The results of experimental verification *in vivo*. **(A-M)** mRNA expression levels of *Tnf α*, *Il6*, *Il1β*, *Nfκb1*, *Bax*, *Caspase3*, *Bcl2*, *Tlr4*, *Mmp9*, *Ptgs2*, *Mapk3*, *Pi3k*, and *Akt1*. *#p* < 0.05, *##p* < 0.01, *###p* < 0.001 vs. CON group; **p* < 0.05, ***p* < 0.01, ****p* < 0.001 vs. CCl_4 group.

higher in the CCl_4 group than in the CON group, which was significantly reduced by YCSND treatment at all doses (Figure 4D). Changes in serum ALT and AST activities are vital indices for evaluating the degree of ALI. ALT and AST levels were significantly higher in the CCl_4 group, indicating that the ALI model was successfully established (Figures 4E, F). Compared with the model group, ALT and AST levels were significantly lower in all YCSND treated groups, except for the YCSNDH group, which exhibited a decreasing trend in ALT but not significant (Figures 4E, F). Additionally, YCSND suppressed CCl_4-induced oxidative stress by reducing MDA content and increasing serum GSH and SOD levels compared with the CCl_4 group (Figures 4G–I). Overall, these results confirmed that YCSND protects against CCl_4-induced ALI by regulating biochemical indices.

3.4 Effects of YCSND on hepatic histopathology

Compared with serum enzyme activities, hepatic histopathology could be more intuitive in reflecting the degree of liver damage. In the CON group, a normal hepatocytic cell structure was observed with the following representative characteristics: uniform arrangement of hepatocytes, rich hepatocytic cytoplasm, clear cellular nucleoli, and prominent central veins (Figure 4J). In contrast, the CCl_4 group showed severe pathological changes, including nuclear pyknosis, extensive necrosis, and inflammatory infiltration around the central vein (Figure 4J). However, YCSND treatments ameliorated the histopathological changes associated with CCl_4-induced liver injury to some extent, especially the YCSNDM and YCSNDH groups, which showed reduced

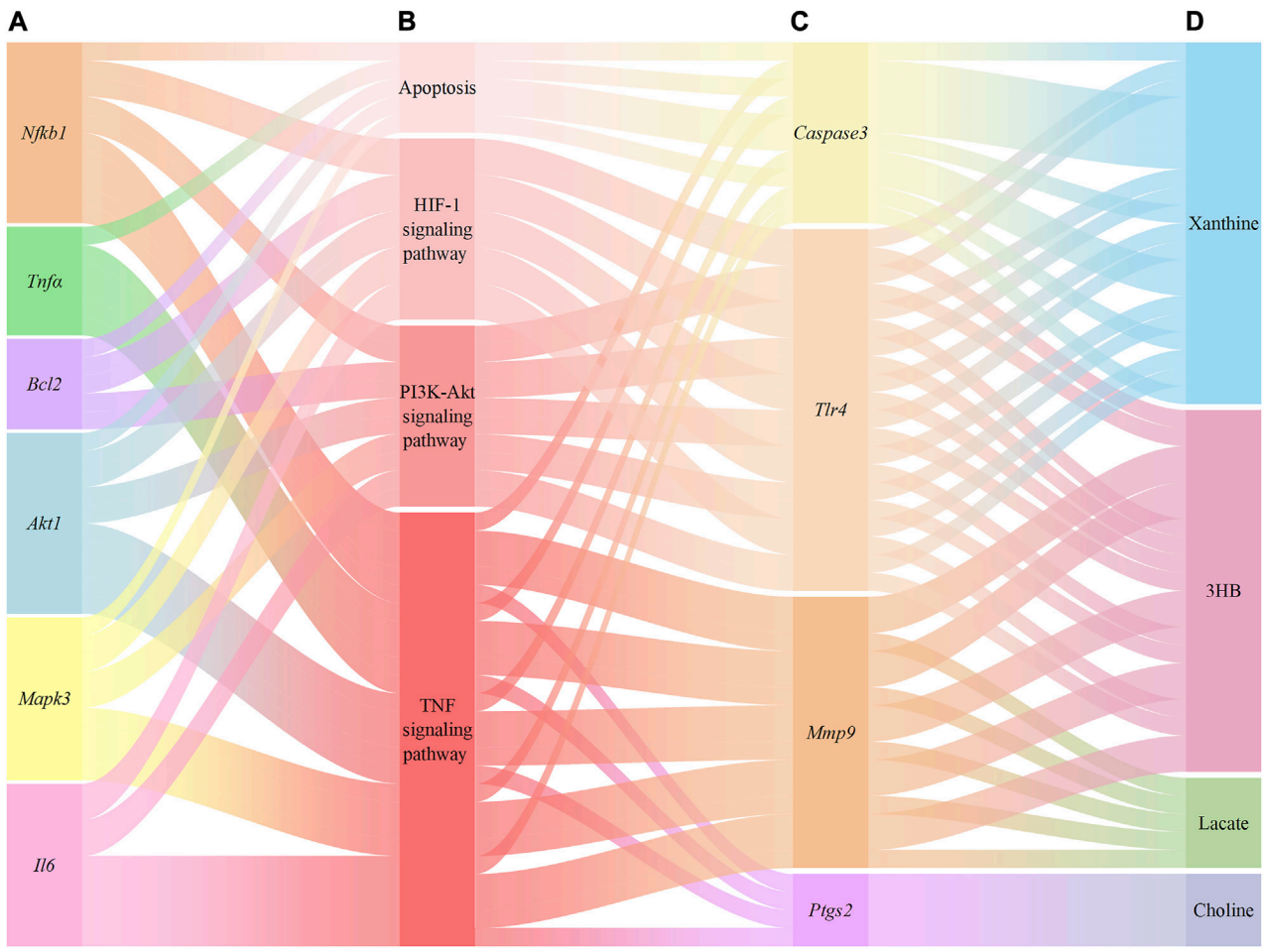

FIGURE 8
The relationship between the targets of network pharmacological prediction and metabolites regulated by Yinchen Sini Decoction (YCSND). **(A)**, the validated targets from pharmacological prediction; **(B)**, pathways associated with acute liver injury (ALI); **(C)**, the validated crossover targets; **(D)**, metabolites regulated by YCSND.

inflammatory infiltration and necrosis compared with that in the CCl_4 group (Figure 4J).

3.5 ^{1}H-NMR metabolomics analysis

^{1}H-NMR metabolomic was used to distinguish differential metabolites in the liver of the mice. OPLS-DA score plots demonstrated a clear separation between the CCl_4 group and the other groups, indicating an abnormal metabolic profile caused by CCl_4 (Supplementary Figures S3A–D). To prevent overfitting of the model between the CON and CCl_4 group, a 200-times permutation test was employed. The Q2 values was <0.05, indicating that the OPLS-DA model (R^2X = 0.854, R^2Y = 0.998, Q^2 = 0.898) was reliable (Supplementary Figures S3E). S-plot and VIP values were applied to screen differential metabolites based on VIP >1 and p < 0.05 (Supplementary Figures S3F), a total of 16 differential metabolites were altered by CCl_4 treatment vs. CON groups, among which nine were upregulated and seven were downregulated (Figure 5A). Interestingly, pretreatment with YCSND significantly affected nine metabolites, including choline, malic acid, glutamate, 3-hydroxybutyric acid (3HB), succinate, trimethylamine oxide (TMAO), acetate, lactate, and xanthine (Figures 5B–J), indicating that YCSND improved the CCl_4-induced abnormal hepatic metabolism. High lactate levels are indicative of CCl_4-induced liver toxicity (Zira et al., 2013). Our results showed that a medium dose of YCSND significantly reduced hepatic lactate content. Li et al. reported elevated acetate and 3HB levels in a CCl_4-induced liver injury model (Li et al., 2017), which is consistent with the results of the present study. Choline is a key component of the cell membrane. In our study, choline content was significantly lower in the CCl_4 group, which is consistent with previous findings (Li et al., 2014; Sun et al., 2020). Patients with cirrhosis had decreased levels of TMAO and choline deficiency could contribute to reduce TMAO levels in liver cirrhosis (van den Berg et al., 2022). TMAO content was significantly lower in the CCl_4 group compared with CON group. These data show that YCSND alleviated ALI by improving hepatic endogenous metabolite profile.

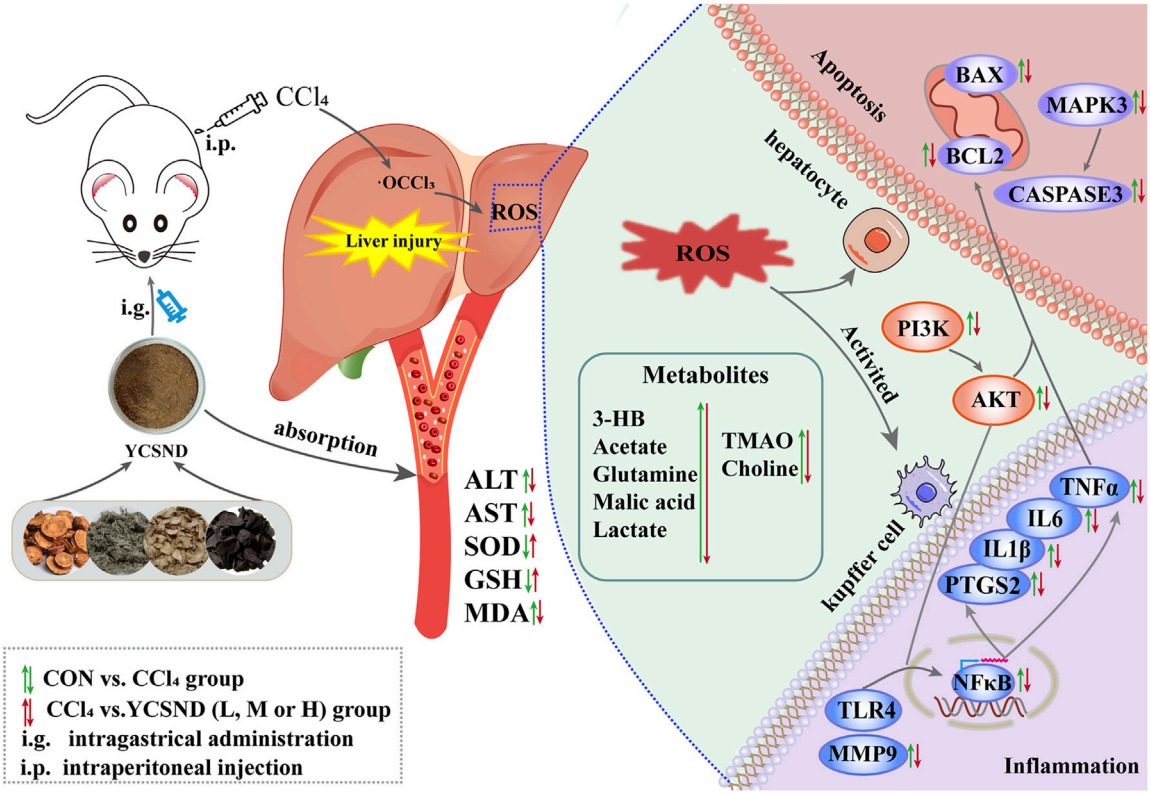

FIGURE 9
The molecular mechanism of Yinchen sini decoction (YCSND) against acute liver injury (ALI).

3.6 Network analysis

3.6.1 Target prediction of YCSND metabolites against ALI

A total of 763 targets of 89 metabolites from the SWISS database and 1,432 targets of liver injury from public databases were identified after removing duplicate targets (Supplementary Material S1). Venn diagram showed 229 overlapping targets, which were identified as key targets of YCSND in liver injury (Supplementary Figure S4A). A network of "metabolite-overlapped target" relationship was constructed and shown in Supplementary Figure S4B.

3.6.2 KEGG pathway and GO enrichment

GO and KEGG pathway enrichment analyses were performed using the Metascape database (Supplementary Material S2, S3), and the top 20 KEGG pathways based on *p*-value are shown in Figure 6A. KEGG pathway analysis showed that several disease-related pathways were enriched, such as pathways in cancer, hepatitis B and C, and influenza A. We focused on five key KEGG pathways (Figure 6B) that were closely related to the mechanism of liver-injury, according to the literature (Zhou et al., 2020; Abdelhamid et al., 2021). Overall, these results suggest that YCSND may play a key role in ALI prevention by regulating several pathways. GO enrichment analysis showed that the targets were mainly enriched in the functions of cell membrane and organelles, including the side of the membrane, receptor complex, and membrane microdomain, in the "cellular components (CC)" category; in kinase activities and cell factor binding, including kinase, protein kinase, and transcription factor binding, in the "molecular functions (MF)" category; and the physiological state of cells and immune responses in the "biological processes (BP)" category (Figures 6C–E).

3.6.3 Construction of metabolite-target-pathway (M-T-P) network

A M-T-P network was constructed to elucidate the relationships among the top 20 KEGG pathways, related targets and metabolites. The network contained 1,451 edges and 208 nodes, including 78 metabolites, 110 targets, and 20 KEGG pathways (Supplementary Figure S5A). Additionally, the target-pathway (T-P) and M-T-P networks were constructed using five key pathways related to ALI (Figure 6F; Supplementary Figure S5B). The T-P network showed that the targets with high degrees in these five pathways were AKT1, NfκB1, MAPK3, PI3KCA, PI3KCB, PI3KR1 and RELA, among which AKT1, PI3KCA, PI3KCB and PI3KR1 are key genes involved in the PI3K-AKT signaling pathway. RELA and NfκB1 are crucial targets involved in the NFκB pathway which regulates inflammatory cytokines. Therefore, we speculated that the PI3K-AKT signaling pathway and inflammation regulation may be involved in the effects of YCSND against ALI. The M-T-P network showed that the five metabolites with the highest degree values were 6-gingerol (degree, 46), scoparone (degree, 41), galangin (degree, 40), 8-shogaol (degree, 40), and morusin (degree, 39). Notably, HPLC confirmed that YCSND has a high scoparone

content. Scoparone is the active ingredient of Artemisia capillaris Thunb. [Asteraceae; Artemisiae scopariae herba] and has positive therapeutic effects on liver diseases (Hui et al., 2020). Overall, the results of the network analysis indicated that YCSND had multifaceted synergistic effects against ALI by integrating multiple metabolites, targets, and multi-pathways against ALI, which is consistent with the theory of TCM.

3.7 The molecular mechanism of YCSND against acute liver injury (ALI)

To explore the molecular mechanisms of YCSND in ALI, we identified multiple targets from five ALI-related pathways predicted by network analysis. These targets included *Pi3k*, *Akt1*, *Mapk3*, *Tlr4*, *Il6*, *Tnf*, *Nfκb1*, *Bcl2*, *Caspase3*, *Mmp9*, *Ptgs2*, *Stat3*, *Vegfa*, and *Egfr*. Additionally, the important inflammatory cytokines *Il1β* and apoptotic gene *Bax* were also included. Network predictions showed that YCSND may have anti-inflammatory activity, which was consistent with the results on the *in vivo* experiments. YCSND demonstrated excellent anti-inflammatory effects against ALI by reducing the mRNA levels of the pro-inflammatory factors *Il6*, *Il1β*, *Tnfα* and the upstream inflammatory regulator *Nfκb1* (Figures 7A–D). TLR4, PTGS2, and MMP9 are closely associated with inflammatory responses, and TLR4 regulates NFκB activation, which can promote PTGS2 expression. Inflammatory response and tissue damage caused by CCl_4 in mice could induce the overexpression of MMP9 (Hafez et al., 2017). CCl_4 increased *Tlr4*, *Ptgs2* and *Mmp9* mRNA levels in the liver (Figures 7E–G), which was consistent with previous findings (Leung et al., 2011; Zhao D. et al., 2022). However, YCSND pretreatment reversed CCl_4-induced changes in inflammation-related genes, but did not significantly affect *Vegfa*, *Efgr*, and *Stat3* mRNA levels, which are mainly involved in the HIF-1 signaling pathway (Supplementary Figures S6A–C). Furthermore, we examined changes in the expression levels of the apoptosis-related genes *Bcl2*, *Caspase3*, and *Bax*. CCl_4 upregulated the expression of the pro-apoptotic genes *Bax* and *Caspase3* and downregulated the anti-apoptotic gene *Bcl2* (Figures 7H–J). In contrast, YCSND pretreatment reversed CCl_4-induced changes in the expression of apoptosis-related genes, indicating an anti-apoptotic effect against ALI. The activation of mitogen-activated protein kinase (MAPK) can accelerate apoptosis by inhibiting *Bcl2* expression and inducing the activation of caspase family proteins (Dong et al., 2015). *Mapk3* expression was upregulated in the CCl_4 group, which was reversed by YCSND treatment (Figure 7K). Additionally, the PI3K-AKT signaling pathway was the most significant pathway closely associated with ALI in computational prediction. Compared with the CCl_4 group, YCSND treatment inhibited *Pi3k* and *Akt* mRNA expression (Figures 7L, M). These results suggest that YCSND improved ALI by regulating PI3K-AKT signaling pathway and ameliorating inflammation and apoptosis.

3.8 Integration of network analysis and metabolomics

A total of 267 targets from 8 metabolites were altered by YCSND, except for acetate (no target was found), based on the SWISS database. Additionally, we identified 19 overlapping targets from the metabolites altered by YCSND and five pharmacological prediction pathways related to ALI (Supplementary Material S4). We also verified that YCSND regulated the targets of *Caspase3*, *Tlr4*, *Mmp9*, and *Ptgs2*, which were mainly linked to the metabolites including xanthine, 3HB, lactate, and choline. *Tlr4*, *Mmp9*, and *Ptgs2* are related to inflammatory response and *Caspase3* is a typical target associated with apoptosis. Finally, we constructed a network to link the metabolites changed by YCSND *in vivo*, crossed targets (metabolites and network analysis), pathways related to ALI, and targets related to pathways affected by YCSND (Figure 8).

4 Discussion

Over the years, several clinical trials have demonstrated the hepatoprotective potential of YCSND in hepatobiliary diseases (Wang et al., 2008); however, the underlying molecular mechanisms remain unclear. The theory of TCM emphasizes the holistic and synergistic effects of multiple metabolites of YCSND. The main metabolites of YCSND, chlorogenic acid, 6-gingerol and scoparone, have been reported to possess therapeutic effects against ALI (Merzouk et al., 2017; Hui et al., 2020; Liu et al., 2023). In the present study, we elucidated the mechanism of the hepatoprotective effects of YCSND using integrating network analysis and metabolomics.

The metabolites of TCM formulas are not simple combinations of plant-derived metabolites; instead, they are influenced by the source of botanical drugs and processing techniques (Li Z. et al., 2022). There was a noticeable discrepancy between the predicted outcomes based on the actual compositions of TCM and the database (Li Z. et al., 2022). Although the predicted YCSND metabolites based on the database were not included in the present study, there were notable discrepancies between the network analysis results obtained from the predicted components and the actual metabolites of YCSND. We attempted to predict the metabolites of YCSND based on a previous database (TCMSP database) and identified 105 effective metabolites, UHPLC-QE-MS identified only 89 metabolites of YCSND detected by UHPLC-QE-MS, indicating that only a small fraction of the actual metabolites of YCSND were consistent with the predictions. Additionally, the top 20 KEGG pathways based on the predicted metabolites appeared unreliable, as these pathways were mainly related to cancer and diabetes, rather than the five pathways related to ALI based on predictions using the actual metabolites. Overall, predictions based on the actual metabolites of YCSND could minimize the inherent prediction bias in network analysis.

Biomarkers are effective tools for monitoring disease progression and assessing treatment effectiveness (Borém et al., 2023). CCl_4-induced ALI can lead to abnormal accumulation or depletion of hepatic endogenous metabolites in the body, affecting a range of metabolic pathways, such as amino acid metabolism, energy metabolism, and lipid metabolism (Zira et al., 2013; Li et al., 2017). Choline deficiency may be related to CCl_4-induced breakdown of cell membrane structure, resulting in the outflow of ALT from the liver into the serum (Li et al., 2014). The tricarboxylic acid (TCA) cycle, an important energy metabolism pathway, is the hub for amino acid and glycolipid metabolism. CCl_4 can induce abnormal

energy metabolism by damaging the hepatocellular mitochondria and inhibiting enzyme activity during the TCA cycle (Zira et al., 2013). However, YCSND can restore malic acid and succinate, which are intermediate metabolites of the TCA cycle. Moreover, glutamate can participate in the glutamic acid and glutamine cycles, and glutamine is degraded into glutamate and ammonia by glutaminase. Liver injury can lead to impaired ammonia metabolism in the body, potentially resulting in hyperammonemia (Jimenez-Torres et al., 2021); however, a decrease in glutamate can reverse this condition. Moreover, low levels of glutamate are beneficial for ROS clearance and the improvement of antioxidant capacity (Demircan et al., 2014; Chen et al., 2023). The excessive oxidation of fatty acids can increase the end-product acetate and induce the accumulation of ketone bodies in the CCl_4-induced ALI model (Huo et al., 2016), which are consistent with our results of increasing acetic acid and ketone body 3HB in CCl_4 group. Notably, we showed that pretreatment with YCSND reversed these changes. Overall, these results support the hypothesis that YCSND has a positive effect on abnormal metabolism in the liver of mice.

The relationship between genes and metabolites is bidirectional and complex, with genes affecting metabolites, and *vice versa*. In the present study, we integrated network analysis and metabolomics to link the differential metabolites to gene targets. Figure 8 depicts the potential associations between metabolites and target genes. Xanthine oxidase converts hypoxanthine to xanthine, which eventually forming uric acid. Elevated xanthine concentrations can contribute to the formation of uric acid, posing potential health risks; the increase of xanthine can activate the expression of CASPASE3, whereas xanthine oxidase inhibitors had the opposite effect (Genesca et al., 2002; Park et al., 2010). High levels of 3HB could initiate ketosis, resulting in the activation of TLR4/NFκB to induce high expression of inflammation under a state of ketosis (Li et al., 2017). Moreover, the inhibition of TLR4 may be beneficial for the regulation of ketone body levels and the decrease in 3HB levels. Choline has been reported to treat LPS-induced inflammation in rats by reducing PTGS2 levels (Baris et al., 2021). And long-term choline deficiency diet can lead to increased hepatic PTGS2 levels (Motino et al., 2016; He et al., 2022). In this study, choline levels increased and *Ptgs2* mRNA level decreased after treatment with YCSND, which is consistent with previous reports (Motino et al., 2016; He et al., 2022). Pyruvate generates lactic acid under the action of lactate dehydrogenase, and lactate dehydrogenase knockout reduces the level of MMP9 (Wang et al., 2017). Moreover, a positive correlation has been reported between lactic acid level and MMP9 (Park et al., 2005; Duda et al., 2020). Overall, these data support the potential association between targets and metabolites that could be regulated by YCSND.

The metabolism-related targets identified in the present study have been reported to be involved in inflammation and apoptosis, which are important regulatory targets in ALI. Exposure to CCl_4 can activate Kupffer cells in the liver, which can promote the expression of pro-inflammatory factors through TLR4/NFκB signaling (Hsieh et al., 2021; Sun et al., 2022). Additionally, the TNF signaling pathway, which is related to the inflammatory response is activated during CCl_4-induced ALI (Zhang J. X. et al., 2022). In the present study, YCSND reduced hepatic inflammation by inhibiting the mRNA expression of the pro-inflammatory factor *Il6*, *Il1β*, and *Tnfα* and the inflammatory regulators *Nfκb1* and *Tlr4*. These results suggest that YCSND effectively inhibited the TNF signaling pathway by downregulating the typical target genes of the pathway, including *Il6*, *Tnfα*, and *Nfkb1*. The upregulation of the pleiotropic cytokine TNFα not only promotes inflammation but also accelerates cell apoptosis (Dong et al., 2016). Additionally, excessive free radicals produced during the hepatic metabolism of CCl_4 can trigger mitochondrial dysfunction and induce hepatic apoptosis. An increase in the pro-apoptotic protein BAX can enhance mitochondrial permeability and activate CASPASE3 to induce apoptosis (Wang Y. et al., 2023). In the present study, there was a decrease in the expression of the anti-apoptotic *Bcl2* mRNA level in damaged cells, which was reversed by treatment with YCSND. Overall, these results indicate that YCSND reduced inflammation and inhibited hepatocyte apoptosis.

Research evidence has shown that the PI3K-AKT pathway contributes to the development of liver injury and fibrosis, including the activation of hepatic stellate cells, synthesis and degradation of the extracellular matrix, and regulation of matrix metalloproteinase (MMP) activity (Gong et al., 2020). TCM has been shown to possess therapeutic effects in ALI by inhibiting the PI3K-AKT pathway (Zhao et al., 2018; Gong et al., 2020; Wang J. M. et al., 2023). For instance, Qinggan Huoxue Recipe attenuated ethanol-induced ALI by downregulating *Pi3k* and *Akt1* mRNA levels. Additionally, the Dahuang Zhechong pill ameliorated CCl_4-induced liver fibrosis by reducing the protein levels of PI3K and phosphorylated AKT and inhibiting the proliferation of HSC, and exerting a synergistic effect with the PI3K inhibitor LY294002. Zhao et al. reported a relationship between the PI3K/AKT/Raptor/Rictor signaling pathway and apoptosis and observed that Erzhi Pill can ameliorate ALI by inhibiting the pathway to reduce hepatic apoptosis (Zhao et al., 2018). Moreover, AKT phosphorylation can exacerbate ALI, whereas AKT inhibitors can suppress hepatic apoptosis by inhibiting the PI3K/AKT/FXR axis *in vitro* (Jiang et al., 2023). The PI3K-AKT signaling pathway is also vital in the regulation of inflammation, especially the PI3K/AKT/NF-κB axis (Zhu et al., 2017; Yang et al., 2020). Phosphorylated AKT enhances the nuclear transcription of NFκB and the release of pro-inflammatory cytokines, and these effects are blocked by PI3K inhibitors, thereby inhibiting hepatocyte apoptosis, reducing inflammation, and alleviating liver damage (Gong et al., 2020). Glycyrrhizic acid (Niu et al., 2022), scoparone (Liu et al., 2020), isorhamnetin (Li et al., 2015), quercetin (Yang et al., 2020), and luteolin (Jiang et al., 2023) have been reported to regulate the PI3K/AKT axis to improve ALI. And these metabolites were detected in YCSND in our study. In the present study, YCSND inhibited *Pi3k* and *Akt1* mRNA expression, indicating that YCSND can regulate the PI3K-AKT pathway to inhibit hepatic apoptosis and inflammatory responses in ALI.

This study had some limitations. Although the accuracy of the network prediction has improved, there was still heterogeneity in the experimental validation and prediction results in the present study. YCSND had only minimal effects on some of the predicted targets, such as *Vegfa*, *Egfr*, and *Stat3*. We suggested that network analysis should be based on the actual constituents of the TCM, rather than botanical drug information from existing databases. However, network analysis still relies heavily on databases, and this inherent bias caused by the databases is a common issue in network analysis. The completeness and timeliness of the Swiss database can particularly impact our study results. For example, delayed data updates and the abundance of potential targets for well-known

active metabolites like quercetin with the less targets of new metabolites can lead to result in false positives or false negatives. To narrow down these biases, continuous improvement and timely information updates of databases should be the common goal of future network analysis research. Moreover, network analysis predictions may not comprehensively reflect the intricate interactions and mechanisms of drugs within the body. Therefore, experimental verification is necessary to ensure the authenticity of network predictions. Meanwhile, regarding the connection between network analysis and metabolism, the target genes related to changes in differential metabolites require further investigation. We validated the highly significant PI3K signaling pathway predicted by network analysis through RT-qPCR analysis. In future studies, other signaling pathways predicted by network analysis should be further considered to expand the molecular mechanisms of YCSND in ALI.

5 Conclusion

In the present study, integrated network analysis and ^{1}H-NMR metabolomics revealed key targets (*Tlr4*, *Ptgs2*, *Mmp9,* and *Caspase3*) and related metabolites (choline, xanthine, lactate, and 3HB) regulated by YCSND in ALI treatment. Our results indicated that YCSND ameliorated ALI by regulating the PI3K-AKT signaling pathway, reducing inflammatory response, and inhibiting apoptosis (Figure 9). Overall, our findings indicate that YCSND has the potential to alleviate ALI, offering a foundational support for the subsequent development and utilization. We have also pointed out the direction for applying network analysis in TCM formulas, stressing the importance of utilizing real metabolites for network analysis and experimental validation. Enhancing the precision of network analysis presents a challenge that future researchers should collectively address.

Data availability statement

The original contributions presented in the study are included in the article/Supplementary Material, further inquiries can be directed to the corresponding authors.

Ethics statement

The animal study was approved by the Animal Care and Use Committee of Jinlin University (approval no: 2021SY0715). The study was conducted in accordance with the local legislation and institutional requirements.

Author contributions

WZ designed the experiment. WZ, YM, and TP performed the animal's experiment. WZ and JP analyzed data and drafted the manuscript. YZ, CS, and KN participate in the modified revision of manuscript. HX and QX provided design ideas, research platforms, and financial support for this work, and reviewed the manuscript. All authors contributed to the article and approved the submitted version.

Funding

This work was supported by Changchun Science and Technology Bureau under Grant 21ZGN11, Jilin Province Development and Reform Commission under Grant 2021FGWCXNLJSSZ11, and Jilin Province Science and Technology Institute under Grant 20220204067YY.

Conflict of interest

The authors declare that the research was conducted in the absence of any commercial or financial relationships that could be construed as a potential conflict of interest.

Publisher's note

Supplementary material

The Supplementary Material for this article can be found online at: https://www.frontiersin.org/articles/10.3389/fphar.2023.1221046/full#supplementary-material

References

Abdelhamid, A. M., Youssef, M. E., Abd El-Fattah, E. E., Gobba, N. A., Gaafar, A. G. A., Girgis, S., et al. (2021). Blunting p38 MAPKa and ERK1/2 activities by empagliflozin enhances the antifibrotic effect of metformin and augments its AMPK-induced NF-kappa B inactivation in mice intoxicated with carbon tetrachloride. *Life. Sci.* 286, 120070. doi:10.1016/j.lfs.2021.120070

Baris, E., Simsek, O., Efe, H., Oncu, S., Gelal, A., Hamurtekin, E., et al. (2021). Effects of CDP-choline and choline on COX pathway in LPS-induced inflammatory response in rats. *Int. J. Pharmacol.* 17 (2), 84–96. doi:10.3923/ijp.2021.84.96

Bilkan, M. T., Çiçek, Z., Kurşun, A. G. C., Özler, M., and Eşmekaya, M. A. (2022). Investigations on effects of titanium dioxide (TiO(2)) nanoparticle in combination with UV radiation on breast and skin cancer cells. *Med. Oncol.* 40 (1), 60. doi:10.1007/s12032-022-01931-5

Borém, F. M., Abreu, G. F., Ferreira, A. G., Santos, M. D. S., Alves, T. D. C., and Alves, A. P. C. (2023). ^{1}H NMR spectroscopy applied to identify chemical aging markers in green coffee (*Coffea arabica* L.). *Food. Chem.* 405, 134667. doi:10.1016/j.foodchem.2022.134667

Chen, D., Liang, Y., Liang, J., Shen, F., Cheng, Y., Qu, H., et al. (2023). Beneficial effects of *m*n rats with nonalcoholic fatty liver disease. *J. Dairy. Sci.* 106 (3), 1533–1548. doi:10.3168/jds.2022-22383

Chen, G., Huang, C., Lu, J., Huang, R., Zhang, J., Chen, Z., et al. (2019). Efficacy and safety of Yinchen Sini decoction in treating biliary atresia patients after Kasai portoenterostomy A systematic review and meta-analysis protocol. *Med.* 98 (2), e13935. doi:10.1097/MD.0000000000013935

Demircan, C., Gül, Z., and Büyükuysal, R. L. (2014). High glutamate attenuates S100B and LDH outputs from rat cortical slices enhanced by either oxygen–glucose deprivation or menadione. *Neurochem. Res.* 39 (7), 1232–1244. doi:10.1007/s11064-014-1301-7

Dong, D., Xu, L., Yin, L., Qi, Y., and Peng, J. (2015). Naringin prevents carbon tetrachloride-induced acute liver injury in mice. *J. Funct. Foods.* 12, 179–191. doi:10.1016/j.jff.2014.11.020

Dong, Y. L., Liu, Y. Z., Kou, X. R., Jing, Y. Y., Sun, K., Sheng, D. D., et al. (2016). The protective or damaging effect of Tumor necrosis factor-alpha in acute liver injury is concentration-dependent. *Cell. Biosci.* 6, 8. doi:10.1186/s13578-016-0074-x

Duda, I., Krzych, Ł., Jędrzejowska-Szypułka, H., and Lewin-Kowalik, J. (2020). Plasma matrix metalloproteinase-9 and tissue inhibitor of matrix metalloproteinase-1 as prognostic biomarkers in critically ill patients. *Open. Med-Warsaw.*15 (1), 50–56. doi:10.1515/med-2020-0008

Genesca, M., Sola, A., Miquel, R., Pi, F., Xaus, C., Alfaro, V., et al. (2002). Role of changes in tissular nucleotides on the development of apoptosis during ischemia/reperfusion in rat small bowel. *Am. J. Pathol.* 161 (5), 1839–1847. doi:10.1016/S0002-9440(10)64460-4

Gong, Z. H., Lin, J. Y., Zheng, J., Wei, L. Y., Liu, L., Peng, Y. Z., et al. (2020). Dahuang Zhechong pill attenuates CCl_4-induced rat liver fibrosis via the PI3K-Akt signaling pathway. *J. Cell. Biochem.* 121 (2), 1431–1440. doi:10.1002/jcb.29378

Guo, C., Kang, X., Cao, F., Yang, J., Xu, Y., Liu, X., et al. (2021). Network pharmacology and molecular docking on the molecular mechanism of Luo-hua-zi-zhu (LHZZ) granule in the prevention and treatment of bowel precancerous lesions. *Front. Pharmacol.* 12, 629021. doi:10.3389/fphar.2021.629021

Hafez, M. M., Hamed, S. S., El-Khadragy, M. F., Hassan, Z. K., Al Rejaie, S. S., Sayed-Ahmed, M. M., et al. (2017). Effect of ginseng extract on the TGF-beta 1 signaling pathway in CCl_4-induced liver fibrosis in rats. *Bmc. Complement. Altern. Med.* 17 (1), 45–47. doi:10.1186/s12906-016-1507-0

He, X. L., Hu, Y. R., Liu, W., Zhu, G. H., Zhang, R. X., You, J. W., et al. (2022). Deciphering the effective constituents and mechanisms of *Portulaca oleracea* L. For treating NASH via integrating bioinformatics analysis and experimental pharmacology. *Front. Pharmacol.* 12, 818227. doi:10.3389/fphar.2021.818227

Hsieh, Y. C., Lee, K. C., Wu, P. S., Huo, T. I., Huang, Y. H., Hou, M. C., et al. (2021). Eritoran attenuates hepatic inflammation and fibrosis in mice with chronic liver injury. *Cells* 10 (6), 1562. doi:10.3390/cells10061562

Hsueh, T. P., Lin, W. L., Dalley, J. W., and Tsai, T. H. (2021). The pharmacological effects and pharmacokinetics of active compounds of Artemisia capillaris. *Biomedicines* 9 (10), 1412. doi:10.3390/biomedicines9101412

Huang, L., Xu, Y., Deng, M., and Zhou, Z. (2021). Research progress on chemical constituents, pharmacological mechanism and clinical application of *Artemisiae scoparia* Herba. *Nat. Prod. Res.* 33 (04), 676–690. doi:10.16333/j.1001-6880.2021.4.018

Hui, Y., Wang, X., Yu, Z., Fan, X., Cui, B., Zhao, T., et al. (2020). Scoparone as a therapeutic drug in liver diseases: Pharmacology, pharmacokinetics and molecular mechanisms of action. *Pharmacol. Res.* 160, 105170. doi:10.1016/j.phrs.2020.105170

Huo, T., Fang, Y., Zhao, L., Xiong, Z., Zhang, Y., Wang, Y., et al. (2016). ^{1}HNMR-based metabonomic study of sub-chronic hepatotoxicity induced by realgar. *J. Ethnopharmacol.* 192, 1–9. doi:10.1016/j.jep.2016.07.003

Huo, X. W., Meng, X. B., Zhang, J., and Zhao, Y. Y. (2020). Hepatoprotective effect of different combinations of 18 alpha-and 18 beta-Glycyrrhizic acid against CCl_4-induced liver injury in rats. *Biomed. Pharmacother.* 122, 109354. doi:10.1016/j.biopha.2019.109354

Jiang, M., Huang, C., Wu, Q., Su, Y., Wang, X., Xuan, Z., et al. (2023). Sini San ameliorates CCl_4-induced liver fibrosis in mice by inhibiting AKT-mediated hepatocyte apoptosis. *J. Ethnopharmacol.* 303, 115965. doi:10.1016/j.jep.2022.115965

Jimenez-Torres, C., El-Kehdy, H., Hernandez-Kelly, L. C., Sokal, E., Ortega, A., and Najimi, M. (2021). Acute liver toxicity modifies protein expression of glutamate transporters in liver and cerebellar tissue. *Front. Neurosci.* 14, 613225. doi:10.3389/fnins.2020.613225

Lee, M. M., Kim, H. G., Lee, J. S., Lee, S. B., Cho, J. H., Lee, D. S., et al. (2020). Synergistic hepatoprotective effects of CG(plus) on CCl_4-induced acute injury. *J. Ethnopharmacol.* 249, 112441. doi:10.1016/j.jep.2019.112441

Leung, T. M., Fung, M. L., Liong, E. C., Lau, T. Y. H., Nanji, A. A., and Tipoe, G. L. (2011). Role of nitric oxide in the regulation of fibrogenic factors in experimental liver fibrosis in mice. *Histol. Histopathol.* 26 (2), 201–211. doi:10.14670/HH-26.201

Li, J., Li, X., Xu, W., Wang, S., Hu, Z., Zhang, Q., et al. (2015). Antifibrotic effects of luteolin on hepatic stellate cells and liver fibrosis by targeting AKT/mTOR/p70S6K and TGFβ/Smad signalling pathways. *Liver. Int.* 35 (4), 1222–1233. doi:10.1111/liv.12638

Li, J., Qiu, J. L., Xu, H., An, J., Cao, L. M., Yang, H. P., et al. (2016b). EGCG induces lung cancer A549 cell apoptosis by regulating Ku70 acetylation. *J. Chin. Med. Mater.* 39 (10), 2339–2347. doi:10.3892/or.2016.4587

Li, J., Qiu, J., and Xu, H. (2016a). Effect of jiawei yinchen sini decoction on the production of Smad7 and CollagenI, III in carbon tetrachloride induced hepatic fibrosis model of mice. *J. Chin. Med. Mater.* 39 (6), 1384–1388. doi:10.13863/j.issn1001-4454.2016.06.045

Li, M., Luo, Q., Tao, Y. Y., Sun, X., and Liu, C. H. (2022a). Pharmacotherapies for drug-induced liver injury: A current literature review. *Front. Pharmacol.* 12, 806249. doi:10.3389/fphar.2021.806249

Li, X., Zhang, F., Wang, D., Li, Z., Qin, X., and Du, G. (2014). NMR-based metabonomic and quantitative real-time PCR in the profiling of metabolic changes in carbon tetrachloride-induced rat liver injury. *J. Pharm. Biomed.* 89, 42–49. doi:10.1016/j.jpba.2013.10.023

Li, Z., Li, Y., Lu, L., Yang, Z., Xue, W., Tian, X., et al. (2017). ^{1}H-NMR based serum metabolomics study to investigate hepatoprotective effect of qin-jiao on carbon tetrachloride-induced acute hepatotoxicity in rats. *Evid-Based. Compl. Alt.* 10, 6091589. doi:10.1155/2017/6091589

Li, Z., Qu, B., Wu, X., Chen, H., Wang, J., Zhou, L., et al. (2022b). Methodology improvement for network pharmacology to correct the deviation of deduced medicinal constituents and mechanism: Xian-Ling-Gu-Bao as an example. *J. Ethnopharmacol.* 289, 115058. doi:10.1016/j.jep.2022.115058

Liu, B., Deng, X., Jiang, Q., Li, G., Zhang, J., Zhang, N., et al. (2020). Scoparone improves hepatic inflammation and autophagy in mice with nonalcoholic steatohepatitis by regulating the ROS/P38/Nrf2 axis and PI3K/AKT/mTOR pathway in macrophages. *Biomed. Pharmacother.* 125, 109895. doi:10.1016/j.biopha.2020.109895

Liu, X. J., Liu, H. L., Zhao, D., Wei, F. X., Wang, Y. Z., Lv, M., et al. (2021). Hepatic metabolomics of the compatibility effect of Xiaoyaosan on CUMS-induced depression based on the TCM theory of "Treating Diseases via Regulating the Liver's Function. *J. Pharm. Biomed.* 201, 114123. doi:10.1016/j.jpba.2021.114123

Liu, X., Tian, X., Ma, Z. P., Chen, J. L., Huang, Q. S., Gao, P. Y., et al. (2022). Efficacy and safety of glycyrrhizic acid preparation treating comorbid liver injury in COVID-19: A systematic review. *Front. Pharmacol.* 13, 1003697. doi:10.3389/fphar.2022.1003697

Liu, Y. Z., Li, D., Wang, S., Peng, Z., Tan, Q., He, Q. F., et al. (2023). 6-Gingerol ameliorates hepatic steatosis, inflammation and oxidative stress in high-fat diet-fed mice through activating LKB1/AMPK signaling. *Int. J. Mol. Sci.* 24 (7), 6285. doi:10.3390/ijms24076285

Merzouk, A. S., Hafida, M., Medjdoub, A., Loukidi, B., Cherrak, S., Merzouk, S. A., et al. (2017). Alterations of hepatocyte function with free radical generators and reparation or prevention with coffee polyphenols. *Free Radic. Res.* 51 (3), 294–305. doi:10.1080/10715762.2017.1307979

Mogadem, A., Naqvi, A., Almamary, M. A., Ahmad, W. A., Jemon, K., and El-Alfy, S. H. (2022). Hepatoprotective effects of flexirubin, a novel pigment from Chryseobacterium artocarpi, against carbon tetrachloride-induced liver injury: An *in vivo* study and molecular modeling. *Toxicol. Appl. Pharm.* 444, 116022. doi:10.1016/j.taap.2022.116022

Motino, O., Agra, N., Contreras, R. B., Dominguez-Moreno, M., Garcia-Monzon, C., Vargas-Castrillon, J., et al. (2016). Cyclooxygenase-2 expression in hepatocytes attenuates non-alcoholic steatohepatitis and liver fibrosis in mice. *Bba-Mol. Basis. Dis.* 1862 (9), 1710–1723. doi:10.1016/j.bbadis.2016.06.009

Niu, Z., Lin, J., Hao, C., Xu, X., Wang, C., Dai, K., et al. (2022). Glycyrrhizic acid attenuates pulmonary fibrosis of silicosis by inhibiting the interaction between HMGB1 and BRG1 through PI3K/Akt/mTOR pathway. *Int. J. Env. Res. Pub. He.* 19 (14), 8743. doi:10.3390/ijerph19148743

Park, K. J., Hwang, S. C., Sheen, S. S., Oh, Y. J., Han, J. H., and Lee, K. B. (2005). Expression of matrix metalloproteinase-9 in pleural effusions of tuberculosis and lung cancer. *Respiration* 72 (2), 166–175. doi:10.1159/000084048

Park, S., Kim, J. A., Choi, S., and Suh, S. H. (2010). Superoxide is a potential culprit of caspase-3 dependent endothelial cell death induced by lysophosphatidylcholine. *J. Physiol. Pharmacol.* 61 (4), 375–381.

Reagan-Shaw, S., Nihal, M., and Ahmad, N. (2008). Dose translation from animal to human studies revisited. *FASEB J.* 22 (3), 659–661. doi:10.1096/fj.07-9574LSF

Ren, X., Xin, L. T., Zhang, M. Q., Zhao, Q., Yue, S. Y., Chen, K. X., et al. (2019). Hepatoprotective effects of a traditional Chinese medicine formula against carbon tetrachloride-induced hepatotoxicity *in vivo* and *in vitro*. *Biomed. Pharmacother.* 117, 109190. doi:10.1016/j.biopha.2019.109190

Ruiz-Rodado, V., Nicoli, E.-R., Probert, F., Smith, D. A., Morris, L., Wassif, C. A., et al. (2016). ^{1}H NMR-linked metabolomics analysis of liver from a mouse model of NP-C1 disease. *J. Proteome. Res.* 15 (10), 3511–3527. doi:10.1021/acs.jproteome.6b00238

Sahayarayan, J. J., Udayakumar, R., Arun, M., Ganapathi, A., Alwahibi, M. S., Aldosari, N. S., et al. (2020). Effect of different Agrobacterium rhizogenes strains for *in-vitro* hairy root induction, total phenolic, flavonoids contents, antibacterial and antioxidant activity of (*Cucumis anguria* L.). *Saudi. J. Biol. Sci.* 27 (11), 2972–2979. doi:10.1016/j.sjbs.2020.08.050

Shrestha, N., Chand, L., Han, M. K., Lee, S. O., Kim, C. Y., and Jeong, Y. J. (2016). Glutamine inhibits CCl_4 induced liver fibrosis in mice and TGF-β1 mediated epithelial–mesenchymal transition in mouse hepatocytes. *Food. Chem. Toxicol.* 93, 129–137. doi:10.1016/j.fct.2016.04.024

Siddhuraju, P., and Manian, S. (2007). The antioxidant activity and free radical-scavenging capacity of dietary phenolic extracts from horse gram (*Macrotyloma uniflorum* (Lam.) Verdc.) seeds. *Food. Chem.* 105 (3), 950–958. doi:10.1016/j.foodchem.2007.04.040

Sun, L. L., Zhang, Y. Z., Wen, S., Li, Q. H., Chen, R. H., Lai, X. F., et al. (2022). Extract of *Jasminum grandiflorum* L. alleviates CCl_4-induced liver injury by decreasing inflammation, oxidative stress and hepatic CYP2E1 expression in mice. *Biomed. Pharmacother.* 152, 113255. doi:10.1016/j.biopha.2022.113255

Sun, L., Zhao, M., Zhao, Y., Wang, M., Man, J., and Zhao, C. (2020). Investigation of the therapeutic effect of Shaoyao Gancao decoction on CCL_4-induced liver injury in rats by metabolomic analysis. *Biomed. Chromatogr.* 34 (11), e4940. doi:10.1002/bmc.4940

Unsal, V., Cicek, M., and Sabancilar, I. (2021). Toxicity of carbon tetrachloride, free radicals and role of antioxidants. *Rev. Environ. Health.* 36 (2), 279–295. doi:10.1515/reveh-2020-0048

van den Berg, E. H., Flores-Guerrero, J. L., Garcia, E., Connelly, M. A., de Meijer, V. E., Bakker, S. J. L., et al. (2022). High plasma levels of betaine, a trimethylamine N-Oxide-related metabolite, are associated with the severity of cirrhosis. *Liver. Int.* 43 (2), 424–433. doi:10.1111/liv.15310

Wang, J. M., Lu, Y. F., Zhang, C. Y., Tian, S. X., Xiang, H. J., Ding, P. L., et al. (2023a). Qinggan Huoxue Recipe attenuates Alcoholic Liver Disease by suppressing PI3K/AKT signaling pathway based on network pharmacology. *Int. J. Med. Sci.* 20 (3), 346–358. doi:10.7150/ijms.80329

Wang, M. F., Zhao, S. S., Thapa, D. M., Song, Y. L., and Xiang, Z. (2021a). Metabolomics of Fuzi-Gancao in CCl_4 induced acute liver injury and its regulatory effect on bile acid profile in rats. *World. J. gastroentero.* 27 (40), 6888–6907. doi:10.3748/wjg.v27.i40.6888

Wang, Q., Li, Y., Yan, D., Su, H., Tan, B., Jin, J., et al. (2020a). Clavukoellians G-K, new nardosinane and aristolane sesquiterpenoids with angiogenesis promoting activity from the marine soft coral *lemnalia* sp. *Shanghai J. Traditional Chin. Med.* 54, 171–176. doi:10.3390/md18030171

Wang, Q., Luo, Z., Li, D., Qin, J., Pan, Z., Guo, B., et al. (2022). Investigation of the therapeutic effect of total alkaloids of corydalis saxicola bunting on CCl_4-induced liver fibrosis in rats by LC/MS-Based metabolomics analysis and network pharmacology. *Metabolites* 13 (1), 9. doi:10.3390/metabo13010009

Wang, X. J., Wu, M. Z., Zhao, L., and Yan, G. L. (2008). The historical evolution of Yinchen Sini Decoction in the treatment system of yin jaundice syndrome. *Mod. Traditional Chin. Med. Materia Medica-World Sci. Technol.* 03 (2), 12–14.

Wang, X. S., Xu, L. X., Wu, Q. L., Liu, M. Y., Tang, F., Cai, Y., et al. (2017). Inhibition of LDHA deliver potential anticancer performance in renal cell carcinoma. *Urol. Int.* 99 (2), 237–244. doi:10.1159/000445125

Wang, Y., Guo, Y., Liu, H., Du, X., Shi, L., Wang, W., et al. (2023b). Hawthorn fruit extract protect against MC-LR-induced hepatotoxicity by attenuating oxidative stress and apoptosis. *Environ. Toxicol.* 38 (6), 1239–1250. doi:10.1002/tox.23760

Wang, Y., Xie, Q., Zhang, Y., Ma, W., Ning, K., Xiang, J., et al. (2020b). Combination of probiotics with different functions alleviate DSS-induced colitis by regulating intestinal microbiota, IL-10, and barrier function. *Appl. Microbiol. Biot.* 104 (1), 335–349. doi:10.1007/s00253-019-10259-6

Wang, Y., Zhang, H., Wang, J., Yu, M., Zhang, Q., Yan, S., et al. (2021b). Aconiti lateralis Radix Praeparata inhibits Alzheimer's disease by regulating the complex regulation network with the core of GRIN1 and MAPK1. *Pharm. Biol.* 59 (1), 311–320. doi:10.1080/13880209.2021.1900879

Wei, X. C., Luo, C. H., He, Y. N., Huang, H. Z., Ran, F., Liao, W., et al. (2021). Hepatoprotective effects of different extracts from triphala against CCl_4-induced acute liver injury in mice. *Front. Pharmacol.* 12, 664607. doi:10.3389/fphar.2021.664607

Wu, T., Li, S., Huang, Y., He, Z., Zheng, Y., Stalin, A., et al. (2021). Structure and pharmacological activities of polysaccharides from *Anoectochilus roxburghii* (Wall.) Lindl. *J. Funct. Foods* 87, 104815. doi:10.1016/j.jff.2021.104815

Xie, J., Wang, W., Dong, C., Huang, L., Wang, H., Li, C., et al. (2018). Protective effect of flavonoids from *Cyclocarya paliurus* leaves against carbon tetrachloride-induced acute liver injury in mice. *Food. Chem. Toxicol.* 119, 392–399. doi:10.1016/j.fct.2018.01.016

Yang, L., Fu, W.-l., Zhu, Y., and Wang, X.-g. (2020). T beta 4 suppresses lincRNA-p21-mediated hepatic apoptosis and fibrosis by inhibiting PI3K-AKT-NF-kappa B pathway. *Gene* 758, 144946. doi:10.1016/j.gene.2020.144946

Yang, Q., Wu, X., Pan, Z., Guan, R., Yang, P., Liu, Y., et al. (2023). Integration of pharmacodynamics, network pharmacology and metabolomics to elucidate effect and mechanism of *Artemisia capillaris* Thunb. in the treatment of jaundice. *J. Ethnopharmacol.* 303, 115943. doi:10.1016/j.jep.2022.115943

Yu, H., Fu, Q., Huang, Z., Lin, J., Chen, Q., Wang, Q., et al. (2019). Apoptosis induced by ursodeoxycholic acid in human melanoma cells through the mitochondrial pathway. *Oncol. Rep.* 41 (1), 213–223. doi:10.3892/or.2018.6828

Zhang, H. Y., Wang, H. L., Zhong, G. Y., and Zhu, J. X. (2018). Molecular mechanism and research progress on pharmacology of traditional Chinese medicine in liver injury. *Pharm. Biol.* 56 (1), 594–611. doi:10.1080/13880209.2018.1517185

Zhang, J. X., Yang, Y., Huang, H., Xie, H. B., Huang, M., Jiang, W., et al. (2022a). TNF-α/TNFR1 regulates the polarization of Kupffer cells to mediate trichloroethylene-induced liver injury. *Ecotox. Environ. Safe.* 230, 113141. doi:10.1016/j.ecoenv.2021.113141

Zhang, Q., Yang, T., Li, D., Ma, M., Liang, X., Ma, Z., et al. (2022b). The synergistic effect of Angelica sinensis (Oliv.) Diels and Rehmannia glutinosa (Gaertn.) DC. on antioxidant activity and protective ability against cell injury. *J. Food. Biochem.* 46 (8), e14196. doi:10.1111/jfbc.14196

Zhao, D., Xue, C., Yang, Y. F., Li, J. Q., Wang, X. L., Chen, Y., et al. (2022a). Lack of Nogo-B expression ameliorates PPARγ deficiency-aggravated liver fibrosis by regulating TLR4-NF-κB-TNF-α axis and macrophage polarization. *Biomed. Pharmacother.* 153, 113444. doi:10.1016/j.biopha.2022.113444

Zhao, H. M., Zhang, X. Y., Lu, X. Y., Yu, S. R., Wang, X., Zou, Y., et al. (2018). Erzhi PillProtected experimental liver injury against apoptosis via the PI3K/Akt/Raptor/Rictor pathway. *Front. Pharmacol.* 9, 283. doi:10.3389/fphar.2018.00283

Zhao, Q., Ren, X., Song, S.-Y., Yu, R.-L., Li, X., Zhang, P., et al. (2022b). Deciphering the underlying mechanisms of formula le-cao-shi against liver injuries by integrating network pharmacology, metabonomics, and experimental validation. *Front. Pharmacol.* 13, 884480. doi:10.3389/fphar.2022.884480

Zhou, S., Ai, Z., Li, W., You, P., Wu, C., Li, L., et al. (2020). Deciphering the pharmacological mechanisms of taohe-chengqi decoction extract against renal fibrosis through integrating network pharmacology and experimental validation *in vitro* and *in vivo*. *Front. Pharmacol.* 11, 00425. doi:10.3389/fphar.2020.00425

Zhu, M., Zhou, X., and Zhao, J. (2017). Quercetin prevents alcohol-induced liver injury through targeting of PI3K/Akt/nuclear factor-κB and STAT3 signaling pathway. *Exp. Ther. Med.* 14 (6), 6169–6175. doi:10.3892/etm.2017.5329

Zira, A., Kostidis, S., Theocharis, S., Sigala, F., Engelsen, S. B., Andreadou, I., et al. (2013). ^{1}H- NMR-based metabonomics approach in a rat model of acute liver injury and regeneration induced by CCl_4 administration. *Toxicology* 303 (1), 115–124. doi:10.1016/j.tox.2012.10.015

Ziyatdinova, G., and Kalmykova, A. (2023). Electrochemical characterization of the antioxidant properties of medicinal plants and products: A review. *Molecules* 28 (5), 2308. doi:10.3390/molecules28052308

Frontiers in Pharmacology

Explores the interactions between chemicals and living beings

The most cited journal in its field, which advances access to pharmacological discoveries to prevent and treat human disease.

Discover the latest Research Topics

See more →

Frontiers

Avenue du Tribunal-Fédéral 34
1005 Lausanne, Switzerland
frontiersin.org

Contact us

+41 (0)21 510 17 00
frontiersin.org/about/contact